

The 4th  
**INTERNATIONAL  
CONFERENCE  
ON THE PHYSICS OF OPTICAL  
MATERIALS AND DEVICES**

**ICOM 2015**

**BOOK OF ABSTRACTS**

**The 4<sup>TH</sup> International Conference on the Physics of Optical Materials and Devices**

**BOOK OF ABSTRACTS**

**Editors: Dr. Miroslav Dramićanin**

**Dr. Bruno Viana**

**Dr. Rachid Mahiou**

**Published and printed by: Institut za nuklearne nauke "Vinča" Beograd**

**Print run: 300**

**ISBN: 978-86-7306-134-4**

**August 2015, Budva, Montenegro**

CIP - Каталогизacija у публикацији - Народна библиотека Србије, Београд

538.9(048)(0.034.2)

INTERNATIONAL Conference on Physics of Optical Materials and Devices (4 ; 2015 ; Budva)

Book of Abstracts [Elektronski izvor] / The 4th International Conference on the Physics of Optical Materials and Devices - ICOM 2015, Budva, Montenegro, August 31st - September 4th, 2015 ; [editors Miroslav Dramićanin, Bruno Viana, Rachid Mahiou]. - Beograd : Institut za nuklearne nauke "Vinča", 2015 (Beograd : Institut za nuklearne nauke "Vinča"). - 1 USB fleš memorija ; 1 x 3 x 6 cm

Sistemska zahtevi: Nisu navedeni. - Nasl. sa naslovne strane dokumenta. - Tiraž 300. - Bibliografija uz većinu apstrakata.

ISBN 978-86-7306-134-4

а) Физика кондензоване материје - Апстракти б) Физика чврстог стања - Апстракти  
COBISS.SR-ID 216811788

# **ICOM 2015**

**The 4<sup>TH</sup> International Conference on the Physics of  
Optical Materials and Devices**

**BOOK OF ABSTRACTS**

**Budva, Montenegro**

**August 31<sup>st</sup> – September 4<sup>th</sup>, 2015**

## Scientific advisory committee

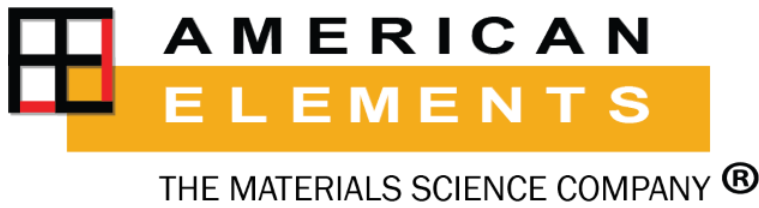
- G. Boulon (France)
- O. Malta (Brasil)
- P. Dorenbos (The Netherlands)
- M. Popova (Russia)
- J. Holsa (Finland)
- M. Brik (Estonia)
- M. Bettinelli (Italy)
- L. Carlos (Portugal)
- Ph. Boutinaud (France)
- S. Jobic (France)
- B. Moine (France)
- J. Nedeljković (Serbia)
- J. Capobianco (Canada)
- S. Fujihara (Japan)
- S. Tanabe (Japan)
- M. Peng (China)
- W. Strek (Poland)
- A. Djurišić (China)
- D. Jaque Garzía (Spain)
- Ph. Goldner (France)
- A. Ferrier (France)
- T.M. Chen (Taiwan)
- P.Deren (Poland)
- A. Meijerink (The Netherlands)
- L.Bausa (Spain)
- J.L.Adam (France)
- M. Ferrari (Italy)
- C. V. Santilli (Brasil)
- W. Ka-Leung (Hong Kong)
- M. Marinović-Cincović (Serbia)
- M. Ferrari (Italy)

## Organizing and Program committee

- M. Dramićanin (Serbia)
- Ž. Antić (Serbia)
- K. Vuković (Serbia)
- M. Sekulić (Serbia)
- M. Antonov (Serbia)
- R. Krsmanović (Serbia)
- V. Đorđević (Serbia)
- D. Jovanović (Serbia)
- B. Milićević (Serbia)
- M. Medić (Serbia)
- S. Čulubrk (Serbia)
- T. Gavrilović (Serbia)
- B. Viana (France)
- Ph. Goldner (France)
- Ph. Boutinaud (France)
- R. Mahiou (France)
- G. Chadeyron (France)
- M. Ferrari (Italy)



Sponsored by:



## **FOREWORD**

The 4<sup>th</sup> Conference of Physics and Optical Material (ICOM 22015) will be held in Budva, Montenegro, from 31<sup>st</sup> of August to 4<sup>th</sup> of September 2015 and is organized by the Vinca Institute of Nuclear Sciences, University of Belgrade (Serbia) and the Institut de Chimie de Clermont-Ferrand, Université Blaise Pascal (France) and IRCP Chimie Paristech.

The 4<sup>th</sup> Edition of ICOM Conference will celebrate 2015 - International Year of Light and Light-based Technologies. Light plays a vital role in our daily lives and is an imperative crosscutting discipline of science in the 21st century. The special conference session will highlight the importance of light and light-based technologies in everyday lives, for the futures, and for the development of society.

The ICOM 2015 Conference brings together scientists and technology users who investigate or develop materials for optical applications. The conference presents the state of the art in preparation methods, optical characterization and usage of optical materials and devices in various photonic fields.

We are grateful for sponsorships which have assisted us by providing some financial support.

We wish to express our thanks to the members of the International committee for their suggestion of oral speakers and we are also grateful to the members of the local organizing committee in Montenegro for their effort and time during preparation of the conference.

The 4<sup>th</sup> ICOM 2015 Conference is bigger every time and we are very happy to welcome you all in beautiful Budva. We wish you to meet other people at our conference and start new friendship and collaboration right here.

## List of contribution

### **NANOMATERIAL-BASED FLUORESCENT BIOSENSING AND IMAGING**

Otto S. Wolfbeis ..... 1

### **ADVANCED OPTICAL MANIPULATION EXPLOITING MATERIALS SCIENCE**

Kishan Dholakia ..... 2

### **ORGANOMETALLIC MOLECULAR MATERIALS FOR NLO, OLED AND**

Wai-Yeung Wong ..... 3

### **NOVEL RED PERSISTENT PHOSPHORS DEVELOPED BY BAND GAP ENGINEERING**

Setsuhisa Tanabe, Jian Xu, Jumpei Ueda ..... 4

### **OPTICAL CHALCOGENIDE GLASSES, FIBERS, AND DEVICES**

Jean-Luc Adam ..... 5

### **SPECTROSCOPIC PROPERTIES OF Sr<sub>2</sub>CeO<sub>4</sub> NANOCRYSTALS CO-DOPED WITH RARE-EARTH IONS**

Dariusz Hreniak, Łukasz Marciniak, Robert Tomala, Mariusz Stefański, Wiesław Stręk ..... 6

### **OPTICAL SPECTROSCOPY OF FLUORIDE AND OXIDE HOST LATTICES ACTIVATED WITH Dy<sup>3+</sup>**

Enrico Cavalli ..... 7

### **ASSIGNMENT OF Nd<sup>3+</sup>/Yb<sup>3+</sup> ENERGY LEVELS IN THE C<sub>2</sub> AND C<sub>3i</sub> CENTERS OF Lu<sub>2</sub>O<sub>3</sub> SESQUIOXIDE CERAMICS/CRYSTAL**

Georges Boulon, Guillaume Alombert-Goget, Yannick Guyot, Malgorzata Guzik, Jan Pejchal, Akira Yoshikawa, Akihiko Ito, Takashi Goto ..... 8

### **FASCINATING OPTICAL PROPERTIES OF THE COPPER METABORATE**

Marina N. Popova ..... 9

### **SPECTROSCOPY OF TRANSITION METAL IONS IN SOLIDS – THEORETICAL MODELING**

Mikhail G. Brik ..... 10

### **Ln<sup>3+</sup> 4f ENERGY LEVELS AND LUMINESCENCE IN YTTRIUM ALUMINATE PEROVSKITE**

Kazushige Ueda, Yuhei Shimizu ..... 11

### **INTERVALENCE CHARGE TRANSFER LUMINESCENCE: AB INITIO CALCULATIONS AND CONFIGURATION COORDINATE DIAGRAMS**

Zoila Barandiarán, Luis Seijo ..... 12

### **FLUORESCENCE SPECTROMICROSCOPY OF MYRIAD SINGLE DYE MOLECULES IN SOLID MATRICES: TOOL FOR HYPERSPECTRAL MATERIAL NANODIAGNOSTICS**

Andrei V. Naumov ..... 13

### **NANOMECHANICS OF PHOTOTHERMAL AND PHOTOACOUSTIC SPECTROSCOPY**

Thomas Thundat ..... 14

### **Nd<sup>3+</sup>, Eu<sup>3+</sup> AND Yb<sup>3+</sup> IONS AS STRUCTURAL PROBES IN THE SCHEELITE-TYPE CADMIUM MOLYBDATE WITH VACANCIES**

Malgorzata Guzik, Elzbieta Tomaszewicz, Yannick Guyot, Janina Legendziewicz, Georges Boulon .... 15

### **RARE-EARTH DOPED FLUORIDE LASER CRYSTALS: RECENTLY EXPLORED “EXOTIC” PROPERTIES**

Biao Qu, Simone Normani, Zhiping Cai, Patrice Camy, Jean-Luis. Doualan, Alain Braud, Richard Moncorgé ..... 16

### **THE LUMINESCENCE OF Bi<sup>3+</sup> IN SOLIDS**

Alok M. Srivastava ..... 17

### **CATHODOLUMINESCENCE IN ELECTRON MICROSCOPY: FROM PHOSPHOR EVALUATION TO SINGLE PARTICLE ANALYSIS**

Philippe F. Smet, Lisa I.D.J. Martin, Jeroen Watzet, Filip Strubbe, Dirk Poelman ..... 18

<b>NEAR INFRARED LIGHT MEDIATED DRUG RELEASE, PHOTODYNAMIC THERAPY USING UPCONVERSION NANOPARTICLES</b>	
John A. Capobianco .....	19
<b>NUCLEATION, AGGREGATION AND GROWTH OF QUANTUM DOTS PREPARED BY SOL-GEL CHEMISTRY</b>	
Sandra H. Pulcinelli .....	20
<b>ENERGY TRANSFER IN RARE-EARTH DOPED SYSTEMS</b>	
A. Meijerink, T. Senden, D. Yu, F.T. Rabouw .....	21
<b>LUMINESCENT NANOTHERMOMETRY. NANOTHERMOMETERS AND NANOHEATERS GET CLOSER</b>	
Luís D. Carlos .....	22
<b>NOVEL RED PERSISTENT PHOSPHORS DEVELOPED BY BAND GAP ENGINEERING</b>	
Setsuhisa Tanabe, Jian Xu, Jumpei Ueda.....	23
<b>DEFECT STATES OF 3d, 4d, AND 5d ELECTRONS OF TRANSITION METALS AND LANTHANIDES IN INORGANIC COMPOUNDS</b>	
Pieter Dorenbos, Edith G. Rogers .....	24
<b>LuPO<sub>4</sub>:Eu SINTERED CERAMICS - AN OLD PHOSPHOR WITH NEW LUMINESCENT FUNCTIONALITIES</b>	
Justyna Zeler, Joanna Cybińska, Eugeniusz Zych .....	25
<b>UPCONVERSION LUMINESCENCE PROPERTIES OF SINGLE PCONVERSION LiY/LuF<sub>4</sub>:Yb<sup>3+</sup>/Er<sup>3+</sup> MICROCRYSTAL</b>	
Hairong Zheng, Wei Gao, Qingyan Han .....	26
<b>BISMUTH OXIDE AS HOST FOR RARE-EARTH DOPANTS IN UCNP<sub>s</sub></b>	
Michele Back, Enrico Trave, Pietro Riello .....	27
<b>ENCAPSULATION OF UP-CONVERTING NaYF<sub>4</sub> NANOCRYSTALS IN MULTIFUNCTIONAL POLYMERIC NANOCONTAINERS<sub>4</sub></b>	
Dominika Wawrzyńczyk, Urszula Bazylińska, Bartłomiej Cichy, Artur Bednarkiewicz, Marek Samoć, Kazimiera A. Wilk.....	28
<b>LiY<sub>0.3</sub>Lu<sub>0.7</sub>F<sub>4</sub>: Ce<sup>3+</sup>, Pr<sup>3+</sup> MIXED CRYSTAL AS A PERSPECTIVE UP-CONVERSIONALLY PUMPED UV ACTIVE MEDIUM<sub>4</sub></b>	
Viktoria Gorieva, Vadim Semashko, Stella Korableva, Mikhail Marisov, Vitaly Pavlov.....	29
<b>UP-CONVERSION LUMINESCENCE, RAMAN AND THERMAL STABILITY OF BaTiO<sub>3</sub>:Er<sup>3+</sup></b>	
Mauricio Vega, I.R. Martin, Sandra Fuentes, Jaime Llanos .....	30
<b>UPCONVERSION LUMINESCENCE IN Ho<sup>3+</sup>-DOPED FLUORIDE MATERIALS UNDER EXCITATION OF <sup>5</sup>I<sub>7</sub> AND <sup>5</sup>I<sub>5</sub> LEVELS</b>	
Andrey A. Lyapin, Pavel P. Fedorov, Polina A. Ryabochkina .....	31
<b>UP-CONVERTIONAL LUMINESCENCE IN GERMANATE GLASSES</b>	
Ksenya S. Moskaleva, Vladimir A. Aseev, Nickolay V. Nikonorov, Yu.K. Fedorov, Ya.A Nekrasova, I.M. Sevastianova, A.O. Larin .....	32
<b>OPTICAL PROPERTIES OF K<sub>2</sub>SiF<sub>6</sub>: Mn<sup>4+</sup> AT AMBIENT AND HIGH HYDROSTATIC PRESSURES</b>	
Sebastian Mahlik, Agata Lazarowska, Marek Grinberg, Chun-Che Lin, Ru-Shi Liu.....	33
<b>NONLINEAR OPTICAL PROPERTIES OF PbOGeO<sub>2</sub> GLASS CODOPED BY Yb<sup>3+</sup>/Tm<sup>3+</sup> AND INCORPORATED Si NANOPARTICLES</b>	
Izabela Fuks-Janczarek, Rafał Miedziński, Luciana R. P. Kassab .....	34
<b>FAR-INFRARED SPECTROSCOPY OF MULTIFERROIC RFe<sub>3</sub>(BO<sub>3</sub>)<sub>4</sub> (R=Gd,Tb): PHASE TRANSITIONS AND COUPLING BETWEEN LATTICE PHONONS AND CRYSTAL-FIELD EXCITATIONS</b>	
Sergei A. Klimin.....	35

<b>CHARACTERIZATION OF MAGNETO-OPTIC HEXAFERRITES BY TERAHERTZ TIME DOMAIN SPECTROSCOPY</b>	
Martin Mičica, Kamil Postava, Mathias Vanwolleghem, Jean-François Lampin, Jaromír Pištora .....	36
<b>APPLICATION OF MULTI-WAY ANALYSIS FOR DECOMPOSITION OF LUMINESCENCE SPECTRA OF PHOSPHOR MIXTURES</b>	
Lea Lenhardt, Ivana Zeković, Miroslav Dramićanin.....	37
<b>INTRA- AND INTER-CONFIGURATIONAL LUMINESCENCE SPECTROSCOPY OF Pr<sup>3+</sup> - DOPED YTTRIUM ORTHOPHOSPHATES YPO<sub>4</sub> NANOPHOSPHORS SYNTHESIZED BY SOL GEL METHOD</b>	
L. Guerbous and B. Kahoudji, .....	38
<b>THE NEW MATERIALS BASED ON DOPED BY CU ZNS DEPOSITED INTO POROUS ANODIC ALUMINA FOR ELECTROLUMINESCENT LIGHT EMITTING DEVICES</b>	
Rishat G. Valeev, Andrey I.Chukavin, Artemii N. Beltukov, Dmitri I. Petukhov, Vladimir M. Vetoshkin, Alexander L. Trigub.....	39
<b>PERSISTENT NANOPHOSPHORS FOR BIOIMAGING<sup>4</sup></b>	
Morgane Pellerin, Corinne Chaneac, Bruno Viana.....	40
<b>SPECTRAL FEATURES OF HIGH-FIELD ELECTROLUMINESCENCE IN AlN FILAMENTARY NANOCRYSTALS</b>	
Ilya A.Weinstein, Alexander S. Vokhmintsev, Dmitry V. Chaikin, Yuri .D. Afonin .....	41
<b>SYNTHESES AND MORPHOLOGIES OF GdVO<sub>4</sub> POWDERS:FROM BULK TO NANO</b>	
Dragana J. Jovanović, Tamara V. Gavrilović, Sanja Čulubrk, Goran Dražić, Miroslav Dramićanin .....	42
<b>SYNTHESIS AND OPTICAL PROPERTIES OF TRANSPARENT GLASS-CERAMICS WITH (Eu,Yb,Y)NbO<sub>4</sub> NANOCRYSTALS</b>	
I. Alekseeva, O. Dymshits, M. Tsenter, A. Zhilin, S. Zapalova, P. Loiko, A.M. Malyarevich, N. Scoptsov, K. Yumashev, E. Vilejshikova, K. Bogdanov .....	43
<b>RESEARCH THE NATURE OF THE LUMINESCENCE OF COPPER-DOPED QUANTUM DOTS CDSE</b>	
T.N. Nurakhmetov, A.K. Kainarbay, D.H. Daurenbekov, K. A. Kuterbekov, P. Kotin, S. Bubenov, O.B. Tleugabylov .....	44
<b>CALCULATION OF THE DISPERSION OF ELECTRO-OPTIC AND NONLINEAR COEFFICIENTS</b>	
Marc Fontana, Mustapha Abarkan and Jean-Paul Salvestrini.....	45
<b>Yb:YVO<sub>4</sub>-BASED CPA SYSTEM</b>	
Alexander Rudenkov, Viktor Kisel, Vladimir Matrosov, and Nikolai Kuleshov .....	46
<b>LARGE TI-DOPED SAPPHIRE SINGLE CRYSTALS GROWN BY THE KYROPOULOS TECHNIQUE FOR PETAWATT POWER LASER APPLICATION</b>	
Guillaume Alombert-Goget, Gourav Sen, Cyril Pezzani, Nicolas Barthalay, Thierry Duffar, Kheirreddine Lebbou .....	47
<b>THE EFFECTS OF DIFFRACTION AND SPHERICAL ABERRATION AT THE FEMTOSECOND LASER FABRICATION EXTENDED MICROSTRUCTURE BY DIFFERENT FOCUSING SYSTEMS.</b>	
Daniil Ganin, Alexey Z. Obidin, Konstantin Lapshin and Sergey K. Vartapetov.....	48
<b>EFFICIENT IN-BAND PUMPED Er:KY(WO<sub>4</sub>)<sub>2</sub> LASER</b>	
Konstantin Gorbachenya, Viktor Kisel, Anatol Yasukevich, Anatoly Pavlyuk, Nikolai Kuleshov .....	49
<b>SILVER COMPLEX NANOSTRUCTURES FOR SHG ENHANCEMENT IN RbTiOPO<sub>4</sub></b>	
L. Sánchez-García, P. Molina, M.O. Ramírez, J.J. Carvajal, M. Aguiló, F. Díaz, C. Heras, L.E. Bausá.....	50
<b>STABILIZATION OF P-TYPE N-DOPED Zn-DEFICIENT ZnO NANOPARTICLES</b>	
A. Renaud, B. Chavillon, X. Rocquefelte, E. Faulques, P. Deniard, M. Boujtita, Y. Pellegrin, E. Blart, F. Odobel, F. Cheviré, F. Tessierc, L. Cario, Stephane Jobic .....	51

## **LASER INDUCED WHITE EMISSION FROM GRAPHENE CERAMICS**

Wiesław Stręk, Bartłomiej Cichy, Łukasz Radosiński, Paweł Głuchowski, Łukasz Marciniak, Mikołaj Łukaszewicz, Dariusz Hreniak ..... 52

## **LUMINESCENCE PROPERTIES OF CeO<sub>2</sub> DOPED WITH Ln IONS UNDER OPTICAL AND X-RAY EXCITATION MODES**

Daniel Avram, Bogdan Cojocar, Mihaela Florea, Vasile Parvulescu, Carmen Tiseanu ..... 53

## **LUMINESCENCE PROPERTIES OF GAS-PHASE MASS-SELECTED LANTHANOID COMPLEXES**

Jean-François Greisch, Michael E. Harding, Jiří Chmela, Wim Klopper, Detlef Schooss, Manfred M. Kappes ..... 54

## **SPECTROSCOPIC PROPERTIES OF YZnPO POLYCRYSTALS DOPED WITH Nd<sup>3+</sup> IONS**

Karol Lemański, Michael Babij, Przemysław J. Dereń ..... 55

## **SPECTRAL-KINETIC AND COLOR CHARACTERISTICS OF THE LUMINESCENCE OF ZnWO<sub>4</sub>:Eu<sup>3+</sup> CRYSTALS**

D. Valiev, E. Poliadova, V. Lisitsyn and I. Tupitsyn ..... 56

## **HIGH-TEMPERATURE SINTERING OF SrS:Ce TOWARDS THE NEW RED-IR Ce EMISSION**

Dagmara Kulesza, Karolina Fiaczyk, Joanna Cybińska, Aneta Wiatrowska, Eugeniusz Zych ..... 57

## **LOCATION OF THE Ce<sup>3+</sup> GROUND STATE IN THE BANDGAP AND LUMINESCENCE EFFICIENCY IN Y<sub>3</sub>Al<sub>2</sub>Ga<sub>3</sub>O<sub>12</sub>:Ce<sup>3+</sup> AND Y<sub>3</sub>Ga<sub>5</sub>O<sub>12</sub>:Ce<sup>3+</sup>**

Sebastian Mahlik, Agata Lazarowska, Marek Grinberg, Jumpei Ueda, Setsuhisa Tanabe ..... 58

## **SURFACE-MODIFIED TiO<sub>2</sub> NANOPARTICLES ON POLYMER SUPPORT: SYNTHESIS, CHARACTERIZATION AND PHOTOCATALYTIC PERFORMANCE**

Ivana D. Vukoje, Lidija V. Trandafilović, Tijana S. Radoman, Enis S. Džunuzović, S. Phillip Ahrenkiel, Jovan M. Nedeljković ..... 59

## **INVERTED QUANTUM DOT LIGHT EMITTING DIODES USING POLYETHYLENIMINE ETHOXYLATED MODIFIED ZNO ELECTRON TRANSPORT LAYER**

Hong Hee Kim, Do Kyeong Hwang, Won Kook Choi ..... 60

## **EXCITED STATES RELAXATION IN HIGHLY CONFINED AgInS<sub>2</sub> AND AgInS<sub>2</sub>/ZnS QUANTUM DOTS EVALUATED BY SINGLE PARTICLE SPECTROSCOPY**

Bartłomiej Cichy, Ryan Rich, Zygmunt Gryczynski, Wiesław Stręk ..... 61

## **MULTI-SPECTRAL FLUORESCENT NANOPROBES: TRIPLE Re<sup>3+</sup>-DOPED NIR-EMITTING NaGdF<sub>4</sub> NANOPARTICLES (793NM-NIR) ALSO PLAYING AS *IN VITRO* (980NM-VIS) IMAGING AND THERMOMETRY PROBES**

Antonio Benayas, W. F. Silva, B. del Rosal, F. Sanz-Rodriguez, Vetrone, Fiorenzo ..... 62

## **TYPE-II EXCITONS IN (Ga,In)As/Ga(N,As)-QUANTUM WEELS**

Sebastian Gies, Carsten Kruska, Philip Hens, Wolfgang Stolz, Kerstin Volz, Wolfram Heimbrodt ..... 63

## **PHOTO-IONIZATION OF 3d IONS IN GLASSES**

Doris Möncke, Doris Ehrt ..... 64

## **LOCAL, ELECTRONIC AND GLOBAL STRUCTURE OF MOLYBDENUM-LEAD-GERMANATE GLASSES AND GLASS CERAMICS**

Marius Rada, Nicolae Aldea, Simona Rada, Ramona - Crina Suci, Sergiu Macavei, Adrian Bot, Eugen Culea and Radu Balan ..... 65

## **REDOX STATE OF RE IONS EMBEDDED IN ALUMINOBOROSILICATE GLASSES**

Eugenia Malchukova, Bruno Boizot, Alexey Abramov and Eugeni Terukov ..... 66

## **THE DE-CLUSTERING INFLUENCE OF ALUMINUM IONS ON THE GREEN EMISSION EFFICIENCY OF Tb<sup>3+</sup> IONS IN BARIUM BOROPHOSPHATE GLASSES**

M. Piaeck, T. Kalpana, M.G. Brik, S. Sudarsan, N. Veeraiah .....	67
<b>SPECTROSCOPY OF THE Er-DOPED BORATE GLASSES</b>	
Bohdan V. Padlyak, Radoslaw Lisiecki, Witold Ryba-Romanowski.....	68
<b>FLUORESCENT CLAY HYBRIDS IN TRANSPARENT AQUEOUS MEDIA: INTERACTION WITH BIOINTERFACES</b>	
Tom Felbeck, Marina Lezhnina, Christian Radunsky, Jens Müller, Anna Nickisch-Hartfiel, Peter Klauth, Ulrich Kynast.....	69
<b>ALL OPICALLY CONTROLLED ORGANIC-INORGANIC HYBRID DEVICE</b>	
Vera Marinova, Etienne Goovaerts, Ren Chung Liu, Shiuan Huei Lin, Yi Hsin Lin, Ken Yuh Hsu .....	70
<b>PHOTON CONVERSION FROM 4.4<math>\mu</math>M Dy<sup>3+</sup> DOPED FLUORESCENT FIBERS TO 800NM IN Er<sup>3+</sup> DOPED FIBERS FOR ALL-OPTICAL GAS SENSING</b>	
A.L. Pelé, A. Braud, J.L. Doualan, R. Chahal, V. Nazabal, R. Moncorgé, and P. Camy.....	71
<b>LOCALIZED SURFACE PLASMON RESONANCE BASED BIOSENSOR USING ALCOHOL OXIDASE FOR FORMALDEHYDE DETECTION</b>	
Vivi Fauzia, Nur Intan Pratiwi, Nurlely, Dede Djuhana, Adhi Harmoko, Cuk Imawan .....	72
<b>INNOVATIVE COPPER-DOPED GLASSES AND FIBERS AS SENSITIVE MATERIALS FOR IONISING BEAM DOSIMETRY</b>	
Bruno Capoen, Hicham El Hamzaoui, Mohamed Bouazaoui, Laurent Bigot, Géraud Bouwmans, Youcef Ouerdane, Aziz Boukenter, Sylvain Girard, Geneviève Chadeyron, Rachid Mahiou, Claude Marcandella, Olivier Duhamel.....	73
<b>CHARACTERISATION OF BAM:Eu<sup>2+</sup> AND ZnO PHOSPHOR PARTICLES FOR TEMPERATURE IMAGING IN FLUIDS</b>	
Christopher Abram, Benoit Fond, Frank Beyrau .....	74
<b>ADVANCED OPTICAL REMOTE SENSORS FOR AIRBORNE AND SPACEBORNE PLATFORMS</b>	
M. M. Cazacu, A. Timofte, O. Rusu, B. Albina, G. Bulai, L. Leontie, and S. Gurloi .....	75
<b>EVOLUTION OF Eu AND Mn OXIDATION STATE IN DOPED BaMgAl<sub>10</sub>O<sub>17</sub> DURING X-RAY IRRADIATION</b>	
Lucia Amidani, Katleen Korthout, Marte Van der Linden, Andries Meijerink, Philippe Smet, Dirk Poelman, Pieter Glatzel .....	76
<b>GLASS-BASED 1-D DIELECTRIC MICROCAVITIES</b>	
Alessandro Chiasera, Francesco Scotognell, Sreeramulu Valligatla, Stefano Varas, Jacek Jasieniak, Luigino Criante, Anna Lukowiak, Davor Ristic, Stefano Taccheo, Mile Ivanda, Giancarlo C. Righini, Roberta Ramponi, Alessandro Martuccim, Maurizio Ferrari .....	77
<b>THE CHEMICAL BOND OVERLAP POLARIZABILITY AND COVALENCY. CONCEPTS AND APPLICATIONS: FROM DIATOMIC MOLECULES TO SOLIDS</b>	
Renaldo T. Moura Jr., Ricardo L. Longo, Oscar L. Malta .....	78
<b>MOLECULAR IMAGING AND KILLING OF LATENTLY EBV-INFECTED TUMOR CELLS BY THE DEVELOPMENT OF EBNA1-SPECIFIC LANTHANIDE BIOPROBES</b>	
Ka-Leung Wong .....	79
<b>RARE EARTH-DOPED NANOPARTICLES AS NEW PHOTOTHERMAL AGENTS: FUNDAMENTALS AND IN VIVO APPLICATIONS</b>	
Blanca del Rosal, Elisa Carrasco, Francisco Sanz-Rodríguez, Ángeles Juarranz de la Fuente, Ueslen Rocha, Kagola Upendra Kumar, Carlos Jacinto, D. J. Jovanović, M. D. Dramićanin, José García Soléand Daniel Jaque .....	80
<b>NIR EMITTING QUANTUM DOTS AND RE<sup>3+</sup>-DOPED NANOPARTICLES: PROSPECTS AT THE MULTIFUNCTIONALITY BATTLEGROUND FOR BIO-IMAGING AND THERMAL SENSING</b>	

A. Benayasa, F. Rena, D. Ortgies, E. Carrasco, E. Navarro, B. del Rosal, A. Juarranz, F. Sanz-Rodríguez, G.A. Hirata, D. Jaque, F. Vetrone, E. Martin-Rodríguez, D.L. Ma .....	81
<b>CO-ENCAPSULATION OF CdSe-ZnS QUANTUM DOTS AND PHTHALOCYANINE IN NANOCARRIERS FOR PHOTODYNAMIC THERAPY</b>	
Janusz Szeremeta, Slawomir Drozdek, Marcin Nyk, Kazimiera A. Wilk, Marek Samoc.....	82
<b>CARBON DOTS (C-DOTS) FROM COW MANURE WITH IMPRESSIVE SUBCELLULAR SELECTIVITY TUNED BY SIMPLE CHEMICAL MODIFICATION</b>	
Cintya D'Angelis do E. S. Barbosa, José R. Corrêa, Gisele M. Alves, Gabrielle Barreto, Kelly G. Magalhães, Aline L. de Oliveira, John Spencer, Brenno A. D. Neto, Marcelo O. Rodrigues.....	83
<b>TUNABLE LUMINESCENT PROPERTIES AND CONCENTRATION-DEPENDENT, SITE-PREFERABLE DISTRIBUTION OF Eu<sup>2+</sup> IONS IN SILICATE GLASS FOR WHITE LEDS APPLICATIONS</b>	
Jing Wang, Xuejie Zhang.....	84
<b>CONTROLLING THE MORPHOLOGY OF YPO<sub>4</sub>:Eu<sup>3+</sup> BY CHEMICAL PROCESSING PARAMETERS</b>	
Joanna Cybińska .....	85
<b>EFFICIENCY DROOP IN AlGa<sub>n</sub> EPITAXIAL LAYERS AND MULTIPLE QUANTUM WELLS</b>	
J. Jurkevičius, J. Mickevičius, A. Kadys, G. Tamulaitis, M. Shur, M. Shatalov, J. Yang, and R. Gaska ....	86
<b>BRIGHTENING GaN:Eu RED LED BY BACK-AND-FORCE MOTION OF INJECTION CHARGES AND ITS APPLIED TO SITE-SELECTIVE ANALYSES OF EMISSION CENTRES</b>	
Masashi Ishii, Atsushi Koizumi, Yasufumi Fujiwara .....	87
<b>YAG BASED PHOSPHORS FOR WHITE LED – A REVIEW</b>	
Pooja Yadav, Charusheela Joshi, S.V. Moharil.....	88
<b>STRUCTURE AND LATTICE DYNAMICS OF CRYSTALS WITH RARE EARTH SUBLATTICE: AB INITIO CALCULATIONS</b>	
Vladimir A. Chernyshev, Anatoliy E. Nikiforov, Vladislav P. Petrov, Alexander V. Serdcev.....	89
<b>CORRELATION BETWEEN COORDINATION ENVIRONMENT OF Ce<sup>3+</sup> AND LUMINESCENCE PROPERTIES IN YELLOW-EMITTING Sr<sub>2</sub>Si<sub>7</sub>Al<sub>3</sub>ON<sub>13</sub>:Ce<sup>3+</sup> PHOSPHOR</b>	
Yumi Fukuda, Iwao Mitsuishi, Ariane Keiko Albessard, Yasushi Hattori, Aoi Okada, Kunio Ishida, Katsuyoshi Oh-ishi, and Masahiro Kato.....	90
<b>MODELING THE STRUCTURAL, VIBRATIONAL, ELECTRONIC AND OPTICAL PROPERTIES OF LANTHANIDE-DOPED MATERIALS</b>	
Chong-Geng Ma, Mikhail Brik.....	91
<b>LINewidths OF THE 4f-4f ELECTRONIC TRANSITIONS AND ELECTRONIC STRUCTURE OF Ce<sup>3+</sup> DOPANT IN YTTRIUM AND LUTETIUM ORTHOALUMINATE CRYSTALS</b>	
Aleksander Wittlin, Hanka Przybylińska, Agata Kamińska, Piotr Sybilski, Yaroslav Zhydachevskii, Chong-Geng Ma, Mikhail G. Brik, Michal Malinowski, Andrzej Suchocki.....	92
<b>INVESTIGATION OF THE QUENCHING MECHANISMS OF Tb<sup>3+</sup> DOPED SCHEELITES</b>	
Katrien W. Meert, Jonas J. Joos, Dirk Poelman, Philippe F. Smet .....	93
<b>MODELLING THE INFLUENCE OF SILVER NANOPARTICLES ON THE f-f LUMINESCENCE OF THE EuEDTA COMPLEX IN THE POLYVINYLPIRROLIDONE POLYMER</b>	
M. A. Couto dos Santos, O. L. Malta, R. Reisfeld .....	94
<b>PHOTOPHYSICAL STUDIES AND APPLICATION OF COMPUTER MODELLING AND HARTREE-FOCK METHOD FOR INTERPRETATION OF SPECTROSCOPIC PROPERTIES AND STRUCTURAL CHANGES OF AXIALLY SUBSTITUTED Yb(III) MONOPHTHALOCYANINES IN DIFFERENT MEDIA</b>	
Yu. Gerasymchuk, L. Tomachynski, M. Guzik, A. Koll, J. Jański, Y. Guyot, W. Stręk, G. Boulon, J. Legendziewicz.....	95



<b>EMPIRICAL ENERGY LEVEL MODELING OF LANTHANIDE DEFECTS IN CaGa<sub>2</sub>S<sub>4</sub> AND SrGa<sub>2</sub>S<sub>4</sub>: UNCERTAINTY ANALYSIS AND UNEXPECTED BEHAVIOR</b>	
Jonas J. Joos, Dirk Poelman, Philippe F. Smet .....	96
<b>THE ORIGIN OF FERROELECTRIC DISTORTION IN HEXAGONAL MULTIFERROICS RMnO<sub>3</sub> (R = Y, Lu)</b>	
M. V. Lalic, A. M. Sousa, W. S. Coutinho, A. F. Lima .....	97
<b>HIGH-RESOLUTION OPTICAL ABSORPTION SPECTROSCOPY OF Si-VACANCY COLOR CENTER IN MONOISOTOPIC DIAMOND <sup>13</sup>C</b>	
Kirill N. Boldyrev, Viktor G. Ralchenko, Vadim S. Sedov, Andrey P. Bolshakov, Andrey A. Khomich, Anatoly V. Krasilnikov .....	98
<b>MULTI-PHOTON QUANTUM CUTTING IN Gd<sub>2</sub>O<sub>2</sub>S:Tm<sup>3+</sup></b>	
D.C. Yu, R. Martín-Rodríguez, Q.Y. Zhang, A. Meijerink, F.T. Rabouw .....	99
<b>INFLUENCE OF DIFFERENT ATMOSPHERES ON PHOTOPHYSICAL AND STRUCTURAL PROPERTIES OF ZINC OXIDE</b>	
Sergio A. M. Lima, Fernando A. Sigoli, Miguel Jafelicci Jr., Marian R. Davolos .....	100
<b>RADIOMETRICALLY CALIBRATED HYPERSPECTRAL PHOTOLUMINESCENCE IMAGING OF DIAMOND</b>	
R. E. Cross, M. Gunn, D. P. Langstaff, D. A. Evans .....	101
<b>THE d-f LUMINESCENCE OF Eu<sup>2+</sup> AND Ce<sup>3+</sup> IONS IN Cs<sub>2</sub>(Ca,Sr)P<sub>2</sub>O<sub>7</sub></b>	
Tim Senden, Andries Meijerink .....	102
<b>SUBMICRON DIAMOND PILLARS WITH SILICON-VACANCY COLOR CENTERS AS LOCALIZED NEAR INFRA-RED PHOTOEMITTERS</b>	
Dmitry N. Sovyk, Victor G. Ralchenko, Konstantin N. Tukmakov, Andrew A. Khomich, Vladimir A. Shershulin, Vadim V. Vorobyov, Alexey V. Akimov. ....	103
<b>DECAY RATE OF THE LUMINESCENCE CENTER LOCATED NEAR METALLIC NANOPARTICLE</b>	
Konstantin K. Pukhov.....	104
<b>CRYSTAL GROWTH, OPTICAL AND SCINTILLATION PROPERTIES OF BULK Eu-DOPED SrI<sub>2</sub> SINGLE CRYSTALS</b>	
Akira Yoshikawa, Yasuhiro Shoji, Yuui Yokota, Shunsuke Kurosawa, Valery I. Chani, Tomoki Ito, Kei Kamada, Yuji Ohashia, Vladimir Kochurikhin .....	105
<b>COMPOSITION ENGINEERING OF THE SINGLE CRYSTALLINE FILM SCINTILLATORS BASED ON THE MULTICOMPONENT GARNET COMPOUNDS</b>	
Yuriy Zorenko, Vitaliy Gorbenko, Tetyana Zorenko, Oleg Sidletskiy, Alexander Fedorov.....	106
<b>CO-DOPING EFFECTS ON LUMINESCENCE AND SCINTILLATION PROPERTIES OF Ce DOPED (Lu,Gd)<sub>3</sub>(Ga,Al)<sub>5</sub>O<sub>12</sub> SCINTILLATOR</b>	
Hiroaki Yamaguchi, Kei Kamada, Shunsuke Kurosawa, Jan Pejchal, Yasuhiro Shoji, Yuui Yokota, Yuji Ohashi, Akira Yoshikawa .....	107
<b>DIFFRACTIVE OPTICS FOR ASTRONOMY: VOLUME PHASE HOLOGRAPHIC GRATINGS BASED ON PHOTOPOLYMERS</b>	
Alessio Zanutta, Andrea Bianco.....	108
<b>EFFICIENT POLYMER SOLAR CELLS FABRICATED BY TUNING COUPLED ELECTRICAL-OPTICAL PROPERTIES AT THE INTERFACE</b>	
Gopalan Sai-Anand, Anantha-Iyengar Gopalan, Kwang-Pill Lee, Byoung-Ho Kang, Jae-Sung Lee, Sang- Won Lee, Dae-Hyuk Kwon, Shin-Won Kanga .....	109
<b>THEORETICAL CALCULATION OF OPTICAL AND ELECTRICAL PROPERTIES OF V DOPED ZnO USING IN SOLAR CELLS APPLICATIONS</b>	
M. Boujnah, A. Benyoussef and A. El Kenz.....	110

<b>3D OPTICAL MEASUREMENT OF COMPOSITE STRAIN AND DISPLACEMENT IN RESTORED TEEH</b> Dragica Manojlovic, Milos Milosevic, Nenad Mitrovic, Vesna Miletic .....	111
<b>A NANOPOROUS SILICON - ALUMINUM LIGHT EMITTING SCHOTTKY STRUTURE INCORPORATED INTO SILICON CHIP</b> Aliaksandr G. Smirnov, Andrey A. Stepanov, Yugene V. Mukha .....	112
<b>A RECOMBINATION LUMINESCENCE IN THE FIELD OF TRANSITION TEMPERATURE OF KDP CRYSTAL</b> Temirgaly Koketai, Ainura Tussupbekova, Elmira Mussenova, Anel Ibrayeva, Nurbolat Saidrakhimov.....	113
<b>AHARONOV-BOHM OSCILLATION MODES IN NON-UNIFORM QUASI-ONE-DIMENSIONAL RING UNDER LATERAL ELECTRIC FIELD</b> William Gutiérrez, Iliia D. Mikhailov, Marlon R. Fulla, and Jairo H. Marín.....	114
<b>ALTERNATIVE SYNTHESIS METHODS OF PERSISTENT LUMINESCENT MATERIALS</b> Leonnam G. Merízio, Ian P. Machado, Lucas C.V. Rodrigues, Jorma Hölsä, Hermi F. Brito .....	115
<b>SENSITIZER-LIMITED EXCITON DIFFUSION IN LIGHT-UPCONVERTING DIPHENYLANTHRACENE/PMMA FILMS</b> Steponas Raisys, Karolis Kazlauskas, Saulius Jursenas, Yoan Simon .....	116
<b>ANALYSIS OF THERMOLUMINESCENCE GLOW CURVES OF Ga<sub>2</sub>SeS LAYERED CRYSTALS</b> Mehmet Isik, Serdar Delice, Nizami Hasanli.....	117
<b>ATOMIC LAYER DEPOSITION OF Al-DOPED ZnO FILMS: OPTICAL PROPERTIES TUNING</b> Dimitre Z. Dimitrov, Blagoy Blagoev, Vladimir Mehandzhiev, Jerome Leclercq, Peter Sveshtarov....	118
<b>ATOMIC ORDERING AND BIAxIAL STRAIN WITHIN MOVPE- GROWN III-V SEMICONDUCTOR ALLOYS: ANALYSIS OF PHOTOLUMINESCENCE EMISSION POLARIZATION</b> T. Prutskija, N. Makarova, G. Attolinib .....	119
<b>AXIAL SELF-TRAPPED EXCITON CONFIGURATIONS IN BERYLLIUM OXIDE</b> Michael A. Botov, Aleksey Yu. Keznetsov, Aleksandr B. Sobolev .....	120
<b>BiFeO<sub>3</sub> CERAMICS: PROCESSING, OPTICAL AND MAGNETIC PROPERTIES</b> Maria Čebela, Radmila Hercigonja, Marija Prekajski, Miljana Mirković, Jelena Pantić, Jelena Luković, Branko Matović .....	121
<b>BISMUTH SILICATE NANOPARTICLES: STRUCTURAL CONTROL AND RARE EARTH DOPING FOR UPCONVERSION</b> Michele Back, Enrico Trave, Patrizia Canton, Pietro Riello .....	122
<b>BLUE TO GREEN TUNABLE LUMINESCENCE OF Ce<sup>3+</sup> DOPED YTTRIUM SILICATE PHOSPHORS</b> Adrian I. Cadis, Laura.E. Muresan, Ioana Perhaita, Dan T. Silipas .....	123
<b>BRANCHED RELAXATION OF ELECTRONIC EXCITATIONS DURING PHOTOELECTRON SCATTERING IN N<sub>2</sub> DOPED SOLID Kr</b> O.N. Bliznjuk, N.Yu. Masalitina, A.N. Ogurtsov .....	124
<b>CATHODOLUMINESCENCE STUDY OF LuAG:CeGdGa SINGLE CRYSTALLINE FILMS</b> Ondrej Lalinsky, Petr Schauer, Miroslav Kucera, Zuzana Onderisinova, Martin Hanus.....	125
<b>CHARACTERIZATION OF Ge-Ga-Se GLASSES USING OPTICAL AND POSITRON ANNIHILATION TECHNIQUE</b> Halyna Klym, Adam Ingram, Oleh Shpotyuk, Ivan Karbovnyk.....	126
<b>TEMPERATURE DEPENDANCE OF LUMINESCENCE OF Eu<sup>3+</sup>-DOPED TiO<sub>2</sub> THIN FILMS</b> Željka Antić, Kovur Prashanthi, Vesna Đorđević, Miroslav D. Dramićani, Thomas Thundat .....	127
<b>COMPARARISON OF Cr<sup>3+</sup>:ZnGa<sub>2</sub>O<sub>4</sub> and Bi<sup>3+</sup>:ZnGa<sub>2</sub>O<sub>4</sub> PERSISTENT NANOPHOSPHORS ELABORATED BY VARIOUS METHODS</b>	

Morgane Pellerin, Bruno Viana, Corinne Chaneac, Elliott Teston, Cyrille Richard, Jian Xu, Setsuhisa Tanabe.....	128
<b>COMPARATIVE STUDY OF NONDOPED AND Eu-DOPED SrI<sub>2</sub> SCINTILLATOR</b>	
Takayuki Yanagida, Masanori Koshimizu, Go Okada, Takahiro Kojima, Jyunya Osada.....	129
<b>CRYSTAL SIZE EFFECT IN POLARITONIC LUMINESCENCE FROM SOLID XENON</b>	
A.N. Ogurtsov, O.N. Bliznjuk, N.Yu. Masalitina .....	130
<b>CU-DOPED PHOTOVOLTAIC GLASSES BY ION EXCHANGE FOR SUNLIGHT DOWN-SHIFTING</b>	
Marco Mardegan and Elti Cattaruzza.....	131
<b>DETECTIVE QUANTUM EFFICIENCY OF PHOSPHORS FOR X-RAY IMAGING</b>	
Goran S. Ristić.....	132
<b>DONOR-ACCEPTOR SYSTEMS CONTAINING 1,8-NAPHTHALIMIDE AS MULTICOLOR EMITTERS</b>	
Regimantas Komskis, Arunas Miasojedovas, Rokas Skaisgiris, Alytis Gruodis, Vygintas Jankauskas, Dalius Gudeika, Juozas Vidas Grazulevicius, Saulius Jursenas.....	133
<b>NEW Eu(III) B-DIKETONATE COMPLEXES CONTAINING A 2-(4-MORPHOLINYLMETHYL)PHENOL: AN EXPERIMENTAL AND THEORETICAL INVESTIGATIONS</b>	
Khodzhaberdi Allaberdiev .....	134
<b>EARLY AGE MONITORING OF INNOVATIVE CEMENTS BY USING FIBER BRAGG GRATING SENSORS</b>	
Stefania Campopiano, Agostino Iadicicco, Rajeev Ranjan, Giovanna Palumbo, Flavio Esposito, Francesco Messina, Francesco Colangelo, Claudio Ferone, Raffaele Cioffi .....	135
<b>EFFECT OF EUROPIUM CONCENTRATION ON THE LUMINESCENCE PROPERTIES OF Eu<sup>3+</sup> AND Tb<sup>3+</sup> DOPED PHOSPHATE-BORATE-FLUORIDE GLASSES</b>	
Elena Polisadova, Damir Valiev, Konstantin Belikov, Nataliya Yegorova, Vitaliy Vaganov .....	136
<b>EFFECT OF THERMAL TREATMENT ON MORPHOLOGIES AND OPTICAL PROPERTIES OF DOWNCONVERSION AND UPCONVERSION NaYF<sub>4</sub>:Ln<sup>3+</sup> CRYSTALS</b>	
Marcos A. Calil Junior, Marcelo O. Rodrigues .....	137
<b>EFFECTS OF PRESSURE AND TEMPERATURE ON THE LUMINESCENCE OF Ba<sub>2</sub>K(PO<sub>3</sub>)<sub>5</sub> DOPED WITH Eu<sup>2+</sup> AND Eu<sup>3+</sup></b>	
Anna Baran, Sebastian Mahlik, Marek Grinberg, Adam Watras, Robert Pązik, Przemysław Dereń....	138
<b>ELECTRIC FIELD EFFECT ON PHOTOLUMINESCENCE OF QUANTUM DOTS CdSe / ZnS IN NEMATIC LIQUID CRYSTAL</b>	
Kurochkina Marharyta, Shcherbinin Dmitry, Konshina Elena .....	139
<b>ELECTRON-VIBRATIONAL EFFECT IN MgO: M<sup>2+</sup> (M=V, Fe, Mn)</b>	
C.N.Avrám, M.G.Brik, A.S.Gruia and A.M.Barb .....	140
<b>ENERGY TRANSFER FROM Gd<sup>3+</sup> TO Er<sup>3+</sup> IN MATRIX Gd<sub>2</sub>O<sub>3</sub></b>	
Yu A Kuznetsova, A F Zatsepin.....	141
<b>ERBIUM-DOPED LEAD SILICATE GLASSES FOR UP-CONVERSION LUMINESCENCE TEMPERATURE SENSORS</b>	
Wojciech A. Pisarski, Joanna Pisarska, Radosław Lisiecki, Witold Ryba-Romanowski.....	142
<b>EVOLUTION OF THE OPTICAL PROPERTIES OF CHROMIUM DOPED CALCIUM TETRABORATE GLASS UNDER HIGH PRESSURE</b>	
Tadeusz Lesniewski, Marek Grinberg, Justyna Barzowska, Sebastian Mahlik, Bohdan V. Padyak ....	143
<b>EXPERIMENTAL INVESTIGATION OF FLUORESCENT SENSORS FOR THE DETECTION NITRO EXPLOSIVES</b>	
Anna A. Baranova, Konstantin O. Khokhlov .....	144

<b>EXPLORING AND DEEPENING THE USE OF ALGAL CHLOROPHYLLS INTO DYE SENSITIZED SOLAR CELLS</b>	
Emmanuele Ambrosi, Simona Armeli Minicante, Michele Back, Jessica Barichello, Elti Cattaruzza, Francesco Gonella, Enrico Scantamburlo, Enrico Trave .....	145
<b>FABRICATION AND SPECTROSCOPIC PROPERTIES OF TRANSLUCENT LuPO<sub>4</sub>:Ce FILMS</b>	
Justyna Zeler, Joanna Cybińska, Eugeniusz Zych .....	146
<b>FIRST INVESTIGATIONS OF CUBIC Yb<sup>3+</sup>-DOPED La<sub>2</sub>(MoW)<sub>2</sub>O<sub>9</sub> FOR OPTICAL CERAMICS</b>	
M. Bieza, M. Guzik, E. Tomaszewicz, Y. Guyot, E. Zych, G. Boulon .....	147
<b>FLUORESCENT ORGANIC NANOPARTICLES BASED ON INERT CARBON FREE RADICALS</b>	
Davide Blasi, Domna Maria Nikolaidou, Francesca Terenziani, Imma Ratera, Jaume Veciana.....	148
<b>FORMATION FEATURES OF COPPER THIN FILMS ON THE PHOSPHATE GLASS</b>	
Elena Kolobkova, Ba Minh Dinh, Nikolay Nikonorov, Rustam Nuryev, Alexandr Trofimov .....	149
<b>FORMATION OF THE LUMINESCENT CENTERS IN ZINC-PHOSPHATE GLASSES DOPED WITH Ag AND Cu IONS BY X-RAY AND NANOSECOND LASER RADIATION</b>	
Klyukin D.A., Leontieva V.A., Stolyarchuk M.V., Sidorov A.I., Ignatiev A.I., Nikonorov N.V. ....	150
<b>GENERALIZED CLAUSIUS-MOSSOTTI RELATION FOR SEMI-INFINITE ARTIFICIAL PERIODIC STRUCTURE</b>	
Maxim N. Anokhin, Alexey A. Tishchenko, Mikhail N. Strikhanov .....	151
<b>ANALYSIS OF INTACT CEREAL FLOURS BY FLUORESCENCE SPECTROSCOPY COUPLED WITH PARAFAC</b>	
Ivana Zeković, Lea Lenhardt, Bojana Milićević, Tatjana Dramićanin, Miroslav D. Dramićanin .....	152
<b>STRUCTURAL PHASE TRANSITIONS AND PHOTOLUMINESCENCE PROPERTIES OF OXONITRIDOSILICATE PHOSPHORS UNDER HIGH HYDROSTATIC PRESSURE</b>	
Agata Lazarowska, Sebastian Mahlik, Marek Grinberg, Guogang Li, Ru-Shi Liu .....	153
<b>EFFECT OF TEMPERATURE ON PHOTOLUMINESCENCE OF Gd DOPED ZnO NANOCRYSTALS</b>	
Deepika Mithal, Tapanendu Kundu.....	154
<b>PERSISTENT LUMINESCENCE OF TERBIUM AND PRASEODYMIUM DOPED LUTETIA PREPARED BY THE RAPID MICROWAVE ASSISTED METHOD</b>	
C. C. S. Pedroso, J. M. Carvalho, L. C. V. Rodrigues, H. F. Brito, J. Hölsä .....	155
<b>DIFFRACTION GRATING PROFILE RECONSTRUCTION USING SAMPLE-ROTATION MUELLER MATRIX ELLIPSOMETRIC MEASUREMENTS</b>	
Lukáš Halagačka, Kamil Postavaa, Martin Mičica, Jaromír Pištora.....	156
<b>SYNTHESIS AND CHARACTERIZATION OPTICAL PROPERTIES OF Bi<sub>4</sub>Ti<sub>3</sub>O<sub>12</sub>:Er NANOPARTICLES</b>	
S. Fuentes, P. Muñoz and J. Llanos, I.R. Martin.....	157
<b>STRUCTURAL AND PHOTOLUMINESCENCE INVESTIGATION OF Pr<sup>3+</sup>-DOPED Gd<sub>2</sub>O<sub>3</sub> NANOMATERIALS BY SOL-GEL PROCESS</b>	
M. Seraiche, L. Guerbous .....	158
<b>GROWTH AND LUMINESCENCE PROPERTIES OF Ce DOPED LaCl<sub>3</sub>/CaCl<sub>2</sub> EUTECTIC SCINTILLATOR</b>	
Kei Kamada, Kosuke Hishinuma, Shunsuke Kurosawa, Akihiro Yamaji, Yasuhiro Shoji, Jan Pejchalb, Yuji Ohashi, Yuui Yokota, and Akira Yoshikawa .....	159
<b>PHOTOLUMINESCENCE AND THERMOLUMINESCENCE STUDY ON TI<sub>2</sub>Ga<sub>2</sub>S<sub>3</sub>Se LAYERED CRYSTALS</b>	
Nizami Hasanli, Mehmet Isik, Serdar Delice.....	160
<b>GROWTH AND SPECTROSCOPIC CHARACTERIZATION OF YbF<sub>3</sub> DOPED BaF<sub>2</sub> CRYSTALS</b>	
Marius Stef, Irina Nicoara.....	161
<b>HALOGEN-FREE IMMERSION FOR OPTICAL ELEMENTS WITH HIGH REFRACTIVE INDEX</b>	

Valery M. Volynkin, Yury A. Gatchin, Konstantin V. Dukelskiy, Sergey K. Evstropiev, Anatoly G. Korobeynikov .....	162
<b>HIGH SENSITIVE POLYMER MEDIUMS FOR OPTICAL GAS SENSORS</b>	
Bohdan R.Tsizh B., Olena I. Aksimentyeva O.....	163
<b>HIGH-EFFICIENT LUMINESCENCE OF SILVER CLUSTERS IN SODIUM-ZINC-ALIMINOSILICATE GLASSES DOPED WITH ANTIMONY OXIDE</b>	
Yevgeniy Sgibnev, Nikolay Nikonorov, Alexander Ignatiev .....	164
<b>HYBRID MATERIAL ORGANIC-INORGANIC WITH LUMINESCENCE PROPERTIES AND BIOMEDICAL APPLICATIONS</b>	
Adina Segneanu, Daniel Damian, Cristian Vaszilcsin, Paulina Vlazan, Ioan Grozescu.....	165
<b>IMPROVED LUMINESCENCE AND SCINTILLATION PROPERIES OF MULTICOMPONENT GARNET SCINTILLATORS</b>	
Miroslav Kucera, Zuzana Onderisinova, Martin Hanus, Ondrej Lalinsky, Jiri A.Mares,Martin Nikl....	166
<b>STRENGTHENING OF QUARTZ CERAMIC MATERIALS FOR OPTICAL AND LASER GLASS MELTING</b>	
Yury A. Gatchin, Konstantin V. Dukelskiy, Sergey K. Evstropiev, Anatoly G. Korobeynikov, Valery M. Volynkin, Alexander V. Shashkin .....	167
<b>INFLUENCE OF MO/MF<sub>2</sub> MODIFIERS (M = Ca, Sr, Ba) ON SPECTROSCOPIC PROPERTIES OF Eu<sup>3+</sup> IONS IN GERMANATE AND BORATE GLASSES</b>	
Lidia Žur, Joanna Janek, Marta Sołtysa, Joanna Pisarska, Wojciech A. Pisarski .....	168
<b>INFLUENCE OF REACTION MEDIUM ON THE MORPHO-STRUCTURAL PROPERTIES OF KNbO<sub>3</sub> POWDERS</b>	
P. Vlazan, M. Poienar, M. Stoia, P. Sfirloaga .....	169
<b>INFLUENCE OF RESTORATIVE PROCEDURES ON ENDODONTICALLY TREATED PREMOLARS: FINITE ELEMENT ANALYSIS OF A CT-SCAN BASED MATHEMATICAL MODEL</b>	
Tatjana Maravić, Darko Vasiljević, Ivana Kantardžić, Tijana Lainović, Ognjan Lužanin and Larisa Blažić .....	170
<b>INFLUENCE OF SYNTHESIS, THERMAL TREATMENT, AND ELECTRON IRRADIATION CONDITIONS ON THE FORMATION OF BISMUTH CENTERS IN BARIUM FLUORIDE CRYSTAL</b>	
O.K. Alimov, M.E. Doroshenko, V.A. Konyushkin, V.V. Osiko.....	171
<b>INFLUENCE OF Yb<sup>3+</sup> ION CO-DOPING ON ZnO:X (X=Eu<sup>3+</sup>, Er<sup>3+</sup>, Ho<sup>3+</sup>) PROPERTIES</b>	
Lidija V. Trandafilović, Dragana Jovanović, Miroslav Dramićanin .....	172
<b>INTELLIGENT MAGNETO-OPTICAL CORROBORATOR WITH FERROFLUIDS</b>	
David C. A. Saravia, José A. Siqueira D. Suhaila Maluf Shibli, Saulo Finco.....	173
<b>INTRINSIC LUMINESCENCE IN ALKALI METAL SULPHATES</b>	
T.N. Nurakhmetov, K. A. Kuterbekov, D.H. Daurenbekov, Zh.M. Salikhodzha, A.K. Kainarbay, A. M. Zhunusbekov, K. Bekmyrza.....	174
<b>INVESTIGATION OF ENERGY TRANSFER BETWEEN RARE EARTH IONS OF A 3D LANTHANIDE-ORGANIC FRAMEWORK</b>	
Carime V. Rodrigues, Marcelo Oliveira Rodrigues, Leonis L. Luz, Ricardo O. Freire, Severino A. Junior.....	175
<b>DISCOLORATION EFFECTS OF DENTAL COMPOSITE MATERIALS STAINED IN BEER</b>	
Milica Antonov, Bojana Milićević, Lea Lenhardt, Ivana Zeković, Dragica Manojlović, Miroslav D. Dramićanin .....	176
<b>INVESTIGATION OF THE OPTICAL AND LUMINESCENT PROPERTIES OF THE PURE QUARTZ USING SYNCHROTRON RADIATION</b>	
Vitaly N. Kolobanov, Igor A. Markov, Peter P. Shvansky .....	177

<b>IR SPECTROSCOPY STUDY OF THE ORIENTATION ORDER OF NEMATIC LIQUID CRYSTALS DOPED QUANTUM DOTS</b>	
Cavrish E.O., Konshina E.A., Vangonen A.I. ....	178
<b>K<sub>2</sub>SiF<sub>6</sub>:Mn<sup>4+</sup> AS A RED PHOSPHOR FOR REMOTE LEDs</b>	
Heleen F. Sijbom, Koen Van den Eeckhout, Dirk Poelman, Philippe F. Smet.....	179
<b>KINETICS OF HOLOGRAM RECORDING IN REVERSIBLE HOLOGRAPHIC MEDIUM BASED ON CALCIUM FLUORIDE CRYSTALS WITH COLOR CENTERS</b>	
Aleksandr S. Shcheulin, Aleksandr E. Angervaks, Aleksandr I. Ryskin.....	180
<b>LANGASITE AND LANGATATE CRYSTALS: OPTICAL CHARACTERIZATION AND POINT DEFECTS</b>	
Oleg A. Buzanov, Nina S. Kozlova, Anna P. Kozlova, Dmitriy A. Spassky, Nikita A. Siminel, Evgeniya V. Zabelina .....	181
<b>LANTANIDES BASED LUMINESCENT MATERIAL INCORPORATED INTO SILICA MATRIXES</b>	
Joanna Cybińska, Magdalena Wilk, Marta Kargol, Katarzyna Komorowska .....	182
<b>LATTICE DYNAMICS OF Ca<sub>2</sub>Ge<sub>7</sub>O<sub>16</sub>: A COMBINED EXPERIMENTAL-THEORETICAL STUDY</b>	
Vladislav P. Petrov, Vladimir A. Chernyshev, Ivan I. Leonidov, Ekaterina I. Konstantinova, Emma G. Vovkotrub, Anatoliy E. Nikiforov .....	183
<b>COLLOID SYNTHESIS, PHOTOCATALYTIC AND PHYSICO-CHEMICAL PROPERTIES OF BiVO<sub>4</sub> NANOPARTICLES</b>	
Slobodan D. Dolić, Dragana J. Jovanović, Milena Marinović Cincović, Biljana Babić, Krisjanis Smits, Miroslav D. Dramićanin .....	184
<b>LINEAR AND NONLINEAR OPTICAL ABSORPTION COEFFICIENTS IN AN OFF-CENTER SPHERICALLY CONFINED HYDROGEN ATOM</b>	
Vladan Pavlović, Ljiljana Stevanović.....	185
<b>LOCALIZED SURFACE PLASMON RESONANCE IN THE IR REGIME</b>	
N. Sardana, J.Schilling.....	186
<b>LOW-TEMPERATURE COMBUSTION SYNTHESIS AND PHOTOLUMINESCENCE PROPERTIES OF Y<sub>2-x-y</sub>Eu<sub>x</sub>Bi<sub>y</sub>WO<sub>6</sub></b>	
Darío Espinoza, Jaime Llanos.....	187
<b>LUMINESCENCE AND SCINTILLATION PROPERTIES OF A Cs<sub>3</sub>BiCl<sub>6</sub> CRYSTAL</b>	
Makoto Shimizu, Masanori Koshimizu, Yutaka Fujimoto, Takayuki Yanagida, Shingo Ono, Keisuke Asai.....	188
<b>LUMINESCENCE OF CO-DOPED Sr<sub>5</sub>MgLa<sub>2</sub>(BO<sub>3</sub>)<sub>6</sub>:Ce<sup>3+</sup>,Mn<sup>2+</sup> PHOSPHOR</b>	
Matthias Müller, Stefan Fischer, Thomas Jüstel .....	189
<b>LUMINESCENCE OF InP/ZnS QUANTUM DOTS IN NANOPOROUS ANODIC ALUMINA</b>	
Sergey S. Savchenko, Ilya A. Weinstein, Alexander S. Vokhmintsev, Denis O. Ilin.....	190
<b>LUMINESCENCE OF NEUTRON-IRRADIATED BERYLLIUM OXIDE CRYSTALS</b>	
Maxim D. Petrenko, Igor N. Ogorodnikov, Vladimir Yu. Ivanov, Alexander V. Kruzhlov.....	191
<b>LUMINESCENCE OF RARE EARTH IONS IN PHOSPHATE GLASSES</b>	
Marta Sołtysa, Joanna Pisarskia, Joanna Janeka, Lidia Żura, Wojciech A. Pisarskia.....	192
<b>LUMINESCENCE PROPERTIES AND INFLUENCE OF AGING TIME ON STRUCTURE OF Sr<sub>3</sub>SiO<sub>5</sub> DOPED WITH Eu<sup>3+</sup> AND Eu<sup>2+</sup></b>	
J. Barzowska, N. Górecka, K. Szczodrowski, M. Grinberg.....	193
<b>LIGHT EMISSION FROM IONIC NHC-CYCLOPLATINATED COMPOUNDS</b>	
Andres Chueca, Sara Fuertes, Violeta Sicilia. ....	194

<b>INVESTIGATION OF PHYSICAL AND CHEMICAL PROPERTIES OF WO<sub>3</sub>-FILMS OBTAINED BY SOL-GEL METHOD</b>	
Alexandr O. Trofimov, Elena V. Kolobkova, Nikolay V. Nikonorov .....	195
<b>EFFECT OF ANNEALING CONDITIONS ON Eu<sup>3+</sup>-DOPED Gd<sub>2</sub>Ti<sub>2</sub>O<sub>7</sub> THIN FILM LUMINESCENCE</b>	
Željka Antić, K. Prashanthi, Sanja Čulubrk, Miroslav D. Dramićanin and Thomas Thundat .....	196
<b>Multisite excitation and emission properties of the Nd<sup>3+</sup> and Lu<sup>3+</sup> doped CaF<sub>2</sub> laser crystals</b>	
S. Normani, A. Braud, J.L. Doualan, R. Moncorgé, C. Maunier, D. Penninck, P.Camy .....	197
<b>GRAPHENE UNROLLED FROM MULTI-WALLED CARBON NANOTUBES BY HIGH-INTENSITY ULTRASOUND</b>	
Jiří Henych, Václav Štengl, Petra Ecorchard, Hynek Benešb .....	198
<b>STRUCTURAL AND PHOTOLUMINESCENCE INVESTIGATION OF Pr<sup>3+</sup>-DOPED Gd<sub>2</sub>O<sub>3</sub> NANOMATERIALS BY SOL-GEL PROCESS</b>	
M. Seraiche, L. Guerbous .....	199
<b>PHOTOCATALYTIC PERFORMANCE OF Mg<sub>2</sub>TiO<sub>4</sub> NANOPOWDER</b>	
Mina Medić, Marija Vasić, Aleksandra Zarubica, Lidija Trandafilović, Miroslav D. Dramićanin, Jovan M. Nedeljković .....	200
<b>FABRICATION OF Y<sub>2</sub>O<sub>3</sub> and Y<sub>1.94</sub>Yb<sub>0.05</sub>Er<sub>0.01</sub>O<sub>3</sub> THIN FILMS BY PULSED LASER DEPOSITION</b>	
Djordje Veljović, Natalia Mihailescu, Angela Stefan, G. E. Stan, Catalin Luculescu, Djordje Janačkovic, Vesna Đorđević, Miroslav D. Dramićanin, Radenka Krsmanović Whiffen, Carmen Ristoscu, Serban Georgescu, Ion N. Mihailescu .....	201
<b>SUBSTITUTIONAL METHODS IN SPECTRAL PARAMETERS' MANAGEMENT OF LED GARNET PHOTOLUMINOPHORES</b>	
Naum Soschin, Vladimir Bolshukhin, Vladimir Ulasyuk .....	202
<b>X-RAY SENSITIVE DETECTOR WITH A MATRIX OF SILICON PHOTODIODES FOR ENTERING THE X-RAY IMAGE INTO A COMPUTER</b>	
Vladimir Ulasyuk, Lyudmila Bikova, Nina Jelyabovskaya, Irina Lobanova, Vladimir Shukhtin, Naum Soschin .....	203
<b>STRUCTURE AND LUMINESCENCE PROPERTIES OF PURE AND EUROPIUM-DOPED Zn<sub>2</sub>SnO<sub>4</sub></b>	
Tamara B. Ivetić, Mirjana R. Dimitrievska, Goran R. Štrbac, Kristina O. Čajko, Ljubica R. Đačanin, Dragoslav M. Petrović, Svetlana R. Lukić-Petrović .....	204
<b>DIELECTRIC AND STRUCTURAL CHARACTERISTICS OF THE Bi-As<sub>2</sub>S<sub>3</sub> QUASIBINAR CHALCOGENIDES</b>	
M.V. Šiljegović, S.R. Lukić Petrović, D.M. Petrovića D. L. Sekulić, G.R. Štrbac, F. Skuban .....	205
<b>RE<sup>3+</sup>-DOPED GdVO<sub>4</sub> THIN FILMS OBTAINED BY PULSED LASER DEPOSITION METHOD</b>	
Željka Antić, K. Prashanthi, Dragana Jovanović, Miroslav D. Dramićanin and Thomas Thundat .....	206
<b>RARE-EARTH DOPED SILVER EXCHANGED SILICA-HAFNIA WAVEGUIDES FOR BROADBAND DOWNCONVERSION TO IMPROVE THE EFFICIENCY OF PV SOLAR CELLS</b>	
A. Bouajaj, F. Enrichi, C. Armellini, G. Battaglin, F. Belluomo, E. Cattaruzza, F. Gonella, A. Łukowiak, M. Mardegan, S. Polizzi, C. Sada, M. Ferrari .....	207
<b>RARE EARTH DOPED LEAD-FREE GERMANATE GLASSES FOR OPTICAL ACTIVE FIBER TECHNOLOGY</b>	
Joanna Pisarska, Wojciech A. Pisarski, Marcin Kochanowicz, Jacek Żmojda, Dominik Dorosz, Jan Dorosz .....	208
<b>RADIOPHOTOLUMINESCENCE PROPERTIES OF Ag-DOPED PHOSPHATE GLASSES</b>	
Hironori Tanaka, Yutaka Fujimoto, Masanori Koshimizu, Takayuki Yanagida, Keiichiro Saeki, Takuma Yahaba, Keisuke Asai .....	209

<b>RADIATION RESISTANCE DIAGNOSTICS OF OPTICAL MATERIALS</b>	
Eduard Feldbach, Eliko Töldsepp, Marco Kirm, Aleksandr Lushchik, Kenichiro Mizohata, Jyrki Räisänen .....	210
<b>QUANTUM MECHANICAL TRANSMISSION WITH ABSORPTION OF ZnO THIN FILMS</b>	
Petya Petkova, Darina Bachvarova, Petko Vasilev, Karem Boubaker, Refka Mimouni.....	211
<b>PHOTOLUMINESCENCE PROPERTIES OF Sr<sub>2</sub>GeO<sub>4</sub>:Ce,Na</b>	
Karolina Fiaczyk, Eugeniusz Zych.....	212
<b>PHOTOLUMINESCENCE FROM MAGNETOEXCITON IN NON-UNIFORM NANORING</b>	
Luis C. Porras, William. Gutiérrez Niño, Ilia D. Mikhailov.....	213
<b>GROWTH AND SCINTILLATION PROPERTIES OF Eu and Tb DOPED LiGdF<sub>4</sub>/LiF EUTECTIC SCINTILLATOR FOR NEUTRON DETECTION</b>	
Kei Kamada, Kosuke Hishinuma, Shunsuke Kurosawa, Akihiro Yamaji, Yasuhiro Shoji, Jan Pejchal, Yuji Ohashi, Yuui Yokota, and Akira Yoshikawa .....	214
<b>PHOTOLUMINESCENCE AND RADIATION PROPERTIES OF Ce<sup>3+</sup>-DOPED CsCaCl<sub>3</sub> CRYSTALLINE SCINTILLATOR</b>	
Yutaka Fujimoto, Keiichiro Saeki, Hironori Tanaka, Takuma Yahaba, Takayuki Yanagida, Masanori Koshimizu, Keisuke Asai, .....	215
<b>PHOTOIONIZATION OF Ce<sup>3+</sup> IONS IN YAG:Ce<sup>3+</sup>, LiCaAlF<sub>6</sub>:Ce<sup>3+</sup>, LiY<sub>x</sub>Lu<sub>1-x</sub>F<sub>4</sub>:Ce<sup>3+</sup> (X = 0, 0.5, 1) AND SrAlF<sub>5</sub>:Ce<sup>3+</sup> CRYSTALS</b>	
Vitaly Pavlov, Vadim Semashko, Rafail Rakhmatullin, Stella Korableva.....	216
<b>PHOSPHOR IN GLASS BASED ON HIGH REFRACTIVE INDEX GLASSES DOPED WITH Eu<sup>3+</sup> AND Mn<sup>2+</sup> IONS FOR LEDs</b>	
Yana A. Nekrasova, Vladimir A. Aseev, Anastasiya Y. Bibik, Julia V. Tuzova, Mariya A. Shvaleva, Nicolay V. Nikonorov, Elena V. Kolobkova, Oleg A. Usov.....	217
<b>PHONON SPECTRA OF EULYITE CRYSTALS Bi<sub>4</sub>M<sub>3</sub>O<sub>12</sub> (M=Ge, Si):AB INITIO STUDY</b>	
N. M. Avram, V.A.Chernyshev, E.-L.Andreici, V.P. Petrov, P. Petkova .....	218
<b>PHONON SPECTRA AND ELASTIC CONSTANTS OF RARE-EARTH TITANATE PYROCHLORES R<sub>2</sub>Ti<sub>2</sub>O<sub>7</sub> (R = Gd, Tb, Dy, Ho, Er, Tm, Yb, Lu, Y) FROM FIRST PRINCIPLES</b>	
Vladislav P. Petrov, Vladimir A. Chernyshev, Anatoliy E. Nikiforov.....	219
<b>PERMITTIVITY AND PERMEABILITY OF SEMI-INFINITE METAMATERIAL</b>	
Olga V. Porvatkina, Alexey A. Tishchenko, Mikhail N. Strikhanov.....	220
<b>OPTICALLY- AND THERMALLY-STIMULATED LUMINESCENCES OF Ce-DOPED SiO<sub>2</sub> GLASS PREPARED BY SPARK PLASMA SINTERING</b>	
Go Okada, Safa Kasap, Takayuki Yanagida .....	221
<b>NON-ISOTHERMAL CRYSTALLIZATION PROCESS OF Eu<sup>3+</sup> DOPED Zn<sub>2</sub>SiO<sub>4</sub> POWDERS</b>	
Milena Marinović-Cincović, Bojan Janković, Miroslav D. Dramićanin.....	222
<b>OPTICAL PROPERTIES OF HYBRID ASSOCIATES COLLOIDAL Ag<sub>2</sub>S QUANTUM DOT WITH J-AGGREGATES OF DEC ORGANIC DYE</b>	
Tamara Shatskikh, Oleg Ovchinnikov, Irina Grevtseva, Michail Smirnov.....	223
<b>OPTICAL PROPERTIES OF CONVENTIONAL AND LOW-SHRINKAGE MODEL COMPOSITES</b>	
Dragica Manojlovic, Miroslav D. Dramićanin, Maja Lezaja, Pong Pongprueksa, Bart Van Meerbeek, Vesna Miletic .....	224
<b>OPTICAL PROPERTIES OF CdMoO<sub>4</sub>:RE<sup>3+</sup> (RE = Nd, Eu, Yb) SINGLE CRYSTALS</b>	
Małgorzata Guzik, Elżbieta Tomaszewicz, Yannick Guyot, Marek Berkowski, Kheirredine Lebbou, Janina Legendziewicz, Georges Boulon.....	225



<b>OPTICAL PROPERTIES OF <math>^{40}\text{Ca}^{100}\text{MoO}_4</math> SINGLE CRYSTALS FOR THEIR APPLICATION IN THE CRYOGENIC SCINTILLATION DETECTOR</b>	
Anastasiia Chernykh, Oleg Buzanov, Marina Bykova, Evgeniya Zabelina, Anna Kozlova, Nina Kozlova .....	226
<b>OPTICAL PROPERTIES OF DOPED TRANSPARENT <math>\text{Y}_2\text{O}_3</math> AND <math>\text{Y}_3\text{Al}_5\text{O}_{12}</math> CERAMICS</b>	
V.V.Balashov, Y.L.Kopylov, V.B.Kravchenko, K.V.Lopukhin, V.V.Shemet .....	227
<b>Optical characterization of ZnSe/CdSe nanocrystals with <math>\pi</math>-conjugated organic ligands</b>	
Takuma Yahaba, Shigeru Kaida, Masanori Koshimizu, Yutaka Fujimoto, Keisuke Asai.....	228
<b>OPTICAL BIOSENSOR FOR DETECTION OF FORMALDEHYDE BASED ON AOX ENZYME ON POLY-N-BUTYL ACRYLIC-CO-N-ACRYLOXSUCCINIMIDE FILM</b>	
Nurlely Kusuma, Musa Ahmad, Lee Yook Heng .....	229
<b>OPTICAL AND MORPHOLOGICAL PROPERTIES OF NEW RED <math>\text{Y}_2\text{Hf}_2\text{O}_7:\text{Eu}^{3+}</math> NANOPHOSPHORS</b>	
Jelena Papan, Milica Sekulić, Dragana J. Jovanović, Vesna Đorđević, Miroslav Dramićanin .....	230
<b>OPTICAL AND LUMINESCENT PROPERTIES OF RARE-EARTH GALLIUM BORATES <math>\text{RGa}_3(\text{BO}_3)_4</math>, WHERE <math>R = \text{Nd, Sm} - \text{Er, Y}</math></b>	
Elena A. Dobretsova, Kirill N. Boldyrev, Elena Yu. Borovikova.....	231
<b>NONLINEAR OPTICAL PROPERTIES OF <math>\text{TeO}_2\text{-P}_2\text{O}_5\text{-ZnO-LiNbO}_3</math> GLASSES DOPED BY <math>\text{Er}_2\text{O}_3</math>, <math>\text{Nd}_2\text{O}_3</math> AND <math>\text{Gd}_2\text{O}_3</math> RARE EARTH IONS</b>	
Rafał Miedziński, Izabela Fuks-Janczarek, El Sayed Yousef .....	232
<b>Non-isothermal kinetic behavior OF crystallization process of <math>\text{Y}_2\text{Ti}_2\text{O}_7</math></b>	
Bojana Milićević, Sanja Čulubrk, Željka Antić, Miroslav Dramićanin, Milena Marinović-Cincović.....	233
<b>OPTICAL STUDIES OF THE ABSORPTION CURVES OF KDP CRYSTAL</b>	
Temirgaly Koketai, Ainura Tussupbekova, Askhat Baltabekov, Batima Tagayeva, Anel Ibrayeva, Elmira Mussenova .....	234
<b>NATURE AND FORMATION ENERGY OF absorbing CENTRES caused BY reducing heat treatment in <math>\text{LiNbO}_3</math>, <math>\text{LiNbO}_3:\text{Mg}</math> AND <math>\text{LiNbO}_3:\text{Fe}</math> crystals</b>	
Dmitro Sugak, Oleg Buryy, Yuriy Sugak, Klaus-Dieter Becker, Ivan Solskii, Sergii Ubizskii.....	235
<b>MODEL OF NANOCONE STRUCTURE WITH GIANT POLARIZABILITY</b>	
William Gutiérrez Niño, Luis Francisco Garcia, Iliia D. Mikhailov.....	236
<b>LUMINESCENCE PROPERTIES, JUDD-OFELT ANALYSIS AND EMISSION ON UP-CONVERSION UNDER 612 NM EXCITATION IN A NEW ERBIUM DOPED GERMANO-TELLURITE GLASS</b>	
Y. Benmadani, A. Kermaoui, R. Si Fodil, A. Kellou, M.Benabdesselam .....	237
<b>Luminescence spectroscopy of <math>\text{Eu}^{3+}</math> ions in <math>\text{Lu}_3\text{Ga}_5\text{O}_{12}</math> garnet</b>	
A.P. Luचेchko, I.I. Syvorotka, I.M. Syvorotka .....	238
<b>LUMINESCENT LABELING OF NANOCRYSTALS: <math>\text{SiO}_2 @ \text{LaPO}_4</math></b>	
Jacobine van Hest, Andries Meijerink .....	239
<b>LUMINESCENT PROPERTIES OF FLUOROPHOSPHATE GLASS DOPED WITH COPPER IONS</b>	
Anastasiia N. Babkina, Pavel S. Shirshnev, Nikolay V. Nikonorov, Elena V. Kolobkova.....	240
<b>LUMINESCENT PROPERTIES OF SILVER MOLECULAR CLUSTERS IN PHOTO-THERMO-REFRACTIVE GLASSES CONTAINING CHLORIDE AND BROMIDE AGENTS</b>	
Victor D. Dubrovin, Aleksander I. Ignatiev, Nikolai V. Nikonorov .....	241
<b>LUMINESCENT PROPERTIES OF YAG: Gd, CePHOSPHORS UNDER PHOTO- AND ELECTRONIC EXCITATION</b>	
Damir Valiev, Sergey Stepanov, Viktor Lisitsyn .....	252

<b>MAGNETIC FEATURES AND PHASE TRANSITIONS OF Ni<sub>3</sub>(BO<sub>3</sub>)<sub>2</sub> SINGLE CRYSTAL</b>	
Anastasiia D. Molchanova, Kirill N. Boldyrev, Roman V. Pisarev.....	253
<b>SYNTHESIS AND PROPERTIES OF Eu<sup>3+</sup> DOPED Lu<sub>2</sub>Ti<sub>2</sub>O<sub>7</sub></b>	
Sanja Čulubrk, Katarina Vuković, Milena Marinović-Cincović, Miroslav D. Dramićanin .....	244
<b>MOLTEN LIGAND SYNTHESIS METHOD AND LUMINESCENCE STUDY OF RE<sup>3+</sup> COMPLEXES WITH PIMELATE</b>	
Israel P. Assunção, Hermi F. Brito, Maria C.F.C. Felinto, Oscar L. Malta .....	245
<b>MONOCRYSTALLINE PHOSPHOR WITH ENHANCED LIGHT EXTRACTION</b>	
Tomáš Fidler, Jan Kubát, Peter Matvija, Ondřej Bečička, Martin Rejman, , Štěpán Novotný.....	246
<b>LIGHT EMITTERS BASED ON ELECTROCHEMILUMINESCENT PHENOMENA IN NANOSIZED CAVITIES</b>	
Aliaksandr Smirnov, Andrei Stepanov .....	247
<b>OSL PROPERTIES OF NEW HYBRID DETECTORS</b>	
Ewa Mandowska, Arkadiusz Mandowski, Barbara Marczevska, Paweł Bilski, .....	248
<b>AN EXOTIC REMOTE PHOSPHOR WITH HIGH QUANTUM YIELD FOR WARM WHITE LIGHT PRODUCTION: MANIFESTATION OF SILICA NANOPARTICLES</b>	
Kiwan Jang, Sakthivel Gandhi, Ho Sueb Lee, Dong Soo Shin, Jung Hyun Jeong .....	249
<b>DUAL-MODE LUMINESCENCE WITH BROAD NEAR UV AND BLUE EXCITATION BAND FROM Sr<sub>2</sub>CaMoO<sub>6</sub>:Sm<sup>3+</sup> PHOSPHOR FOR WHITE LEDs</b>	
Lili Wang, Byung Kee Moon, Byung Chun Choi, Jung Hyun Jeong, Jung Hwan Kim, Kiwan Jang, Ho Sueb Lee, Dong Soo Shin .....	250
<b>WHITE UPCONVERSION EMISSION AND TEMPERATURE DEPENDENCE OF Er<sup>3+</sup>, Yb<sup>3+</sup> AND Tm<sup>3+</sup> TRI-DOPED Y<sub>2</sub>O<sub>3</sub> NANOPHOSPHORS</b>	
Hyeon Mi Noh, Jung Hyun Jeong, Jung Hwan Kim, Kiwan Jang, Ho Sueb Lee, Dong Soo Shin .....	251
<b>BLUE LUMINESCENCE IN MWO<sub>4</sub>:Tm<sup>3+</sup> (M= Ba, Sr) PHOSPHORS</b>	
Edson L. Gaiollo, Renan P. Moreira, Heliomar P. Barbosa, Cassio C. S. Pedroso, Lucas C.V. Rodrigues, Oscar M. L. Malta, Hermi F. Brito, Maria C.F.C. Felinto.....	252
<b>ZNO NANOPOWDERS BY A MICROWAVE HYDROTHERMAL METHOD – INFLUENCE OF EUROPIUM DOPING ON LUMINESCENCE PROPERTIES</b>	
E. Wolska- Kornio, J. Kaszewski, B.S. Witkowski, Ł. Wachnicki, M. Godlewski .....	253
<b>WHITE-LIGHT-EMITTING KCl:Eu<sup>2+</sup>/KCN CRYSTAL</b>	
Luis H. Andrade, Sandro M. Lima, Rogerio Ventura da Silva, Mauro L. Baesso, Yannick Guyot, Luiz Antonio de Oliveira Nunes .....	254
<b>OPTIMIZATION OF EMULSION POLYMERIZATION OF SELF-ASSEMBLED COLLOIDAL CRYSTALS FOR LASER APPLICATION</b>	
S.H. Vakili Tahami, S. Pourmahdian, B. Shirkavand, M. M. Tehranchi .....	255
<b>WAVELENGTH-CONVERSION EFFICIENCY ENHANCEMENT IN NANO-TEXTURED FLUORESCENT 6H-SiC PASSIVATED BY ATOMIC LAYER DEPOSITED TITANIUM OXIDE</b>	
Weifang Lu, Yiyu Ou, Valdas Jokubavicius, Ahmed Fadil, Mikael Syväjärvi, Paul Michael Petersen, and Haiyan Ou .....	256
<b>UPCONVERSION WHITE LIGHT AND MULTICOLOR LUMINESCENCE IN GdVO<sub>4</sub>:Ln<sup>3+</sup>/Yb<sup>3+</sup> (Ln<sup>3+</sup> = Ho<sup>3+</sup>, Er<sup>3+</sup>, Tm<sup>3+</sup>, Ho<sup>3+</sup>/Er<sup>3+</sup>/Tm<sup>3+</sup>) NANORODS</b>	
Tamara Gavrilović, Dragana J. Jovanović, Sanja Čulubrk, Krisjanis Smits, Miroslav D. Dramićanin ....	257
<b>UPCONVERSION LUMINESCENCE IN LaInO<sub>3</sub>:Er<sup>3+</sup></b>	
Nina Mironova-Ulmane, Vera Skvorcova, Kristaps Strals, Guna Kriekē, Anatolijs Sarakovskis, Leonid Bashkirov, Elena Juhno.....	258

<b>UPCONVERSION LUMINESCENCE IN <math>\text{CaYb}_{2-x}\text{Er}_x\text{Ge}_3\text{O}_{10}</math> (<math>x = 0-2</math>)</b>	
Olga A. Lipina, Ivan I. Leonidov, Ludmila L. Surat, Alexander P. Tyutyunnik, Vladimir G. Zubkov .....	259
<b>UP-CONVERSION EMISSIONS IN WATER-SOLUBLE <math>\text{Yb}^{3+}</math>, <math>\text{Tm}^{3+}</math>, <math>\text{Gd}^{3+}</math> DOPED <math>\beta\text{-NaYF}_4</math> NANOPARTICLES FOR IN VIVO THERANOSTIC</b>	
N. Francolon, F. Leccia, E. Jouberton, D. Boyer, I. Miladi, Delphine Felder-Flesch, Sylvie Begin-Colin, L. Morel, E. Miot-Noirault, J-M. Chezal, R.Mahiou .....	260
<b>UPCONVERSION STUDIES ON <math>\text{Mg}^{2+}</math> DOPED <math>\text{La}_2\text{O}_3</math>: <math>\text{Er}^{3+}/\text{Yb}^{3+}</math> NANOPHOSPHORS FOR TEMPERATURE SENSING AND SECURITY</b>	
Surya P. Tiwari, Sanjeet Singh, Kaushal Kumar, Vineet K. Rai .....	261
<b>UNCONTROLLED IMPURITY OF <math>\text{Bi}^{3+}</math> IN RARE-EARTH IRON BORATES <math>\text{RFe}_3(\text{BO}_3)_4</math></b>	
Kirill N. Boldyrev, Marina N. Popova, Leonard N. Bezmaternykh, Irina A. Gudim .....	262
<b>TUNING OF THE PHOTOPHYSICAL PROPERTIES OF PYRIMIDINE AND PYRROLO [2, 3-D] PYRIMIDINE CORE BASED DERIVATIVES AND THEIR APPLICATIONS FOR FLUORESCENCE SENSING</b>	
Arunas Miasojedovas, Lina Skardžiūtė, Justina Jovaišaitė, Jelena Dodonova, Jonas Bucevičius, Sigitas Tumkevičius, Saulius Juršėnas .....	263
<b>THEORY OF OPTICAL CENTRES WITH JAHN-TELLER EFFECT IN EXCITED STATES – CONTRIBUTION OF PHONONS</b>	
Kaja Pae, Vladimir Hizhnyakov .....	264
<b>THEORETICAL STUDY ON ZNHGSSE ALLOYS FOR WIDE RANGE OPTOELECTRONIC APPLICATIONS</b>	
Mehmet Ustundag, Sadik Bagci, Battal G. Yalcin, Metin Aslan .....	265
<b>THE UNIT CELL PARAMETER OF THE CUBIC BIXBYITE SESQUIOXIDES VS. STARK SPLITTING OF THE EUROPIUM <math>^7\text{F}_1</math> MANIFOLD</b>	
Željka Antića, Vesna Đorđević, Miroslav D. Dramićanin, Thomas Thundat .....	266
<b>The effect of <math>\text{Li}^+</math> co-doping on structural, morphological and optical properties of <math>\text{TiO}_2:\text{Eu}^{3+}</math> nanopowders</b>	
Vesna Đorđevića, Bojana Milićević, Goran Dražić, Miroslav D. Dramićanin .....	267
<b>THE LUMINESCENCE BUILD UP OF EXCITON-LIKE NATURE IN ALKALI HALIDE CRYSTALS AT REDUCED LATTICE SYMMETRY</b>	
Kuanyszbek Sh. Shunkeyev, Shynar Zh. Sagimbayeva, Zuchra K. Aimaganbetova, Sagynbek K. Shunkeyev, Daulet M. Sergeyev .....	268
<b>THE LORENTZ OSCILLATOR MODEL AND COVALENT BONDS OF AQUEOUS SOLUTIONS</b>	
Petya Petkova, Darina Bachvarova and Petko Vasilev .....	269
<b>SPECTRAL-LUMINESCENT PROPERTIES OF ZINC ALUMINOSILICATE GLASS-CERAMICS DOPED WITH NiO</b>	
Alexandr Zhilin, Irina Alekseeva, O Dymshits, Valery Golubkov, Marina Tsenter, Michael Shepilov, Pavel Loiko, Konstantin Yumashev, Kirill Bogdanov .....	270
<b>THE EFFECT OF ELECTRON BEAM AND THERMAL TREATMENTS ON THE SODIUM NANOPARTICLES FORMATION IN SODA-LIME GLASSES</b>	
Elizaveta. S. Bochkareva, Nikolay V. Nikonorov, Oleg A. Podsvirov, Mikhail A. Prosnikov, Alexander.I. Sidorov .....	271
<b>THE EFFECT OF CHARGE COMPENSATION BY MEANS OF <math>\text{Na}^+</math> IONS ON THE LUMINESCENT PROPERTIES OF <math>\text{Nd}^{3+}</math>-DOPED <math>\text{CaAl}_4\text{O}_7</math> AND <math>\text{CaGa}_4\text{O}_7</math></b>	
Malgorzata Puchalska .....	272
<b>TEMPERATURE DEPENDENT LUMINESCENCE OF <math>\text{Cr}^{3+}</math> DOPED <math>\text{YAl}_3(\text{BO}_3)_4</math> AND <math>\text{GdAl}_3(\text{BO}_3)_4</math></b>	
Beata Malysa, Andries Meijerink, Thomas Jüstel .....	273

<b>TEMPERATURE DEPENDENCE OF Y-ADMIX GAGG SCINTILLATOR GROWN BY THE CZOCHRALSKI PROCESS</b>	
Shunsuke Kurosawa, Mafuyu Seki, Kei Kamada, Jan Pejchal, Yasuhiro Shoji, Yuji Ohashi, Yuui Yokota, Akira Yoshikawa.....	274
<b>SYNTHESIS, STRUCTURE AND LUMINESCENT PROPERTIES OF Eu<sup>3+</sup>- DOPED Zn<sub>2</sub>TiO<sub>4</sub> NANOPARTICLES</b>	
Mina Medić, Vesna Lojpur, Željka Antić, Miroslav Dramićanin.....	275
<b>SYNTHESIS, LUMINESCENCE AND SILICA COATING OF Eu<sup>3+</sup>-DOPED LaVO<sub>4</sub> NANOPARTICLES</b>	
Robin Geitenbeek and Andries Meijerink .....	276
<b>Ag AND TiO<sub>2</sub> NANOPARTICLES ON POLYMER SUPPORT</b>	
Ivana D. Vukoje, Lidija V. Trandafilović, Tijana S. Radoman, Enis S. Džunuzović, S. Phillip Ahrenkiel, Jovan M. Nedeljković.....	277
<b>Study of luminescence mechanisms and excitation energy transfer in the Yb-doped PbWO<sub>4</sub> crystals</b>	
Oksana Chukova, Sergiy G. Nedilko.....	278
<b>STUDIES ON YSO:Ce BASED PHOSPHORS PREPARED BY GEL COMBUSTION USING NEW SILICON SOURCE</b>	
Ioana Perhaita, Laura E. Muresan, Adrian I. Cadis, Oana Ponta, Laima Trinkler.....	279
<b>STRUCTURAL PROPERTIES OF BISMUTH–LEAD–GERMANATE GLASSES</b>	
Simona Rada, Marius Rada, Nicolae Aldea, Ramona - Crina Suciuc, Sergiu Macavei, Adrian Bot, Eugen Culea and Radu Balan.....	280
<b>STRUCTURAL AND OPTICAL PROPERTIES OF PEROVSKITE–TYPE COMPOUNDS: NaTaO<sub>3</sub> AND NaNbO<sub>3</sub></b>	
Paula Sfirloaga, Maria Poienar, Marcela Stoia, Paulina Vlazan .....	281
<b>STANDARD THERMAL CONTRAST DEPENDENCE ON THE SUBSURFACE DEFECT DEPTH FOR THE DIFFERENT MATERIALS</b>	
Ljubiša D. Tomić, Vesna M. Damnjanović, Goran D. Dikić, Bojan Č. Milanović, Boban M. Bondžulić ....	282
<b>SPECTROSCOPIC STUDY OF LUMINESCENT PROPERTIES OF Li-DOPED SCREEN-PRINTED ZnO FILMS</b>	
T.V. Zashivailo, V.I. Kushnirenko .....	283
<b>SPECTROSCOPIC PROPERTIES OF TRIVALENT SAMARIUM IONS IN BORATE GLASSES</b>	
Ihor I. Kindrat, Bohdan V. Padlyak.....	284
<b>SPECTROSCOPIC PROPERTIES OF Lu<sub>2</sub>O<sub>3</sub>:Pr,Ti</b>	
Paulina Bolek, Aneta Wiatrowska, Dagmara Kulesza, Eugeniusz Zych .....	285
<b>THE OPTICAL SPECTRUM OF TERNARY ALLOY BBI<sub>1-x</sub>AS<sub>x</sub></b>	
Battal G. Yalcin, M. Aslan, M. H. Ozcan, H. A. Rahnamaye Aliabad .....	286
<b>SPECTRAL-LUMINESCENCE PROPERTIES OF ZrO<sub>2</sub>-Y<sub>2</sub>O<sub>3</sub>-Er<sub>2</sub>O<sub>3</sub> CRYSTALS</b>	
Natalya V. Sidorova, Elena E. Lomonova, Andrey A. Lyapin, Alexey N. Chabushkin, Polina A. Ryabochkina .....	287
<b>SIMULATION AND NUMERICAL ANALYSIS OF HIGHLY BIREFRINGENT PHOTONIC CRYSTAL FIBER TEMPERATURE SENSOR</b>	
R.Boufenar, M. Bouamar, A.Hocini .....	288
<b>SCINTILLATION PROPERTIES OF Eu-DOPED CsCl AND CsBr CRYSTALS</b>	
Keiichiro Saeki, Masanori Koshimizu, Takayuki Yangida, Yutaka Fujimoto, Takuma Yahaba, Hironori Tanaka, Keisuke Asai .....	289
<b>ROOM TEMPERATURE TIME-RESOLVED LUMINESCENCE OF OXYGEN-VACANCY DEFECT IN ZnO NANOSTRUCTURES SYNTHESIZED BY HYDROTHERMAL ROUTE</b>	
Widad Bekhti, Mostefa Ghamnia, Lakhdar Guerbus.....	290

<b>RELATIONSHIP BETWEEN STRUCTURE AND LUMINESCENCE PROPERTIES IN Ce<sup>3+</sup> OR Ce<sup>3+</sup>, Mn<sup>2+</sup>-DOPED GARNET PHOSPHORS FOR USE IN WHITE LEDS</b>	
Damian Pasiński, Eugeniusz Zych, Jerzy Sokolnicki .....	291
<b>REFRACTIVE INDEX SENSING USING TAPERED MICROCAVITIES PHOTONIC-CRYSTAL</b>	
Ahlam Harhouz, Abdesselam Hocini .....	292
<b>RED-TO-GREEN PHOTON UPCONVERTING MICROCRYSTALS FOR TEMPERATURE SENSING</b>	
Gary Degliame, Nathalie Trannoy, Jean-Pierre Jouart, Madjid Diaf.....	293
<b>OPTICAL CHARACTERIZATION OF RADIATION-INDUCED STRUCTURAL TRANSFORMATIONS IN CHALCOGENIDE SEMICONDUCTOR GLASSES</b>	
Oleh I. Shpotyuk, Mykhaylo V. Shpotyuk, Sergii B. Ubizskii .....	294
<b>NEW METHODS FOR STUDYING EXTREMELY LONG LASTING LUMINESCENCE PHENOMENA IN OSL DETECTORS</b>	
Arkadiusz Mandowski, Ewa Mandowska, Magdalena Biernacka, Renata Majgier, .....	295
<b>NANOSCALE CHARACTERISATION OF OPTICAL MATERIALS BY MAPPING OF LOCAL REFRACTIVE INDEX VALUES AS MEASURED WITH SINGLE-MOLECULE SPECTROMICROSCOPY</b>	
Tatiana A. Anikushina, Maxim G. Gladush, Aleksei A. Gorshelev, Andrei V. Naumov .....	296
<b>FABRICATION OF Y<sub>2</sub>O<sub>3</sub> and Y<sub>1.94</sub>Yb<sub>0.05</sub>Er<sub>0.01</sub>O<sub>3</sub> THIN FILMS BY PULSED LASER DEPOSITION</b>	
Djordje Veljović, Natalia Mihailescu, Angela Stefan, G. E. Stan, Catalin Luculescu, Djordje Janačkovic, Vesna Đorđević, Miroslav D. Dramićanin, Radenka Krsmanović Whiffen, Carmen Ristoscu, Serban Georgescu, Ion N. Mihailescu.....	297
<b>MODELLING LIGHT EMISSION FROM DC DISCHARGE TUBE FILLED WITH CH<sub>4</sub> GAS</b>	
V. Stojanović, Ž. Nikitović and Z. Lj. Petrović.....	298
<b>NOVEL ENERGY-SAVING (NANO) PHOSPHORS</b>	
Claudia Wickleder.....	299
<b>STAINING KINETICS OF DENTAL RESIN COMPOSITES</b>	
D. Manojlović, M. Antonov, B. Milićević, L. Lenhardt, M.D. Dramićanin .....	300
<b>THE EFFECTS OF DOPING ON CRYSTAL STRUCTURE AND PHOTOLUMINESCENCE OF LaVO<sub>4</sub>:Eu<sup>3+</sup></b>	
Andrii Shyichuk, Mohammad Zarad, Marcin Runowski, Agata Szczeszak, Renaldo T. Moura Jr., Albano N. Carneiro Neto, Stefan Lis, Oscar L. Malta .....	301
<b>IMPROVEMENT OF MATERIAL SURFACE PROPERTIES BY USING LASER SHOCK WAVE TECHNIQUE</b>	
Abdulhadi Kadhim , Haitham T. Hussein , Zahraa J. Muhammad, Ayad Zwayen Mohammed .....	302

# NANOMATERIAL-BASED FLUORESCENT BIOSENSING AND IMAGING

Otto S. Wolfbeis

*Institute of Analytical Chemistry, Chemo- and Biosensors, University of Regensburg,  
93040 Regensburg (Germany)*

Nanoparticles (NPs) often possess luminescence properties that are entirely different from those of bulk materials and from respective molecular species. Hence, they are highly attractive in terms of luminescent labels, markers, probes or imaging agents. Examples for nanomaterials commonly used in luminescence imaging include (a) the so-called quantum dots, most often of the CdSe and CdTe type; (b) carbon nanodots, (c) lanthanide-based upconversion NPs that can convert near-IR light into visible light, (d) gold nanoclusters, and – less often – carbon nanotubes, other noble metal clusters, or dyed silica particles. The surface of most NPs has to be modified in order to make them biocompatible or functional, and this is often more complicated than just making the NPs. The presentation first will cover nanomaterials for use in plain imaging and targeted imaging of cells and tissue. Such NPs also are quite useful in terms of sensing on a nanoscale because their use enables to view processes and properties of living cells that cannot be visualized by other methods (such as NMR spectroscopy). Examples include sensing of temperature, pH values or oxygen, and even monitoring of fundamental enzymatic reactions. More recently, NPs have been designed that have bimodal functionality. Examples include NPs for simultaneous optical and magnetic resonance imaging (with improved contrast) or CT of cancerous tissue, NPs for optical imaging and thermally induced lysis of cancer cells, and imaging along with drug delivery or photodynamic/photothermal therapy. Current challenges in the field include inadequate light penetration depths when working with (colored) biomatter, the complexity of methods for surface modification of NPs, and the lack of (affordable) methods for characterizing modified NPs. Also, issues of toxicity have to be addressed in each single case, and nanotechnology therefore is often said to be a boon to science and medicine.

[1] An Overview of Nanoparticles Commonly Used in Fluorescent Bioimaging. O. S. Wolfbeis, *Chem. Soc. Rev.* (2015), on the web. DOI: 10.1039/c4cs00392f.

[1] Upconversion Nanoparticles: From Hydrophobic to Hydrophilic Surfaces. V. Muhr, S. Wilhelm, Th. Hirsch, O. S. Wolfbeis; *Acc. Chem. Res.* 47 (2014) 3481–3493.

[1] Photon Upconverting Nanoparticles for Luminescent Sensing of Temperature. A. Sedlmeier, D. E. Achatz, L. H. Fischer, H. H. Gorris, O. S. Wolfbeis; *Nanoscale* 4 (2012) 7090-7096.

[1] Fluorophore-Doped Polymer Nanomaterial for Referenced Imaging of pH and Temperature with Sub-Micrometer Resolution. X. Wang, R. J. Meier, O. S. Wolfbeis; *Adv. Funct. Mat.* 22 (2012) 4202-4207.

[1] Targetable Phosphorescent Oxygen Nanosensors for the Assessment of Tumor Mitochondrial Dysfunction by Monitoring Respiratory Activity. X. Wang, H. Peng, L. Yang, F. You, F. Teng, L. Hou, O. S. Wolfbeis; *Angew. Chem. Int. Ed.* 53 (2014) 12471-12475.

[1] Spectrally Matched Upconverting Luminescent Nanoparticles for Monitoring Enzymatic Reactions. S. Wilhelm, M. del Barrio, J. Heiland, S. F. Himmelstoss, J. Galbán, O. S. Wolfbeis, T. Hirsch; *ACS Appl. Mat. Interf.* 6 (2014) 15427–15433.

<sup>1</sup> Multifunctional nanoprobe for fluorescence, magnetic resonance and computed tomography trimodal imaging. H. Xing, W. Bu, S. Zhang, J. Shi, *Biomaterials* 4 (2012) 1079-1089.

<sup>1</sup> Chemical modifications and bioconjugate reactions of nanomaterials for sensing, imaging, drug delivery and therapy. V. Biju, *Chem. Soc. Rev.* 43 (2014) 744-7

## ADVANCED OPTICAL MANIPULATION EXPLOITING MATERIALS SCIENCE

Kishan Dholakia,

*<sup>a</sup>SUPA, School of Physics and Astronomy, University of St Andrews, St Andrews, North Haugh UK KY16 9SS, kd1@st-andrews.ac.uk*

In the domain of science fiction, one is quite familiar with the idea of moving objects using laser beams (a “tractor beam”). In the laboratory science fiction turns into science fact: a powerful technique known as “optical tweezers” (OT) is analogous to this where micrometre-sized particles (and even biological material and atoms) can be grabbed, moved and generally manipulated without any physical contact. This is a stark demonstration of the optical dipole or gradient force in action. Such “optical tweezers”, based primarily on Newton’s laws and fundamental optics have enabled unprecedented insight about biological molecules such as DNA and molecular motors. In the microscopic world of optical tweezers, researchers are now harnessing these systems to study a host of science: this includes advanced colloidal interactions, dynamics of particles in various potentials (with strong analogues to atomic systems), insights into superconductivity, optically bound matter, studies of the optical angular momentum of light, magnetic flux line pinning, thermodynamics, microfluidics and motor protein transport. The list is ever growing.

This talk will give a new perspective on this field using materials science. This includes the use of new particles with specific properties for new studies. This can include the rotation of particles in liquid and vacuum [1] and the use of anti-reflection coated particles for enhanced optical forces [2].

[1] Y. Arita, M. Mazilu, and K. Dholakia, *Nat Commun* 4, (2013) 2374

[2] Anita Jannasch, Ahmet F. Demirörs, Peter D. J. van Oostrum, Alfons van Blaaderen & Erik Schäffer, *Nature Photonics* 6, (2012) 469–473

## ORGANOMETALLIC MOLECULAR MATERIALS FOR NLO, OLED AND OPV

Wai-Yeung Wong

*Institute of Molecular Functional Materials and Department of Chemistry, Hong Kong Baptist University, Waterloo Road, Hong Kong, rwywong@hkbu.edu.hk*

Inclusion of transition metal elements into organic scaffolds allows the hybridization of the interesting physical characteristics of metal complexes such as electronic, optical and magnetic properties with the solubility and processability inherent to the organic-based molecules. This lecture highlights the recent development of some multifunctional metallopolyynes and metallophosphors which can exhibit easily tunable luminescent and electronic properties (Figure 1). Considerable focus is placed on the evaluation of their suitability as emitters in OLEDs for display and lighting applications, optical power limiters for sensor protection as well as semiconductors in organic photovoltaic cells for solar power generation. The approaches based on structural modification of the organic chromophore to achieve multiple-color phosphorescence emission and to tune the optical (both linear and non-linear) and photovoltaic properties of these organometallic materials will be presented.

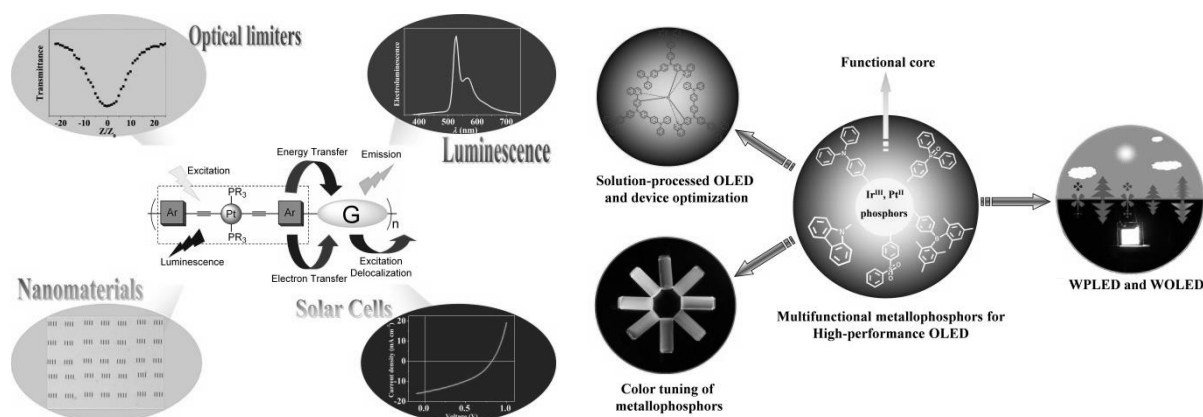


Figure 1. Multifunctional metallopolyynes and metallophosphors.

- [1] W.-Y. Wong, X.-Z. Wang, Z. He, A.B. Djurišić, C.-T. Yip, K.-Y. Cheung, H. Wang, C.S.K. Mak, W.-K. Chan, *Nat. Mater.* 6 (2007) 521.
- [2] W.-Y. Wong, C.-L. Ho, *Acc. Chem. Res.* 43 (2010) 1246.
- [3] J. Zou, H. Wu, C.-S. Lam, C. Wang, J. Zhu, S. Hu, C. Zhong, C.-L. Ho, G.-J. Zhou, H. Wu, W.C.H. Choy, J. Peng, Y. Cao, W.-Y. Wong, *Adv. Mater.* 23 (2011) 2976.
- [4] B. Zhang, G. Tan, C.-S. Lam, B. Yao, C.-L. Ho, L. Liu, Z. Xie, W.-Y. Wong, J. Ding, L. Wang, *Adv. Mater.* 24 (2012) 1873.
- [5] W.-Y. Wong, C.-L. Ho, *C.-L. J. Mater. Chem.* 19 (2009) 4457.
- [6] G. Zhou, W.-Y. Wong, *Chem. Soc. Rev.* 40 (2011) 2541.



## NOVEL RED PERSISTENT PHOSPHORS DEVELOPED BY BAND GAP ENGINEERING

Setsumi Tanabe, Jian Xu, Jumpei Ueda

*Graduate School of Human and Environmental Studies, Kyoto University, Kyoto 606-8501m  
Japan*

Long red persistent phosphors are expected for *in vivo* bio-imaging. The key point to design persistent phosphors is the possibility of tuning the “trap depth” between the bottom of conduction band, CB and the electron trap. If the binding energy of an electron trap is predicted, this strategy to control the trap depth by changing the CB energy level is regarded as “CB engineering”. Recently, we have applied the CB engineering to develop new persistent phosphors in some aluminate/ gallate based garnets (i.e. Ce<sup>3+</sup>-doped YAGG (green) [1] and GAGG (yellow) [2] phosphors), in which the probability of photoionization from the excited Ce<sup>3+</sup>: 5d<sub>1</sub> level to CB with blue illumination can be increased by increasing Ga<sup>3+</sup> substitution for Al<sup>3+</sup>. We have also developed red persistent phosphor (~690 nm) of Cr<sup>3+</sup> doped YAGG, where Cr<sup>3+</sup> ions act both as emission centers and trap centers [3]. The persistent behavior and TL glow peak temperature of these materials can systematically be tuned by changing Ga<sup>3+</sup> content. The persistent radiance (mW/Sr/m<sup>2</sup>) of the optimized composition was higher than that of the ZnGa<sub>2</sub>O<sub>4</sub>:Cr<sup>3+</sup> phosphor, which is used widely for *in vivo* bio-imaging applications [4]. We report a bright deep-red persistent phosphors of Cr<sup>3+</sup>-Eu<sup>3+</sup> codoped Gd<sub>3</sub>Al<sub>5-x</sub>Ga<sub>x</sub>O<sub>12</sub> garnet (GAGG: Cr<sup>3+</sup>-Eu<sup>3+</sup>), in which only Cr<sup>3+</sup> ion shows emission bands centered at 730 nm and Eu<sup>3+</sup> ion acts as an excellent electron trap. The design concept is based on a theoretical assumption and zigzag curves in the Dorenbos theory for garnet compounds [5]. The zigzag curve representing the ground state of divalent lanthanide ions show a minimum bottom at 4f<sup>7</sup> configuration (Eu<sup>2+</sup>). Because of its deep level, GGG (x=5) with the lowest CB level showed the best persistent behavior and longest emission wavelength due to the weakest crystal field strength. The persistent radiance of the GGG:Cr<sup>3+</sup>-Eu<sup>3+</sup> (x = 5) sample at 1 h after ceasing UV light was approximately 25 times higher than that of the Cr<sup>3+</sup> singly doped GGG sample, and is over 6 times higher than the ZnGa<sub>2</sub>O<sub>4</sub>: Cr<sup>3+</sup> red persistent phosphor.

[1] J. Ueda, K. Kuroishi, and S. Tanabe, *Appl. Phys. Lett.* 104, 101904 (2014).

[2] J. Ueda, K. Kuroishi, and S. Tanabe, *Appl. Phys. Express* 7, 062201 (2014).

[3] J. Xu, J. Ueda, Y. Zhuang, B. Viana, and S. Tanabe, *Appl. Phys. Express* 8, 042602 (2015).

[4] A. Bessière, S. Jacquart, et al., *Opt. Express* 19, 10131 (2011).

[5] P. Dorenbos, *J. Lumin.* 134, 310 (2013).

## OPTICAL CHALCOGENIDE GLASSES, FIBERS, AND DEVICES

Jean-Luc Adam

*Glasses & Ceramics Research Group, Institut des Sciences Chimiques de Rennes, UMR  
CNRS 6226, Université Rennes 1, Campus de Beaulieu, 35042 Rennes Cedex, France*

Compared to oxide based glasses, vitreous materials composed of chalcogen elements (S, Se, Te) show large transparency windows in the infrared. Indeed, chalcogenide glasses can be transparent from the visible up to 12-15  $\mu\text{m}$ , depending on their compositions. This is due to the lower phonon energies of chalcogenides, which are also responsible for enhanced luminescence of rare-earth ions embedded in such matrices. Thus, sulfide glasses, for instance, allow light emission at wavelengths not accessible with silica. In addition, chalcogenide glasses contain large polarisable atoms and external lone electron pairs which induce exceptional non-linear properties. Consequently, the non-linear properties can be 100 or 1000 times as high as the non-linearity of silica.

Applications are directly related to these unique optical properties. Thus, chalcogenide glasses possess a high potential for applications as mid-infrared sources above 3  $\mu\text{m}$ , where rare-earth-doped silica glass cannot operate. Also, chalcogenide photonic crystal fibers (PCF) might lead to new devices with unique optical properties in the mid-infrared domain like multimode or endlessly single-mode transmission of light, small or large mode area fibers, non-linear properties for wavelength conversion or generation of supercontinuum sources. Optical fiber sensors for the mid-IR region between 2 and 14  $\mu\text{m}$  are another promising area of applications. The IR signatures of most molecules, including biomolecules, are located in this spectral domain, which allows in situ, non-invasive and real-time detection of molecules by means of Fiber Evanescent Wave Spectroscopy (FEWS).

Future trends concern the development of composite materials like chalcogenide glass ceramics for energy or environment-oriented applications. This includes glass ceramics with enhanced properties for the conversion of solar light in photovoltaic cells, the generation of large photocurrent, thermoelectricity, and photocatalysis.

## **SPECTROSCOPIC PROPERTIES OF Sr<sub>2</sub>CeO<sub>4</sub> NANOCRYSTALS CO-DOPED WITH RARE-EARTH IONS**

Dariusz Hreniak, Łukasz Marciniak, Robert Tomala, Mariusz Stefański, Wiesław Stręk  
*Institute of Low Temperature and Structure Research, Polish Academy of Sciences, 50-950  
Wrocław, Poland, d.hreniak@int.pan.wroc.pl*

Spectroscopic properties of the Sr<sub>2</sub>CeO<sub>4</sub> nanocrystals under UV excitation were investigated. Blue emission associated with charge transfer (CT) Ce<sup>4+</sup>-O<sup>2-</sup> transition was observed. The absorption, excitation and emission spectra of obtained Sr<sub>2</sub>CeO<sub>4</sub> nanocrystals were analysed in details. In particular, the influence of the average grain size of Sr<sub>2</sub>CeO<sub>4</sub> nanocrystals on their optical properties was studied. It was observed that with increasing the average grain size of Sr<sub>2</sub>CeO<sub>4</sub> nanocrystals the emission decay times decreased significantly. From the other hand broad band emission under a high power NIR excitation was observed. The impact of the excitation density on the luminescent properties was analysed in details. The power and pressure dependence of emission intensity were discussed.

### Acknowledgement

The authors acknowledge the support from NCN grant no. 2012/06/A/ST5/00212.

## OPTICAL SPECTROSCOPY OF FLUORIDE AND OXIDE HOST LATTICES ACTIVATED WITH Dy<sup>3+</sup>

Enrico Cavalli

*Chemistry Department, University of Parma, viale delle Scienze 17/a, I-43124 Parma, Italy,  
enrico.cavalli@unipr.it*

The spectroscopic properties of Dy<sup>3+</sup>-doped oxide and fluoride lattices are reviewed in the light of their perspectives of applications. Their main emission transitions are in the 485 nm and 575 nm regions and make them attractive for the realization of solid state laser operating in the yellow region [1] and of single phase white emitting phosphors [2, 3], then motivating the continuously increasing interest in these compounds. In this connection, it has to be pointed out that most studies are carried out in order to develop new materials or to improve the synthesis conditions and/or the luminescence performance of materials with device potentialities, whereas less attention is dedicated to fundamental investigations. This implies two kinds of consequences: first, it is not uncommon to encounter misconceptions or questionable interpretations of the experimental data and, second, there are aspects concerning the emission dynamics of the Dy<sup>3+</sup> ion, which are still to be fully understood. In this connection it has to be pointed out that the application of known theoretical models, mainly based on the Judd-Ofelt Theory [4, 5] allows to obtain information useful for the evaluation of the host effect on the luminescence characteristics, for the estimate of the efficiencies of the various emission channels and also for the design of new experiments. These aspects will be dealt with by considering the experimental work carried out in the last fifteen years on Dy<sup>3+</sup>-doped materials, in the frame of an unitary approach in which some open questions will be pointed out together with their impact on the understanding of the luminescence mechanisms.

[1] S. R. Bowman, S. O'Connor, N. J. Condon *Opt. Express* 20 (2012) 12906-12911.

[2] F. Angiuli, F. Mezzadri, E. Cavalli, *J. Sol. State Chem.* 184 (2011) 1843-1849.

[3] K. Pavani, J. Suresh Kumar, T. Sasikala, B.C. Jamalajah, Hyo Jin Seo, L. Rama Moorthy, *Mat. Chem. Phys.* 129 (2011) 292-295.

## ASSIGNMENT OF Nd<sup>3+</sup>/Yb<sup>3+</sup> ENERGY LEVELS IN THE C<sub>2</sub> AND C<sub>3i</sub> CENTERS OF Lu<sub>2</sub>O<sub>3</sub> SESQUIOXIDE CERAMICS/CRYSTAL

Georges Boulon<sup>a</sup>, Guillaume Alombert-Goget<sup>a</sup>, Yannick Guyot<sup>a</sup>, Malgorzata Guzik<sup>b</sup>,  
Jan Pejchal<sup>c</sup>, Akira Yoshikawa<sup>c</sup>, Akihiko Ito<sup>c</sup>, Takashi Goto<sup>c</sup>

<sup>a</sup>*Institute Light Matter (ILM), UMR5306 CNRS-UCB Lyon1, University of Lyon,  
69622 Villeurbanne, France*

<sup>b</sup>*Faculty of Chemistry, University of Wrocław, ul. F. Joliot-Curie 14,  
50-383 Wrocław, Poland*

<sup>c</sup>*Institute for Materials Research, Tohoku University, Sendai 980-8577, Japan*

Lu<sub>2</sub>O<sub>3</sub> refractory sesquioxide has been suggested to be a potential laser host when doped either by Nd<sup>3+</sup> or by Yb<sup>3+</sup> rare earth ions, taking into account of the highest thermal conductivity (12.5 W/m/K) and the lowest phonon energy (614 cm<sup>-1</sup>) in comparison with YAG (10.8 W/m/K and 700 cm<sup>-1</sup>, respectively). As a result, spectroscopic data of Nd<sup>3+</sup> and Yb<sup>3+</sup> laser ions are needed in Lu<sub>2</sub>O<sub>3</sub> host, either as single crystal or as ceramics. It is extremely difficult to grow Lu<sub>2</sub>O<sub>3</sub> single crystal using conventional crystal growth methods because of its high melting point (2490 °C) but it is much easier to fabricate Lu<sub>2</sub>O<sub>3</sub> into a ceramic structure since the sintering temperature is about 700 °C lower than its melting point and no expensive crucible is required. In our program, Nd<sup>3+</sup>-doped Lu<sub>2</sub>O<sub>3</sub> single crystals are grown by the  $\mu$ -Pulling Down method and Nd<sup>3+</sup>-doped Lu<sub>2</sub>O<sub>3</sub> ceramics are fabricated by the non-conventional method Spark Plasma Sintering (SPS).

The main goal of this presentation is, first, to show the structure of cubic un-doped Lu<sub>2</sub>O<sub>3</sub> as single crystal and polycrystalline transparent ceramics [1] and, secondly, to assign absorption spectra, emission spectra and decays of Nd<sup>3+</sup> and Yb<sup>3+</sup> energy levels in the two crystallographic non-centrosymmetric C<sub>2</sub> and symmetrical C<sub>3i</sub> sites of the Lu<sub>2</sub>O<sub>3</sub> structure of both ceramics and crystal with the particularity that the population of C<sub>2</sub> sites is three times higher than those of the C<sub>3i</sub> ones [2-5]. Whereas spectroscopic studies of rare earth-doped sesquioxides involve mainly C<sub>2</sub> sites, associated with electric dipole induced type transitions of high probability, site selective laser spectroscopy is especially useful to point out also the transitions of C<sub>3i</sub> sites associated with magnetic-dipole type transitions of much weaker probability. An important result is C<sub>3i</sub> levels are located at higher energy than that of C<sub>2</sub> sites as already observed with other Eu<sup>3+</sup> and Sm<sup>3+</sup> rare earths-doped Lu<sub>2</sub>O<sub>3</sub> sesquioxides. The spectral positions of the two types of Lu<sub>2</sub>O<sub>3</sub> materials are the same.

[1] M. Guzik, M. Siczek, T. Lis, J. Pejchal, A. Yoshikawa, A. Ito, T. Goto, G. Boulon, *Crystal Growth and Design*, 14 (2014) 3327–34.

[2] G. Alombert-Goget, Y. Guyot, M. Guzik, G. Boulon, A. Ito, T. Goto, A. Yoshikawa, M. Kikuchi, *Opt. Mat.*, 41 (2015) 3-11.

[3] G. Toci, M. Vannini, M. Ciofini, A. Lapucci, A. Pirri, A. Ito, T. Goto, A. Yoshikawa, A. Ikesue, G. Alombert-Goget, Y. Guyot, *Opt. Mat.*, 41 (2015) 12–16.

[4] M. Guzik, G. Alombert-Goget, Y. Guyot, J. Pejchal, A. Yoshikawa, A. Ito, T. Goto, G. Boulon, *J. of Luminescence*.doi. 10.1016/j.jlumin.2014.12.063.

[5] Y. Guyot, M. Guzik, G. Alombert-Goget, J. Pejchal, A. Yoshikawa, A. Ito, T. Goto, G. Boulon, *J. of Luminescence*, accepted on April 19, 2015.

## FASCINATING OPTICAL PROPERTIES OF THE COPPER METABORATE

Marina N. Popova

*Institute of Spectroscopy, Russian Academy of Sciences, 5 Fizicheskaya Str., Troitsk, Moscow,  
Russia, popova@isan.troitsk.ru*

Beautiful bright blue crystals of the copper metaborate  $\text{CuB}_2\text{O}_4$  were first mentioned in “Foundations of Chemistry” by D. Mendeleev (St. Petersburg, 1906). Quite recently, in 2008,  $\text{CuB}_2\text{O}_4$  was found as a natural mineral from the Santa Rosa mine (Atacama desert, Chile) and was named *Santarosaitite*. In spite of a simple chemical formula,  $\text{CuB}_2\text{O}_4$  has a complex crystal structure (SG *I42d*) with 12 formula units in the tetragonal crystal unit cell, which has been characterized only in 1960. Magnetic  $\text{Cu}^{2+}$  ions ( $S=1/2$ ) in the unit cell occupy two different crystallographic positions, *4b* and *8d*. The compound exhibits a unique combination of magnetic, magnetoelectric, linear and nonlinear optical properties. To mention some of them,  $\text{Cu}(4b)$  and  $\text{Cu}(8d)$  magnetic sublattices order at different temperatures, 21 K and  $\sim 8$  K, respectively. Multiple frustrated and nonfrustrated antisymmetric exchange interactions within and between the *4b* and *8d* magnetic sublattices result in a rich complex magnetic phase diagram. As for optical properties,  $\text{CuB}_2\text{O}_4$  is the only transition-metal oxide that demonstrates narrow zero-phonon (ZP) exciton lines for all transitions between the crystal-field-split *3d*-states [1]. ZP lines are accompanied by an extremely rich vibronic structure [1,2]. Three types of optical magnetic-field-induced second harmonic generation were detected in  $\text{CuB}_2\text{O}_4$  [3]. In  $(\text{Cu}, \text{Ni})\text{B}_2\text{O}_4$ , nonreciprocal linear dichroism was observed and used to visualize a rotation of magnetization caused by an electric field [4,5].

In the Institute of Spectroscopy, we carry out high-resolution optical studies of  $\text{CuB}_2\text{O}_4$  single crystals. We have found a large sublattice-sensitive optical linear dichroism (LD) on ZP exciton lines which arises below the temperature of the antiferromagnetic ordering in the crystallographically isotropic (*xy*)-plane of  $\text{CuB}_2\text{O}_4$  [6]. We elucidate the nature of this LD attributing it to the magnetic Davydov splitting. Using the LD data we have discovered a splitting of the phase transition at  $\sim 8$  K into two transitions and have found three additional magnetic phase transitions at the temperatures 2.05 K, 2.00 K, and 1.85 K. Moreover, we were able to specify arrangement of spins in different incommensurate phases of the copper metaborate.

As a result, we show that the discovered optical LD can be used as a new efficient method for revealing hidden features of magnetic structures and phase transitions in complex multi-sublattice insulating multiferroics and magnetics.

This work was supported by the Russian Academy of Sciences under the Program for Basic Research “Electron correlations in systems with strong interactions”.

- [1] R.V. Pisarev, A.M. Kalashnikova, O. Schöps, L.N. Bezmaternykh, Phys. Rev. B 84 (2011) 075160 (11 pp).
- [2] R.V. Pisarev, K.N. Boldyrev, M.N. Popova, A.N. Smirnov, V.Yu. Davydov, L.N. Bezmaternykh, M.B. Smirnov, V.Yu. Kazimirov, Phys. Rev. B 88 (2013) 024301 (15 pp).
- [3] R.V. Pisarev, I. Sanger, G.A. Petrakovskii, M. Fiebig, Phys. Rev. Lett. 93 (2004) 037204 (4 pp).
- [4] M. Saito, K. Ishikawa, S. Konno, K. Taniguchi, T. Arima, Nature Materials 8 (2009) 634-638.
- [5] S.W. Lovesey, U. Staub, J. Phys.: Condens. Matter 21 (2009) 142201 (5 pp).
- [6] K.N. Boldyrev, R.V. Pisarev, L.N. Bezmaternykh, M.N. Popova, arXiv:1410.8727 [cond-mat.mtrl-sci].

## SPECTROSCOPY OF TRANSITION METAL IONS IN SOLIDS – THEORETICAL MODELING

Mikhail G. Brik<sup>a,b,c,d</sup>

<sup>a</sup> *College of Sciences, Chongqing University of Posts and Telecommunications, Chongqing 400065, China*

<sup>b</sup> *Institute of Physics, University of Tartu, Ravila 14C, Tartu 50411, Estonia*

<sup>c</sup> *Institute of Physics, Polish Academy of Sciences, al. Lotnikow 32/46, 02-668 Warsaw, Poland*

<sup>d</sup> *Institute of Physics, Jan Dlugosz University, Armii Krajowej 13/15, PL-42200 Czestochowa, Poland E-mail: mikhail.brik@ut.ee*

Transition metal ions find numerous applications in optical devices and materials such as solid state lasers, phosphors for lighting, phosphorescent sensors, solar energy conversion materials etc. The energy levels of these ions arise from the unfilled 3d electron shell, which strongly interacts with the crystal lattice vibrations and actively participates in chemical bonds formation. As a result, the absorption/emission spectra of these ions in solids differ considerably from host to host due to variation in strength of the electron-vibrational interaction and nephelauxetic effect. In the present work an overview of spectroscopic properties of the transition metal ions in a free state and in crystals will be given. Several trends between the main parameters describing the energy levels of the ions with unfilled d electron shell will be highlighted [1-2].

Applications of several different approaches (e.g. crystal field theory, DFT-based computational techniques, configurational coordinate model etc) to various optical materials with 3d ions as impurities will be discussed in details, with special emphasis on how to identify location of the impurity ions energy levels in the host band gap. It will be shown that by combining the crystal field theory and ab initio methods of electronic structure calculations it is possible to build up the complete energy level scheme of a doped crystal, which includes the host's electronic band structure and impurity ion energy levels superimposed onto it [3-5]. Recently developed model for the description of the spin-forbidden transitions of the  $d^3$  ( $Mn^{4+}$ ,  $Cr^{3+}$ ) and  $d^8$  ( $Ni^{2+}$ ) ions [6,7] will be also presented.

All calculated results will be compared with corresponding experimental data; agreement (or the reasons for disagreement) between the theory and experiment will be discussed.

[1] M.G. Brik, A.M. Srivastava, *Opt. Mater.* 35 (2013) 1776-1782.

[2] C.-G. Ma, M.G. Brik, *J. Lumin.* 145 (2014) 402-409.

[3] M.G. Brik, G.A. Kumar, D.K. Sardar, *Mater. Chem. Phys.* 136 (2012) 90-102.

[4] M.G. Brik, M. Nazarov, M.N. Ahmad-Fauzi, L. Kulyuk, S. Anghel, K. Sushkevich, G. Boulon, *J. Lumin.* 132 (2012) 2489-2494.

[5] M.G. Brik, M. Nazarov, M.N. Ahmad-Fauzi, L. Kulyuk, S. Anghel, K. Sushkevich, G. Boulon, *J. Alloys Comps.* 330 (2013) 103-108.

[6] M.G. Brik, A.M. Srivastava, N.M. Avram, A. Suchocki, *J. Lumin.* 148 (2014) 338-341.

[7] M.G. Brik, S.J. Camardello, A.M. Srivastava, *ECS J. Sol. State Sci. Technol.* 4 (2015) R39-R43.

## **Ln<sup>3+</sup> 4f ENERGY LEVELS AND LUMINESCENCE IN YTTRIUM ALUMINATE PEROVSKITE**

Kazushige Ueda<sup>a</sup>, Yuhei Shimizu<sup>a</sup>

<sup>a</sup>*Department of Materials Science, Faculty of Engineering, Kyushu Institute of Technology, 1-1 Sensui, Tobata, Kitakyushu 804-8550, Japan, kueda@che.kyutech.ac.jp*

Information about lanthanide (Ln) 4f energy levels relative to energy bands of host materials is important to understand the Ln luminescence properties. The Ln<sup>3+</sup> 4f energy levels in many various compounds have been reported on the basis of empirical data by Dorenbos [1, 2]. Thiel et al experimentally determined the Ln<sup>3+</sup> 4f energies relative to the valence band maximum (VBM) in yttrium aluminum garnet (YAG) by using resonant ultraviolet photoemission spectroscopy (UPS) [3]. Using the same resonant UPS technique, Sun et al simply examined the Ln<sup>3+</sup> 4f energies in perovskite-type yttrium aluminate, YAlO<sub>3</sub>. In this study, the Ln<sup>3+</sup> 4f ground energy levels in YAlO<sub>3</sub> were investigated by using conventional X-ray photoelectron spectroscopy (XPS). The energy diagram of the Ln<sup>3+</sup> 4f levels was drawn from the observed data and empirical data [2] as shown in Figure 1.

The wide band gap of YAlO<sub>3</sub> enables not only visible luminescence from various Ln<sup>3+</sup> but also uv luminescence from Gd<sup>3+</sup> [5]. The Gd<sup>3+</sup> sharp uv luminescence is usually observed at approximately 310 nm, which is anticipated for medical application such as skin disease phototherapy. Thin films of Gd<sup>3+</sup> doped YAlO<sub>3</sub> were prepared by a RF sputtering method aiming future development of thin film devices. The high quality films of Gd<sup>3+</sup> doped YAlO<sub>3</sub> were grown on LaAlO<sub>3</sub> single crystal substrates and photo- and cathodo-luminescence was observed from the thin films.

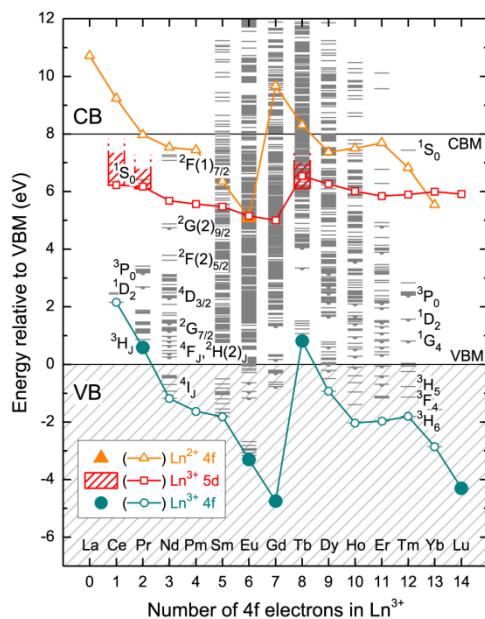


Fig. 1 Ln 4f and 5d energy diagram for YAlO<sub>3</sub>.

[1] P. Dorenbos, *J. Lumin.* 136 (2013) 122-129

[2] P. Dorenbos, *J. Lumin.* 135 (2013) 93-104

[3] C.W. Thiel, H. Cruguel, Y. Sun, G.J. Lapeyre, R. M. Macfarlane, R.W. Equall, R.L. Cone, *J. Lumin.* 94-95 (2001) 1-6

[4] Y. Sun, C.W. Thiel, R.L. Cone, R.W. Equall, R.L. Hutchison, *J. Lumin.* 98 (2002) 281-287

[5] Y. Shimizu, Y. Takano, K. Ueda, *J. Lumin.* 141 (2013) 44-47



## INTERVALENCE CHARGE TRANSFER LUMINESCENCE: AB INITIO CALCULATIONS AND CONFIGURATION COORDINATE DIAGRAMS

Zoila Barandiarán<sup>a,b</sup> and Luis Seijo<sup>a,c</sup>,

<sup>a</sup>*Departamento de Química and Instituto Universitario de Ciencia de Materiales Nicolás Cabrera, Universidad Autónoma de Madrid, Madrid, Spain.*

<sup>b</sup>*zoila.barandiaran@uam.es*

<sup>c</sup>*luis.seijo@uam.es*

We report the existence of intervalence charge transfer (IVCT) luminescence, which we identified in doped phosphor materials.

Although IVCT absorption is a well-known phenomenon in mixed-valence compounds [1], IVCT luminescence has never been reported, to the best of our knowledge. By means of ab initio calculations based on the use of multiconfigurational wave functions, we have shown that the so-called anomalous emissions of Ce<sup>3+</sup> in elpasolites and Yb<sup>2+</sup> in fluorites are, in fact, IVCT emissions [2,3]. In Cs<sub>2</sub>LiLuCl<sub>6</sub>:Ce<sup>3+</sup>, it is a Ce<sup>3+</sup>5d<sub>g</sub>→Ce<sup>4+</sup>4f electron transfer. In CaF<sub>2</sub>:Yb<sup>2+</sup> and SrF<sub>2</sub>:Yb<sup>2+</sup>, it is an Yb<sup>2+</sup>5d<sub>g</sub>→Yb<sup>3+</sup>4f<sub>7/2</sub> electron transfer accompanied by a 4f<sub>7/2</sub>→4f<sub>5/2</sub> de-excitation within the Yb<sup>2+</sup>4f<sup>13</sup> subshell. We also found that the broad orange emission of CaF<sub>2</sub>:Bi<sup>2+</sup>, which was attributed to a Bi<sup>2+</sup>(6s<sup>2</sup>6p) <sup>2</sup>P<sub>3/2</sub>→<sup>2</sup>P<sub>1/2</sub> transition [4], is an electron transfer from an impurity-trapped-exciton of Bi<sup>2+</sup> to the 6p shell of Bi<sup>3+</sup>. We find reasonable to assume that, besides Ce<sup>3+</sup>, Yb<sup>2+</sup>, and Bi<sup>2+</sup>-doped materials, IVCT emissions must be present in many other materials where different oxidation states are likely to coexist, e.g. in Pr<sup>3+</sup> and Eu<sup>2+</sup> containing materials.

IVCT emissions are very much red-shifted with respect to their excitations; and they are very broad. The reason lies in the very different equilibrium structures of the oxidized and reduced centers involved in the IVCT transition: after the electron transfer, which takes place at fixed structures, very large reorganization energy is released which is subtracted from the excitation energy; and the horizontal offset between the minima of two IVCT states is very large.

We also discuss simplified IVCT and metal-to-metal charge transfer (MMCT) configuration coordinate energy diagrams [5]. We discuss their main features and procedures to obtain them from empirical data. Application to Yb-doped YAG suggests that IVCT states of Yb<sup>2+</sup>/Yb<sup>3+</sup> pairs may play an important role in the quenching of the Yb<sup>3+</sup> 4f-4f emission and it provides the details of the quenching mechanism. Application to Ce,Yb-codoped YAG supports and provides details to the interpretation recently given for the energy transfer from Ce<sup>3+</sup> to Yb<sup>3+</sup> via a MMCT Ce<sup>4+</sup>-Yb<sup>2+</sup> state [6].

[1] G. C. Allen and N. S. Hush, *Prog. Inorg. Chem.* 8 (1967) 357.

[2] L. Seijo and Z. Barandiarán, *J. Chem. Phys.* 141 (2014) 214706.

[3] Z. Barandiarán and L. Seijo, *J. Chem. Phys.* 141 (2014) 234704.

[4] R. Cao, F. Zhang, C. Liao, and J. Qiu, *Opt. Express* 21 (2013) 15728.

[5] Z. Barandiarán, A. Meijerink, and L. Seijo, submitted.

[6] D. C. Yu, F. T. Rabouw, W. Q. Boon, T. Kieboom, S. Ye, Q. Y. Zhang, , and A. Meijerink, *Phys. Rev. B* 90 (2014) 165126.

## FLUORESCENCE SPECTROMICROSCOPY OF MYRIAD SINGLE DYE MOLECULES IN SOLID MATRICES: TOOL FOR HYPERSPETRAL MATERIAL NANODIAGNOSTICS

Andrei V. Naumov<sup>a,b</sup>

<sup>a</sup>*Institute for Spectroscopy of the Russian Academy of Sciences, Molecular Spectroscopy  
Department, Troitsk Moscow, 142190 Russia*

<sup>b</sup>*Moscow State Pedagogical University, Theoretical Physics Chair, Moscow, Russia  
E-mail: a\_v\_naumov@mail.ru, Web-page: www.single-molecule.ru*

Laser fluorescence spectromicroscopy of single probe molecules (SMSM) in transparent solids is a widely recognized field of science. The SMSM methods are especially informative at cryogenic temperatures, when *zero-phonon lines (ZPL)* of emitting centres are reachable for observation with the use of a narrowband laser light source [1,2]. The extreme sensitivity of the ZPL parameters to the single-molecule (SM) local environment allows us to apply SMSM for the study of doped solids on the nanometer scale. Actually, the high ratio of inhomogeneous absorption bandwidth to the very narrow ZPL homogeneous spectral width gives the opportunity to measure fluorescence excitation spectra and coordinates *for all efficiently fluorescing SMs* in doped bulk solid samples (crystals, glasses, polymers) at low-temperatures. For this purposes some specially developed algorithms and software should be applied for quick SM spectra and images recognition, data processing and specific statistical analyses. Note that the nanometre accuracy is achievable for all *three* spatial coordinates of each SM by adaptive optics based modification and analysis of its point-spread function [3].

In the present talk we overview the advances of SMSM for the materials characterisation on the nanometer scale. We show, that measurements, experimental data postprocessing and numerical analysis give the following opportunities:

- (a) to study comprehensively the photophysical properties of fluorescent media (from single emitter up to bulk sample), in particular to investigate the intermolecular processes, and the phenomena of single quantum objects emission enhancement, bleaching and blinking;
- (b) to probe processes local local fields in doped solids on the microscopic/nanoscale level (single low-energy elementary excitations, energy/charge transfer, aging);
- (c) to study anomalies and artifacts (sub-ppm chemical contamination);
- (d) to construct synthetic distributions of SM parameters, which have physical meaning, compare them with ensemble averaged data obtained by classic experiments;
- (e) to map the SM parameters in relation to sample nanoscale structure, thus to search and analyze physical nature of various correlations between local parameters of a sample, i.e. realise *far-field hyperspectral material nanodiagnosics*.

[1] A.V. Naumov, Phys.-Usp. 56 (2013) 605.

[2] A.V. Naumov, I.Yu. Eremchev, A.A. Gorshelev, Eur. Phys. J. D 68 (2014) 348.

[3] S.R.P. Pavani, M.A. Thompson, J.S. Biteen, S.J. Lord, N. Liu, R.J. Twieg, R. Piestun, W.E. Moerner, PNAS 106 (2009) 2995–□□□□□

[4] A.V. Naumov, A.A. Gorshelev, Y.G. Vainer, L. Kador, J. Kohler, Phys.Chem.Chem.Phys. 13 (2011) 1734–1742.

(\*) The support is acknowledged from Russian Foundation for Basic Researches (14-02-00822: experiments with the technique for cryogenic DHPSF SMSM) and Russian Science Foundation (14-12-01415: development of the methods for statistical analysis of SMSM-data). The study is included into the RAS Research Program of (“Basic Optical Spectroscopy and its Applications”). The results were obtained in our department, and in collaboration with the Univeristy of Bayreuth, Germany (Prof. L.Kador, Prof. J. Köhler). [1,2,4]

## **NANOMECHANICS OF PHOTOTHERMAL AND PHOTOACOUSTIC SPECTROSCOPY**

Thomas Thundat

*Dept. of Chemical and Materials Engineering, University of Alberta, Edmonton, AB, Canada*

Photothermal and photoacoustic effects accompanying pulsed resonant excitation of molecules are routinely used for material characterization. Photothermal and photoacoustic effects can also result in mechanical motion that can be observed using microfabricated devices. Recent advances in microfabricating structures that can detect extremely small forces open up possibilities for photothermal and photoacoustic spectroscopy of femto and pico gram quantities of molecules. This technique can be extended into pico liters of confined liquids in micro and nanoscale structures. Recent advances in the nanomechanical spectroscopy and its integration into multi-modal signal generation to achieve selectivity, sensitivity, and rapid regeneration will be discussed.

## Nd<sup>3+</sup>, Eu<sup>3+</sup> AND Yb<sup>3+</sup> IONS AS STRUCTURAL PROBES IN THE SCHEELITE-TYPE CADMIUM MOLYBDATE WITH VACANCIES

Malgorzata Guzik<sup>a</sup>, Elzbieta Tomaszewicz<sup>b</sup>, Yannick Guyot<sup>c</sup>, Janina Legendziewicz<sup>a</sup>,  
Georges Boulon<sup>c</sup>

<sup>a</sup>*Faculty of Chemistry, University of Wrocław, Joliot-Curie 14, 50-383 Wrocław, Poland*

<sup>b</sup>*Department of Inorganic and Analytical Chemistry, West Pomeranian University of  
Technology, Al. Piastów 42, 71-065 Szczecin, Poland*

<sup>c</sup>*Institute Light Matter (ILM), UMR5306 CNRS-UCB Lyon1, University of Lyon,  
69622 Villeurbanne, France*

A series of micro-crystalline scheelite-type cadmium molybdate with vacancies ( $\square$ ) of chemical formula  $\text{Cd}_{1-3x}\text{RE}_{2x}\square_x\text{MoO}_4$  ( $\text{RE}^{3+}=\text{Nd}^{3+}, \text{Eu}^{3+}, \text{Yb}^{3+}$ ) were synthesized by mean of high-temperature solid state reaction. X-ray diffraction patterns indicate that the samples show only one phase and crystallize in the tetragonal scheelite-type structure (the space group  $I4_1/a.$ , with point symmetry  $S_4$ ), when the concentration of  $\text{RE}^{3+}$  ions with respect to  $\text{Cd}^{2+}$  ions is in the range from 0.05 mol% to 66.67 mol% for  $\text{Eu}^{3+}$  and  $\text{Nd}^{3+}$  ions and from 0.05 mol% to 33.36 mol% for  $\text{Yb}^{3+}$  ions. Substitution of divalent  $\text{Cd}^{2+}$  by trivalent  $\text{RE}^{3+}$  cations leads to the formation of cationic vacancies in the framework due to the charge compensation:  $3\text{Cd}^{2+}\square + 2\text{RE}^{3+} + \square$  vacancy. Vacancy concentration dependence brings some originality to this research program in optical materials. Our objective is to take advantage of the  $\text{RE}^{3+}$  spectroscopic probes to analyze in details the structural properties of the cationic environment in the lattice as complementarity data to XRD diffraction techniques.

Multisite character of  $\text{RE}^{3+}$  sites has been pointed out from the important role played by laser techniques, like site selective spectroscopy and time-resolved spectroscopy using tuneable laser pumping at cryogenic temperature (4K, 77K). Only specific lines of the unique  $\text{Eu}^{3+}$   $^5\text{D}_0 \leftrightarrow ^7\text{F}_0$ ,  $\text{Nd}^{3+}$   $^4\text{I}_{9/2} \rightarrow ^2\text{P}_{1/2}$  and  $\text{Yb}^{3+}$  0-phonon line  $^2\text{F}_{5/2} \leftrightarrow ^2\text{F}_{7/2}$  transitions respectively, and the double  $\text{Nd}^{3+}$   $^4\text{I}_{9/2} \rightarrow ^4\text{F}_{3/2}$  absorption transitions, have been analysed.

$\text{RE}^{3+}$ -doped samples exhibit very intense luminescence, so that could be applied for WLEDs with  $\text{Eu}^{3+}$  ions and for laser materials with  $\text{Nd}^{3+}/\text{Yb}^{3+}$  ions.

[1] M. Guzik, E. Tomaszewicz, Y. Guyot, J. Legendziewicz, G. Boulon, J. Mat. Chem. C, 3 (2015) 4057- 4069.

[2] M. Guzik, E. Tomaszewicz, Y. Guyot, J. Legendziewicz, G. Boulon, J. Lumin. 2015, accepted on February 19. doi.org/10.1016/j.jlumin.2015.02.043.

[3] M. Guzik, E. Tomaszewicz, Y. Guyot, J. Legendziewicz, G. Boulon, J. Mat. Chem. C, submitted on April 18, 2015.

## RARE-EARTH DOPED FLUORIDE LASER CRYSTALS: RECENTLY EXPLORED “EXOTIC” PROPERTIES

Biao Qu<sup>a,b</sup>, Simone Normani<sup>a</sup>, Zhiping Cai<sup>b</sup>, Patrice Camy<sup>a</sup>, Jean-Luis. Doualan<sup>a</sup>, Alain Braud<sup>a</sup>, Richard Moncorgé<sup>a</sup>

<sup>a</sup>*Centre de recherche sur les Ions, les Matériaux et la Photonique (CIMAP)  
UMR 6252 CEA-CNRS-ENSICAEN, Université de Caen, 6 Blvd Maréchal Juin*

<sup>b</sup>*Department of Electronic Engineering, Xiamen University, Xiamen 361005, China  
richard.moncorgé@ensicaen.fr*

Two kinds of recently explored properties will be presented: Pr<sup>3+</sup> broadband laser emission properties of various Pr-doped fluoride crystals and glasses around 900nm and Nd<sup>3+</sup> broadband laser emission and thermo-mechanical properties of Nd-doped CaF<sub>2</sub> and SrF<sub>2</sub> single crystals.

Rather unexpectedly and almost completely ignored in the past literature, it was recently proved that rather efficient and broadband laser emission could be obtained around 900nm in Pr:LiYF<sub>4</sub> as well as in other well-known Pr-doped materials due to a combination of spin-forbidden and spin-allowed thermalized optical transitions. It will be shown that pumping Pr:LiYF<sub>4</sub> with a blue InGaAn laser diode at about 444nm or with an optically pumped semiconductor laser (OPSL) at 479 nm, it was possible to lase around 915nm with laser efficiencies of more than 30% and that continuous laser wavelength tunability could be achieved in the continuous-wave laser regime between about 865 and 935nm, thus over 70nm.

Rather unexpectedly again, it was also recently demonstrated that broadband and ultrashort-pulse laser operation was possible with Nd-doped CaF<sub>2</sub> and SrF<sub>2</sub> single crystals around 1.055μm. Such laser emission, known as completely quenched because of cross-relaxation energy transfers in the singly doped materials, indeed increases spectacularly by co-doping the crystals with non-optically active “buffer” ions like Y<sup>3+</sup> or Lu<sup>3+</sup>. As a matter of fact, broadband laser emission and sub-100fs laser operation could be already demonstrated and large scale high peak power diode-pumped amplifiers, also thanks to favorable thermo-mechanical properties, can be already anticipated.

More details about the spectroscopy, the laser performance and the thermo-mechanical properties of the various systems will be given at the conference.

## THE LUMINESCENCE OF Bi<sup>3+</sup> IN SOLIDS

Alok M. Srivastava

*GE global research, One research circle, Niskayuna, New York 12309*

The interest in the luminescence of ions with ns<sup>2</sup> electronic configuration is driven by the many potential applications in lighting and scintillator technologies [1]. Fundamental explorations pertaining to the luminescence of ns<sup>2</sup> ions in solids can assist technologists in designing new materials where the optical properties can be tuned to satisfy the device requirements.

The evolution of the optical properties of the Bi<sup>3+</sup> ion as a function of host lattice composition is reviewed in terms of new results and data which are available in the archival literature [2]. In particular the Bi<sup>3+</sup> luminescence in materials is discussed. Particular emphasis is placed on identifying emission from isolated Bi<sup>3+</sup> ions, emission from pairs (or clusters) of Bi<sup>3+</sup> ions and photoionized emission. The specific cases which will be considered are the materials with the pyrochlore, perovskite and zircon crystal structures [3-6].

[1] G. Blasse, B. C. Grabmaier, *Luminescent Materials*, Springer-Verlag, Berlin Heidelberg, 1994.

[2] Philippe Boutinaud, *Inor. Chem.* 52 (2013) 6028.

[3] A. M. Srivastava, W. W. Beers, *J. Lumin.* 71 (1990) 285.

[4] A. M. Srivastava, *Mat. Res. Bull.* 37 (2002) 745.

[5] A. M. Srivastava, A. Szarowski, *J. Solid St. Chem.* 146 (1999) 494.

[6] A. M. Srivastava, S. J. Camardello, *Opt. Mat.*, 39 (2015) 130.

## CATHODOLUMINESCENCE IN ELECTRON MICROSCOPY: FROM PHOSPHOR EVALUATION TO SINGLE PARTICLE ANALYSIS

Philippe F. Smet<sup>a,b</sup>, Lisa I.D.J. Martin<sup>a,b</sup>, Jeroen Wattez<sup>a,b,c</sup>, Filip Strubbe<sup>b,c</sup>, Dirk Poelman<sup>a,b</sup>

<sup>a</sup>*Lumilab, Department of Solid State Sciences, Ghent University, Belgium*

<sup>b</sup>*Center for Nano- and Biophotonics (NB-Photonics), Ghent University, Belgium*

<sup>c</sup>*Liquid Crystals and Photonics Group, Ghent University, Belgium*

Impurity doped phosphors often show a close relationship between their luminescent and structural properties. When a phosphor is characterized by a distribution of structural properties (such as local compositional variations, dopant clustering, impurity phases or particle size inhomogeneity), the luminescence can show similar variations. If synthesized phosphors are only evaluated at the macroscopic scale, all contributions are averaged out, which can lead to a broadened emission spectrum, a luminescence decay profile featuring multiple exponential contributions or a peculiar thermal behavior [1,2].

In this presentation we discuss cathodoluminescence (CL) spectroscopy in a scanning electron microscope (SEM) as a tool to study emission characteristics in phosphors at the microscopic scale [1,3]. In SEM-CL simultaneous identification of the morphology, the chemical composition and the spectral distribution can be performed in imaging mode. When using a fast beam blaster, local decay time analysis and spectrally resolved decay time mapping can be performed [1]. A temperature stage allows to evaluate thermal quenching at the sub-micron scale [4].

Correlation of simultaneously obtained structural, compositional and luminescence properties leads to a profound understanding of a phosphor's behavior. It can be used to identify minority phases in phosphors, e.g. the formation of  $\text{EuGa}_2\text{S}_4$  when preparing  $\text{ZnGa}_2\text{S}_4:\text{Eu}$  [3]. The light outcoupling of single phosphor particles can be studied, as well as the occurrence of whispering gallery modes in highly symmetric particles [5].

[1] D. Poelman, P.F. Smet, *Physica B* 439 (2014), 35-40.

[2] K. Takahashi, B. Dierre, YJ Cho, T. Sekiguchi, R.J. Xie, N. Hirosaki, *J. Am. Cer. Soc.* 98 (2015) 1253-1258.

[3] D. den Engelsen, P. Harris, T. Ireland, J. Silver, *ECS J. Sol. Stat. Sci. Tech.* 4 (2015) R1-R9.

[3] J.J. Joos, K. Korthout, S. Nikitenko, D. Poelman, P.F. Smet, *Opt. Mater. Exp.* 3 (2013), 1338-1350.

[4] P.F. Smet, J. Botterman, A.B. Parmentier, D. Poelman, *Opt. Mater.* 35 (2013) 1970-1975.

[5] K. Korthout, P.F. Smet, D. Poelman, *Appl. Phys. Lett.* 94 (2009) 051104.

## **NEAR INFRARED LIGHT MEDIATED DRUG RELEASE, PHOTODYNAMIC THERAPY USING UPCONVERSION NANOPARTICLES**

John A. Capobianco

*Department of Chemistry and Biochemistry, Centre for NanoScience Research Concordia  
University, 7141 Sherbrooke Street West, Montreal, Quebec, Canada  
John.Capobianco@concordia.ca*

Lanthanide doped nanoparticles have the ability to undergo upconversion. Upconversion is a non-linear anti-Stokes process that efficiently converts two or more low-energy excitation photons, which are generally near infrared (NIR) light, into a higher energy photon (e.g., NIR, visible, ultraviolet) through the use of long lifetime and real ladder-like energy levels of trivalent lanthanide ions embedded in an appropriate inorganic host lattice. Thus, these materials are quickly emerging as candidates in novel biological applications. This stems from their unique optical and chemical properties, such as non-blinking, non-photobleaching, absence of autofluorescence, low-toxicity, low photodamage to live cells, and their remarkable ability to penetrate light in tissues. Here, we present the characterization and optical properties of lanthanide-doped fluoride nanoparticles and subsequent strategies to impart biological functionality. We show relevant biological applications of these upconverting nanoparticles as a platform for photodynamic therapy and drug delivery.



## NUCLEATION, AGGREGATION AND GROWTH OF QUANTUM DOTS PREPARED BY SOL-GEL CHEMISTRY

Sandra H. Pulcinelli

*Institute of Chemistry, UNESP, PO Box 355, Araraquara, SP, Brazil, sandrap@iq.unesp.br*

Nanocrystal semiconductor technology has emerged in the early 1980's when Efros and Brus independently observed striking differences of colour for solutions made from the same colloidal species. The origin of this unusual optoelectronic property is the quantum size effect observed when the Bohr exciton size is bigger than the semiconductor nanocrystal size, this is the so-called "quantum dots" (Qdot). In the Qdot the optical band gap and the energy of the emitted light can be tuned by changing the nanocrystal size. A typical semi-conductor presenting this striking property is the zinc oxide, a wide band-gap semiconductor (3.7 eV) with high exciton binding energy (60 meV) which ensures efficient excitonic UV emission at room temperature. In addition, ZnO Qdot is currently attracting great interest as potential labels for biological applications, such as theranostic devices, due to their luminescent properties and low toxicity *in vivo*. In this talk we aim to give experimental evidence of the mechanism involved in the process of ZnO nanoparticles formation and growth. To reach this goal, the structural evolution of zinc species in solution and in condensed phase were examined in deep by *in situ* and simultaneous time resolved monitoring of UV-Vis absorption spectra combined with small angle X-rays scattering (SAXS) and with X-ray absorption fine structure (EXAFS). The formation and growth of ZnO nanoparticle from zinc acetate as well as the effect of doping was followed at 40°C and hydrolysis ratio  $[OH]/[Zn] = 0.5$ . The results of this *in situ* and combined techniques investigation show that the kinetic of formation of colloidal ZnO nanocrystal is a stepped process composed of four main stages: (i) ZnO Qdot nucleation and growth; (ii) growth of compact ZnO Qdot aggregates; (iii) growth of fractal aggregates; (iv) secondary nucleation and fractal aggregate growth. Nucleation and growth of ZnO Qdot occur at the expense of the zinc oxy-acetate leading to a conversion of about 13% of zinc precursors in ZnO, at the early stage of the kinetics. Then, at longer period of time, the reaction of ZnO colloid formation is characterized by an equilibrium state between two species, and an aggregation growth described by the oriented attachment induced by grain-rotation model that favors the subsequent coalescence of ZnO Qdot. At the advanced stage the coarsening of ZnO Qdot presents a kinetic behavior characteristic of the Ostwald ripening process. In fact, complementary experiments done at very well controlled kinetics have shown that during the very first instants of the reaction, the growth is governed by oriented aggregation, a model specifically proposed for crystal growth. This observation leads us to propose this conventional model is more general than previously proposed. In addition, as  $Mg^{2+}$  ions were incorporated into the ZnO wurtzite lattice owing to the very close values of the  $Mg^{2+}$  and  $Zn^{2+}$  ion radii, the growth and final size of ZnO nanocrystals were strongly influenced. The presence of Mg prevented the aggregation of primary nanoparticles, widened the band gap of ZnO Qdot and enhanced their visible luminescence. With increasing proportion of  $Mg^{2+}$  ions, both the absorption and emission spectra experienced a blue shift and the quantum yield increased about 6 times as compared to the pristine ZnO suspension.

This work is supported by CNPq and FAPESP.

## ENERGY TRANSFER IN RARE-EARTH DOPED SYSTEMS

A. Meijerink, T. Senden, D. Yu, F.T. Rabouw

Debye Institute, Utrecht University, P.O. Box 80000, 3508 TA Utrecht, The Netherlands  
a.meijerink@uu.nl

Lanthanides have transformed the world of lighting in the past 40 years. Presently, almost all artificial light sources rely on emission of light by lanthanide ions. In many luminescent materials energy transfer is involved and plays a crucial role in obtaining the desired luminescence characteristics: for example, in the lamp phosphor  $\text{LaPO}_4:\text{Ce},\text{Tb}$  absorption of UV radiation by  $\text{Ce}^{3+}$  is followed by energy transfer to the green emitting  $\text{Tb}^{3+}$  ion. In the well-known upconversion phosphor  $\text{NaYF}_4:\text{Yb},\text{Er}$  energy transfer from two  $\text{Yb}^{3+}$  ions to  $\text{Er}^{3+}$  is involved. The opposite process of downconversion relying on the lanthanide couples ( $\text{Er}^{3+}, \text{Yb}^{3+}$ ), ( $\text{Tb}^{3+}, \text{Yb}^{3+}$ ) and ( $\text{Pr}^{3+}, \text{Yb}^{3+}$ ) involves either two-step energy transfer or cooperative energy transfer. Modelling energy transfer is not trivial but is needed to understand the mechanism and efficiency of spectral conversion processes involving energy transfer.

In this presentation a short historical introduction to modelling energy transfer will be followed by an overview of recent developments, demonstrating the need for modelling using microscopic models based on actual distributions of lanthanide ions taking into account distributions of donor-acceptor distances imposed by the crystal structure of the host material. As an illustrative example, energy transfer from  $\text{Ce}^{3+}$  to  $\text{Yb}^{3+}$  will be discussed. In the literature cooperative energy transfer from  $\text{Ce}^{3+}$  to two  $\text{Yb}^{3+}$  ions has been reported but based on modelling we show that in fact the energy transfer is dominated by single step energy transfer via a metal-to-metal charge transfer state. The second illustration involves energy transfer in nanocrystals. Research on lanthanide doped nanocrystals is booming. Modelling energy transfer in nanocrystals is complicated by the confined geometry but accurate modelling can be realized. Experimental luminescence decay curves of the  $\text{Ce}^{3+}$  emission in  $\text{Ce}^{3+}, \text{Tb}^{3+}$  co-doped  $\text{LaPO}_4$  NCs are reproduced by our model for a wide range of  $\text{Tb}^{3+}$  acceptor concentrations, using only one donor-acceptor interaction parameter (Figure 1). Experiments for energy transfer in nanocrystals surrounded by solvents of different refractive index demonstrate that the absolute energy transfer rate is not affected by the refractive index of the medium surrounding the NC which makes it possible to tune the energy transfer efficiency by embedding the NC in different photonic environments. Finally, an outlook into the future of modelling energy transfer will be given.

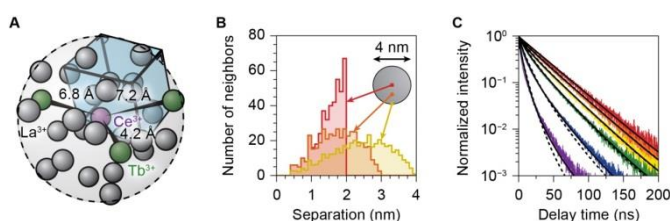


Figure 1 – Modelling of donor emission decay curves for ET in confined geometries **A** Schematic of a doped  $\text{LaPO}_4$  nanocrystal with a  $\text{Ce}^{3+}$  donor (purple) and  $\text{Tb}^{3+}$  acceptors (green). **B** The distribution of distances to nearby sites from a central donor ion, in a 4 nm  $\text{LaPO}_4$  NC with the central ion at different depths. **C** Luminescence decay curves of the  $\text{Ce}^{3+}$  emission for  $\text{Tb}^{3+}$  concentrations ranging from 0% (red) to 40% (purple). Broken lines represent the best fits for a bulk model while the drawn black lines represent the fits for the position dependent distributions in B.

## LUMINESCENT NANOTHERMOMETRY. NANOTHERMOMETERS AND NANOHEATERS GET CLOSER

Luís D. Carlos

*Physics Department and CICECO, Universidade de Aveiro, 3810–193 Aveiro, Portugal*

Nanothermometry has indeed experienced an unprecedented growth over the past five years following, in most examples, the technological trends of sub-micron miniaturization, namely in the temperature mapping of microcircuits and microfluidic devices.<sup>1</sup> There is also a high demand of nanothermometry for biomedical uses, like the development of intracellular thermometers capable of accurate temperature determination in living cells.<sup>2</sup>

Despite promising progresses on the temperature mapping of microfluidic devices and living cells, precision control of fluid temperature by accounting for local temperature gradients, heat propagation and accurate temperature distributions have not yet been satisfactorily addressed. The major obstacle for this has been the unavailability of a thermometer with the following requirements: i) high temperature resolution (ca. 0.1 degree); ii) ratiometric temperature output; iii) high spatial resolution ( $< 1 \times 10^{-6}$  m); iv) functional independency of changes in pH, ionic strength and surrounding biomacromolecules; and v) concentration-independent output.

Moreover, magnetic-, plasmonic- and phonon-induced nanoparticles thermal heating are noninvasive techniques for drug release, remote control of single cell functions, plasmonic devices and hyperthermia therapy. To be effective, local heating requires measuring the nanoheater's local temperature. Single nanoparticles integrating heaters and thermometers are then crucial for this purpose and numerous attempts were reported, namely within the last year.<sup>3-5</sup>

The lecture presents a general revision of the work done at the GFHybrids in Aveiro in the last couple of years on luminescent nanothermometers and in heater/thermometer nanoplatfoms, with particular emphasis on examples comprising lanthanide-based nanoparticles with potential application in cellular thermometry and hyperthermia therapy.

[1] C. D. S. Brites, P. P. Lima, N. J. O. Silva, A. Millán, V. S. Amaral, F. Palacio, L. D. Carlos, *Nanoscale* 4 (2012) 4799–829.

[2] D. Jaque, B. del Rosal, E. M. Rodriguez, L. M. Maestro, P. Haro-Gonzalez, J. G. Solé, *Nanomedicine-UK* 9 (2014) 1047–1062.

[3] M. L. Debasu, D. Ananias, I. Pastoriza-Santos, L. M. Liz-Marzan, J. Rocha, L. D. Carlos, *Adv. Mater.* 25 (2013) 4868–4874.

[4] J. Dong, J. I. Zink, *ACS Nano* 8 (2014) 5199–5207.

[5] Piñol, R.; Brites, C. D.; Bustamante, R.; Martínez, A.; Silva, N. J.; Murillo, J. L.; Cases, R.; Carrey, J.; Estepa, C.; Sosa, C., et al. *ACS Nano* 2015, 9, 3134–42.

## NOVEL RED PERSISTENT PHOSPHORS DEVELOPED BY BAND GAP ENGINEERING

Setsuhisa Tanabe, Jian Xu, Jumpei Ueda

*Graduate School of Human and Environmental Studies, Kyoto University, Kyoto 606-8501m Japan*

Long red persistent phosphors are expected for *in vivo* bio-imaging. The key point to design persistent phosphors is the possibility of tuning the “trap depth” between the bottom of conduction band, CB and the electron trap. If the binding energy of an electron trap is predicted, this strategy to control the trap depth by changing the CB energy level is regarded as “CB engineering”. Recently, we have applied the CB engineering to develop new persistent phosphors in some aluminate/ gallate based garnets (i.e. Ce<sup>3+</sup>- doped YAGG (green) [1] and GAGG (yellow) [2] phosphors), in which the probability of photoionization from the excited Ce<sup>3+</sup>: 5d<sub>1</sub> level to CB with blue illumination can be increased by increasing Ga<sup>3+</sup> substitution for Al<sup>3+</sup>. We have also developed red persistent phosphor (~690 nm) of Cr<sup>3+</sup> doped YAGG, where Cr<sup>3+</sup> ions act both as emission centers and trap centers [3]. The persistent behavior and TL glow peak temperature of these materials can systematically be tuned by changing Ga<sup>3+</sup> content. The persistent radiance (mW/Sr/m<sup>2</sup>) of the optimized composition was higher than that of the ZnGa<sub>2</sub>O<sub>4</sub>:Cr<sup>3+</sup> phosphor, which is used widely for *in vivo* bio-imaging applications [4]. We report a bright deep-red persistent phosphors of Cr<sup>3+</sup>-Eu<sup>3+</sup> codoped Gd<sub>3</sub>Al<sub>5-x</sub>Ga<sub>x</sub>O<sub>12</sub> garnet (GAGG: Cr<sup>3+</sup>-Eu<sup>3+</sup>), in which only Cr<sup>3+</sup> ion shows emission bands centered at 730 nm and Eu<sup>3+</sup> ion acts as an excellent electron trap. The design concept is based on a theoretical assumption and zigzag curves in the Dorenbos theory for garnet compounds [5]. The zigzag curve representing the ground state of divalent lanthanide ions show a minimum bottom at 4f<sup>7</sup> configuration (Eu<sup>2+</sup>). Because of its deep level, GGG (x=5) with the lowest CB level showed the best persistent behavior and longest emission wavelength due to the weakest crystal field strength. The persistent radiance of the GGG:Cr<sup>3+</sup>-Eu<sup>3+</sup> (x = 5) sample at 1 h after ceasing UV light was approximately 25 times higher than that of the Cr<sup>3+</sup> singly doped GGG sample, and is over 6 times higher than the ZnGa<sub>2</sub>O<sub>4</sub>: Cr<sup>3+</sup> red persistent phosphor.

[1] J. Ueda, K. Kuroishi, and S. Tanabe, *Appl. Phys. Lett.* 104, 101904 (2014).

[2] J. Ueda, K. Kuroishi, and S. Tanabe, *Appl. Phys. Express* 7, 062201 (2014).

[3] J. Xu, J. Ueda, Y. Zhuang, B. Viana, and S. Tanabe, *Appl. Phys. Express* 8, 042602 (2015).

[4] A. Bessière, S. Jacquart, et al., *Opt. Express* 19, 10131 (2011).

[5] P. Dorenbos, *J. Lumin.* **134**, 310 (2013).

## DEFECT STATES OF 3d, 4d, AND 5d ELECTRONS OF TRANSITION METALS AND LANTHANIDES IN INORGANIC COMPOUNDS

Pieter Dorenbos<sup>a</sup>, Edith G. Rogers <sup>a</sup>

<sup>a</sup> *Delft University of Technology, Faculty of Applied Science, Department of Radiation Science and Technology(FAME-LMR), 2629 JB Delft, The Netherlands,  
p.dorenbos@tudelft.nl*

Methods and models to establish the location of the 4f levels of divalent and trivalent lanthanides within the band gap of inorganic compounds are nowadays frequently used. The top of the valence band is then chosen as the level of reference. In 2012 the chemical shift model was developed [1]. The positively charged lanthanide is always screened by an equal amount of negative charge at a distance dictated by the size of the lanthanide and how strongly electrons are bonded on the surrounding anions. Chemical shift, which is caused by that screening charge, is then the shift in binding energy of an electron from the free ion value to the value that applies for the lanthanide in a compound. With the model one may establish the vacuum referred binding energy (VRBE) of electrons in lanthanide states.

4f-electron orbitals are well screened from the crystalline environment. This does not apply to d-electrons that have a strong interaction with the surrounding anion ligands. Different d-orbitals have different orientation in space and depending on the shape of the coordinating anion polyhedron strong crystal field splitting of d-states occurs. d-orbitals also overlap with ligand orbitals leading to covalence and correlated ligand electron and d-electron motion which lead to the so called centroid shift. Crystal field splitting and centroid shift can be treated as chemical shift differences.

We started with determining the VRBE of the single 5d-electron in divalent and trivalent lanthanides. Next we collected data on the 3d<sup>1</sup>, 4d<sup>1</sup>, and 5d<sup>1</sup> transition metal elements like Ti<sup>3+</sup>, Nb<sup>4+</sup>, and W<sup>5+</sup> and determined the VRBE for different compounds. The VRBE of nd<sup>1</sup> electrons shows about ± 1 eV compound to compound whereas that of 4f electrons only ±0.2 eV. The much larger variation is attributed to the much larger variation in crystal field splitting of nd-levels. The average nd<sup>1</sup> VRBE shows clear trends with changing charge of the TM or Ln (2+, 3+, 4+, or 5+) and with changing type of d-orbital (3d, 4d, or 5d). Trends that follow the same trends as of the free TM and Ln ions [2].

With knowledge on 4f<sup>n</sup> and nd<sup>1</sup> VRBEs in compounds and knowledge on the VRBE of conduction band and valence band electrons one may understand and better predict luminescence, carrier storage and preferred valence of Ln and TM defects in compounds. Various examples from experiment will be presented. First ideas and data on level locations of TM with more than one d-electron like in Cr<sup>3+</sup> will be presented.

[1] P. Dorenbos, P. Dorenbos, Phys. Rev. B 85 (2012) 165107.

[2] E.G. Rogers, P. Dorenbos, ECS Journal of Sol. State Sci. and Techn. 3 (2014) R173.

## LuPO<sub>4</sub>:Eu SINTERED CERAMICS - AN OLD PHOSPHOR WITH NEW LUMINESCENT FUNCTIONALITIES

Justyna Zeler<sup>a</sup>, Joanna Cybińska<sup>a,b</sup>, Eugeniusz Zych<sup>a</sup>

<sup>a</sup>*Faculty of Chemistry, University of Wrocław*

*14 F. Joliot-Curie Street, Wrocław, Poland; Justyna.zeler@chem.uni.wroc.pl;*

*Joanna.cybinska@chem.uni.wroc.pl; Eugeniusz.zych@chem.uni.wroc.pl*

<sup>b</sup>*Wrocław Research Centre EIT+, 147/149 Stabłowicka Street, Wrocław, Poland*

LuPO<sub>4</sub> activated with lanthanide ions have been reported as efficient phosphors, also upon ionizing radiation [1]. Since this composition melts incongruently, large single crystals cannot be obtained by the classic Czochralski method [2]. Therefore, we decided to experiment with sintering of LuPO<sub>4</sub>:Eu to produce its high-density compact bodies.

We soon noted that the LuPO<sub>4</sub>:Eu sintered ceramics showed significant red-color afterglow after exposure to X-rays. Its efficiency was found to depend on the Eu concentration, but was observed for Eu content spanning at least the range of 0.1-15 mol%. The courses of thermoluminescence glow curves were also Eu concentration dependent to some extent, though they all peaked around 200 °C (Fig. 1). In general, with increasing Eu concentration the glow curves were broader with more TL components reflecting more types of traps.

These results, which we shall discuss in detail at the presentation, are surprising as recent publications of the Dorenbos group on YPO<sub>4</sub>, a structural analogue of LuPO<sub>4</sub>, seemed to conclude that energy storage in these phosphates can occur when *two* specific lanthanides are doped into the host [3]. While in [3] a TL peak around 190 °C (close to our 200 °C) was also seen for Ce-activated YPO<sub>4</sub> it had much different characteristics compared to what is seen in our LuPO<sub>4</sub>:Eu. We shall show that singly activated LuPO<sub>4</sub>:Eu processed in specific conditions turns into an efficient storage/persistent phosphor, without a need of co-doping.

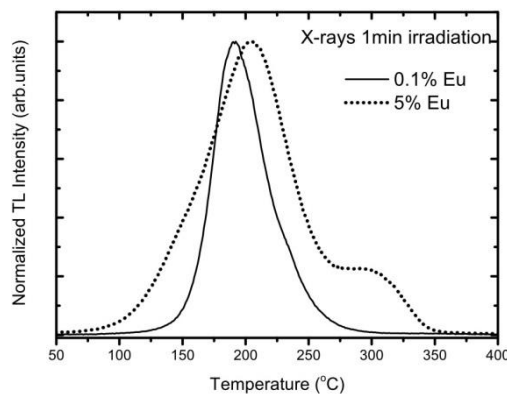


Figure 1. The glow curves of LuPO<sub>4</sub>:Eu sintered ceramics with two different contents of the activator.

[1] L. Boatner, L. Keefer, J. M. Farmer, D. Wisniewski, A. J. Wojtowicz, SPIE - The International Society of Optical Engineering 5540 (2004) 73–87.

[2] J. S. Neal, L. Boatner, M. Spurrier, P. Szupryczynski, C. L. Melcher, Proc. of SPIE 6319 (2006) 631907–1.

[3] A. Dobrowolska, A. J. J. Bos and P. Dorenbos, J. Phys. D: Appl. Phys. 47 (2014) 335301. doi:10.1088/0022-3727/47/33/335301.

## UPCONVERSION LUMINESCENCE PROPERTIES OF SINGLE PCONVERSION $\text{LiY/LuF}_4:\text{Yb}^{3+}/\text{Er}^{3+}$ MICROCRYSTAL

Hairong Zheng, Wei Gao, Qingyan Han

*School of Physics and Information Technology, Shaanxi Normal University, No. 620, West Chang'an Avenue, Chang'an District, Xi'an, China, hrzheng@snnu.edu.cn*

$\text{Yb}^{3+}/\text{Er}^{3+}$  codoped tetragonal  $\text{LiY/LuF}_4$  octahedral microcrystals are synthesized by a facile hydrothermal method. The crystal structure and morphology of the samples are characterized by XRD and SEM. The strong upconversion emission of single  $\text{LiY/LuF}_4:\text{Yb}^{3+}/\text{Er}^{3+}$  microcrystal is observed under 980 nm laser excitation[1]. It is found that upconversion emission intensity of single  $\text{LiLuF}_4:\text{Yb}^{3+}/\text{Er}^{3+}$  microcrystal is stronger than  $\text{LiYF}_4:\text{Yb}^{3+}/\text{Er}^{3+}$  microcrystals when replacing  $\text{Y}^{3+}$  with  $\text{Lu}^{3+}$  in the  $\text{LiYF}_4$  host lattice. Meanwhile, the upconversion emission of different parts of the single particle is also investigated in detail. The current study suggests that the luminescence observation with single microparticle can effectively avoid the influence of environment and neighbor particles, which is important for investigating the luminescence properties of micro-or nano-crystals and for extending their application.

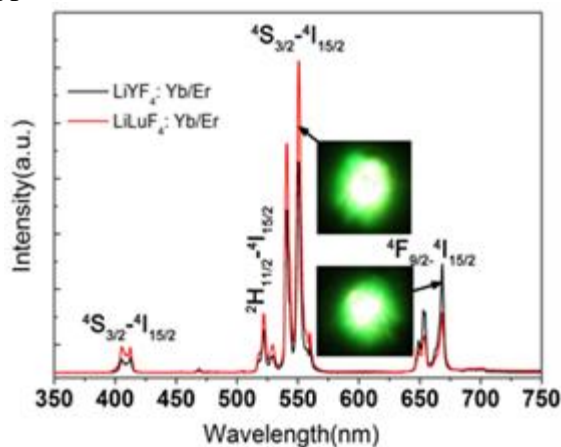


Figure 1. UC emission spectra emissions of single  $\text{LiY/LuF}_4:\text{Yb}^{3+}/\text{Er}^{3+}$  microparticle under 980 nm excitation.

[1] X. P. Chen, W. J. Zhang, Q. Y. Zhang. *Physica B*. 406 (2011) 1248–1252.

**BISMUTH OXIDE AS HOST FOR RARE-EARTH DOPANTS IN UCNPs**

Michele Back, Enrico Trave, Pietro Riello

*Dept. of Molecular Sciences and Nanosystems, Ca' Foscari University of Venice, Via Torino 155/b, 30170 Mestre, VE, Italy, michele.back@unive.it*

In the last decade, the uniqueness of the upconversion phenomenon, together with the progressive nanotechnology advent, has led to a relevant interest from the scientific community for the development of new nanoparticles for upconversion (UCNPs) with promising potentialities for applications in different scientific and technological fields [1].

Bismuth oxide ( $\text{Bi}_2\text{O}_3$ ) is a semiconductor with band gap energy in the blue-green spectral region ( $E_g \sim 2.4$  eV). By incorporating suitable dopants, gap engineering was achieved resulting in a controlled blue-shift of the  $\text{Bi}_2\text{O}_3$  absorption edge. Moreover, the existence of a wide range of  $\text{Bi}_2\text{O}_3$  crystalline polymorphs [2] can be a further parameter for controlling the optical response of the system. Therefore, these features make  $\text{Bi}_2\text{O}_3$  appealing as host for luminescent rare-earth ions, since it is possible to modulate the chromaticity of the generated radiation directly acting on both crystalline and electronic structure of the matrix.

Aiming at this, different types of trivalent ions ( $\text{Y}^{3+}$ , firstly) were incorporated in sol-gel Pechini synthesized  $\text{Bi}_2\text{O}_3$  nanoparticles, together with  $\text{Er}^{3+}$  as an optical probe to account for the matrix influence on the activation of both fluorescence and non-linear optical processes, such as upconversion (UC). Indeed, Er ions have different absorption lines in the near-IR that may give rise to excited state absorption (ESA) mechanisms, with conversion of IR photons into visible luminescence radiation.

Next step consisted in realizing  $\text{Bi}_2\text{O}_3$  based UCNPs embedding pairs of lanthanide ions  $\text{Yb}^{3+}$ - $\text{Ln}^{3+}$  ( $\text{Ln}^{3+} = \text{Er}^{3+}, \text{Ho}^{3+}, \text{Tm}^{3+}$ ), in order to study the UC mechanisms and to identify the appropriate strategies for the realization of materials with high luminescence yield. Particular care was dedicated to the research of the optimized procedure for the realization of selective emitting UCNPs, extremely appealing for multicolor upconversion imaging [3].

[1] J. Zhou, Q. Liu, W. Feng, Y. Sun, F. Li, Chem. Rev. 115 (2015) 395-465.

[2] N. M. Sammes, G. A. Tompsett, N. Nafe, F. Aldinger, J. Eur. Ceram. Soc. 19 (1999) 1801-1826.

[3] G. Chen, H. Qiu, P. N. Prasad, X. Chen, Chem. Rev. 114 (2014) 5161-5214.



## ENCAPSULATION OF UP-CONVERTING NaYF<sub>4</sub> NANOCRYSTALS IN MULTIFUNCTIONAL POLYMERIC NANOCONTAINERS

Dominika Wawrzyńczyk<sup>a</sup>, Urszula Bazylińska<sup>b</sup>, Bartłomiej Cichy<sup>c</sup>, Artur Bednarkiewicz<sup>c,d</sup>, Marek Samoć<sup>a</sup>, Kazimiera A. Wilk<sup>b</sup>

<sup>a</sup>*Advanced Materials Engineering and Modelling Group, Faculty of Chemistry, Wrocław University of Technology, Wyb. Wyspiańskiego 27, 50-370 Wrocław, Poland*

<sup>b</sup>*Department of Organic and Pharmaceutical Technology, Faculty of Chemistry, Wrocław University of Technology, Wybrzeże Wyspiańskiego 27, 50-370 Wrocław, Poland*

<sup>c</sup>*Institute of Low Temperature and Structure Research, PAS, Okólna 2, 50-422 Wrocław, Poland*

<sup>d</sup>*Wrocław Research Centre EIT+, Stabłowicka 147, 54-066 Wrocław, Poland*

Rapid development of wet chemistry synthetic routes in the last decade gave the possibility to obtain colloidal, lanthanide-doped nanocrystals (NCs) with precisely designed optical and magnetic properties [1]. The versatility of the synthesized and characterized nanomaterials opened new perspectives for real life applications, with great attention paid to the use of up-converting NaYF<sub>4</sub> NCs as optical agents for bioimaging and nanomedicine [2]. However, as the wet chemistry synthesis techniques usually yield hydrophobic NaYF<sub>4</sub> NCs, the efficient and straightforward surface functionalization remains the main challenge [3]. Well known NCs surface hydrophilization techniques are often time consuming, complicated and require further steps for conjugation of NCs with different functional components such as therapeutic agents, e.g. porphyrins or cytostatic drugs. The use of up-converting NaYF<sub>4</sub> NCs as markers for fluorescence imaging is additionally well established, and only “smart” theranostic agents, which combine both functions of nano-engineered therapeutic and diagnostic tools, can further broaden the application of those NCs in biophotonics and nanomedicine.

With this in mind, we have designed three types of nanocontainers for efficient encapsulation of up-converting NaYF<sub>4</sub> NCs. Polymeric nanocapsules were obtained by layer-by-layer coating of silicone core with polyelectrolyte shells, which allowed for nanocontainers engineering on the nano-level: the structure and surface of nanocarriers was intentionally designed for specific applications, including functionalization with sugar-based polyelectrolytes or polyethylene glycol. As the polymeric nanocapsules acted as the targeting factor, the active cargo composed of either the Tm<sup>3+</sup> and Yb<sup>3+</sup> co-doped NaYF<sub>4</sub> up-converting NCs, or mixed NaYF<sub>4</sub>:Tm<sup>3+</sup>,Yb<sup>3+</sup> NCs and Verteporphyrin<sup>®</sup> molecules was designed for biodetection and therapeutic applications, including photodynamic cancer treatments. Upon 980 nm laser diode excitation, the encapsulated, water soluble NaYF<sub>4</sub>:Tm<sup>3+</sup>,Yb<sup>3+</sup> NCs showed bright emission in the blue and near-infrared (NIR) region of light, due to the <sup>1</sup>G<sub>4</sub>→<sup>3</sup>H<sub>6</sub> and <sup>3</sup>H<sub>4</sub>→<sup>3</sup>H<sub>6</sub> transitions in Tm<sup>3+</sup> ions, respectively. The latter transition (800 nm) was used for NIR to NIR cancer and healthy cells fluorescence bioimaging, while the light emitted at 480 nm could be absorbed by the co-encapsulated molecules of Verteporphyrin<sup>®</sup>, and led to reactive oxygen species generation. The obtained nanostructures exhibited long term colloidal stability, high loading capacity, enhanced biocompatibility and better internalization by tumor cells. The proposed solution allowed for omitting the cumbersome functionalization of individual NCs surfaces, and allowed for theranostic application of up-converting NaYF<sub>4</sub> NCs.

**Acknowledgements:** This work was financed by the National Science Center (Poland) under Grant No. 2012/05/B/ST4/00095.

[1] G. Wang, Q. Peng, Y. Li, *Acc. Chem. Res.* 44 (2011) 322–332.

[2] A. Gnach, T. Lipiński, A. Bednarkiewicz, J. Rybka, J. A. Capobianco, *Chem. Soc. Rev.* 44 (2015) 1561–1584.

[3] A. Gnach, A. Bednarkiewicz, *Nano Today*, 7 (2012) 532–563.

## **LiY<sub>0.3</sub>Lu<sub>0.7</sub>F<sub>4</sub>: Ce<sup>3+</sup>, Pr<sup>3+</sup> MIXED CRYSTAL AS A PERSPECTIVE UP-CONVERSIONALLY PUMPED UV ACTIVE MEDIUM**

Viktoria Gorieva, Vadim Semashko, Stella Korableva, Mikhail Marisov, Vitaly Pavlov  
*Institute of Physics, Kazan Federal University, 18 Kremlevskaya st, Kazan, Russia,*  
*ekorre\_v@mail.ru, ua4pcy@mail.ru, safkorstella@mail.ru, m.a.marisov@gmail.com,*  
*vitaly.v.pavlov@gmail.com*

Currently tunable solid-state optical quantum generators of UV range are most easily implemented on interconfigurational  $4f^{n-1}5d - 4f^n$  transitions of rare-earth ions in wide-bandgap dielectric crystals. In this case the pumping of the laser is usually carried out by UV harmonics of visible and infrared radiation generated by of commercially available lasers, or powerful UV radiation of excimer lasers. However, UV pumping radiation induces in solid-state active elements various photodynamic processes (PDP), which cause degradation of the optical properties of active media. One of the ways to avoid or significantly reduce harmful manifestations of PDP is to use up-conversion pumping [1]. Finding ways to realize such up-conversion pumping is a topic problem in the view of future implementation of effective solid-state UV-active media with the use of semiconductor lasers as a pumping source and compact solid-state quantum electronics devices of UV range in general.

Here we investigate an opportunity of effective population of states of 5d-configuration of Ce<sup>3+</sup> ions in LiY<sub>0.3</sub>Lu<sub>0.7</sub>F<sub>4</sub> (LYLF) crystals by stepwise <sup>3</sup>H<sub>4</sub>-4f5d up-conversion excitation of states of 4f5d-configuration of Pr<sup>3+</sup> ions, followed by the transfer of excitation energy from Pr<sup>3+</sup> to Ce<sup>3+</sup> ions.

We determine the real concentrations of Pr<sup>3+</sup> and Ce<sup>3+</sup> ions in LYLF crystals. Such parameters as excited 4f5d state photoionization cross-section of Pr<sup>3+</sup> ions, ground state cross-section of Ce<sup>3+</sup> ions at 266 nm wavelengths and energy transfer coefficients of energy transfer from Pr<sup>3+</sup> to Ce<sup>3+</sup> ions were estimated. The results of pump-probe experiments on 5d-4f transitions of Ce<sup>3+</sup> ions in LYLF crystals are presented. Due to non-optimal pumping conditions just small-signal gain was observed. The optimal parameters for getting maximal gain (about 1,5) on 5d-4f transitions of Ce<sup>3+</sup> ions were determined by mathematical modeling.

Obtained results of pump-probe experiments and results of mathematical modeling demonstrate good prospects of using crystal LiY<sub>0.3</sub>Lu<sub>0.7</sub>F<sub>4</sub>:Ce<sup>3+</sup>, Pr<sup>3+</sup> as an active medium of solid-state laser with up-conversion pumping.

This work was funded by the subsidy of the Russian Government (agreement # 02.A03.21.0002) to support the Program of Competitive Growth of Kazan Federal University among World's Leading Academic Centers, the subsidy allocated to Kazan Federal University for the state assignment in the sphere of scientific activities and Russian Foundation for Basic Research grand 15-02-05309.

[1] V. V. Semashko, M. F. Joubert, E. Descroix, et.al. Proc. of SPIE. 4061 (2000) 306–316.

## UP-CONVERSION LUMINESCENCE, RAMAN AND THERMAL STABILITY OF BaTiO<sub>3</sub>:Er<sup>3+</sup>

Mauricio Vega<sup>a</sup>, I.R. Martín<sup>b</sup>, Sandra Fuentes<sup>c</sup>, Jaime Llanos<sup>d</sup>

<sup>a</sup>*Dept. of Chemistry, Universidad de Chile, Las Palmeras 3425, Santiago, Chile, mvega02@ucn.cl*

<sup>b</sup>*Departamento de Física Fundamental, Experimental, Electrónica y Sistemas, Universidad de La Laguna, 38206 La Laguna, Tenerife, Spain, imartin@ull.edu.es*

<sup>c</sup>*Dept. of Pharm. Sciences, Universidad Católica del Norte, Avda. Angamos 0610, Antofagasta, Chile, sfuentes@ucn.cl*

<sup>d</sup>*Dept. of Chemistry, Universidad Católica del Norte, Avda. Angamos 0610, Antofagasta, Chile, jllanos@ucn.cl*

One of the most important challenge for physics and chemists of materials is to reach in a single phase interesting physical properties like as ferromagnetic ordering or luminescent properties. In this sense, special interest has been focused in compounds exhibiting perovskite-like structure with general formula ABO<sub>3</sub> (A=Ba, B=Ti) [1,2]. The incorporation of rare-earth cations (Er<sup>3+</sup>, Yb<sup>3+</sup>) in this type of materials is an interesting field of research, in order to obtain up-conversion phosphors for potential application in photovoltaic solar cells [3,4].

In this work, we report on the synthesis, Raman spectroscopy and up-conversion properties of BaTiO<sub>3</sub> doped with Er<sup>3+</sup>, and thermal stability at high temperature. To verify the purity of the phases, PXRD were collected, the experimental powder pattern were in perfect agreement with those registered in ICSD database [5]. The Raman spectra show the four characteristic bands of BaTiO<sub>3</sub>, the bands at 260 and 520 cm<sup>-1</sup> can be assigned to the cubic phase of the BaTiO<sub>3</sub>, whereas the bands at 305 and 720 cm<sup>-1</sup> corresponding to the tetragonal phase of the titanate. The effect of the Er<sup>3+</sup> dopant concentration on the Raman spectra is show in the variation of the band at 305 cm<sup>-1</sup>.

The emission spectrum of BaTiO<sub>3</sub>:Er<sup>3+</sup> at a wavelength of 1480 nm shows three different emission peaks, corresponding to the transitions <sup>4</sup>S<sub>3/2</sub> → <sup>4</sup>I<sub>15/2</sub> (548 nm, green emission); <sup>4</sup>F<sub>9/2</sub> → <sup>4</sup>I<sub>15/2</sub> (660 nm, red emission), and the IR emission at 980 nm, corresponding to the transition <sup>4</sup>I<sub>11/2</sub> → <sup>4</sup>I<sub>15/7</sub>.

Finally, the simultaneous thermal analysis (TG/DSC) of the most efficient phosphor BaTiO<sub>3</sub>:Er<sup>3+</sup> 5% at., performed up to 873K, shows that during the all process the mass changed by only 5 micrograms demonstrating the excellent long-term stability of the as prepared phase.

[1] S.K.Jo, J.S. Park, Y.H. Han, J. Alloys and Comp. 501 (2010) 259

[2] X. Cheng, Y. Li, F. Kong, L. Li, Q. Sun, F. Wang, J. Alloys and Comp. 541 (2012) 505

[3] H.X. Zhang, C.H. Kam, Y. Zhou, X.Q. Han, S. Buddhudu, Y. L. Lam, Opt. Mater. 15 (2000) 47

[4] S. Fuentes, N. Barraza, E. Veloso, R. Villarroel, J. Llanos, J. Alloys and Compd. 569 (2013) 52

[5] ICSD: The inorganic crystal structure database, FIZ, Karlsruhe, Release 2014/1

Acknowledgment: The authors acknowledge Conicyt-Chile for financial support (Anillo Grant ACT 1204).. J.LI and I.R.M. acknowledge Fondecyt (Grant 1130248) for international cooperation.

## UPCONVERSION LUMINESCENCE IN Ho<sup>3+</sup>-DOPED FLUORIDE MATERIALS UNDER EXCITATION OF <sup>5</sup>I<sub>7</sub> AND <sup>5</sup>I<sub>5</sub> LEVELS

Andrey A. Lyapin<sup>a</sup>, Pavel P. Fedorov<sup>b</sup>, Polina A. Ryabochkina<sup>a</sup>

<sup>a</sup>*N.P. Ogarev Mordovian State University, 68 Bolshevistskaya. Str., Saransk, Russia, andrei\_lyapin@mail.ru*

<sup>b</sup>*Prokhorov General Physics Institute, Russian Academy of Sciences, 38 Vavilova Str., Moscow, Russia, ppf@lst.gpi.ru*

Study of mechanisms responsible for upconversion luminescence of rare-earth ions is useful for developing IR visualizer, up conversion lasers and IR Quantum Counter [1-2]. Early we have shown that CaF<sub>2</sub>:Ho crystals and ceramics are possible candidates for visualizer of two-micron laser radiation [3]. The purpose of the present paper is to study the mechanisms of near-infrared to visible upconversion luminescence in CaF<sub>2</sub>:Ho and BaF<sub>2</sub>:Ho crystals under excitation of <sup>5</sup>I<sub>7</sub> and <sup>5</sup>I<sub>5</sub> levels by the two-micron laser radiation.

Fig. 1 shows luminescence spectra of Ho<sup>3+</sup> ions in the visible region upon excitation of <sup>5</sup>I<sub>7</sub> level by two-micron laser. To identify mechanisms of upconversion luminescence we recorded luminescence rise and decay from <sup>5</sup>I<sub>7</sub>, <sup>5</sup>I<sub>6</sub>, <sup>5</sup>F<sub>5</sub>, <sup>5</sup>S<sub>2</sub>(<sup>5</sup>F<sub>4</sub>) and <sup>5</sup>F<sub>3</sub> levels of Ho<sup>3+</sup> ions upon excitation of <sup>5</sup>I<sub>7</sub> level. Also dependences of the intensity of upconversion luminescence on the excitation intensity of LiYF<sub>4</sub>:Tm laser were investigated. The energy efficiency of the conversion of two-micron laser radiation to radiation in the red spectral range by the CaF<sub>2</sub>:Ho and BaF<sub>2</sub>:Ho crystals were estimated. Using experiment results, channels of populating of <sup>5</sup>F<sub>3</sub>, <sup>5</sup>F<sub>5</sub>, <sup>5</sup>S<sub>2</sub>(<sup>5</sup>F<sub>4</sub>), <sup>5</sup>I<sub>4</sub>, <sup>5</sup>I<sub>5</sub>, <sup>5</sup>I<sub>6</sub> and <sup>5</sup>I<sub>7</sub> levels under excitation of <sup>5</sup>I<sub>7</sub> level were suggested.

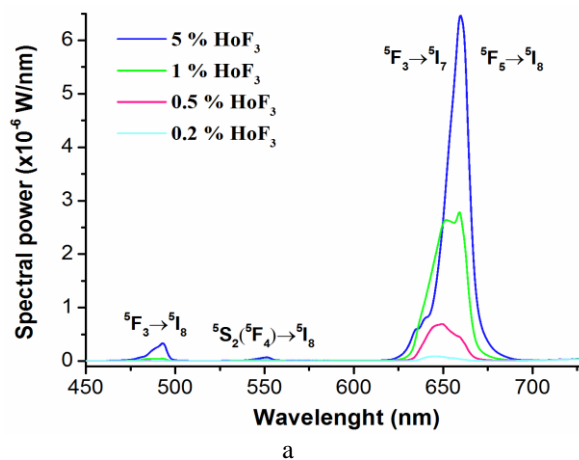


Fig. 1. The spectral power of the upconversion luminescence of Ho<sup>3+</sup> ions doped CaF<sub>2</sub> in the range from 450 nm to 730 nm.

Also mechanisms responsible for upconversion luminescence of Ho<sup>3+</sup> ions in CaF<sub>2</sub>:Ho and BaF<sub>2</sub>:Ho crystals under excitation of <sup>5</sup>I<sub>5</sub> level were studied.

This work were supported by the The Ministry of Education and Science of the Russian Federation State Order for Research (Project No. 3.384.2014/K and Project No. 07080210059611).

[1] N. Bloembergen, Phys. Rev. Letters 2 (1959) 84-85.

[2] S.R. Bullock, B.R. Reddy, P. Venkateswarlu, J. Opt. Soc. Am. B. 14 (1997) 553-559.

[3] A.A. Lyapin, P.A. Ryabochkina, S.N. Ushakov, P.P. Fedorov, Quantum Electron 44 (2014) 602-650.

## UP-CONVERTIONAL LUMINESCENCE IN GERMANATE GLASSES

Ksenya S. Moskaleva, Vladimir A. Aseev, Nickolay V. Nikonorov, Yu.K. Fedorov, Ya.A. Nekrasova, I.M. Sevastianova, A.O. Larin

*ITMO University, 4 Birzhevaya liniya, Saint-Petersburg, Russia, ks.moskaleva@gmail.com*

The luminescent properties of germanate glasses doped with ytterbium and erbium ions have been studied. The luminescence spectra of glasses in the visible and near-IR ranges under their pumping at a wavelength of 975 nm have been measured. Changes in the luminescence spectra of glasses depending on the different additives into the glass composition have been examined.

Germanate glasses are promising materials for photonic applications, due to their high-frequency threshold of vibration spectrum is sufficiently lower than those of silicate or phosphate glasses [1, 2]. Also germanate glasses have high refractive index ( $\sim 2$ ), which leads to increasing of rate of radiative transitions [3]. Both of these facts result in increasing of quantum yield of luminescence for transitions, which are usually quenched in silicate and phosphate glasses [4]. Erbium, in turn, is one of the most commonly used ions for conversion from IR to visible range.

In the work, we investigated samples of the following composition:

$\text{Na}_2\text{O-GeO}_2\text{-Yb}_2\text{O}_3\text{-La}_2\text{O}_3$ . The concentration of erbium was constant, being 0.25 mol%. The glass compositions have been varied by introducing on the following additives:

$\text{SiO}_2$ ,  $\text{TiO}_2$ ,  $\text{Al}_2\text{O}_3$ ,  $\text{Nb}_2\text{O}_5$ ,  $\text{PbO}$ ,  $\text{MgO}$ ,  $\text{BaO}$ ,  $\text{B}_2\text{O}_3$  (5 % mol), or  $\text{P}_2\text{O}_5$  (6 % mol).

Thereby the object of the present work is investigation of effect of different additives in glass composition on the spectral and luminescent properties and especially on up-convertional luminescence of erbium ions in the germanate glasses.

[1] R. Xu, Y. Tian, M. Wang, L. Hu, J. Zhang, *Opt. Mater.* 33 (2011) 299–302.

[2] W.A. Pisarski, J. Pisarska, D. Dorosz, J. Dorosz, *Mater. Chem. Phys.* 148 (2014) 485–489.

[3] S. Tanabe, *Proc. Int. Soc. Opt. Eng.* 4282 (2001) 85–92.

[4] M. Naftaly, S. Shen, A. Jha  $\text{Tm}^{3+}$ -doped tellurite glass for a broadband amplifier at 1.47  $\mu\text{m}$ . *Appl. Opt.* 39 (2000) 4979–4984.

## OPTICAL PROPERTIES OF $K_2SiF_6:Mn^{4+}$ AT AMBIENT AND HIGH HYDROSTATIC PRESSURES

Sebastian Mahlik<sup>a</sup>, Agata Lazarowska<sup>a</sup>, Marek Grinberg<sup>a</sup>, Chun-Che Lin<sup>b</sup>, Ru-Shi Liub,<sup>c</sup>  
<sup>a</sup>*Institute of Experimental Physics, University of Gdansk, Wita Stwosza 57, 80-952 Gdansk, Poland*

*E-mail: s.mahlik@ug.edu.pl*

<sup>b</sup>*Department of Chemistry, National Taiwan University, Taipei 106, Taiwan*

<sup>c</sup>*Department of Mechanical Engineering and Graduate Institute of Manufacturing Technology, National Taipei University of Technology, Taipei 106, Taiwan*

In this work effects of pressure and temperature on the luminescence of the  $K_2SiF_6:Mn^{4+}$  system have been presented. It was found that at ambient pressure luminescence spectrum of  $Mn^{4+}$  consists of several lines attributed to phonon repetitions of the  ${}^2E_g \rightarrow {}^4A_{2g}$  transition, and does not contained the zero phonon line (ZPL). At pressure above 0.9 GPa additional line at about 624 nm occurs, which can be attributed to the ZPL of the  ${}^2E_g \rightarrow {}^4A_{2g}$  transition in the  $Mn^{4+}$  ions. This change in the emission spectrum was accompanied by shortening of the luminescence decay time. Further increasing pressure up to 220 kbar does not cause a significant change in the spectrum only the red shift of all lines. Upon releasing pressure all observed lines are going back to their previous positions. However, ZPL remains visible below 9 kbar and was observed even at ambient pressure. This means that the changing of the structure persists to ambient conditions. Taking into account XRD and Raman spectra at ambient pressure before and after compression-decompression (no significant change was observed in the spectra) we have attributed these changes to pressure-induced local structure changing of  $K_2SiF_6:Mn^{4+}$ .

## **NONLINEAR OPTICAL PROPERTIES OF PbOGeO<sub>2</sub> GLASS CODOPED BY Yb<sup>3+</sup>/Tm<sup>3+</sup> AND INCORPORATED Si NANOPARTICLES**

Izabela Fuks-Janczarek<sup>a</sup>, Rafał Miedziński<sup>b</sup>, Luciana R. P. Kassab<sup>c</sup>

<sup>a</sup>*Institute of Physics, J. Dlugosz University, Al. Armii Krajowej 13/15, Czestochowa,  
Poland, i.fuks@ajd.czyst.pl*

<sup>b</sup>*Institute of Physics, J. Dlugosz University, Al. Armii Krajowej 13/15, Czestochowa, Poland,  
r.miedzinski@ajd.czyst.pl*

<sup>c</sup>*Laboratório de Tecnologia em Materiais Fotônicos e Optoeletrônicos, Faculdade de  
Tecnologia de São Paulo, CEETEPS, 01124-060 São Paulo, SP, Brazil,  
kassablm@osite.com.br*

Nowadays, it has become an essential task to characterize the nonlinear optical response of new materials, in order to identify suitable candidates for ultrafast processing in all-optical devices. One of the most widely used techniques for this purpose is the Z-scan, which consists on measuring the nonlinear refractive and absorptive responses of a material by scanning the sample along the optical path of a convergent Gaussian beam. We will analyze the nonlinear response of new glasses. The two-photon absorption (TPA) coefficient  $\beta$  and nonlinear refractive index  $n_2$  are obtained, while the maximum pulse intensity was 30 (GW/cm<sup>2</sup>). The concentration of Si nanoparticles was 0.05%, 0.50%, 1.00% and 2.00%. The highest TPA coefficient was obtained for 1.00% Si concentration, the smallest ones for 0.50% Si concentration.

## FAR-INFRARED SPECTROSCOPY OF MULTIFERROIC $R\text{Fe}_3(\text{BO}_3)_4$ ( $R=\text{Gd},\text{Tb}$ ): PHASE TRANSITIONS AND COUPLING BETWEEN LATTICE PHONONS AND CRYSTAL-FIELD EXCITATIONS

Sergei A. Klimin

*Institute of Spectroscopy RAS, 5, Fizicheskaya, Troitsk, Russia, klimin@isan.troitsk.ru*

Multiferroic materials are known to demonstrate strong interactions between different degrees of freedom, e.g., magnetic, charge, or lattice. Such a behavior is interesting both for fundamental investigations to understand mechanisms of interactions, and for practice taking into account new possibilities for sensing one parameter via another, e.g., magnetization via electricity. The family of rare-earth (RE) iron borates  $R\text{Fe}_3(\text{BO}_3)_4$  ( $R = \text{RE}$ ) is recognized to be a model system with multiferroic features [1,2]. Studying of phonon subsystem is a good tool to demonstrate the interplay between the crystal lattice and other subsystems, e.g., magnetic sublattice. For instance, a previous study of Raman-active phonons [3] allowed us to get information about spin-lattice interaction, as well as about phase transitions, namely, structural and magnetic ones ( $T_S=156$  K,  $T_N=38$  K for  $\text{GdFe}_3(\text{BO}_3)_4$  [3,4] and  $T_S=199$  K,  $T_N=40$  K for  $\text{TbFe}_3(\text{BO}_3)_4$ ). Information about a behavior of infrared (IR) phonons is scarce (see, e.g., [5]). In this work, we present a comprehensive study of infrared phonons in  $\text{GdFe}_3(\text{BO}_3)_4$  and  $\text{TbFe}_3(\text{BO}_3)_4$ , discuss phase transitions, and demonstrate a strong spin-lattice interaction in both compounds and appearance of electron-phonon coupled mode in  $\text{TbFe}_3(\text{BO}_3)_4$  (Fig. 1).

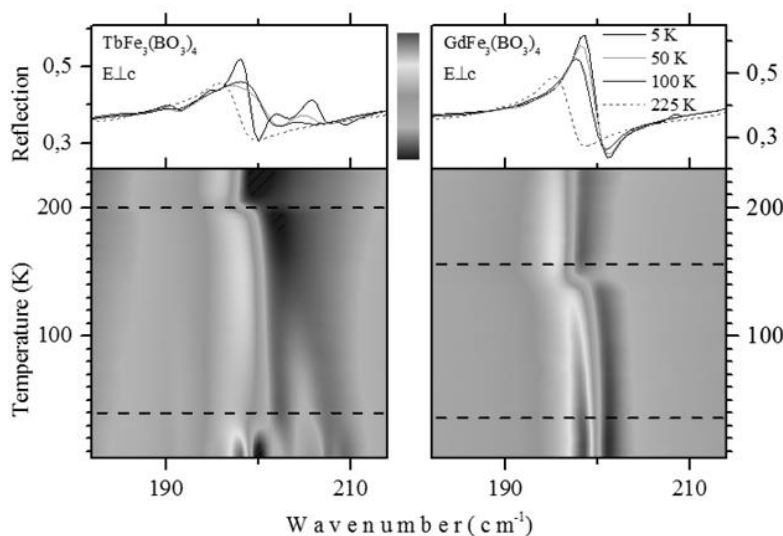


Fig. 1.  $E_g$  phonon at  $195\text{ cm}^{-1}$  in  $\text{GdFe}_3(\text{BO}_3)_4$  and  $\text{TbFe}_3(\text{BO}_3)_4$ , and formation of electron-phonon coupled mode in  $\text{TbFe}_3(\text{BO}_3)_4$ .

Support of the Russian Science Foundation (Grant No. 14-12-01033) is acknowledged.

- [1] A.K. Zvezdin, et al., JETP Lett., 81 (2005) 272-277.
- [2] F. Yen, et al., Phys. Rev. B 73 (2006) 054435 (pp. 1-6).
- [3] D. Fausti et al., Phys. Rev. B 74 (2006) 024403 (pp. 1-12).
- [4] S. Klimin, et al., Acta Cryst. B 61 (2005) 481-485.
- [5] K.N. Boldyrev, et al., Phys. Lett. A 376 (2012) 2562-2564.



## CHARACTERIZATION OF MAGNETO-OPTIC HEXAFERRITES BY TERAHERTZ TIME DOMAIN SPECTROSCOPY

Martin Mičica<sup>a</sup>, Kamil Postava<sup>a</sup>, Mathias Vanwolleghem<sup>b</sup>, Jean-François Lampin<sup>b</sup>,  
Jaromír Pištora<sup>a</sup>

<sup>a</sup>*Nanotechnology Centre and Department of Physics, VŠB-Technical University of Ostrava,  
17. listopadu 15, 708 33 Ostrava – Poruba, Czech Republic, martin.micica@vsb.cz*

<sup>b</sup>*Institut d'Electronique, Microelectronique et Nanotechnologie, CNRS UMR 8520  
Avenue Poincaré BP 60069, 59652 Villeneuve d'Ascq CEDEX, France,  
mathias.vanwolleghem@univ-lille1.fr*

Terahertz (THz) radiation consists of the electromagnetic waves with frequency between 0.1 and 10 THz. This band was referred as terahertz gap because of the lack of suitable sources and detectors. Nowadays with development of new THz sources new materials active in this region and also new methods that will be able to reliably characterize properties of these materials in THz band are required.

Terahertz time domain spectroscopy (THz-TDS) has been proved in the last years as reliable method for THz material characterization. THz-TDS measures actual waveform of the electric field in time, from which we are able to obtain not only the intensity but also the phase information.

Hexaferrites are partially transparent to the THz radiation and have magneto-optical properties in this spectral range, which can be useful for design of nonreciprocal THz devices for THz waveguiding and isolating applications.

In this paper we present results from measurement of the optical properties by THz-TDS of hexaferrite samples in the spectral range 0.06 – 3 THz (2 – 100 cm<sup>-1</sup>). Used samples were single crystals of SrFe<sub>12</sub>O<sub>19</sub> and BaFe<sub>12</sub>O<sub>19</sub>. Results show high absorptions in the lowest part of the measured spectra around 0.06 THz (2 cm<sup>-1</sup>) caused by resonance in magnetic permeability [1], very high absorptions at 0.6 THz (20 cm<sup>-1</sup>) for BaFe<sub>12</sub>O<sub>19</sub> and at 1.2 THz (40 cm<sup>-1</sup>) for SrFe<sub>12</sub>O<sub>19</sub>, which leaves partially transparent band between this frequencies for both samples.

[1] K. Korolev, L. Subramanian, M. Afsar, J. Appl. Phys. 99 (2006)

## **APPLICATION OF MULTI-WAY ANALYSIS FOR DECOMPOSITION OF LUMINESCENCE SPECTRA OF PHOSPHOR MIXTURES**

Lea Lenhardt, Ivana Zeković, Miroslav Dramićanin

*University of Belgrade, Vinča Institute of Nuclear Sciences, P.O. Box 522, Belgrade, 11001, Serbia, lea@vinca.rs*

One of the main challenges in a characterization of mixtures of rare earth based phosphors is decomposition of luminescence spectra into contribution from individual components present in the mixture. Parallel factor analysis (PARAFAC) [1] is the method frequently used for decomposition of multi-way data. Mixtures of europium(III) doped  $Gd_2O_3$ ,  $Gd_2Ti_2O_7$  and  $GdVO_4$  powders were measured using time-resolved luminescence spectroscopy with the emission range from 570 to 650 nm and the time delays varying between 0 and 10 ms. PARAFAC was used to detect the presence and the relative concentrations of each single component in the powder mixture samples. By modeling measured time-resolved spectra it was also possible to extract emission spectra and emission decay profiles of individual phosphors. Calibration of the obtained model was carried out using known concentrations of single phosphors present in the samples which were used for the building of the model. The model was cross-validated with unknown samples and showed 0.1% accuracy and the prediction error  $\leq 0.034\%$ . Based on given results we can conclude that PARAFAC method combined with time-resolved spectroscopy could be promising tool for characterization of multi-component phosphor materials.

[1] R. Bro, Chemometr. Intell. Lab. 38 (1997) 149-171.

**INTRA- AND INTER-CONFIGURATIONAL LUMINESCENCE  
SPECTROSCOPY OF Pr<sup>3+</sup> - DOPED YTTRIUM ORTHOPHOSPHATES  
YPO<sub>4</sub> NANOPHOSPHORS SYNTHESIZED BY SOL GEL METHOD**

L. Guerbous<sup>1</sup> and B. Kahoudji<sup>1,2</sup>,

<sup>1</sup>*Laser Department/ Nuclear Research Centre of Algiers (CRNA), 02, Boulevard Frantz  
Fanon, B.P. 399, Algiers (16000), Algeria, Fax: +(213) 21 434280,*

*Correspondence author : L. Guerbous E-mail: guerbous@yahoo.fr*

<sup>2</sup>*Faculté des sciences Exactes, Département de Physique, Université de Béjaia, 06000, Algeria*

In the last years there was an intense research devoted with the synthesis of the orthophosphates doped by the trivalent rare earth ions. Among them, YPO<sub>4</sub> matrix doped by Pr<sup>3+</sup> ions because which presents a good physical and chemical properties and that is why it considered as good candidate for the manufacture of the scintillators and phosphors. In this work, Pr<sup>3+</sup>- doped YPO<sub>4</sub> nanophosphors have been prepared by the sol gel method under different synthesis conditions, such as Pr<sup>3+</sup> content, pH values and annealing temperatures. The room temperature interconfigurational ( $4f^n \leftrightarrow f^{n-1}5d$ ) and intraconfigurational ( $4f^n \leftrightarrow 4f^n$ ) emission-excitation transitions spectra are measured and investigated. It is found that under UV excitation (230 nm), all the samples present two bands fluorescence emission spectra attributed to the ( $f^{n-1}5d \rightarrow {}^3H_6$ ,  $f^{n-1}5d \rightarrow {}^2F_4$ ) and ( $f^{n-1}5d \rightarrow {}^3P_j$ ,  $I_6$ ). Under the same excitation wavelength, they present an intense phosphoresce emission spectra located at 590 nm attributed to the  ${}^1D_2 \rightarrow {}^3H_4$  transition. Also, exciting at 449 nm wavelength they present emission at 590 nm attributed also to the  ${}^1D_2 \rightarrow {}^3H_4$ . In addition, under UV excitation (230nm), the photon cascade emission phenomena (PCE), attributed to the ( $f^{n-1}5d \rightarrow {}^1D_2 \rightarrow {}^3H_4$ ) is observed. The time-resolved photoluminescence has been studied and discussed and it has been found that it depend on the excitation wavelength.

## THE NEW MATERIALS BASED ON DOPED BY CU ZNS DEPOSITED INTO POROUS ANODIC ALUMINA FOR ELECTROLUMINESCENT LIGHT EMITTING DEVICES

Rishat G. Valeev<sup>a</sup>, Andrey I.Chukavin<sup>a</sup>, Artemii N. Beltiukov<sup>a</sup>, Dmitri I. Petukhov<sup>a,b</sup>, Vladimir M. Vetoshkin<sup>a</sup>, Alexander L. Trigub<sup>a,c</sup>

<sup>a</sup>*Physical-Technical Institute of UB RAS, 132 Kirova str., Izhevsk, Russia, rishatvaleev@mail.ru*

<sup>b</sup>*Dept. of Materials Sciences, Lomonosov's State University, 1 Leniskie Gory, Moscow, Russia, di.petukhov@gmail.com*

<sup>c</sup>*NSC "Kurchatov's Institute", 1 Akademika Kurchatova pl., Moscow, Russia, alexander.trigub@gmail.com*

One of the first and most effective materials for electroluminescent light emitters is ZnS doped by different elements (Cu, Mn, Tb, Cl, etc.). For example, there unique light emitting properties of ZnS doped by Cu are caused by the fact that each phosphorus grain can be represented as heterojunctions of n(ZnS:Cu)-p(Cu<sub>2</sub>SZn)-n(ZnS:Cu) with effective emission of luminescence. Electroluminescent emitters with powder and thin film phosphors are widely used in different applications, such as electroluminescent panels, displays and others. However, there have mediocre characteristics of light intensity in comparison to light emitting diodes. The best way to increasing of light emission is formation of large number of nanosized individual light sources. The coherent addition of light from single emitters should lead to increasing of total photoemission of device.

In this work we have proposed to use ZnS:Cu nanostructures embedded into porous anodic alumina (AAO) matrix as the phosphorus layer of electroluminescent light-emitting panels (LEP). In this case a single nanostructure synthesized in the pore is the dot-type light emitter. Filling the pores has performed by the method of thermal deposition of ZnS and Cu<sub>2</sub>S powders mixture. A modeling of deposition process by thermodynamical calculations was also performed that was allows to establish the conditions for the maximal filling of pores. A depth profile of chemical composition has been studied by XPS. It is necessary to show the stoichiometry of phosphor in the depth of matrix pores and to obtain the maximum depth of phosphor penetration into pores. EXAFS and XANES studies were allowed to determine chemical bonds parameters and to describe principles of light emission.

Electroluminescence spectra were recorded under the AC signal with the amplitude 220 Volt and frequency 50 Hz. In the spectrum a maximum with wavelength of 550 nm is observed.

## PERSISTENT NANOPHOSPHORS FOR BIOIMAGING

Morgane Pellerin<sup>a, b</sup>, Corinne Chaneac<sup>a</sup>, Bruno Viana<sup>b</sup>

<sup>a</sup>*Sorbonne Universités, UPMC Univ Paris 06, CNRS, Collège de France, Laboratoire de Chimie de la Matière Condensée de Paris, 11 place Marcelin Berthelot, 75005 Paris, France.*  
*morgane.pellerin@etu.upmc.fr, corinne.chaneac@upmc.fr*

<sup>b</sup>*PSL Research University, Chimie ParisTech – CNRS, Institut de Recherche de Chimie Paris, 11 Rue Pierre et Marie Curie, 75005 Paris, France, bruno.viana@chimie-paristech.fr*

*In vivo* optical imaging allows structural and functional imaging (early diagnosis of tumours, following of the cells' biodistribution *in vivo* for instance). However two main limitations exist: the light is strongly absorbed by the tissues outside the therapeutic window (between 600 and 1200nm) and the tissue autofluorescence hides the probe's signal. Recently, to overcome these limitations a new class of persistent luminescence nanoparticles (PLNPs) has been developed.<sup>[1]</sup> These nanoparticles present a bright near-infrared persistent luminescence after UV excitation.

Herein, small size zinc gallate nanoparticles doped with chromium ( $\text{ZnGa}_2\text{O}_4:\text{Cr}^{3+}$ ) are synthesized by soft chemistry using microwave heating in aqueous medium. Microwave heating offers a reduction of the reaction time (30min) in comparison to traditional hydrothermal synthesis. These very small size nanophosphors (around 9nm) present interesting long lasting persistent luminescence after annealing at 1000°C and they can be excited both under UV and under LED excitation. The nanoparticles keep their small size as they are coated with a silica layer which can then be removed by a chemical leaching treatment with  $\text{NH}_5\text{F}_2$ .

Bismuth can also be added, as a co-dopant, to the zinc gallate oxide nanoparticles doped with chromium.<sup>[2]</sup> The incorporation of bismuth allows the improvement of the persistent luminescence properties of the nanomaterials without any size change (Figure 1).

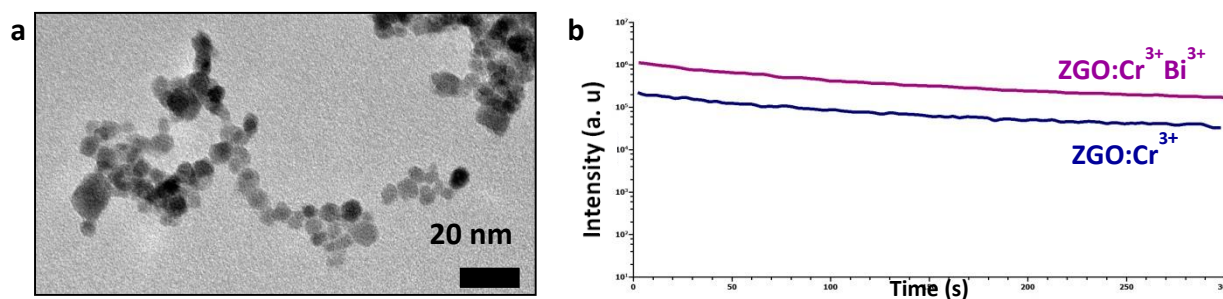


Figure 1: a. TEM picture of  $\text{ZnGa}_2\text{O}_4:\text{Cr}^{3+}$ ,  $\text{Bi}^{3+}$  nanoparticles after annealing and after removal of the silica layer. b. Persistent luminescence decay after 2 min ultraviolet excitation

[1] Le Masne de Chermont Q., Chanéac C., Seguin J., Pellé F., Maîtrejean S., Jolivet J.-P., Scherman D. PNAS, 104 (22) (2007), 9266-9271

[2] Zhuang, Y., Ueda J., Tanabe S. Applied Physics Express, 6(5) (2013), 052602

## SPECTRAL FEATURES OF HIGH-FIELD ELECTROLUMINESCENCE IN AlN FILAMENTARY NANOCRYSTALS

Ilya A. Weinstein, Alexander S. Vokhmintsev, Dmitry V. Chaikin, Yuri .D. Afonin  
*Ural Federal University, NANOTECH Centre,  
Ekaterinburg, Mira str., 19, Russia, 620002, i.a.weinstein@urfu.ru*

Currently significant attention is given to filamentary nanocrystals or nanowhiskers based on various III-V semiconductors because of possible use for fabrication of short wavelength light-emitting nanodiodes, high efficiency nanodetectors, chemical and biological nanosensors, etc. In particular AlN nanowhiskers can be applied for new emission sources in the ultraviolet and visible ranges due to wide bandgap (6.2 eV) of the material [1]. So analysis and optimization of luminescent characteristics of one-dimensional AlN nanostructures are extremely important task. Recently we have investigated the photoluminescence (PL) processes in AlN nanowhiskers by comparison with analogous properties of bulk single crystals [2]. The objective of this work is to study spectral characteristics of high-field electroluminescence (EL) in AlN nanowhiskers, synthesized by the original technology.

The AlN filamentary nanocrystals under investigation have been grown by simultaneous treatment of liquid aluminum in an aluminum chloride and nitrogen vapor environment, when condensed on a polycrystalline aluminum nitride substrate. Morphological characteristics of the samples have been analyzed by a Carl Zeiss Sigma VP scanning electron microscope. The chemical analysis of AlN whiskers has been carried out using an energy dispersive detector, X-max Oxford Instruments. X-ray diffraction measurements and evaluation of structural parameters have been performed with use of XPert Pro MPD PANalytical diffractometer by Rietveld full-profile analysis technique. Spectral features of EL processes in the filamentous samples have been studied at room temperature with a Perkin Elmer LS 55 spectrometer equipped by recently developed EL cell [1]. Design of the cell has provided the luminescent layer of thickness of 20  $\mu\text{m}$  and 10 mm in diameter.

The spectral dependencies for high-field electroluminescence in Al-rich AlN nanowhiskers with average diameter of 70 nm were measured under variation of applied voltage ( $U = 75 - 200$  V) and frequency ( $f = 0.05 - 10.0$  kHz) of the exciting harmonic signal. EL spectra were registered in the range of  $\lambda = 310 - 700$  nm. It was demonstrated that EL emission was mainly observed in the blue region of the spectrum (band with  $E_{\text{max}} = 2.7$  eV and halfwidth of  $\omega = 0.4$  eV) and the shape of experimental curves was independent on U values. Semiquantitative empirical description of the voltage effects on EL intensity in synthesized nanowhiskers was fulfilled. It was suggested using chemical analysis of the samples and review of published data on luminescence in various AlN structures that release of trapped charge carriers took place from levels of  $\text{O}_{\text{N}^-}$  and  $\text{V}_{\text{N}}$ -centers under varying the electric field parameters. It was concluded that investigated AlN nanowhiskers were very promising solid state luminophore for fabrication of modern emitters in blue spectral region.

[1] A.S. Vokhmintsev, I.A. Weinstein, D.V. Chaikin, M.D. Fedorov, Yu.D. Afonin, *Technical Physics Letters*. 41 (2015) 332–335.

[2] A.S. Vokhmintsev, I.A. Weinstein, D.V. Chaikin, D.M. Spiridonov, Yu.D. Afonin, *Functional Materials*. 21 (2014) 21–25.

## SYNTHESES AND MORPHOLOGIES OF GdVO<sub>4</sub> POWDERS: FROM BULK TO NANO

Dragana J. Jovanović<sup>a</sup>, Tamara V. Gavrilović<sup>a</sup>, Sanja Čulubrk<sup>a</sup>, Goran Dražić<sup>b</sup>, Miroslav Dramićanin<sup>a</sup>

<sup>a</sup>*Vinča Institute of Nuclear Sciences, University of Belgrade, P.O. Box 522, 11001 Serbia, draganaj@vinca.rs*

<sup>b</sup>*Department of Nanostructured Materials, Jožef Stefan Institute, Jamova 39, SI-1000 Ljubljana, Slovenia*

Over recent years, synthesis and characterization of luminescent materials based on vanadates (or orthovanadates) of the general formula RVO<sub>4</sub> (R = Sc, Y, La, Gd, or Lu) have attracted much attention due to their superior properties: high luminescence quantum efficiencies and stability of matrices. Herein, we show design and synthesis of doped-GdVO<sub>4</sub> with various types Re<sup>3+</sup> (Eu<sup>3+</sup>, Dy<sup>3+</sup>, Sm<sup>3+</sup>, Ho<sup>3+</sup>/Yb<sup>3+</sup>, Er<sup>3+</sup>/Yb<sup>3+</sup>, Tm<sup>3+</sup>/Yb<sup>3+</sup>) ions. Four different methods have been used for synthesis of Re<sup>3+</sup>-doped GdVO<sub>4</sub> particles (from micro- to nano-sized) and influence of particle size on their structural and optical properties have been systematically studied. A standard *high-temperature solid-state reaction* method [1-5] have been used for preparing large irregular spherical particles with an average diameter in the range of 1-3 μm. For preparing nano-rods (diameter ~ 5 nm, length to 20 nm) a *chemical co-precipitation* [6] have been utilized. The nano-rods are self-organized in bundles, and with increasing of annealing temperature T<sub>a</sub>, the particles grow respectively into single ellipsoidal particles (about 30 nm in size) (at T<sub>a</sub> = 600°C) and long rods (diameter about 1-2 μm, several μm in length) (at T<sub>a</sub> = 1000°C). An *inverse micelle* technique [7] have been used for preparing nanoparticles with diameter about 4 nm. Finally, it is very important to note that in our work the GdVO<sub>4</sub> nanoparticles have been synthesized for the first time in *colloidal form* with well-dispersed nanoparticles of 2 nm. All recorded XRD patterns clearly show the presence of a tetragonal zircon-type GdVO<sub>4</sub> crystal structure corresponding to the reference card. No other phases are detected, indicating that Re<sup>3+</sup> ions have been effectively incorporated into all size GdVO<sub>4</sub> host lattice. We have recorded luminescent emissions of all prepared particles with various Re<sup>3+</sup> ions for both down-conversion and up-conversion.

- [1] T. Gavrilović, M.G. Nikolić, D.J. Jovanović, M.D. Dramićanin, Phys. Scripta T157 (2013) 014055 (4pp).
- [2] M.G. Nikolić, D.J. Jovanović, V. Đorđević, Ž. Antić, R. Krsmanović, M.D. Dramićanin, Phys. Scripta T149 (2012) 014063 (4pp).
- [3] M.G. Nikolić, D.J. Jovanović, M.D. Dramićanin, Appl. Opt. 52 (2013) 1716-1724.
- [4] T.V. Gavrilović, D.J. Jovanović, V.M. Lojpur, V. Đorđević, J. Solid State Chem. 217 (2014) 92–98.
- [5] T.V. Gavrilović, D.J. Jovanović, L.V. Trandafilović, M.D. Dramićanin, Opt. Mater. 45 (2015) 76-81.
- [6] D.J. Jovanović, Ž. Antić, R.M. Krsmanović, M. Mitrić, V. Đorđević, B. Bártová, M.D. Dramićanin, Opt. Mater. 35 (2013) 1797- 1804.
- [7] T.V. Gavrilović, D.J. Jovanović, V. Lojpur, M.D. Dramićanin, Sci. Rep. 4 (2014) 4209.

## SYNTHESIS AND OPTICAL PROPERTIES OF TRANSPARENT GLASS-CERAMICS WITH (Eu,Yb,Y)NbO<sub>4</sub> NANOCRYSTALS

I. Alekseeva<sup>a</sup>, O. Dymshits<sup>a</sup>, M. Tsenter<sup>a</sup>, A. Zhilin<sup>a</sup>, S. Zapalova<sup>a</sup>, P. Loiko<sup>b</sup>, A.M. Malyarevich<sup>b</sup>, N. Skoptsov<sup>b</sup>, K. Yumashev<sup>b</sup>, E. Vilejshikova<sup>b</sup>, K. Bogdanov<sup>d</sup>  
<sup>a</sup>*NITIOM Vavilov State Optical Institute, 36/1, Babushkina ul., St. Petersburg, Russia, vodym1959@gmail.com*

<sup>b</sup>*Center for Optical Materials and Technologies, Belarusian National Technical University, 65/17 Nezavisimosti Ave, Minsk, Belarus, kinetic@tut.by*

<sup>d</sup>*National Research University of Information Technologies, Mechanics and Optics, Kronverkskiy pr., 49, St. Petersburg, Russia, kirw.bog@gmail.com*

Rare-earth orthoniobates are promising luminescent materials. Recently, we prepared transparent glass-ceramics containing RE niobate nanocrystals, (Er,Yb)NbO<sub>4</sub> and YbNbO<sub>4</sub>, by the secondary heat-treatment of lithium aluminosilicate glasses doped with niobium and rare-earth oxides [1].

In the present work, we synthesized transparent glass-ceramics with Eu,Yb:YNbO<sub>4</sub> nanocrystals. Glasses (300 g in weight) were melted in crucibles made of quartz ceramics in a laboratory electric furnace at 1580 °C for 4 hours with stirring and cast onto a steal plate. Annealed glasses were heat-treated in the temperature range from 700 to 1000 °C for 6 - 24 h. The structure of the parent glasses and glass-ceramics was studied with the aid of Raman and optical absorption spectroscopy and X-ray diffraction analysis. Visible luminescence was recorded under direct excitation of Eu<sup>3+</sup> ions by blue GaN diodes, as well as near-IR excitation by InGaAs diodes via the 2Yb<sup>3+</sup>→Eu<sup>3+</sup> cooperative energy-transfer process.

Heat treatments result in volume crystallization of (Eu,Yb,Y)NbO<sub>4</sub> with sizes of 7 – 15 nm. Crystals with tetragonal structure appear at 740 °C, and at 1000 °C the transformation to a monoclinic form begins. The sizes and crystallinity fraction of orthoniobates grow with temperature and time of heat treatment. Rare-earth niobates act as nucleating agent for bulk crystallization of β-quartz solid solutions, the main crystalline phase of glass-ceramics prepared in the temperature range of 800-1000 °C.

The optical properties of glass-ceramics are directly linked to crystallization and the structure of rare-earth niobates; appearance of the monoclinic phase has a pronounced effect on their spectral-luminescent properties. The analysis of the luminescence parameters of glass-ceramics led to conclusion that at heat-treatment at 1000 °C almost all Eu<sup>3+</sup> ions enter the niobate crystals.

### Acknowledgments

This work was partially supported by the RFBR (Grant 13-03-01289 A) and performed under the task of Ministry of Education and Science of Russian Federation (task No. 3.109.2014/K).

[1] O.S Dymshits, I.P. Alekseeva, A.A. Zhilin, M.Ya. Tsenter, P.A. Loiko, N.A.Skoptsov, A.M. Malyarevich, K.V. Yumashev, X. Mateos, A.V. Baranov, J. Lumin. 160 (2015) 337–345.



## RESEARCH THE NATURE OF THE LUMINESCENCE OF COPPER-DOPED QUANTUM DOTS CDSE

T.N. Nurakhmetov, A.K. Kainarbay, D.H. Daurenbekov, K. A. Kuterbekov, <sup>a</sup>P. Kotin, S. Bubenov, O.B. Tleugabylov

*010000, Kazakhstan, Astana, 13 Munaitpasov str., L. N. Gumilyov Eurasian National University, duke.ddx@yandex.kz*

<sup>a</sup>*119991. Russia, Moscow, Faculty of Materials Science, M.V. Lomonosov Moscow State University, kotin-pa@mail.ru*

The interest to the synthesis and studies of quantum dots (QDs) in semiconductors is generated by their energy spectra and practical applications. Of particular interest are luminescent QDs embedded into various transparent matrices. Varying methods of synthesis and sizes of active luminescent QDs, it is possible to obtain matrices with given spectral characteristics. The main role in optical properties of the QDs is played by quantum size effects, therefore it is easy to control spectral characteristics varying sizes of the quantum dots. There is a series of papers describing the use of quantum dots as radiation sources or converters of ultraviolet and visible radiation in the desired spectral range. One of the methods used to increase the efficiency of solar cells is the use of QDs directly in constructions of photoelectric converters (PEC), which can give a significant extension of the total bandgap of solar cells and, thus, extension of the spectral range of the effective electric conversion. These effects are achieved by the down-conversion of the solar radiation spectra in the most efficient area of the photoelectric converter.

We synthesized and studied pure and activated CdSe-Cu nanocrystals. Quantum dots were formed in CdSe nanocrystals by pulsed nucleation at a temperature of 230 K in a highly boiling solvent. We observed the kinetics of the QD appearance in CdSe by fluorescent methods. In the CdSe-Cu we experimentally observed the emission bands with maxima at 570 nm (750 - 780) nm created by emission of an exciton and some surface defects after irradiation by 400-510nm photons. We studied the influence of the concentration of impurities, temperature, and methods of synthesis on the intensity and spectral location of individual emission bands. It was shown experimentally that the maximum intensity of the luminescence of the exciton emission band (570 nm) is observed in the CdSe-Cu quantum dot with impurity concentration of 1%. As the copper concentration increases from 3 to 15%, the intensity of exciton luminescence band decreases several times, and the intensity of the impurity-defect wavelength band at 750-780 nm increases. It is assumed that the long-wave emission bands with maxima at 750-780 nm (in CdSe-Cu) are formed by the radiative decay of excitons near surface defects located near Cu admixture.

We studied the relationship with the influence of copper and introduced rare-earth ions. We also studied the influence of copper and rare earth ion impurities introduced into nanocrystals on the intensity of the long-wavelength bands, which can create additional electron-hole pairs increasing the efficiency of solar cells.

## **CALCULATION OF THE DISPERSION OF ELECTRO-OPTIC AND NONLINEAR COEFFICIENTS**

Marc Fontana, Mustapha Abarkan and Jean-Paul Salvestrini  
*Laboratoire Matériaux Optiques, Photonique et Systèmes,  
Université de Lorraine and CentraleSupélec, 2 rue Edouard Belin, 57070 Metz, France.  
marc.fontana@supelec.fr*

The use of non-linear optical (NLO) crystals in several devices usually requires the knowledge of the wavelength dependence of the electro-optic (EO) or NLO coefficients over a wide range. But generally only some values at a few discrete wavelengths are experimentally available. This is due to the fact that the measurement of these coefficients needs relatively large crystals with good optical quality, different geometrical configurations for phase matching, and therefore is time consuming.

We propose a model able to predict the frequency dependence of NLO coefficients using a simple model based on pioneering studies of non linear polarization [1, 2]. This model provides the dependence of second-harmonic generation (SHG) and EO coefficients [3].

It is shown that within our model the wavelength dependence of the EO or SHG coefficients can be calculated from the dispersion of the linear refractive indices only, without any adjustable parameter. Solely a value of NLO coefficient measured at one wavelength is needed [3].

The validity of our approach is proved on several EO and NLO crystals as KTP, KNbO<sub>3</sub>, SBN, DAST and BBO by the comparison of our results with the experimental data [3].

[1] J. Bloembergen, Non Linear Optics, Benjamin, New York, 1965.

[2] S.K. Kurtz and F.N.H. Robinson, Appl. Phys. Letters, 10 (1967) 62

C.G.B. Garrett and F.N.H. Robinson, Journal of Quantum Electronics, QE 2, (1966). 328

[3] M.D Fontana, M. Abarkan and J.P. Salvestrini, Optical Materials 36 (2014) 764

## Yb:YVO4-BASED CPA SYSTEM

Alexander Rudenkov<sup>a</sup>, Viktor Kisel<sup>a</sup>, Vladimir Matrosov<sup>b</sup>, and Nikolai Kuleshov<sup>a</sup>

<sup>a</sup>. Center for Optical Materials and Technologies, Belarusian National Technical University, 65/17 Nezavisimosti Ave., Minsk, 220013 Belarus, alex\_electron@bk.ru

<sup>b</sup>.Solix Ltd., 77 Partizanski Ave., Minsk, Belarus.

Schematic of the laser system is shown in Fig. 1. As a seed Yb:YVO4 femtosecond laser was used with pulse duration about 120 fs, pulse repetition frequency (PRF) 70 MHz and pulse energy about 4 nJ. The pulses were stretched to the duration of about 150 ps. The BBO-electro optic based pulse-picker unit deliver pulse train with adjustable PRF from 1 to 200 kHz. Amplifier cavity was formed by two concave folding mirrors (M1, M2) and flat back mirror (FM). 4mm-long a-cut Yb(2at.%):YVO4 crystal was used as a gain medium. A novel “off-axes” pump layout was developed for longitudinal pumping of the active element (Fig. 2). As a pump source a multiple single emitter InGaAs fiber coupled laser diode ( $\varnothing 105 \mu\text{m}$ , NA=0.15) with maximum output power of about 28 W was used. The crystal was kept at 15°C by means of thermoelectrical cooling. BBO-based electro-optic Pockels cell together with the thin-film polarizer were used. The last unit of the amplifier system is compressor based on reflective diffraction grating with 1800 grooves per millimeter which is the same as grating in the stretcher. The dependencies of average output power and pulse energy on pulse repetition frequency for Yb:YVO4 regenerative amplifier system (before compression) are presented in Fig.3. The maximum average output power of 5.5 W was obtained at a PRF higher than 100 kHz. The corresponding incident pump power was 26.6 W. Maximum pulse energy was obtained at a PRF up to 15 kHz witch amounted 140 uJ. The amplified spectrum width at half maximum was about 8.5 nm with compressed pulse duration of about 200 fs and central wavelength 1018 nm. The compressor unit has transmission of about 76 %. The output beam profile was Gaussian up to maximum pump powers with M2 factor lower than 1.2 thus indicating negligible thermo-optical aberrations.

In conclusion, Yb:YVO4 based regenerative amplifier with 4.2 W output power and 200 fs pulse duration is demonstrated.

Diode-pumped femtosecond laser sources with pulse repetition rate of tens kHz and pulse energies of tens microjoules are of practical importance for diverse applications. Room-temperature quasi-three-level Yb-doped YVO4 laser crystal has attractive spectroscopic properties which makes it promising material for femtosecond laser systems. They have a reasonable large emission cross section ( $\sim 1.0 \times 10^{-20} \text{ cm}^2$ ), long upper-level lifetime (247  $\mu\text{s}$ ), small quantum defect (<4%), and broadband absorption and emission spectra. Here we present the results of experimental study of Yb<sup>3+</sup>:YVO4 based regenerative amplifier.

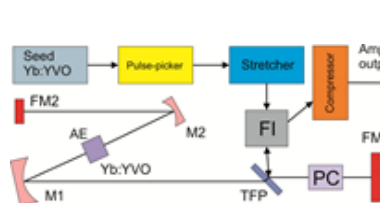


Fig. 1 Schematic of the system

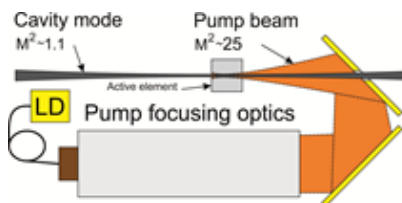


Fig. 2. Pump layout.

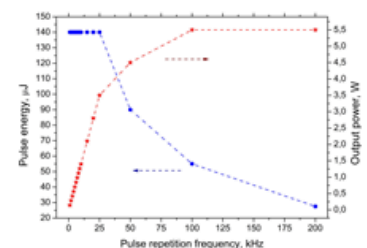


Fig. 3. Average output power and pulse energy versus PRF.

## LARGE TI-DOPED SAPPHIRE SINGLE CRYSTALS GROWN BY THE KYROPOULOS TECHNIQUE FOR PETAWATT POWER LASER APPLICATION.

Guillaume Alombert-Goget<sup>a</sup>, Gourav Sen<sup>b</sup>, Cyril Pezzani<sup>c</sup>, Nicolas Barthalay<sup>c</sup>,  
Thierry Duffar<sup>b</sup>, Kheirreddine Lebbou<sup>a</sup>

<sup>a</sup>*Institut Lumière Matière, Université Lyon 1—UMR 5306 CNRS, 69622 Villeurbanne, France*

<sup>b</sup>*SIMAP-EPM, UMR 5266 CNRS, 38402 Saint Martin d'Hères, France*

<sup>c</sup>*RSA le rubis SA, BP 16, 38560 Jarrie/Grenoble, France*

Ti-sapphire presented a broad luminescence emission bandwidth from 660 to 1180 nm making it one of the principal laser materials to produce ultra-short pulse. In order to generate high-energy pulse and obtain petawatt peak power laser, large diameters Ti-sapphire are requested [1]. Therefore, the improvement of crystal growth methods to produce large diameter and high quality Ti-doped sapphire crystals is a huge challenge for the future development of this technology. Grow large boules was attempted by the HEM [1], Czochralski [2,3], and Kyropoulos processes [4,5] but it is difficult to produce them with the required high optical quality and homogeneous Ti concentration. As the titanium (effective) segregation coefficient differs from unity ( $K = C_s/C_l < 1$ ), both a high proportion of ( $Ti^{3+}$ ) active ions and a good homogeneity in their spatial distribution are key factors to obtain good quality Ti:Al<sub>2</sub>O<sub>3</sub> laser crystals.

In this study, we have succeeded to grow large Ti-doped sapphire crystals by Kyropoulos technique (figure 1a). We presented luminescence (figure 1b), transmittance and wave front measurement characterizations. The obtained results were promising to control the distribution of titanium concentrations to improve the factor of merit (FOM) of the grown crystals.

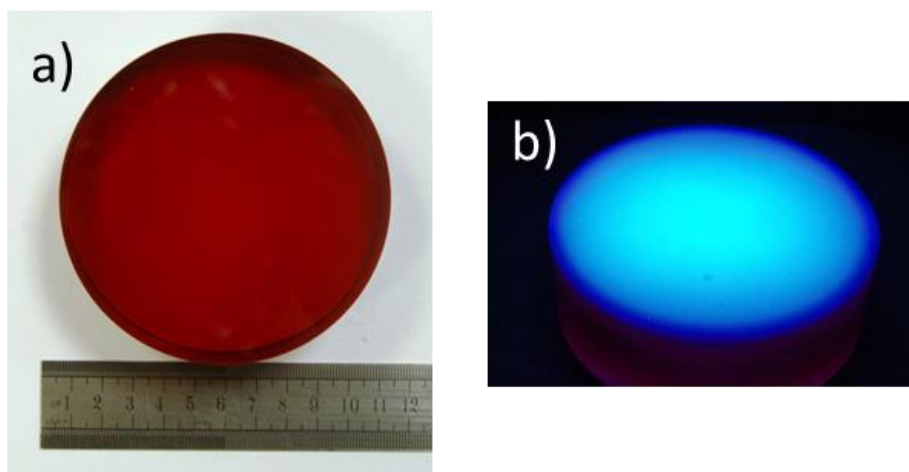


Figure 1: Picture of 10 cm diameter Ti-doped sapphire crystal:  
a) on white light, b) on 256 nm light

- [1] D.B. Joyce, F. Schmid, J. Cryst. Growth 312 (2010) 1138.
- [2] T. Fukuda, Y. Okano, N. Kodama, F. Yamada, S. Hara, D.H. Yoon, Cryst. Res. Technol. 30 (1995) 185.
- [3] H. Li, E. a Ghezal, A. Nehari, G. Alombert-Goget, A. Brenier, K. Lebbou, Opt. Mater. 35 (2013) 1071.
- [4] A. Nehari, A. Brenier, G. Panzer, K. Lebbou, J. Godfroy, S. Labor, H. Legal, G. Chériaux, J.P. Chambaret, T. Duffar, R. Moncorgé, Cryst. growth & design 11 (2011) 445-448 .
- [5] G. Alombert-Goget, K. Lebbou, N. Barthalay, H. Legal, G. Chériaux, Opt. Mater. 36 (2014) 2004–2006.

## **THE EFFECTS OF DIFFRACTION AND SPHERICAL ABERRATION AT THE FEMTOSECOND LASER FABRICATION EXTENDED MICROSTRUCTURE BY DIFFERENT FOCUSING SYSTEMS.**

Daniil Ganin<sup>a,b</sup>, Alexey Z. Obidin<sup>b</sup>, Konstantin Lapshin<sup>b</sup> and Sergey K. Vartapetov<sup>b</sup>  
<sup>a</sup>*National Research Nuclear University “MEPhI”, 31 Kashirskoe Shosse, Moscow, Russian Federation, ganin@pic.troitsk.ru*

<sup>b</sup>*Physical Instrumentation Center of Prokhorov General Physics Institute, 40 kilometr Kaluzhskoe shosse, Troitsk, Moscow, Russian Federation*

In this paper, we present the results of experiments on creation graphitized cylindrical microstructures (filaments) by focusing the single femtosecond (FS) laser pulses in a bulk of transparent polymer - polycarbonate (PC). At the same time, the graphite-like microstructure is covered by shell with a refractive index change that has waveguide properties. The electrical conductivity of the obtained structures is 1 S/m.

There were two types of structural modifications formed in a bulk by single FS pulse. The first type is the destruction in the form of a filament, the length of which depends on the focusing depth and does not exceed 150  $\mu\text{m}$ , that is formed by using a aberration corrected focusing objective. In this case, the interface spherical aberration (interface SA) that occurs at the air-sample interface is the cause of the filament. The second type is a sequence of destruction of graphitized filaments disposed on the optical axis, an overall length greater than 1 mm. Filaments separated by a region with modified refractive index. The reason for the formation of this sequence is diffraction. This type of modification is fabricated by a ordinary spherical lens. The lengths of the filaments do not depend on the focusing depth.

By varying the pulse energy and focusing depth, we have found the optimal parameters to achieve a graphitized filaments with the length more than 2 mm and constant diameter of 2  $\mu\text{m}$  by single femtosecond pulse. Arrays of these cavities can be used to produce diffractive elements.

- [1] Q. Sun, H. Jiang, Y. Liu, Y. Zhou, H. Yang, Gong, J. Opt. A: Pure Appl. Opt. 7 (2005) 655-659.
- [2] A. Couairon, L. Sudrie, M. Franco, B. Prade, A. Mysyrowicz, Phys. Rev. B 71 125435 (2005).
- [3] N. Morita, Y. Shimotsuma, M. Nishi, M. Sakakura, K. Miura, K. Hirao, Appl. Phys. Lett 105 201104 (2014).
- [4] Vartapetov S.K., Khudyakov D.V., Lapshin K.E., Obidin A.Z., Shcherbakov I.A., Quantum Electronics, 42 (3), 262–268, (2012).
- [5] White Y. V. *et al.*, Optics Express 16, 14411 (2008).
- [6] S. Vartapetov, D. Ganin, K. Lapshin, A. Z. Obidin, Proceedings of IV International Conference on Photonics and Information Optics, Russia, Moscow, 276-277, (2015).

## EFFICIENT IN-BAND PUMPED Er:KY(WO<sub>4</sub>)<sub>2</sub> LASER

Konstantin Gorbachenya<sup>a</sup>, Viktor Kisel<sup>a</sup>, Anatol Yasukevich<sup>a</sup>, Anatoly Pavlyuk<sup>b</sup>, Nikolai Kuleshov<sup>a</sup>

<sup>a</sup>*Center for Optical Materials and Technologies, Belarusian National Technical University, 65/17 Nezavisimosti Ave., 220013 Minsk, Belarus, gorby@bntu.by*

<sup>b</sup>*Nikolaev Institute for Inorganic Chemistry, Siberian Branch of Russian Academy of Sciences, 630090 Novosibirsk, Russia*

Erbium lasers emitting near 1.6  $\mu\text{m}$  are attractive for applications in eye-safe laser range finding, ophthalmology, fiber-optic communication systems and optical location. In-band pumping of the  $^4I_{15/2} \rightarrow ^4I_{13/2}$  transition of  $\text{Er}^{3+}$  reduces the quantum defect and thermal load of the crystal and enables to increase strongly laser efficiency in comparison with pumping of Yb,Er-codoped crystals near 1  $\mu\text{m}$ .

Recently we demonstrated laser performance of in-band pumped Er:KY(WO<sub>4</sub>)<sub>2</sub> (KYW) crystal for the first time to the best of our knowledge [1]. However, maximum slope efficiency of 27% in that case was limited by strong up-conversion losses in the crystal due to high erbium concentration. In this report we demonstrate that reducing of the erbium concentration resulted in an increase of the slope efficiency as well as maximum output power of in-band pumped Er:KYW laser.

The laser experiments were performed with a 3-mirror cavity (Fig. 1). The plane-plane  $N_p$ -cut Er(1at.%):KYW crystal with a length of 20 mm antireflection coated for both pump and lasing wavelengths was mounted on the copper heatsink without active cooling. As a pump source a compact diode-pumped Er,Yb:YAB laser at 1522 nm with  $M^2 < 1.2$  was used. The pump beam was focused inside the active element into a spot with the diameter of 60  $\mu\text{m}$ .

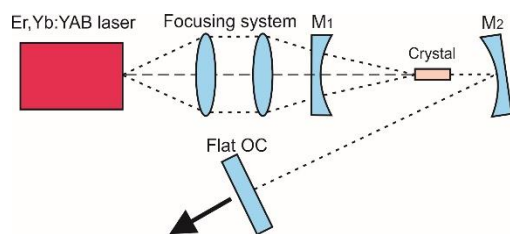


Fig. 1 Setup for laser experiments

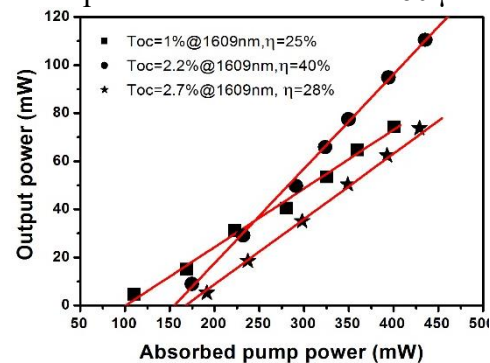


Fig. 2 Input-output characteristics

Input-output characteristics of continuous-wave in-band pumped Er:KYW laser are shown in Fig. 2. The slope efficiency of 25% and output power of 75 mW were realized at 1609 nm for output coupler with transmission of 1%. For 2.2% output coupler slope efficiency increased up to 40% resulting in maximum output power of 110 mW. For the output coupler of 2.7% an output power of 70 mW with slope efficiency of 28% was demonstrated. The spatial profile of the output beam was close to TEM<sub>00</sub> mode with  $M^2 < 1.2$  during all laser experiments. The intensity of green fluorescence measured during lasing was much lower in comparison with that for 2at.% Er-doped crystal at the same pump powers, that confirmed reduction of up-conversion losses in Er(1at.%):KYW.

In conclusion, efficient in-band pumped continuous-wave Er:KYW laser operation with maximal slope efficiency of 40% and output power of 110 mW at 1609 nm was demonstrated for 1at.% Er-doped crystal.

[1] K.N. Gorbachenya, V.E. Kisel, A.S. Yasukevich, A.A. Pavlyuk, and N.V. Kuleshov, *Laser Phys.* **23** (2013) 125005.

## SILVER COMPLEX NANOSTRUCTURES FOR SHG ENHANCEMENT IN RbTiOPO<sub>4</sub>

L. Sánchez-García<sup>1</sup>, P. Molina<sup>1</sup>, M.O. Ramírez<sup>1</sup>, J.J. Carvajal<sup>2</sup>, M. Aguiló<sup>2</sup>, F. Díaz<sup>2</sup>, C. Heras<sup>1</sup>, L.E. Bausá<sup>1</sup>

1. Dept. Física de Materiales and Instituto Nicolas Cabrera, Universidad Autónoma de Madrid, 28049-Madrid, Spain

2. Física i Cristallografia de Materials, Universitat Rovira i Virgili 43007-Tarragona, Spain

Despite the well-known capability of metallic nanostructures to act as optical nanoantennas to confine and enhance electric fields, little work has been devoted to the interaction of localized surface plasmons (LSP) and the  $\chi^{(2)}$  response of dielectric materials as a way to improve SHG processes. Recently, the authors have demonstrated, by means of a simple and low cost photochemical method, the deposition of nearly monodispersive Ag nanocubes on the polar surface of RbTiOPO<sub>4</sub> (RTP), a nonlinear ferroelectric crystal. The quadratic SHG response of the RTP substrate at the blue region was intensified in a factor of 3 due to the presence of LSP provided by the Ag nanocubes [1].

Here we go a step further to show that the SHG of the hybrid metal-RTP system can be enhanced in a factor higher than 50 by means of complex silver nanostructures. Moreover, depending on the type of Ag metallic nanostructure, the plasmonic response can be tuned from the visible to the NIR region, matching either the blue SHG or the NIR fundamental radiation. In this latter case the output SHG intensity can be quadratically boosted, in agreement with the nonlinear character of the frequency conversion process, which needs the participation of two fundamental photons to generate a single blue one.

The results are of technological interest since they open the pathway to new efficient frequency doubling nano-devices in a scalable and low-cost way.

[1] L. Sanchez-Garcia, M.O. Ramirez, P. Molina, F. Gallego-Gómez, L. Mateos, E. Yraola, J.J. Carvajal, M. Aguiló, F. Díaz, C. de las Heras and L.E. Bausá, Adv. Mat. 26 (2014), 6447.

## STABILIZATION OF p-TYPE N-DOPED Zn-DEFICIENT ZnO NANOPARTICLES

A. Renaud<sup>a</sup>, B. Chavillon<sup>a</sup>, X. Rocquefelte<sup>a</sup>, E. Faulques<sup>a</sup>, P. Deniard<sup>a</sup>, M. Boujtita<sup>b</sup>, Y. Pellegrin<sup>b</sup>, E. Blart<sup>b</sup>, F. Odobel<sup>b</sup>, F. Cheviré<sup>c</sup>, F. Tessier<sup>c</sup>, L. Cario<sup>a</sup>, Stephane Jobic<sup>a</sup>

<sup>a</sup>*Institut des Matériaux Jean Rouxel, Université de Nantes, CNRS, 2 rue de la Houssinière, 44322 Nantes cedex 3, France*

<sup>b</sup>*CEISAM, Université de Nantes, CNRS, 2 rue de la Houssinière, 44322 Nantes cedex 03, France*

<sup>c</sup>*Institut des Sciences Chimiques de Rennes, Université de Rennes 1, CNRS, 263 Avenue du General Leclerc, 35042 Rennes cedex, France*

\*stephane.jobic@cnrs-immn.fr

Nowadays zinc oxide is regarded as a very promising material deemed to compete in the near future with GaN for optoelectronic applications. Unfortunately, the durability of p-type ZnO is yet a blockage that singularly slows down the launching of ZnO based devices. In that context, we embarked recently on the synthesis as powdered samples of a p-type zinc oxide material with the wurtzite structure by ammonolysis at low temperature (e.g. 250 °C) of zinc peroxide [1]. The nature of the charge carriers was identified without ambiguity by photo-electrochemistry, complex impedance spectroscopy and transient spectroscopy. P-typeness in ZnO would result from an extraordinary huge amount of Zn vacancies (up to 20%) coupled with the insertion of nitrogen within nanoscale spherical particles. Remarkably, the p-type conductivity remains stable for periods longer than two years and a half in ambient conditions. Here the chemical route to produce p-type ZnO, as well the optical and electrical properties of the synthesized material, will be described. In addition, the origin of the strong Zn deficit, which probably plays a major role in the establishment of p-typeness, will also be addressed [2].

[1] B. Chavillon, L. Cario, A. Renaud, F. Tessier, F. Cheviré, M. Boujtita, Y. Pellegrin, E. Blart, A. Smeigh, L. Hammarström, F. Odobel, S. Jobic, *J. Am. Chem. Soc.* 134 (2012) 464–470.

[2] A. Renaud et al., submitted (2015).



## LASER INDUCED WHITE EMISSION FROM GRAPHENE CERAMICS

Wiesław Strek<sup>a</sup>, Bartłomiej Cichy<sup>a</sup>, Łukasz Radosiński<sup>b</sup>, Paweł Głuchowski<sup>a</sup>,  
 Łukasz Marciniak<sup>a</sup>, Mikołaj Łukaszewicz<sup>a</sup>, Dariusz Hreniak<sup>a</sup>

<sup>a</sup> *Institute of Low Temperature and Structure Research, Polish Academy of Sciences,  
 Wrocław, Poland, W.Strek@int.pan.wroc.pl*

<sup>b</sup> *Wrocław University of Technology, Department of Chemistry, Wrocław, Poland*

The laser induced white (LIW) emission from graphene ceramics was investigated. The intense white broadband emission centred at 650 nm was measured. It was observed that LIW emission from graphene ceramics was characterized by the threshold process that decreased with incident photon energy of laser beam.

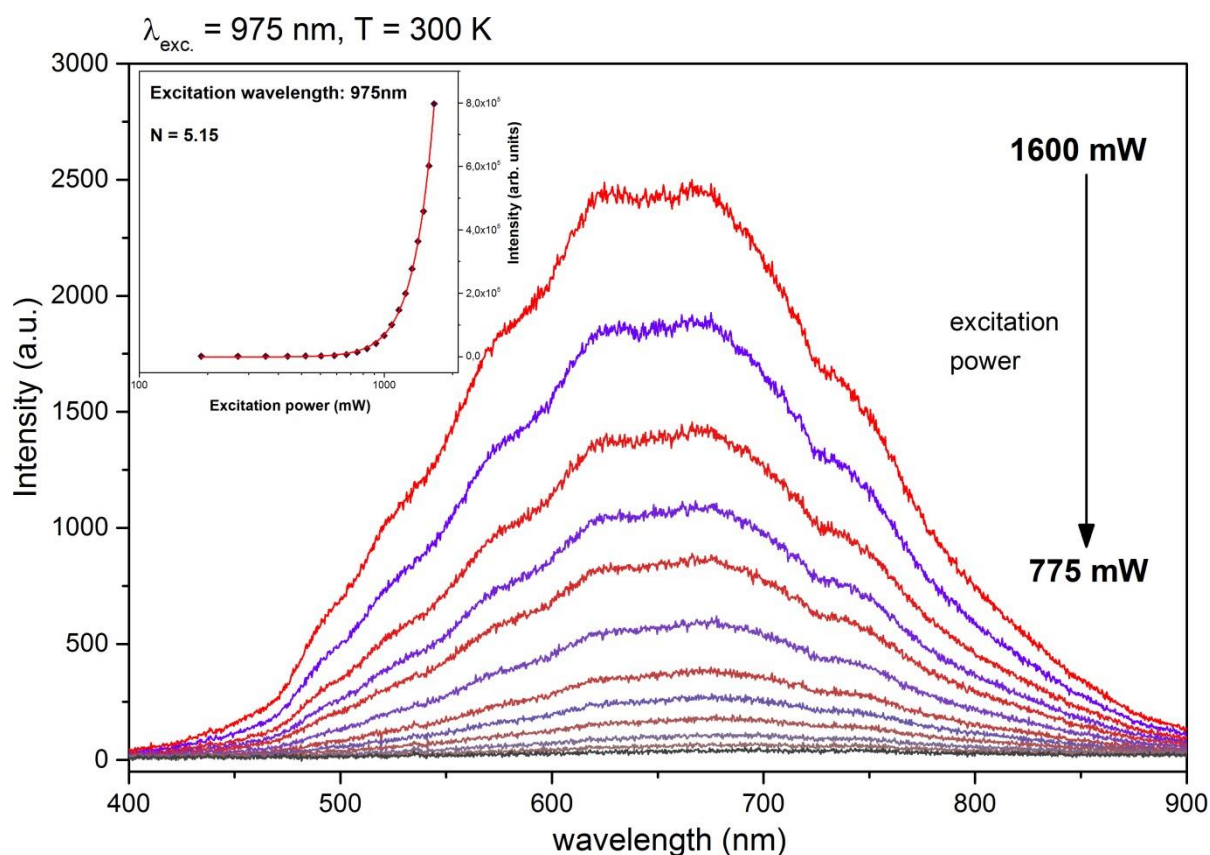


Fig. 1. Power dependence of laser induced white emission from graphene ceramics.

The LIW emission from the graphene ceramic shown in the Fig.1 was excited with  $\lambda_{exc}=975$  nm of CW LD as a function of laser power. An inset shows the power dependence of LIW emission. The value of N represents the order of the multiphoton absorption.

An origin of LIW emission in graphene ceramic was discussed within the concept of photoinduced gap opening associated with the transient domain-like phase  $sp^2 \rightarrow sp^3$  transition [1].

[1] W. Strek, B. Cichy, L. Radosinski, P. Gluchowski, L. Marciniak, M. Lukasiewicz, D. Hreniak, *Light: Science & Applications* (2015) 4, e237; doi:10.1038/lisa.2015.10

## LUMINESCENCE PROPERTIES OF CeO<sub>2</sub> DOPED WITH Ln IONS UNDER OPTICAL AND X-RAY EXCITATION MODES

Daniel Avram<sup>a</sup>, Bogdan Cojocaru<sup>b</sup>, Mihaela Florea<sup>b</sup>, Vasile Parvulescu<sup>b</sup>, Carmen Tiseanu<sup>a</sup>

<sup>a</sup>National Institute for Laser, Plasma and Radiation Physics, P.O.Box MG-36, RO 76900, Bucharest-Magurele, Romania, radu.avram@inflpr.ro, carmen.tiseanu@inflpr.ro

<sup>b</sup>University of Bucharest, Faculty of Chemistry, Department of Organic Chemistry, Biochemistry and Catalysis, 4–12 Regina Elisabeta Bvd., Bucharest, Romania, bogdan.cojocaru@g.unibuc.ro, mihaela.florea@chimie.unibuc.ro, vasile.parvulescu@g.unibuc.ro

Herein we present the latest results of our group on down-conversion, up-conversion and X-ray excited optical luminescence of Ln (Ln: Nd, Sm, Eu, Dy, Ho, Er, Tm, Yb) doped CeO<sub>2</sub> nanoparticles.

The aliovalent substitution of tetravalent Ce with trivalent Ln generates oxygen vacancies (V<sub>O</sub>) which interact with Ln either in the nearest-neighbour (NN) or next nearest neighbour (NNN) modes [1, 2]. We show that, by use of low temperature (10 and 80 K) time-gated site selective emission spectroscopy (spectral resolution of up to 0.05 nm) in the range of 210 to 1600 nm, the fingerprint emission, excitation and decay of Ln - V<sub>O</sub>(NNN) and Ln - V<sub>O</sub>(NN) can be discriminated. Further, we discuss the roles of ceria properties (such as cation local symmetry, low lying O<sup>2-</sup> - Ce<sup>4+</sup> charge-transition, well known ability to dissolve lanthanide oxides followed by charge-compensation induced oxygen vacancies) as well as the ionic radius and concentration of Ln in shaping the emission properties and mechanisms.

Finally, we present some possible applications of Ln doped CeO<sub>2</sub> in optical and X-ray imaging as well as photovoltaics.

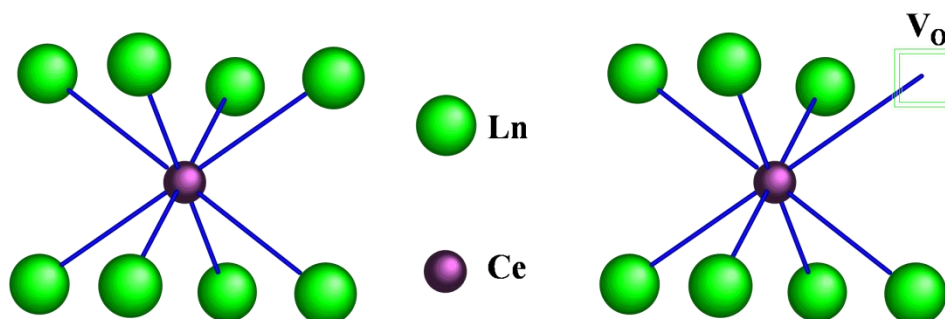


**Figure 1.** Illustration of the two main Ln centers in Ln doped CeO<sub>2</sub>. Both centers substitute for the Ce lattice sites but have distinct oxygen environments with cubic symmetry for Ln - V<sub>O</sub>(NNN) and low symmetry for Ln - V<sub>O</sub>(NN).

### Acknowledgements

D. Avram, B. Cojocaru and C. Tiseanu acknowledge the Romanian National Authority for Scientific Research (CNCS-UEFISCDI), project number PN-II-ID-PCE-2011-3-0534 and ANCS LAPLAS project PN 09.39 for the financial support.

[1] C. Tiseanu, B. Cojocaru, D. Avram, V.I. Parvulescu, A.V. Vela-Gonzalez, M. Sanchez-Dominguez, J. Phys. D: Appl. Phys. 46 (2013) 275302.

[2] D. Avram, C. Rotaru, B. Cojocaru, M. Sanchez-Dominiguez, M. Florea, C. Tiseanu, J. Mater. Sci. 49 (2014) 2117–2126.

## LUMINESCENCE PROPERTIES OF GAS-PHASE MASS-SELECTED LANTHANOID COMPLEXES

Jean-François Greisch<sup>a</sup>, Michael E. Harding<sup>a</sup>, Jiří Chmela<sup>b</sup>, Wim Klopper<sup>a,b</sup>, Detlef Schooss<sup>a,b</sup>,  
Manfred M. Kappes<sup>a,b</sup>

<sup>a</sup> *Institute of Nanotechnology, Karlsruhe Institute of Technology (KIT),  
Hermann-von-Helmholtz-Platz 1, 76344 Eggenstein-Leopoldshafen, Germany*

<sup>b</sup> *Institute of Physical Chemistry, Karlsruhe Institute of Technology (KIT),  
Fritz-Haber-Weg 2, 76131 Karlsruhe, Germany*

Charged lanthanoid-antenna complexes are technologically relevant light convertors and emitters. The present work focuses on the interplay between stoichiometry, symmetry, and overall charge state in affecting luminescence properties. To this aim use is made of mass spectrometric methods allowing the isolation and mass-selection of charged species.[1-2] Two techniques, in particular, are combined: gas-phase-ion laser-induced luminescence and ion mobility spectroscopy. The gas-phase energy level splittings, in particular related to the Stark levels, and the excited state lifetimes of mono- and multinuclear lanthanoid (e.g. europium) complexes are investigated in relation to their environment. The observed shifts and splittings are rationalized in terms of structural changes, which are in turn determined with the support of ion mobility measurements. The role of the ligand shell and the induced ligand field on the lanthanoid's energy levels and the corresponding optical transitions are interpreted with the support of density functional theory in combination with ligand field theory.[1]

[1] J. F. Greisch, M. Harding, B. Schaefer, M. Rotter, M. Ruben, W. M. Klopper, M. M. Kappes, D. Schooss. *J. Phys. Chem. A*, 118 (2014) 94-112.

[2] J. F. Greisch, M. Harding, B. Schaefer, M. Ruben, W. Klopper, M. M. Kappes, D. Schooss. *J. Phys. Chem. Lett.* 5 (2014) 1727-1731.

## SPECTROSCOPIC PROPERTIES OF YZnPO POLYCRYSTALS DOPED WITH Nd<sup>3+</sup> IONS

Karol Lemański, Michael Babij, Przemysław J. Dereń

*Institute of Low Temperature and Structure Research Polish Academy of Sciences,  
Department of Spectroscopy of Excited States, ul. Okólna 2, 50-422 Wrocław, Poland,*

*\*Corresponding author: P.Deren@int.pan.wroc.pl*

YZnPO phosphide oxide possesses trigonal crystal structure with a space group R-3m [1]. The YZnPO compound has the interesting properties, also because of its specific crystal structure, where the phosphate ions (P<sup>3-</sup>) are ligands, together with the oxygen ions. The ytterbium atoms in the trigonal structure have four oxygen and three phosphorus neighbours [2].

Polycrystals of YZnPO doped with neodymium ions were synthesized using the solid state reaction method. The crystal structure was confirmed using X-ray powder diffraction. The absorption and emission spectra, as well as the luminescence decay curves measurement were performed. The crystal field energy levels of Nd<sup>3+</sup> ions were obtained from the absorption and emission spectra.

The Nd<sup>3+</sup> emission occurs from the <sup>4</sup>F<sub>3/2</sub> energy levels. The strongest luminescence band was assigned to the <sup>4</sup>F<sub>3/2</sub>→<sup>4</sup>I<sub>11/2</sub> transition, which is in the range of 1070–1115 nm, with the maximum at 1084 nm (see Fig. 1). Also significant is the <sup>4</sup>F<sub>3/2</sub>→<sup>4</sup>I<sub>13/2</sub> emission, which is present from 890 to 935 nm. The energy transfer from the host lattice (HL) to the doped neodymium(III) ions has been also observed.

The investigated compound may find applications as a material, to improve solar cell efficiency working as a downshifter phosphor. The YZnPO absorption band is very broad and absorbed energy is transferred to the Nd<sup>3+</sup> ions which emission matches well the maximum sensitivity of silicon solar cells.

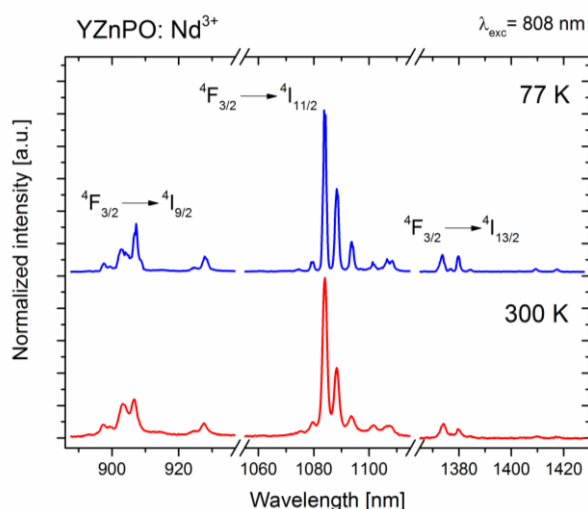


Fig.1. The emission spectrum of YZnPO doped with 1% of Nd<sup>3+</sup> ions, measured at different temperatures.

[1] H. Lincke, R. Glaum, V. Dittrich, M. Tegel, D. Johrendt, W. Hermes, M. H. Möller, T. Nilges, R. Pöttgen, *Z. Anorg. Allg. Chem.* 2008, 1339.

[2] A.T. Nientiedt, W. Jeitschko, *Inorg. Chem.* 37 (1998) 386.

### Acknowledgement

This work was supported by POIG.01.01.02-02-006/09 project co-funded by European Regional Development Fund within the Innovative Economy Program. Priority I, Activity 1.1. Sub-activity 1.1.2, which is gratefully acknowledged.

## SPECTRAL-KINETIC AND COLOR CHARACTERISTICS OF THE LUMINESCENCE OF ZnWO<sub>4</sub>:Eu<sup>3+</sup> CRYSTALS

D. Valiev<sup>a</sup>, E. Polissadova<sup>a</sup>, V. Lisitsyn<sup>a</sup> and I. Tupitsyna<sup>b</sup>

<sup>a</sup>*National Research Tomsk Polytechnic University 634050, Tomsk, 30, Lenin Avenue, Russia, dtdamirka@gmail.com*

<sup>b</sup>*Institute for Scintillation Materials, 61001, Kharkov, 60, Lenin Avenue, Ukraine*

Luminescent properties of zinc tungstate are well studied since it is widely used as a scintillator crystal [1, 2]. As self-activated phosphor zinc tungstate possesses good properties such as chemical stability, high absorption coefficient of X-ray, high light yield, short decay time and low afterglow. ZnWO<sub>4</sub> crystal exhibits intensive intrinsic luminescence in the blue-green region. Doping with rare-earth ions emitting in the red region makes it promising as a white-light phosphor [3, 4] to produce "white LEDs." Therefore, the study of the processes occurring in ZnWO<sub>4</sub>:Eu<sup>3+</sup> crystals and affecting their luminescent properties is considered to be of relevant importance.

Zinc tungstate crystals grown by Czochralski method have been studied. Europium was added to the mix as Eu<sub>2</sub>O<sub>3</sub> oxide, its concentration being of 3, 6 and 9 mol% before growing.

The spectra of the optical transmittance were studied with Lomo-Photonics UVI-256 spectrophotometer. The AvaSpec-2048 spectrometer with the integration time of 100 ms was used to measure the integrated luminescence spectra under photo- and electron excitation. The time-resolved pulsed cathodoluminescence (PCL) spectra and decay kinetics were investigated with the pulsed optical spectrometer based on a high-current electron accelerator GIN- 600.

It is shown that the ratio of the intensity of intrinsic luminescence and activator luminescence (bands at 485 nm and 614 nm, respectively) depends on the excitation mode and concentration of Eu<sup>3+</sup> in the crystal. The luminescence efficiency of the europium ions is higher in electronic excitation. Increasing the concentration of Eu<sup>3+</sup> causes an increase in the emission intensity in the bands at 614 nm and 628 nm. In case the concentration of Eu is 9 mol%, the luminescence intensity of the crystal matrix decreases.

The excitation spectrum of intrinsic luminescence for ZnWO<sub>4</sub> ( $\lambda_{em} = 485$  nm) is shown to be the band  $\lambda_{ex} = 320$  nm. A number of bands at 360, 385, 394, 417, 465 and 539 nm are observed in the excitation spectrum of the europium ions ( $\lambda_{em} = 614$  nm). The most intense peak of excitation Eu<sup>3+</sup>  $\lambda_{max} = 465$  nm corresponds to the transition  ${}^7F_0 \rightarrow {}^6L_6$ , and it overlaps the emission spectrum of the ZnWO<sub>4</sub> matrix. This proves the possibility of energy transfer from the lattice ZnWO<sub>4</sub> to Eu<sup>3+</sup> ions in ZnWO<sub>4</sub>:Eu occurs through the re-absorption intrinsic emission of ZnWO<sub>4</sub>.

If the concentration of europium changes, the kinetics of the PCL decay in the band at 614 nm does not significantly change,  $\tau_{slow}$  of the slow component is about 500  $\mu$ s, and  $\tau_{fast}$  of the fast component can vary within 0.8-0.1  $\mu$ s. The kinetic of the luminescence decay in the band at 485 nm (intrinsic luminescence) is similar to the kinetic in nonactivated crystal. The decay time of the initial stage varies within 1  $\mu$ s, and the final stage decays after  $\tau \sim 14-16$   $\mu$ s. However, if the amount of europium ions increases, the luminescence decay time of zinc tungstate tends to decrease.

- [1] V. Nagirnyi, E. Feldbach, L. J. Onsson Nucl. Instr. and Meth. in Phys. Res. A. 486 (2002) 395–398.  
 [2] L. L. Nagornaya, B. V. Grinyov, A. M. Dubovik et al. IEEE Trans. Nucl. Sci. 56 ( 2009) 994–997.  
 [3] V. Lisitsyn, D. Valiev, I. Tupitsyna, E. Polissadova et al. Advanced Mater. Res. 872 (2014) 128-133  
 [4] T. Dong, Z. Li, Z. Ding, L. Wu Mater.Res. Bull. 43 (2008) 1694-1701.

## HIGH-TEMPERATURE SINTERING OF SrS:Ce TOWARDS THE NEW RED-IR Ce EMISSION

Dagmara Kulesza<sup>a</sup>, Karolina Fiaczyk<sup>a</sup>, Joanna Cybińska<sup>a,b</sup>, Aneta Wiatrowska<sup>c</sup>,  
Eugeniusz Zych<sup>a,b</sup>

<sup>a</sup>*Faculty of Chemistry, University of Wrocław*

*14. F. Joliot-Curie Street, 50-383 Wrocław, Poland, dagmara.kulesza@chem.uni.wroc.pl*

<sup>b</sup>*Wrocław Research Centre EIT+, 147 Stabłowicka Street, 54-066 Wrocław, Poland*

<sup>c</sup>*Philips Research, Materials Technology Department*

*High Tech Campus 04, 5656 AE Eindhoven, The Netherlands*

SrS:Ce is an old phosphor well-known for its efficient bluish-green emission, which can be slightly broadened and red-shifted to some extent when Ce<sup>3+</sup> concentration increases [1-3]. Contrary to these literature data, our experiments with both low- and high-concentration SrS:Ce *sintered ceramics* showed the possibility to create a new Ce<sup>3+</sup> luminescent center producing intense luminescence in the red and infrared range of spectrum (Fig.1.).

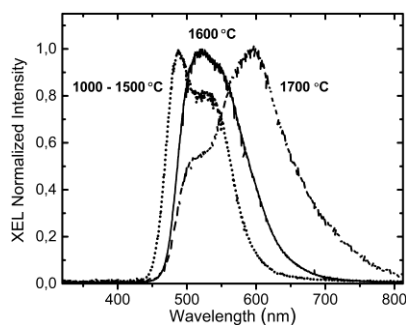


Fig. 1. Normalized X-ray excited luminescence of SrS:Ce sintered at different temperatures.

In this presentation we shall show an evolution of the luminescent properties of SrS:Ce upon sintering at elevated temperatures, from 1000 °C to 1700 °C. We shall show, that a never reported red-IR emission of Ce<sup>3+</sup> evolves and becomes continuously stronger as the sintering temperature increases. This spectroscopic effect occurs parallel to proceeding densification of the SrS:Ce body. The changes in the morphology of the material mirrored with variations in excitation and emission spectra and in decay traces of the both emissions in wide range of temperatures will be presented and discussed.

The excitation spectrum of the long-wavelength luminescence differs entirely from the spectrum of the regular luminescence proving a greatly different local symmetry of the new luminescent center. The spectroscopic data allowed to suggest that the new center is composed of [Ce<sup>3+</sup>-S<sup>2-</sup>-Ce<sup>3+</sup>] aggregates formed as a result of high temperature of the sintering.

### Acknowledgement

This work was supported by POIG.01.01.02-02-006/09 project co-funded by European Regional Development Fund within the Innovative Economy Program. Priority I, Activity 1.1. Sub-activity 1.1.2, which is gratefully acknowledged.

[1] B. Hüttl, U. Troppenz, K.O.Velthaus, C.R. Ronda, R.H. Mauch, J. Appl. Phys. 78 (12) (1995) 7282-7287.

[2] P.F. Smet, I. Moreels, Z. Hens, D. Poelman, Materials 3 (2010) 2834-2883.

[3] Y. Zhao, F.T. Rabouw, T. van Puffelen, C.A. van Walree, D.R. Gamelin, C. de Mello Donegá, A. Meijerink, J. Am. Chem. Soc., 136 (47) (2014) 16533–16543.

## LOCATION OF THE Ce<sup>3+</sup> GROUND STATE IN THE BANDGAP AND LUMINESCENCE EFFICIENCY IN Y<sub>3</sub>Al<sub>2</sub>Ga<sub>3</sub>O<sub>12</sub>:Ce<sup>3+</sup> AND Y<sub>3</sub>Ga<sub>5</sub>O<sub>12</sub>:Ce<sup>3+</sup>

Sebastian Mahlik<sup>1</sup>, Agata Lazarowska<sup>1</sup>, Marek Grinberg<sup>1</sup>, Jumpei Ueda<sup>2</sup>, Setsuhisa Tanabe<sup>2</sup>

<sup>1</sup>*Institute of Experimental Physics, University of Gdansk, Wita Stwosza 57, 80-952 Gdańsk, Poland*

<sup>2</sup>*Graduate School of Human and Environmental Studies, Kyoto University, Kyoto 606-8501, Japan*

Recently, some of us reported the blue light chargeable persistent luminescence related to Ce<sup>3+</sup> in Y<sub>3</sub>Al<sub>2</sub>Ga<sub>3</sub>O<sub>12</sub> (YAGG) doped with Ce<sup>3+</sup> and Cr<sup>3+</sup> [1]. On the other hand, Y<sub>3</sub>Ga<sub>5</sub>O<sub>12</sub> (YGG):Ce<sup>3+</sup>, Cr<sup>3+</sup> does not show persistent luminescence as well as photoluminescence at ambient pressure. In this contribution we present the pressure and temperature dependence of the luminescence of both materials. Photoluminescence and photoluminescence kinetics have been measured for pressure range up to 325 kbar for temperature range from 10 K to ambient.

In YAGG:Ce<sup>3+</sup>, Cr<sup>3+</sup> it has been found that Ce<sup>3+</sup> luminescence spectrum consists of two overlapping bands at 19100 cm<sup>-1</sup> and 16900 cm<sup>-1</sup>, related to transitions from the 5d state to the 2F<sub>5/2</sub> and 2F<sub>7/2</sub> states of 4f electronic configuration of Ce<sup>3+</sup>. Energies of the bands diminish with increasing pressure with the rates; 7cm<sup>-1</sup>/kbar and 7.9 cm<sup>-1</sup>/kbar, respectively. In the case of YGG:Ce<sup>3+</sup>, Cr<sup>3+</sup> the Ce<sup>3+</sup> luminescence appeared at pressure 50 kbar as two overlapping bands which energetically coincide with YAGG:Ce<sup>3+</sup> luminescence.

Above 50 kbar the Ce<sup>3+</sup> luminescence bands in YGG and YAGG hosts have the same energies and the same pressure shifts. It means that the intrinsic crystal field splitting strength for Ce<sup>3+</sup> in YGG and YAGG is the same and only difference is in the location of the conduction band (CB). In YAGG the CB is located above the excited state of Ce<sup>3+</sup>, whereas in the YGG the 5d excited state is degenerated with conduction band at ambient pressure due to the CB lowering.

Analysis of dependence of YGG:Ce<sup>3+</sup> luminescence lifetime on pressure above 50 kbar and temperature allowed to obtain value of the energy of the 5d state with respect to the conduction band. It was found that this energy diminish with respect the energy of the conduction band edge by value 6 cm<sup>-1</sup>/kbar with increasing g pressure. As the result we obtained that value of the energy of the ground state of Ce<sup>3+</sup> increases with respect to conduction band edge in YGG by approximately 1.9 cm<sup>-1</sup>. Obtained results were discussed in the framework of the models describing the location of the ground state and excited 4f-15d state of lanthanides in the bandgap and the model of impurity trapped exciton.

[1] J. Ueda, K. Kuroishi, S. Tanabe, Appl. Phys. Lett. 104, 101904 (2014)

## **SURFACE-MODIFIED TiO<sub>2</sub> NANOPARTICLES ON POLYMER SUPPORT: SYNTHESIS, CHARACTERIZATION AND PHOTOCATALYTIC PERFORMANCE**

Ivana D. Vukoje<sup>a</sup>, Lidija V. Trandafilović<sup>a</sup>, Tijana S. Radoman<sup>b</sup>, Enis S. Džunuzović<sup>c</sup>,  
S. Phillip Ahrenkiel<sup>d</sup>, Jovan M. Nedeljković<sup>a</sup>

<sup>a</sup>*Institute of Nuclear Sciences Vinča, University of Belgrade, P. O. Box 522,  
Belgrade, Serbia, ivanav@vinca.rs*

<sup>b</sup>*Innovation center, Faculty of Technology and Metallurgy, University of Belgrade,  
Karnegijeva 4, 11120 Belgrade, Serbia*

<sup>c</sup>*Faculty of Technology and Metallurgy, University of Belgrade, Karnegijeva 4,  
11120 Belgrade, Serbia*

<sup>d</sup>*South Dakota School of Mines and Technology, 501 E Saint Joseph Street, Rapid City,  
SD 57701, USA*

Poly(GMA-*co*-EGDMA) macroporous copolymer decorated with TiO<sub>2</sub> nanoparticles was prepared by a modification of poly(GMA-*co*-EGDMA) in the reaction with dopamine, and consequent hydrolysis of titanium(IV) isopropoxide. In addition, this synthetic approach lead to the formation of charge transfer complex between dopamine and surface Ti atoms from TiO<sub>2</sub> nanoparticles followed with the significant red shift of the onset of optical absorption. Obtained nanocomposite was characterized using elemental analysis, transmission electron microscopy and X-ray diffraction analysis. UV-Vis reflection spectroscopy was used for optical characterization of surface-modified TiO<sub>2</sub> nanoparticles, while the coordination of TiO<sub>2</sub> nanoparticles to the poly(GMA-*co*-EGDMA) copolymer was studied using infrared spectroscopy. The photocatalytic ability of red-shifted TiO<sub>2</sub> nanoparticles on polymer support was tested under visible light illumination by following the degradation of organic dye crystal violet. The low energy band-pass 450 nm cut-off filter was used to eliminate photons with energy higher than 2.75 eV. The preliminary results clearly indicate that surface-modified TiO<sub>2</sub> nanoparticles are able to photocatalytically perform under visible light illumination.



## **INVERTED QUANTUM DOT LIGHT EMITTING DIODES USING POLYETHYLENIMINE ETHOXYLATED MODIFIED ZNO ELECTRON TRANSPORT LAYER**

Hong Hee Kim<sup>a</sup>, Do Kyeong Hwang<sup>b</sup>, Won Kook Choi<sup>c</sup>

<sup>a</sup>*Center for Optoelectronic Materials, Korea Institute of Science and Technology (KIST),  
Seoul, 136-791, Korea, t12551@kist.re.kr*

<sup>b</sup>*Center for Optoelectronic Materials, Korea Institute of Science and Technology (KIST),  
Seoul, 136-791, Korea, dkhwang@kist.re.kr*

<sup>c</sup>*Materials and Life Science Research Division, Korea Institute of Science and Technology  
(KIST), Seoul, 136-791, Korea, wkchoi@kist.re.kr*

Colloidal quantum dots (QDs) are an emerging class of new materials due to their unique physical properties. In particular, colloidal QD based light emitting diodes (QDLEDs) have been extensively studied and developed for the next generation displays and solid-state lighting. Among a number of approaches to improve performance of the QDLEDs, the most practical one is optimization of charge transport and charge balance in the recombination region. Here, we suggest a polyethylenimine ethoxylated (PEIE) modified ZnO nanoparticles (NPs) as electron injection and transport layer for inverted structure red CdSe-ZnS based quantum dot light emitting diode (QDLED). The PEIE surface modifier, incorporated on the top of the ZnO NPs film, facilitates the enhancement of both electron injection into the CdSe-ZnS QD emissive layer by lowering the workfunction of ZnO from 3.58 eV to 2.87 eV and charge balance on the QD emitter. As a result, this device exhibit a low turn-on voltage of 2.0–2.5 V and have maximum luminance and current efficiency values of 8600 cd/m<sup>2</sup> and current efficiency of 1.53 cd/A, respectively.[1] The same scheme with ZnO NPs/PEIE layer has also been used to successfully fabricate green, blue, and white QDLEDs style

[1] H.H. Kim, S. Park, Y. Yi, C.Park, D.I. Son, D.K. Hwang, and W.K. Choi, *Sci. Rep.* 5 (2015) 8968-8972 (2015)

## **EXCITED STATES RELAXATION IN HIGHLY CONFINED AgInS<sub>2</sub> AND AgInS<sub>2</sub>/ZnS QUANTUM DOTS EVALUATED BY SINGLE PARTICLE SPECTROSCOPY**

Bartłomiej Cichy<sup>a</sup>, Ryan Rich<sup>b</sup>, Zygmunt Gryczynski<sup>b</sup>, Wiesław Strek<sup>a</sup>

<sup>a</sup>*Institute of Low Temperatures and Structural Research, Polish Academy of Science,  
Okólna 2 50-422 Wrocław, Poland, b.cichy@int.pan.wroc.pl*

<sup>b</sup>*University of North Texas Health Science Center, Center for Fluorescence Technologies  
and Nanomedicine, Fort Worth Texas 15676, United States of America*

There is continuous interest in looking for a new bio-probes for fluorescent bio-detection and imaging. Different studies have already indicated that quantum confined nanocrystalline semiconductors are able to match the requirements expected from fluorescent probes. This interest is caused mainly due to their unique properties e.g. tunable absorption and emission bands, resulting from quantum confinement of the fundamental excitations as well as finite crystal nature.

Recently, lot of scientific attention was devoted to cadmium-free compounds e.g. carbon nanotubes (CNTs), Ag<sub>2</sub>S, PbS, and also to the group of A<sup>I</sup>B<sup>III</sup>IX<sup>VI</sup><sub>2</sub> ternary chalcopyrites where A = Cu, Ag; B = Al, In, Ga and the X = S, Se, Te. Beneath multitude of the group's compounds, the AgInS<sub>2</sub> (AIS) quantum dots (QDs) seems to be of particular interest as their composition is free of Se, Te and Ga, their emission band may be tuned from VIS to NIR spectral range and their quantum yield (QY) is higher than for the CuInS<sub>2</sub> (CIS). Moreover, particular interest is also devoted to the time-domain properties of AIS QDs, as their luminescence lifetime is in the range of hundreds of nanoseconds being well suited for fluorescence lifetime imaging (FLIM) experiments.

Although, the first impression of AIS quantum dots (QDs) is very positive, there is a major drawback concerning complicated kinetics of the excited states affecting both the emission band as well as the time-resolved spectra. Understanding of the excited states relaxation kinetics in such compounds is crucial for proper interpretation of the experimental results and getting deeper insight into many physicochemical properties occurring at the interface of QDs and living matter.

In this work we report on the recombination pathways in confined AIS and AIS/ZnS nanostructures, leading to deviations from the first order rate law on the basis of single particle spectroscopy. The nonradiative processes in A<sup>I</sup>B<sup>III</sup>X<sup>VI</sup><sub>2</sub> nanoparticles are still far from well understanding especially in the highly confined compounds where high correlation of electrons, pendulum uncertainty, high electron-hole Coulomb interaction and diminished translational momentum conservation are dominating. Formation of structural defects is discussed with regard to their impact on the decay kinetics.

B. Cichy acknowledges support from the National Science Center Poland (NCN) under the SONATA program (DEC-2013/11/D/ST5/02989).

## MULTI-SPECTRAL FLUORESCENT NANOPROBES: TRIPLE $\text{Re}^{3+}$ -DOPED NIR-EMITTING $\text{NaGdF}_4$ NANOPARTICLES (793NM-NIR) ALSO PLAYING AS *IN VITRO* (980NM-VIS) IMAGING AND THERMOMETRY PROBES

*Antonio Benayasa*<sup>\*a</sup>, *W. F. Silva*<sup>b</sup>, *B. del Rosal*<sup>c</sup>, *F. Sanz-Rodriguez*<sup>c</sup>, *Vetrone, Fiorenzo*<sup>a</sup>

<sup>a</sup> *Energie Matériaux Télécommunications, Institut National de la Recherche Scientifique, Varennes, QC, Canada.*

<sup>b</sup> *Universidade Federal de Alagoas, Maceió, Brazil.*

<sup>c</sup> *Fluorescence Imaging Group Universidad Autónoma de Madrid, Cantoblanco, Madrid, Spain.*

*antonio.benayas@uam.es, vetrone@emt.inrs.ca*

Nowadays, the use of fluorescence imaging is at the forefront of biomedical investigations. That powerful tool is thoroughly applied for *in vitro* and *in vivo* sensing, detection, targeting therapy and as assistance for surgery process, as well. Among the phosphors and fluorophores that could play a significant role for bioimaging and sensing, fluorescent nanoparticles (NPs) present a number of features that make them interesting for *in vivo* imaging, such as tunable pharmacokinetics, large surface areas so that multiple targeting groups and therapeutic agents can be conjugated to them, and resistance to photo-bleaching.

This work proposes using a different pumping route from the usual one in fluorescent  $\text{RE}^{3+}$ -doped  $\text{NaGdF}_4$  nanoparticles. In our case,  $\text{Tm}^{3+}$  ions are pumped at 793 nm, i.e. in the 1<sup>st</sup> Biological Window (700-950nm), then supplying a rich near-infrared (NIR) emission spectrum from  $\text{Yb}^{3+}$  and  $\text{Tm}^{3+}$  emissions. The usual roles of the  $\text{Yb}^{3+}$  ions as sensitizers and  $\text{Tm}^{3+}$  ions as “pure emitters” are here reversed. Upon energy transfer of the Thulium-absorbed optical pumping to  $\text{Yb}^{3+}$  ions, a multi-band NIR emission arises both from  $\text{Yb}^{3+}$  and  $\text{Tm}^{3+}$  ions, its spectral range entirely matching the Second Biological Window (1000-1350nm), what makes it a perfectly suitable fluorescent nanoprobe by improving the expected penetration depth for eventual *in vivo* applications.

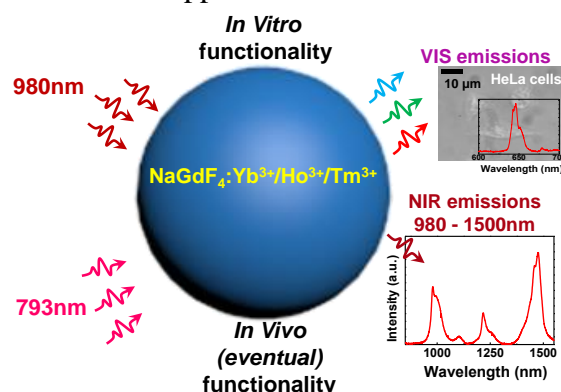


Figure 1: scheme of the two routes of excitation (980 and 793 nm) and the two sets of fluorescence emissions, suitable for both ways of bio-applications, VIS range (*in vitro*) and NIR for (future) *in vivo*.

Moreover, this  $\text{NaGdF}_4:\text{Yb}^{3+}/\text{Ho}^{3+}/\text{Tm}^{3+}$  nanoparticle is gifted with multifunctional optical properties: upon the “usual” optical excitation of Ytterbium ions at 980nm, and after that optical energy is transferred to both Thulium and Holmium ions, a blue-green-red palette of visible emissions is obtained. That supplies a multicolor platform for *in vitro* imaging, together with a three-photon fluorescent nanothermometer at cellular level, with a great deal of potential high-spatial resolution to offer. A proof-of-concept of the latter is here presented, subsequently applied to HeLa cells.

## TYPE-II EXCITONS IN (Ga,In)As/Ga(N,As)-QUANTUM WEELS

Sebastian Gies<sup>a</sup>, Carsten Kruska<sup>a</sup>, Philip Hens<sup>a</sup>, Wolfgang Stolz<sup>a</sup>, Kerstin Volz<sup>a</sup>,  
and Wolfram Heimbrodt<sup>a</sup>

<sup>a</sup>*Faculty of Physics and Materials Science Center, Philipps University Marburg,  
Renthof 5, D-35032 Marburg, Germany, sebastian.gies@physik.uni-marburg.de*

Nitrogen containing quantum well (QW) structures are promising materials for solar cell and lasers. Because of the band anticrossing interaction between the N-impurity and the GaAs conduction band a huge redshift occurs, pushing the bandgap towards 1.55  $\mu\text{m}$ . On the other hand nitrogen introduces a huge disorder. The N-related disorder in the bulk material and in QWs has been studied extensively, while knowledge about the influence of N on the QW-interfaces (IF) is very scarce. However, interfaces are an important part of any device considering charge carrier confinement and transport properties. To address the interfaces in particular, we use type-II excitons as an IF-sensitive probe. Since the recombination of type-II excitons takes place across the interface they are an excellent probe for the interface properties. Here we present a systematic and comprehensive analysis of the influence of the interface on spatially indirect (type-II) excitons in (Ga,In)As/Ga(N,As)-QWs on GaAs.

The QW-structures under investigation were grown epitaxially using metal-organic vapor-phase epitaxy. On the GaAs substrates a 10 nm thick (Ga<sub>0.76</sub>,In<sub>0.24</sub>)As-layer was grown. This layer is followed by a GaAs-interlayer and a QW of Ga(N,As). The final capping consists of 45 nm GaAs. Samples with two different nitrogen contents in the Ga(N,As)-QW have been manufactured. A low nitrogen concentration of  $x_{\text{N}}=0.5\%$  yields type-I behavior with the energetically lowest electron and heavy hole states confined in the (Ga,In)As-QW, while a higher nitrogen concentration of  $x_{\text{N}}=5\%$  results in a type-II structure with the energetically lowest electron state in the Ga(N,As)-QW.

To analyze the interface in a systematic manner the thickness of the GaAs-interlayer between heavy-hole confining (Ga,In)As-QW und electron confining Ga(N,As)-QW has been modified. Furthermore, the roughness of either QW-interface has been modified by introducing a growth interruption during sample growth.

Using photoluminescence (PL) spectroscopy we can clearly identify the type-II transition between Ga(N,As)-QW and (Ga,In)As-QW. Combining the PL results with photo-modulated reflectance spectroscopy we are able to determine the ground and excited states of the respective QWs. Finally, the conjunction of experiment and theory enables us to precisely determine the hetero-offset between Ga(N,As)-QW and GaAs barrier and therefore to produce an exact picture of the bandstructure. Moreover, we will present time-resolved PL measurements revealing the recombination dynamic of the type-II excitons. These will not only be compared to the behavior of the corresponding type-I structure but also analyzed regarding the influence of the GaAs-interlayer. This yields a direct correlation between interface roughness and optical properties of the type-II excitons.

To sum up, we present a comprehensive analysis of the interconnection of the real interface and the optical and electronic properties of (Ga,In)As/Ga(N,As)-QWs.

## PHOTO-IONIZATION OF 3d IONS IN GLASSES

Doris Möncke, Doris Ehrt

<sup>a</sup>*Otto-Schott-Institute of Materials Research, Friedrich-Schiller-University Jena,  
Fraunhoferstr.6, 07743 Jena, Germany, dorismoencke@uni-jena.de*

The interaction of radiation with glasses often modifies the materials properties (e.g. the refractive index), or, most noticeable might cause a loss in transmission. Such processes can be exploited for photo-sensitive materials such as radiation sensors or photochromic glasses. On the other hand, such modifications are to be avoided in many other applications in the field of high performance optics.

In order to improve the understanding of defect generation processes, a systematic comparison of defect formation in (fluoride-)phosphate glasses doped with low concentrations of 3d ions was attempted. Samples doped with 10 to 5000 ppm of Ti, V, Cr, Mn, Fe, Co, or Ni were irradiated in the UV-range using excimer lasers. Defects, which generally form in levels of several ppm, were characterized by optical and Electron Spin Resonance (ESR) spectroscopy [1].

Extrinsic defects replaced intrinsic defects or like charge and their formations often enhanced also the formation of intrinsic defects of the opposite charge.

$V^{4+}$  was photo-oxidized to the empty valence shell  $d^0$  ion while  $Co^{2+}$ ,  $Mn^{2+}$  and  $Fe^{2+}$  were all photo-oxidized to the trivalent state. On the other hand, divalent  $Ni^{2+}$  was photo-reduced to the monovalent ion, acting as electron center (EC) [2-4]. The fully oxidized  $Ti^{4+}$  was also photo-reduced.  $Cr^{3+}$  showed photo-disproportionation into  $(Cr^{3+})^-$  EC (or  $Cr^{2+}$  ion) and  $(Cr^{3+})^{+++}$  HC (or  $Cr^{6+}$  ion). Qualitative and quantitative changes in defect formation rates depend not only on the ion, but also on the radiation parameters, e.g. the wavelength of the excimer lasers used (193, 248, 351 nm) or the initial transmission of the glass samples at the chosen laser wavelength [5].

Defect recovery was followed over time up to ten years after ending the irradiation experiments, while the samples were stored in the dark at room-temperature. Often extrinsic hole center (HC) of photo-oxidized ions were more stable than intrinsic HC and a transformation of phosphate related oxygen hole center (POHC) into  $(Fe^{2+})^+$  HC or  $(Co^{2+})^+$  HC was observed. Similarly, the  $(Ni^{2+})^-$  EC and the oxygen hole center form a very stable defect pair, the induced absorption of these two defects increasing over the decade following the irradiation experiment, enhancing the transmission loss in the visible wavelength region.

[1] D. Möncke, D. Ehrt, Irradiation induced defects in glasses resulting in the photoionization of polyvalent dopants, *Opt. Mater.*, 25 (2004) 425-437.

[2] D. Möncke, D. Ehrt, Irradiation-induced defects in different glasses demonstrated on a metaphosphate glass, *Glass Sci. Technol. - Glas Techn. Ber.*, 74 (2001) 199-209.

[3] D. Möncke, D. Ehrt, Radiation-induced defects in CoO- and NiO-doped fluoride-phosphate glasses, *Glass Sci. Technol. - Glas Techn. Ber.*, 74 (2001) 65-73.

[4] D. Möncke, D. Ehrt, Radiation-induced defects in CoO- and NiO-doped fluoride, phosphate, silicate and borosilicate glasses, *Glass Sci. Technol.*, 75 (2002) 243-253.

[5] D. Möncke, D. Ehrt, Photoionization of polyvalent ions, in: H.P. Glick (Ed.) *Materials Science Research Horizons*, Nova Science Publishers Inc., 2007, pp. 1-56.

## LOCAL, ELECTRONIC AND GLOBAL STRUCTURE OF MOLYBDENUM–LEAD–GERMANATE GLASSES AND GLASS CERAMICS

Marius Rada<sup>a</sup>, Nicolae Aldea<sup>a</sup>, Simona Rada<sup>b</sup>, Ramona - Crina Suciua<sup>a</sup>, Sergiu Macavei<sup>a</sup>, Adrian Bot<sup>a</sup>, Eugen Culea<sup>b</sup> and Radu Balan<sup>c</sup>

<sup>a</sup> *National Institute for Research and Development for Isotopic and Molecular Technologies, 400293 Cluj-Napoca, Romania*

<sup>b</sup> *Department of Physics & Chemistry, Technical University of Cluj-Napoca, 400020 Cluj-Napoca, Romania*

<sup>c</sup> *The Department of Mechanisms, Fine Mechanics and Mechatronics, Technical University of Cluj-Napoca, 400020 Cluj-Napoca, Romania*

Glasses and glass ceramics of the  $x\text{MoO}_3$  (100-x)[7GeO<sub>2</sub>•3PbO] system where x=0–30 mol% MoO<sub>3</sub> were synthesized and characterized in order to obtain information about the structural correlations and the relationship between structure and physical properties in these materials. Changes of the FTIR, UV–vis, XRD, XAS and EPR data are discussed in view of the glass network structural changes determined by the evolution of molybdenum ions state, glass composition and MoO<sub>3</sub> concentration[1,2,3]. The spectroscopic studies indicate that with increasing of MoO<sub>3</sub> content a fraction of the Mo<sup>6+</sup> ions convert Mo<sup>3+</sup> and Mo<sup>5+</sup> ions. Accordingly, these modifications cause the depolymerization of the host network, the increase of the structural disorder and formation of GeO<sub>2</sub> and PbMoO<sub>4</sub> crystalline phases[4]. The shape of EPR spectra is modified by the increase of the MoO<sub>3</sub> concentration indicating that molybdenum ions exists in glass and glass ceramics in more than one valence state. The EPR spectra contain a broad line located at  $g \approx 5.2$  and, for the samples with a MoO<sub>3</sub> content up to  $x \geq 15$  mol%, the presence of the hyperfine structure characteristic for the Mo<sup>5+</sup> ions can be observed, too. The electrochemical performances of the glass and glass ceramics samples with x=10 and 30 mol% MoO<sub>3</sub> were demonstrated by cyclic voltammetry.

[1] L. Abbas, L. Bih, A. Nadiri, Y. El Amraoui, D. Mezzane, B. Elouadi, Properties of mixed Li<sub>2</sub>O and Na<sub>2</sub>O molybdenum phosphate glasses, *Journal of Molecular Structure* 876 (1–3) (2008)194–198.

[2] S.M. Abo-Naf, FTIR and UV–vis optical absorption spectra of gamma-irradiated MoO<sub>3</sub> -doped lead borate glasses, *Journal of Non-Crystalline Solids* 358 (2012) 406–413.

[3] S. Hazra, A. Ghosh, Structural properties of unconventional lead cuprate glass, *Journal of Materials Research* 10 (1995) 2374–2378.

[4] A. Ghosh, Electrical-properties of lead vanadate glasses, *Physical Review B* 49 (1994) 3131–3135.

## REDOX STATE OF RE IONS EMBEDDED IN ALUMINOBOROSILICATE GLASSES

Eugenia Malchukova<sup>a</sup>, Bruno Boizot<sup>b</sup>, Alexey Abramov<sup>a</sup> and Eugeni Terukov<sup>a</sup>

<sup>a</sup>*Ioffe Physical Technical Institute, Polytechnicheskaya St., 26, Saint-Petersburg, 194021, Russia, evguenia.malchukova@polytechnique.edu*

<sup>b</sup>*Dept. CEA, IRAMIS, Laboratoire des Solides Irradiés, Ecole Polytechnique, CNRS, 91128 Palaiseau, France, bruno.boizot@polytechnique.edu*

The confinement of high-level nuclear waste (HLW) into borosilicate glass is an internationally accepted technology for the immobilization of this radioactive material [1]. For use in the immobilization of nuclear waste, borosilicate glasses must be durable over the thousands of years that the waste will remain hazardous. Therefore, prediction of the long-term behaviour and stability of these glasses is of great importance. It is known that structural evolution of the nuclear glass due to self-irradiation during such long-term storage can modify its confinement properties [2]. To study of the consequences of  $\beta$ -decay, the effect of  $\beta$ -irradiation on the structure of simplified borosilicate glasses has been investigated. Rare earth elements should be immobilized in the glass matrix as fission products of self-irradiation decay. Lanthanides are not radioactive, and can therefore be easily handled and used as surrogates for actinides (because of their similar physical and chemical properties) [3]. For instance, neodymium may be used as a surrogate for the trivalent minor actinides: americium and curium. Cerium - which exhibits both “+3” and “+4” oxidation states - is used as a surrogate for uranium and plutonium when both oxidation states need to be considered [3].

The aim of this work is to explore the behaviour of the RE elements a namely their reduction ability in the pristine and b-irradiated aluminoborosilicate glasses, since depending on the charge state these elements can occupy different position in glass matrix.

It was found that among polyvalent RE ions only europium and cerium reveal changes in charge state under melting process in air. These results are explained in the frame of the optical basicity theory. In fact for example for Eu-doped glass value of calculated optical basicity is lower than critical magnitude known from literature. Sm ions in as-prepared glass samples remain stable in “3+” charge state. At the same time irradiation leads to the strong reduction both Eu, Ce and Sm ions. Gd and Nd ions are known to be stable in only one charge state. In fact neither luminescence not transmission measurements show other valence of elements studied except “3+”. However features observed in luminescence spectra of these RE ions in dependence on RE concentration or irradiation dose let us to assume some re-arrangement in the RE local environment.

Thus it's concluded that RE ions can change both valence and local environment in aluminoborosilicate glass under. The mechanisms influenced this phenomena are presented.

[1] M.J. Plodinec, J. Non-Cryst. Solids, 84, (1986), p.206.

[2] W. Weber, J. Nucl.Instr. and Meth. B, 32, (1988), p.471.

[3] H.Li, J.D. Vienna, D.E.Smith, P.Hrma, M.I.Gong, Ceram. Trans., 72, (1997), p.399.

## THE DE-CLUSTERING INFLUENCE OF ALUMINUM IONS ON THE GREEN EMISSION EFFICIENCY OF Tb<sup>3+</sup> IONS IN BARIUM BOROPHOSPHATE GLASSES

M. Piaeck<sup>a</sup>, T. Kalpana<sup>b</sup>, M.G. Brik<sup>c</sup>, S. Sudarsan<sup>d</sup>, N. Veeraiah<sup>b</sup>

<sup>a</sup>*Institute of Physics, Jan Dlugosz University, Armii Krajowej 13/15, 42-200 Czestochowa, Poland, m.piaeck@ajd.czyst.pl*

<sup>b</sup>*Department of Physics, Acharya Nagarjuna University, Nagarjuna Nagar, 522 510, A.P., India*

<sup>c</sup>*Institute of Physics, University of Tartu, Ravila 14C, Tartu 50411, Estonia*

<sup>d</sup>*Bhabha Atomic Research Centre, Chemistry Division, Mumbai 400085, India*

In this work we have studied the declustering influence on the emission characteristics of Tb<sup>3+</sup> by Al<sup>3+</sup> ions in barium borophosphate glasses. The content of Al<sub>2</sub>O<sub>3</sub> is varied from 1 to 5 mol% with a step of 1 %. The glasses were prepared by the conventional melt- quenching technique. The optical absorption, luminescence spectra and fluorescence decay curves of these glasses were recorded at room temperature.

The emission spectra of all these glasses excited at 375 nm have exhibited prominent bands in the blue and green regions, which were due to the <sup>5</sup>D<sub>3</sub>→<sup>7</sup>F<sub>5,4,3</sub> and <sup>5</sup>D<sub>4</sub>→<sup>7</sup>F<sub>6,5,4,3</sub> transitions of the Tb<sup>3+</sup> ions, respectively. From these spectra, various radiative parameters including spontaneous emission probability A, the total emission probability, the radiative lifetime τ, the fluorescent branching ratio β of different transitions of Tb<sup>3+</sup> ions have been evaluated. A clear increase in the quantum efficiency and luminescence emission of the prominent bands of Tb<sup>3+</sup> ions in the green region is observed with increase in the concentration of Al<sub>2</sub>O<sub>3</sub>. This increase has been attributed to the declusterization of Tb<sup>3+</sup> ions by Al<sup>3+</sup> ions in the glass network and also to the possible admixing of wave functions of opposite parities.



## SPECTROSCOPY OF THE Er-DOPED BORATE GLASSES

Bohdan V. Padlyak<sup>a,b</sup>, Radoslaw Lisiecki<sup>c</sup>, Witold Ryba-Romanowski<sup>c</sup>

<sup>a</sup>*Vlokh Institute of Physical Optics, Sector of Spectroscopy, 23 Dragomanov Str., 79-005 Lviv, Ukraine, bohdan@mail.lviv.ua*

<sup>b</sup>*University of Zielona Góra, Institute of Physics, Division of Spectroscopy of Functional Materials, 4a Szafrana Str., 65-516 Zielona Góra, Poland*

<sup>c</sup>*Institute of Low Temperatures and Structure Research of the Polish Academy of Sciences, 2 Okólna Str., 50-422 Wrocław, Poland, R.Lisiecki@int.pan.wroc.pl*

The Er-doped glasses with Li<sub>2</sub>B<sub>4</sub>O<sub>7</sub>:Er, LiCaBO<sub>3</sub>:Er, and CaB<sub>4</sub>O<sub>7</sub>:Er compositions were investigated by electron paramagnetic resonance (EPR) and optical spectroscopy techniques. The investigated borate glasses of high optical quality were obtained from corresponding polycrystalline compounds by standard glass synthesis. The Er impurity was added to the raw materials as Er<sub>2</sub>O<sub>3</sub> compound in amounts 0.5 and 1.0 mol. %.

The EPR spectroscopy in the 4.2 ÷ 300 K temperature range and optical spectroscopy at room temperature show that the Er impurity is incorporated into the network of borate glasses as Er<sup>3+</sup> ions (4f<sup>11</sup>, <sup>4</sup>I<sub>15/2</sub>), exclusively. All observed EPR signals and optical absorption and luminescence bands corresponding to the Er<sup>3+</sup> centres in the Li<sub>2</sub>B<sub>4</sub>O<sub>7</sub>:Er, LiCaBO<sub>3</sub>:Er, and CaB<sub>4</sub>O<sub>7</sub>:Er glasses were identified. The Er<sup>3+</sup> EPR signal with effective *g*-factor  $g_{\text{eff}} \cong 9.78$  are clearly observed in the 4 ÷ 20 K temperature range and disappear at higher temperatures due to homogeneous broadening, caused by shortening of the Er<sup>3+</sup> paramagnetic relaxation time. The EPR and optical spectroscopy clearly shows that the Er impurity is incorporated into the borate glass network as isolated Er<sup>3+</sup> centres in samples with low (0.5 mol. %) and high (1.0 mol. %) amount of the Er<sub>2</sub>O<sub>3</sub>.

The ground state optical absorption, luminescence excitation, and emission spectra as well as luminescence kinetics for main *f* – *f* transitions of the Er<sup>3+</sup> centres in the Li<sub>2</sub>B<sub>4</sub>O<sub>7</sub>:Er, LiCaBO<sub>3</sub>:Er, and CaB<sub>4</sub>O<sub>7</sub>:Er glasses were detailed investigated and analysed. On the basis of standard Judd-Ofelt theory the oscillator strength ( $P_{\text{theor}}$ ) for all observed absorption transitions and phenomenological intensity parameters ( $\Omega_2$ ,  $\Omega_4$ , and  $\Omega_6$ ) for Er<sup>3+</sup> centres in the investigated were determined. Spectroscopic parameters of relevance for laser applications, including radiative decay rates (emission probabilities of transitions),  $W_r$ , branching ratios,  $\beta$ , and radiative lifetime,  $\tau_{\text{rad}}$ , have been calculated for all main electric dipole transitions of the Er<sup>3+</sup> centres in the Li<sub>2</sub>B<sub>4</sub>O<sub>7</sub>:Er, LiCaBO<sub>3</sub>:Er, and CaB<sub>4</sub>O<sub>7</sub>:Er glasses.

The luminescence kinetics for infrared emission band (<sup>4</sup>I<sub>13/2</sub> → <sup>4</sup>I<sub>15/2</sub> transition,  $\lambda_{\text{max}} \cong 1530$  nm) of the Er<sup>3+</sup> centres in the investigated borate glasses were satisfactory described by single exponential decay, whereas the luminescence kinetics for green emission band (<sup>4</sup>S<sub>3/2</sub> → <sup>4</sup>I<sub>15/2</sub> transition,  $\lambda_{\text{max}} \cong 560$  nm) of the Er<sup>3+</sup> centres were described by non-exponential decay with average lifetime values. The obtained experimental lifetimes were compared with those calculated and quantum efficiency ( $\eta$ ) for green and infrared emission transitions were estimated and compared with corresponding quantum efficiencies of the Er<sup>3+</sup> laser glasses and crystals. The calculated quantum efficiencies show that the Li<sub>2</sub>B<sub>4</sub>O<sub>7</sub>:Er<sup>3+</sup> glasses are promising materials for LED-pumped lasers, operating in the green (<sup>4</sup>S<sub>3/2</sub> → <sup>4</sup>I<sub>15/2</sub> channel) and LiCaBO<sub>3</sub>:Er<sup>3+</sup> glass – for LED-pumped lasers, operating in the IR (<sup>4</sup>I<sub>13/2</sub> → <sup>4</sup>I<sub>15/2</sub> channel) ranges.

Incorporation peculiarities and local structure of the Er<sup>3+</sup> luminescence centres in the network of Li<sub>2</sub>B<sub>4</sub>O<sub>7</sub>, LiCaBO<sub>3</sub>, and CaB<sub>4</sub>O<sub>7</sub> glasses are considered and discussed based on the obtained spectroscopic results and referenced structural data for investigated glasses and their crystalline analogies.

## FLUORESCENT CLAY HYBRIDS IN TRANSPARENT AQUEOUS MEDIA: INTERACTION WITH BIOINTERFACES

Tom Felbeck<sup>a,b</sup>, Marina Lezhnina<sup>a</sup>, Christian Radunsky<sup>b</sup>, Jens Müller<sup>b</sup>, Anna Nickisch-Hartfiel<sup>c</sup>, Peter Klauth<sup>c</sup>, Ulrich Kynast<sup>a</sup>

<sup>a</sup>Münster University of Applied Sciences, Stegerwaldstr. 39, Steinfurt, Germany, tom.felbeck@fh-muenster.de

<sup>b</sup>Westfälische Wilhelms-Universität Münster, Corrensstr. 28/30, Münster, Germany

<sup>c</sup>Hochschule Niederrhein University of Applied Sciences, Adlerstr. 32, Krefeld, Germany

Nanoclay dispersions have recently been used as convenient shuttles for hydrophobic guest molecules for their promotion into aqueous systems.[1] Such dispersions have numerous advantages, like low cost of starting materials, ease of dye-loading, small sizes and hence minimum scattering of visible light, ease of surface modification, low toxicity and excellent long-term stability.

Laponite constitute the inorganic core of our investigations on optically functionalized nanoclays. They possess a chemical composition of  $\text{Na}_{0.7}(\text{H}_2\text{O})_n\{(\text{Li}_{0.3}\text{Mg}_{5.5})[\text{Si}_8\text{O}_{20}(\text{OH})_4]\}$ , and morphologically form platelets of 25 nm in diameter and a thickness of 1 nm, which are commercially available for numerous fields of industrial applications. Beside the modification with fluorophores and complexes via an adsorption route, [2] it is also possible to modify the particles via covalent conjugation to the rim of the particle.[3] Both hybrid materials, with adsorbed and covalently attached dyes, have been compared with regard to secondary interactions with bio-macromolecular interfaces.

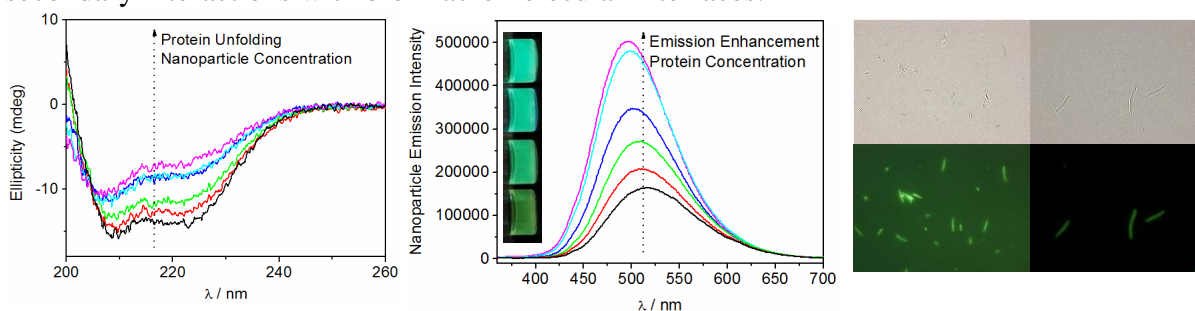


Figure 1: BSA unfolding with increasing laponite concentration monitored via circular dichroism (left), emission enhancement of laponite-dansyl hybrid with increasing protein concentration (center) and laponite-dansyl interactions with gram negative bacteria *Pseudomonas fluorescens* (right).

Several effects can be observed on interaction of proteins with the nano-clay hybrids. Due to intercalation, the sheet silicate layer-layer distances are increased, at the same time, the folding of the proteins can be altered (Figure 1, left), furthermore, solvatochromic fluorophores can be used to monitor the formation of the protein corona (Figure 1, center). Additionally, those hybrids can be used for the labeling of bacteria (Figure 1, right), which proves nanoclays to be an interesting tool in the design of bio-nanomaterials for sensing, analysis and imaging.

[1] M.M. Lezhnina, T. Grewe, H. Stoehr, U. Kynast, *Angew. Chem. Int. Ed.* 51 (2012) 10652–10655.

[2] T. Felbeck, S. Munding, M.M. Lezhnina, M. Staniford, U. Resch-Genger, U.H. Kynast, *Chem. Eur. J.* 21 (2015) 7582–7587.

[3] T. Felbeck, K. Hoffmann, U. Resch-Genger, M. Lezhnina, U. H. Kynast, *J. Phys. Chem. C* 119 (2015) 12978–12987.

## ALL OPTICALLY CONTROLLED ORGANIC-INORGANIC HYBRID DEVICE

Vera Marinova<sup>a,b</sup>, Etienne Goovaerts<sup>c</sup>, Ren Chung Liu<sup>b</sup>, Shiuan Huei Lin<sup>d</sup>, Yi Hsin Lin<sup>b</sup>, Ken Yuh Hsu<sup>b</sup>

<sup>a</sup> Institute of Optical Materials and Technologies, Sofia, Bulgaria, vmarinova@iomt.bas.bg

<sup>b</sup> Department of Photonics, National Chiao Tung University, Hsinchu 30010, Taiwan

<sup>c</sup> Department of Physics, University of Antwerpen, Antwerpen, Belgium

<sup>d</sup> Department of Electrophysics, National Chiao Tung University, Hsinchu 30010, Taiwan

Development of advanced hybrid structures assembled by combination of organic and inorganic materials attract essential scientific and technological interest in order to meet the requirements of 3D display technologies, optical processing and light manipulation. The outstanding properties as large anisotropy and strong birefringence typical for organics [1] and high photosensitivity and charge carrier motilities of inorganics [2] open possibilities to optimize their properties independently and combine them into a single device with enhanced functionality.

We report a hybrid device, based on excellent photoconductivity of doped sillenite photorefractive crystals [3] and strong birefringence of polymer dispersed liquid crystal (PDLC) layer (fig.1). The photoexcited charge carriers generated in photorefractive substrate create an optically induced space charge field, sufficient to penetrate into the PDLC layer and to re-orient the LC molecules inside the droplets. Beam-coupling measurements at Bragg regime are performed showing prospective amplification values and high spatial resolution.

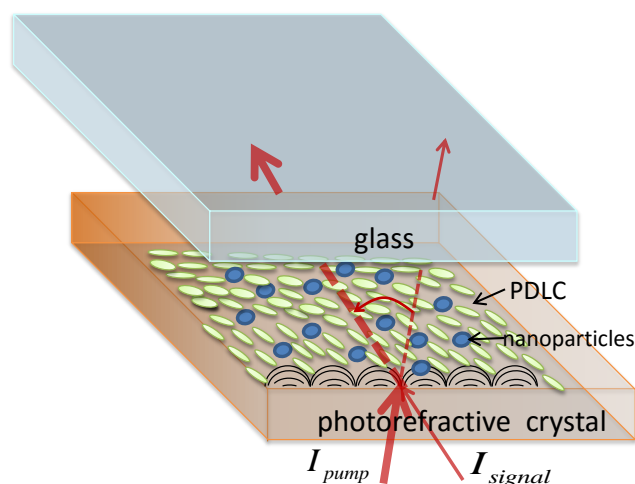


Fig.1 All optically controlled organic-inorganic hybrid structure

The proposed novel organic-inorganic hybrid structure is simple and easy to fabricate, without requirements for conductive layer deposition (ITO contacts), alignment layers and use of polarizers. Such device allows all the processes to be controlled by light, thus opens further potential for real-time image processing at the near infrared spectral range [4].

[1] P. Yeh, C. Gu, Optics of liquid crystal display, second ed., Wiley Interscience, New York, 2010.

[2] J. Frejlich, Photorefractive materials, Wiley Interscience, 2007.

[3] V. Marinova, I. Ahmad, E. Goovaerts, J. Appl. Phys 107 (2010) 113106.

[4] R.C. Liu, V. Marinova, S.H. Lin, M.S. Chen, Y.H. Lin, K.Y. Hsu, Opt. Lett. 39 (2014) 3320–3323.

## PHOTON CONVERSION FROM 4.4 $\mu\text{m}$ Dy<sup>3+</sup> DOPED FLUORESCENT FIBERS TO 800NM IN Er<sup>3+</sup> DOPED FIBERS FOR ALL-OPTICAL GAS SENSING

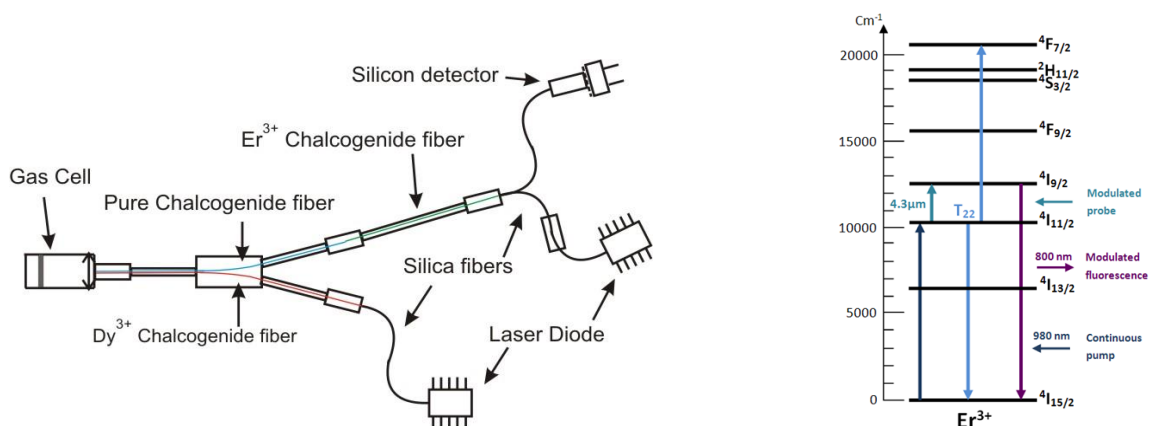
A.L. Pelé<sup>1</sup>, A. Braud<sup>1</sup>, J.L. Doualan<sup>1</sup>, R. Chahal<sup>2</sup>, V. Nazabal<sup>2</sup>, R. Moncorgé<sup>1</sup>, and P. Camy<sup>1</sup>

<sup>1</sup> Centre de Recherche sur les ions, les matériaux et la photonique (CIMAP), Caen, France  
UMR 6252 CEA-CNRS-ENSICAEN, Université de Caen, 6 bd Maréchal Juin, 14050 Caen

<sup>2</sup> Equipe EVC, UMR 6226, Institut Sciences Chimiques de Rennes, Rennes, France

Many radicals spectroscopic signatures associated to gases of interest are in the 2.5 – 15  $\mu\text{m}$  spectral range (4000-350  $\text{cm}^{-1}$ ). This spectral range can be addressed by emissions from rare-earth ions embedded into chalcogenide glasses which are well-known for having low phonon energies. We will show results concerning the development of an all-optical sensor at 4.4 $\mu\text{m}$  based on rare-earth doped chalcogenide glasses. The sensor schematic is presented in figure 1: a diode pumped Dy<sup>3+</sup> doped chalcogenide fiber first produces the infrared signal, which is then sent to the gas cell to probe the gas absorption at 4.4  $\mu\text{m}$ . The probe IR signal is then converted to 800nm by excited state absorption within an Er<sup>3+</sup> doped chalcogenide fiber making possible to transport the probe signal through a silica optical fiber over large distances considerably increasing the scope of possible applications.

The optimization of the Dy<sup>3+</sup> doped 2S2G fiber as the IR source, which will be presented, is based on a comparison between experimental data and the modeling of the luminescent fiber. The energy conversion mechanism from 4.4  $\mu\text{m}$  to 800 nm presented in figure 2 has been recently successfully implemented in Er<sup>3+</sup> doped GeGaSb(Se) chalcogenide fibers [1]. The IR probe signal is modulated while the pump is kept continuous. As a consequence, the 800 nm converted signal from the <sup>4</sup>I<sub>9/2</sub> level is itself modulated at the IR signal frequency which allows the discrimination between the 800nm “gas” signal and parasitic 800nm luminescence due to upconversion mechanisms (T<sub>22</sub> in Figure 2) by energy transfer among Er<sup>3+</sup> ions. Like for the Dy<sup>3+</sup> doped 2S2G fiber, the Er<sup>3+</sup> doped 2S2G fiber was optimized to obtain the best signal to noise ratio and the maximum fluorescence at 800nm. Different energy conversion schemes and the corresponding dependence of the converted signal with the pump and probe wavelengths and with photon fluxes will be presented. We will also discuss, using



experimental results and simulations, critical parameters for the energy conversion and the sensor itself such as the dopant concentrations, the fibers geometry or the impact of the pump upconversion parasitic signal on the converted signal to noise ratio.

[1] AL. Pelé, A. Braud, JL. Doualan, R.Chahal, V. Nazabal, B.Bureau, R. Moncorgé, and P. Camy, Optics Express, Vol. 23, Issue 4, pp. 4163-4172 (2015).

## **LOCALIZED SURFACE PLASMON RESONANCE BASED BIOSENSOR USING ALCOHOL OXIDASE FOR FORMALDEHYDE DETECTION**

Vivi Fauzia<sup>1</sup>, Nur Intan Pratiwi<sup>2</sup>, Nurlily<sup>3</sup>, Dede Djuhana<sup>4</sup>, Adhi Harmoko<sup>5</sup>, Cuk Imawan<sup>6</sup>  
*Department of Physics, Faculty of Mathematics and Natural Sciences,  
University of Indonesia, Depok, Indonesia, <sup>1</sup>vivi@sci.ui.ac.id, <sup>2</sup>nurintan15@gmail.com,  
<sup>3</sup>kusuma\_lily@yahoo.com <sup>4</sup>dede.djuhana@sci.ui.ac.id <sup>5</sup>adhi@sci.ui.ac.id,  
<sup>6</sup>imawan.cuk@gmail.com*

Noble metal nanoparticles has attracted much attention because of its unique physical and chemical properties that is different with those of bulk state. One of the unique optical properties of metal nanoparticles is the enhanced absorption and scattering of light around metal nanoparticles commonly called localized surface plasmon resonance (LSPR). Their resonance property has tremendous potential to be applied in the optical sensor devices that has advantages over conventional sensors such as ultra high refractive index sensitivity, fast response, label-free and real-time. In this work, we developed a new formaldehyde biosensor utilizing the LSPR properties of gold nanoparticles. Gold nanoparticles was grown directly on indium tin oxide coated glass using seed-mediated growth method, and further coated by mixture of butyl acrylate, 1.6 hexanedioldiacrylate and acrylic acid N-hydroxysuccinimide ester for immobilization of enzyme alcohol oxidase. By monitoring the LSPR peak wavelength shift in UV-VIS spectrophotometer, the limit of the sensor will be discovered. The mechanism of gold nanoparticles response to the presence of formaldehyde will be discussed.

## INNOVATIVE COPPER-DOPED GLASSES AND FIBERS AS SENSITIVE MATERIALS FOR IONISING BEAM DOSIMETRY

Bruno Capoen<sup>a</sup>, Hicham El Hamzaoui<sup>a</sup>, Mohamed Bouazaoui<sup>a</sup>, Laurent Bigot<sup>a</sup>, Géraud Bouwmans<sup>a</sup>, Youcef Ouerdane<sup>b</sup>, Aziz Boukenter<sup>b</sup>, Sylvain Girard<sup>b</sup>, Geneviève Chadeyron<sup>c</sup>, Rachid Mahiou<sup>c</sup>, Claude Marcandella<sup>d</sup>, Olivier Duhamel<sup>d</sup>

<sup>a</sup> *Laboratoire PhLAM/IRCICA, CNRS-Université Lille 1, Villeneuve d'Ascq, France*

<sup>b</sup> *Laboratoire Hubert Curien, CNRS-Université Jean Monnet, Saint-Etienne, France*

<sup>c</sup> *ICCF, CNRS-Université Blaise Pascal, Aubière, France*

<sup>d</sup> *CEA-DAM, Bruyères-le-Châtel, France*

In the field of ionizing radiation dosimetry, the optical fiber architecture is particularly suitable for applications requiring real time monitoring over a long distance both for dose measurements and spatial cartography. To this purpose, scintillating fibers exist, generally made of tissue-equivalent organic materials, which are particularly interesting to measure X-ray dose in radiotherapy applications. However, these plastic optical fibers exhibit rather poor guiding properties. Moreover, increased attenuation losses and degradation of the scintillating dopant may occur in those devices when exposed to high dose rates, which is a problem in nuclear applications in which radiation hardening is crucial. Inorganic radio-sensitive optical elements, such as doped silicate glasses and optical fibers, can overcome these difficulties.

Up to now, inorganic fibered dosimeters have been invented in the form of a radiosensitive element, for instance a piece of doped glass, coupled to one or several standard optical fibers that bring the light signal to the detector. In this configuration, the Radio-Luminescence (RL) and Optically Stimulated Luminescence (OSL) of copper-doped silica glasses have been previously investigated and exploited for 6 MeV photons and for doses of up to 50 Gy [1, 2].

In this paper, we show that such a radio-sensitive glass compound may be obtained with a high doping concentration using the sol-gel process. These sol-gel silica copper-doped rods have been successfully used as starting materials to achieve microstructured fibers [3]. All the obtained materials were optically characterized by using several spectroscopic tools (absorption, photoluminescence under UV excitation, decay times). A high visible emission quantum efficiency was evidenced and highlighted when the Cu-doped material was heat-treated under neutral atmosphere, which is due to the promotion of Cu<sup>+</sup> ions [4].

We also present RL and OSL measurements of a copper-doped sol-gel vitreous rod exposed to high dose rates of X-rays. The sample exhibited a reversible linear RL intensity versus the dose rate (up to 40 Gy/s), confirming the potentialities of this material for in vivo or remote dosimetry measurements. The OSL signal was also strong enough and did not saturate for doses up to 2500 Gy. However, a few limitations were identified, like a spontaneous thermal recombination phenomenon (fading) or a permanent darkening effect after the highest dose exposition (15 kGy) and some solutions are under study.

[1] B.L. Justus, P.L. Falkenstein, A.L. Huston, M.C. Plazas, H. Ning, R.W. Miller, *Appl. Opt.* 43 (2004) 1663-1668.

[2] A.L. Huston, B.L. Justus, P.L. Falkenstein, R.W. Miller, H. Ning, R. Altemus, *Nucl. Instr. Meth. Phys. Res. B* 184 (2001) 55-67.

[3] H. El Hamzaoui, Y. Ouerdane, L. Bigot, G. Bouwmans, B. Capoen, A. Boukenter, S. Girard, M. Bouazaoui, *Opt. Express* 20 (2012) 29751-29760.

[4] H. El Hamzaoui, G. Bouwmans, B. Capoen, Y. Ouerdane, G. Chadeyron, R. Mahiou, S. Girard, A. Boukenter, M. Bouazaoui, *Mater. Res. Express* 1 (2014) 026203.

## CHARACTERISATION OF BAM:Eu<sup>2+</sup> AND ZnO PHOSPHOR PARTICLES FOR TEMPERATURE IMAGING IN FLUIDS

Christopher Abrama, Benoit Fondb, Frank Beyraua

aLehrstuhl für Technische Thermodynamik, Otto-von-Guericke-Universität Magdeburg,  
39106 Magdeburg, Germany, christopher.abram@ovgu.de, frank.beyrau@ovgu.de

bDepartment of Mechanical Engineering, Imperial College London, London SW7 2AZ, UK,  
b.fond10@imperial.ac.uk

Laser-based measurement techniques are essential for fundamental studies of fluid-mechanical turbulence, convective heat transfer and reacting flows. In recent work, we developed a novel technique for simultaneous temperature and velocity imaging based on thermographic phosphor particles, which are seeded in the flow as a tracer [1,2]. The particles are excited using a pulsed (ns) UV laser, and the ensuing temperature-dependent luminescence emission is imaged to measure the particle temperature using a two-colour, ratio-based method. Simultaneously, laser light scattered by the particles is imaged to determine the flow velocity using conventional particle image velocimetry (PIV). Micrometre-size particles follow the turbulent flow motion, and the particle temperature matches that of the surrounding gas [1]. This approach permits simultaneous temperature-velocity imaging, using simple instrumentation and a single chemically inert, robust tracer.

Suitable phosphors should have a large absorption cross-section, high quantum efficiency and short ( $\sim\mu\text{s}$ ) luminescence lifetime. Additionally, to measure at temperatures  $>1000\text{ K}$  or with a high precision, delayed onset of thermal quenching and a pronounced temperature-dependence of the emission spectrum are essential. We have identified two suitable phosphors, BAM:Eu<sup>2+</sup> and ZnO. We seek to determine the benefits and limitations of these tracer particles, and gain a deeper understanding of the interaction of the excitation laser with particles dispersed in a fluid.

Toward this aim, we present characterisation measurements of both BAM:Eu and ZnO particles. A particle counting tool [3] is used to measure the emission intensity per particle and compare the temperature precision attained with each phosphor. ZnO is shown to be more than three times more sensitive in the range 300-500 K. The thermal quenching of BAM:Eu is characterised, with the conclusion that this phosphor can be used up to 920 K with a precision of 45 K (5%). The emission of BAM:Eu is shown to be insensitive to oxygen partial pressures in the range 0-200 mbar.

Saturation of the luminescence signal at laser fluences  $>5\text{ mJ/cm}^2$  is identified for both phosphors. Excitation at 355 and 266 nm (spectral bandwidth  $<1\text{ cm}^{-1}$ ) and 376 nm ( $200\text{ cm}^{-1}$ ) does not alter the saturation behavior of BAM:Eu. Potential laser-induced heating of the particles is investigated, and for ZnO an additional effect of excitation irradiance on the luminescence emission is confirmed.

These phosphors are shown to be suitable tracers for measurements in fluid flows, affording new capabilities for simultaneous vector-scalar imaging. Most importantly, there is an infinite variety of thermographic phosphors, the vast majority of which are unexplored for thermometry. Thus there are broad perspectives for further development of this promising technique, which will involve novel particle characterisation methods and new or optimised phosphors with enhanced luminescence properties.

[1] B. Fond, C. Abram, A.L. Heyes, A.M. Kempf, F. Beyrau, *Opt. Express* 20 (2012) 22118-22133.

[2] C. Abram, B. Fond, A.L. Heyes, F. Beyrau, *Appl. Phys. B-Lasers O.* 111 (2013) 155-160.

[3] B. Fond, C. Abram, F. Beyrau, *Appl. Phys. B-Lasers O.* 118 (2015) 393-399

## ADVANCED OPTICAL REMOTE SENSORS FOR AIRBORNE AND SPACEBORNE PLATFORMS

M. M. Cazacu<sup>a,b</sup>, A. Timofte<sup>a,c</sup>, O. Rusu<sup>a</sup>, B. Albina<sup>a</sup>, G. Bulai<sup>a</sup>,  
L. Leontie<sup>a</sup>, and S. Gurlui<sup>a</sup>

<sup>a</sup>*Faculty of Physics, Alexandru Ioan Cuza University of Iasi, Bulevardul Carol I, nr. 11,  
700506 Iasi, Romania, sgurlui@uaic.ro*

<sup>b</sup>*Physics Department, Gheorghe Asachi Technical University of Iasi, 59A Mangeron Blvd.,  
700050 Iasi, Romania, cazacumarius@gmail.com*

<sup>c</sup>*National Meteorological Administration, Regional Forecast Center Bacau, 3 Timpului Str.,  
Bacau, Romania, timofte.adrian@gmail.com*

Study of the atmospheric aerosol optics and behavior of ultra trace amounts of organic or inorganic compounds plays a key role in Earth physics. To determine physico-chemical properties of divers species, their concentrations and associated human health risk, as well as impact on climate changes, different sensors, both ground-based and satellite optical instruments are currently extensively used. Moreover, satellite spectral instruments which provide continuous, long-term data sets, indispensable for environmental forecasting and global climate studies have, in particular, a great potential for atmospheric pollutants detection, as well as for estimation of water amount, brightness temperatures, etc. Thus, satellite remote sensing provides global coverage (latitude and longitude), but it also can encounter difficulties in analyzing a specific altitude range: time (magnitude of seconds)-space (magnitude of few km) resolution of measurements is insufficient for measuring and understanding fast chemical and optical processes induced by various physical atmospheric factors. In order to better understand the fundamentals of some critical physico-chemical transformations of the atmospheric compounds and for practical purpose, our study relies on a new optical power instrument. It is able to capture a fast plume airborne image (2 ns gate time) and can be used to real-time investigate the behavior of several chemical compounds at a given point of the free atmosphere, with a spatial resolution of up to 1 cm. This new remote sensing optical instrument is based on the fast imaging and space-time resolved Raman Spectroscopy of both airborne and spaceborne plumes. Formation and dynamics of the airborne plume were studied by means of an optical telescope and a high-resolution monochromator (Acton SP2750i) coupled to a Princeton Instruments ICCD camera (Roper Scientific PIMAX3- UNIGEN2, 1024 × 1024 pixels, 2 ns minimum gate time). To investigate the scattered radiation of the chemical species we used a laser beam with a continuously variable wavelength (205–700 nm), generated by a High Resolution-UV/Visible-Optical Parametric Oscillator (HR-UV/V-OPO), pumped by the 3<sup>rd</sup> harmonic of a Q-switched Nd:YAG Laser (Quantel Brilliant EaZy). Preliminary optical measurements of airborne plume found over Iasi County (Romania) reveal interesting dynamics of several chemical compounds in altitude, including dust, nitrogen, carbonate molecules or ice in special structural forms etc.

### Acknowledgements

This work was financially supported by the Romanian Space Agency (ROSA) within Space Technology and Advanced Research (STAR) Program (Project nr. 98/29.11.2013) and by the strategic grant POSDRU/159/1.5/S/137750, Project “Doctoral and Postdoctoral programs support for increased competitiveness in Exact Sciences research” cofinanced by the European Social Found within the Sectorial Operational Program Human Resources Development 2007 – 2013.



## EVOLUTION OF Eu AND Mn OXIDATION STATE IN DOPED BaMgAl<sub>10</sub>O<sub>17</sub> DURING X-RAY IRRADIATION

Lucia Amidani<sup>a</sup>, Katleen Korthout<sup>b</sup>, Marte Van der Linden<sup>c</sup>, Andries Meijerink<sup>d</sup>, Philippe Smet<sup>b</sup>, Dirk Poelman<sup>b</sup>, Pieter Glatzel<sup>a</sup>

<sup>a</sup>*ESRF, 71 Avenue des Martyrs, Grenoble, France, Amidani@esrf.fr, Glatzel@esrf.fr*

<sup>b</sup>*Department of Solid State Science, Lumilab, Ghent University, Krijgslaan 281-S1, Gent, Belgium, Katleen.Korthout@UGent.be, Philippe.Smet@UGent.be, Dirk.Poelman@UGent.be*

<sup>c</sup>*Inorganic Chemistry and Catalysis, Debye Institute for Nanomaterials Science, Utrecht University, Universiteitslaan 99, 3584 CG Utrecht, The Netherlands,*

*M.vanderLinden1@uu.nl*

<sup>d</sup>*CMI, Debye Institute for Nanomaterials Science, Utrecht University, 3508 TA, Utrecht, The Netherlands, A.Meijerink@uu.nl*

BaMgAl<sub>10</sub>O<sub>17</sub> (BAM) is a technologically very important host for luminescent impurities: when doped with Eu it is one of the best blue phosphors on the market, when doped with Mn it is a green emitting phosphor, albeit with poor efficiency. Doping with both Mn and Eu greatly improves the green emission from Mn and opens the way to the use of BAM:Eu,Mn as an alternative to more expensive rare-earth based green phosphors.

Optimization of BAM based phosphors is of great importance for modern lighting applications. The interplay of structural and electronic properties at the atomic level on the luminescent efficiency is still not well understood.

High resolution x-ray absorption spectroscopy (XAS) is a chemically selective technique probing the local coordination and electronic structure of a selected atomic species and can be used to investigate both Eu and Mn in singly doped and co-doped BAM phosphors. When applied to inorganic phosphors, x-rays do not only act as a probe but also as a source of excitation and potential irreversible damage. By collecting the radioluminescence from the sample in parallel to x-ray spectra a complete view on sample efficiency and evolution of impurities local structure is obtained.

We systematically investigated Eu and Mn singly and co-doped BAM phosphors with high resolution XAS at Eu L<sub>III</sub>- and Mn K- edges in two sets of BAM samples. Mn is always found in 2+ oxidation state and preferentially in tetrahedral sites. Eu impurities on the contrary are found in both 2+ and 3+ oxidation states, with Eu<sup>2+</sup>/Eu<sup>3+</sup> ratio varying from sample to sample. X-ray irradiation at high flux induces relevant variations to this scenario: Eu undergoes fast oxidation to Eu<sup>3+</sup> while the local structure of Mn is unaffected. In parallel, the luminescence of both Mn and Eu degrades at a rate following Eu oxidation.

Our investigation confirms that the stability of the conduction layer, where Eu is incorporated, plays a central role in determining luminescence properties of BAM [1,2]. The rate of Eu oxidation was found sample dependent, indicating that growing conditions and/or co-doping may affect the stability of the conduction layer.

[1] P. Boolchand, K. C. Mishra, M. Raukas, A. Ellens, P. C. Schmidt, Phys. Rev. B 66 (2002) 134429.

[2] G. Bizarri, B. Moine, J. of Luminesc. 113 (2005) 199-213.

## GLASS-BASED 1-D DIELECTRIC MICROCAVITIES

Alessandro Chiasera<sup>a</sup>, Francesco Scotognella<sup>b,c</sup>, Sreeramulu Valligatla<sup>a,d,e</sup>, Stefano Varas<sup>a</sup>, Jacek Jasieniak<sup>f</sup>, Luigino Criante<sup>c</sup>, Anna Lukowiak<sup>g</sup>, Davor Ristic<sup>h,i</sup>, Stefano Taccheo<sup>j</sup>, Mile Ivanda<sup>h,i</sup>, Giancarlo C. Righini<sup>k,l</sup>, Roberta Ramponi<sup>b</sup>, Alessandro Martucci<sup>m</sup>, Maurizio Ferrari<sup>a,k</sup>

<sup>a</sup>*IFN - CNR CSMFO Lab. & FBK CMM, via alla Cascata 56/C Povo, 38123 Trento, Italy, maurizio.ferrari@ifn.cnr.it*

<sup>b</sup>*Politecnico di Milano, Dipartimento di Fisica and IFN-CNR, Piazza Leonardo da Vinci 32, 20133 Milano, Italy, francesco.scotognella@polimi.it; roberta.ramponi@polimi.it*

<sup>c</sup>*Center for Nano Science and Technology@PoliMi, Istituto Italiano di Tecnologia, Via Giovanni Pascoli, 70/3, 20133, Milan, Italy, Luigino.Criante@iit.it*

<sup>d</sup>*Dipartimento di Fisica, Università di Trento, via Sommarive 14, Povo, 38123 Trento, Italy.*

<sup>e</sup>*School of Physics, University of Hyderabad, Hyderabad 500046, India, srihcu08@gmail.com*

<sup>f</sup>*CSIRO Manufacturing Flagship, Ian Wark Laboratory, - 3168 – Clayton, Australia, Jacek.Jasieniak@csiro.au*

<sup>g</sup>*Institute of Low Temperature and Structure Research, PAS, 2 Okolna St., 50-422 Wrocław, Poland, A.Lukowiak@int.pan.wroc.pl*

<sup>h</sup>*Ruđer Bošković Institute, Division of Materials Physics, Laboratory for Molecular Physics, Bijenička c. 54, Zagreb, Croatia, Davor.Ristic@irb.hr*

<sup>i</sup>*Center of Excellence for Advanced Materials and Sensing Devices, Research unit New Functional Materials, Bijenička c. 54, Zagreb, Croatia, ivanda@irb.hr*

<sup>j</sup>*College of Engineering, Swansea University, Singleton Park, Swansea, UK, s.taccheo@swansea.ac.uk*

<sup>k</sup>*Centro di Studi e Ricerche Enrico Fermi, P.zza Viminale 1, 00184 Roma, Italy, giancarlo.righini@centrofermi.it*

<sup>l</sup>*IFAC - CNR, MiPLab, Via Madonna del Piano 10, 50019 Sesto Fiorentino, Italy.*

<sup>m</sup>*Dipartimento di Ingegneria Industriale, Università di Padova, via Marzolo 9, 35122, Padova, alex.martucci@unipd.it*

The development of optically confined structure is a major topic in both basic and applied physics including information engineering, biological and medical sciences, sensing. One-dimensional photonic crystals have been widely investigated and still remain an outstanding tool for new photonics, being the simplest system to exhibit a so-called photonic bandgap and therefore one of the easiest to handle in order to obtain tailored optical devices. RF sputtering techniques has demonstrated to be a viable technique for fabrication of 1D-photonic crystals allowing management and manipulation of the optical and spectroscopic properties [1,2]. Here we will present recent results obtained by our consortium regarding: (i) 1D photonic crystals allowing Er<sup>3+</sup> luminescence enhancement concerning the <sup>4</sup>I<sub>13/2</sub>-<sup>4</sup>I<sub>15/2</sub> transition; (ii) disordered 1D photonic structures that are very interesting for the modelization and realization of broad band filters and light harvesting devices; (iii) 1D microcavities, activated by a layer based on poly-laurylmethacrylate matrix containing CdSe@Cd<sub>0.5</sub>Zn<sub>0.5</sub>S quantum dots, leading to coherent emission.

[1] A. Chiasera, J. Jasieniak, S. Normani, S. Valligatla, A. Lukowiak, S. Taccheo, D.N. Rao, G.C. Righini, M. Marciniak, A. Martucci, M. Ferrari, *Ceramics International* 41(2015)7429-7433.

[2] F. Scotognella, A. Chiasera, L. Criante, S. Varas, I. Kriegel, M. Bellingeri, G.C. Righini, R. Ramponi, M. Ferrari, *Proc. of SPIE* 9364 (2015) 93640Y-1/8.

## THE CHEMICAL BOND OVERLAP POLARIZABILITY AND COVALENCY. CONCEPTS AND APPLICATIONS: FROM DIATOMIC MOLECULES TO SOLIDS

Renaldo T. Moura Jr., Ricardo L. Longo, Oscar L. Malta

*Departamento de Química Fundamental-CCEN- Universidade Federal de Pernambuco, Cidade Universitária, 50.740-560, Recife, PE-Brazil. \* oscar.malta@ufpe.br*

The concepts of chemical bond overlap polarizability (OP) and ionic specific valence (ISV) have been introduced, about a decade ago (2002), in the context of the ligand field theory applied to lanthanide compounds. These concepts led to relevant conclusions on the interpretation of the non-spherical ligand field interaction in terms of covalency. They have also been explored in a more general context outside the scope of ligand field theory. Thus, they have proven to be useful in the case of diatomic molecules, allowing to establish a new covalency scale in excellent agreement with Pauling's scale and analytically quantifiable in terms of the OP.

An analysis on this subject in 2005, in which the overlap region is regarded as a localized plasmon-like mode of oscillation (chemical bond overlap plasmon - CBOP), characterized by the OP, has raised the possibility of absorption and inelastic scattering of radiation, specifically by the overlap region, in an oscillation mode distinguishable from the collective plasmon of the system. Predicted oscillator strengths and scattering cross sections for diatomic molecules are considerably high and can be measured in the UV up to the near soft-X-rays spectral regions. The possibility of detecting the CBOP in diatomic molecules by electron energy-loss measurements has also been analyzed. Different treatments by using the Valence Bond Theory and a Localized Molecular Orbital approach have been evoked to describe the OP concept and the CBOP proposal, in polyatomic molecules and hydrogen bond. The CBOP has been shown as a promising tool for quantifying covalency also in solid-state materials, opening a way to classifying materials in terms of average covalent fractions. Interesting questions could be raised on possible relationships between macroscopic properties of materials and the OP concept. For instance, a good correlation has been found between the non-linear index of refraction ( $n_2$ ) and the OP, though the comparison has been made between the precursor diatomic molecule and the solid-state material.

Some unassigned bands in the electron energy-loss and absorption spectra of crystalline alkaline-earth chalcogenides and some alkali and alkali-earth metals in solid-state systems have been discussed in terms of the CBOP, raising the possibility of new assignments alternative to exciton or band-to-band transitions [1].

**Acknowledgements** This work was supported by CNPq, FACEPE, PRONEX, INCT-INAMI

[1] Moura Jr., RT, Malta OL, Longo RL, *Int. J. Quant. Chem.* 2005, **111**, 1626 – 1638, and Refs therein.

## **MOLECULAR IMAGING AND KILLING OF LATENTLY EBV- INFECTED TUMOR CELLS BY THE DEVELOPMENT OF EBNA1- SPECIFIC LANTHANIDE BIOPROBES**

Ka-Leung Wong

*Department of Chemistry, Hong Kong Baptist University, Kowloon Tong, Hong Kong*

Epstein-Barr virus (EBV) is etiologically implicated in several lymphoid and epithelial malignancies, substantially contributing to the development of a diversity of lymphomas and carcinomas. Such presence of EBV in the tumor cells of EBV-associated cancers can, therefore, provide overarching basis for specific therapy.

Although current treatments for EBV-associated carcinoma, such as radiotherapy and chemotherapy have long been adopted, the former is inadequate either to kill advanced, metastatic tumor or to prevent their recurrence, while the latter is still under development. The dimeric viral oncoprotein, Epstein-Barr nuclear antigen (EBNA1), is known to be responsible for the development of EBV-related malignancies and the maintenance of EBV episome. Given that carcinogenesis of EBV-associated carcinoma is symbiotically connected with EBV infection and EBNA1 can function (e.g. replication, DNA binding and transactivation) only upon dimerization (formation of the active form), we hypothesize that a fluorescent probe consisting of a chromophore and an EBNA1-specific molecule which hampers the dimer formation can be used for the imaging and inhibition of latent EBV-infected cells.

In the poster, we are going to show some of our progress in the development of responsive bioprobes for inhibition of EBNA1 dimerization. Our study are provided a novel strategy to interfere the growth of EBV-associated tumor cells. All our europium complexes are all water-soluble and cell-permeable for EBNA1 *in vitro* imaging and inhibition. We hope our work here can bring to society a more powerful tool (especially able to combine multi-photon and time-resolved technology) to unveil the mystery and understand the very role of EBNA1 in EBV-associated carcinoma for further cancer therapy and research.

[1] L. Jiang, L.L. Lau, H. Li, C.F. Chan, R.F. Lan, W.L. Chan, T.C.K. Lau, G.S.W. Tsao, N.K. Mak, K.L. Wong, *Chem. Commun.*, 50 (2014) 6517-6519

## RARE EARTH-DOPED NANOPARTICLES AS NEW PHOTOTHERMAL AGENTS: FUNDAMENTALS AND *IN VIVO* APPLICATIONS

Blanca del Rosal<sup>a</sup>, Elisa Carrasco<sup>b</sup>, Francisco Sanz-Rodríguez<sup>a,c,d</sup>, Ángeles Juarranz de la Fuente<sup>b,c</sup>, Ueslen Rocha<sup>a</sup>, Kagola Upendra Kumar<sup>e</sup>, Carlos Jacinto<sup>e</sup>, D. J. Jovanović<sup>f</sup>, M. D. Dramićanin<sup>f</sup>, José García Solé<sup>a</sup> and Daniel Jaque<sup>a</sup>

<sup>a</sup>*Fluorescence Imaging Group. Departamento de Física de Materiales, Facultad de Ciencias. Campus de Cantoblanco, Universidad Autónoma de Madrid. Madrid 28049, Spain*

<sup>b</sup>*Instituto de Investigaciones Biomédicas “Alberto Sols”, CSIC-UAM. Madrid 28029, Spain*

<sup>c</sup>*Departamento de Biología, Facultad de Ciencias. Campus de Cantoblanco. Universidad Autónoma de Madrid. Madrid 28049, Spain*

<sup>d</sup>*Instituto Ramón y Cajal de Investigación Sanitaria, Hospital Ramón y Cajal, Madrid 28034, Spain*

<sup>e</sup>*Grupo de Fotônica e Fluidos Complexos. Instituto de Física, Universidade Federal de Alagoas 57072-970, Maceió, Alagoas, Brazil*

<sup>f</sup>*Vinča Institute of Nuclear Sciences, University of Belgrade, P.O. Box 522, 11001, Serbia*

Photothermal therapy, which relies on light-induced heating to irreversibly damage cancer cells is nowadays attracting a great deal of attention as an effective and low cost technique for treating malignant tumors.[1] Different types of nanoparticles have been successfully used to achieve localized heating in cancer tumors in animal models.

Most recently, the attention is focused on obtaining multifunctional platforms which, besides releasing a significant amount of heat upon laser irradiation, allow for simultaneous imaging and temperature sensing. For this purpose, neodymium-doped nanoparticles arise as excellent candidates thanks to their infrared luminescence properties, including the temperature sensitivity of some of its emission bands.

Using these nanoparticles, fluorescence imaging can be used to evaluate their incorporation in the tumor to be treated. Moreover, intratumoral temperature can be measured through spectral analysis of the fluorescence signal, thus allowing for a temperature-controlled photothermal treatment that cannot be achieved traditional thermometry techniques.

In this work, Nd<sup>3+</sup>:LaF<sub>3</sub> and NdVO<sub>4</sub> nanoparticles have been explored as photothermal agents during *in vivo* experiments in animal models. Moreover, Nd<sup>3+</sup>:LaF<sub>3</sub> nanocrystals have been used for continuous intratumoral temperature monitoring during photothermal therapy. These infrared-emitting nanoparticles double as efficient *in vivo* heating agents and temperature sensors. The use of this kind of nanoparticles for temperature-controlled therapy opens the way for highly efficient and minimally invasive photothermal treatments of cancer tumors.

[1] D. Jaque L. Martínez Maestro, B. del Rosal, P. Haro-Gonzalez, A. Benayas, J. L. Plaza, E. Martín Rodríguez and J. García Solé. *Nanoscale*, 6 (2014) 9494-9530

## NIR-II EMITTING QUANTUM DOTS AND RE<sup>3+</sup>-DOPED NANOPARTICLES: PROSPECTS AT THE MULTIFUNCTIONALITY BATTLEGROUND FOR BIO-IMAGING AND THERMAL SENSING

A. Benayas<sup>a</sup>, F. Ren<sup>a</sup>, D. Ortgies<sup>b</sup>, E. Carrasco<sup>c,d</sup>, E. Navarro<sup>b</sup>, B. del Rosal<sup>b</sup>, A. Juarranz<sup>c,d</sup>, F. Sanz-Rodríguez<sup>c</sup>, G.A. Hirata<sup>e</sup>, D. Jaque<sup>b</sup>, F. Vetrone<sup>a\*</sup>, E. Martín-Rodríguez<sup>b</sup>, D.L. Ma<sup>a</sup>

<sup>a</sup>Univ Quebec, INRS, 1650 Blvd Lionel Boulet, Varennes, PQ J3X 1S2, Canada

<sup>b</sup>Univ Autonoma Madrid, Fac. Ciencias, Fluorescence Imaging Group, Dept. Fis. Mat, E-28049 Madrid, Spain. <sup>3</sup>Univ Autonoma Madrid,

<sup>c</sup>Fac Med, CSIC, Inst. Invest. Biomed. Alberto Sols, Dept Bioquim, E-28029 Madrid, Spain.

<sup>d</sup>Univ Autonoma Madrid, Fac. Ciencias, Dept. Biol., E-28049 Madrid, Spain.

<sup>e</sup>CNyN, Ensenada, 22800 Baja California, Mexico

antonio.benayas@uam.es

Near infrared (NIR) nanoprobes, such as NIR-emitting quantum dots (QDs), or NIR-emitting rare earth (RE<sup>3+</sup>) doped nanoparticles, are deservedly attracting a great deal of attention for imaging and sensing purposes[1]. Here we report, first, on the imaging and nanothermometry remarkable features achieved by building up biocompatible PbS/CdS/ZnS core/shell/shell QDs. They emit slightly above 1250nm, in the so-called Second Biological Window (2<sup>nd</sup> BW, that is 1000-1350nm)[2], thus reaching higher sub-tissue penetration depths in the biological context. Our outstanding *in vivo* imaging results, regarding both injected nanoprobes' low-dose and all-optical biodistribution tracking, are discussed within the current state-of-the-art with respect to competitors such as Ag<sub>2</sub>S nanoprobes.

On the other hand we are also here reporting the development of efficient Nd:YAG fluorescent nanothermometers, that have demonstrated remarkable thermal sensitivity performance on NIR-1<sup>st</sup> BW (700-950nm) temperature-monitoring applications (electrical circuits, sub-tissue measurements and optical trapping context)[3]. Continuing with the comparative aim along this work, we illustrate the major insights of the YAG host that may eventually make it an advantageous player among other widely used fluoride hosts.

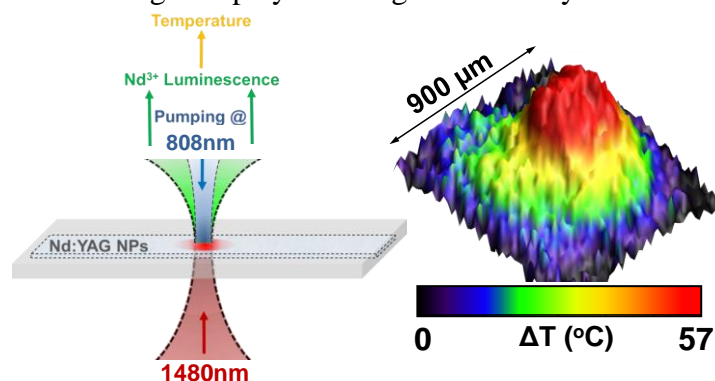


Figure 1. Schematic representation of the experimental set up (left) and thermal image (right) of the T-gradient created upon 1480 nm laser pumping of a microchannel filled with Nd:YAG NPs.

Finally, we discuss the encapsulated hybrid 2<sup>nd</sup> BW nanothermometers: the QDs discussed above together with RE<sup>3+</sup>-doped NaGdF<sub>4</sub> nanoparticles (NPs). In a single polymeric nanocapsule, we benefit from the very different temperature-dependent fluorescence emission behaviour by playing together the T-independent emission intensity from RE<sup>3+</sup>-doped NPs with the T-quenched emission form the NIR-QDs. Thus, we got a high-sensitivity, real-time fluorescence nanothermometry platform, that arguably paves the way for temperature-based diagnosis and therapeutic techniques. Prospects in that field are also thoroughly discussed.

[1] N.G.Horton, et al. Nat. Photonics 7 (2013) 205-209 [2] T. Lim et al Mol. Imaging 2 (2003) 50-64 [3] A. Benayas et al. Ad. Opt. Mat 3 (2015) 687-694

## CO-ENCAPSULATION OF CdSe-ZnS QUANTUM DOTS AND PHTHALOCYANINE IN NANOCARRIERS FOR PHOTODYNAMIC THERAPY

*Janusz Szeremeta, Sławomir Drozdek, Marcin Nyk, Kazimiera A. Wilk, Marek Samoc  
Faculty of Chemistry, Wrocław University of Technology Wybrzeże Wyspińskiego 27,  
50-370 Wrocław, Poland*

In the photodynamic therapy (PDT) the photoexcited sensitizer molecules generate reactive oxygen species (ROS) in order to destroy cancer tissues. There are two important issues that have to be considered in the design of the efficient therapeutic systems. Firstly, the highly cytotoxic sensitizer has to be delivered straight into diseased tissue without harming healthy cells. This is possible by delivering the drug enclosed into capsules that will penetrate selectively into tumour cells, where the drug will then be released. Secondly, to extend the depth of the penetration into the tissue it is convenient to use near-infrared (NIR) photosensitization, because it utilizes the biological window of optical transparency. However, this requires a process of the energy upconversion so that the electronic energy level of the photosensitizer is higher than the singlet oxygen energy level and this can be achieved e.g. by two-photon absorption (2PA). Because photosensitizers usually possess rather low 2PA cross sections, it is necessary to couple them with other strongly multi-photon absorbing species. [1]

To meet these requirements we designed a new theranostic system, in which core-shell CdSe<sub>x</sub>S<sub>1-x</sub>/ZnS quantum dots (QDs) together with zinc phthalocyanine (ZnPc) were encapsulated in biocompatible polymer nanocapsules. The idea is to excite the QDs by two-photon absorption process, which will be followed by transfer of the energy to the photosensitizer (ZnPc), able to produce reactive oxygen species (ROS).

We report a new approach to fabricate nanocapsules prepared via solvent/evaporation method, where Poloxamer 403 was applied as the polymer component; Cremophor EL<sup>®</sup> as the nonionic surfactant and silicone oil with hydrogenated caprylyl olive oil esters as the oil phase. Dynamic light scattering (DLS), transmission electron microscopy (TEM) and atomic force microscopy (AFM) examinations confirmed the particle diameter below 150 nm and polydispersity of ca. 0.2-0.3. UV-Vis absorption and fluorescence studies confirmed successful encapsulation of the optically active QDs/ZnPc system. For use as the reference in the optical studies we also obtained nanocapsules with only QDs or ZnPc. The size of the QDs was chosen so that their fluorescence spectrum efficiently overlapped the absorption spectrum of ZnPc in order to enable the Förster resonance energy transfer (FRET). Proof of the existence of this interaction in a homogeneous solution was reported previously [2]. QDs are known as strong two-photon absorbers [3], therefore under irradiation with NIR fs pulse laser significant fluorescence of both QDs and ZnPc is observed. The shortening of the QDs fluorescence lifetimes confirmed FRET between both species. Finally, we confirmed the generation of the ROS by quenching of the bovine serum albumin, under irradiation in the presence of the nanocapsules filled with both QDs and ZnPc.

**Acknowledgements:** This work was financed by the National Science Center (Poland) under Grant No. 2012/05/B/ST4/00095.

[1] A. V. Kachynski, A. Pliss, A. N. Kuzmin, T. Y. Ohulchansky, A. Baev, J. Qu, P. N. Prasad, *Nat Photonics* 8 (2014) 455-461.

[2] M. Nyk, K. Palewska, L. Kepinski, K. Wilk, W. Strek, M. Samoć, *J. Luminescence* 130 (2010) 2487-2490.

[3] M. Nyk, D. Wawrzyńczyk, J. Szeremeta, M. Samoc, *Appl. Phys. Lett.* 100 (2012) 041102.

## CARBON DOTS (C-DOTS) FROM COW MANURE WITH IMPRESSIVE SUBCELLULAR SELECTIVITY TUNED BY SIMPLE CHEMICAL MODIFICATION

Cintya D'Angelis do E. S. Barbosa, José R. Corrêa, Gisele M. Alves, Gabrielle Barreto, Kelly G. Magalhães, Aline L. de Oliveira, John Spencer, Brenno A. D. Neto, Marcelo O. Rodrigues  
 Instituto de Química, Campus Universitário Darcy Ribeiro, Brasília-DF, Brazil,  
 marcelozohio@gmail.com

*Department of Chemistry, School of Life Sciences, University of Sussex, Falmer, Brighton, East Sussex, BN1 9QJ, United Kingdom.*

Carbon quantum dots, also known as C-dots, are a class of nanomaterials which present optical properties similar to conventional quantum dots, but with advantage of good biocompatibility coupled to a low toxicity.<sup>1</sup> Based in our interest in the development of more selective bioprobes we report that C-dots synthesized from cow manure (or from glucose) by chemical oxidation, are capable of selectively staining the cell nuclei of breast cancer cells lineage (MCF-7) after a simple chemical modification with ethylenediamine. Four other cellular models were equally tested and showed excellent results using the modified C-dots.

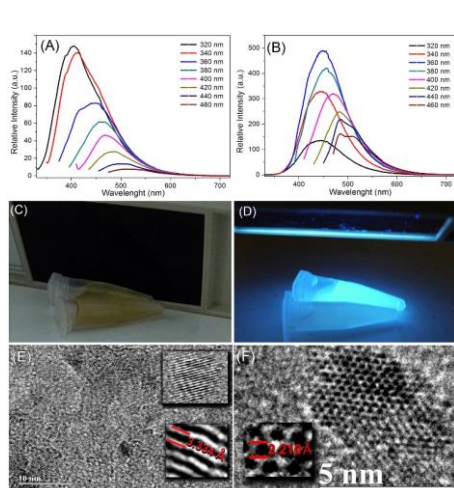


**Figura 1:** (A) and (B) Emission spectra of the C-dots and modified C-dots (respectively) (C) and (D) C-dots under white light and UV-light irradiation ( $\lambda_{exc} = 365 \text{ nm}$ ). (E) HRTEM images for the modified C-dots

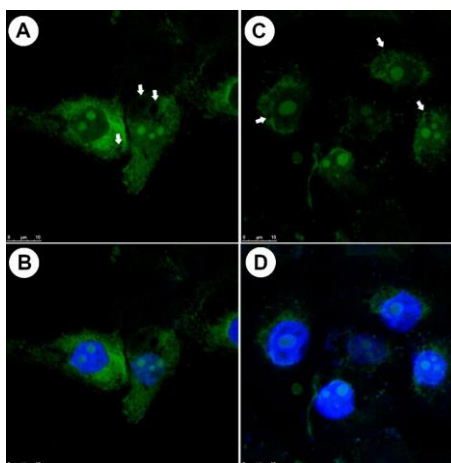


**Figura 2:** (A) and (B) show the modified C-dots stain pattern (green) for the fixed cells whereas (C) and (D) show the staining for live cells (MCF-7 cells). The cytoplasmic associations (pattern and distribution) are with ribosomal components. Bar scale of 10 μm.

Figure 1 shows the emission spectra of the C-dots and of the modified C-dots (treated with ethylenediamine), the luminescence images of the samples under UV-light irradiation and the HRTEM, respectively. Emission spectra of the samples show a gradual decrease of the fluorescence as a function of the excitation wavelength. The high bright fluorescence emission, especially for that exhibited by the modified C-dot, may be justified by the presence of surface energy trapping sites, which were stabilized by the passivating agent. The modified C-dots present a very precise subcellular localization with a real and impressive nucleoli selection (Figure 2). The predominance of acidic regions found in the nucleoli machinery is most probably responsible for the subcellular direction of the modified C-dots.<sup>1</sup>

[1]- C. D'Angelis do E. S. Barbosa, J. R. Corrêa, G. A. Medeiros, G. Barreto, K. G. Magalhães, A. L. de Oliveira, J. Spencer, M. O. Rodrigues and B. A. D. Neto, *Chem. - A Eur. J.*, 2015, **21**, 5055–5060.



## TUNABLE LUMINESCENT PROPERTIES AND CONCENTRATION-DEPENDENT, SITE-PREFERABLE DISTRIBUTION OF $\text{Eu}^{2+}$ IONS IN SILICATE GLASS FOR WHITE LEDS APPLICATIONS

Jing Wang, Xuejie Zhang

<sup>a</sup>State Key Laboratory of Optoelectronic Materials and Technologies, School of Chemistry and Chemical Engineering, Sun Yat-sen University, Guangzhou, Guangdong 510275, China, ceswj@mail.sysu.edu.cn

The design of luminescent materials with widely and continuously tunable excitation and emission is still a challenge in the field of advanced optical applications. In this paper, we reported a  $\text{Eu}^{2+}$ -doped  $\text{SiO}_2\text{-Li}_2\text{O-SrO-Al}_2\text{O}_3\text{-K}_2\text{O-P}_2\text{O}_5$  (abbreviated as SLSAKP: $\text{Eu}^{2+}$ ) silicate luminescent glass. Interestingly, it can give an intense tunable emission from cyan (474 nm) to yellowish-green (538 nm) simply by changing excitation wavelength and adjusting the concentration of  $\text{Eu}^{2+}$  ions. The absorption spectra, photoluminescence excitation (PLE) and emission (PL) spectra, and decay curves reveal that there are rich and distinguishable local cation sites in SLSAKP glasses and that  $\text{Eu}^{2+}$  ions show preferable site distribution at different concentrations, which offer the possibility to engineer the local site environment available for  $\text{Eu}^{2+}$  ions. Luminescent glasses based color and white LED devices were successfully fabricated by combining the as-synthesized glass and a 385 nm n-UV LED or 450 nm blue LED chip, which demonstrates the potential application of the site engineering of luminescent glasses in advanced solid-state lighting in the future.

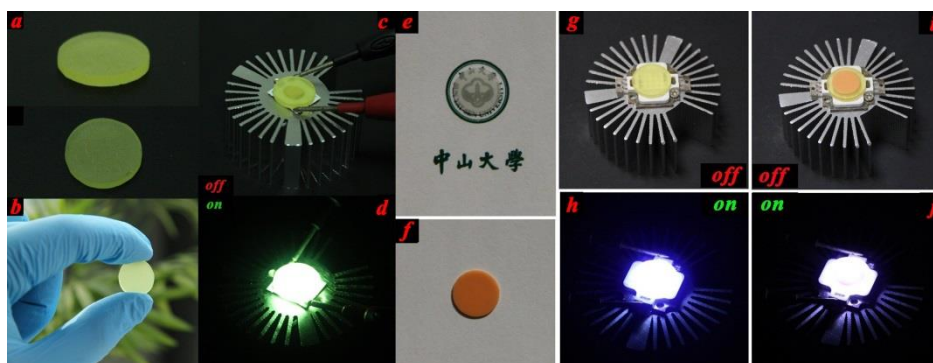


Figure 1. Photographs of SLSAKP:1.0%  $\text{Eu}^{2+}$  glass (a, b), glass without (e) and with (f) red phosphor  $\text{CaAlSiN}_3\text{:Eu}^{2+}$ , the fabricated luminescent glasses based green (c,d) and white LEDs without (g,h) and with (i,j) red phosphor  $\text{CaAlSiN}_3\text{:Eu}^{2+}$  driven by 100 mA current;

[1] X.J. Zhang, J. Wang, L. Huang, F.J. Pan, Y. Chen, B.F. Lei, M.Y. Peng, M.M. Wu, ACS Appl. Mater. Interfaces. 7 (2015), 10044-10054.

[2] X.J. Zhang, L. Huang, F.J. Pan, M.M. Wu, J. Wang, Y. Chen, Q. Su, ACS Appl. Mater. Interfaces. 2014, 6 (2014), 2709-2717.

[3] S. Zhou, Q. Guo, H. Inoue, Q. Ye, A. Masuno, B. Zheng, Y. Yu, J. Qiu, Adv. Mater. 26(2014), 7966-7972.

[4] M. Eichelbaum, K. Rademann, Adv. Funct. Mater., 19(2009), 2045-5252.

## CONTROLLING THE MORPHOLOGY OF $\text{YPO}_4:\text{Eu}^{3+}$ BY CHEMICAL PROCESSING PARAMETERS

Joanna Cybińska<sup>a,b</sup>

<sup>a</sup> Faculty of Chemistry, University of Wrocław, Poland, [jcybinska@chem.uni.wroc.pl](mailto:jcybinska@chem.uni.wroc.pl)

<sup>b</sup> Department of Nanotechnology, Wrocław Research Centre EIT+, Poland

Phosphor materials based on orthophosphates have been widely investigated in the past. They combine high energy fundamental with excellent chemical and mechanical stability. These non-hygroscopic crystal matrices are able to accommodate high concentrations of lanthanide ions without suffering from concentration quenching of the luminescence [1].  $\text{YPO}_4$  as nanopowder material can be obtained by a variety of synthesis processes, for examples solid state, sol-gel, Pechini's, hydrothermal, combustion methods. However, to get full benefit of all the advantages of the nanocrystalline phosphors potentials it is necessary to find a synthesis route giving a control over the products morphology. This, in turn, allows to manage their spectroscopic properties.

In this work the studies of the influence of synthesis route on the optical properties and the morphology of the nano- and microscale  $\text{YPO}_4$  doped with  $\text{Eu}^{3+}$  ions (5%) are presented. The investigated samples were prepared by classic hydrothermal method and its ionic-liquids-assisted modification. By changing the conditions of the reaction (pH, T or time) it is possible to control the shape and size of the particles. Based on the results obtained from electron microscope studies (TEM and SEM) it was possible to correlate the morphology of the nanophosphates with their optical properties such as decay times or emission quantum yield.

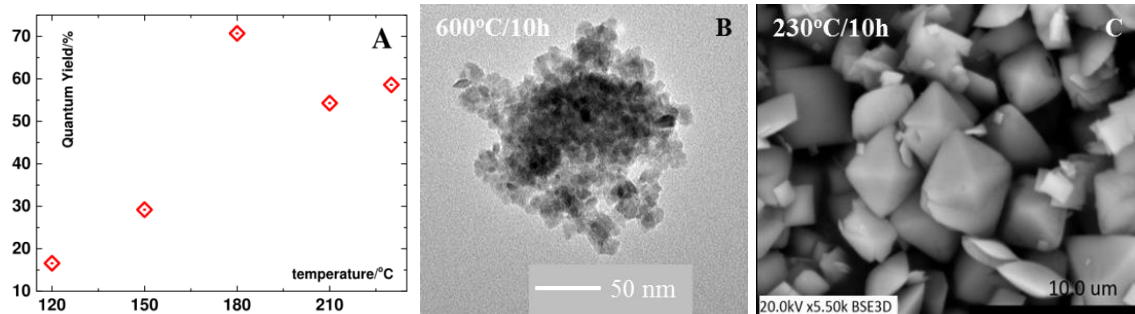


Fig. Absolute quantum efficiency of the  $\text{YPO}_4:\text{Eu}$  obtained by hydrothermal method as a function of the synthesis temperature (A). TEM and SEM micrographs of  $\text{YPO}_4:\text{Eu}$  synthesized using IL assisted hydrothermal method 600°C (B) and hydrothermal method at 230°C (C).

### Acknowledgement

This work was partially supported under grant # POIG.01.01.02-02-006/09 of the Minister of Science and Higher Education (Poland).

[1] J. Cybinska, C. Lorbeer, E. Zych, A.V. Mudring, *ChemSusChem*, 4, 595 (2011)

## EFFICIENCY DROOP IN AlGa<sub>N</sub> EPTAXIAL LAYERS AND MULTIPLE QUANTUM WELLS

J. Jurkevičius<sup>a</sup>, J. Mickevičius<sup>a</sup>, A. Kadys<sup>a</sup>, G. Tamulaitis<sup>a</sup>, M. Shur<sup>b</sup>, M. Shatalov<sup>c</sup>, J. Yang<sup>c</sup>,  
and R. Gaska<sup>c</sup>

<sup>a</sup>*Semiconductor Physics Department and Institute of Applied Research, Vilnius University,  
Saulėtekio av. 9-III, Lithuania*

<sup>b</sup>*Department of ECE and CIE, Rensselaer Polytechnic Institute, 110 8th St, Troy, USA*

<sup>c</sup>*Sensor Electronic Technology, Inc., 1195 Atlas Rd, Columbia, USA*

The development of high power AlGa<sub>N</sub>-based light emitters requires deeper understanding of the processes governing the luminescence efficiency in this material and its structures. We report on the origin of the luminescence efficiency droop in AlGa<sub>N</sub> epitaxial layers and multiple quantum wells (MQWs) with different carrier localization conditions and in a wide range of temperatures.

The epilayers and MQWs under study were grown on sapphire substrates by either MOCVD or migration-enhanced MOCVD techniques. The aluminum content ranged from 17% to 78% and from 8% to 35% in the epilayers and MQWs, respectively. PL spectroscopy was performed under quasi steady state conditions in the temperature range from 8 K to 300 K. The fourth harmonic (266 nm) of a Q-switched YAG:Nd laser radiation and the radiation of a tunable optical parametric oscillator at 213 nm were used for the photoexcitation.

The analysis of the PL measurement results show that samples with weak carrier localization exhibit a higher droop onset and a more rapid increase of the droop onset with increasing temperature. The investigation of the links between the carrier thermalization and efficiency droop shows that the ratio of thermal energy and localization parameter  $k_B T / \sigma$ . (where T is temperature and  $\sigma$  is the characteristic energy fluctuation scale) and thermalization temperature are the key parameters determining the carrier dynamics.

We could distinguish three regions in the PL efficiency droop onset dependence on  $k_B T / \sigma$  with each of the regions representing the different mechanisms of PL efficiency droop. For nonthermalized carriers at low values of  $k_B T / \sigma$ , the droop onset occurs at low excitation intensities and does not depend on  $k_B T / \sigma$ . These features might be explained by filling-in of the states at the local potential minima. In this case, the nonradiative recombination is enhanced due to the carrier mobility increase. In the intermediate region of the droop onset versus  $k_B T / \sigma$  dependence, the PL efficiency droop onset is increasing rapidly. This is the result of a more efficient carrier thermal redistribution and faster radiative recombination of the free carriers. The saturation of the increase of the droop onset is observed in the third region (thermalized carriers,  $k_B T > \sigma$ ). This feature is discussed in view of a possible influence of the stimulated emission in AlGa<sub>N</sub> MQWs and of the fast nonradiative recombination at extended defects.

# BRIGHTENING GaN:Eu RED LED BY BACK-AND-FORCE MOTION OF INJECTION CHARGES AND ITS APPLIED TO SITE-SELECTIVE ANALYSES OF EMISSION CENTRES

Masashi Ishii<sup>a</sup>, Atsushi Koizumi<sup>b</sup>, Yasufumi Fujiwara<sup>b</sup>

<sup>a</sup>National Institute for Materials Science, Tsukuba, Japan, [ISHII.Masashi@nims.go.jp](mailto:ISHII.Masashi@nims.go.jp)

<sup>b</sup>Osaka University, Suita, Osaka, Japan, [fujiwara@mat.eng.osaka-u.ac.jp](mailto:fujiwara@mat.eng.osaka-u.ac.jp)

As for GaN-based LEDs, blue and green light can be obtained using the well-established band gap control of InGaN, while red light is difficult to obtain. Eu-doped GaN (GaN:Eu) has been extensively studied as a candidate of red LED in which the intra-4*f* transition of the Eu dopants emits the red light. Despite the attractive luminescent color of GaN:Eu, since the emission centers originate from low-density Eu dopants, many injection charges penetrate through the GaN:Eu active layer built into LED and cannot contribute to the red light emission. In this study, we propose pulse drive to suppress the penetration loss, and applied the practically advantageous operation to diagnosis of the emission centers.

The GaN:Eu red LED (Eu concentration of  $4.5 \times 10^{19} \text{ cm}^{-3}$ ) was fabricated on a sapphire wafer using OMVPE.[1] For the LED, the built-in potential sweeps the electrons in the GaN:Eu active layer into the n layer under no forward bias,  $V_F = 0$ , whereas electrons are injected into the active layer from the n layer for  $V_F$  sufficiently above the diode threshold. Therefore, the ON/OFF pulse drive results in the back-and-forth motion of the injected charges in the GaN:Eu active layer and suppresses the penetration loss.

Figure 1 shows the suppression of penetration loss by the back-and-forth motion. The total emission intensity with respect to pulse frequency  $f$  indicates that optimal back-and-forth transport for the suppression occurs at  $f = f_r$ , resulting in the maximum emission intensity.

The GaN:Eu LED has two bright sites.[2] We found that the emission intensity versus  $f$  depends on emission sites: Monochromatic detection tuned at slightly different colors of the bright sites (1.996 eV and 2.007 eV) can characterize these bright sites selectively. This new characterization technique (site-selective pulse driven-emission spectroscopy, PDES) [3] quantified size of the emission centers. The result indicated that the spatially larger site is more favorable for capture of injection charges, resulting in the bright emission.

This work was partly supported by KAKENHI with a Grand-in-Aid for Scientific Research (26420287).

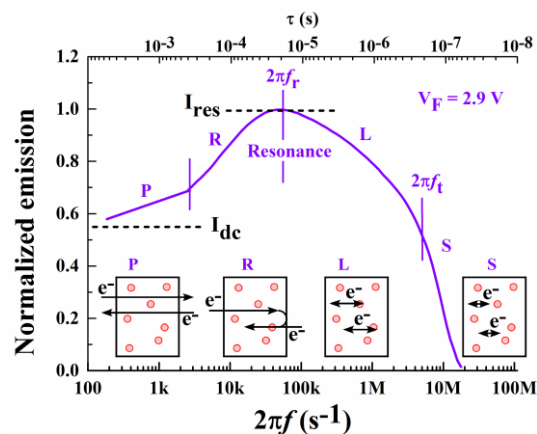


Fig. 1 Total intensity of GaN:Eu red LED with respect to pulse frequency

[1] A. Nishikawa, T. Kawasaki, N. Furukawa, Y. Terai, and Y. Fujiwara, *Appl. Phys. Express* 2, 071004 (2009).

[2] M. Ishii, A. Koizumi, and Y. Fujiwara, *J. Appl. Phys.* 117, 155307 (2015).

[3] M. Ishii, A. Koizumi, and Y. Fujiwara, *Appl. Phys. Lett.*, 105, 171903 (2014).

## YAG BASED PHOSPHORS FOR WHITE LED – A REVIEW

Pooja Yadav<sup>a</sup>, Charusheela Joshi<sup>a</sup>, S.V. Moharil<sup>b</sup>

<sup>a</sup> Physics Department, Shri Ramdeobaba College of Engg. and Management, Nagpur, India;  
email: charusheela\_4253@yahoo.co.in ; joshicp@rknc.edu

<sup>b</sup>Dept. of Physics, RTM Nagpur University, Nagpur, India, svmoharil@yahoo.com

For over the last decade, the world has witnessed rapid shift from conventional Hg based lighting to LED based solid state lighting (SSL). Commercial YAG: Ce<sup>3+</sup> phosphor plays important role in LED industry in converting blue light from (In,Ga)N LED chip to yellow. The combination of blue and yellow gives a bright white light source with an overall energy efficiency exceeding that of a compact fluorescent lamp.

However, the color impression of YAG:Ce on the basis of a blue diode is too “cold”, a red component is missing [3]. Co-dopants [4] are known to be able to act as co activators [5] and as wavelength shifters [6–8]. In case of YAG:Ce<sup>3+</sup>, Gd<sup>3+</sup> and La<sup>3+</sup> are known to shift the  $5d \rightarrow 4f$  yellow luminescence of the Ce<sup>3+</sup> defects to longer wavelengths (red shift) whereas co-doping with Ga<sup>3+</sup> and In<sup>3+</sup> shifts the luminescence to shorter wavelengths (blue shift).

We have carried out extensive work on combustion synthesis of doped YAG, with relevant co-dopings and fabrication of LEDs with developed phosphors. For example fig 1 shows the red shift in excitation and emission both, whereas fig.2 shows the phosphor converted yellow emission of blue LED with much improved CRI up to 85 from 65-70. A review of this work is presented here.

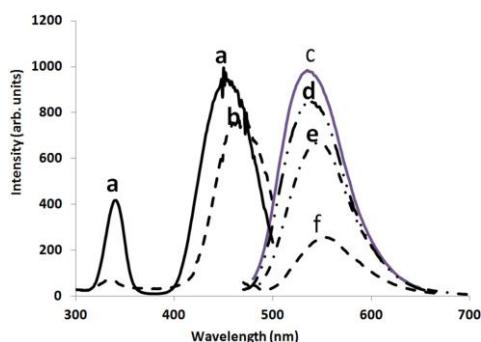


Fig. 1 PL characteristics of (a) exc of YAG:Ce with em at 535 nm, (b) exc of GdAG:Ce with em at 545 nm, (c) em of YAG:Ce at 460 nm, (d) em of (Y,Gd)AG:Ce at 460 nm exc, (e) em of Gd(Al,Ga)G:Ce at 470 nm exc, and (f) em of GdAG:Ce at 470 nm exc

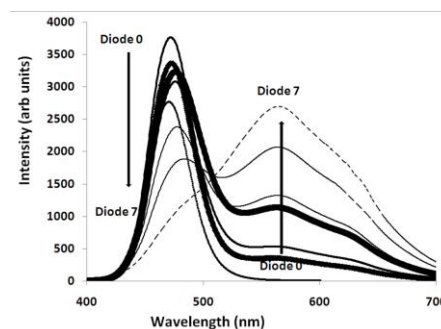


Fig. 2 Emission spectra of fabricated LEDs: LED0 represents the uncoated blue diode, while LED 7 represents the diode with white emission. LED2-LED6 occupy intermediate positions.

- [1] S.Kuck, I.Sokolska, M.Henke, M. Doring, T. Scheferc, *J. Lumin.* 102–103 (2003) 176–181
- [2] H.S. Janga, W.B. Ima, D.C. Leeb, D.Y Jeona, S.S. Kim, *J. Lumin.* 126 (2007) 371–377
- [3] M.Batentschuk, A.Osvet , G.Schierninga, A.Kliera, J.Schneiderb, A.Winnackera, *Radiat. Meas.* 38 (2004) 539–543
- [4] A.B. Muñoz García, J.L. Pascual, Z.Barandiarán, and L.Seijo, *Phys. Rev. B* 82 (2010) 64114–64121
- [5] Y.S Lin, R.S. Liu, B.M. Cheng, *J. Electrochem. Soc.*152 (2005) J41–J45
- [6] G. Blasse, A. Bril, *J. Chem. Phys.*, 47 (1967) 5139–5145
- [7] T.Y. Tien, E.F. Gibbons, R.G. DeLosh, P.J. Zacmanidis, D.E. Smith, and H.L.Stadler, *J. Electrochem. Soc.* 120 (1973) 278–281
- [8] Y. Pan, M. Wu, Q. Su, *J. Phys. Chem. Solids*, 65 (2004) 845–850

## STRUCTURE AND LATTICE DYNAMICS OF CRYSTALS WITH RARE EARTH SUBLATTICE: AB INITIO CALCULATIONS

Vladimir A. Chernyshev<sup>a</sup>, Anatoliy E. Nikiforov<sup>a</sup>, Vladislav P. Petrov<sup>a</sup>, Alexander V. Serdcev<sup>a</sup>

<sup>a</sup>*Ural Federal University, Mira 19 str., Ekaterinburg, Russia, vchern@inbox.ru*

The approach developed for the electronic structure and phonon spectra of crystals with rare-earth ions sublattice. The possibility of replacing the inner orbitals of rare earth ions by pseudopotential allows us to done the calculation for an acceptable computing time. Calculations for the crystal types of elpasolites, pyrochlores, non-stoichiometric cyclogermanates have been done. The rare earth impurity centers in fluorites have been investigated too. The calculations have been performed in the framework of the density functional theory using the MO LCAO method with hybrid DFT functionals in the CRYSTAL09 [1] program developed for the simulation of periodic structures. The lattice dynamics and band structure have been calculated for elpasolites  $\text{Cs}_2\text{NaRF}_6$  ( $R = \text{Y}, \text{Yb}$ ), pyrochlores  $\text{R}_2\text{Ti}_2\text{O}_7$  ( $R = \text{Gd}, \text{Tb}, \text{Dy}, \text{Ho}, \text{Er}, \text{Tm}, \text{Yb}, \text{Lu}$ ) and non-stoichiometric cyclogermanate  $\text{Y}_2\text{CaGe}_4\text{O}_{12}$  [2]. Rare earth impurity centers (Tm, Eu) have been investigated in  $\text{MeF}_2$  ( $\text{Me} = \text{Ca}, \text{Sr}, \text{Ba}$ ) and  $\text{SrCl}_2$  matrices. The results of the calculations are in a good agreement with available IR and Raman data, ENDOR data.

[1] R. Dovesi, V. R. Saunders, C. Roetti, R. Orlando, C. M. Zicovich-Wilson, F. Pascale, B. Civalleri, K. Doll, N. M. Harrison, I. J. Bush, P. D'Arco, and M. Llunell, CRYSTAL09 User's Manual (University of Torino, Torino, 2009).

[2] I.I. Leonidov, V.P. Petrov, V.A. Chernyshev, A.E. Nikiforov, E.G. Vovkotrub, A.P. Tyutyunnik, V.G. Zubkov, J. of Phys. Chem. C 118 (2014), 8090-8101



## CORRELATION BETWEEN COORDINATION ENVIRONMENT OF $\text{Ce}^{3+}$ AND LUMINESCENCE PROPERTIES IN YELLOW-EMITTING $\text{Sr}_2\text{Si}_7\text{Al}_3\text{ON}_{13}:\text{Ce}^{3+}$ PHOSPHOR

Yumi Fukuda<sup>a</sup>, Iwao Mitsuishi<sup>a</sup>, Ariane Keiko Albessard<sup>a</sup>, Yasushi Hattori<sup>a</sup>, Aoi Okada<sup>a</sup>,  
Kunio Ishida<sup>a</sup>, Katsuyoshi Oh-ishi<sup>b</sup>, and Masahiro Kato<sup>a</sup>

<sup>a</sup>Corporate Research & Development Center, Toshiba Corporation, Kawasaki, Japan,

<sup>b</sup>Faculty of Science and Engineering, Chuo University, Tokyo, Japan,

yumi.fukuda@toshiba.co.jp

Recently, nitrides and oxynitrides have been intensively studied as phosphor materials for white light-emitting diodes. We previously reported that  $\text{Eu}^{2+}$  doped Sr-containing sialon  $\text{Sr}_2\text{Si}_7\text{Al}_3\text{ON}_{13}:\text{Eu}^{2+}$  is a red-emitting phosphor with high luminous efficiency[1]. We showed that the white LEDs using  $\text{Sr}_2\text{Si}_7\text{Al}_3\text{ON}_{13}:\text{Eu}^{2+}$  combined with a green-emitting phosphor  $\text{Sr}_3\text{Si}_{13}\text{Al}_3\text{O}_2\text{N}_{21}:\text{Eu}^{2+}$  and a blue LED have excellent color rendering[2].

On the other hand, a yellow-emitting phosphor that can be excited by a blue LED is a key material for realizing white LEDs with high luminance. Based on the prediction that the change of activator of  $\text{Sr}_2\text{Si}_7\text{Al}_3\text{ON}_{13}:\text{Eu}^{2+}$  from  $\text{Eu}^{2+}$  to  $\text{Ce}^{3+}$  would provide the yellow emission, we succeeded in synthesizing  $\text{Sr}_2\text{Si}_7\text{Al}_3\text{ON}_{13}:\text{Ce}^{3+}$  that emits light with a wavelength of around 550 nm. The host crystal is of the same structural type as  $\text{SrAlSi}_4\text{N}_7:\text{Ce}^{3+}$  [3-6].

In this work, we studied the detail of the crystal structures of a series of yellow-emitting  $\text{Sr}_2\text{Si}_7\text{Al}_3\text{ON}_{13}:\text{Ce}^{3+}$  phosphors by Rietveld analysis of powder X-ray diffraction pattern. The lattice parameters of the host crystal were correlated with the crystal composition and the luminescence properties of these phosphors. Moreover, we also found that the efficiency strongly depended on a certain  $\text{Ce}^{3+}$ -N bond distance, which can be explained by the ligand field theory and the configuration coordinate model.

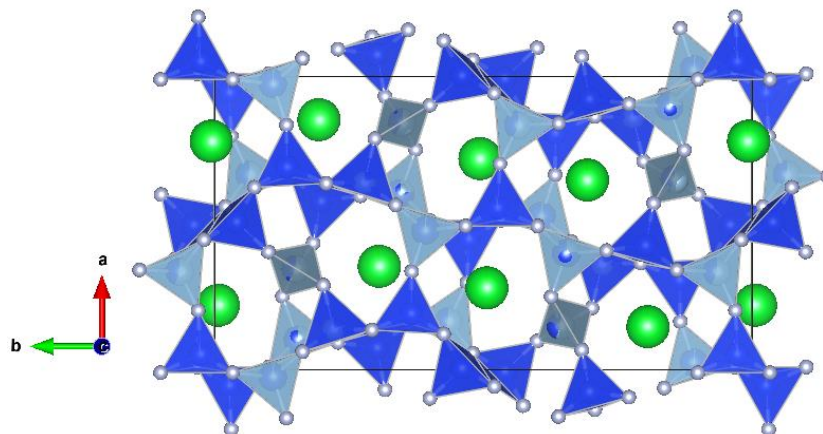


Figure 1 The crystal structure of  $\text{Sr}_2\text{Si}_7\text{Al}_3\text{ON}_{13}:\text{Ce}^{3+}$ [7].

[1] Y. Fukuda, A. Okada, A. K. Albessard, *Appl. Phys. Express* 5 (2012) 062102.

[2] Y. Fukuda, T. Sato, *Jpn. J. Appl. Phys.* 51 (2012) 122103.

[3] Z. Zhang, O. M. ten Kate, A. C. A. Delsing, Z. Man, R.-J. Xie, Y. Shen, M. J. H. Stevens, P. H. L. Notten, P. Dorenbos, J. Zhao, H. T. Hintzen, *J. Mater. Chem. C* 1 (2013) 7856-7865.

[4] L. Zhang, J. Zhang, X. Zhang, Z. Hao, H. Zhao, Y. Luo, *ACS Appl. Mater. Interfaces* 5 (2014) 12839-12846.

[5] J. Ruan, R.-J. Xie, S. Funahashi, Y. Tanaka, T. Takeda, T. Suehiro, N. Hirotsaki, Y.-Q. Li, *J. Solid State Chem.* 208 (2013) 50-57.

[6] G. King, K. Ishida, K. Page, Y. Fukuda, A. K. Albessard, Y. Hattori, R. Hiramatsu, I. Mitsuishi, A. Okada, M. Kato, N. Fukushima, *J. Mater. Chem. C* 3 (2015) 3135-3140.

[7] K. Momma, F. Izumi, *J. Appl. Crystallogr.* 44 (2011) 1272-1276.

## MODELING THE STRUCTURAL, VIBRATIONAL, ELECTRONIC AND OPTICAL PROPERTIES OF LANTHANIDE-DOPED MATERIALS

Chong-Geng Ma<sup>a</sup>, Mikhail Brik<sup>a,b</sup>

<sup>a</sup> *College of Sciences, Chongqing University of Posts and Telecommunications, No.2  
Chongwen Road, Chongqing 400065, P.R. China, cgma.ustc@gmail.com*

<sup>b</sup> *Institute of Physics, University of Tartu, Ravila 14C, Tartu 50411, Estonia,  
mikhail.brik@ut.ee*

In the last decades, the discovery and the optimization of lanthanide activated luminescent materials for lighting and display applications have been implemented mainly by using the smart combination of various experimental techniques, such as XRD structural refinement, Infrared and Raman spectra, and excitation and emission spectra [1]. Nowadays, the quick development of quantum chemistry theory for strongly-correlated lanthanides [2], together with an increase of the computational resources, has made it possible to propose a systematical calculation strategy to understand the physics picture behind those measurements and build up the link between the structural and optical properties of lanthanide-doped materials.

In this talk, we will demonstrate how the theoretical calculations support the experimental studies of the structural, vibrational, electronic and optical properties of lanthanide-doped materials. Ce<sup>3+</sup> and Eu<sup>2+</sup> ions will be paid more attention to due to their applications for white LED phosphors. Three questions will be answered as follows: 1) What can we get from first-principles calculations? 2) What is the real reason resulting in the red or blue shift of the lowest 5d-4f emissions of Eu<sup>2+</sup> and Ce<sup>3+</sup> ions [3]? 3) Is there a general relationship between the lowest 4f-5d excitation energies of Eu<sup>2+</sup> and Ce<sup>3+</sup> ions as Dorenbos's model [4] successfully works for the lanthanide series? The combined theoretical scheme of modern first-principles and conventional crystal-field models will be introduced and emphasized [5]. The successful applications including the recent unpublished work on the solid solution phosphors will be shown in order to highlight what we can serve for experimental studies. In addition, the misunderstanding about the position of the lowest 4f<sup>6</sup>5d energy level in the 4f-5d excitation spectra of Eu<sup>2+</sup> ions will be clarified, and thus the Stokes shift can be properly reproduced and further fed into understanding the electron-phonon coupling effect of Eu<sup>2+</sup> ions with host lattices [6].

[1] C. Liu, Z. Qi, C.-G. Ma, P. Dorenbos, D. Hou, S. Zhang, X. Kuang, J. Zhang, H. Liang, *Chem. Mater.* 26 (2014) 3709–3715.

[2] C.-G. Ma, D.-X. Liu, B. Feng, Y. Tian, L. Li, M.G. Brik, *J. Lumin.* (2015) available online at <http://dx.doi.org/10.1016/j.jlumin.2015.01.012>

[3] G. Li, C.C. Lin, W.-T. Chen, M.S. Molokeev, V.V. Atuchin, C.-Y. Chiang, W. Zhou, C.-W. Wang, W.-H. Li, H.-S. Sheu, T.-S. Chan, C.-G. Ma, R.-S. Liu, *Chem. Mater.* 26 (2014) 2991–3001.

[4] P. Dorenbos, *J. Lumin.* 91 (2000) 91.

[5] C.-G. Ma, M.G. Brik, *Phys. Status Solidi B* 250 (2013) 858-863.

[6] D. Hou, C.-G. Ma, H. Liang, M.G. Brik, *ECS J. Solid State Sci. Technol.* 3 (2014) R39-R42.



## LINEWIDTHS OF THE 4f-4f ELECTRONIC TRANSITIONS AND ELECTRONIC STRUCTURE OF Ce<sup>3+</sup> DOPANT IN YTTRIUM AND LUTETIUM ORTHOALUMINATE CRYSTALS

Aleksander Wittlin<sup>a,b</sup>, Hanka Przybylińska<sup>a</sup>, Agata Kamińska<sup>a</sup>, Piotr Sybilski<sup>a</sup>, Yaroslav Zhydachevskii<sup>a</sup>, Chong-Geng Ma<sup>c</sup>, Mikhail G. Brik<sup>d</sup>, Michal Malinowski<sup>e</sup>, Andrzej Suchocki<sup>a,f</sup>

<sup>a</sup> *Institute of Physics, Polish Academy of Sciences, Al. Lotników 32/46, 02-668 Warsaw, Poland*

<sup>b</sup> *Cardinal Stefan Wyszyński University in Warsaw, ul. Dewajtis 5, 01-815 Warsaw, Poland*

<sup>c</sup> *College of Mathematics and Physics, Chongqing University of Posts and Telecommunications, Chongqing 400065, PR China*

<sup>d</sup> *Institute of Physics, University of Tartu, Riia 142, Tartu 51014, Estonia*

<sup>e</sup> *Institute of Microelectronics and Optoelectronics, Technical University of Warsaw, Warsaw, Poland*

<sup>f</sup> *Institute of Physics, Kazimierz Wielki University, Weysenhoffa 11, 85-072 Bydgoszcz, Poland*

Low temperature, infrared transmission spectra of yttrium orthoaluminate and lutetium orthoaluminate bulk crystals doped with Ce<sup>3+</sup> are presented. In the region of intra-configurational 4f – 4f transitions the spectra of the bulk LuAG crystals exhibit existence of at least three different Ce<sup>3+</sup> related centers, a major one associated with Ce in regular positions substituting yttrium or lutetium and at least two others additional center, most probably related to so called antisite positions of rare-earth ions in this host, i.e. ions in the Al positions. Crystal field analysis based on exchange charge model exhibit excellent agreement with the experimental data for the major Ce<sup>3+</sup> center. Unusual broadening of some of the 4f-4f absorption lines is observed, which we associate with the coincidence of phonon energies of these hosts with the differences between the energies of the particular 4f crystal field levels.

### Acknowledgements:

The cooperation program between Estonian and Polish Academies of Sciences for the years 2013–2015 is kindly acknowledged. This work was partially supported by the Project DEC-2012/07/B/ST5/02080 of the National Science Center of Poland.

## INVESTIGATION OF THE QUENCHING MECHANISMS OF Tb<sup>3+</sup> DOPED SCHEELITES

Katrien W. Meert<sup>a,b</sup>, Jonas J. Joos<sup>a,b</sup>, Dirk Poelman<sup>a,b</sup>, Philippe F. Smet<sup>a,b</sup>

<sup>a</sup>Lumilab, Department of Solid State Sciences, Ghent University, Belgium

<sup>b</sup>Center for Nano- and Biophotonics (NB-Photonics), Ghent University, Belgium

Scheelites are ABO<sub>4</sub> compounds for which a variety of ions can be chosen for A and/or B cations. Some among these scheelites show intrinsic luminescence and doping with rare earth elements results in additional 4f-4f emission. Here, the investigated material was PbWO<sub>4</sub>:Tb<sup>3+</sup>. The host emission consists of two emission bands, in the blue and green region respectively, however strongly suppressed by the Tb<sup>3+</sup> emission, including transitions from the <sup>5</sup>D<sub>4</sub> and <sup>5</sup>D<sub>3</sub> level.

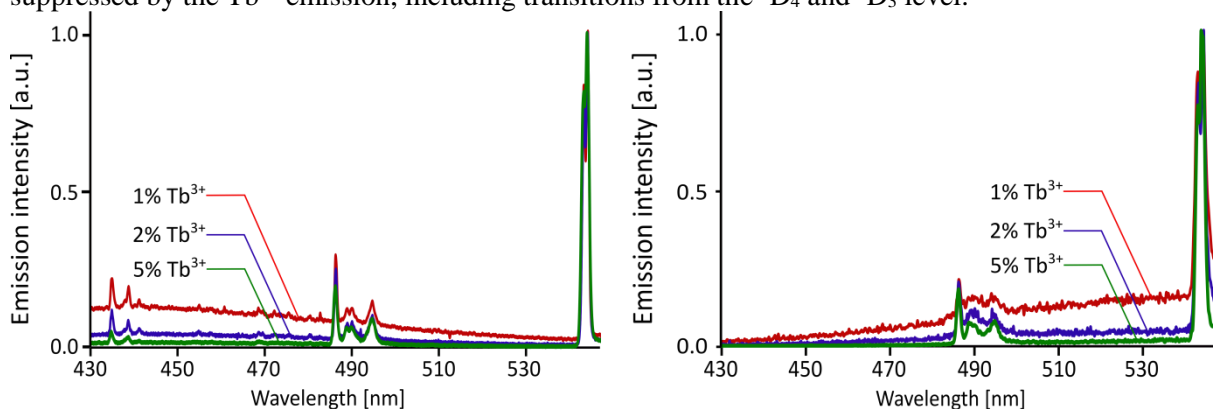


Fig 1. Emission spectra of PbWO<sub>4</sub>:Tb<sup>3+</sup> (1%, 2% and 5% Tb<sup>3+</sup>) upon excitation at 270 nm (left) and 320 nm (right) at 10K.

Both the host emission and the Tb<sup>3+</sup> emission possess a strong temperature dependence. Elucidation of this behavior is not straightforward as several transfer mechanisms are involved. The thermal quenching profiles of both the host emission and the Tb<sup>3+</sup> emission are recorded for different excitation wavelengths, making the distinction between host excitation and direct excitation into the 4f-levels of Tb<sup>3+</sup>. Divergent quenching profiles of the host emission for the un-doped versus doped materials reveal a temperature dependent energy transfer process from the host towards the Tb<sup>3+</sup> ions. Performing these measurements for samples with different Tb<sup>3+</sup> concentrations allowed discriminating between the different processes involved. In addition, time resolved measurements are carried out to unravel the energy transfer mechanisms. Based on the available data a detailed energy level scheme of host and dopant is proposed.

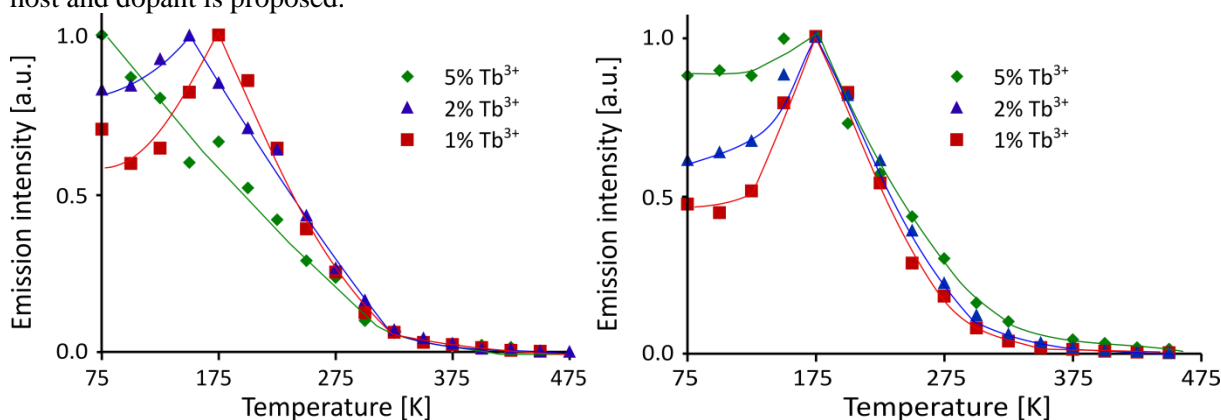


Fig 2. Thermal quenching of the integrated emission intensities from the <sup>5</sup>D<sub>3</sub> (left) and <sup>5</sup>D<sub>4</sub> level (right) after excitation in the host ( $\lambda_{exc} = 270$  nm). The solid lines serve as a guide to the eye.

## MODELLING THE INFLUENCE OF SILVER NANOPARTICLES ON THE f-f LUMINESCENCE OF THE EuEDTA COMPLEX IN THE POLYVINYLPIRROLIDONE POLYMER

M. A. Couto dos Santos<sup>a</sup>, O. L. Malta<sup>b</sup>, R. Reisfeld<sup>c</sup>

<sup>a</sup>*Depto de Física, Universidade Federal de Sergipe/CCET, São Cristóvão/SE, 49100-000 Brazil, marcoscouto@ufs.br*

<sup>b</sup>*Depto de Química Fundamental, Universidade Federal de Pernambuco/CCEN, Recife/PE 50670-901, Brazil, oscar@inct-inami.com.br*

<sup>c</sup>*The Hebrew University of Jerusalem, Chemistry Institute, E. Safra Campus, 91904 Jerusalem, Israel, renata.reisfeld@mail.huji.ac.il*

A theoretical analysis on experimental results previously obtained on the influence of silver nanoparticles in a polyvinylpirrolidone (PVP) polymer film containing a trivalent europium complex with EDTA ligand is made. Depending on the excitation source (at 393 nm with a xenon lamp or at 532 nm with a focused diode laser) the characteristic Eu<sup>3+</sup> luminescence is observed to be enhanced by factors between 5 and 50 [1].

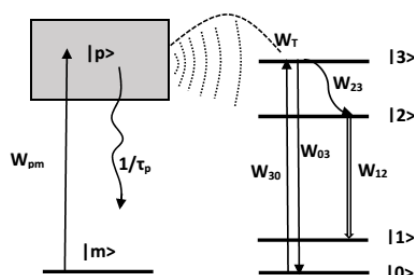


Figure 1.

The theoretical analysis presumes a migration process of the EuEDTA complex units towards the silver nanoparticles and subsequently the treatment of the competition between local high field gradient effects and Eu<sup>3+</sup> ion to the silver nanoparticles energy transfer successfully accounts for the observed luminescence enhancement factors.

Table 1. The enhancement ratio,  $c_R$ , for a confinement radius  $R_0 = 25$  nm and the non-radiative transition rates associated to the different excitations. The experimental enhancement ratios are in parenthesis [2].

Excitation (nm)	$W_{23}(s^{-1})$	$c_R$
393	$10^4$	5.2 (3)
532	$10^6$	50.0 (50)

[1] O.L. Malta, M.A. Couto dos Santos, Chem. Phys. Lett 174 (1990) 13-18

[2] R. Reisfeld, T. Saraidarov, G. Panzer, V. Levchenko, M. Gaft, Opt. Mater. 34 (2011) 351-355

**PHOTOPHYSICAL STUDIES AND APPLICATION OF COMPUTER MODELLING AND HARTREE-FOCK METHOD FOR INTERPRETATION OF SPECTROSCOPIC PROPERTIES AND STRUCTURAL CHANGES OF AXIALLY SUBSTITUTED Yb(III) MONOPHTHALOCYANINES IN DIFFERENT MEDIA**

Yu. Gerasymchuk<sup>a</sup>, L. Tomachynski<sup>b</sup>, M. Guzik<sup>c</sup>, A. Koll<sup>c</sup>, J. Jański<sup>c</sup>, Y. Guyot<sup>d</sup>, W. Stręka<sup>a</sup>,  
G. Boulon<sup>d</sup>, J. Legendziewicz<sup>c</sup>

<sup>a</sup>*Institute of Low Temperature and Structure Research, 2 Okólna str., 50-422 Wrocław, Poland*

<sup>b</sup>*V.I. Vernadskii Institute of General and Inorganic Chemistry, 32/34 Palladin Ave., Kiev, Ukraine*

<sup>c</sup>*Faculty of Chemistry Wrocław University, F. Joliot-Curie 14 str., 50-383 Wrocław, Poland*

<sup>d</sup>*Institute Light Matter, UMR5306 CNRS-University of Lyon 1, University of Lyon, Bat. Kastler, 69622 Villeurbanne, France*

Lanthanide complexes with phthalocyanines (Pc) and porphyrins belong to the group of most investigated compounds because of their unique luminescence properties and variety of applications. The special interest is directed to medical applications, mainly in photodynamic therapy. This paper is devoted to photophysical studies of acetato- and chloro-ytterbium monophtalocyanine complexes in the solid state, solutions, silica matrices and PMMA polymer which can design their applicability. The structures, IR, and Raman spectra were calculated applying Hartree-Fock and Density Functional Theory methods and further correlated with experimental findings. The theory reproduces reasonably spectroscopic frequencies of YbPcOAc<sub>2</sub>DMSO chelate. Two molecules of DMSO with somewhat different spectroscopic behaviour were found to exist in this complex.

The mechanism of the effect of conformation changes, steric obstacles, extra-coordination of solvent molecules and molecule immobilization in polymer and inorganic matrices on lanthanide and phthalocyanine emission spectra was discussed. Attention was paid to the radiative and non-radiative processes, intramolecular energy transfer and the role of charge-transfer state in this process, electron-phonon coupling, multiion cooperative interactions, non-linear processes and dynamics in excited states. The role of solvent molecule exchange dynamic in possible interaction of Yb(III) complexes with biological systems was also analysed.

## **EMPIRICAL ENERGY LEVEL MODELING OF LANTHANIDE DEFECTS IN $\text{CaGa}_2\text{S}_4$ AND $\text{SrGa}_2\text{S}_4$ : UNCERTAINTY ANALYSIS AND UNEXPECTED BEHAVIOR**

Jonas J. Joos, Dirk Poelman, Philippe F. Smet

*LumiLab, Dept. of Solid State Sciences, Ghent University, Krijgslaan 281-S1, 9000 Gent, Belgium*

*Center for Nano- and Biophotonics (NB Photonics), Ghent University, Gent, Belgium*

Lanthanides (Ln) are remarkable elements. As the valence electrons in the 4f shell are shielded from the environment by filled 5s and 5p shells in the case of lanthanide ions, unique physical and chemical properties are found. In particular, systematic behavior in the electronic structure emerges.

This systematic behavior can be used to set up empirical relations to describe the electronic structure of lanthanide ions [1]. Because these ions usually show luminescence upon incorporation of in inorganic matrices, a large number of empirical rules are already available describing the optical and luminescence properties of lanthanide defects. It has even become standard practice to obtain the electronic structure of a lanthanide doped semiconductor or insulator, purely from optical spectroscopy [2].

In this work, empirical energy level modeling is applied to the lanthanide doped alkaline earth thiogallates  $\text{CaGa}_2\text{S}_4$  and  $\text{SrGa}_2\text{S}_4$ . These sulfides are well-known for their excellent luminescence properties upon lanthanide doping [3-4]. The crucial parameters, describing the electronic structure and optical properties of these compounds are calculated from optical measurements. In addition, a dedicated uncertainty analysis is carried out to pinpoint the accuracy of the obtained parameters.

By comparing the obtained energy level schemes and the luminescence spectra of these compounds, it is shown that  $\text{CaGa}_2\text{S}_4:\text{Ln}$  behaves as an ideal case concerning the empirical rules. In contrast,  $\text{SrGa}_2\text{S}_4:\text{Ln}$  shows a behavior which cannot be explained from the energy level schemes. It is argued that the local geometry of the  $\text{Ln}^{3+}$  defect is different in the case of  $\text{Ce}^{3+}$ , compared to the other  $\text{Ln}^{3+}$ . The repercussions of this deviating behavior on the energy level scheme are discussed.

[1] C.W. Thiel, H. Cruguel, H. Wu, Y. Sun, G.J. Lapeyre, R.L. Cone, R. W. Equall, R. M. Macfarlane, *Phys. Rev. B* 64 (2001) 085107.

[2] P. Dorenbos, *J. Solid State Sci. Technol.* 2 (2013) R3001–R3011.

[3] P. Benalloul, P.C. Barthou, C. Fouassier, A.N. Georgobiani, L.S. Lepnev, Y.N. Emirov, A.N. Gruzintsev, B.G. Tagiev, O.B. Tagiev, R.B. Jabbarov, *J. Electrochem. Soc.* 150 (2003) G62–G65.

[4] J.J. Joos, K.W. Meert, A.B. Parmentier, D. Poelman, P.F. Smet, *Opt. Mater.* 34 (2012) 1902–1907.

## THE ORIGIN OF FERROELECTRIC DISTORTION IN HEXAGONAL MULTIFERROICS $\text{RMnO}_3$ ( $\text{R} = \text{Y}, \text{Lu}$ )

M. V. Lalic, A. M. Sousa, W. S. Coutinho, A. F. Lima

*Physics Department, Federal University of Sergipe, São Cristóvão, Brazil, mlalic@ufs.br*

The hexagonal  $\text{YMnO}_3$  and  $\text{LuMnO}_3$  are multiferroic materials in which the ferroelectricity and antiferromagnetism take simultaneously place at low temperatures [1]. Both compounds, together with other members of the same  $\text{RMnO}_3$  ( $\text{R} = \text{Ho}, \text{Er}, \text{Tm}, \text{Yb}, \text{Lu}, \text{Y}, \text{Sc}, \text{In}$ ) family, are extensively studied due to numerous promising applications in the area of novel optoelectronic and spintronic devices [2]. One of the most intriguing questions about hexagonal manganites is about the origin of ferroelectric distortion that causes formation of spontaneous electric moment when  $\text{RMnO}_3$  undergo the phase transition between paraelectric (PE) and ferroelectric (FE) crystal structures. There are several proposed theories in the literature, but still without definite answer.

With a motivation to clarify this issue, we performed thorough theoretical study of Lu-O, Y-O and Mn-O bonds in  $\text{YMnO}_3$  and  $\text{LuMnO}_3$  in both of their PE and FE phases. The study was based on analysis of the electronic structure determined by the first-principles DFT calculations in which the Mn ions were treated either as non-spin-polarized or as spin-polarized (exhibiting the G-type antiferromagnetic arrangement). By applying a semi-local mBJ [3] exchange-correlation potential we succeeded to describe the band gap and energies of the Mn bands better than the previous calculations. The chemical bonds were analyzed in 3 different manners: (1) by comparing densities of electron states in the PE and the FE phase, (2) by comparing electronic density maps projected onto suitable planes, and (3) by performing Bader's topological analysis [4] of electronic densities in both PE and FE phases of the compounds. The results strongly indicate that the Mn-O bonds do not exhibit significant changes when the systems undergo the PE to FE phase transition, while the Y-O apical bonds become more covalent due to enhanced hybridization between empty Y  $d_z^2$  orbital and partially occupied neighboring O  $p_z$  orbital. This hybridization can be driving force that causes asymmetric movements of the Y and Lu ions from their centrosymmetric positions. On the basis of this conclusion, the present study substantiates the Y and Lu  $d^0$ -ness model to explain the origin of ferroelectric distortion in the  $\text{YMnO}_3$  and  $\text{LuMnO}_3$  compounds. The details of the study are published recently in refs [5,6].

[1] S. Lee et al, Nature (London) 451(2008) 805.

[2] W. Eerenstein, N. D. Mathur, and J. F. Scott, Nat. Rev. 442 (2006) 759.

[3] F. Tran and P. Blaha, Phys. Rev. Lett. 102 92009) 226401.

[4] R. F. W. Bader, *Atoms in Molecules* (Oxford University Press: Oxford, 1990).

[5] A. M. Sousa, W. S. Coutinho, A. F. Lima, and M. V. Lalic, J. Chem. Phys. 142 (2015) 074703.

[6] W. S. Coutinho, A. F. Lima and M. V. Lalic, J. Alloys and Compounds (2015) submitted.

## HIGH-RESOLUTION OPTICAL ABSORPTION SPECTROSCOPY OF Si-VACANCY COLOR CENTER IN MONOISOTOPIC DIAMOND $^{13}\text{C}$

Kirill N. Boldyrev<sup>a</sup>, Viktor G. Ralchenko<sup>b</sup>, Vadim S. Sedov<sup>b</sup>, Andrey P. Bolshakov<sup>b</sup>,  
Andrey A. Khomich<sup>b</sup>, Anatoly V. Krasilnikov<sup>c</sup>

<sup>a</sup>*Institute of Spectroscopy, Russian Academy of Sciences, 5 Fizicheskaya str., Troitsk,  
Moscow, Russia, kn.boldyrev@gmail.com*

<sup>b</sup>*General Physics Institute, Russian Academy of Sciences, 38 Vavilov str., 119991 Moscow,  
Russia, ralchenko@nsc.gpi.ru*

<sup>c</sup>*Project Center ITER, Build. 3, Kurchatov sq. 1, 123182 Moscow, Russia*

Currently, the study of color centers in diamond attracts a great attention of researchers in view of potential applications of these bright emission centers in physics, biology, quantum informatics [1]. Among other impurity-related defects in diamond the silicon-vacancy centers (Si-V) emitting a narrow zero-phonon-line at 737 nm wavelength, are of a special interest for development of biological markers [1], single-photon emitters [2,3], and also spintronic devices and quantum computers [4].

In the previous works [5,6] the photoluminescence and optical absorption spectra of the Si-V centers with natural isotopic composition (1.07%  $^{13}\text{C}$ ) were investigated in detail. Here we studied the Si-V centers in a monoisotopic  $^{13}\text{C}$  (99.96%) diamond by high-resolution optical spectroscopy at low temperatures. The single crystal  $^{13}\text{C}$  diamond samples were grown by a chemical vapor deposition technique. The fine spectral structure is measured, and a noticeable isotopic shift of spectral lines compared to those for normal diamond is revealed. The energy diagram of the Si-V center in  $^{13}\text{C}$  diamond is considered, and the cause of the observed isotope effects is discussed.

This work was supported by the Russian Foundation for Basic Research under Grant No 13-02-01091.

- [1] I. Aharonovich, E. Neu, Adv. Opt. Mater. 2 (2014) 911.
- [2] C. Wang et al., J. Phys. B.: At. Mol. Opt. Phys. 39 (2006) 37.
- [3] L.J. Rogers, et al., Nature Communications 5 (2014) 4739.
- [4] T. Müller et al., Nature Commun. 5 (2014) 3328.
- [5] C. D. Clark et al., Phys. Rev. B., 51 (1995) 16681.
- [6] C. Hepp et al., Phys. Rev. Lett. 112 (2014) 036405.

## MULTI-PHOTON QUANTUM CUTTING IN $\text{Gd}_2\text{O}_2\text{S}:\text{Tm}^{3+}$

D.C. Yu<sup>a,b</sup>, R. Martín-Rodríguez<sup>b</sup>, Q.Y. Zhang<sup>a</sup>, A. Meijerink<sup>b</sup>, F.T. Rabouw<sup>b</sup>

<sup>a</sup>South China University of Technology, Guangzhou 510641, P. R. China

<sup>b</sup>Utrecht University, P.O. Box 80000, 3508 TA Utrecht, The Netherlands  
f.t.rabouw@uu.nl

Conventional photoluminescence yields at most one emitted photon for each absorption event. Downconversion (or quantum cutting) materials can yield more than one photon, by virtue of energy transfer processes between luminescent centers. We introduce  $\text{Gd}_2\text{O}_2\text{S}:\text{Tm}^{3+}$  as a multi-photon quantum cutter. It can convert near-infrared, visible, or ultraviolet photons into respectively two, three, or four infrared photons of  $\sim 1800$  nm.

The cross-relaxation steps between  $\text{Tm}^{3+}$  ions that lead to quantum cutting are identified from photoluminescence (PL) emission spectra as a function of  $\text{Tm}^{3+}$  concentration in the crystal. From an analysis of the PL decay dynamics as a function of  $\text{Tm}^{3+}$  concentration, we quantify the rate constants of the cross-relaxation steps [1,2]. A consistent model is presented reproducing how the  $\text{Tm}^{3+}$  concentration affects the relative intensities of the various emission lines and the excited state dynamics. It provides an analytical formula for the quantum cutting efficiency as a function of  $\text{Tm}^{3+}$  concentration. Fig. 1 shows an example of our analysis, for the case of excitation in the  $^1\text{D}_2$  level where two consecutive quantum cutting processes  $^1\text{D}_2 \rightarrow 2\ ^3\text{H}_4$  followed by  $^3\text{H}_4 \rightarrow 2\ ^3\text{F}_4$  can give a quantum yield close to 400%. Finally, we discuss the potential application of  $\text{Gd}_2\text{O}_2\text{S}:\text{Tm}^{3+}$  for spectral conversion to improve the efficiency of next-generation photovoltaics. Challenges are to increase the effective absorption of the material, and to suppress concentration quenching of the emitting  $^3\text{F}_4$  level.

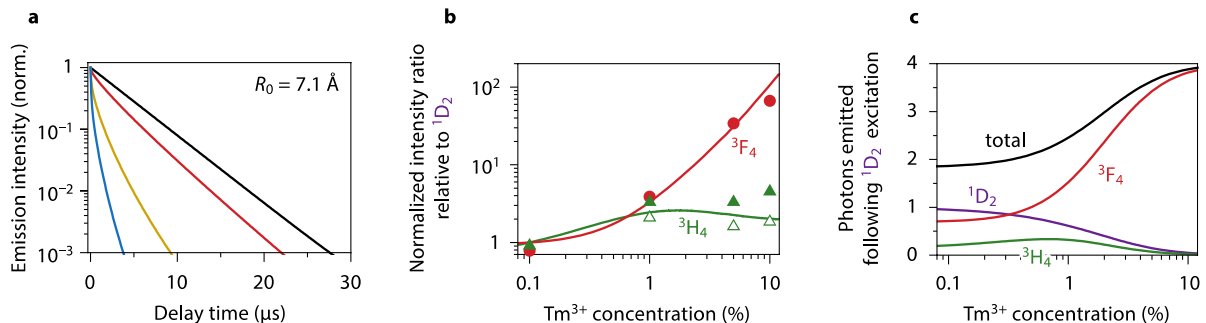


Figure 1 - Downconversion from the  $^1\text{D}_2$  level. (a) The decay dynamics of the  $^1\text{D}_2$  level as a function of  $\text{Tm}^{3+}$  concentration are fitted to find the critical radius for cross-relaxation of  $R_0 = 7.1$  Å. (b) Using this parameter, we can reproduce the experimental intensities of emission lines in the spectrum. (c) The model yields analytical expressions for the photon yield from the different excited states of  $\text{Tm}^{3+}$ , following excitation in the  $^1\text{D}_2$  level. The total photon yield increases to nearly 4 emitted photons per absorption event as cross-relaxation becomes more efficient at increasing  $\text{Tm}^{3+}$  concentration.

[1] F.T. Rabouw, S.A. den Hartog, T. Senden, A. Meijerink, Nat. Comm. 5 (2014) 3610.

[2] D.C. Yu, F.T. Rabouw, W.Q. Boon, T. Kieboom, S. Ye, Q.Y. Zhang, A. Meijerink, Phys. Rev. B 90 (2014) 165126.



## INFLUENCE OF DIFFERENT ATMOSPHERES ON PHOTOPHYSICAL AND STRUCTURAL PROPERTIES OF ZINC OXIDE

Sergio A. M. Lima<sup>a,b</sup>, Fernando A. Sigoli<sup>b,c</sup>, Miguel Jafelicci Jr.<sup>b</sup>, Marian R. Davolos<sup>b</sup>

<sup>a</sup>*Faculdade de Ciências e Tecnologia – Univ. Estadual Paulista –Unesp- R. Roberto Simonsen, 305, Presidente Prudente-SP, Brazil, samlima@fct.unesp.br*

<sup>b</sup>*Institute of Chemistry – Univ. Estadual Paulista –Unesp- R. Francisco Degni, 55, Araraquara-SP, Brazil, jafeli@iq.unesp.br, davolos@iq.unesp.br*

<sup>c</sup>*Institute of Chemistry – Univ. Estadual de Campinas –Unicamp- Zeferino Vaz, Campinas-SP, Brazil, fsigoli@iqm.unicamp.br*

Zinc oxide is a non-stoichiometric compound due to the existence of several structural defects, especially oxygen vacancies, which are determined by thermodynamic equilibrium. Such equilibrium depends on temperature and partial pressure of oxygen. It is reasonable to think that lower oxygen pressure causes an increase of oxygen vacancies, but the effect of the temperature is not that obvious [1]. In this sense, an oxygen-poor, or an oxygen-rich atmosphere would cause different structural defects during the synthesis of ZnO obtained via thermal decomposition of zinc hydroxycarbonate (ZHC). Luminescence property depends on the electronic structure, which in turn depends on crystalline structure, which in turn is strongly dependent on the identity and quantity of lattice defects. In this work we evaluated the presence of these defects through crystalline micro-strain and correlated them with the luminescence of ZnO. The atmosphere effects on samples were also investigated by thermogravimetric (TG) and differential thermal analysis (DTA), X-ray diffraction (XRD), Scanning Electron Microscopy (SEM), and Photoluminescence Spectroscopy (PL). ZHC was obtained via homogeneous precipitation from a solution of urea and zinc chloride at 90 °C/1.5h. The obtained ZHC was then decomposed by thermal treatment at 285 °C, 600 °C or 900 °C under either argon flow (oxygen-poor), or dynamic air (oxygen-rich) atmosphere. By SEM we observed that ZHC was obtained as micro-rods bunched as spherulites of about 7 μm, after thermal treatment in either atmosphere the formed ZnO kept the micro-rods format suggesting topotactic decomposition, although as temperature rises spherulites change into acicular form. For both atmospheres a peak was observed by DTA indicating the decomposition process occurs at 270 °C. Complete decomposition was observed at 500 °C and 530 °C, respectively for air and argon atmosphere. Further increase in temperature causes a mass increase corresponding to oxygen reabsorption by the samples, obviously in an oxygen-rich atmosphere the absorption corresponds to a much higher variation than that observed in argon atmosphere. We investigated the presence of micro-strain within crystalline structure of all ZnO samples through Williamson-Hall analysis from X-ray diffractograms. Crystallite size was also determined by the same method. While micro-strain tends to decrease as the temperature rises, the crystallite size tends to increase. However, oxygen-rich atmosphere results in smaller crystalline size, and higher micro-strain value. Micro-strain is dependent on the temperature and the atmosphere, but not related exclusively to oxygen vacancies. Other structural defects must be considered in order to explain micro-strain into the ZnO lattice, i.e., interstitial zinc, ionized oxygen/zinc vacancy, etc. All these defects contribute to electronic structure of the material, which regulate the luminescence properties. Samples treated at 285 °C and 600 °C exhibit broad band centred at the red region, while samples treated at 900 °C emit a broad band centred at the green region. All three samples treated under argon atmosphere exhibit higher intensity of emission compared to those treated under air. From these we may conclude that although micro-strain is essential to the luminescence of ZnO, a smaller value is desired when it comes to higher intensity of emission.

[1] S. A. M. Lima, F. A. Sigoli, M. Jafelicci Jr, M. R. Davolos, *Int. J. Inorg. Mat.* 3 (2001) 749–754.

## **RADIOMETRICALLY CALIBRATED HYPERSPECTRAL PHOTOLUMINESCENCE IMAGING OF DIAMOND**

R. E. Cross, M. Gunn, D. P. Langstaff, D. A. Evans

*Department of Physics, Aberystwyth University, Aberystwyth, UK, SY23 3BZ,  
rac21@aber.ac.uk*

Diamond is a very promising material due to its mechanical, thermal and electrical properties. Optical methods are widely used for defect characterization in diamonds, identifying defect centres that can be attributed to amorphous carbon phases and non-carbon inclusions in the lattice. Diamonds can be found in nature in a range of colours, of which brown is the most abundant. In spite of much research, the underlying cause of brown colouration in diamonds is yet to be resolved.

Current high-resolution photoluminescence spectroscopy enables the identification of defects present as an average for a sampled area, however spatial detail and the correlation of defects to regions of interest is lost. In order to correlate photoluminescence emission with local structure a new instrument has been designed, fabricated and calibrated to probe a material's chemical state via luminescence using a range of excitation sources.

The capabilities and benefits of hyperspectral imaging for remote sensing applications are well known, however the use of hyperspectral imaging in microscopy is less well established. Here we present a hyperspectral luminescence microscope, HeLIOS (Hyperspectral Luminescence Imaging for Optical Spectroscopy) which has received full radiometric calibration, traceable to National Institute of Standards and Technology (NIST). HeLIOS builds on previous instrumentation development in Aberystwyth and hyperspectral imaging development and is currently employed in a diverse range of interdisciplinary research including Material Physics, Computer Science, Astrobiology and Earth Sciences.

Spatially resolved photoluminescence of a natural type Ia banded diamond under UV excitation at low temperatures (14K) has been compared to high-resolution conventional spectroscopy to reveal a correlation between dislocation related spectral features and the brown colouration in natural diamonds. Due to the radiometric processing these data can be expressed in real physical units as opposed to arbitrary luminescence intensity. This enables direct comparisons and quantifications not previously possible.

## THE d-f LUMINESCENCE OF $\text{Eu}^{2+}$ AND $\text{Ce}^{3+}$ IONS IN $\text{Cs}_2(\text{Ca,Sr})\text{P}_2\text{O}_7$

Tim Senden<sup>a</sup>, Andries Meijerink<sup>a</sup>

<sup>a</sup>*Condensed Matter and Interfaces, Debye Institute for Nanomaterials Science, Utrecht University, P.O. Box 80000, 3508 TA Utrecht, The Netherlands, t.senden@uu.nl*

Currently there is a worldwide search for narrow band red emitting phosphors that are excitable in the blue, as these phosphors are crucial for developing efficient warm white light LEDs (w-LEDs). Narrow band red emission has recently been reported for  $\text{Eu}^{2+}$  in  $\text{Cs}_2\text{CaP}_2\text{O}_7$  [1]. The  $\text{Eu}^{2+}$  luminescence in this phosphate is characterized by a high luminescence quenching temperature and a large Stokes shift (see Figure 1a), which is promising for use in w-LEDs. The combination of a large Stokes shift with a narrow emission band and high quenching temperature are unusual. This indicates that the  $\text{Eu}^{2+} 4f^65d^1$  excited state undergoes a relaxation in the excited state, possibly a Jahn-Teller (JT) distortion.

In this work we have investigated the occurrence of a JT effect in the  $4f^65d^1$  excited state by studying the d-f luminescence of  $\text{Eu}^{2+}$  in  $\text{Cs}_2(\text{Ca,Sr})\text{P}_2\text{O}_7$  at cryogenic temperatures. Furthermore, we studied the optical properties of  $\text{Yb}^{2+}$  and  $\text{Ce}^{3+}$  ions in  $\text{Cs}_2(\text{Ca,Sr})\text{P}_2\text{O}_7$ , as the d-f luminescence of  $\text{Eu}^{2+}$ ,  $\text{Yb}^{2+}$  and  $\text{Ce}^{3+}$  are normally related.

In the low temperature luminescence spectra of  $\text{Eu}^{2+}$  (Figure 1a) no zero-phonon lines were observed and no information on the position of the electronic origins of lowest  $4f^65d^1$  state in absorption and emission can be obtained. Hence, this provides no direct evidence for the presence of a JT effect. For  $\text{Ce}^{3+}$ , two types of d-f luminescence were observed in  $\text{Cs}_2(\text{Ca,Sr})\text{P}_2\text{O}_7$  (green and grey line in Figure 1b), which is ascribed to sites with local and distant charge compensation. Interestingly, we observe a ‘normal’ Stokes shift for the  $\text{Ce}^{3+}$  luminescence, which is not comparable to the anomalously large Stokes shift observed for  $\text{Eu}^{2+}$ . This implies that the anomalous relaxation for the  $4f^65d$  state of  $\text{Eu}^{2+}$  does not occur for the 5d state of  $\text{Ce}^{3+}$ .

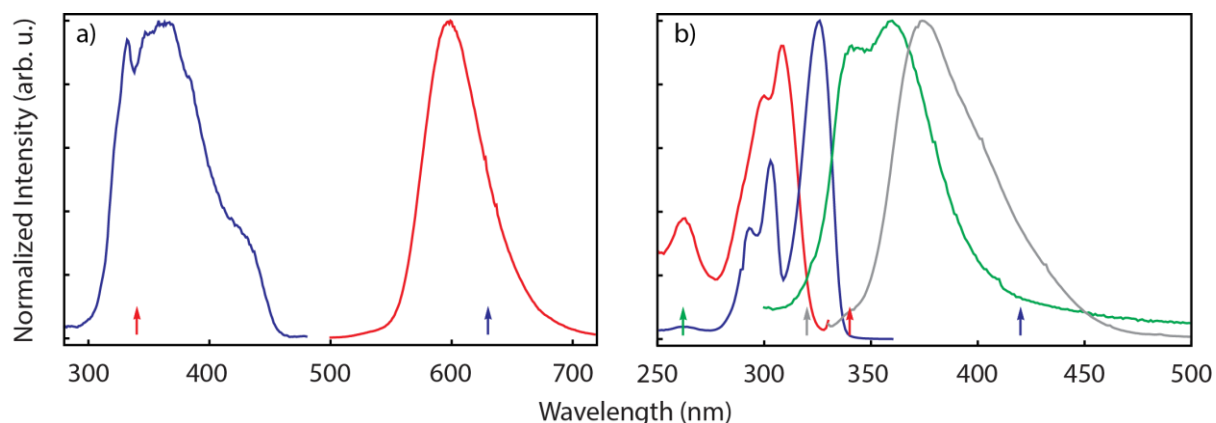


Figure 1 – Spectroscopic properties of  $\text{Eu}^{2+}$  and  $\text{Ce}^{3+}$  in  $\text{Cs}_2\text{CaP}_2\text{O}_7$  at  $T = 4$  K. a) Excitation (blue) and emission spectra (red) of  $\text{Cs}_2\text{CaP}_2\text{O}_7:\text{Eu}^{2+}$ . b) Excitation (red and blue) and emission spectra (green and grey) of  $\text{Cs}_2\text{CaP}_2\text{O}_7:\text{Ce}^{3+}$ .

[1] A.M. Srivastava, H.A. Comanzo, S. Camardello, S.B. Chaney, M. Aycibin, U. Happek, J. Lumin. 129 (2009) 919–925.

## SUBMICRON DIAMOND PILLARS WITH SILICON-VACANCY COLOR CENTERS AS LOCALIZED NEAR INFRA-RED PHOTOEMITTERS

Dmitry N. Sovyk<sup>a,b</sup>, Victor G. Ralchenko<sup>a,b</sup>, Konstantin N. Tukmakov<sup>c</sup>, Andrew A. Khomich<sup>a</sup>, Vladimir A. Shershulin<sup>a,d</sup>, Vadim V. Vorobyov<sup>e,f</sup>, Alexey V. Akimov<sup>f,g</sup>.

<sup>a</sup> *A.M. Prokhorov General Physics Institute of Russian Academy of Sciences, 38 Vavilov str., Moscow, Russia, sovyk@nsc.gpi.ru*

<sup>b</sup> *National Research Nuclear University "MEPhI", 31 Kashirskoye road, Moscow, Russia*

<sup>c</sup> *Samara State Aerospace University, 34 Moskovskoye road, Samara, Russia*

<sup>d</sup> *National Research University of Electronic Technology, 5 4806 str., Zelenograd, Moscow, Russia*

<sup>e</sup> *Moscow Institute of Physics and Technology, 9 Institutskiy lane, Dolgoprudny, Moscow region, Russia*

<sup>f</sup> *P.N. Lebedev Physical Institute of Russian Academy of Sciences, 53 Leninsky prosp., Moscow, Russia*

<sup>g</sup> *Russian Quantum Center, 100A Novaya str., Skolkovo, Moscow region, Russia*

We report on direct growth of submicron-scale single crystal diamond pillars doped with silicon to form photoemitters based on color centers silicon-vacancy (SiV) demonstrating a bright photoluminescence (PL) around 738 nm wavelength. The fabrication of the pillared structures utilizing total internal reflection effect is one of the ways to improve the collection of single photon emission used in quantum technologies [1]. We applied a bottom-up approach [2,3] as an alternative to well-known reactive ion etching of diamond substrate [1] for preparation of pillar structures with aspect ratio  $A = \text{height/width} > 2$ .

The diamond pillars have been epitaxially grown in microwave plasma CVD reactor through windows (holes) in amorphous Si mask of 1  $\mu\text{m}$  in thickness deposited on HPHT diamond substrate. Arrays of the holes of 400 nm in diameter were perforated in the mask by focus ion beam (FIB) milling. The further diamond deposition using methane-hydrogen gas mixtures is confined by the hole's walls, thus directing the pillars growth. The Si mask, etched by atomic hydrogen from the plasma, supplies  $\text{SiH}_x$  radicals which result in diamond doping with Si, and forming optically active SiV centers. After the mask removal a strong PL emission of the SiV centers at 738.6 nm localized within the pillars was detected with a confocal microscope connected to Hanbury-Brown-Twiss interferometer. High PL contrast between the pillars and the background (the substrate) was revealed. We observed sevenfold enhancement in PL intensity for the pillars with  $A=2.0-2.8$  in comparison with the flat surface. In addition, the SiV PL decay time of 1.1 ns has been measured upon excitation by 60 ps laser pulses at 532 nm.

[1] T.M. Babinec, B.J.M. Hausmann, M. Khan, Y. Zhang, J.R. Maze, P.R. Hemmer, M. Lončar. *Nat. Nanotechnol.* 5 (2010) 195-199.

[2] I. Aharonovich, J.C. Lee, A.P. Magyar, D.O. Bracher, E.L. Hu. *Laser Photonics Rev.* 7 (2013) L61-L65.

[3] D. Sovyk, V. Ralchenko, M. Komlenok, A. Khomich, et al. *Appl. Phys. A.* 118 (2015) 17–21.

## DECAY RATE OF THE LUMINESCENCE CENTER LOCATED NEAR METALLIC NANOPARTICLE

Konstantin K. Pukhov

*Prokhorov General Physics Institute of the RAS, 38 Vavilov Street, Moscow, Russia,  
pukhov@lst.gpi.ru*

The general expression is derived for the probability of the spontaneous electric-dipole transitions in an emitter located near subwavelength nanoparticle (NP). This expression takes into account arbitrary orientation of the dipole moment of the emitter with respect to NP surface and has the simple form

$$A = n_{med} f_L \frac{4\omega^3}{3\hbar c^3} \left[ |\mathbf{d}|^2 - 2\text{Re}\gamma \frac{|\mathbf{d}|^2}{r^3} + 6\text{Re}\gamma \frac{|\mathbf{dn}|^2}{r^3} + |\gamma|^2 \frac{|\mathbf{d}|^2 + 3|\mathbf{dn}|^2}{r^6} \right]$$

Here  $n_{med}$  is the refractive index of the medium that surround NP,  $f_L$  is local-field correction,  $\omega$  and  $\mathbf{d}$  are the transition frequency and the transition dipole moment, respectively;  $\gamma = \text{Re}\gamma + i\text{Im}\gamma$  is the NP polarizability,  $\mathbf{r} = r\mathbf{n}$  is the radius-vector of an emitter with respect to the center of NP.

The obtained expression coincides with the previously found particular expressions (see e.g. [1]) for cases when a dipole is perpendicular to the particle surface ( $|\mathbf{dn}| = 0$ ) and when a dipole is parallel to it ( $|\mathbf{dn}|^2 = |\mathbf{d}|^2$ ).

A similar expression is also obtained for an emitter located inside the shell of core-shell NP with the metallic core. Of course, these expressions are valid for dielectric NPs as well. Nonradiative contribution to decay rate is also discussed.

[1] G. Colas des Francs, A. Bouhelier, E. Finot, J.C. Weeber, A. Dereux, C. Girard, E. Dujardin, *Opt. Express*, 16 (2008) 17654–17666.

## CRYSTAL GROWTH, OPTICAL AND SCINTILLATION PROPERTIES OF BULK Eu-DOPED SrI<sub>2</sub> SINGLE CRYSTALS

Akira Yoshikawa<sup>a,b,c</sup>, Yasuhiro Shoji<sup>a,c</sup>, Yuui Yokota<sup>b</sup>, Shunsuke Kurosawa<sup>a,b</sup>, Valery I. Chani<sup>a</sup>, Tomoki Ito<sup>a</sup>, Kei Kamada<sup>b,c</sup>, Yuji Ohashi<sup>a</sup>, Vladimir Kochurikhin<sup>c,d</sup>  
<sup>a</sup>*Institute for Materials Research (IMR), Tohoku University, 2-1-1, Katahira, Aoba-ku, Sendai, Miyagi, 980-8577, Japan, yoshikawa@imr.tohoku.ac.jp*  
<sup>b</sup>*New Industry Creation Hatchery Center (NICHe), Tohoku University, 6-6-10, Aramaki, Aoba, Aoba-ku, Sendai, Miyagi, 980-8579, Japan*  
<sup>c</sup>*C&A Corporation, 6-6-40, Aramaki, Aoba, Aoba-ku, Sendai, Miyagi, 980-8579, Japan*  
<sup>d</sup>*General Phys. Institute, Russ. Academy of Sci. 119991, Moscow, Vavilov Str., 38, Russia*

Eu doped SrI<sub>2</sub> (Eu:SrI<sub>2</sub>) single crystal have been energetically investigated and re-discovered as a next-generation gamma-ray scintillator with high light yield and energy resolution. Eu:SrI<sub>2</sub> scintillator crystals with strong hygroscopic nature have been grown by the Vertical Bridgman (VB) method using a quartz ampoule [1]. On the other hand, we developed a modified micro-pulling-down ( $\mu$ -PD) method with a removable chamber in order to grow single crystals of halide materials at higher growth rate than the VB method [2]. We reported the results of crystal growth and scintillation properties of halide scintillator crystals as represented by CeBr<sub>3</sub>, Ce:LaBr<sub>3</sub> and Eu:SrI<sub>2</sub> using the modified  $\mu$ -PD method.

However, the modified  $\mu$ -PD method couldn't grow a bulk single crystal with more than 10 mm in diameter. Therefore, we developed a novel VB method using the  $\mu$ -PD furnace with the removable chamber to grow bulk single crystals of hygroscopic halide materials. There are some advantages of the novel VB method using  $\mu$ -PD furnace compared to the conventional VB method. In the result, 1 inch Eu:SrI<sub>2</sub> bulk crystal could be grown by the VB method using the  $\mu$ -PD furnace. In this study, we developed bulk Eu:SrI<sub>2</sub> bulk single crystal by the VB method using  $\mu$ -PD furnace and investigated the scintillation properties.

In this study, Eu-doped SrI<sub>2</sub> crystals were grown from the melt using modified bridgeman method with vacuum tight removable chamber.

The carbon crucible is designed for the growth of bulk Eu:SrI<sub>2</sub> single crystal. SrI<sub>2</sub> and EuI<sub>2</sub> powders (> 4N, APL Japan) were used as a starting material and the mixed powder with nominal composition of (Sr<sub>0.98</sub>Eu<sub>0.02</sub>)I<sub>2</sub> (Eu2%:SrI<sub>2</sub>) was set into the crucible. Undoped SrI<sub>2</sub> single crystal grown by the  $\mu$ -PD method used as a seed crystal and it was set in the bottom of crucible. All the processes mentioned above were performed in a glove box filled with Ar gas. The removable chamber was taken out from the glove box after the hotzone set up. The chamber was connected with a Turbo Molecular pump and was vacuumed up to 10<sup>-4</sup> Pa at ~300°C. After the baking process, high-purity Ar gas (99.9999%) was introduced in the chamber. The carbon crucible was heated by a high-frequency induction coil up to the melting point of Eu:SrI<sub>2</sub>. The mixed powder was melted and then, the crucible was pulled down for crystal growth. After the crystal growth procedure, the crucible was cooled down to room temperature. The grown crystal was taken out from the chamber in the glove box.

In the result, the bulk Eu:SrI<sub>2</sub> bulk crystal without visible crack was obtained. It had high transparency and there was no visible inclusion in the crystal. The crystal was cut and polished in the glove box and was sealed into the aluminum container with an optical window. The detail of crystal growth, optical and scintillation properties of bulk Eu:SrI<sub>2</sub> bulk crystal will be reported in the presentation.

[1] E. V. van Loef, N. J. Cherepy, et.al., IEEE Trans. on Nucl. Sci., 56(3) (2009) 869-872.

[2] Y. Yokota, A. Yoshikawa, et. al., J. Cryst. Growth 375 (2013) 49–52.

## COMPOSITION ENGINEERING OF THE SINGLE CRYSTALLINE FILM SCINTILLATORS BASED ON THE MULTICOMPONENT GARNET COMPOUNDS

Yuriy Zorenko<sup>a</sup>, Vitaliy Gorbenko<sup>a,b</sup>, Tetyana Zorenko<sup>a</sup>, Oleg Sidletskiy<sup>c</sup>, Alexander Fedorov<sup>d</sup>

<sup>a</sup>*Institute of Physics, Kazimierz Wielki University in Bydgoszcz, 85090 Bydgoszcz, Poland,  
zorenko@ukw.edu.pl*

<sup>b</sup>*Department of Electronics, Ivan Franko National University of Lviv, 79017 Lviv, Ukraine*

<sup>c</sup>*Institute for Scintillation Materials NAS of Ukraine, 61001 Kharkiv, Ukraine*

<sup>d</sup>*Institute for Single Crystals NAS of Ukraine, 61178 Kharkiv, Ukraine*

This report presents our last achievements in the creation of new types of single crystalline film (SCF) scintillators based on the  $A_{3-x}Al_{5-y}Ga_yO_{12}:Ce$  garnet compounds; A= Gd, Lu, Tb and their combination at  $x=0\div 3.0$  and  $y=1.5\div 3.0$ , using the Liquid Phase Epitaxy (LPE) method from PbO and BaO based fluxes onto  $Y_3Al_5O_{12}$  (YAG) and  $Gd_3Al_{2.5}Ga_{2.5}O_{12}$  (GAGG) substrates. The bulk crystals of multicomponent garnets are now on the top list of most efficient oxide scintillators with the light yield (LY) up to 50000 Ph/MeV [1]. Therefore, the growth of SCF analogues of such garnets is now very actual task, first of all for the creation of scintillation screens for X-ray imaging with submicron spatial resolution [2].

In our work, we have applied the following research concepts: (i) “host band gap engineering” [3]; (ii) “engineering of  $Ce^{3+}$  ion energy structure” [1]; (ii) “enhancing the energy transfer from the host to  $Ce^{3+}$  ion” [4] to basic scintillation materials –  $Lu_3Al_5O_{12}:Ce$  (LuAG:Ce) SCF using the alloying of the  $Gd^{3+}$  and  $Tb^{3+}$  ions in the decahedral positions and  $Ga^{3+}$  ions in the octahedral positions of the garnet host. Namely, we have found that from all the studied SCF of  $Gd_{3-x}Lu_xAl_{5-y}Ga_yO_{12}:Ce$  compositions at  $x=0\div 3$  and  $y=1.5\div 3.0$  the best scintillation properties are realized in the  $Lu_{1.5}Gd_{1.5}Al_{2.75}Ga_{2.25}O_{12}$  SCF whose LY under  $\alpha$ -particles excitation exceeds 1.3-1.4 times the LY of YAG:Ce SCF but is by a factor of 1.4 lower than the LY of the best reference LuAG:Ce SCF scintillator.

With the aim of enhancing the energy transfer from the host of multicomponent garnet to the  $Ce^{3+}$  ions, the SCF of  $Tb_{3-x}Gd_xAl_{5-y}Ga_yO_{12}:Ce$  garnet at  $x=0\div 3$  and  $y=1.5\div 3.0$  were crystallized by the LPE method onto GAGG substrates and the luminescent and scintillation properties of these SCFs were studied as well. Due to the composition engineering and efficient and  $Gd^{3+}\rightarrow Tb^{3+}\rightarrow Ce^{3+}$  energy transfer in the mentioned garnet matrices, we have observed strong increasing the LY of SCFs of the these compounds in comparison with LuAG:Ce SCF counterpart. Namely, the LY of the best samples of  $Tb_{3-x}Gd_xAl_3Ga_2O_{12}:Ce$  SCF at  $x=1.0\div 1.5$ , grown from PbO-based flux, under  $\alpha$ -particles is equal to 120-150% with respect to LuAG:Ce SCF and is comparable with the LY of  $Gd_3Al_{2.5}Ga_{3.25}O_{12}:Ce$  bulk crystals. To our knowledge, these are the highest LY of SCF scintillators so far, prepared from PbO based flux.

The role of  $Ga^{3+}$  doping in the improvement of the efficiency of energy transfer processes in  $A_{3-x}Al_{5-y}Ga_yO_{12}:Ce$  garnets was discussed in detail. The comparison between the luminescent and scintillation properties of  $A_{3-x}Al_{5-y}Ga_yO_{12}:Ce$  SCF; A=Gd, Lu, Tb, grown from PbO and BaO based fluxes was considered as well.

[1] K. Kamada, T. Endo, K. Tsutumi, J. Pejchal, M. Nikl, et al, *Cryst. Growth Des.*, 11 (2011) 4484.

[2] T. Martin, A. Koch, *Journal of Synchrotron Radiation*, 13 (2006) 180.

[3] Fasoli, M., Vedda, A., Nikl, *Phys. Rev.*, B 84 (2011) 081102(R).

[4] J. Ogiegło, A. Zych, K. Ivanovskikh, et al, *J. Phys. Chem. A*, 116 (2012) 8464.

This work was realized within the Polish NCN No 2012/07/B/ST5/02376 and Ukrainian SL-20F projects.

## Co-doping effects on luminescence and scintillation properties of Ce doped (Lu,Gd)<sub>3</sub>(Ga,Al)<sub>5</sub>O<sub>12</sub> scintillator

Hiroaki Yamaguchi<sup>a</sup>, Kei Kamada<sup>b,c</sup>, Shunsuke Kurosawa<sup>a,c</sup>,  
Jan Pejchal<sup>d</sup>, Yasuhiro Shoji<sup>a,b</sup>, Yuui Yokota<sup>c</sup>, Yuji Ohashi<sup>a</sup>, Akira Yoshikawa<sup>a,b,c</sup>

<sup>a</sup> Tohoku University, Institute for Material Research, 2-1-1 Katahira Aoba-ku, Sendai, Miyagi 980-8577, Japan, h\_yamaguchi@imr.tohoku.ac.jp

<sup>b</sup> C&A Corporation, T-Biz, 6-6-10 Aoba, Aramaki, Aoba-ku, Sendai, Miyagi 980-8579, Japan

<sup>c</sup> Tohoku University, New Industry Creation Hatchery Center, 6-6-10 Aoba, Aramaki, Aoba-ku, Sendai, Miyagi 980-8579, Japan

<sup>d</sup> Institute of Physics CAS, Cukrovarnicka 10, 16253 Prague, Czech Republic

Scintillator materials combined with photo detectors are widely used to detect high energy photons and particles, e.g. in high energy physics, oil well logging, security, medical imaging techniques [1] such as X-ray computed tomography, positron emission tomography (PET) and other applications. Oxide scintillation materials based on garnet structure like Ce-doped Lu<sub>3</sub>Al<sub>5</sub>O<sub>12</sub> (Ce:LuAG) are promising candidates for scintillator applications because of well mastered technology developed for laser hosts and other applications, optical transparency and easy doping by rare-earth elements [2]. LuAG admixed with balanced Gd and Ga ratio was proved to be an excellent scintillator where the effect of shallow traps was suppressed; the spectrally corrected light yield value exceeded 40,000 photons/MeV, and the scintillation decay was dominated by a 53 ns decay component which is close to that of Ce<sup>3+</sup> photoluminescence decay in this host [3]. Positive role of Ce<sup>4+</sup> centers stabilized by divalent ion co-doping has been proposed to explain the enhancement of light yield in Mg,Ce:LuAG [4] and decay time acceleration in Mg,Ce: Gd<sub>3</sub>Ga<sub>3</sub>Al<sub>2</sub>O<sub>12</sub> [5].

In this report, Mg co-doping effects on scintillation properties of Ce:(Lu,Gd)<sub>3</sub>(Ga,Al)<sub>5</sub>O<sub>12</sub> (LGGAG) were investigated. Mg 200 ppm co-doped Ce:LGGAG single crystals were prepared by micro pulling down method (Fig.1). Ce<sup>4+</sup> charge transfer absorption was observed below 300nm in Mg,Ce:LGGAG which is in good agreement with previous reports [2]. Figure 2 shows scintillation decay curves. The scintillation decay times were accelerated by Mg co-doping. In our presentation, details of crystal growth, crystal structure and chemical composition analysis will be reported. Furthermore, relation between chemical composition of LGGAG and Mg co-doping effects on scintillation properties considering the band structure will be reported.

### References:

- [1] M. Nikl, Meas. Sci. Techn. 17 (2006) R37.
- [2] M. Nikl, A. Yoshikawa *et al*, Cryst. Growth Des. 14 (2014) 4827–4833
- [3] K. Kamada, A. Yoshikawa *et al*, Cryst. Growth Des. 11(2011) 4484–4490.
- [4] K. Kamada, A. Yoshikawa *et al*, Nucl. Instrum. Meth. A 782 (2015) 9–12.
- [5] K. Kamada, A. Yoshikawa *et al*, Opt. Mater. 41(2015) 63–66.

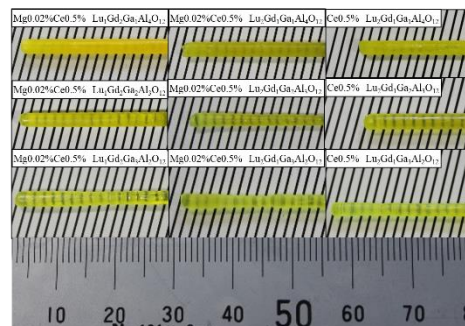


**Fig. 1.** Photographs of single crystals grown by the u-PD method.

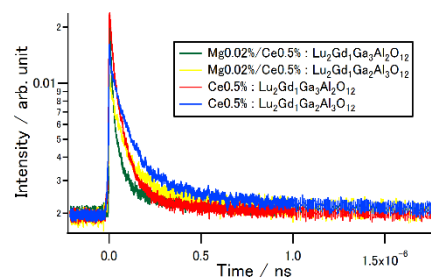


**Fig. 2** Scintillation decay curves of the Mg co-doped and non co-doped Ce:(Lu,Gd)<sub>3</sub>(Ga,Al)<sub>5</sub>O<sub>12</sub> crystals (excitation 662 keV of <sup>137</sup>Cs radioisotope).



## DIFFRACTIVE OPTICS FOR ASTRONOMY: VOLUME PHASE HOLOGRAPHIC GRATINGS BASED ON PHOTOPOLYMERS

Alessio Zanutta<sup>a</sup>, Andrea Bianco<sup>a</sup>

<sup>a</sup>INAF – Osservatorio Astronomico di Brera, via E. Bianchi 46, 23807, Merate (LC) – Italy – [alessio.zanutta@brera.inaf.it](mailto:alessio.zanutta@brera.inaf.it)

The improvement of astronomical instrumentations is fundamental in order to face the open issues of modern astronomy. A key contribution of this progress comes from the dispersing element, thanks to the introduction of Volume Phase Holographic Gratings (VPHGs)[1,2], which especially operate into low and medium resolution spectrographs. A key point for the manufacturing of such VPHGs is the development of new photosensitive materials that match the stringent requirements of the astronomical environment. Here we report on the performances of VPHGs based on Bayfol® HX solid photopolymer films, developed by Bayer MaterialScience AG, designed for volume gratings[3]. The most important features of these materials are the self-development and the fine-tuning of the final index modulation by the adjustment of the writing power. Moreover, the thickness homogeneity, material's reliability and the optical properties are very good.

Different Bayfol® HX materials have been characterized especially in terms of film thickness  $d$  and refractive index modulation  $\Delta n$ , which are the parameters responsible of the performances of VPHGs in the VIS-NIR region. Based on these results, we have proven the applicability in the astronomical field, developing VPHGs for spectrographs at the Asiago's telescope and at the Nordic Optical Telescope. Great performances have been obtained performing the observation of different sky objects[4,5].

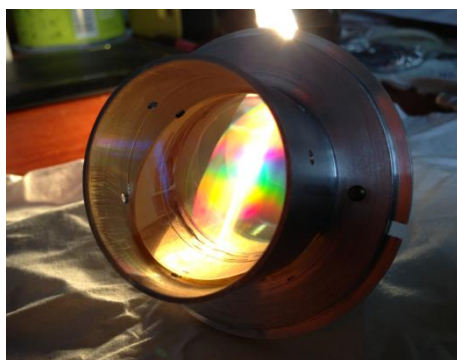


Figure 1: Example of astronomical dispersing element (VPHG and prisms), based on Bayfol® HX material used in the Asiago's spectrograph.

- [1] J. A. Arns, W. S. Colburn, S. C. Barden, Proc. of SPIE 3779 (1999) 313–323;
- [2] E. Molinari, A. Bianco, P. Conconi et al., Proc. of SPIE 6269 (2006) 6269N–8;
- [3] H. Berneth, F.-K. Bruder, T. Fäcke, R. Hagen, D. Hönel, T. Rölle, G. Walze, M.-S. Weiser, Proc. SPIE 8776 (2013) 877603-3;
- [4] A. Zanutta, M. Landoni, A. Bianco, L. Tomasella, S. Benetti, E. Giro, PASP 126 (2014) 264-269;
- [5] A. Zanutta, M. Landoni, A. Bianco et al., Proc. of SPIE 9147 (2014) 91474E-1.

## EFFICIENT POLYMER SOLAR CELLS FABRICATED BY TUNING COUPLED ELECTRICAL-OPTICAL PROPERTIES AT THE INTERFACE

Gopalan Sai-Anand<sup>a</sup>, Anantha-Iyengar Gopalan<sup>b</sup>, Kwang-Pill Lee<sup>c</sup>, Byoung-Ho Kang<sup>a</sup>,  
Jae-Sung Lee<sup>a</sup>, Sang-Won Lee<sup>a</sup>, Dae-Hyuk Kwon<sup>d</sup>, Shin-Won Kang<sup>a</sup>

<sup>a</sup>*School of Electronics Engineering, Kyungpook National University,  
Daegu 702-701, Republic of Korea, \*swkang@knu.ac.kr*

<sup>b</sup>*Department of Nano-Science & Technology, Kyungpook National University,  
Daegu 702-701, Republic of Korea*

<sup>c</sup>*Department of Chemistry Education, Kyungpook National University,  
Daegu 702-701, Republic of Korea*

<sup>d</sup>*School of Electronics Engineering, Kyungil University,  
Gyeongsan 712-702, Republic of Korea*

Polymer solar cells (PSCs) have been developed and demonstrated their potential as renewable and low cost energy resources because of the high possibility of commercialization based on the ease of processing [1]. Several approaches have been considered to improve the photo/power conversion efficiency (PCE) of the polymer bulk heterojunction (BHJ) solar cells, which include synthesizing new photoactive materials and tuning electrical and optical properties of the fabricated devices. Buffer layer plays a crucial role in achieving highly efficient PSCs [2]. Recent developments in BHJ PSCs are addressed to increase the PCE by the introduction of plasmonic particles into polymer layers for utilizing the plasmonic field effect and scattering of light [3]. However, the full exploitation of plasmonic aspects has not been extracted through adequate design of polymer structure in the BHJ PSCs. In recent years, the distribution of plasmonic nanostructures into conducting polymer (CP) matrix has infused a new area of research and applications [4][5]. In this work, we design and demonstrate that the inclusion of a buffer layer composed of the new functionalized CP and plasmonic nanoparticles (PNP) in the device configuration, enhances the light harvesting efficiency and electrical-optical properties at the polymer interface, leading to improved photovoltaic characteristics for the PSCs. As a proof of concept, we synthesized the new functionalized polyaniline (PANI-F) which can generate ‘*in situ*’ electric dipole at the interface and at the same time augments light absorption efficiency via the PNP anchored onto the PANI-F matrix. The new PANI-F/PNP nanocomposites (PANI-F/PNP-NC) was characterized by cyclic voltammetry, UV-Visible spectroscopy, X-ray diffraction, X-ray photoelectron spectroscopy and Atomic force microscopy. The current density-voltage curves of the devices fabricated with PANI-F/PNP-NC as buffer layer informed that the PCE of PSCs showed ~ 12 % improvement in the overall PCE, compared with the PSCs having pristine PANI-F. The superior photovoltaic characteristics observed for PANI-F/PNP-NC incorporated PSCs, is due to the synergistic tuning of electro-optical properties and the enhanced molecular ordering in the photoactive layer. The proposed device architecture with the inclusion of PANI-F/PNP NC as buffer layer is extendable to various other CP-PNP combinations and possibly opens up a new avenue for fabrication of the range of highly efficient PSCs.

[1] Y. Huang, E. J. Kramer, A. J. Heeger, G. C. Bazan, *Chem. Rev.*, 114 (2014) 7006-7043.

[2] R. Po, C. Carbonera, A. Bernardi, N. Camaioni, *Energ Environ Sci.*, 4 (2011) 285-310.

[3] J. L. Wu, F. C. Chen, Y. S. Hsiao, F. C. Chien, P. Chen, C. H. Kuo, C. S. Hsu, *ACS Nano.*, 5 (2011), 959-967.

[4] G. Sai-Anand, A.-I. Gopalan, S.-W. Kang, K.-P. Lee, *IEEE Elec. Dev. Lett.*, 34 (2013) 1065-1067.

[5] G. Sai-Anand, A.-I. Gopalan, S.-W. Kang, S. Komathi, K.-P. Lee, *Sci. Adv. Mater.*, 6 (2014) 1356-1364.

## **THEORETICAL CALCULATION OF OPTICAL AND ELECTRICAL PROPERTIES OF V DOPED ZnO USING IN SOLAR CELLS APPLICATIONS**

M. Boujnah<sup>1</sup>, A. Benyoussef<sup>1,2</sup> and A. El Kenz<sup>1</sup>

<sup>1</sup> *Laboratory of Magnetism and Physics of High Energies, Department of Physics, B.P. 1014, Faculty of Sciences, Mohammed V- Agdal University, Rabat, Morocco*

<sup>2</sup> *Institute of Nanomaterials and Nanotechnology, MASCIR Foundation, Rabat, Morocco*

*Corresponding author: boujnah.mourad@gmail.com*

Using the full-potential linearized augmented plane wave method (FP-LAPW) based on density functional theory (DFT) and Boltzmann's Transport theory, we study the electronic structure, Optical and electrical properties of Vanadium -doped wurtzite ZnO with different concentrations (3.125, 6.25, 12.5, 25%). The FP-LAPW based on the new potential approximation known as the Tran–Blaha modified Becke–Johnson exchange potential approximation (TB-mBJ). The calculated band structure and density of states (DOS) exhibit a band gap of pure ZnO (3.3 eV) closer to the experimental one. As well, our results indicate the average transmittance in the 400 to 1000 nm wavelength region was 93%. The optimized composition of the V doped ZnO, which had the highest conductivity ( $3,2 \cdot 10^3 \Omega \cdot \text{cm}$ ) and transmittance was  $\text{Zn}_{96.875}\text{V}_{3.125}\text{O}$ . We further identify that the lower concentration of heavily of V doped ZnO, the conductivity is stronger.

### **3D OPTICAL MEASUREMENT OF COMPOSITE STRAIN AND DISPLACEMENT IN RESTORED TEETH**

Dragica Manojlovic<sup>a</sup>, Milos Milosevic<sup>b</sup>, Nenad Mitrovic<sup>c</sup>, Vesna Miletic<sup>a</sup>

<sup>a</sup>*University of Belgrade, School of Dental Medicine, DentalNet Research Group, Rankeova 4, Belgrade, Serbia*

<sup>b</sup>*University of Belgrade, Innovation Center of Faculty of Mechanical Engineering, Kraljice Marije 16, Belgrade, Serbia*

<sup>c</sup>*University of Belgrade, Faculty of Mechanical Engineering, Kraljice Marije 16, Belgrade, Serbia*

Despite constant improvements, polymerization shrinkage and stress remain drawbacks of dental composites contributing to microleakage, secondary caries and pulpal damage. None of the currently marketed low-shrinkage composites is able to eliminate polymerization shrinkage.

The aim of this study was to measure strain and displacement of experimental composites using the 3D digital image correlation method.

An experimental low-shrinkage composite based on monomer FIT-852 (FIT; Esstech) and a conventional, control composite based on bisphenol A-glycidyl methacrylate (BisGMA; Sigma-Aldrich) were prepared by mixing resin/photoinitiator matrix with silanated barium-glass fillers in the amount of 70wt% or 74wt%. Modified Class 2 restorations were prepared in plastic and extracted human molars (n=5/group). Teeth were restored with composite either without an adhesive (plastic teeth) or with adhesive Optibond Solo Plus (Kerr) (human teeth). 3D optical measurements were done with a two-camera system (Aramis) with images taken immediately before and after light-curing. Data were statistically analyzed in Minitab 16 using a general linear model ( $\alpha=0.05$ ).

In plastic teeth, strain ranged from  $2.7\pm 1.4\%$  (FIT\_70) to  $4.7\pm 2.1\%$  (BisGMA\_70) whilst displacements varied between  $34\pm 22\ \mu\text{m}$  (BisGMA\_70) and  $69\pm 19\ \mu\text{m}$  (FIT\_70). Differences in strain between FIT\_70 and BisGMA\_70 in both plastic and human teeth were statistically significant ( $p<0.05$ ). Displacements between FIT\_70 and BisGMA\_70 were significant only in plastic teeth ( $p<0.05$ ). FIT\_74 showed lower displacements (mean  $38\text{-}47\ \mu\text{m}$ ) than FIT\_70 ( $60\text{-}69\ \mu\text{m}$ ) in plastic and human teeth ( $p<0.05$ ).

Lower strain i.e. polymerization shrinkage and displacement was confirmed for FIT-based composite. Higher filler content reduces material flow and displacement thereby increasing strain in the FIT-based composite.

## **A NANOPOROUS SILICON - ALUMINUM LIGHT EMITTING SCHOTTKY STRUCTURE INCORPORATED INTO SILICON CHIP**

*Aliaksandr G. Smirnov, Andrey A. Stepanov, Yugene V. Mukha  
Belarusian State University of Informatics and Radioelectronics, 220013 Minsk,  
Belarus*

To fabricate a LED integrated to a silicon chip we are using nanoporous silicon/aluminum Schottky structure. High current densities and high concentrations of hydrofluoric acid are generally needed during the electrochemical etching process to fabricate high porosity nanostructured silicon films [1]. However, short process time (non-controllability/uniformity of ultrathin films formation), and toxic (high HF vapor pressure), fluidity and aggressive reagents (etching Al layers and interconnections in the meanwhile) are serious concerns associated with it. Therefore, it is highly demanded to seek alternatives to fabricate ultrathin nanoporous Si films using lower current densities at low F<sup>-</sup> ion concentrations. We have developed an ultrathin nanoporous silicon fabrication process by electrochemical etching in ammonia fluoride water solution. It was shown that highly uniform and ultrathin high porosity nanoporous silicon films can be fabricated under very low current densities and fluorine ion concentration in a reproducible manner. Structural and electro optical properties of nanoporous silicon films will be discussed [2].

N-type <100> oriented phosphorous doped silicon substrates (0.1 Ohm cm and 0.01 Ohm cm) were used. The samples were anodized in NH<sub>4</sub>F:H<sub>3</sub>PO<sub>4</sub>:C<sub>2</sub>H<sub>5</sub>OH:H<sub>2</sub>O at current densities of 0.01 – 1 mA/cm<sup>2</sup> and 5 – 25 % H<sub>3</sub>PO<sub>4</sub> concentrations with halogen lamp illumination. At about 10 mA/cm<sup>2</sup> the behaviour turns and morphology of nanoporous silicon changes from regular vertical holes (at higher current densities) to sponge like structure (at lower current densities).

Pores size and structure of nanoporous silicon films were observed on the scanning electron microscope LEO 1550 Gemini. Its thickness and porosity was measured by Spectroscopic Ellipsometer VB-250 and then calculated. Photoluminescence and electroluminescence are measured by spectrometer, photoluminescence was excited by discrete 330 nm mercury lamp. For electroluminescent measurements 0.7 micron Al was PVD and anodized through photoresist mask. 200x200 micron pads leaves on the nanoporous silicon layer. Electrical measurements of the Schottky diodes are carried out by special equipment [3].

So, in this paper we report the stable and reproducible regimes of nanoporous silicon layers formation at ultra small current densities and fluorine ion concentrations which allows to fabricate effective light emitters incorporated into Si chips.

[1] L. T. Canham, A. G. Cullis, C. Pickering, O. D. Dossor, T. I. Cox, and T. P Lunch, Nature 368, 133 (1994)

[2] P. Jaguiro, P. Katsuba, S. Lazarouk, M. Farmer and A. Smirnov, Si-based emissive microdisplays, Physica E 41, 927 (2009)

[3] A.Smirnov, A.Hubarevich, A. Stsiapanau et al., in Mat. 9<sup>th</sup> Int. Conference Porous Semiconductor-Science and Technology PSST-2014, P. 170-172

## **A RECOMBINATION LUMINESCENCE IN THE FIELD OF TRANSITION TEMPERATURE OF KDP CRYSTAL**

Temirgaly Koketai, Ainura Tussupbekova, Elmira Mussenova, Anel Ibrayeva, Nurbolat Saidrakhimov

*Academician Y.A.Buketov Karaganda State University, 28 Universitetskaya Street  
Karaganda, Kazakhstan, aintus\_070482@mail.ru*

A recombinational luminescence in the field of transition temperature of KDP is observed obviously. It is connected to that for this exemplar light sum in TSL peak in the field of 110-130K is much more, than in KDP to a heat processing.

The result received at studying of spectral composition of peak of TSL at 125K is represented as more important. As well as earlier, it consists of two emission bands with maxima at 2.6 eV and 4.75 eV. It is established that the relation of radiation intensities in these optical strips does not change from temperature and duration of a heat processing [1]. Partial leaving of molecules of water leads to the considerable increase of preradiation deficiency of crystals. Besides, concentration of L-defects increases. Irrespective of it the ratio of intensity in strips of recombinational radiation does not change. It shows interrelation of two recombinational processes giving these emission bands.

[1] L.M. Kim, T.A. Kuketayev, B.S. Tagayeva. Book of the abstracts of 7th International Conf. Nuclear and Radiation Physics (2009) 132.

## AHARONOV-BOHM OSCILLATION MODES IN NON-UNIFORM QUASI-ONE-DIMENSIONAL RING UNDER LATERAL ELECTRIC FIELD

William Gutiérrez <sup>a</sup>, Iliia D. Mikhailov <sup>a</sup>, Marlon R. Fulla <sup>b,c</sup>, and Jairo H. Marín <sup>b</sup>

<sup>a</sup> *Escuela de Física, Universidad Industrial de Santander, Bucaramanga, Colombia*

<sup>b</sup> *Escuela de Física, Universidad Nacional de Colombia, Medellín, Colombia,*  
*jhmarin@unal.edu.co*

<sup>c</sup> *Institución Universitaria Pascual Bravo, AA 6564, Medellín, Colombia*

Low-lying states of a narrow one-electron nanoring with variable thickness in the presence of threading magnetic and lateral electric fields are analysed by using the adiabatic approximation [1-2]. In this technique the problem is reduced to a one-dimensional Schrödinger equation that describes the rotation of the electron along the ring in an axially non-homogeneous effective field whose potential depends on both the variation of the nanoring thickness and the external electric and magnetic fields. We solve this equation by using the Fourier method and present novel curves for energies of lower levels and the magnetization as functions of the magnetic and electric fields for structures with different profiles given by periodical dependencies of the ring thickness on the azimuthal angle. We show that the electronic properties of narrow nano-rings are very sensitive to both the external electric field and the structural non-homogeneity. Particularly, the non-homogeneous height of the ring and the in-plane electric field provide each one the electron localization and a quenching of the Aharonov Bohm oscillations for lower states, but if they act together the oscillations reinforcement instead of their quenching can be achieved. This opens a new possibility to control nanoring properties by external electric field.

[1] F. Rodríguez-Prada, L. F. García, and I. D. Mikhailov, *Physica E* 56 (2014) 393.

[2] M. R-Fulla, J. H. Marín, Y. A. Suaza, C. A. Duque, M. E. Mora-Ramos, *Phys. Lett. A*, 378 (2014) 2297.

## ALTERNATIVE SYNTHESIS METHODS OF PERSISTENT LUMINESCENT MATERIALS

Leonnam G. Merízio<sup>a</sup>, Ian P. Machado<sup>a</sup>, Lucas C.V. Rodrigues<sup>a</sup>, Jorma Hölsä<sup>b,c</sup>, Hermi F. Brito<sup>a</sup>

<sup>a</sup>Chemistry Institute, University of São Paulo, São Paulo-SP, Brazil, leomerizio@usp.br

<sup>b</sup>University of Turku, Department of Chemistry, Turku, Finland, jholasa@utu.fi

<sup>c</sup>Turku University Centre for Materials and Surfaces (MatSurf), Turku, Finland

Persistent luminescence materials emit light for several hours after ceasing irradiation. They consist usually of inorganic hosts with wide bandgap doped with emitters, *e.g.* rare earth ions such as  $\text{Eu}^{2+}$ ,  $\text{Pr}^{3+}$  and  $\text{Tb}^{3+}$  [1]. Studies on these materials have proliferated in recent years due to their diverse applications: emergency lighting, luminescent paints, radiation detectors and biological markers. The disilicate hosts are used due to their stable structure and the bandgap favorable to persistence luminescence [2]. The current challenges include the search for new synthesis methods to control of the parameters as particle size and morphology to yield improved persistent intensity and duration.

In this work,  $\text{Sr}_2\text{MgSi}_2\text{O}_7:\text{Eu}^{2+},\text{Dy}^{3+}$  materials were synthesized with two methods to improve the efficiency and to obtain small particle size. The materials were synthesized with i) a solid state method by annealing the intimately ground mixture of  $\text{SrCO}_3$ ,  $\text{MgCO}_3$ ,  $\text{SiO}_2$  and  $\text{R}_2\text{O}_3$  (R: Eu, Dy) and ii) by a co-precipitation method using the reaction between  $\text{SrCl}_2$ ,  $\text{MgCl}_2$ ,  $\text{RCl}_3$  and  $\text{Na}_2\text{SiO}_3$ . The precursors were heated in static air at 700 °C for 2 h and then at 1150 °C for 5 h in CO in both methods. The materials were characterized by infrared absorption spectroscopy, X-ray Powder Diffraction (XPD), Scanning Electronic Microscopy (SEM) and luminescence spectroscopy. The XPD patterns indicate the formation of the desired  $\text{Sr}_2\text{MgSi}_2\text{O}_7$  phase with a small amount of a  $\text{MgSiO}_3$  impurity in the co-precipitation material. The Scherrer calculations indicate smaller crystallite size for the co-precipitation method. The excitation spectra (Fig. 1, left) show two broad bands centered from 250 to 450 nm assigned to the  $\text{Eu}^{2+} 4f^7 \rightarrow 4f^65d^1$  transitions. Several  $\text{Eu}^{3+} 4f-4f$  absorption lines are observed in these spectra centered at *e.g.* 396, 420 and 450 nm. The emission spectra (Fig. 1, right) of the materials are similar with a broad band centered at 470 nm (blue) arising from the  $\text{Eu}^{2+}$  parity allowed  $4f^65d^1 \rightarrow 4f^7$  transition. This indicates energy transfer from  $\text{Eu}^{3+}$  to  $\text{Eu}^{2+}$ . Both materials can be efficiently excited in the visible range allowing applications in the storage of sun light energy.

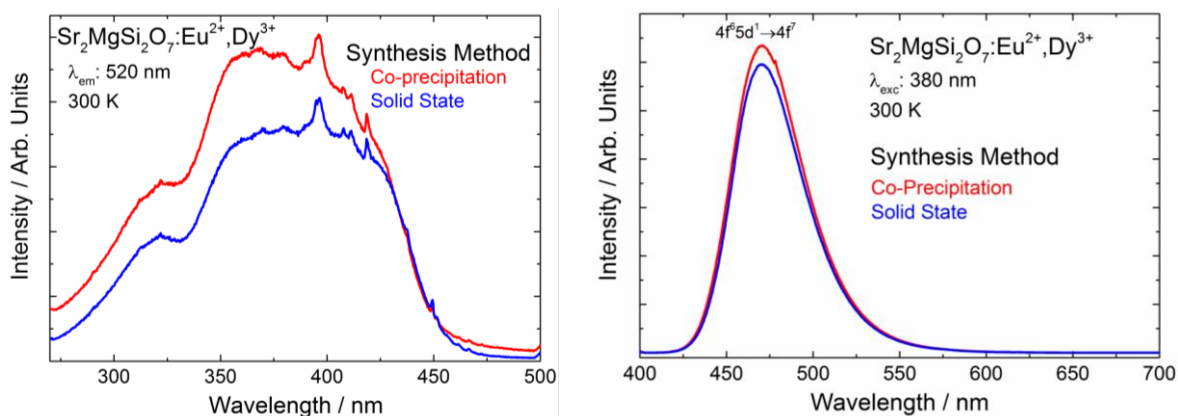


Fig. 1 – Excitation (left) and emission (right) spectra of  $\text{Sr}_2\text{MgSi}_2\text{O}_7:\text{Eu}^{2+},\text{Dy}^{3+}$  materials prepared with the solid state and co-precipitation methods.

[1] H.F. Brito, J. Hölsä, T. Laamanen, M. Lastusaari, M. Malkamäki, L.C.V. Rodrigues, Opt. Mater. Express 2 (2012) 371–381.

[2] M. Lastusaari, H. Jungner, A. Kotlov, T. Laamanen, L.C.V. Rodrigues, H.F. Brito, J. Hölsä, Z. Naturforsch. B 69 (2014) 17–182.



## SENSITIZER-LIMITED EXCITON DIFFUSION IN LIGHT-UPCONVERTING DIPHENYLANTHRACENE/PMMA FILMS

Steponas Raisys<sup>a</sup>, Karolis Kazlauskas<sup>a</sup>, Saulius Jursenas<sup>a</sup>, Yoan Simon<sup>b</sup>

<sup>a</sup>*Institute of Applied Research, Vilnius University, Sauletekio 9-III, Vilnius, Lithuania, steponas.raisys@tmi.vu.lt*

<sup>b</sup>*Adolphe Merkle Institute, University of Fribourg, Chemin Verders 4, Fribourg, Switzerland*

Low power upconversion *via* triplet-triplet annihilation (TTA) is considered to be very promising for enhancing performance of photovoltaic cells, since the power density of the sun light is sufficient to accomplish the upconversion process. Despite the fact that upconversion efficiency ( $\Phi_{UC}$ ) in a solution exceeds 30%, [1] in a solid state it drops down by more than one order of magnitude. Although all the factors responsible for the efficiency drop are still unclear, they are believed to be emitter concentration-dependent and associated with inefficient singlet/triplet exciton diffusion and emitter self-quenching. Reduced emitter concentration may indeed prevent quenching, however, it will also impede exciton hopping and hence lower the probability of TTA. Thus, for maximization of  $\Phi_{UC}$ , the influence of each process needs to be evaluated as a function of emitter concentration. For this, evaluation of diffusion length ( $L_D$ ) of both singlet and triplet excitons at different emitter concentration is crucial.

In this work, singlet and triplet exciton diffusion in the poly(methyl methacrylate) (PMMA) films containing 9,10-diphenylanthracene (DPA) as an emitter and platinum octaethylporphyrin (PtOEP) as a triplet exciton sensitizer was investigated. The films were prepared by melt-processing technique [2] for suppressed emitter aggregation at high concentrations. Exciton diffusion was determined from the emission quenching efficiency in the DPA:PtOEP:PMMA films with randomly distributed quenchers. Monte Carlo simulations and Stern-Volmer approach were applied to quantitatively model excited state relaxation dynamics in DPA:PtOEP:PMMA/quencher blends with increasing quencher concentration (0 – 2 wt%) for the evaluation of  $L_D$ . [3,4] Optimization of  $\Phi_{UC}$  vs emitter concentration revealed optimal DPA concentration (25 wt%) necessary to achieve maximal  $\Phi_{UC}$  in the solid DPA:PtOEP:PMMA films. In the absence of sensitizer,  $L_D$  for the singlet excitons was found to increase from 27 nm up to 41 nm with increasing DPA concentration from 20% to 35%, respectively. Meanwhile in the presence of small amount of sensitizer (0.05%),  $L_D$  remained independent (~15 nm) of DPA concentration. In contrast, in the case of triplet excitons, an increase of  $L_D$  from 31 nm up to 50 nm with increasing DPA concentration by the same amount was observed even with the present of sensitizer.

The results imply efficient exciton diffusion for both singlets and triplets. While for the triplets long  $L_D$  ensures enhanced TTA and upconversion, for the singlets it implies additional losses due to the energy transfer to sensitizer. Insensitivity of  $L_D$  to the amount of DPA in the DPA:PtOEP:PMMA films indicates sensitizer-limited singlet exciton diffusion.

[1] Y. Y. Cheng, T. Khoury, R. G. C. R. Clady, M. J. Y. Tayebjee, N. J. Ekins-Daukes, M. J. Crossley, T. W. Schmidt, *Phys. Chem. Chem. Phys.*, 12 (2010) 66–71.

[2] S. H. Lee, J. R. Lott, Y. C. Simon, C. Weder, *J. Mater. Chem. C*, 1 (2013) 5142–5148.

[3] O. V. Mikhnenko, H. Azimi, M. Scharber, M. Morana, P. W. M. Blom, M. A. Loi, *Energy Environ. Sci.* 5 (2012) 6960–6965.

[4] H. Y. Hsu, J. H. Vella, J. D. Myers, J. Xue, K. S. Schanze, *Phys. Chem. C* (2014) 118, 24282–24289.

## ANALYSIS OF THERMOLUMINESCENCE GLOW CURVES OF Ga<sub>2</sub>SeS LAYERED CRYSTALS

Mehmet Isik<sup>a</sup>, Serdar Delice<sup>b</sup>, Nizami Hasanli<sup>b</sup>

<sup>a</sup>*Dept. of Electrical and Electronics Engineering, Atilim University, Ankara, Turkey,*  
*mehmet.isik@atilim.edu.tr*

<sup>b</sup>*Dept. of Physics, Middle East Technical University, Ankara, Turkey, sdelice@metu.edu.tr,*  
*nizami@metu.edu.tr*

GaSe and GaS semiconducting compounds have been attractive materials used in optoelectronic devices in red and blue regions. The large optical non-linearity properties of these materials make them very promising materials in the areas of optical switching devices and photo-detectors. The researches on both compounds showed that GaSe can be especially used in nonlinear optical application whereas GaS is a promising material for near-blue light emitting devices. Ga<sub>2</sub>SeS is one of the GaS<sub>x</sub>Se<sub>1-x</sub> mixed crystals formed from GaSe and GaS. Taking into consideration the role of constituent compounds in the technological applications, Ga<sub>2</sub>SeS mixed crystal can be thought as a promising candidate to be used in the fabrication of long-pass filter, light emitting devices and optical detecting systems.

Thermoluminescence (TL) is a technique used to characterize the trapping centers arising due to the defects and/or impurities which are one of the principal factors affecting the performance of optoelectronic devices such as LEDs, lasers. Low-temperature (10–300 K) TL measurements were performed on the Ga<sub>2</sub>SeS crystals grown by Bridgman method. The characterization of trapping centers was accomplished using various methods for analysis of TL glow curves. The presence of three trapping centers located at 6, 30 and 72 meV was revealed from the analysis. Heating rate dependence of the observed TL peaks was studied for the rates between 0.4 and 1.0 K/s (Fig. 1). Distribution of the traps was also investigated using an experimental technique [ $T_m(E_a) - T_{stop}$ ] based on thermal cleaning (Fig. 2). The distributed levels with activation energies increasing from 6 to 136 meV were revealed by rising the stopping temperature from 10 to 52 K.

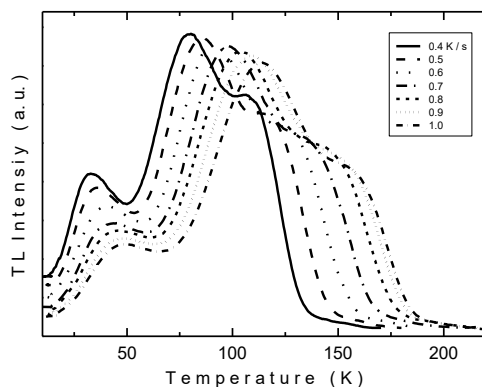


Fig. 1. Experimental TL curves of Ga<sub>2</sub>SeS crystals with various heating rates.

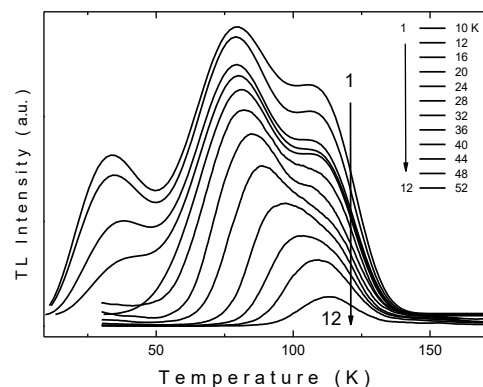


Fig. 2. TL glow curves of Ga<sub>2</sub>SeS crystals at different  $T_{stop}$  temperatures.

## **ATOMIC LAYER DEPOSITION OF Al-DOPED ZnO FILMS: OPTICAL PROPERTIES TUNING**

Dimitre Z. Dimitrov, Blagoy Blagoev, Vladimir Mehandzhiev, Jerome Leclercq and Peter Sveshtarov

*Institute of Solid State Physics, Bulgarian Academy of Sciences, Blvd. Tzarigradsko Chaussee 72, Sofia, Bulgaria, dzdimitrov@issp.bas.bg*

Optical and electrical properties of ZnO can be tailored by doping using, for instance, aluminum or/and aluminum oxide ( $\text{Al}_2\text{O}_3$ ). Al-doped ZnO (AZO) films were deposited by atomic layer deposition (ALD) on silicon, borosilicate glass and sapphire substrates. The Al composition of the films was varied from 1% to 5% by controlling the ratio of Zn:Al pulses. Film resistivity was measured as a function of Al content and the substrate temperature used for ALD deposition in order to obtain the minimum of resistivity. X-ray diffraction (XRD) was performed on the films, showing a reduction in lattice parameter, as a function of Al concentration, indicating that  $\text{Al}^{3+}$  ions occupy substitutional sites in the ZnO lattice. The resistivity of films deposited on different substrates was measured and related to the structure. The surface morphology of the films on silicon, glass and sapphire was compared using scanning electron microscopy (SEM), which showed similar grain sizes on each substrate, suggesting that the difference in conductivity was due to grain orientation rather than microstructural differences. Optical properties were measured using spectrophotometry and ellipsometry. It was found that the transparency was  $>80\%$  for wavelengths of 370–1600 nm.

## **ATOMIC ORDERING AND BIAxIAL STRAIN WITHIN MOVPE-GROWN III-V SEMICONDUCTOR ALLOYS: ANALYSIS OF PHOTOLUMINESCENCE EMISSION POLARIZATION**

T. Prutskij<sup>a</sup>, N. Makarov<sup>a</sup>, G. Attolini<sup>b</sup>

<sup>a</sup> *Instituto de Ciencias, BUAP, Privada 17 Norte, No 3417, col. San Miguel Huyeotlipan, 72050, Puebla, Pue., México, tatiana.prutskij@correo.buap.mx*

<sup>b</sup> *IMEM/CNR, Parco Area delle Scienze 37/A - 43010, Parma, Italy*

Knowledge and understanding of light waves polarization is important in the use of several optical devices, such as lasers and light-emitting diodes. On the other hand many optoelectronic light-emitting devices are based on ternary and quaternary semiconductor III-V alloys. It is widely known that within III-V ternary or quaternary alloys grown by Metalorganic Vapor Phase Epitaxy (MOVPE), atomically ordered clusters are spontaneously formed during the epitaxial growth. [1] The atomic ordering within GaInP alloy corresponds to the presence of a superlattice structure consisting of alternated In-rich and Ga-rich {111} diagonal planes, with interleaving planes of P atoms. The resulting symmetry of the crystal lattice of ordered alloy causes reduction of the band-gap energy (with respect to its value in the disordered material) and splitting of the valence band. Another factor that changes the symmetry of the alloy is an internal biaxial strain due to a mismatch between the epitaxial layer and the substrate. As a consequence, the PL emission of the alloy becomes polarized.

We analyze here the linear polarization of the photoluminescence (PL) emission of GaInP and GaInAsP epitaxial layers grown by MOVPE technique on Ge and GaAs substrates. We measured angular polarization dependences of the PL emission intensity from the (001) surface plane and from (110) and (1-10) edge planes of the epitaxial layer at different temperatures. The PL measurements were performed using the backscattering geometry for the PL emission propagating along the [001] crystallographic direction and the right-angle scattering geometry for that propagating along [110] and [1-10] directions. In order to estimate the degree of atomic ordering and biaxial strain within the layer, the measured angular dependencies were compared with that calculated using the model based on symmetry considerations. [2]

With decreasing temperature, the elastic biaxial strain changes due to different temperature dependences of dilatation coefficients of the layer and the substrate, while the value of the ordering parameter of the layer remains. Thus, studying the temperature dependence of the PL emission polarization, one can separate contributions of atomic ordering and of biaxial “epitaxial” strain. We measured and calculated the polarization angular dependences of the PL emission propagating along the [001] crystallographic direction at different temperatures and analyzed their temperature evolution. We estimated the value of the elastic biaxial strain within the layer at different temperatures by fitting experimental and calculated polarization patterns. Our study demonstrate that the increase of the PL emission polarization at low temperatures can be explained by the change of the biaxial strain due to the difference of the thermal expansion coefficients of the layer and the substrate. We also discuss the limits of application of the model developed for ternaries III-V alloys to quaternaries.

[1] A. Gomyo, T. Suzuki, S.Kawata, I. Hino, T. Yuasa, Appl. Phys. Lett., 50 (1987) 673-675

[2] S.-H. Wei and A. Zunger, Phys. Rev. B 49 (1994) 14337-14351.

## AXIAL SELF-TRAPPED EXCITON CONFIGURATIONS IN BERYLLIUM OXIDE

Michael A. Botov<sup>a</sup>, Aleksey Yu. Keznetsov<sup>b</sup>, Aleksandr B. Sobolev<sup>a</sup>

<sup>a</sup>*Dept. of High Mathematics, Ural Federal University, 19 Mira St., Yekaterinburg, Russia, scibma@gmail.com*

<sup>b</sup>*Dept. of Experimental Physics, Ural Federal University, 19 Mira St., Yekaterinburg, Russia,*

Presented work is devoted to theoretical investigation of two axial self-trapped exciton (STE) configurations in beryllium oxide crystal. Our study is based on *ab-initio* calculations performed in CRYSTAL09 package using Hartree-Fock (HF) approximation and density functional theory (B3LYP). Atoms were described by their full-electron basis set (5-11G for Be and 8-411G for O) with optimized valence shells. Supercell (SC) for defect calculation contains 109 atoms. All calculations were performed using periodic boundary conditions and full SC geometry relaxation.

We study two STE orientation: co directional to z-axis (STE electron density center is localized mainly inside beryllium-oxygen tetrahedron) and reversed situation - contra directional to z-axis.

As far as electronic structure is concerned it is presented in density of states (DOS) chart and charge density distribution maps (e.g. Fig.1 (a), (b) and (c))

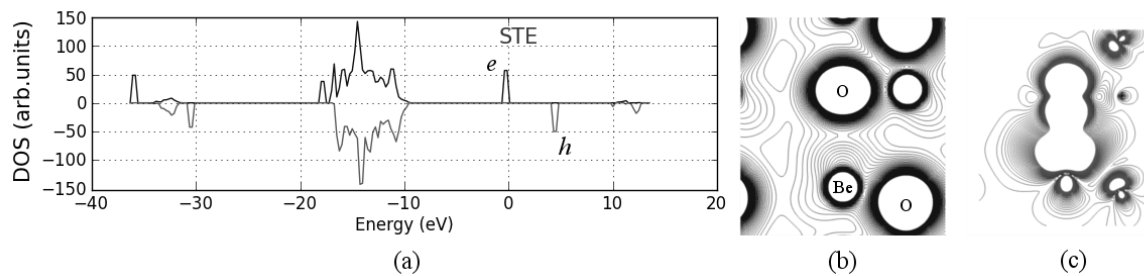


Fig.1 (a) DOS for axial STE in BeO. (b) Charge density maps of STE. (c) Spin density maps of STE. Both of maps belong to “co directional” configuration. Slice represents zx-plane. (HF, 109 atoms SC)

Electron and hole levels are clearly observable. Two defect levels in band structure of material are shown up in luminescence spectrum also. Our results as to luminescence are presented in Table 1.

Table1. Axial STE luminescence bands (SC 109 atoms)

Configuration	HF	B3LYP30	Exp.[1,2]
co directional	6.0	6.5	4.9
contra directional	9.2	7.8	6.7

[1] K.N. Giniyatulin, A.F. Malysheva, A.V. Kruzhalov, T.N. Kyarner, Tr.Inst.Fiz.Akad.Nauk Estonii, 53 (1982) 71

[2] V.Y. Ivanov, V.A. Pustovarov, A.V. Kruzhalov, B.V. Shulgin, Nucl.Instr.Meth.Phys.Res.A 282 (1989) 559

## **BiFeO<sub>3</sub> CERAMICS: PROCESSING, OPTICAL AND MAGNETIC PROPERTIES**

Maria Čebela<sup>a</sup>, Radmila Hercigonja<sup>b</sup>, Marija Prekajski<sup>a</sup>, Miljana Mirković<sup>a</sup>, Jelena Pantić<sup>a</sup>,  
Jelena Luković<sup>a</sup>, Branko Matović<sup>a</sup>

<sup>a</sup>*"Vinca" Institute of Nuclear Sciences, Materials Science Laboratory, University of  
Belgrade, P.O. Box 522, Serbia, mcebela@vinca.rs*

<sup>b</sup>*Faculty of Physical Chemistry, University of Belgrade, Serbia, rada@ffh.bg.ac.rs*

Nanosized bismuth ferrite powder has a potential application in the production of lead free piezoelectric materials for actuators as well as magnetoelectric sensors. The simple, low-costing and energy-saving hydrothermal method has advantages over the conventional methods. Crystalline bismuth ferrite (BiFeO<sub>3</sub>) powder was synthesized via hydrothermal method at 200°C using Bi(NO<sub>3</sub>)<sub>3</sub>×5H<sub>2</sub>O and Fe(NO<sub>3</sub>)<sub>3</sub> ×9H<sub>2</sub>O, as starting materials and 8 M KOH as a mineralizer. The X-ray diffraction (XRD), IR and Raman spectroscopy have been performed on the synthesized bismuth ferrite (BFO) powders in order to confirm the formation of pure and well-crystallized BFO nanocrystallites. <sup>57</sup>Fe Mössbauer spectroscopy was performed in order to provide information on Fe cation arrangement in the BiFeO<sub>3</sub> phase. The magnetic and optical properties of BFO samples were characterized by SQUID magnetometry, and ultraviolet–visible spectroscopy. Temperature dependence of magnetization shows antiferromagnetic-paramagnetic phase transition at T<sub>N</sub>= 220 K, while below this temperature weak ferromagnetic ordering is detected.

## **BISMUTH SILICATE NANOPARTICLES: STRUCTURAL CONTROL AND RARE EARTH DOPING FOR UPCONVERSION**

Michele Back, Enrico Trave, Patrizia Canton, Pietro Riello

*Department of Molecular Sciences and Nanosystems, Ca' Foscari University of Venezia, Via Torino 155/b, 30170 Mestre - Venezia, Italy*

This research deals with the development of a new class of nanophosphors, consisting in bismuth silicate crystalline matrices doped with lanthanide ions. The high selectivity of the emissions generated by the luminescent ions and the consequent control of the spectral features for the emitted radiation open for the use of the here investigated systems in several technological areas, ranging from bioimaging to anticounterfeiting, from temperature sensing to photocatalysis, from LED to solar cell technology.

The interest in  $\text{Bi}_x\text{Si}_y\text{O}_z$  compounds (primarily  $\text{Bi}_2\text{SiO}_5$ ) as host for luminescent systems is mainly due to the silicate nature, which implies a refined control of the nanoparticle surface functionalization and the possibility of interfacing with different optical and optoelectronic devices.

Due to the high reactivity of the bismuth with the silica, the procedure adopted for the synthesis of the bismuth silicate nanostructures was based on impregnation of mesoporous silica nanoparticles (MSNs) with Bi and lanthanide salt solutions. Peculiar core-shell self-assembling mechanism for nanoparticle formation was evidenced by TEM analysis. Dedicated synchrotron XRD experiment during sample heating at different temperature was performed to follow the silicate structural evolution by “in situ” WAXS analysis.

Bismuth silicate doping with  $\text{Yb}^{3+}$  and other rare earth ions as  $\text{Er}^{3+}$ ,  $\text{Tm}^{3+}$  and  $\text{Ho}^{3+}$  was done in order to realize near IR pumped upconverting nanoparticles (UCNPs). We explored the chromaticity variation of the synthesized UCNPs by adjusting the molar ratios between the different doping rare earth ions. It is worth to emphasize the possibility to achieve the realization of a white light emitting system under near IR pumping. The dynamics of the energy transfer mechanism involved in the UC process was investigated, together with the effect of both power variation and photoexciting pulse modulation on the UCNP emission spectrum.

## BLUE TO GREEN TUNABLE LUMINESCENCE OF Ce<sup>3+</sup> DOPED YTTRIUM SILICATE PHOSPHORS

Adrian I. Cadis<sup>a</sup>, Laura.E. Muresan<sup>a</sup>, Ioana Perhaita<sup>a</sup>, Dan T. Silipas<sup>b</sup>

<sup>a</sup>Raluca Ripan Institute for Research in Chemistry-UBB, 30 Fantanele, Cluj-Napoca, Romania, laura\_muresan2003@yahoo.com

<sup>b</sup>National Institute R&D for Isotopic and Molecular Technologies, 67-103 Donath, Cluj-Napoca, Romania, dan\_silipas@yahoo.com.

In the present study, the luminescent properties of rare earth (cerium and/or terbium) activated yttrium silicate phosphors (YSO:RE), were investigated in order to elucidate the role of the activator system for color tuning of the phosphor emission as well as to identify the energy transfer processes. Synthesis of the mixed rare earth silicates phosphors was carried out using the gel combustion method.

The synthesis takes place in three stages: (1) preparation of the gels; (2) formation of ashes by the combustion of gels and (3) preparation of the phosphors by thermal treatment of the ashes at 1400°C for 4 hrs in air atmosphere.

The phosphor samples were characterized by SEM, FT-IR, XRD, ICP-OES and PL investigations.

Under different excitation wavelength, YSO:RE phosphors exhibit various emission colors from blue to green depending on the activator system and amount of rare earth (Figure1). The photoluminescent characteristics of the phosphor powders are correlated with their morpho-structural characteristics.

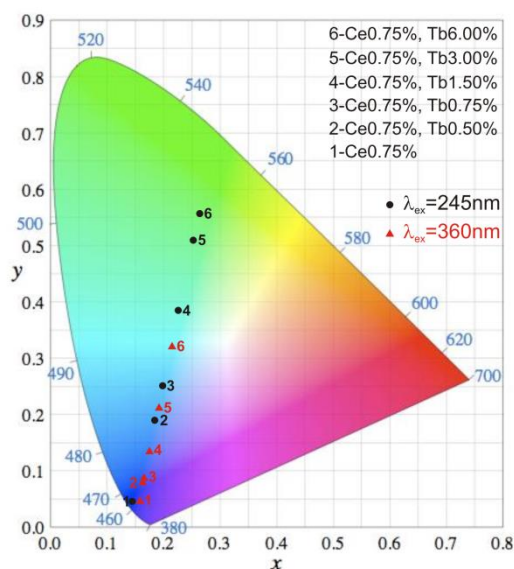


Figure 1 Chromatic coordinates of YSO:RE samples

### Acknowledgments

This work was supported by a grant of the Romanian National Authority for Scientific Research, CNCS – UEFISCDI, project number PN-II-RU-TE-2012-3-0360.



## BRANCHED RELAXATION OF ELECTRONIC EXCITATIONS DURING PHOTOELECTRON SCATTERING IN N<sub>2</sub> DOPED SOLID Kr

O.N. Bliznjuk, N.Yu. Masalitina, A.N. Ogurtsov

*National Technical University "KhPI", Frunse Str. 21, Kharkov, 61002, Ukraine  
onbliznjuk@ukr.net*

In rare-gas solids the energy loss rate of photoelectrons with energies above the band gap energy is mainly determined by electron-electron scattering [1]. The scattering of a hot photoelectron by a valence electron results in the formation of an additional electron-hole pair which can be bound or free. Such processes of multiplication of excitations with well-defined thresholds lead to prominent structures in the photoluminescence excitation spectra [2]. The influence of inelastic electron-electron scattering processes on quantum efficiency of intrinsic photoluminescence have been the subject of continuous interest as a powerful tool to investigate the relaxation mechanisms in rare-gas solids [3].

Solid krypton doped with N<sub>2</sub> was extensively used to investigate intra- and intermolecular energy relaxation into the impurity subsystem [4]. Because of the fast electronic relaxation by the intersystem crossing to the lowest excited  $A^3\Sigma_u^+$  state and the pronounced Vegard-Kaplan bands emission, N<sub>2</sub> can be used as a sensitive luminescent probe to detect electronic relaxation at an impurity [5].

This paper reports the observation of the influence of inelastic photoelectron scattering on luminescence of N<sub>2</sub> doped solid Kr.

The photoluminescence experiments were carried out at the SUPERLUMI experimental station at HASYLAB, DESY, Hamburg [6]. Solid krypton exhibit strong effects of neutral and charged defect formation induced by electronic transitions[2]. Therefore all measurements were carried out after saturation of dose effects at steady concentration of point defects and ionic centers.

Under selective excitation by synchrotron radiation the threshold energies for multiplication of electronic excitations were measured. The data obtained suggest that in N<sub>2</sub> doped solid Kr three types of photoelectron scattering exist: (i) long-range photoelectrons are scattered inelastically by the impurity molecules, (ii) short-range photoelectrons with energies about  $E_g + E_{\text{exciton}}$  form electronic polaron complexes, (iii) photoelectrons with energies above  $2E_g$  can create intrinsic ionic centers as a result of formation of secondary electron-hole pairs during scattering. The influence of mean free path of photoelectrons on scattering process is discussed.

[1] A.N. Ogurtsov, E.V. Savchenko, J. Becker, M. Runne, G. Zimmerer. Chem. Phys. Lett. 281 (1997) 281–284.

[2] A.N. Ogurtsov, Cryocrystals Modification by Electronic Excitations, NTU "KhPI", Kharkov, 2009.

[3] A.N. Ogurtsov, in: E.C. Faulques, D.L. Perry, A.Y. Yeremenko (Eds.), Spectroscopy of Emerging Materials, Kluwer, Dordrecht, 2004, 45–56.

[4] S.L. Pan, G. Zumofen, K. Dressler. J. Chem. Phys. 87 (1987) 3482–3491.

[5] A.N. Ogurtsov, O. N. Bliznjuk, N. Yu. Masalitina, ITE 1 (2013) 54–58.

[6] N.Yu. Masalitina, O. N. Bliznjuk, A. N. Ogurtsov, HASYLAB Jahresbericht (2008) 1117–1118.

## CATHODOLUMINESCENCE STUDY OF LuAG:CeGdGa SINGLE CRYSTALLINE FILMS

Ondrej Lalinsky<sup>a</sup>, Petr Schauer<sup>a</sup>, Miroslav Kucera<sup>b</sup>, Zuzana Onderisinova<sup>b</sup>, Martin Hanus<sup>b</sup>

<sup>a</sup>*Institute of Scientific Instruments of the CAS, Kralovopolska 147, 612 64 Brno, Czech Republic, xodr@isibrno.cz*

<sup>b</sup>*Charles University, Faculty of Mathematics and Physics, 121 16 Prague, Czech Republic*

Cerium activated single crystals of lutetium aluminum garnet (LuAG:Ce) are prospective scintillation materials for detection of X-rays, gamma rays or high energy particles [1]. However, the LuAG:Ce single crystals usually contain various unwanted structural defects (mainly antisite defects) which can result in nonradiative recombination and in delayed luminescence decay (afterglow). It was shown previously [2] that the concentration of these defects decreases with the decreasing temperature of the crystal growth. Therefore, single crystalline epitaxial films have attracted a lot of attention recently because the growth temperature of LuAG:Ce films is about a half (1000 °C) of the bulk ones (2000 °C). Although some new defects can be created due to strain in the film, the concentration of the antisite defects is highly reduced, as shown in this work. Moreover, the influence of Gd and Ga substitution on the cathodoluminescence (CL) properties was studied.

Specimens of the LuAG:CeGdGa multicomponent epitaxial films with different concentration of Ce, Gd and Ga were grown from lead-free BaO-B<sub>2</sub>O<sub>3</sub>-BaF<sub>2</sub> flux. The films were excited by an electron beam with energy of 10 keV using a specialized CL apparatus [3]. CL spectra, CL intensity decays and thermoluminescence glows in the temperature range between 100 and 500 K were obtained.

It was shown, that a balanced Gd and Ga admixture into the LuAG:Ce film provided an excellent scintillator where the effect of unwanted structural defects was suppressed, the spectrally corrected CL light yield value exceeded 150 % of the commercially available bulk LuAG:Ce single crystal, and CL decay was dominated by a component with 50-80 ns decay time which is close to that of Ce<sup>3+</sup> (5d-4f) photoluminescence decay. Moreover, a weak fast decay component with 11 ns decay time was observed. Since now, comparable component has been published only in one work related to similar structures [4]. The origin of this component could be in the strain in the film due to different lattice parameter of the film and the layer. Measured CL decays of approximately homoepitaxial film and of a bulk LuAG:Ce affirm this theory because the 11 ns fast component wasn't observed here.

[1] M. Nikl, A. Yoshikawa, K. Kamada, K. Nejezchleb, C.R. Stanek, J.A. Mares, K. Blazek, Prog. Cryst. Growth Charact. Mater. 59 (2013) 47.

[2] M. Nikl, E. Mihokova, J. Pejchal, A. Vedda, Y. Zorenko, K. Nejezchleb, Phys. Status Solidi B 242 (2005) R119-R121.

[3] J. Bok, P. Schauer, Rev. Sci. Instrum. 82 (2011) 113109.

[4] M. Kucera, M. Hanus, Z. Onderisinova, P. Prusa, A. Beitlerova, M. Nikl, IEEE Trans. Nucl. Sci. 61 (2014) 286-287.

## CHARACTERIZATION OF Ge-Ga-Se GLASSES USING OPTICAL AND POSITRON ANNIHILATION TECHNIQUE

Halyna Klym<sup>a</sup>, Adam Ingram<sup>b</sup>, Oleh Shpotyuk<sup>c,d</sup>, Ivan Karbovnyk<sup>e</sup>

<sup>1</sup>*Lviv Polytechnic National University, 12 Bandera str., 79013 Lviv, Ukraine,  
klymha@yahoo.com*

<sup>2</sup>*Physics Faculty of Opole University of Technology, 75 Ozimska str., 45370, Opole, Poland*

<sup>3</sup>*Vlokh Institute of Physical Optics, 23, Dragomanov str., 79005, Lviv, Ukraine*

<sup>4</sup>*Institute of Physics of Jan Dlugosz University,  
13/15 al. Armii Krajowej, 42201 Czestochowa, Poland*

<sup>5</sup>*Ivan Franko National University of Lviv, Department of Electronics  
107 Tarnavskogo str., 79017 Lviv, Ukraine*

Ge-Ga-Se chalcogenide glasses (ChG) possessing good transparency in 0.8-16  $\mu\text{m}$  spectral range are widely used in optoelectronic systems exploring thermal and optical imaging effects in both atmospheric telecommunication windows (3-5 and 8-12  $\mu\text{m}$ ). It is known that crystallization of such ChG can improve their physical, mechanical and thermal properties considerably, but it is difficult to produce IR transmitting glass-ceramics properly because growing crystals is generally out of control during heat treatment, which makes the material opaque. However, the row of experimental probes available to study atomic-deficient void structure of such materials is rather limited, especially at nanometer and sub-nanometer scale. One of the best techniques capable to identify such finest free-volume voids is positron annihilation lifetime (PAL) spectroscopy, the method grounded on physical phenomenon of electron interaction with its antiparticle (positron) in a matter. In the present paper, we imply, the PAL and optical methods to study of crystallized 80GeSe<sub>2</sub>-20Ga<sub>2</sub>Se<sub>3</sub> ChG caused by thermally-activated treatment above- $T_g$  annealing for 10, 25, 50 and 80 h.

It is shown that crystallization process in 80GeSe<sub>2</sub>-20Ga<sub>2</sub>Se<sub>3</sub> glasses influences their optical transmission spectra. The non-annealed glassy samples show maximum optical transmittance at the level of 65 %. Annealing at 380 °C decreases this transmittance and shifts optical transmission edge in a long-wave side. The appearance of growing of Ga<sub>2</sub>Se<sub>3</sub> and GeGa<sub>4</sub>Se<sub>8</sub> nanocrystals inside glassy matrix induces light scattering at shorter wavelengths. With increasing heat treatment to 80 h, the crystallization of GeSe<sub>2</sub> on glass surface provokes decrease in optical transmittance. Generally, this phenomenon shows the presence of large crystals that deteriorate optical transparency of the material rapidly, leading progressively to its whole opacity in IR range. It can be concluded that large GeSe<sub>2</sub> crystallites are precipitated on the surface of glasses crystallized for a long time. The sizes of inner Ga<sub>2</sub>Se<sub>3</sub> and GeGa<sub>4</sub>Se<sub>8</sub> nanocrystallites are much smaller than those of GeSe<sub>2</sub> crystals on the surface, and do not change with heat-treatment above 50 h. It means that new Ga<sub>2</sub>Se<sub>3</sub> and GeGa<sub>4</sub>Se<sub>8</sub> nanocrystallites do not appear in a bulk under prolonged annealing, while void fragmentation further proceeds in thermally-relaxed glassy matrix.

Modification of free-volume structure of ChG leading to specific fragmentation of larger free-volume entities (positron trapping voids) into a greater number of smaller ones with a previous nucleation process in the initial stage of annealing. Such effect reveals an increase of the second lifetime component and a decrease of its intensities testifying in a favour of increased number of smaller free volumes. In accordance to PAL spectroscopy, the studied ChG cannot be classified as typical pseudo-binary system based on non-additivity of defect-free bulk lifetimes  $\tau_b$  of its constituting components (GeSe<sub>2</sub> and Ga<sub>2</sub>Se<sub>3</sub>).

HK and IK thank EU CALIPSO program under FP7

## TEMPERATURE DEPENDANCE OF LUMINESCENCE OF $\text{Eu}^{3+}$ -DOPED $\text{TiO}_2$ THIN FILMS

Željka Antić<sup>a</sup>, Kovur Prashanthi<sup>a</sup>, Vesna Đorđević<sup>b</sup>, Miroslav D. Dramićani<sup>b</sup>, Thomas Thundat<sup>a</sup>

<sup>a</sup>Department of Chemical and Materials Engineering, University of Alberta, Edmonton, Canada, zeljkaa@gmail.com, antic@ualberta.ca

<sup>b</sup>Vinča Institute of Nuclear Sciences, University of Belgrade, P.O.Box 522, 11001 Belgrade, Serbia

This report is on temperature dependence of luminescence of 3at%  $\text{Eu}^{3+}$ -doped  $\text{TiO}_2$  thin films. Film composition was chosen according to our previous study on  $\text{TiO}_2:\text{Eu}^{3+}$  nanopowders where we showed that relative sensor sensitivity ranges from 0.25 to 2.7%  $\text{K}^{-1}$  and that it is among the highest recorded for inorganic nanosensors [1]. Ceramic target was prepared starting from the above mentioned powder which detail synthesis and characterization we reported previously [2]. Pellet prepared from the powder under a load of 5 tons and with no additives was calcinated for 24 hours at 420°C and used as a target for pulsed laser deposition. Due to applied pressure and intense calcination, structure of the target pellet is checked and confirmed with XRD. Deposition was carried out on thermally grown  $\text{SiO}_2$  substrate at 600°C temperature. After deposition thin film structure was confirmed to be anatase. Photoluminescent spectra were taken with sample placed in a custom-made temperature controlled furnace and the data were collected via an optical fiber bundle. In photoluminescent emission spectra two distinct spectral regions are observed: the high energy spectral region associated with the trap emission of the  $\text{TiO}_2$  host which is fairly dependent on the temperature and the low energy spectral region with well resolved emission peaks of the  $\text{Eu}^{3+}$  ions whose intensity decrease fast with the temperature. These two spectral regions are tested for possible use in temperature sensing.

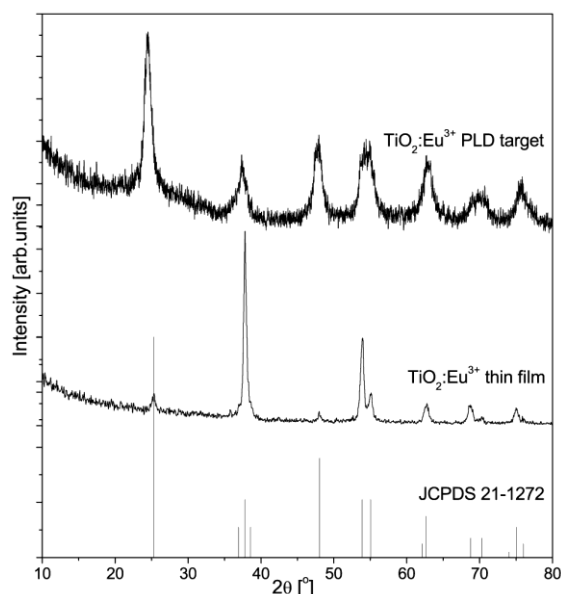


**Figure 1.** XRD diffractograms of  $\text{Eu}^{3+}$ -doped  $\text{TiO}_2$  ceramic target and obtained thin film with presented JCPDS card No. 21-1272.

[1] M.G. Nikolić, Ž. Antić, S. Čulubrk, J.M. Nedeljković, M.D. Dramićanin, *Sensor. Actuat. B-Chem.* 201 (2014) 46-50.

[2] Ž. Antić, R. M. Krsmanović, M. G. Nikolić, M. Marinović-Cincović, M. Mitrić, S. Polizzi, M. D. Dramićanin, *Mater. Chem. Phys.* 135 (2012) 1064-1069

## COMPARARISON OF Cr<sup>3+</sup>:ZnGa<sub>2</sub>O<sub>4</sub> and Cr<sup>3+</sup>, Bi<sup>3+</sup>:ZnGa<sub>2</sub>O<sub>4</sub> PERSISTENT NANOPHOSPHORS ELABORATED BY VARIOUS METHODS

Morgane Pellerin<sup>a, b</sup>, Bruno Viana<sup>a</sup>, Corinne Chaneac<sup>b</sup>, Eliott Teston<sup>c</sup>, Cyrille Richard<sup>c</sup>, Jian Xu<sup>d</sup>, Setsuhisa Tanabe<sup>d</sup>

<sup>a</sup>*PSL Research University, Chimie ParisTech – CNRS, Institut de Recherche de Chimie Paris, 11 Rue Pierre et Marie Curie, 75005 Paris, France, bruno.viana@chimie-parisetch.fr*

<sup>b</sup>*Sorbonne Universités, UPMC Univ Paris 06, CNRS, Collège de France, Laboratoire de Chimie de la Matière Condensée de Paris, 11 place Marcelin Berthelot, 75005 Paris, France*

<sup>c</sup>*UTCBS, CNRS, INSERM, Université Paris Descartes, Chimie-Paristech, Sorbonne Paris Cité, Faculté des Sciences Pharmaceutiques et Biologiques, Paris, F-75270 cedex France*

<sup>d</sup>*Graduate School of Human and Environmental Studies, Kyoto University, Kyoto 606-8501, Japan*

Persistent luminescence is a singular property of some materials which are able to store the excitation light before slowly releasing it within several hours. Such compounds are prepared as nanoparticles (NPs), and when functionalization is realized to get colloidal materials well dispersed in aqueous medium, such nanoprobe open the use of the persistent luminescence for bioimaging applications (see for instance [1]). The numbers of *in vivo* applications increased with new modalities and new expectations.

Recently, small size zinc gallate nanoparticles doped with chromium (ZnGa<sub>2</sub>O<sub>4</sub>:Cr<sup>3+</sup>) were synthesized by several methods including hydrothermal [1], [2] and biphasic hydrothermal route [3], co-precipitation and microwave heating in aqueous medium and in non- aqueous medium [4]. These different ways of synthesis lead to NPs sizes ranging in the sub-10 nm up to 100 nm with various optical features. In some case, Bi<sup>3+</sup> cation was also added, as a co-dopant [5]. The incorporation of bismuth allows the improvement of the persistent luminescence properties.

Here we report a comparison of the synthesis methods with the advantages and the drawbacks in relation to the *in-vivo* bioimaging applications. Several samples are compared with a focus on the size -TEM and DLS are the usual procedure to compare the actual size of the NPs- the morphology, the optical properties and the persistence of the luminescence. The effect of the excitation sources and the excitation time will also be compared.

[1] T. Maldiney, A. Bessiere, J. Seguin, E. Teston, S.K. Sharma, B. Viana, A.J.J. Bos, P. Dorenbos, M. Bessodes, D. Gourier, D. Scherman, C. Richard, *Nature Materials*, 13 (2014), 418-426

[2] Z. Li, Y. Zhang, X. Wu, L. Huang, D. Li, W. Fan, G. Han. *J. Am. Chem. Soc.*, 137 (16) (2015), 5304–5307

[3] B.B. Srivastava, A. Kuang, Y. Mao. *Chem. Commun*, 51(34) (2015), 7372–7375

[4] E. Teston, S. Richard, T. Maldiney, N Lièvre, G. Wang, L. Motte, L.,Y. Lalatonne. *Chem. Eur. J.*, 21(20) (2015), 7350–7354

[5] Y. Zhuang, J. Ueda, S. Tanabe. *Applied Physics Express*, 6(5) (2013), 052602

## COMPARATIVE STUDY OF NONDOPED AND Eu-DOPED SrI<sub>2</sub> SCINTILLATOR

Takayuki Yanagida<sup>a</sup>, Masanori Koshimizu<sup>b</sup>, Go Okada<sup>a</sup>, Takahiro Kojima<sup>c</sup>, Jyunya Osada<sup>c</sup>

<sup>a</sup>*Graduate School of Materials Science, Nara Institute of Science and Technology (NAIST),  
8916-5 Takayama-Cho, Ikoma, Nara 630-0192, Japan, t-yanagida@ms.naist.jp*

<sup>b</sup>*Dept. of Applied Chemistry, Graduate School of Engineering, Tohoku University, 6-6-07  
Aoba, Aramaki, Aoba-ku, Sendai 980-8579, Japan*

<sup>c</sup>*Oxide Corporation, 1741-1 Makihara, Takegawa-cho, Hokuto-shi, Yamanashi, 408-0302  
Japan*

Scintillating materials which convert the absorbed energy of ionizing radiation to UV-Vis photons have played an important role in radiation detectors [1-2]. Especially, halide materials have attracted much attention due to their high scintillation light yields. Common examples are Tl-doped NaI [3] and CsI [4]. Most recently, Eu-doped SrI<sub>2</sub> was introduced, and it showed very good scintillation properties [5-6]. Though the light yield is inferior to the Eu-doped one, a non-doped SrI<sub>2</sub> also exhibits a scintillation, and the emission spectrum is very complicated to interpret. Therefore, there is a room to study and discuss the origin of the scintillation in non-doped SrI<sub>2</sub>. The aim of this work is to investigate basic optical and scintillation properties of 3% Eu doped SrI<sub>2</sub> and non-doped SrI<sub>2</sub> crystalline scintillators.

Eu-doped and non-doped SrI<sub>2</sub> crystals were prepared by Oxide Corporation using a Bridgeman technique. The sample size were 0.5 inch × 0.5 inch-high and encapsulated. Characterization of optical and scintillation properties were carried out at NAIST, Nara, Japan. The basic optical characterization including photoluminescence (PL), PL excitation spectrum, and PL decay time were studied. The X-ray induced radioluminescence (RL) spectrum and scintillation decay time profiles were evaluated under X-ray and  $\gamma$ -ray excitation. Then, temperature dependence of scintillation spectrum from 8 to 300 K was investigated. In order to study excitation bands of the emission precisely, we used a Synchrotron facility (UVSOR, Aichi, Japan).

In X-ray induced RL spectra at different temperatures, intense emission peaks appeared at 430 nm in the Eu-doped sample. The emission is due to 5d-4f transitions of Eu<sup>2+</sup>. In the non-doped SrI<sub>2</sub>, some emission bands around 360, 410, 430, and 540 nm were observed. These emissions were also observed in PL evaluations. In the scintillation decay curve, the 5d-4f emission of Eu<sup>2+</sup> is dominant and the decay time constant is 1.3  $\mu$ s, while the time constant is much smaller (450 ns) without Eu-doping. In the afterglow profile, Eu-doped sample showed the normalized intensity of ~ 0.1% at several tens of milliseconds after X-ray excitation was cut off. This long afterglow may partially affected by the emission of Eu<sup>3+</sup> due to the 4f-4f transitions, which typically has a lifetime in the range of milliseconds. When <sup>137</sup>Cs 662 keV  $\gamma$ -ray was irradiated, scintillation light yields of nondoped and Eu-doped SrI<sub>2</sub> were ~ 70000 and ~ 82000 ph/MeV, respectively. In the conference, the nature of the emission from nondoped SrI<sub>2</sub> will be discussed based on optical and scintillation characteristics.

- [1] T. Yanagida, *Opt. Mater.*, 35 1987-1992 (2013).
- [2] T. Yanagida, *J. Lumin.*, doi:10.1016/j.jlumin.2015.01.006 (2015).
- [3] J. T. M. d. Haas, P. Dorenbos, *IEEE Trans. Nucl. Sci.*, 55 1086-1092 (2008).
- [4] E. Sakai, *IEEE Trans. Nucl. Sci.*, 34 418-422 (1987).
- [5] N. J. Cherepy, G. Hull, A. D. Droshoff, S. A. Payne, E. Van Loef, C. M. Wilson, K. S. Shah, U. N. Roy, A. Burger, L. A. Boatner, W. S. Choong, W. W. Moses, *Appl. Phys. Lett.*, 92 083508 (2008).
- [6] V. A. Pustovarov, I. N. Ogorodnikov, A. A. Goloshumova, L. I. Isaenko, A. P. Yelisseyev, *Opt. Mater.*, 34 926-930 (2012).

## CRYSTAL SIZE EFFECT IN POLARITONIC LUMINESCENCE FROM SOLID XENON

A.N. Ogurtsov, O.N. Bliznjuk, N.Yu. Masalitina  
*National Technical University "KhPI", Frunse Str. 21, Kharkov, 61002, Ukraine*  
*anogurtsov@ukr.net*

The exciton-photon interaction leads to the formation of polaritonic states energetically positioned at both sides of the initial exciton. In a large ideal crystal of cubic symmetry, where the interval of the longitudinal-transverse splitting does not contain excitonic levels, the polaritonic dispersion branches lie beyond this interval at both sides of its boundaries. On the contrary, in a crystalline grain comparable or less in size than the wavelength in the substance, the interval of the longitudinal-transverse splitting is filled in continuously by excitonic states intercepting a significant part of the oscillator strength of the excitonic transition.

In the previous experiments with polycrystalline samples of solid xenon the formation of the lower polaritonic state was traced by the red shift of the luminescence spectrum relative to the bottom  $E_1=8.36$  eV of the lowest excitonic band [1].

In the present paper we explore the new crystal growing technique, which allowed to obtain the solid Xe samples with essentially improved crystallographic properties [2] and to resolve the internal structure of the luminescence bands at the edge of exciton absorption [3]. The photoluminescence experiments were carried out at the SUPERLUMI experimental station at HASYLAB, DESY, Hamburg.

Unlike previous works, where the observed red polaritonic shift was small commensurably with a weak inelastic polariton-photon scattering, a large polaritonic shift of luminescence is not due to energy dissipation, the energy conservation law being met due to equal probabilities for opposite-sign energy shifts. Such effect is possible if the crystalline grains are comparable in size with light wavelength, which provides the filling in the interval of the longitudinal-transverse splitting by excitons with sufficient oscillator strength. And the sample structure must be perfect enough to lowering the exciton scattering rate with respect to the rate of the polariton formation through exciton-photon coupling.

For the first time the excitation spectra of free-exciton luminescence band were recorded simultaneously below  $E_1$  and within the interval of the longitudinal-transverse splitting. The luminescence of non-equilibrium polaritons was observed both within the longitudinal-transverse splitting interval and at photoexcitation below the bottom of the excitonic band. The excitation spectrum below  $E_1$  is determined by competition of two processes. The first one is the creation of excitons by photons with energy  $E_1$  at the Lorenz tail of excitonic absorption. The second process is a competing absorption related to the direct formation of two-site excitonic polarons (self-trapped excitons). Both excitation spectra of polaritonic luminescence below  $E_1$  and within the longitudinal-transverse splitting interval show high sensitivity to crystal quality of the samples.

[1] A.N. Ogurtsov, *Cryocrystals Modification by Electronic Excitations*, NTU "KhPI", Kharkov, 2009.

[2] A.N. Ogurtsov, in: E.C. Faulques, D.L. Perry, A.Y. Yeremenko (Eds.), *Spectroscopy of Emerging Materials*, Kluwer, Dordrecht, 2004, 45–56.

[3] A.N. Ogurtsov, A.M. Ratner, *Phys. Lett. A* 332 (2004) 441–448.

## CU-DOPED PHOTOVOLTAIC GLASSES BY ION EXCHANGE FOR SUNLIGHT DOWN-SHIFTING

Marco Mardegan and Elti Cattaruzza

*Center for Nanosciences and Nanobiomaterials, Department of Molecular Sciences and Nanosystems, Università Ca' Foscari Venezia, via Torino 155/b, 30172 Venezia-Mestre, Italy, cattaruz@unive.it*

Ion exchange process is a widely studied synthesis technique for the controlled modification of silicate glass composition and properties, being moreover an easy and cheap approach. Luminescent metal-doped silicate glass sheets suitable as down-shifters to be used for covering solar cells have been prepared by thermal ion exchange [1,2].

In particular, silicate glasses containing copper are known to exhibit a broad luminescent band peaked around 500 nm, ascribed to  $4d^{10} - 4d^95s^1$  electronic transition of  $Cu^+$  ions; this band turns out to be much promising for the realization of down-shifting systems, being excited in the UV and near-UV region. Synthesis of the Cu-doped glasses has been done by dipping pure silicate sheets (commercially used as cover of the PV panels) into a fused copper salt mixture at the temperature of  $400^\circ C$ , for duration between a few minutes and some hours; two different types of copper chloride salt mixtures were explored, with the aim at obtaining luminescent glasses able to improve the Si cell yield. Absorption and luminescence glass features were collected and compared. The performance of the different samples was tested by a solar simulator, measuring the output power of a Si solar cell covered with the Cu-doped glass slides.

[1] E.Cattaruzza, M.Mardegan, T.Pregolato, G.Ungaretti, G.Aquilanti, A.Quaranta, G.Battaglin, E.Trave, Sol. Energy Mater. Sol. Cells 130 (2014) 272–280

[2] E.Cattaruzza, V.M. Caselli, M.Mardegan, F.Gonella, G.Bottaro, A.Quaranta, G.Valotto, F.Enrichi, Ceram. Int. 41 (2015) 7221–7226



## DETECTIVE QUANTUM EFFICIENCY OF PHOSPHORS FOR X-RAY IMAGING

Goran S. Ristić

*Applied Physics Laboratory, Faculty of Electronic Engineering, University of Nis, Serbia,  
goran.ristic@elfak.ni.ac.rs*

The Detective Quantum Efficiency (DQE), Modulation Transfer Functions (MTF), and the Noise Power Spectrum (NPS) of the phosphors for X-ray medical imaging have been considered. The slit method was used for the determination of presampling MTF. The slit is positioned at a slight angle to the direction perpendicular to the scanning direction to derive the Line Spread Function (LSF). The presampling MTF is then obtained by the Fourier transformation of the composite LSF. RadEye1 CMOS image sensor developed by Rad-Icon Imaging Corp., suitable for digital radiography was used. The RadEye1 image sensor consists of a two-dimensional array of photodiodes along with CMOS structures for scanning and readout, incorporated into Shad-o-Box camera. The tungsten slit camera manufactured by Radiation Measurements Inc. (model: 07-624-1000) with nominal slit width of 10  $\mu\text{m}$  and 4° relief angles on each jaw are used. Thus, the measured presampling MTF is the product of presampling MTF and slit camera MTF. The effect of geometrical unsharpness is caused by the magnification factor, and the size and shape of the focal spot. The focal spot of used x-ray tube was very small and can be neglected. The MTF measurements were made using polyenergetic beam spectrum with 2 mm Al filtration. The tube voltage was 70 kV and tube currents were 5 and 10 mA. The scintillators used: Min-R Medium (conventional phosphor), and two types of the storage phosphor (manufactured by AGFA company): 5QAQME (standard MD-30 screen with a protective layer) and D7379/1 (the phosphor with a protective layer, but on a transparent substrate). The transparent backing replacing the reflective backing helps reduce blurring but consequently reduces the amount of light escaping the front of the screen. Although it is usual to use a laser beam for the forming of the image by storage phosphor, the images in these experiments were formed only by electrons that were not deeply trapped, i.e. in the same manner as in the case of the conventional phosphor. Namely, the electrons liberated in the storage phosphor during the irradiation either produce light promptly or are stored in the traps. It is very important to know which part of the electrons created during x-ray exposure produces the "prompt" light. Regarding to the application of the storage phosphor, the prompt light is not of interest, and the aim is to increase the probability of electron trapping. On the other hand, when these electrons are released by the stimulating light during readout, the probability of their retrapping instead of producing light, would then be higher, so that the efficiency of readout would be reduced. The optimum balance occurs where the probabilities of an excited electron being retrapped or stimulating fluorescence are equal, meaning that  $\approx 50\%$  electrons released during x-ray irradiation form prompt light. The energy spectra of polyenergetic x-ray beams were not measured, but obtained using *TASMIP model* in which measured spectral data were characterized using polynomial expressions. To find the NPS, the two full images for each scintillator are firstly acquired, and the differences of these images represented the basic matrix for further calculation. Finally, the DQE can be calculated using the equation:  $DQE(f) = S^2 MTF(f) / (\Phi \cdot NPS(f))$ , where  $S$  is the average output signal,  $\Phi$  is the total number of incident quanta per unit area.  $\Phi$  is calculated on the basis of the energy spectra and the dose exposure. The obtained results showed that Min-R Medium has the highest DQE, while DQE of D7379/1 storage phosphor is the smallest.

## DONOR-ACCEPTOR SYSTEMS CONTAINING 1,8-NAPHTHALIMIDE AS MULTICOLOR EMITTERS

Regimantas Komskis<sup>a</sup>, Arunas Miasojedovas<sup>a</sup>, Rokas Skaisgiris<sup>a</sup>, Alytis Gruodis<sup>a</sup>, Vygintas Jankauskas<sup>a</sup>, Dalius Gudeika<sup>b</sup>, Juozas Vidas Grazulevicius<sup>b</sup>, Saulius Jursenas<sup>a</sup>

<sup>a</sup>*Institute of Applied Research, Vilnius University, Sauletekio 9-III, LT-10222, Vilnius, Lithuania, arunas.miasojedovas@ff.vu.lt*

<sup>b</sup>*Department of Organic Technology, Kaunas University of Technology, Radvilenu 19, LT-50254, Kaunas, Lithuania, juozas.grazulevicius@ktu.lt*

Organic electroactive molecules possessing both donor and acceptor substituents are of increasing importance for the application in optoelectronic devices such as organic light emitting diodes, bulk heterojunction solar cells and sensors. The unique structure of donor-acceptor molecules allows their optical and electrochemical properties to be tuned finely over a wide range by appropriate chemical modification of the donor and acceptor moieties. The further progress in the design and synthesis of the donor-acceptor systems depend on understanding the structure-property relationship of such compounds. Excitation relaxation pathways in donor-acceptor systems are intricate due to intramolecular charge transfer, which is highly sensitive to the wavefunction overlap between the electron-donating and electron-accepting systems and the twisting angle of the conjugated fragments. Excitation relaxation includes charge transfer and  $n-\pi$  states that are highly sensitive to the twisting angle and polarity of the surrounding medium.

In this work we analyze the properties of 1,8-naphthalimide derivatives, which represent an attractive class of electron-deficient organic materials, singly bonded at C-4 position by aromatic substituent, which vary in polarity and size of their  $\pi$ -conjugated system. The intramolecular twisting of the donor and acceptor moieties and the wave function overlap are assessed by DFT modelling, supplemented by experimental data on the optical properties of the compounds in various surrounding. Remarkable tuning possibilities of the emission quantum yield and colour as well as drift mobilities are demonstrated for compounds possessing steric and polar substituents. Moreover, these compounds were subjected to studies of the susceptibility of the fluorescence properties to a range of metal ions in various surroundings. Extreme sensitivity (of more than 4000 times) and selectivity to mercury ions was disclosed for naphthalimide substituted with dimethylamine. Heat sensing ability demonstrated organic molecules containing triphenylamine units.

## NEW Eu(III) B-DIKETONATE COMPLEXES CONTAINING A 2-(4-MORPHOLINYLMETHYL)PHENOL: AN EXPERIMENTAL AND THEORETICAL INVESTIGATIONS

Khodzhaberdi Allaberdiev

*Ukraine State Scientific Research Institute for Plastics, 97, pr. Il'icha, Donetsk, 83059,  
Ukraine*

allaberdiev@mail.ru

Two luminescent complexes  $[\beta\text{-diketonate}]_3\text{Eu}[2\text{-(4-morpholinylmethyl)phenol}]$  were synthesized with of anhydrous  $\beta$ -diketonates europium(III),  $\text{Eu(L)}_3$  ( $\text{L} = \text{fod}^-$  -2,2-dimethyl-6,6,7,7,8,8,8-heptafluoro-3,5-octandione,  $\text{tta}^-$  -4,4,4-trifluoro-1-(2-thienyl)-1,3-butandione) and 2-(4-morpholinylmethyl)phenol (MMPh) as an ancillary ligand. The complexes were characterized by IR spectroscopy, and elemental and thermogravimetric analyses and luminescence spectroscopy. These materials show not only the characteristic red emission of Eu(III), but also the emission of ligand the MMPh which extends the range of the spectrum. It is found that the introduction of the MMPh in  $\beta$ -diketonates europium (III) structure in comparison with the tris( $\beta$ -diketonate) and tetrakis( $\beta$ -diketonate) europium complexes has enhances the photophysical properties these materials. Influence of chemical structure of the  $\beta$ -diketones on properties obtained complexes was analyzed. Additionally, the ground and excited states geometrical and electronic structures, charge transfer behavior, absorption, and emission properties of the two europium(III) complexes have been investigated using density functional theory (DFT) and time-dependent density functional theory (TD-DFT). These theoretical estimations are in good agreement with the corresponding observations. Furthermore, the theoretical and experimental IR spectroscopic data suggest the possible modes of coordination of the coligand with the metal. Influences the pyramidal nitrogen inversion and the conformation of morpholine ring on properties of the studied compounds are discussed. The thermogravimetric results demonstrate thermal stability these complexes.

## EARLY AGE MONITORING OF INNOVATIVE CEMENTS BY USING FIBER BRAGG GRATING SENSORS

Stefania Campopiano, Agostino Iadicicco, Rajeev Ranjan, Giovanna Palumbo, Flavio Esposito, Francesco Messina, Francesco Colangelo, Claudio Ferone, Raffaele Cioffi  
*Department of Engineering, Univ.Naples Parthenope, Centro Direz Isola C4, 80143 Napoli, campopiano@uniparthenope.it*

Geopolymer matrices represent one of the main sustainable alternatives to ordinary Portland cement (OPC) and other clinker-based blended cements [1]. Real scale applications are limited and, so, a relevant amount of data is still needed to assess the actual early age and long-term behavior of these systems. Particularly, the early-age monitoring of geopolymers represent a key parameter for mix design optimization. In this work, we have successfully measured the early-age shrinkage and temperature changes of metakaolin-based geopolymers by using properly embedded FBG-based sensors [2, 3] (see fig. 1).

Starting from a case study by authors related to the design of externally bonded fiber reinforced geopolymers for strengthening of existing structures, the matrix was optimized in terms of quartz filler content. Quartz is a quite expensive admixture, which can be added in order to mitigate shrinkage phenomena as far as it acts as a rigid skeleton opposing to volumetric contraction. The measurements carried out by means of FBG sensors allowed to reduce filler content respect to the abovementioned work. Particularly, quartz content can be reduced by 50%. Together with this, an accurate measurement of inner temperatures was also carried out. The relevant temperature associated to polycondensation (about 65°C) limit the designed metakaolin geopolymer to non- massive structures, since thermal cracking could occur, unless research will be able to assess the viability of retardants already available for traditional cements or develop specific ones for geopolymers.

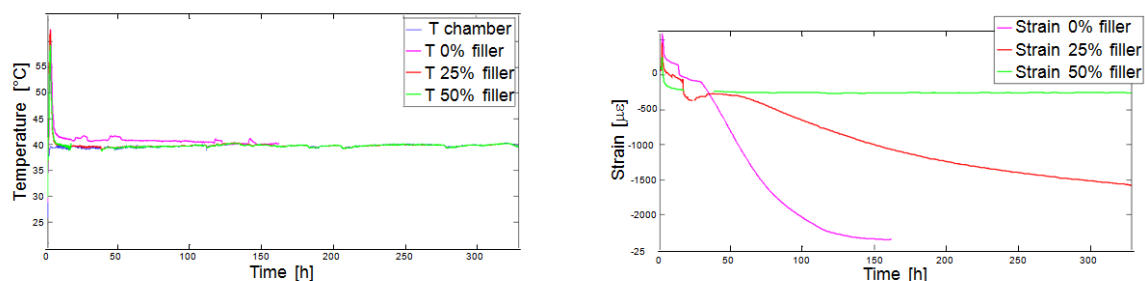


Figure 1: Temperature and shrinkage curves for different filler percentages obtained by means of FBG

[1] <http://www.geopolymer.org/science/world-wide-increase-in-geopolymer-research>. (last access: 18th December,2014).

[2] K.O. Hill, G. Meltz, "Fiber Bragg Grating Technology Fundamentals and Overview," *Journal of Lightwave Technology* 15, 1263 (1997)

[3] S. Campopiano, A. Iadicicco, F. Messina, C. Ferone, R. Cioffi. "Fiber Bragg grating sensors as a tool to evaluate the influence of filler on shrinkage of geopolymer matrices", *Proc. SPIE 9506, 95061J*, (2015)

## EFFECT OF EUROPIUM CONCENTRATION ON THE LUMINESCENCE PROPERTIES OF $\text{Eu}^{3+}$ AND $\text{Tb}^{3+}$ DOPED PHOSPHATE-BORATE-FLUORIDE GLASSES

Elena Polissadova<sup>a</sup>, Damir Valiev<sup>a</sup>, Konstantin Belikov<sup>b</sup>, Nataliya Yegorova<sup>b</sup>, Vitaliy Vaganov<sup>c</sup>

<sup>a</sup> National Research Tomsk Polytechnic University, Lenin Avenue 30, 634050, Tomsk, Russia, [elp@tpu.ru](mailto:elp@tpu.ru)

<sup>b</sup> Institute for Single Crystals, Lenin Avenue 60, Kharkov 61001, Ukraine

Glasses doped of  $\text{Eu}^{3+}$  and  $\text{Tb}^{3+}$  are used as scintillators [1] and how multi-colored phosphors [2]. The main problem of using glasses with REI as scintillators or radiation sources is low light yield compared to crystals. Therefore, development of scintillation materials with high light yield is being conducted to find combinations of dopants to sensitize luminescence. The aim of the research is to study the effect of  $\text{Eu}^{3+}$  ions of different concentrations on spectral and decay kinetic properties of photo- and pulse cathodoluminescence (PCL) of  $\text{Li}_2\text{O}-\text{B}_2\text{O}_3-\text{P}_2\text{O}_5-\text{CaF}_2$  (LPBC) glasses, doped  $\text{Tb}/\text{Eu}$ . The glasses composition LPBC:  $\text{Tb}_2\text{O}_3$  (5 wt%),  $\text{Eu}_2\text{O}_3$  (X wt%), where  $X = 0,5; 0,7; 1$  were investigated. The samples were synthesized at the Institute for Single Crystals of the National Academy of Sciences of Ukraine (Kharkiv). The glasses have a low melting point, high solubility of rare earth components, homogeneity, good transparency and moisture resistance [3].

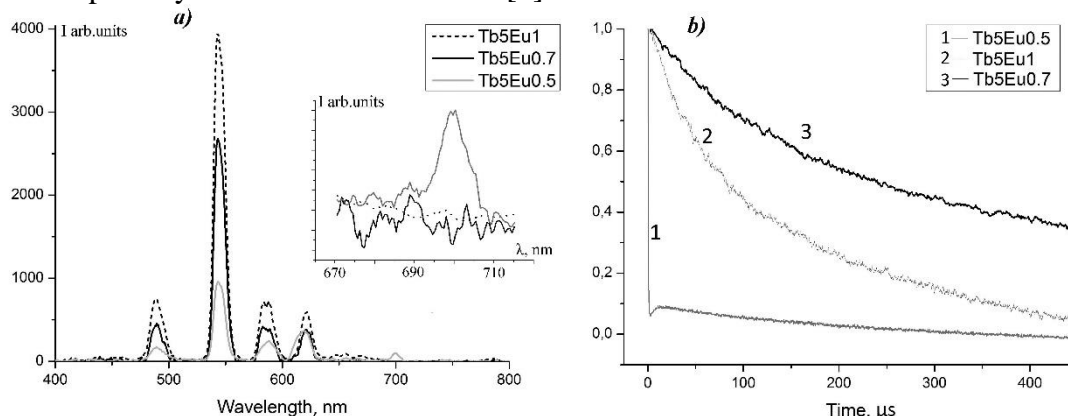


Fig. 1 PCL spectra of LPBC: $\text{Tb}_5\text{Eu}_X$  (0.5; 0.7; 1 wt%) measured by “spectrum per pulse” technique (a); PCL decay kinetic curves for glasses with different concentrations of  $\text{Eu}^{3+}$  ions for the  $\lambda=544$  nm. The PCL was studied by time-resolved spectrometry. For excitation was used the compact high-current electron accelerator; duration of electron pulse at FWHM 10–15 ns, the average energy was 250 keV. The luminescence decay kinetics was recorded with a photomultiplier PMT-84-6 using a monochromator MDR-3 and a digital oscilloscope LeCROY (350 MHz). It was found that increasing the concentration of europium from 0,7 to 1 wt% leads to a quenching the luminescence band at 700 nm (fig.1a) and to a changing in the decay kinetics of band 544 nm (fig.1b) and increasing the intensity of the luminescence of terbium ions (fig.1a). The decay kinetics of luminescence glasses excited electrons beams was studied in detail. Temperature dependencies of decay time for luminescence bands of  $\text{Eu}^{3+}$  and  $\text{Tb}^{3+}$  ions in interval 80-500 K are presented. The stage of emission buildup after pulse electron excitation in the kinetics of luminescence in the band 544 nm at low concentration of Eu was found. The mechanism of energy transfer between ions  $\text{Eu}^{3+}$  and  $\text{Tb}^{3+}$  is discussed.

The reported study was supported by RFBR, research project No. 14-02-31297 mol\_a

[1] G.V. Reddy, L.R. Moorthy, T. Chengaiah, B.C. Jamalaih Ceramics International. 40 (2014) 3399–3410.

[2] X.-Y. Sun, Z.-P. Ye, Z.-J. Zhang at all. J. Am. Ceram. Soc., (2014) 1–7.

[3] K.N. Belikov, N.N. Grebenyuk, Ye.V. Grishina at all. Funct. Mat. 17 (2010) 262–265.

## EFFECT OF THERMAL TREATMENT ON MORPHOLOGIES AND OPTICAL PROPERTIES OF DOWNCONVERSION AND UPCONVERSION NaYF<sub>4</sub>:Ln<sup>3+</sup> CRYSTALS

Marcos A. Calil Junior<sup>a</sup>, Marcelo O. Rodrigues<sup>a</sup>

<sup>a</sup>Laboratory of Inorganic and Materials, Institute of Chemistry, University of Brasilia, Brasilia, Brazil, macaliljr@hotmail.com

Inorganic crystals doped with lanthanides (Ln) ions have been considered as an excellent choice to produce luminescent nanomaterials. Among the diversity of Ln-doped crystals, sodium yttrium fluoride (NaYF<sub>4</sub>) is considered to be one of the most efficient host matrixes because it presents a high refractive index (1.430-1.470 m<sup>2</sup>W<sup>-1</sup>) and low lattice phonon energy (< 400 cm<sup>-1</sup>). Moreover, it shows high transparency in ultraviolet and visible regions.<sup>1</sup> In this work, we present a simple and effective hydrothermal route for controlling the morphologies of  $\alpha$ -NaYF<sub>4</sub>:Ln<sup>3+</sup> and  $\beta$ -NaYF<sub>4</sub>:Ln<sup>3+</sup> crystals, using tartaric acid for controlling particle size and morphology. Silica spheres were used to improve the biocompatibility of the NaYF<sub>4</sub>:Ln<sup>3+</sup> crystals. The downconversion (DC) and upconversion (UC) luminescence properties of NaYF<sub>4</sub> doped with different lanthanides ions have been investigated.

Fig. 1-A displays the UC emission spectra of  $\alpha$ -NaYF<sub>4</sub>:Yb<sup>3+</sup>/Er<sup>3+</sup> crystals excited with different laser powers. We have found that two photons are involved in producing both green and red emissions. Fig. 1-B and Fig. 1-C show HRTEM images of the  $\alpha$ -NaYF<sub>4</sub>:Yb<sup>3+</sup>/Er<sup>3+</sup> crystals. These crystals are uniform with spherical shapes and an average diameter of 50 nm. Figure 1-D shows HRTEM image of the  $\alpha$ -NaYF<sub>4</sub>:Yb<sup>3+</sup>/Er<sup>3+</sup>@SiO<sub>2</sub> nanocomposites. The silica shell is composed of highly uniform spheres and an average diameter of 350 nm. Fig. 1-E shows HRSEM image of  $\beta$ -NaYF<sub>4</sub>:Yb<sup>3+</sup>/Er<sup>3+</sup> crystals. These crystals are highly uniform hexagonal micro-prisms with an average diameter of 2,5  $\mu$ m and an average length of 6  $\mu$ m. In conclusion,  $\alpha$ -NaYF<sub>4</sub>:Ln<sup>3+</sup> and  $\beta$ -NaYF<sub>4</sub>:Ln<sup>3+</sup> crystals have been synthesized using an effective hydrothermal route. These materials can be used in bioprobe applications and photodynamic therapy.

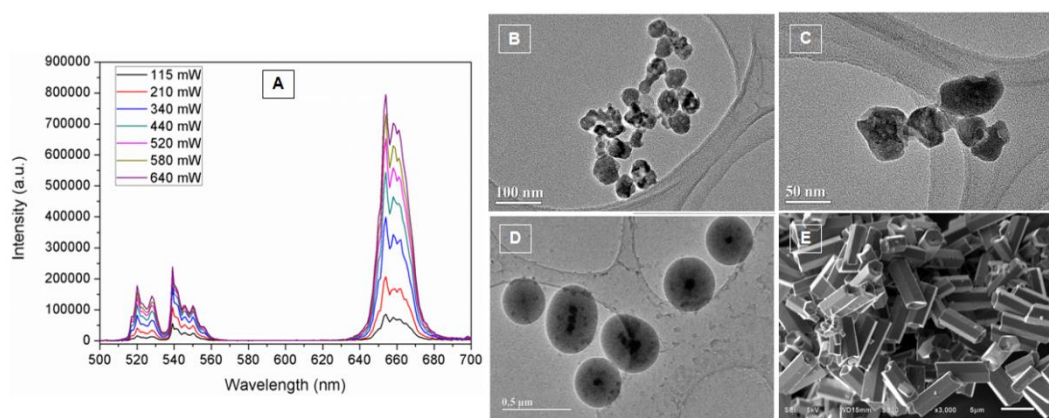


Figure 2 - (A) Pump power dependence of UC emission intensities under 980 nm excitation of NaYF<sub>4</sub>:Yb<sup>3+</sup>/Er<sup>3+</sup> crystals. HRTEM images of (B-C)  $\alpha$ -NaYF<sub>4</sub>:Yb<sup>3+</sup>/Er<sup>3+</sup> and (D)  $\alpha$ -NaYF<sub>4</sub>:Yb<sup>3+</sup>/Er<sup>3+</sup>@SiO<sub>2</sub> nanocomposites. (E) HRSEM image of  $\beta$ -NaYF<sub>4</sub>:Yb<sup>3+</sup>/Er<sup>3+</sup> crystals.

[1] Y. I. Park, K.T. Lee, Y.D. Suh, T. Hyeon. Chem. Soc. Rev. 44 (2015) 1302–1317.

## EFFECTS OF PRESSURE AND TEMPERATURE ON THE LUMINESCENCE OF $\text{Ba}_2\text{K}(\text{PO}_3)_5$ DOPED WITH $\text{Eu}^{2+}$ AND $\text{Eu}^{3+}$

Anna Baran<sup>a</sup>, Sebastian Mahlik<sup>b</sup>, Marek Grinberg<sup>c</sup>,  
Adam Watras<sup>d</sup>, Robert Pązik<sup>e</sup>, Przemysław Dereń<sup>f</sup>

<sup>a</sup> *Institute of Experimental Physics, University of Gdansk, Wita Stwosza 57, 80-952 Gdansk, Poland, anna.baran@ug.edu.pl*

<sup>b</sup> *Institute of Experimental Physics, University of Gdansk, Wita Stwosza 57, 80-952 Gdansk, Poland, s.mahlik@ug.edu.pl*

<sup>c</sup> *Institute of Experimental Physics, University of Gdansk, Wita Stwosza 57, 80-952 Gdansk, Poland, fizmgr@ug.edu.pl*

<sup>d</sup> *Institute of Low Temperature and Structure Research, Polish Academy of Sciences, 2 Okólna Street, 50-422 Wrocław, Poland, a.watras@int.pan.wroc.pl*

<sup>e</sup> *Institute of Low Temperature and Structure Research, Polish Academy of Sciences, 2 Okólna Street, 50-422 Wrocław, Poland, r.pazik@int.pan.wroc.pl*

<sup>f</sup> *Institute of Low Temperature and Structure Research, Polish Academy of Sciences, 2 Okólna Street, 50-422 Wrocław, Poland, p.deren@int.pan.wroc.pl*

Barium potassium phosphate ( $\text{Ba}_2\text{K}(\text{PO}_3)_5$ ) doped with europium belongs to a very limited number of hosts able to accommodate both  $\text{Eu}^{3+}$  and  $\text{Eu}^{2+}$  ions, which might make it useful for white light emitting diodes (WLEDs) based on UV chip technology.

In this work effects of pressure and temperature on the luminescence of  $\text{Eu}^{2+}$  and  $\text{Eu}^{3+}$ -doped  $\text{Ba}_2\text{K}(\text{PO}_3)_5$  are presented. Depending on the excitation wavelength phosphor shows different luminescence spectra. The emission color was bluish green, when only  $\text{Eu}^{2+}$  was excited, reddish orange when only  $\text{Eu}^{3+}$  was excited or white over simultaneous excitation of both ions. At room temperature under excitation with near UV light, the luminescence spectrum consists of broad emission band peaking at 480 nm due to the  $4f^65d^1 \rightarrow 4f^7$  ( $^8S_{7/2}$ ) transitions of  $\text{Eu}^{2+}$  and several sharp lines between 580 and 710 nm region, ascribed to the  $^5D_0 \rightarrow ^7F_J$  ( $J = 0, 1, 2, 3$  and  $4$ ) transitions in  $\text{Eu}^{3+}$ . At low temperatures, we observed three different bands related to the  $4f^65d^1 \rightarrow 4f^7$  transitions in different Eu sites (at 415 nm (A), 450 nm (B) and 505 nm (C)). We assumed existence two Eu sites substituting for  $\text{Ba}^{2+}$  and one Eu site substituting for  $\text{K}^+$ .

Under fixed excitation wavelength the effect of increasing of the intensity of  $\text{Eu}^{2+}$  emission with respect to  $\text{Eu}^{3+}$  emission was observed for temperature range 5 – 100 K. The nonradiative intersystem crossing responsible for decreasing of the relative intensity of the  $\text{Eu}^{2+}$  luminescence for temperature range 150 – 500 K was also responsible for decreasing of the  $\text{Eu}^{2+}$  to  $\text{Eu}^{3+}$  luminescence intensity ratio for temperature higher than 150 K.

Luminescence decays were measured for selected temperatures and pressures. At 10 K the decays of  $\text{Eu}^{3+}$  luminescence were single-exponential, with time constant being 3.6 ms. When temperature increases all emissions decay faster and become multiexponential. Decay times slightly decreased with increasing pressure. In the range of 10 – 400 K the decays of  $4f^65d \rightarrow 4f^7$  emission in the  $\text{Eu}^{2+}$  were single-exponential, with time constant being 0.65  $\mu\text{s}$ , 0.62  $\mu\text{s}$  and 0.35  $\mu\text{s}$  for A, B and C emission bands, respectively, and did not depend on temperature. At higher temperatures (from 400 K to 500 K) the luminescence decays got shorter and non-exponential, indicating thermal quenching. When pressure increases all emissions decay faster.

Energy of the band related to  $4f^65d \rightarrow 4f^7$  transition of  $\text{Eu}^{2+}$  decreases with increasing pressure with the rate  $-9.5 \text{ cm}^{-1}/\text{kbar}$ , whereas energy the luminescence, related to the  $\text{Eu}^{3+}$  ion emission change slightly with the rates from 0,15 to  $-0,54 \text{ cm}^{-1}/\text{kbar}$ .

## **ELECTRIC FIELD EFFECT ON PHOTOLUMINESCENCE OF QUANTUM DOTS CdSe / ZnS IN NEMATIC LIQUID CRYSTAL**

Kurochkina Marharyta, Shcherbinin Dmitry, Konshina Elena  
*ITMO University, Kronverkskii pr. 49A, 197101, Saint Petersburg, Russia*

Creating colloidal media based on liquid crystals doped by nanoparticles is one of the nanotechnology developing areas. Interest in such environments is associated primarily with their great scientific and technical potential [1]. Doping of liquid crystals (LC) with semiconductor quantum dots (QDs) allows varying their optical properties [2,3]. The main goal of this work is to study the photoluminescence (PL) of the LC/QDs suspension and the impact of an external electric field on it.

Investigations were carried out with a nematic liquid crystal (NLC) based on cyanobiphenyls LC-1289 (NIOPIK, Moscow) and hydrophobic semiconductor QDs CdSe/ZnS with a core diameter 3.5 nm, coated TOPO. The suspension was prepared from QD powders and LC in the nematic phase by mixing them with ultrasound. The concentration of the quantum dots was 10 wt. %. Prepared suspension was put into a thin cell with thickness of 20  $\mu\text{m}$ . The cell was assembled from two quartz substrates coated the conductive and alignment layers with the inner sides which ensure a homogeneous unidirectional molecular orientation of the NLC and possibility to apply of electrical field.

The red shift of the PL maximum of suspension about 83 nm was observed in comparison with the PL spectrum of QDs in toluene with the same concentration. The cause of bathochromic shift could be the formation of nanoparticles agglomerates under the influence of the elastic forces in the oriented NLC layer.

The hypsochromic shift by 5nm was obtained under applying of the electric field strength of 0.25 V/m to the layer of NLC/QD and then the maximum of PL spectra did not change its position during further increase of strength. The PL intensity decreases exponentially with increasing of a field strength and halved at a field strength of 1 V/m. These results open up new possibilities for the using of NLC doped quantum dots to optical devices with controlled luminescence.

[1] Choudhary A., Singh G., M. Biradar A.M., *Nanoscale*. V. 6 (2014)

[2] Rodarte A. L., Ferri C. G. L., Gray C., Hirst L. S., Ghosh S., *Proc. of SPIE*. V. 8279 (2010)

[3] Kurochkina M. A., Konshina E. A., *Opt. and Spectr.* V. 118 (2015)



## ELECTRON-VIBRATIONAL EFFECT IN MgO: M<sup>2+</sup> (M=V, Fe, Mn)

C.N.Avr<sup>a</sup>, M.G.Brik<sup>b</sup>, A.S.Gruia<sup>a</sup> and A.M.Barb<sup>a</sup>

<sup>a</sup> *Department of Physics, West University of Timisoara, Bd. V. Parvan 4, Timisoara 300223, Romania,*

<sup>b</sup> *Institute of Physics, University of Tartu, Ravila 14C, Tartu 50411, Estonia*

*E-mail: acalin@physics.uvt.ro*

Magnesium oxide single crystal is usually regarded as a model system to investigate optical properties and electron-vibrational interactions of doped transition-metal 3d<sup>n</sup> ions. The M<sup>2+</sup> (M=V,Fe,Mn) ion, doped in MgO crystal will substitute Mg<sup>2+</sup> ion and will be coordinated by a perfect octahedron of oxygen ions. Therefore, the doped MgO: M<sup>2+</sup> represents a prototypical system for study and testing of theoretical models of crystal field theory and electron-vibrational interaction formalism. The last type of interaction is characterized by typical parameters (TP) as electron vibrational coupling constants, Huang-Rhys factors and Jahn-Teller stabilization energy .

The aim of this paper is the estimations of TP, in <sup>4</sup>T<sub>2g</sub> excited state of M<sup>2+</sup> (M=V, Fe, Mn) doped in MgO crystal, using two methods of calculation.

First method is based on the exchange charge model of crystal field [1] and has been applied to determine the dependence of the crystal field strength 10Dq on interionic distances R, between the M<sup>2+</sup> impurity ion and O<sup>2-</sup> ligands, in cubic MgO: M<sup>2+</sup> system. The obtained results were extrapolated by the power law and was shown that 10Dq depends on R as 1/R<sup>n</sup>, with n ≠ 5. The deviations from the value n = 5 (predicted by the simple point charge model of crystal field) are explained by the covalent and exchange effects. The 10Dq functions obtained as result of our calculations were used for estimating the TP [2].

The second method is based on Ham effect which serves as a firm experimental evidence of the dynamic Jahn-Teller effect in MgO:M<sup>2+</sup>. The quenching of the spin-orbit splitting of <sup>4</sup>T<sub>2g</sub> excited state, due to interactions between optical electrons of the metal ion and a<sub>1g</sub> and e<sub>g</sub> Jahn-Teller active vibrational modes of MgO host matrix, was used to estimate the Ham reduction parameter and Jahn-Teller stabilization energy. All the calculations were done using the optimized geometry of MgO: M<sup>2+</sup> system with DFT ab initio method implemented in CRYSTAL 09 code [3].

The obtained results are compared between them and with experimental data and the results are quite satisfactory.

### Acknowledgements

The work of A.M. Barb was supported by the strategic grant POSDRU/159/1.5/S/137750, Project “Doctoral and Postdoctoral programs support for increased competitiveness in Exact Sciences research” cofinanced by the European Social Fund within the Sectoral Operational Programme Human Resources Development 2007 – 2013.

[1] B.Z. Malkin, Crystal field and Electron-Phonon Interaction in Rare-Earth Ionic Paramagnets, in A.A. Kaplyanskii, B.M. Macfarlane(Eds.), Spectroscopy of solids containing rare-earth ions, North-Holland, Amsterdam, 1987,pg.30.

[2] M.G. Brik and N. M. Avram, J. Phys:Condens.Matt. 21 (2009) 155502.

[3] R.Dovesi, R.Orlando, B.Civalleri, C.Roetti, Saunders V R and Zicovich-Wilson C M, Z.Kristallogr. 220 571 (2005)

## ENERGY TRANSFER FROM Gd<sup>3+</sup> TO Er<sup>3+</sup> IN MATRIX Gd<sub>2</sub>O<sub>3</sub>

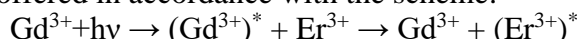
Yu A Kuznetsova, A F Zatsepin

*Ural Federal University, Yekaterinburg, Russia, kuznetsova.bess@mail.ru*

In recent years, there is great interest in the development of new functional materials for a variety application purposes such as solid-state lasers, optoelectronic devices, sensors, solar energy convertors and so on. Due to specialty of energy levels structure in the UV, visible and infrared regions rare-earth ions are promising as optical centers in luminescent energy converter materials based on down-conversion and up-conversion mechanisms. Furthermore, rare earth oxides have been considered as excellent luminescent host matrices because of their optical and chemical properties (broad band gap, low phonon energy) and the ability of being easily doped with rare earth ions in high concentrations. It is known that energy conversion efficiency is determined by the quantum efficiency of optically active ions photoluminescence [1]. In present work the quantum efficiency of the Er<sup>3+</sup> ions luminescence in host lattice Gd<sub>2</sub>O<sub>3</sub> under different excitation was determined.

Compacted powder samples of Gd<sub>2</sub>O<sub>3</sub>: Er<sup>3+</sup> were prepared by sol-gel method at the Institute of Physics Polish Academy of Sciences, Warsaw, Poland. The photoluminescence and excitation spectra and luminescence decay kinetics were obtained at room temperature using a fluorescence spectrometer PerkinElmer LS 55. The temperature luminescence intensity dependence was investigated using a spectrometer McPherson.

Upon excitation 220 nm (interband transitions in host lattice Gd<sub>2</sub>O<sub>3</sub>) the emission spectrum of Gd<sub>2</sub>O<sub>3</sub>: Er<sup>3+</sup> demonstrates the intense lines at 522 and 544 nm attributed to the transitions of Er<sup>3+</sup> ion (<sup>2</sup>H<sub>11/2</sub>→<sup>4</sup>I<sub>15/2</sub> and <sup>4</sup>S<sub>3/2</sub>→<sup>4</sup>I<sub>15/2</sub>). Excitation spectra monitored at 544 nm demonstrates the lines at 247, 277 и 312 nm corresponded to the transitions of Gd<sup>3+</sup> and the lines at 409, 380 и 367 nm assigned to the transitions of Er<sup>3+</sup> [2,3]. Excitation of Gd<sup>3+</sup> ions through the mentioned above transitions in the region of Gd<sub>2</sub>O<sub>3</sub> band gap indicate that such ions cannot be located at regular lattice positions and may be associated with intrinsic defects of host lattice Gd<sub>2</sub>O<sub>3</sub>. So there are several excitation channels of Er<sup>3+</sup> luminescence: interband transitions, the energy transfer from imperfect Gd<sup>3+</sup> ions and intracenter excitation. The mechanism of energy transfer from Gd<sup>3+</sup> ions to Er<sup>3+</sup> optical centers are offered in accordance with the scheme:



Using the data obtained from emission decay curves approximation and temperature quenching curve fitting the quantum efficiency of the Er<sup>3+</sup> ions luminescence under intracenter excitation ( $\eta_1=0,5$ ) and excitation by imperfect Gd<sup>3+</sup> ions ( $\eta_2=0,4$ ) are calculated.

The results indicate that the efficiencies of direct and indirect excitation of Er<sup>3+</sup> ions luminescence are characterized by the same order. It is found that the most decay time of the Er<sup>3+</sup> ions luminescence is observed under excitation by Gd<sup>3+</sup> ions, however, the quantum efficiency in this case is less. It means that the major losses under indirect excitation take place at intermediate stages. So there is a reserve for minimizing these losses and the quantum efficiency of the Er<sup>3+</sup> ions luminescence can be controlled by changes the defectiveness of host lattice Gd<sub>2</sub>O<sub>3</sub>.

[1] Jiayue Sun, Guangchao Sun, Yining Sun and Liu Han 2014 *Optical Materials* **36** 1097- 1100

[2] Gai S., Yang P., Wang D., Li C. 2011 *CrystEngComm* **13** 5480-5487

[3] Baryshnikov V.I., Krivorotova V.V. 2008 *Physics of the Solid State* **50** 1664–1666

## ERBIUM-DOPED LEAD SILICATE GLASSES FOR UP-CONVERSION LUMINESCENCE TEMPERATURE SENSORS

Wojciech A. Pisarski<sup>a</sup>, Joanna Pisarska<sup>a</sup>, Radosław Lisiecki<sup>b</sup>, Witold Ryba-Romanowski<sup>b</sup>

<sup>a</sup> *Institute of Chemistry, University of Silesia, Katowice, Poland*

<sup>b</sup> *Institute of Low Temperature and Structure Research, PAS, Wrocław, Poland,  
wojciech.pisarski@us.edu.pl*

Lead silicate glasses belong to materials emitting light in wide spectral region under UV-vis or NIR laser excitation. The advantage of these glass systems are large transparency from UV to NIR spectral ranges, good thermal stability, high values of refractive indices and quite easy incorporation of rare earth ions into glass matrices. Recently, the spectroscopic aspects for  $\text{Eu}^{3+}$ ,  $\text{Dy}^{3+}$  and  $\text{Tb}^{3+}$  ions in lead silicate glasses were presented and discussed in details [1].

In this work, the up-conversion luminescence spectra of  $\text{Er}^{3+}$  ions in lead silicate glasses have been examined. A special attention has been paid for lead silicate glasses to optical sensor applications. Up-conversion luminescence spectra were recorded in 500-580 nm spectral ranges under excitation by 975 nm line by cw laser-diode. In this spectral region, two green luminescence bands are observed, which correspond to transitions originating from thermally coupled  $^2\text{H}_{11/2}$  and  $^4\text{S}_{3/2}$  excited states to  $^4\text{I}_{15/2}$  ground state of  $\text{Er}^{3+}$ . The relative luminescence band intensities of  $^2\text{H}_{11/2} - ^4\text{I}_{15/2}$  and  $^4\text{S}_{3/2} - ^4\text{I}_{15/2}$  transitions of  $\text{Er}^{3+}$  ions were determined with temperature. The fluorescence intensity ratio defined usually as FIR (or R) from each thermally coupled  $^2\text{H}_{11/2}$  and  $^4\text{S}_{3/2}$  states to the  $^4\text{I}_{15/2}$  ground state was analyzed. In order to evaluate the temperature sensing ability of glass sample, the rate of R varying with temperature was calculated. For the optical temperature sensor based on the FIR technique of the green up-conversion luminescence in the lead silicate glass, the maximum sensitivity is approximately  $26.4 \times 10^{-4} \text{K}^{-1}$  at  $T = 590 \text{ K}$  in the temperature range of 296-650 K, respectively.

Acknowledgment: The National Science Centre (Poland) supported this work under research project 2014/13/B/ST7/01729.

[1] L. Żur, J. Janek, M. Sołtys, J. Pisarska, W.A. Pisarski, *Physica Scripta* T157 (2013) 014035.

## EVOLUTION OF THE OPTICAL PROPERTIES OF CHROMIUM DOPED CALCIUM TETRABORATE GLASS UNDER HIGH PRESSURE.

Tadeusz Lesniewski<sup>a</sup>, Marek Grinberg<sup>a</sup>, Justyna Barzowska<sup>a</sup>, Sebastian Mahlik<sup>a</sup>,  
Bohdan V. Padlyak<sup>b,c</sup>

<sup>a</sup> *Institute of Experimental Physics, University of Gdansk, Wita Stwosza 57, 80-952  
Gdansk, Poland, tadeusz.lesniewski@phdstud.ug.edu.pl*

<sup>b</sup> *Sector of Spectroscopy, Vlokh Institute of Physical Optics, Dragomanov Str. 23,  
79-005 Lviv, Ukraine*

<sup>c</sup> *Division of Spectroscopy of Functional Materials, Institute of Physics, University of  
Zielona Gora, Szafrana Str. 4a, 65-516 Zielona Gora, Poland*

In this contribution, we present luminescence properties of calcium tetraborate glass (CaB<sub>4</sub>O<sub>7</sub>) doped with Cr<sup>3+</sup> ions. Excitation spectra, steady state and time resolved luminescence spectra at temperatures between 10 K and 300 K and at high hydrostatic pressure up to 120 kbar were measured.

The excitation spectrum consists of two broad bands peaking at 420 nm and 580 nm related to transitions from the <sup>4</sup>A<sub>2g</sub> ground state to <sup>4</sup>T<sub>1g</sub> and <sup>4</sup>T<sub>2g</sub> excited states, respectively. Ambient pressure luminescence spectrum consists of two bands peaking at 690 nm and 850 nm. First band is related to the spin forbidden <sup>2</sup>E<sub>g</sub> → <sup>4</sup>A<sub>2g</sub> transition, whereas second, broad band is related to the spin allowed <sup>4</sup>T<sub>2g</sub> → <sup>4</sup>A<sub>2g</sub> transition. Widths of both bands are significantly greater than natural due to inhomogeneous broadening. Emission from both <sup>2</sup>E<sub>g</sub> and <sup>4</sup>T<sub>2g</sub> states exhibits strong thermal quenching, however the ratio between intensities of these bands is also strongly temperature and pressure dependent – relative contribution of <sup>2</sup>E<sub>g</sub> → <sup>4</sup>A<sub>2g</sub> luminescence decreases with increasing temperature, whereas applying pressure increases the relative intensity of <sup>2</sup>E<sub>g</sub> → <sup>4</sup>A<sub>2g</sub> emission band.

Electronic structure of Cr<sup>3+</sup> ions is described by Tanabe-Sugano diagram for *d*<sup>3</sup> electronic configuration. The order of two lowest excited states <sup>4</sup>T<sub>2g</sub> and <sup>2</sup>E<sub>g</sub> and their energy separation  $\Delta = E(^4T_{2g}) - E(^2E_g)$  depend on crystal field strength exerted by ligands surrounding the Cr<sup>3+</sup> ion, represented by crystal field strength parameter *Dq/B*. If *Dq/B* < 2.3 then <sup>4</sup>T<sub>2g</sub> is the lowest excited state ( $\Delta < 0$ ) and the chromium ion is said to be in low crystal field. For *Dq/B* > 2.3 <sup>2</sup>E<sub>g</sub> becomes the lowest excited state ( $\Delta > 0$ ) and the ion is in high crystal field. Simultaneous luminescent transitions from two excited crystal levels observed even at low temperatures indicate existence of chromium sites of both types. This, together with observed inhomogeneous broadening implies broad distribution of values of local crystal field strength, which is a result of distorted nature of chromium sites in glassy host. Relative intensification of <sup>4</sup>T<sub>2g</sub> band for higher temperatures is a result of thermal population of <sup>4</sup>T<sub>2g</sub> in high field sites. Applying pressure reduces the interatomic distances and thus increases the crystal field. This elevates the <sup>4</sup>T<sub>2g</sub> state relative to <sup>2</sup>E<sub>g</sub> and therefore reduces the amount of low field sites as well as suppresses the thermal population of <sup>4</sup>T<sub>2g</sub> in high field sites. Both effects contribute to relative decrease of <sup>4</sup>T<sub>2g</sub> emission band with increasing pressure.

## EXPERIMENTAL INVESTIGATION OF FLUORESCENT SENSORS FOR THE DETECTION NITRO EXPLOSIVES

Anna A. Baranova, Konstantin O. Khokhlov

*Ural Federal University, Mira St. 19, Yekaterinburg, Russia, a.a.baranova@urfu.ru*

The aim of this work was researching optical spectral properties of fluorescent materials which are sensitive to nitro explosives (HE) vapors, detecting more sensitive material and creating on its base the device for explosives detection.

In development of devices and analytical methods for HE detection it is guided by the key property of these compounds - it is the vapors formation of typical chemical composition near, and as the sensors the materials are used, certain properties of which are changed in HE vapors presence.

In this study it was examined the fluorescent materials such as copolymer of terephthalic aldehyde and melamine [1], 5,5-bis (1-pyrenyl)-2,2; 5.2-tertiofen [2], 1,3,6,8 tetra (trimetilsilitinil) pyrene [3], [Cd<sub>3</sub>(ox)<sub>2</sub>(bipy)<sub>5</sub>](ClO<sub>4</sub>)<sub>2</sub> [4] for further application as replaceable cartridges of sensors for HE detection portable device. The synthesized samples were nanopowders dissolved in organic solvent and coated on cellulose substrate.

Photoluminescence and photoluminescence excitation spectra were measured to determine the excitation and detection energy ranges.

It was found that 5,5-bis (1-pyrenyl)-2,2; 5.2-tertiofen substance has the best luminescence excitation characteristics. To maximize the material sensitivity to HE, to excite efficient luminescence it is necessary to use the efficient photon radiation with energy of ~ 500 nm). Having compared the luminescence intensity fall under the HE vapors influence and properties recovery it was observed that 5,5-bis (1-pyrenyl)-2,2; 5.2-tertiofen was more sensitive substance as well.

As a result the device was designed on the basis of this sensor material, sensitivity dependences of the sensor material in interaction with TNT vapors were revealed. The quantitative evaluation of luminescence intensity fall under the HE vapors influence was determined.

[1]W. Zhanga, L. Qiu, Y.-P. Yuana, A.-J. Xiea, Y.-H. Shena, J.-F. Zhub. *Journal of Hazardous Materials* 221– 222 (2012) 147– 154.

[2]T. Liu, K. Zhao, K. Liu, L. Ding, Sh. Yin, Y. Fang. *Journal of Hazardous Materials* 246– 247 (2013) 52– 60.

[3]S. Shanmugaraju, S. A. Joshi, P. S. Mukherjee. *J. Mater. Chem.*, 2011, 21, 9130.

[4]A. Bhunia, E. Zangrando, S. Mistri, S. C. Manna. *Inorganica Chimica Acta* 409 (2014) 528–537.

## EXPLORING AND DEEPENING THE USE OF ALGAL CHLOROPHYLLS INTO DYE SENSITIZED SOLAR CELLS

Emmanuele Ambrosi<sup>a</sup>, Simona Armeli Minicante<sup>b</sup>, Michele Back<sup>a</sup>, Jessica Barichello<sup>b</sup>, Elti Cattaruzza<sup>a</sup>, Francesco Gonella<sup>a</sup>, Enrico Scantamburlo<sup>a</sup>, Enrico Trave<sup>a</sup>

<sup>a</sup>*Department of Molecular Sciences and Nanosystems, Ca' Foscari University of Venezia, Via Torino 155/b, 30170 Mestre - Venezia, Italy*

<sup>b</sup>*Department of Environmental Sciences, Informatics and Statistics, Ca' Foscari University of Venezia, Dorsoduro 2137, 30123 Venezia, Italy*

One of the main targets of contemporary scientific research is finding a solution to the urgent need for a clean and cheap energy source. The sun energy is the most promising alternative because it is clean, abundant and is not concentrated in limited geographical areas. In recent years, the photovoltaic (PV) technologies experimented many advances in efficiency, cost and robustness. There are three main types of PV systems: the p-n semiconductor junction cells, the dye sensitized solar cells (DSSCs) and the organic photovoltaic cells (OPVCs). Since their appearance, DSSCs have drawn a lot of attention from the scientific community due to their ease of fabrication, low cost and competitiveness with different PV systems based on p-n junctions. A DSSC is a device based on the sensitization of large energy band-gap semiconductor by a dye that plays a key role: typically, high porosity TiO<sub>2</sub> nanoparticles are sensitized by dye molecules that, when illuminated, capture the incident photons and generate electron/hole pairs with consequent charge injection into the TiO<sub>2</sub> conduction band.

Since this mechanism resembles the natural photosynthesis process involving light-energy absorption and charge separation, the idea is to employ a photosynthetic pigments for fabricating a DSSC system. In this context chlorophylls (Chls), which act as effective photosensitizer in photosynthesis process, have the potential to be an environment friendly dye source. Among the various types of Chls, Chl-*c* can adsorb efficiently on TiO<sub>2</sub> by means of an anchoring group, typically carboxylic or hydroxyl groups. Moreover it absorbs solar radiation strongly with absorption bands in the UV-visible region, covering a broad range of wavelengths. Therefore, they have potential for ensuring efficient electron injection into the TiO<sub>2</sub> conducting band. Between different plants, marine algae are a rich reserve of natural dyes (Chl-*a*, Chl-*b* and Chl-*c*) but, although show a broad range of applications and a steadily increasing importance in several sectors, they are still an underexploited resource in the photovoltaic field.

This research aims to deepen the possible use of algal Chls as dye within the DSSCs. Two brown macroalgae were tested, namely, *Undaria pinnatifida* and *Sargassum muticum*; they are both largely present in the Venice lagoon area. The main issues addressed were: definition of a protocol for the extraction of the photosynthetic pigments and preparation of the coloured solutions using appropriate solvents; fabrication of TiO<sub>2</sub>-based DSSCs and test of the photovoltaic performances for the Chl-based devices by measuring the usual figure-of-merit parameters (current-voltage curves I-V, incident photocurrent efficiency IPCE); characterization of the spectrophotometric and luminescence properties of the extracted Chls for evaluating also the possible use as fluorescent dye.

## FABRICATION AND SPECTROSCOPIC PROPERTIES OF TRANSLUCENT LuPO<sub>4</sub>:Ce FILMS

Justyna Zeler<sup>a</sup>, Joanna Cybińska<sup>a,b</sup>, Eugeniusz Zych<sup>a</sup>

<sup>a</sup> Faculty of Chemistry, University of Wrocław 14 F. Joliot-Curie Street, Wrocław, Poland  
Eugeniusz.zych@chem.uni.wroc.pl

<sup>b</sup> Wrocław Research Centre EIT+, 147/149 Stabłowicka Street, Wrocław, Poland  
Joanna.cybinska@eitplus.pl

LuPO<sub>4</sub> activated with lanthanide ions have been reported as efficient phosphors, also upon ionizing radiation and thus possibly useful for medical imaging [1][2]. The host shows perfect chemical stability, lack of hygroscopicity and has a reasonable density of 6.5 g/cm<sup>3</sup>. However, lutetium orthophosphate does not melt congruently, which precludes pulling large single crystals by the most convenient Czochralski method [3]. Since LuPO<sub>4</sub> is optically anisotropic material it also cannot be easily sintered into highly transparent ceramics.

In our presentation we will prove that translucent layers of LuPO<sub>4</sub>:Ce can be prepared and their photo- and radioluminescent properties will be presented. The transparency of a thin layer of LuPO<sub>4</sub>:Ce is illustrated in the photo inserted into Fig. 1. The layers were prepared using hydrothermally synthesized nano-powder precursors. The additional thermal treatment of the films in the temperature range of 1000-1350 °C in vacuum or reducing atmosphere improved their luminescent properties. Fig. 1 presents excitation and emission spectra of the translucent LuPO<sub>4</sub>:0.5%Ce film heated at 1000 °C in vacuum. The spectra are very similar to those reported for single crystals made by means of flux technique. In our presentation we shall give more details on the synthesis process and structural, morphological and spectroscopic properties of the LuPO<sub>4</sub>:Ce ceramics.

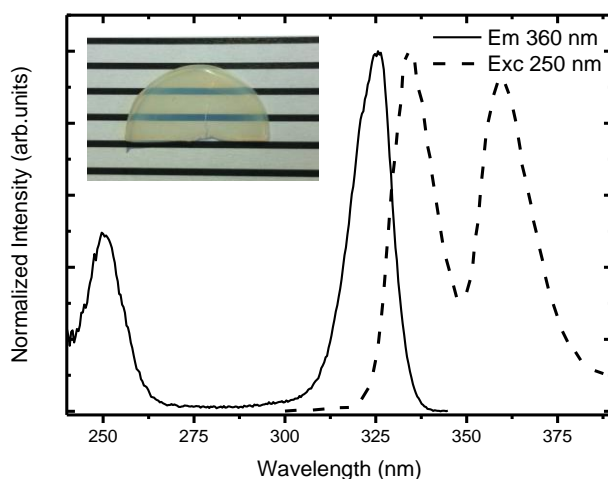


Figure 1. The emission and excitation spectra of LuPO<sub>4</sub>:0.5%Ce film prepared at 1000 °C in vacuum. In the upper left corner a photo of the translucent LuPO<sub>4</sub>:0.5%Ce film is inserted.

### Acknowledgement

This work was supported within the framework of the target subsidy for scientific research or development works and related tasks, contributing to the development of young scientists and PhD students funded within internal competition procedure.

[1] L. Boatner, L. Keefer, J. M. Farmer, D. Wisniewski, A. J. Wojtowicz, SPIE - The International Society of Optical Engineering 5540 (2004) 73–87.

[2] C. Mansuy, J. M. Nedelec, C. Dujardin, R. Mahiou, Journal of Sol-Gel Science and Technology 38 (2006) 97–105.

[3] J. S. Neal, L. Boatner, M. Spurrier, P. Szupryczynski, C. L. Melcher, Proc. of SPIE 6319 (2006) 631907–1

## FIRST INVESTIGATIONS OF CUBIC Yb<sup>3+</sup>-DOPED La<sub>2</sub>(MoW)<sub>2</sub>O<sub>9</sub> FOR OPTICAL CERAMICS

M. Bieza<sup>a</sup>, M. Guzik<sup>a</sup>, E. Tomaszewicz<sup>b</sup>, Y. Guyot<sup>c</sup>, E. Zych<sup>a</sup>, G. Boulon<sup>c</sup>

<sup>a</sup>*Faculty of Chemistry, University of Wrocław, 14 F. Joliot-Curie,  
50-383 Wrocław, Poland,*

<sup>b</sup>*Department of Inorganic and Analytical Chemistry, West Pomeranian University of  
Technology, Al. Piastów 42, 71-065 Szczecin, Poland*

<sup>c</sup>*Institute Light Matter (ILM), UMR5306 CNRS-University Lyon1, University of Lyon, 69622  
Villeurbanne, France*

Rare earth-doped molybdates and tungstates are well-known matrices widely used as phosphors, scintillators and laser materials. Most of laser materials from this family were grown as single crystals by the conventional Czochralski method, and so far are not yet known as optical ceramic materials. The lack of knowledge on optical properties of RE<sup>3+</sup>-doped cubic tungstates and molybdates is the main motivation of our research.

Our previous research on Nd<sup>3+</sup>-doped La<sub>2</sub>Mo<sub>2</sub>O<sub>9</sub> (LAMO<sub>X</sub>) molybdates has shown that the substitution of La<sup>3+</sup> ion by Nd<sup>3+</sup> one until to 15 mol% leads to the creation of the monoclinic structure ( $\alpha$ - form, space group *P2*<sub>1</sub>) and the pure cubic phase ( $\beta$ - form, space group *P2*<sub>1</sub>3) can be obtained when the Nd<sup>3+</sup> contents reached 50 mol%. However the Nd<sup>3+</sup>-doped monoclinic phase might be useful for application in the future as phosphors and ultra-short pulses (pico, femto) laser materials because of very broad absorption and emission bands and very short decay times [1,2].

According to the literature, the partial substitution of cation in the La<sub>2</sub>Mo<sub>2-y</sub>WyO<sub>9</sub> mixed molybdate/tungstate leads to  $\beta$ -polymorph [3]. The series of cubic nano- and microcrystalline Yb<sup>3+</sup>-doped La<sub>2</sub>(MoW)<sub>2</sub>O<sub>9</sub> molybdates/tungstates were obtained by partial substitution of Mo<sup>6+</sup> ions by tungsten W<sup>6+</sup> ones (ratio 1:1) and La<sup>3+</sup> ions by Yb<sup>3+</sup> ones. The samples demonstrate different morphology according to combustion, Pechini and solid state method used for fabrication. The spectroscopic investigations revealed very broad absorption and emission lines even at low temperature, similar to the bands observed in the disordered materials [4]. The fabrication of sintered mixed ceramics is under progress.

[1] M. Guzik, M. Bieza, E. Tomaszewicz, Y. Guyot, G. Boulon, Z. Naturforsch. 69b (2014) 193-204.

[2] M. Guzik, M. Bieza, E. Tomaszewicz, Y. Guyot, E. Zych, G. Boulon, Opt. Mater. 41 (2015) 21-31.

[3] D. Marrero-Lopez, J. Canales-Vazquez, W. Zhou, J.T.S. Irvine, P. Nunez, J. Solid State Chem. 179 (2006) 278–288.

[4] S. Wang, F. Lou, C. Yu, Q. Zhou, M. Wang, S. Feng, D. Chen, L. Hu, W. Chen, M. Guzik, G. Boulon, J. Mater. Chem. C, 2 (2014) 4406.



## FLUORESCENT ORGANIC NANOPARTICLES BASED ON INERT CARBON FREE RADICALS

Davide Blasi<sup>a</sup>, Domna Maria Nikolaidou<sup>b</sup>, Francesca Terenziani<sup>b</sup>, Imma Ratera<sup>a</sup>, Jaume Veciana<sup>a</sup>

<sup>a</sup>*Institut de Ciència de Materials de Barcelona (CSIC) and Ciber-BBN, Campus UAB, 08193, Bellaterra, Barcelona, Spain*

<sup>b</sup>*Dept. of Chemistry, University of Parma, Parco Area delle Scienze 17A, 43124 Parma, Italy*

Polychlorotriphenylmethyl radical derivatives are one of the few examples of persistent and stable free radicals [1]. The particular “open-shell” electronic configuration of these radicals leads to an emission at long wavelengths without the need of an extended  $\pi$ -conjugated structure. Their use in optical and optoelectronic applications is limited by their low photo-stability and fluorescent quantum yield ( $\Phi_f$ ) [2]. During the last years, different molecular approaches have been proposed in order to try to enhance the optical properties of these molecules [3] [4].

In this work we tested a supramolecular strategy to improve the photo-stability and the  $\Phi_f$  of two simple radicals: tris(2,4,6-trichlorophenyl)methyl radical (TTM) and tris(pentachlorophenyl)methyl radical (PTM). Nanoparticles of the non-radical and optically neutral tris(2,4,6-chlorophenyl)methane (TTM- $\alpha$ H) doped with different amounts of TTM and PTM radicals were prepared using the reprecipitation method. Dynamic light scattering and Transmission Electron Microscopy show spherical nanoparticles with a diameter between 50 and 100 nm, with a quite good colloidal stability (Z-potential values between - 32 mV and - 44 mV). Moreover, the nanoparticle suspensions are photo-stable when irradiated at the maximum of absorption (380 nm) of the radical chromophores. The obtained composite nanoparticles with the 1.5% mol. of TTM and PTM radicals are highly luminescent showing  $\Phi_f$  more than ten times higher than in solution. A progressive quenching of emission is observed increasing the amount of radical molecules inside the nanoparticles. In the case of TTM radical, this quenching is accompanied by the appearance of a new emission band at lower energy, characterized by long lifetime, on the order of  $\mu$ s. Because of these characteristics, this new band is assigned to a triplet (or higher multiplicity) state generated by the presence of two or more close radical molecules in this rigid environment.

This work demonstrates that a rigid (nano)environment is able to enhance the luminescence properties of these open-shell molecular materials. Moreover, in the case of TTM it is possible to tune the emission wavelength changing the concentration of radical molecules inside the composite nanoparticles. Due to their intense absorption in the UV-region and their emission in the orange-red region, these materials could be good candidates as fluorescent probes for two-photon microscopy.

- [1] M. Bellester, J. Riera, J. Castañer, C. Badía, J. Monso, *J. Am. Chem. Soc.*, 93 (1971), 2215,
- [2] M.A. Fox, E. Gaillard, C. Chen, *J. Am. Chem. Soc.*, 197 (1987), 7088-7094.
- [3] Y. Hattori, T. Kusamoto, H. Nishihara, *Angew. Chem. Int. Ed.*, 53 (2014), 11845 –11848.
- [4] S. Castellanos, D. Velasco, F. Lopez-Calahorra, E. Brillas, L. Julia, *J. Org. Chem.*, 73 (2008), 3759.

## FORMATION FEATURES OF COPPER THIN FILMS ON THE PHOSPHATE GLASS

Elena Kolobkova, Ba Minh Dinh, Nikolay Nikonorov, Rustam Nuryev, Alexandr Trofimov  
*ITMO University, 49 Kronverksky Pr., Saint Petersburg, Russia, Nuryev@oi.ifmo.ru*

Nanostructured copper oxides are of the great interest for the modern element base of photonics and wide field of photonics applications because of their significant physical and optical properties. The properties of  $\text{Cu}_x\text{O}$  nanomaterials depends on structure, texture, oxidation state etc. Therefore, the investigation of features of formation of copper oxides on surface of phosphate glasses and studying their fundamental parameters have been presented in the work.

The samples of virgin glasses were prepared with two different compositions: 1)  $\text{Na}_2\text{O}-\text{P}_2\text{O}_5-\text{Ga}_2\text{O}_3-\text{AlF}_3-\text{ZnO}$  and 2)  $\text{BaPO}_3-\text{NaPO}_3-\text{AlF}_3$ . The glasses were doped with various concentration of activators  $\text{CuCl}$  and  $\text{Cu}_2\text{O}$  from 2.0 up to 4.0 mol%. The virgin glass was synthesized from melt in an open glassy carbon crucibles at  $950^\circ\text{C}$  under air flow during 40 minutes.  $T_g$  was determined using simultaneous thermal analysis (Netzsch STA 449) and was equal  $400^\circ\text{C}$ . The  $\text{CuO}$  thin films were obtained during secondary heat treatment at range of  $T_g \pm 40^\circ\text{C}$ .

X-ray diffraction (Rigaku Ultima IV) analysis revealed that heat treatment resulted in appearance of  $\text{CuO}$  thin film. The increasing of heat treatment temperature and heating time results in increasing of thickness of copper oxide thin film. The size of  $\text{CuO}$  crystallites weakly depends on the heat treatment time or temperature at range of  $380-440^\circ\text{C}$  and about 16-20 nm. The heat treatment also results in a shift of absorption band into short-wave range. The secondary thermal treatment in strong reduction conditions using graphite powder results in appearance of copper phase (fig. 1)

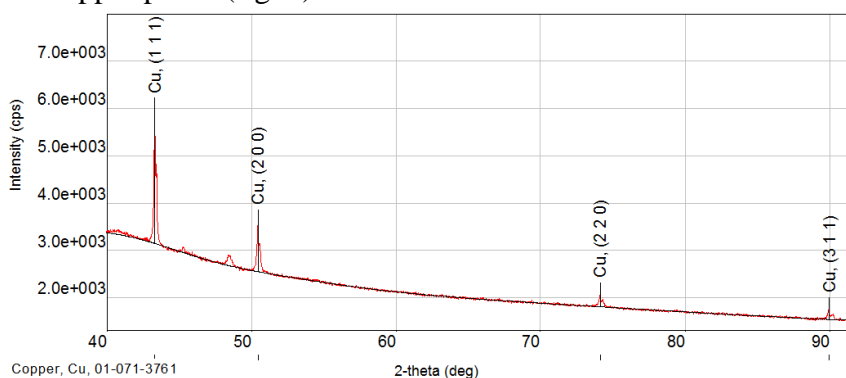


Fig.1 X-ray diffraction patterns of thin film on surface of aluminum-phosphate glass doped with  $\text{Cu}_2\text{O}$  2 mol% after 30 minutes at  $440^\circ\text{C}$

$\text{Cu}_x\text{O}$  are promising candidates for modern photonic applications like optical sensors, solar cells, light emitting diodes and p-type semiconductors. It low-coast material with different properties (optical, conductivity etc.) that could be changed with easily way through conditions of secondary thermal treatment.

[1] B.G. Ganga, P.N. Santhosh, Manipulating aggregation of  $\text{CuO}$  nanoparticles: Correlation between morphology and optical properties, *Journal of Alloys and Compounds* 612 (2014) 456–464.

[2] Yonglong Shen, Meilan Guo, Xiaohong Xiaa, Guosheng Shao, Role of materials chemistry on the electrical/electronic properties of  $\text{CuO}$  thin films, *Acta Materialia* 85 (2015) 122–131.

## FORMATION OF THE LUMINESCENT CENTERS IN ZINC-PHOSPHATE GLASSES DOPED WITH Ag AND Cu IONS BY X-RAY AND NANOSECOND LASER RADIATION

Klyukin D.A., Leontieva V.A., Stolyarchuk M.V., Sidorov A.I., Ignatiev A.I.,  
Nikonorov N.V.

*ITMO University, 49 Kronverksky pr., Russia, valya.leontyeva@yandex.ru*

In this study we present an investigation of the luminescent center formation in zinc-phosphate glasses, containing Ag and Cu ions under the action of X-ray and UV nanosecond laser radiation. Several researches were conducted with X-ray and UV nanosecond laser irradiation of Ag-containing glasses [1].

Several types of zinc-phosphate glasses were synthesized in ITMO University by melting approach. The concentration of silver and copper dopant ions was varied to understand the influence of different glass components on the glass luminescence properties.

It was shown that pure glass without dopants doesn't have significant bands in the luminescence spectrum. Whereas the addition of silver and copper ions to the batch results in a weak orange luminescence that can be assigned to the  $Ag_x-Cu_y$  molecular clusters formation.

The irradiation of (Ag+Cu) glasses by the third harmonic ( $\lambda = 355$  nm) of YAG:Nd nanosecond laser results in the formation of bright luminescent centers in the glass volume. It should be noted that just after the laser irradiation the luminescence intensity is very weak. But approximately after a day keeping at room temperature, or after one hour thermal treatment at a temperature below  $T_g$  the luminescence intensity under UV excitation increases significantly.

Similar results were obtained for X-ray irradiated samples. The dose of irradiation was equal for every sample, but the change of luminescence intensity was quite different for the samples with different concentration of silver and copper. In particular, the silver and copper doped glasses with concentrations of  $Ag_2O$  0,1 mol.% and  $Cu_2O$  0,1 mol. % have a very intense luminescence with the excitation peak at 365 nm and in the nearly whole visible spectral range (Fig.1). The mechanisms of luminescence centers formation and its dynamic are discussed. The obtained results can be used for the creation of luminescent glasses for photonic devices, wavelength convertors, and luminescent sensors.

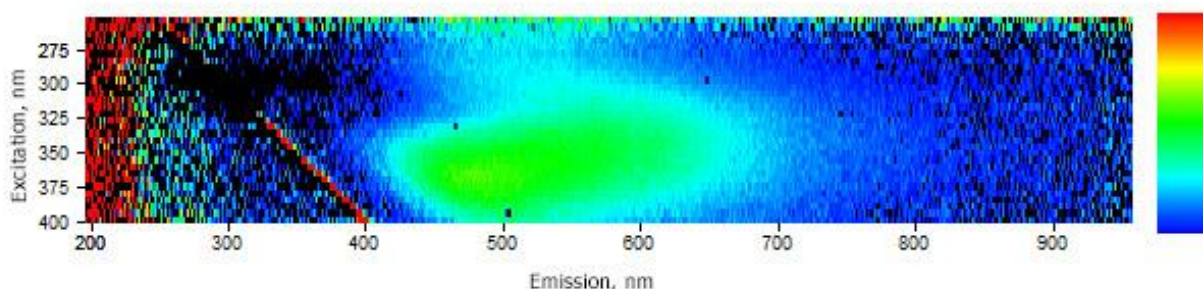


Fig.1. Luminescence intensity via excitation wavelength of (Ag+Cu) doped zinc-phosphate glass after X-ray irradiation.

[1] Y. Miyamoto, T. Ohno, Y., H. Nanto, T. Kurobori, T. Yanagida, A. Yoshikawa, Y. Nagashima, T. Yamamoto, Rad. Measur. 55 (2013) 72–74.

## GENERALIZED CLAUSIUS-MOSSOTTI RELATION FOR SEMI-INFINITE ARTIFICIAL PERIODIC STRUCTURE

Maxim N. Anokhin, Alexey A. Tishchenko, Mikhail N. Strikhanov

*National Research Nuclear University "MEPhI" 31 Kashirskoe Shosse, Moscow, Russia,  
MNAnoxhin@mephi.ru*

Periodicity changes the dielectric properties and, consequently, determines the propagation of electromagnetic waves in periodic structures of various types [1]. Periodic structures are widely used in different applications [1], e.g., in new and perspective class of materials – metamaterials, for producing high-performance filters, in resonators, signal dividers, microwave electronics, etc.

In this work we develop the so called local field theory for the case of semi-infinite artificial periodic structure. In our recent paper [3] we considered an infinite structure and now demonstrate that taking in account the surface leads to the additional anisotropy and thus changes the tensor structure of the dielectric permittivity. The method we use is based on the direct solving of Maxwell's equations, and it is known that in case of amorphous medium the natural changing of the dielectric properties near the surface [3] occur. As a result, we obtain from the first principles a generalized Clausius-Mossotti relation describing the dielectric permittivity for a semi-infinite artificial periodic structure. The expressions obtained include the spatial dispersion and permit to define resonant conditions for propagating waves.

[1] Z. Zhang, S. Satpathy, Phys. Rev. Lett. 65 (1990) 2650.

[2] E. Yablonovitch, J. Optical Soc. America B 10 (1993) 283-295.

[3] M.N. Anokhin, A.A. Tishchenko, M.N. Strikhanov, IOP Conf. Ser. (accepted).

[4] M.I. Ryazanov, JETP 83 (1996) 529.

[5] M.N. Anokhin, A.A. Tishchenko, M.I. Ryazanov, M.N. Strikhanov, IOP Conf. Ser. 541 (2014) 012023.

## **ANALYSIS OF INTACT CEREAL FLOURS BY FLUORESCENCE SPECTROSCOPY COUPLED WITH PARAFAC**

Ivana Zeković, Lea Lenhardt, Bojana Milićević, Tatjana Dramićanin, Miroslav D. Dramićanin  
*University of Belgrade, Institute of Nuclear Sciences Vinča, PO Box 522, 11001 Belgrade, Serbia, email: zekovicivana@gmail.com*

A various types of sensing techniques based on the food fluorescence have been extensively used in recent years for food characterization [1]. Among them, fluorescence spectroscopy coupled with adequate multivariate analysis methods offers several advantages for the characterization of complex food systems [2–4]. In this report, excitation-emission matrices (EEM) were measured on the intact samples of different flour types. Obtained spectra were used to build optimal PARAFAC (parallel factor analysis) model in order to identify fluorophores in flours and their relative concentrations. Results of analysis showed presence of four fluorophores, and their concentration levels are calculated for samples of different flour types. Based on these findings we can conclude that this intact technique offers many advantages for characterization of cereal flours.

- [1] J. Christensen, L. Norgaard, R. Bro, S.B. Engelsen, *Chem. Rev.* 106 (2006) 1979–1994.
- [2] L. Lenhardt, R. Bro, I. Zekovic, T. Dramicanin, M.D. Dramicanin, *Food Chem.* 175 (2015) 284-291
- [3] Lea Lenhardt, Rasmus Bro, Ivana Zeković, Tatjana Dramićanin, Miroslav D. Dramićanin, *Food Chem.* 175, (2015) 284-291.
- [4] Lea Lenhardt, Ivana Zeković, Tatjana Dramićanin, Miroslav D. Dramićanin, Rasmus Bro, *Appl. Spectrosc.* 68, (2014) 557-563

## STRUCTURAL PHASE TRANSITIONS AND PHOTOLUMINESCENCE PROPERTIES OF OXONITRIDOSILICATE PHOSPHORS UNDER HIGH HYDROSTATIC PRESSURE

Agata Lazarowska<sup>a</sup>, Sebastian Mahlik<sup>b</sup>, Marek Grinberg<sup>c</sup>, Guogang Li<sup>d</sup>, Ru-Shi Liu<sup>e</sup>

<sup>a</sup>*Institute of Experimental Physics, University of Gdansk, Wita Stwosza 57, 80-952 Gdansk, Poland, a.lazarowska@ug.edu.pl*

<sup>b</sup>*Institute of Experimental Physics, University of Gdansk, Wita Stwosza 57, 80-952 Gdansk, Poland, s.mahlik@ug.edu.pl*

<sup>c</sup>*Institute of Experimental Physics, University of Gdansk, Wita Stwosza 57, 80-952 Gdansk, Poland, fizmgr@ug.edu.pl*

<sup>d</sup>*Department of Chemistry, National Taiwan University, Taipei 106, Taiwan.  
Faculty of Materials Science and Chemistry, China University of Geosciences, Wuhan  
430074, China, ggli8312@gmail.com*

<sup>e</sup>*Department of Mechanical Engineering and Graduate Institute of Manufacturing  
Technology, National Taipei University of Technology, Taipei 106, Taiwan, rslu@ntu.edu.tw*

Photoluminescence properties of  $(\text{Sr}_{0.98-x}\text{Ba}_x\text{Eu}_{0.02})\text{Si}_2\text{O}_2\text{N}_2$ : $x=0.98$  (*Phase A; orthorhombic; Pbcn*),  $x=0.49$  (*Phase B; triclinic; P1*) (*c*)  $x=0.75$  (*Phase C; triclinic; P1*) were studied under high hydrostatic pressures applied in a diamond anvil cell up to 200 kbar. It was found that the  $5d^14f^6 \rightarrow 4f^7$  luminescence of  $\text{Eu}^{2+}$  ions emerges obvious abrupt changes (decay time, maximum and shape) at about 40 kbar and 20 kbar for  $(\text{Sr}_{0.49}\text{Ba}_{0.49}\text{Eu}_{0.02})\text{Si}_2\text{N}_2\text{O}_2$  and  $(\text{Sr}_{0.23}\text{Ba}_{0.75}\text{Eu}_{0.02})\text{Si}_2\text{O}_2\text{N}_2$ , respectively, which indicate the variation of the local symmetry and crystal field strength of  $\text{Eu}^{2+}$  ions. These changes were attributed to the reversible pressure-induced structural phase transition of triclinic  $(\text{Sr}_{0.98-x}\text{Ba}_x\text{Eu}_{0.02})\text{Si}_2\text{O}_2\text{N}_2$   $x=0.49$  and  $x=0.75$  into orthorhombic structure, while orthorhombic  $(\text{Ba}_{0.98}\text{Eu}_{0.02})\text{Si}_2\text{O}_2\text{N}_2$  phase is preserved in the whole range of the applied pressure. The pressure in which phase transition occurs decreases linearly with increasing Ba composition in  $(\text{Sr}_{0.98-x}\text{Ba}_x\text{Eu}_{0.02})\text{Si}_2\text{O}_2\text{N}_2$ . Very different pressure shifts of the  $4f^65d \rightarrow 4f^7$  luminescence of  $\text{Eu}^{2+}$  in *Phase A* and *C* (where it is equal to  $-20 \text{ cm}^{-1}/\text{kbar}$  and  $-40 \text{ cm}^{-1}/\text{kbar}$ ), and in *Phase B* (where it is equal to zero) have been observed. This effect has been explained by different interaction of the 5d electron with the second coordination sphere of positive ions.

## EFFECT OF TEMPERATURE ON PHOTOLUMINESCENCE OF Gd DOPED ZnO NANOCRYSTALS

Deepika Mithal, Tapanendu Kundu

*Department of Physics, Indian Institute of Technology Bombay, Mumbai 400076, India,  
deepika@phy.iitb.ac.in, tkundu@phy.iitb.ac.in*

ZnO semiconductor nanocrystals provide an opportunity to have applications in the field of photonics due to its UV and visible emissions. These emissions can be tailored by doping rare earth ions into the host matrix introducing structural modifications along with the energy level interactions. Recently, we have communicated a systematic study of the effect of Gd incorporation in ZnO nanocrystals ( $\sim 6.7$  nm in diameter) by analyzing the change in photoluminescence with structural parameters [1]. The particle size reduction and weakening of the crystallinity were observed as the Gd concentration was increased. As a result, the  $A_1$  symmetry phonon modes in the wurtzite crystal structure were found to be Raman active with the extent of Gd doping. Since the phonon vibrations in material govern the nonradiative decay of the photoexcitation energy, the radiative distribution gets modified. Since phonon vibrations are temperature sensitive, temperature dependent photoluminescence study provides effective information about these distributions and enables to measure the interaction of phonons with photogenerated excitons. Fig 1(a) and (b) show the variation of the UV emission with temperature for ZnO and Gd doped ZnO nanocrystals (Gd/Zn,  $x = 0.34$ ), respectively. As seen, the variations in excitonic (UV) emission intensities and its shape with temperature are different in undoped and doped samples. The blue shift of this emission is also observed. From the effect of temperature on integration intensity of the UV emission as shown in fig 1(c), exciton binding energy ( $E_b$ ) was measured by  $I(T) = I(0)/[1 + A \cdot \exp(-E_b/k_B T)]$  where  $I(T)$  is the integrated intensity of the emission at a temperature  $T$ ,  $I(0)$  is integrated intensity at absolute zero,  $A$  is a constant and  $k_B$  is the Boltzmann's constant [2]. The exciton binding energy was found to vary with Gd ions concentration. The extent of exciton phonon interaction with doping concentration was also estimated using the variation of peak shift of the excitonic emission with temperature. Detailed analysis of our observation will be presented.

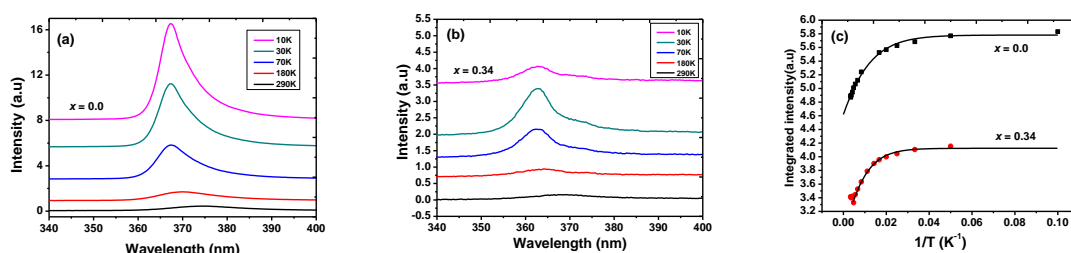


Fig. 1 The variation of UV emission with temperature for (a) ZnO, and (b)  $x = 0.34$  Gd doped ZnO nanocrystals. (c) Variation of integrated intensity as a function of inverse temperature.

[1] D.Mithal, S.Dhar, B.P.Singh, T.Kundu, *Material Research Express* (Communicated).

[2] W-T Hsu, K-F Lin, W-F Hsieh, *Appl. Phys. Lett.* 91 (2007) 181913.

## PERSISTENT LUMINESCENCE OF TERBIUM AND PRASEODYMIUM DOPED LUTETIA PREPARED BY THE RAPID MICROWAVE ASSISTED METHOD

C. C. S. Pedroso<sup>a</sup>, J. M. Carvalho<sup>a</sup>, L. C. V. Rodrigues<sup>a</sup>, H. F. Brito<sup>a</sup>, J. Hölsä<sup>a-c</sup>

<sup>a</sup>Institute of Chemistry, University of São Paulo, São Paulo, Brazil, hefbrito@iq.usp.br

<sup>b</sup>Department of Chemistry, University of Turku, Turku, Finland, jholsa@utu.fi

<sup>c</sup>Turku University Centre for Materials and Surfaces (MatSurf), Turku, Finland

Persistent luminescence is a phenomenon where the material emits radiation (usually in visible) for seconds to hours after the removal of the irradiation source, *e.g.* light, UV radiation, or electron beam. Despite dominance of  $\text{Eu}^{2+}$  as a dopant in persistent luminescence materials, other dopants as trivalent rare earths ( $\text{R}^{3+}$ ) have emerged [1]. For example, the  $\text{Lu}_2\text{O}_3:\text{R}^{3+}$  (R: Eu, Tb or Pr) materials show efficient persistent luminescence but require preparation at high temperatures (1700 °C) in high vacuum or in  $\text{H}_2\text{-N}_2$  [2]. Possible alternative to the ceramic method is the rapid microwave assisted preparation. The advantages of the microwave method include short processing time, selective dielectric heating, energy savings and the use of inexpensive equipment.

In this work, the preparation of the green ( $\text{Tb}, \text{Ca}^{2+}$ ; 0.03-1.5 & 0.0-3.0 mol-%) and red ( $\text{Pr}, \text{Hf}^{\text{IV}}$ ; 0.03-1.5 & 0.0-1.5 mol-%) emitting  $\text{Lu}_2\text{O}_3:\text{R}^{3+}, \text{M}$  persistent luminescence materials by the rapid microwave assisted method is presented. The  $\text{Lu}_2\text{O}_3$ ,  $\text{Pr}_6\text{O}_{11}$ ,  $\text{Tb}_4\text{O}_7$  (all 99.99 %, CSTARM),  $\text{CaO}$  (>98 %, Merck) and  $\text{HfO}_2$  (98 %, Sigma-Aldrich) precursors were mixed and ground using stoichiometric amounts to prepare the polycrystalline  $\text{Lu}_2\text{O}_3:\text{R}^{3+}, \text{Ca}^{2+}/\text{Hf}^{\text{IV}}$ . The mixtures were then heated in a domestic microwave oven (2.45 GHz) with 900-1000 W power for ~25 min with boric acid (5.0 w-%) as a flux in the presence of carbon (microwave susceptor). The SR-XPD pattern (Fig. 1, left) confirms the cubic C-type oxide (lutetia) as the main phase together with a rhombohedral  $\text{LuBO}_3$  (vaterite) impurity. The persistent luminescence of the  $\text{Lu}_2\text{O}_3:\text{Tb}^{3+}, \text{Ca}^{2+}$  phosphor (Fig. 1, middle) consists of emission mainly in green due to the  $^5\text{D}_4 \rightarrow ^7\text{F}_{6-0}$  transitions of  $\text{Tb}^{3+}$ . The  $^5\text{D}_3$  emission is largely quenched indicating this level to overlap with the conduction band of  $\text{Lu}_2\text{O}_3$ . The  $\text{Lu}_2\text{O}_3:\text{Pr}^{3+}, \text{Hf}^{\text{IV}}$  persistent luminescence (Fig. 1, right) shows only emission of the  $\text{Pr}^{3+}$  4f-4f transitions in red ( $^1\text{D}_2 \rightarrow ^3\text{H}_4$ ) and near-infrared. The nearly pure  $\text{Lu}_2\text{O}_3:\text{Tb}^{3+}, \text{Ca}^{2+}$  and  $\text{Lu}_2\text{O}_3:\text{Pr}^{3+}, \text{Hf}^{\text{IV}}$  persistent luminescence materials were thus successfully synthesized with the rapid microwave assisted preparation without the use of high vacuum or  $\text{H}_2\text{-N}_2$ .

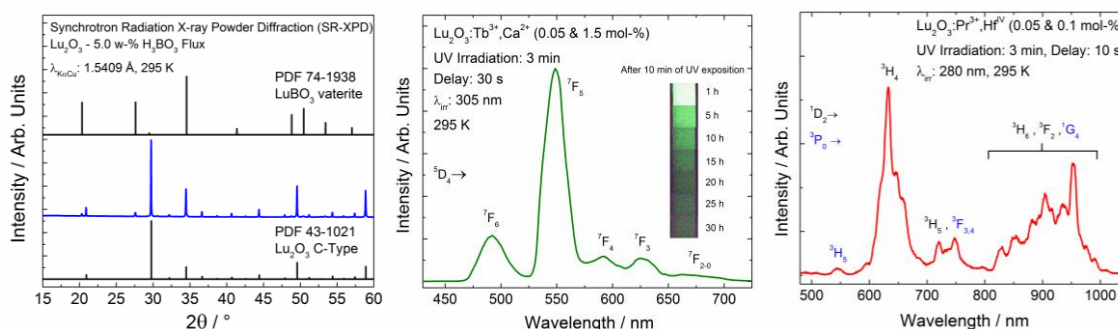


Figure 1. The SR-XPD pattern of  $\text{Lu}_2\text{O}_3$  with  $\text{H}_3\text{BO}_3$  flux (left) as well as the persistent luminescence spectra of  $\text{Lu}_2\text{O}_3:\text{Tb}^{3+}, \text{Ca}^{2+}$  (middle) and  $\text{Lu}_2\text{O}_3:\text{Pr}^{3+}, \text{Hf}^{\text{IV}}$  (right).

[1] L.C.V. Rodrigues, J. Hölsä, M. Lastusaari, M.C.F.C. Felinto, H.F. Brito, J. Mater. Chem. C 2 (2014) 1612–1618.

[2] J. Trojan-Piegza, E. Zych, J. Hölsä, J. Niittykoski, J. Phys. Chem. C 113 (2009) 20493–20498.



## DIFFRACTION GRATING PROFILE RECONSTRUCTION USING SAMPLE-ROTATION MUELLER MATRIX ELLIPSOMETRIC MEASUREMENTS

Lukáš Halagačka<sup>a</sup>, Kamil Postava<sup>a,b,c</sup>, Martin Mičica<sup>a,b</sup>, Jaromír Pištora<sup>a,b</sup>

<sup>a</sup>*IT4 Innovations, National Supercomputing center, VŠB – Technical University of Ostrava, 17. listopadu 15, Ostrava, Czech Republic, Lukas.Halagacka@gmail.com, Matrin.Micica@vsb.cz, Jaromir.Pistora@vsb.cz*

<sup>b</sup>*Nanotechnology Centre, VŠB – Technical University of Ostrava, 17. listopadu 15, Ostrava, Czech Republic,*

<sup>c</sup>*Department of Physics, VŠB – Technical University of Ostrava, 17. listopadu 15, Ostrava, Czech Republic, Kamil.Postava@vsb.cz*

Reconstruction of the geometry of fabricated structures is an important task for the optimization of the technological process and further design of required structures. In this work we analyze 1D periodic gold gratings developed using electron-beam lithography of the positive PMMA photoresist and the lift-off technique. For the characterization the Mueller matrix spectroscopic ellipsometry (MMSE) is used for its zero-impact on the sample and because it provides 16 independent quantities describing changes of polarization states upon reflection (including depolarization effect which is an independent check of the model quality). The presented approach here is based on a well-known change of sensitivity of the optical model parameters at the different azimuthal rotation angle of the structure [1]. The challenge of this work is to combine in one model MMSE data measured with focused probe beam with sample azimuthal rotation. The need of beam focusing is common issue if lateral dimensions of the structure are smaller than spot size and spot size reduction using an iris is not suitable for the light intensity reduction [2]. The presented method includes the beam focusing not only as variation of the incidence angle [3], but it is extended into conical-diffraction configuration with assumption of the incident plane declination from the plane of the sample, which is necessary for description of the depolarization effects in experimental data.

[1] X. Chen, S. Liu, C. Zhang, H. Jiang, Z. Ma, T. Sun, and Z. Xu, *Opt. Express* 22 (2014) 15165-15177.

[2] M. Foldyna, M., Martino, A. D., *Opt. Commun.* 282 (2009) 735–741.

[3] L. Halagačka, K. Postava, M. Vanwolleghem, F. Vaurette, J. Ben-Youssef, B. Dagens, J. Pištora, *J. Opt. Mat. Express* 4, (2014) 1903–191.

## SYNTHESIS AND CHARACTERIZATION OPTICAL PROPERTIES OF $\text{Bi}_4\text{Ti}_3\text{O}_{12}:\text{Er}$ NANOPARTICLES

S. Fuentes<sup>a,c</sup>, P. Muñoz<sup>a</sup> and J. Llanos<sup>b</sup>, I.R. Martín<sup>d</sup>

<sup>a</sup>*Departamento de Ciencias Farmacéuticas, Facultad de Ciencias, Universidad Católica del Norte, Casilla 1280, Antofagasta, Chile, sfuentes@ucn.cl*

<sup>b</sup>*Departamento de Química, Facultad de Ciencias, Universidad Católica del Norte, Casilla 1280, Antofagasta, Chile, jllanos@ucn.cl*

<sup>c</sup>*Center for the Development of Nanoscience and Nanotechnology, CEDENNA, Santiago, Chile.*

<sup>d</sup>*Departamento de Física Fundamental, Experimental, Electrónica y Sistemas, Universidad de La Laguna, 38206 La Laguna, Tenerife, Spain, imartin@ull.edu.es*

Upconversion (UC) materials, which can convert low-energy photons to high-energy photons under continuous-waver near-infra- red (NIR) excitation, have attracted much attention for a wide range of applications, including lasers, optoelectronic devices, color displays, upconversion phosphors, biodetection, and bioimaging [1].

As well known, ferroelectric oxides represent an important class of functional materials exhibiting numerous properties of interest for wide range of applications. Among these oxides, the bismuth titanate ( $\text{Bi}_4\text{Ti}_3\text{O}_{12}$ , BIT) is a member of Aurivillius type layered perovskite oxides with a general formula  $(\text{Bi}_2\text{O}_2) [\text{A}_{m-1}(\text{B})_m\text{O}_{3m+1}]$ . BIT has drawn extensive attention because it is one of the most promising lead-free ferroelectric materials with numerous applications including non-volatile memory, optical memory, electro-optic devices and various types of sensors [2]. In addition, lanthanide element also acts as an important photoluminescence (PL) activator ion which can be used to design luminescent properties of materials [3]. Therefore, it is of interest and significance to study simultaneously the PL and FE properties of Ln-doped BIT from the aspect of development of multi-functional materials. In this work, we will present the results concerning the synthesis of BIT by reaction sol-gel-hydrothermal and their ability of the host matrix, BIT to form solid solutions with the type lanthanide ions  $\text{Er}^{3+}$  and  $\text{Yb}^{3+}$ . The results, obtained by X-ray diffraction show that solid solutions occur throughout the concentration range, from 2 to 8% at. Morphologically, it is possible to observe the formation of nanostructures with strong tendency to form agglomerates.

The results show different morphological and structural features that are dependent on the type of starting reagent and determining their final properties.

[1] C.A. Dearaujo, J. D. Cuchiaro, L.D. McMillan, M.C. Scott, J.F. Scott. Nature 374 (1995) 627.

[2] R. Bokolia, O.P. Thakur, V. K. Rai, S.K. Sharma, K. Sreenivas. Ceramics International 41 (2015) 6055.

[3] T. Wei, C.P. Li, Q.J. Zhou, Y.L. Zou, L.S. Zhang. Materials Letters 118 (2014) 92.

Acknowledgment: The authors acknowledge Conicyt-Chile for financial support (Anillo Grant ACT 1204).

## STRUCTURAL AND PHOTOLUMINESCENCE INVESTIGATION OF Pr<sup>3+</sup>-DOPED Gd<sub>2</sub>O<sub>3</sub> NANOMATERIALS BY SOL-GEL PROCESS

M. Seraiche<sup>a, b</sup>, L. Guerbous<sup>b</sup>

<sup>a</sup> *Department of Materials and Components, Faculty of Physics, USTHB, BP 32 El alia, Bab Ezzouar 16111, Algiers, Algeria. seraiche28@hotmail.fr, mseraiche@usthb.dz*

<sup>b</sup> *Laser Department, Nuclear Techniques Division, Algiers Nuclear Research Center, 02, bd Frantz Fanon, BP 399, Algiers 16000, Algeria. guerbous@yahoo.fr*

Gd<sub>2</sub>O<sub>3</sub>-sesquioxide has been studied many times as the host matrix for rare earth ions for both down-conversion and up-conversion luminescence phenomena, thanks to its interesting physical properties, such as chemical durability, high melting point (2320 °C), thermal stability and its low phonon energy (600 cm<sup>-1</sup>). In addition, it exhibits a high density of Gd<sub>2</sub>O<sub>3</sub> ( $\rho = 7.6$  g/cm<sup>3</sup>), which make it a suitable candidate for RE-doped for X-ray detector scintillators in imaging systems. Moreover, it is well known that the luminescent behavior of all RE-doped phosphors depends on the morphology, size and synthetic route. In this work, we report the results on structural and photoluminescence of Pr<sup>3+</sup>-doped Gd<sub>2</sub>O<sub>3</sub> nanomaterial.

Nano-sized Gd<sub>1-x</sub>Pr<sub>x</sub>O<sub>3</sub> (x=0.5, 1, 2, 4) % mol have been successfully synthesized by sol gel method. X-ray powder diffraction (XRD), FT-IR, steady as well as time-resolved photoluminescence (PL) spectroscopy techniques were employed to characterize the obtained samples. It is found that 0.5 % concentration of Pr<sup>3+</sup> presents the quenching point of emission in Gd<sub>2</sub>O<sub>3</sub> host. Under UV excitation ( $\lambda_{ex}=230$  nm), a number of emission peaks in the red region assigned to <sup>1</sup>D<sub>2</sub>→<sup>3</sup>H<sub>4</sub> intraconfigurational transitions of the Pr<sup>3+</sup>. The luminescence decay curves evolution of Gd<sub>1-x</sub>Pr<sub>x</sub>O<sub>3</sub> monitored by <sup>1</sup>D<sub>2</sub>→<sup>3</sup>H<sub>4</sub> were measured and investigated. In addition, the variation of <sup>1</sup>D<sub>2</sub> lifetime in function of Gd<sub>1-x</sub>Pr<sub>x</sub>O<sub>3</sub> grain size studied and discussed.

## GROWTH AND LUMINESCENCE PROPERTIES OF Ce DOPED LaCl<sub>3</sub>/CaCl<sub>2</sub> EUTECTIC SCINTILLATOR

Kei Kamada<sup>a,b</sup>, Kosuke Hishinuma<sup>c</sup>, Shunsuke Kurosawa<sup>b,c</sup>, Akihiro Yamaji<sup>c</sup>, Yasuhiro Shoji<sup>a,c</sup>, Jan Pejchal<sup>b,d</sup>, Yuji Ohashi<sup>c</sup>, Yuui Yokota<sup>a</sup>, and Akira Yoshikawa<sup>a,b,c</sup>

<sup>a</sup>Tohoku University, New Industry Creation Hatchery Center, Sendai, 980-8579, Japan

<sup>b</sup>C&A corporation, T-Biz, 6-6-10 Aoba, Aramaki, Aoba-ku, Sendai, 80-8579, Japan

<sup>c</sup>Tohoku University, Institute for Material Research, Sendai, 980-8577, Japan

<sup>d</sup>Institute of Physics AS CR, Cukrovarnicka 10, 16253 Prague, Czech Republic

Recently submicron-diameter phase-separated scintillator fibers (PSSFs) were reported and they possessed both the properties of an optical fiber and a radiation-to-light conversion. The PSSFs were fabricated using a directionally solidified eutectic (DSE) system. The DSE systems have been discovered in various materials for many applications. Up to now, CsI/NaCl and GdAlO<sub>3</sub>/Al<sub>2</sub>O<sub>3</sub>[1] have been already reported as PSSFs for high resolution X-ray imaging application. Ce:LaCl<sub>3</sub> has attracted attention due to its high light yield of 50000 photons/MeV and fast decay time of 25ns with enough density of 3.8 g/cm<sup>3</sup> for low energy X-ray detection [2]. In this research, exploration of PSSFs by directional crystal growth method will be reported. In this study, Ce doped LaCl<sub>3</sub>/CaCl<sub>2</sub> eutectics were explored. Crystal growth was performed by Bridgeman (BZ) method at the eutectic point. Investigations of their crystal structure and eutectic phase were performed. Luminescence and scintillation properties were also evaluated.

Ce doped LaCl<sub>3</sub>/CaCl<sub>2</sub> eutectics were grown by the BZ method in a quartz ampoule with 8mm inner diameter. Mixed powder were induced into the ampoule under Ar atmosphere in a glove box. Growth rate was 0.2-1.5 mm/min. Circular samples with 1-mm thickness were obtained from the grown crystal. Fig.1 shows photographs of grown eutectic (a), under UV lump excitation (b) and 1mm thick polished sample along transverse cross-section. The eutectic showed well aligned eutectic structure (Fig.2) and optically transparent (Fig1-c). Grown Ce doped LaCl<sub>3</sub>/CaCl<sub>2</sub> eutectic shows 380 nm emission ascribed to Ce<sup>3+</sup> 4f-5d transition under X-ray excitation. Pulse height spectra of the sample was showed in Fig.3. The light yield was around 1/4 of Ce:Lu<sub>2</sub>SiO<sub>4</sub> (LYSO) standard and 8000 photon/MeV. Scintillation decay time under 662keV gamma-ray was 7ns(5%) 56.8ns(20%) 684ns(74%).

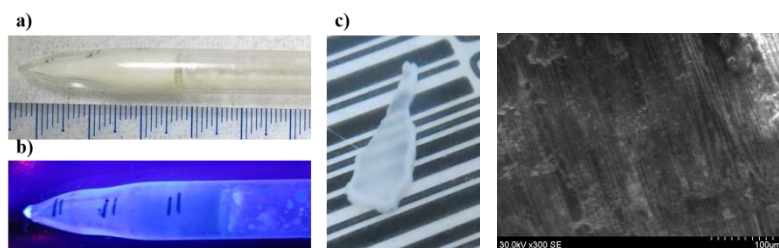


Fig. 1. Photographs of grown eutectic (a), under UV lamp excitation (b) and 1mm thick polished sample along transverse cross-section.

Fig. 2. Back scattered electron image of longitudinal cross-section. (White:LaCl<sub>3</sub>, Black:CaCl<sub>2</sub>)

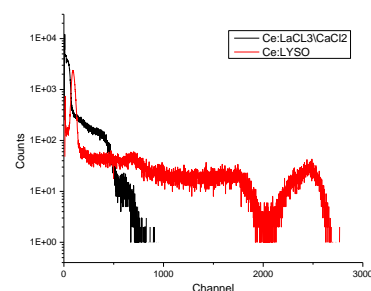


Fig. 3. Pulse height spectra of the grown Ce:LaCl<sub>3</sub>/CaCl<sub>2</sub> eutectic.

[1] Y. Ohashi, et. al., App. Phy. Lett. 102, (2013) 051907.

[2] E. V. D. van Loef et al., Transactions on Nuclear Science, 48 (2001) 341-345.

## PHOTOLUMINESCENCE AND THERMOLUMINESCENCE STUDY ON $\text{Tl}_2\text{Ga}_2\text{S}_3\text{Se}$ LAYERED CRYSTALS

Nizami Hasanli<sup>a</sup>, Mehmet Isik<sup>b</sup>, Serdar Delice<sup>a</sup>

<sup>a</sup>*Dept. of Physics, Middle East Technical University, Ankara, Turkey nizami@metu.edu.tr, sdelice@metu.edu.tr*

<sup>b</sup>*Dept. of Electrical and Electronics Engineering, Atilim University, Ankara, Turkey mehmet.isik@atilim.edu.tr*

Thallium dichalcogenides  $\text{TlBX}_2$  (where B = In or Ga, X = S or Se) compounds have become attractive materials in the optoelectronic applications due to their structural, optical and electrical properties. The quaternary  $\text{Tl}_2\text{Ga}_2\text{S}_3\text{Se}$  compound belonging to layered semiconductor group is a structural analog of  $\text{TlGaS}_2$  in which one quarter of sulfur atoms are replaced by selenium atoms. Photoluminescence (PL) and thermoluminescence (TL) are two basic methods to get information about the energy levels created due to the presence of defects. In this work, we report the results of analysis of PL and TL measurements performed on  $\text{Tl}_2\text{Ga}_2\text{S}_3\text{Se}$  crystals in the temperature ranges of 10–300 K and 10–770 K, respectively. The PL emission band spectra of  $\text{Tl}_2\text{Ga}_2\text{S}_3\text{Se}$  crystals have been studied in the temperature range 10–60 K and in the wavelength region 505–605 nm. A broad band centered at 550 nm (2.25 eV) was observed at  $T = 10$  K. Variation of emission band has been studied as a function of excitation laser intensity in the  $L = 0.3$ –41.5  $\text{mWcm}^{-2}$  range. Radiative transitions from the shallow donor level  $E_d = 0.01$  eV to the moderately deep acceptor level  $E_a = 0.16$  eV were suggested to be responsible for the observed PL band. TL experiments were carried out in the 10–300 K and 290–770 K temperature ranges using home-made and industrial set-ups, respectively. The characterization of trapping centers was accomplished using curve fit method. One trapping center at 16 meV was revealed from the analysis of TL glow curve obtained in the below room temperature region. Two TL peaks nearly at ~373 and 478 K were observed in the above room temperature region. Activation energies of the trapping centers associated with these peaks were calculated as 780 and 950 meV.

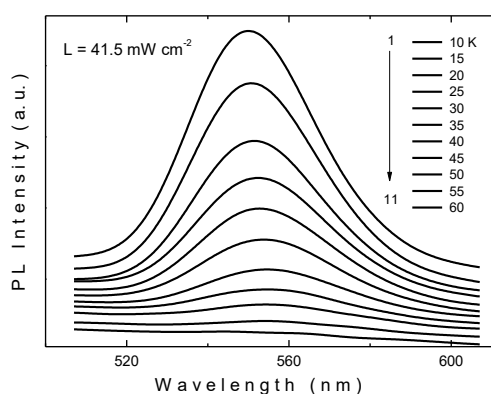


Fig. 1. Temperature dependence of PL spectra from  $\text{Tl}_2\text{Ga}_2\text{S}_3\text{Se}$  crystal.

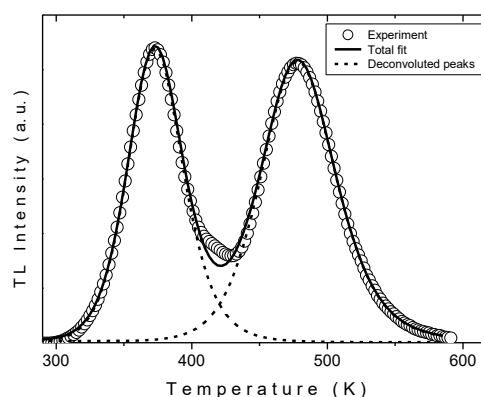


Fig. 2. Above room temperature TL curve of  $\text{Tl}_2\text{Ga}_2\text{S}_3\text{Se}$  crystal and results of curve fit analysis.

## GROWTH AND SPECTROSCOPIC CHARACTERIZATION OF YbF<sub>3</sub> DOPED BaF<sub>2</sub> CRYSTALS

Marius Stef<sup>a</sup>, Irina Nicoara<sup>a</sup>

<sup>a</sup>*West University of Timisoara, Faculty of Physics, Blvd. V. Parvan 4, Timisoara 300223, Romania, marius.stef@e-uvt.ro*

Recently [1-4] it has been shown that MF<sub>2</sub> (M=Ca, Ba, Sr) crystals are efficient laser host for trivalent RE (rare earth) ions. By doping MF<sub>2</sub> crystalline host with YbF<sub>3</sub>, both Yb<sup>2+</sup> and Yb<sup>3+</sup> ions will coexist in the crystal; Yb<sup>3+</sup> ions are responsible for emission in near IR [3,4] spectral domain and Yb<sup>2+</sup> ions are responsible for the emission in UV and VIS domain [5,6]. The properties of the YbF<sub>3</sub> doped MF<sub>2</sub> crystals are strongly dependent on the quality of the crystals and on the YbF<sub>3</sub> concentration. The change of valence can be attained by baking the crystals in a suitable atmosphere [7,8], by electrolytic coloration or exposing them to ionizing radiation [7,9]. The properties of Yb<sup>2+</sup> ions have been less investigated than the properties of the trivalent Yb.

In this work we report the growth and optical characterization of YbF<sub>3</sub>-doped BaF<sub>2</sub> crystals with high divalent Yb ions concentration obtained without any other treatment. Me<sub>1-x</sub>Yb<sub>x</sub>F<sub>2-x</sub> ( $x = 0.0007$  and  $0.017$ ) crystals have been grown using the conventional Bridgman technique [10]. In order to obtain high Yb<sup>3+</sup>→Yb<sup>2+</sup> conversion a special procedure has been developed. The optical absorption spectra of the crystals exhibit intense UV absorption bands, characteristic for divalent Yb ions. It is known that the optical properties of the crystals depend on the relative Yb<sup>2+,3+</sup> and F<sup>-</sup> ions sites in the lattice. The Yb<sup>3+</sup> ions substitute for Ba<sup>2+</sup> ions in the lattice and need charge compensation obtained by an interstitial fluoride ion located in various sites giving rise to a rich multisite structure, which leads to broad absorption and emission bands. The Yb<sup>2+</sup> ions substitute for Ba<sup>2+</sup> ions, do not need charge compensation and possess cubic symmetry. Preliminary luminescence studies reveal a strong concentration dependence of the near UV emission bands. For the first time we studied the emission spectra of the BaF<sub>2</sub> crystals exciting in all absorption bands.

- [1] C. Labbe, J.L. Doualan, P. Camy, R. Moncorgé, and M. Thuau, *Opt. Commun.* 209 (2002) 193-196.
- [2] P. Camy, J.L. Doualan, S. Renard, A. Braud, V. Ménard, and R. Moncorgé, *Opt. Commun.* 236 (2004) 395-398.
- [3] V. Petit, P. Camy, J.L. Doualan, and R. Moncorgé, *Appl. Phys. Lett.* 88 (2006) 051111.
- [4] J. L. Doualan et al. *Laser Physics* 20 (2010) 533-536.
- [5] J. Rubio, *J. Phys. Chem. Solids* 52 (1991)101.
- [6] I. Nicoara, L. Lighezan, M. Enculescu, I. Enculescu, *J. Cryst. Growth* 310 (2007) 2026-2029.
- [7] S. M. Kaczmarek et al. *J. Phys.: Condens. Mater.* 17 (2005) 3771-3774,
- [8] A.S. Shcheulin, A.E. Angervaks, T.S. Semenova, L.F. Koryakina, M.A. Petrova, P.P. Fedorov, V.M. Reiterov, E.A. Garibin, A.I. Ryskin, *Appl. Phys. B* 111 (2013) 551-557.
- [9] D. S. McClure and Z. Kiss, *J. Chem. Phys.* 39 (1963) 3251.
- [10] D. Nicoara and I. Nicoara, *Mater. Science and Eng. A* 102 (1988) L1.

## HALOGEN-FREE IMMERSION FOR OPTICAL ELEMENTS WITH HIGH REFRACTIVE INDEX

Valery M. Volynkin<sup>a</sup>, Yury A. Gatchin<sup>b</sup>, Konstantin V. Dukelskiy<sup>b,c</sup>, Sergey K. Evstropiev<sup>a,b</sup>,  
Anatoly G. Korobeynikov<sup>b</sup>

<sup>a</sup>JVC "Vavilov State Optical Institute", Saint-Petersburg, Kadetskaya linya, 12, Russia.

<sup>b</sup>National Research University of Information Technologies, Mechanics and Optics, Saint-Petersburg, Kronversky pr., 49, Russia.

<sup>c</sup>The Bonch-Bruевич Saint-Petersburg State University of Telecommunications, Saint Petersburg, Moika 61, Russia.

Control and rejection of optical elements include the control of homogeneity of internal areas of the material and the presence of different technological defects (bubbles, inclusions, etc). Usually for this operation different immersion liquids are used. Many traditional immersion liquids having high refractive index contain halogen-organic compounds which are toxic and smelly. Therefore, the development of non-toxic immersion with high refractive index is actual problem, especially for modern large-size optical elements.

To solve these problems new non-toxic immersion liquid has been developed. New immersion contains non-toxic aromatic organic compounds having high refractive index and providing the possibility of formation of stable thin transparent layer on the surface of tested optical element. Formation of this layer allows avoiding the use big amounts immersions at the control of large-size optical elements.

The main component of the immersion is meta-bis (meta phenoxyphenoxy) benzene. Special additives (up to 6 wt/%) (2-naphtol and dibutyl sebacate) are applied for the modification of viscosity and surface tension of the immersion. New immersion is transparent in visible spectral range, has refractive index  $n_D > 1,6$  and dynamic viscosity 3400-3600 cP. New liquid has high adhesion to different modern optical materials having high refractive index (sapphire, garnet, etc.).

The using of new immersion allows to control the homogeneity of optical materials and to find the presence of technological defects (inclusions, bubbles, etc.). Control of optical elements can be performed by their immersion into the new liquid, or by formation of immersion layer on the surface of element by brushing or spraying of this liquid. After measurements the residual parts of the immersion can be easily removed from the surface of optical elements by using organic solvents.

Fig.1 demonstrates the effect of application of new immersion for the control laser garnet crystal. The test sample was cut from single-crystal body by diamond tool (Fig.1a). Formation of immersion layer allows controlling the quality of the crystal (Fig.1b). This photo clearly shows the presence of some inhomogeneities and internal stresses in the structure of tested material.

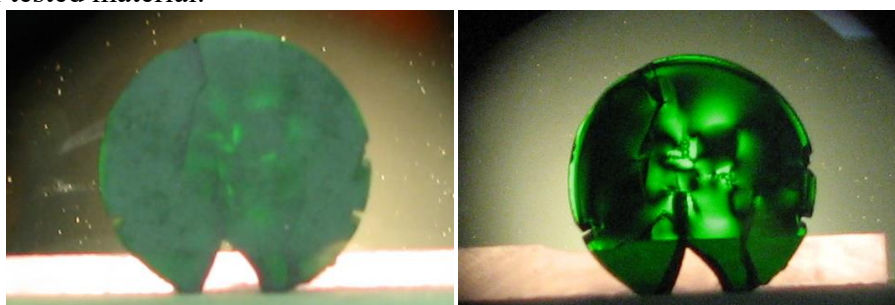


Fig. 1. Photo of the cut Ga-Sc-Gd garnet crystal without (a) and with (b)

## HIGH SENSITIVE POLYMER MEDIUMS FOR OPTICAL GAS SENSORS

Bohdan R. Tsizh B.<sup>a,c)</sup>, Olena I. Aksimentyeva O.<sup>b)</sup>

<sup>a)</sup>*Kazimierz Wielki University in Bydgoszcz, 30 Chodkiewicza, Bydgoszcz, Poland  
tsizhb@ukw.edu.pl,*

<sup>b)</sup>*Ivan Franko National University of Lviv, 6 Kyryla-Mefodia, Lviv, Ukraine,  
aksimen@ukr.net*

<sup>c)</sup>*Stepan Gzytsky Lviv Natoinal University of Veterinary Medicine and Biotechnologies  
50 Pekarska, Lviv, Ukraine*

Optical sensor systems and individual gas sensors now are successfully used for monitoring gas in the industrial atmospheres, transportation, home, for operational monitoring of ecological environment, quality of food and other purposes [1]. However, despite the successful development of such devices, there is a need for simple, reliable and cheap sensors of ammonia, acetone, ethanol and other gases. Organic materials are increasingly used to create sensitive elements. The most promising among them are conductive polymer films due to their high adaptability, simplicity of synthesis and use, lower cost and better performance parameters. The most significant changes of optical absorption of polyaniline (PANI) films under ammonia influence occur in the spectral range of 500...700 nm due to the optical absorption in the conjugated system of polyaminoarenes [2]. A gas sensitivity of the film is defined exactly by this spectral range, so the expansion of the spectral sensitivity will lead to an increase of performance of gas sensors. For this purpose we propose additionally with PANI to use a thin film of poly-3,4-ethylenedioxythiophene (PEDOT) for which maximal changes of optical absorption under ammonia are observed in the spectral range of  $\lambda=350...550$  nm. To create a high sensitive element we investigated the thin film structure with alternately deposited layers of PANI and PEDOT and the thin films deposited from solution of monomer mixture (1:1). It was studied the effect of ammonia on the optical absorption of mentioned films. The optical spectra showed that the bilayer film structure of PANI/PEDOT, and the films based on mixtures of PANI + PEDOT are sensitive to ammonia in a wide spectral range from 350 to 850 nm. Changes in optical absorption under influence of ammonia for PANI/PEDOT structure are more significant as for films based on mixtures, especially for spectral range of  $\lambda > 500$  nm. Increase of integrated optical absorption for PANI/PEDOT bilayer may be explained by the superposition of sensitivity to ammonia of individual films: PANI film in the 470...700 nm and of PEDOT films in the 350...550 nm which occurs in the bilayer structure PANI /PEDOT. Spectral dependence of optical absorption allows doing more detailed comparative analysis of different types of gas sensitive elements. It has found that the change in optical absorption under the action of ammonia for film structure PANI/PEDOT is much larger than similar changes in individual PANI or PEDOT films. For quantitative estimation of integral spectral changes of optical absorption it was evaluated and compared a relation of areas  $S_2/S_1$  under the corresponding spectra. Since changes in the optical absorption is the main indicator of sensitivity, spectral dependence  $\Delta D(\lambda)$  is a kind of coefficient spectral sensitivity. In spectral region of 400...750 nm it was evaluated the relation of areas is  $S_2/S_1 = 1.45$  that gives reason to believe that using film structures PANI/PEDOT as gas sensitive elements increases the sensitivity of ammonia gas sensors.

[1] B.R. Tsizh, M.I. Chokhan', O.I. Aksimentyeva, D.O. Poliovyi, MCLC, 497 (2008) 254–260.

[2] B. R. Tsizh, O.I. Aksimentyeva, Ya. I. Vertsimakha, P.Lutsyk, M.Chokhan, MCLC, 589 (2014) 116 – 123.



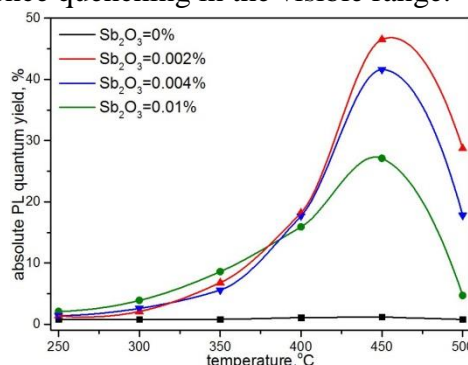
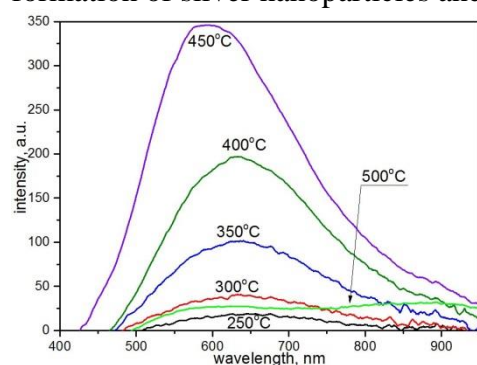
## HIGH-EFFICIENT LUMINESCENCE OF SILVER CLUSTERS IN SODIUM-ZINC-ALIMINOSILICATE GLASSES DOPED WITH ANTIMONY OXIDE

Yevgeniy Sgibnev, Nikolay Nikonorov, Alexander Ignatiev  
ITMO University, 4 Birzhevaya line, St. Petersburg, Russia, sgibnev@gmail.com

Silver molecular clusters (SMCs) in glass have a broadband and intensive luminescence in the visible range [1, 2]. Currently glasses with SMCs are attractive materials for many photonics applications: phosphors for white LEDs, luminescent waveguides, luminescent sensors, down-converters for solar cells, etc. SMCs in glass host can be formed by high temperature synthesis or low temperature ion exchange (IE) [3]. IE is more attractive because it is low cost, flexible and effective method that allows getting high concentration of silver ions on the glass surface.

The goal of this work was research the influence of antimony ions on the luminescent properties of SMCs in sodium-zinc-aluminosilicate glasses. The glasses doped with different quantity of antimony oxide ( $\text{Sb}_2\text{O}_3 = 0\%$ , 0.002%, 0.004% and 0.01% mol) were investigated. Silver ions were introduced in the glass by immersing the samples in a bath with mixture of silver and sodium nitrates (5%  $\text{AgNO}_3/95\%$   $\text{NaNO}_3$  molar) at 320°C for 15 minutes. SMCs were prepared by subsequent thermal treatment (TT) at temperature in the range between 250°C and 500°C for 1-3 hours. Absorption and luminescence spectra were recorded at each step of the experiment with double-beam spectrophotometer Lambda 650 (Perkin Elmer) and absolute photoluminescence quantum yield (QY) measurement system (Hamamatsu), respectively.

Antimony ions play a role of reducing agents for silver ions during the IE and TT processes. However, active reducing process starts only at temperature 350°C or higher. QY grows from 1.5% to 46.5% for glass samples ( $\text{Sb}_2\text{O}_3 = 0.002\%$  mol) as-exchanged and subsequent treated at  $T=450^\circ\text{C}$  for 3 h, respectively. Thermal treatment at  $T=500^\circ\text{C}$  ( $T_g=465^\circ\text{C}$ ) leads to formation of silver nanoparticles and luminescence quenching in the visible range.



PL spectra ( $\lambda_{\text{ex}}=365$  nm) for glass doped with  $\text{Sb}_2\text{O}_3 = 0, 0.002\%$  mol after IE and TT during 3h.

Absolute PL quantum yield dependence on the temperature of subsequent TT for 3h.

As a result, optimal concentration of antimony oxide and treatment conditions for formation of high-efficient SMC's luminescence in the sodium-zinc-aluminosilicate glass have been found. The glass with SMCs can be successfully use as a down-converter for solar cells and phosphor for white LEDs.

[1] Dubrovin V.D., Ignatiev A.I., Nikonorov N.V., Sidorov A.I., Shakhverdov T.A., Agafonova D.S., Opt. Mat. 36 (2014) 753–759.

[2] A.S. Kuznetsov, V.K. Tikhomirov, V.V. Moshchalkov, Opt. Exp. 19 (2012) 21576-21582

[3] A. Tervonen, B. R. West, S. K. Honkanen, Opt. Eng. 50 (2011) 071107.

## **HYBRID MATERIAL ORGANIC-INORGANIC WITH LUMINESCENCE PROPERTIES AND BIOMEDICAL APPLICATIONS**

Adina Segneanu, Daniel Damian, Cristian Vaszilcsin, Paulina Vlazan, Ioan Grozescu  
*National Research Institute for Electrochemistry and Condensed Matter, Plautius  
Andronescu no. 1, Timis, oara 300224, Romania*

The paper study the synthesis and characterisation of an new organic-inorganic hybrid material for biomedical applications. For the synthesis of hybrid material was selected capsaicine an which was functionalized magnetic component, nanoparticles of ferrite. The morfo-structural and luminescence properties of hybrid material were investigate by advanced microscopy and spectroscopic techniques.

## IMPROVED LUMINESCENCE AND SCINTILLATION PROPERTIES OF MULTICOMPONENT GARNET SCINTILLATORS

Miroslav Kucera<sup>a</sup>, Zuzana Onderisinova<sup>a</sup>, Martin Hanus<sup>a</sup>, Ondrej Lalinsky<sup>b</sup>, Jiri A. Mares<sup>c</sup>,  
Martin Nikl<sup>c</sup>

<sup>a</sup> Charles University, Fac. Math. & Physics, 12116 Prague, Czech Rep.,  
kucera@karlov.mff.cuni.cz

<sup>b</sup> Institute of Scientific Instruments, ASCR, 61264 Brno, Czech Republic

<sup>c</sup> Institute of Physics, ASCR, 16000 Prague, Czech Republic

Scintillation properties were studied in multicomponent (GdLu)<sub>3</sub>(GaAl)<sub>5</sub>O<sub>12</sub>:Ce garnet scintillators. The impact of shallow traps on the light yield and timing characteristics were examined using the decay kinetic techniques under e-beam and alpha-particle excitations. Technological breakthrough in the liquid phase epitaxy enabled to grow high purity single crystalline films from BaO-B<sub>2</sub>O<sub>3</sub>-BaF<sub>2</sub> flux with special emphasis on elimination of potential impurities.

The photoelectron yield of Gd, Ga admixed LuAG:Ce epitaxial films with optimized composition approaches that of the best bulk GGAG:Ce single crystals measured so far. Furthermore, the films had excellent timing characteristics: the prompt Ce<sup>3+</sup> (5d-4f) component in the scintillation decay (under alpha-particle or e-beam excitation) was 50-80 ns and very weak slow decay components and afterglow were observed. Cathodoluminescence decay kinetics measured in nano- and milisecond time ranges [1] suggests that the trap centers, which are responsible for “slow light” in the scintillation signal, are completely suppressed in heavily Gd, Ga doped samples. The energy transfer processes involving trap states are thus eliminated and the dominant part of scintillation response is due to the prompt recombination of electrons and holes at the Ce<sup>3+</sup> emission centers. The presented results clearly show that comparable scintillation performance of epitaxial films with that of Czochralski grown bulk crystals can be indeed achieved.

[1] M. Kucera, Z. Onderisinova, J. Bok, et al., J. Lumin., doi:10.1016/j.jlumin.2015.01.034 (2015).

## STRENGTHENING OF QUARTZ CERAMIC MATERIALS FOR OPTICAL AND LASER GLASS MELTING

Yury A. Gatchin<sup>b</sup>, Konstantin V. Dukelskiy<sup>b,c</sup>, Sergey K. Evstropiev<sup>a,b</sup>, Anatoly G. Korobeynikov<sup>b</sup>, Valery M. Volynkin<sup>a</sup>, Alexander V. Shashkin<sup>a</sup>

<sup>a</sup>JVC "Vavilov State Optical Institute", Saint-Petersburg, Kadetskaya linya, 12, Russia.

<sup>b</sup>National Research University of Information Technologies, Mechanics and Optics, Saint Petersburg, Kronversky pr., 49, Russia.

<sup>c</sup>The Bonch-Bruевич Saint-Petersburg State University of Telecommunications, Saint Petersburg, Moika 61, Russia.

To achieve modern high optical and luminescent properties of laser and optical glasses it's necessary to provide very low level of the impurities in glass composition. Traditionally, platinum crucibles and stirrers are used for melting of some types of optical and laser glasses. But high-temperature solubility of platinum in melt leads to formation of the absorbing impurities in glasses. Therefore the development of ceramic refractory materials, which can be used in glass melting instead of platinum, is actual problem.

Quartz ceramics is well-known refractory material used in glass technology. Application this material for large-size (100 liters and more) crucibles and stirrers requires his additional strengthening.

The strengthening method is based on the impregnation of porous ceramics by special colloidal solution at room temperature with followed drying and thermal treatment of the material. Initial samples were prepared by slip casting in gypsum molds, had size 65x8x8 mm and their porosity was about 25%. Composite colloidal solutions containing tetraethyl orthosilicate ( $\text{Si}(\text{OC}_2\text{H}_5)_4$ , propanol-2, water and aluminum nitrate were used for impregnation of porous ceramics. Volatile components were removed from impregnated materials during drying. Thermal treatment of the samples led to the decomposition of aluminum nitrate and to the formation of bonding chains of colloidal silica particles inside ceramic body.

Measurements of bending strength of ceramic samples showed that significant strengthening effect was observed after impregnation even before thermal treatment. Thermal treatment additionally increased the strength of impregnated samples. Fig.1 demonstrates the influence of the temperature of thermal treatment on bending strength of ceramic samples. Experimental results showed that new strengthening method allows increasing the mechanical strength of quartz ceramic samples (+200 %).

The structure of the surface and internal areas of ceramic materials was investigated by SEM method. The results of SEM investigations demonstrated the formation of some chains of silica nanoparticles that additionally bonded together ceramic particles.

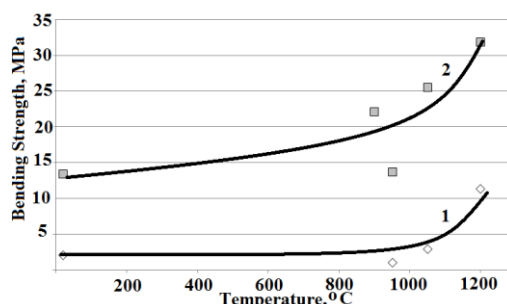


Fig.1 Influence of temperature of thermal treatment on the bending strength of traditional ceramics (curve 1) and strengthened ceramics (curve 2).

## INFLUENCE OF MO/MF<sub>2</sub> MODIFIERS (M = Ca, Sr, Ba) ON SPECTROSCOPIC PROPERTIES OF Eu<sup>3+</sup> IONS IN GERMANATE AND BORATE GLASSES

Lidia Żur<sup>a</sup>, Joanna Janek<sup>a</sup>, Marta Sołtys<sup>a</sup>, Joanna Pisarska<sup>a</sup>, Wojciech A. Pisarski<sup>a</sup>

<sup>a</sup> *Institute of Chemistry, University of Silesia, Katowice, Poland*

Corresponding author: *lidia.zur@us.edu.pl*

In recent years PbO/PbF<sub>2</sub> or CdO/CdF<sub>2</sub> are used as a heavy metal glass components [1], but they are rather prohibited to use in manufacturing due to environment protecting. They have been designated as toxic substances, and consequently they are being eliminated from various applications due to their hazardous effect on health and environment. Alternatively, Pb- and Cd-free glasses were proposed for potential applications in photonics [2]. On the other hand, PbO/PbF<sub>2</sub> or CdO/CdF<sub>2</sub> components were established to play important role in glass formation and further strengthening of glass host network [3].

In our work, Eu<sup>3+</sup>-doped lead-free oxyfluoride germanate and borate glasses were synthesized. The MO glass modifiers (M = Ca, Sr or Ba) were partially or totally substituted by MF<sub>2</sub> in chemical composition. In contrast to samples modified by CaO/CaF<sub>2</sub> or SrO/SrF<sub>2</sub>, the germanate glass samples containing BaO and/or BaF<sub>2</sub> are fully amorphous, while the lead-free borate glasses are fully amorphous, independently from glass modifiers. The luminescence spectra for Eu<sup>3+</sup> ions in lead-free glasses with different BaF<sub>2</sub> content were detected. The ratio of integrated luminescence intensity of the <sup>5</sup>D<sub>0</sub> - <sup>7</sup>F<sub>2</sub> transition to that of the <sup>5</sup>D<sub>0</sub> - <sup>7</sup>F<sub>1</sub> transition (R/O factor), is relative to the strength of covalent/ionic bonding between the Eu<sup>3+</sup> ion and the surrounding ligands. The observed decrease in R/O value with increasing BaF<sub>2</sub> content is due to reduction asymmetry and degree of covalency between Eu<sup>3+</sup> ions and the nearest surroundings. Moreover, the luminescence decay curves were collected and the luminescence lifetimes of <sup>5</sup>D<sub>0</sub> excited state of Eu<sup>3+</sup> ions were determined in function of BaF<sub>2</sub> concentration. The same procedure has been applied to lead-free borate glasses containing CaF<sub>2</sub> and SrF<sub>2</sub> modifiers.

[1] C.R. Kesavulu, K. Kiran Kumar, N. Vijaya, Ki-Soo Lim, C.K. Jayasankar, Mater. Chem. Phys. 141 (2013) 903-911.

[2] H. Lin, E.Y.B. Pun, B.J. Chen, Y.Y. Zhang, J. Appl. Phys. 103 (2008) 056103.

[3] G. Sharma, R. Bagga, N. Mahendru, M. Falconieri, V.G. Achanta, A. Goel, S.N. Rasool, N. Vijaya, J. Lumin. 159 (2015) 38.

## INFLUENCE OF REACTION MEDIUM ON THE MORPHO-STRUCTURAL PROPERTIES OF KNbO<sub>3</sub> POWDERS

P. Vlazan<sup>a</sup>, M. Poienar<sup>a</sup>, M. Stoia<sup>b</sup>, P. Sfirloaga<sup>a</sup>

<sup>a</sup>*National Research Institute for Electrochemistry and Condensed Matter, Plautius Andronescu no. 1, Timisoara 300224, Romania*

<sup>b</sup>*“Politehnica” University of Timisoara, Faculty of Industrial Chemistry and Environmental Engineering, P-ta Victoriei no. 2, Timisoara 300006, Romania*

Ferroelectric nanostructures have attracted much attention recently due to the ongoing demand for miniaturization of devices and discover new phenomena. One of the materials studied intensively in recent years is potassium niobate with perovskite structure is a promising material for electro-optic, nonlinear optical, and photorefractive applications. The synthesis of inorganic nanocrystals with controlled size and shape and the understanding of finite size effects are currently important issues in materials chemistry [1-3].

In this paper we have successfully synthesized KNbO<sub>3</sub> powders by sol-gel and solvothermal method. Particle size, morpho-structural properties of the KNbO<sub>3</sub> materials were investigated by X-ray diffraction (XRD), scanning electron microscopy (SEM), UV-Vis and FTIR spectroscopy.

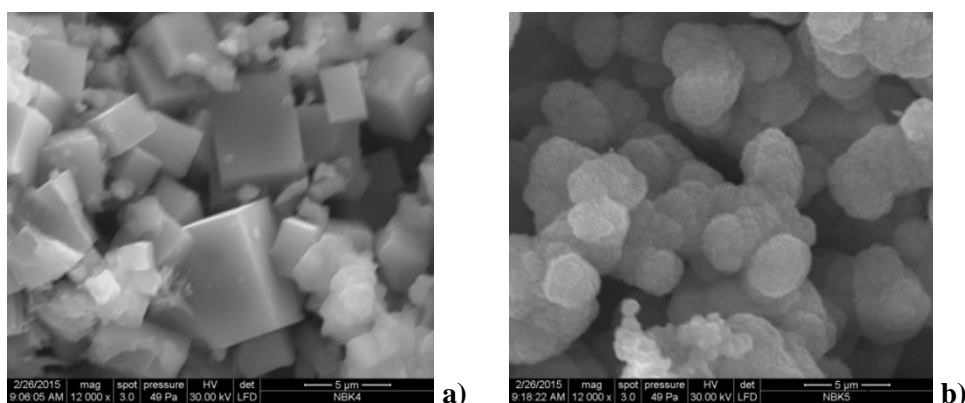


**Figure 1.** SEM images of KNbO<sub>3</sub> obtained by sol-gel (a) and solvothermal method (b)

The morphology of the particles is difference among two structure types depending on the reaction medium and obtaining method. Thus, through sol-gel method have been obtained particle with cubic structure (Figure 1a) and by solvothermal method the particles are spherical shapes, agglomerated in asymmetrical formations (Figure 1b).

**Acknowledgement:** The authors wish to acknowledge the financial support of Partnerships Program - (PCCA 2013) – Project nr. 177/2014.

[1] Haiyan Ge, Yuanye Huang, Yudong Hou, Han Xiao and Mankang Zhu , *RSC Advanced*, 2014, 4, 23344-23350.

[2] Guozhong Wang, Sverre Magnus Selbach, Yingda Yu, Xitian Zhang, Tor Grande and Mari-Ann Einarsrud, *Crst.Eng.Comm.*, 2009,11, 1958-1963.

[3] Gregory K.L. Goh, Fred F. Lange, Sossina M. Haile, Carlos G. Levi, *J. Mater. Res.*, 18, 2003, 338-345.

## **INFLUENCE OF RESTORATIVE PROCEDURES ON ENDODONTICALLY TREATED PREMOLARS: FINITE ELEMENT ANALYSIS OF A CT-SCAN BASED MATHEMATICAL MODEL**

Tatjana Maravić<sup>a</sup>, Darko Vasiljević<sup>b</sup>, Ivana Kantardžić<sup>a</sup>, Tijana Lainović<sup>a</sup>, Ognjan Lužanin<sup>c</sup>  
and Larisa Blažić<sup>d</sup>

<sup>a</sup>*Faculty of Medicine, School of Dentistry, University of Novi Sad, 3 Hajduk Veljkova, Novi Sad, Serbia, vukadinov.tatjana@gmail.com, ivanakantardzic@gmail.com, tijana.lainovic@gmail.com*

<sup>b</sup>*Institute of Physics, University of Belgrade, 118 Pregrevica, Belgrade, Serbia, darko@ipb.ac.rs*

<sup>c</sup>*Faculty of Technical Sciences, Department of Production Engineering, University of Novi Sad, 6 Trg Dositeja Obradovića, Novi Sad, Serbia, luzanin@uns.ac.rs*

<sup>d</sup>*Faculty of Medicine, School of Dentistry, Clinic of Dentistry of Vojvodina, University of Novi Sad, 12 Hajduk Veljkova, Novi Sad, Serbia, larisa.blazic@gmail.com*

In every-day dental practice, an endodontically treated tooth with mesio-occluso-distal (MOD) cavity is usually restored with composite resin. The restorations of these biomechanically weakened teeth are often of limited durability [1]. Thus, additional procedures, such as the inclusion of palatal and buccal cusp into the cavity (MODP, MODPB), and/or fiber-reinforced composite (FRC) posts, are used in an attempt to improve the prognosis of the tooth and the restoration [2,3]. The aim of this study was to determine whether these procedures are beneficial, or the removal of healthy dental tissues during these procedures has a negative effect. Finite element analysis (FEA) has emerged in recent decades as a valid method of research in biomedical sciences due to ethical issues and complexity of factors that influence “in vivo” experimental studies.

In order to make a highly accurate three-dimensional tooth model, a precise medical imaging technique (Computerized Tomography-CT) was used in this study. Based on CT scans of an extracted maxillary second premolar, six tooth models (MOD, MODP, MODPB, MOD+FRC, MODP+FRC, MODPB+FRC) were created in SolidWorks 2014 software (Dassault Systemes SolidWorks Corp, USA). Each model was subjected to a summary force of 150 N on the occlusal surface simulating the natural biting pattern and maximal von Mises stresses were calculated using FEA.

In the presented study, the von Mises stresses in dental tissues (especially enamel), showed lower values in MODP and MODPB preparations, regardless of the use of FRC. MOD+FRC model showed lower stresses in the enamel compared to MOD, and FRC seems to have switched some of the stresses from dental tissues to the composite filling.

### Acknowledgement

Supported by the Serbian Ministry of Education and Science, contract No. III45016 and TR035020.

[1] C.L. Lin, Y.H. Chang, P.R. Liu. *J. Dent.* 36 (2008) 194-203.

[2] K. Kainose, M. Nakajima, R. Foxton, N. Wakabayashi, J. Tagami. *Int. Endod. J.* (2014) doi:10.1111/iej.12397.

[3] I. Kantardzic, D. Vasiljevic, L. Blazic, O. Luzanin. *Croat. Med. J.* 53 (2012) 568-576.

## INFLUENCE OF SYNTHESIS, THERMAL TREATMENT, AND ELECTRON IRRADIATION CONDITIONS ON THE FORMATION OF BISMUTH CENTERS IN BARIUM FLUORIDE CRYSTAL

O.K. Alimov, M.E. Doroshenko, V.A. Konyushkin, V.V. Osiko.

*A.M. Prokhorov General Physics Institute RAS, Vavilov Str. 38, Moscow, Russia.*

*e-mail: olim@lst.gpi.ru*

The spectral and kinetic characteristics of bismuth ions in  $\text{BaF}_2:\text{BiF}_3$  and  $\text{BaF}_2:\text{Bi}_2\text{O}_3$  crystals synthesized by the Bridgman–Stockbarger method are studied. The influence of annealing (in  $\text{HF}^-$  and  $\text{O}_2$  atmospheres) and electron irradiation on the formation of bismuth centers in barium fluoride crystals is considered.

The time-resolved luminescence spectra of bismuth ions in  $\text{BaF}_2:\text{BiF}_3$  and  $\text{BaF}_2:\text{Bi}_2\text{O}_3$  crystals measured at  $T = 300\text{K}$  and two excitation wavelengths ( $\lambda_{\text{exc}} = 337$  and  $532$  nm) showed that the luminescence of  $\text{Bi}^{3+}$  ions in  $\text{BaF}_2:\text{BiF}_3$  crystals is observed only in the visible spectral range  $350\text{--}550$  nm (Fig. 1a, curve 1), while the luminescence of a  $\text{BaF}_2:\text{Bi}_2\text{O}_3$  crystal occurs in the range  $600\text{--}1000$  nm (curve 2).

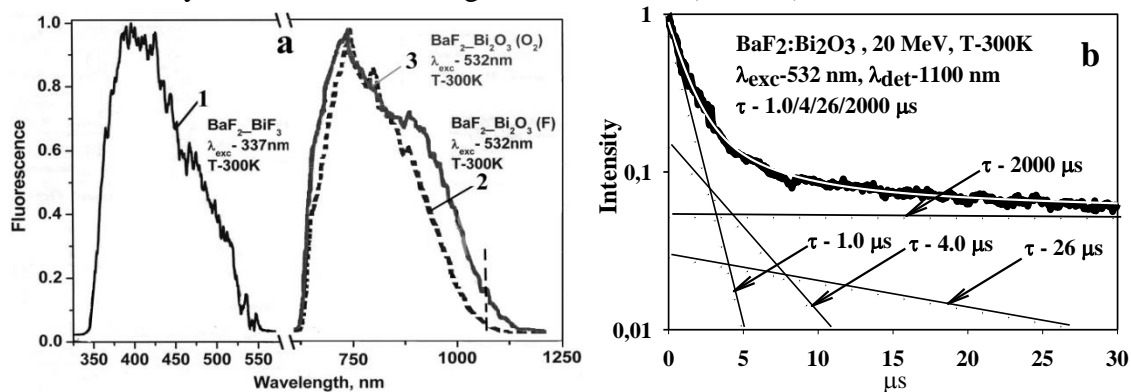


Fig. 1. Luminescence spectra (a) and luminescence decay kinetics (b) of bismuth ions in  $\text{BaF}_2:\text{BiF}_3$  and  $\text{BaF}_2:\text{Bi}_2\text{O}_3$  crystals measured at  $T = 300\text{K}$ .

Annealing of  $\text{BaF}_2:\text{Bi}_2\text{O}_3$  crystals in an  $\text{O}_2$  atmosphere increases the luminescence intensity of bismuth ions in the spectral region of  $1100$  nm (Fig. 1a, curve 3) compared to the luminescence of a  $\text{BaF}_2:\text{Bi}_2\text{O}_3$  crystal annealed in a fluorinating atmosphere.

The luminescence of bismuth ions in a  $\text{BaF}_2:\text{Bi}_2\text{O}_3$  crystal annealed in a fluorinating atmosphere and irradiated by  $150\text{-keV}$  electrons was observed in the spectral range  $600\text{--}1200$  nm, while an increase in the electron energy to  $20\text{-MeV}$  leads to the appearance of additional luminescence bands in the range  $1200\text{--}1800$  nm. The luminescence decay kinetics of bismuth ions has a complex character (Fig. 1b) and depends on the recording ( $670, 730, 790, 1100$  nm) and excitation wavelengths. As follows from Fig. 1b, the luminescence decay kinetics recorded at a wavelength of  $1100$  nm consist of three components with relatively short lifetimes  $\tau = 1.0, 4.0,$  and  $26$  ns and one long component with  $\tau = 2.0$  ms. Such a variety of lifetimes points to a complex structure of the bismuth luminescence band at  $1100$  nm, which is obviously formed by four different types of optical centers. The luminescence bands of bismuth ions in the range  $1200\text{--}1800$  nm probably belong to other optical centers-complexes of radiation defects with closely spaced bismuth ions, which are formed as a result of irradiation by high-energy electrons.



## **INFLUENCE OF Yb<sup>3+</sup> ION CO-DOPING ON ZnO:X (X=Eu<sup>3+</sup>, Er<sup>3+</sup>, Ho<sup>3+</sup>) PROPERTIES**

Lidija V. Trandafilović, Dragana Jovanović, Miroslav D. Dramićanin  
*Vinča Institute of Nuclear Sciences, Belgrade, Serbia, lidija@vinca.rs*

Zinc-oxide (ZnO) is a low-cost material, easily manufactured in various morphologies, has a wide bandgap (3.2-3.4 eV) and large exciton binding energy of 60 meV at room temperature [1]. Due to the presence of defects in the lattice (oxygen vacancies and interstitial zinc) ZnO is a n-type semiconductor [2]. As such, ZnO is a unique host material for lanthanide ions doping. Influence of different molar ratios of lanthanide ions (Eu<sup>3+</sup>, Er<sup>3+</sup>, Ho<sup>3+</sup>) on ZnO matrix characteristics was studied. Emission enhancement was done through Yb<sup>3+</sup> ions co-doping. The prepared samples were characterized using X-ray diffraction (XRD), UV-vis and photoluminescence spectroscopy. Photocatalytic efficiency was studied and result showed system improvement through lanthanide ion doping.

- [1] Y. Sun, N.G. Ndifor-Angwafor, D.J. Riley, M.N.R. Ashfold, Chem. Phys. Lett. 431 (2006) 352.  
[2] A. Janotti and C. G. Van de Walle Rep. Prog. Phys. 72 (2009) 126501 (29pp).

## INTELLIGENT MAGNETO-OPTICAL CORROBORATOR WITH FERROFLUIDS

David C. A. Saravia<sup>a</sup>, José A. Siqueira D.<sup>b</sup> Suhaila Maluf Shibli<sup>c</sup>, Saulo Finco<sup>d</sup>

<sup>a,b</sup> *Dept. instrumentation, semiconductor e photonics, Campinas State University, Barão Geraldo, Campinas, Brazil, davidcesar@yahoo.com*

<sup>c</sup> *Dept. experimental and applied physics, Institute de Physics, University de São Paulo, São Paulo, Brazil, shibli@if.usp.br*

<sup>d</sup> *Dept. of Physics experimental and applied, University, 98A Sunshine Avenue, Philadelphia, USA, saulo.finco@cti.gov.br*

This paper describes the development and application of a magneto-optical corroborator for devices where there are magnetic fields using ferrofluid as the smart sensing material. The current technology in the development and design of ferrofluids, allows the fabrication of these materials almost custom made, and its applications are numerous. Plastic optical fibers are used to transport the light. Alternating magnetic fields were measured at 60.0 Hz (main frequency) and 110 Vrms (at low voltage). The device was designed for measure magnetic fields in function of proximity sensing. The corroborator uses magnetic fluid magnetite Fe<sub>3</sub>O<sub>4</sub> as an active element. It has a simple and compact construction robust elements to adverse electrical conditions and environment, including EMI immunity and flammable atmospheres. The signal presents variations of only -1 dBm.

- [1] D. C. A. Saravia, A. Bee, S. M. Shibli. Blocking Phenomena Studies on Ferronematics. *Journal of Magnetism and Magnetic Materials*. 289 (2005)152-154.
- [2] F. Cecelja, W. Balachandran. Optimized CdTe Sensors for Measurement of Electric and Magnetic Fields in the Near-Field Region, *IEEE Trans. Instrum. Meas.* 49 (2000) 483–487.
- [3] Pan Yingtain, Liu Xiande, Du Chongwu, Li Zaiguang. Fiber Optic Magnetic Field and Current Sensor, Using Magneto - Birefringence of Dense Ferrofluid thin Films. *International Conference on Optical Fibre Sensors in China OFS(C)*. 1572 (1991).
- [4] S. Taketomi et al., Temperature Dependence of Magneto - Optical Effect in Magnetic Fluids. *J. Magn. Soc. Jpn.* 11 (1987) 409 - 412.
- [5] L. M. Maniner, R.T. Rakowski, F. Cecelja. A Novel Magneto-Optic Ferrofluid Material for Sensor Applications Instrumentation and Measurement Technology Conference, Italy 2004.
- [6] B. Andò, S. Baglio, A. Beninato, S. La Malfa, N. Pitrone, Advanced Educational Tools in Measurement and Sensors: from remote monitoring systems to magnetic fluids, *Inter. Journal of Education and Information Technologies*. 3(2009)75-84.
- [7] P. Kaewtrakulpong, Magneto-optical residual current devices, MSc. Industrial Measurement Systems Dissertation, Dept. of Manufacturing and Engineering Systems, London: Brunel University, 1998.
- [8] T. Jayakumar, C. Babu Rao, John Philip, C. K. Mukhopadhyay, J. Jayapandian, C. Pandian. Sensors for Monitoring Components, Systems and Processes. *International Journal on Smart Sensing and Intelligent Systems*. 3 (1) (2010) 61-74.
- [9] A. Sibli, J. Monin, G. Noyel, O Brevet-Philibert. An AC Magnetic Field Remote Sensor Using a Ferrofluid Material: application to the measurement of off-centring sleeves of HV transmission lines. *Meas. Sci. Technol.* 3 (11) (1992) 1068.
- [10] Wei Li, Xiaoping Lu, Yonggang Lin. Novel Absolute Displacement Sensor with Wide Range Based on Malus Law. *Sensors*. 9 (2009)10411-10422.

## INTRINSIC LUMINESCENCE IN ALKALI METAL SULPHATES

T.N. Nurakhmetov, K. A. Kuterbekov, D.H. Daurenbekov, Zh.M. Salikhodzha, A.K. Kainarbay, A. M. Zhunusbekov, K. Bekmyrza  
010000, Kazakhstan, Astana, 13 Munaitpasov str., L. N. Gumilyov Eurasian National University [duke.ddx@yandex.ru](mailto:duke.ddx@yandex.ru)

This paper describes the nature of the intrinsic luminescence of  $\text{Na}_2\text{SO}_4$  and  $\text{LiKSO}_4$  crystals first investigated by the authors at 80 and 300 K under excitation by ultraviolet photons with an energy of 4-6.2 eV.

Based on the band structure of alkali metal sulfates, it may be supposed that their self-luminescence could be caused by two groups of electron transitions. During excitation of alkali metal sulfates, bound electrons (in the valence band) move to the conduction band, consisting of s-cation or antibonding orbital  $3a_1^*$  and  $\text{SO}_4^{2-}$  anion. The authors [1] on the basis of measurements of the diffuse reflection of  $\text{Na}_2\text{SO}_4$  and  $\text{LiKSO}_4$  powders and analysis of calculations of the electron structure of the  $\text{SO}_4^{2-}$  anion showed the existence of three electron transitions in s-states of the cation and three transitions in the antibonding orbital  $3a_1^*$  and  $\text{SO}_4^{2-}$  anion. About 2/3 of these groups are low-energy transitions with energies 4.4, 5.5 and 6eV. Earlier, we and other authors studied natural luminescence of sulfates excited by X-rays and synchrotron radiation with a photon energy of more than 9 eV. In these experiments, for some sulfates a broad radiation band ranging from 2 to 4 eV, with the maxima at 3.5 and 3.9 eV, was detected. After the transfer of electrons, in orbitals or bonds holes are formed, which move from the valence band in the forbidden band. Different local states from the ceiling of the valence band correspond to these localized holes. Self-radiation of alkali metal sulfates should occur during the recombination transition of electrons from the excited state to the hole molecular orbitals  $1t_1$ ,  $3t_2$ , e,  $2t_2$  of the  $\text{SO}_4^{2-}$  ion. Therefore, the emission spectra must have a broad band with a few peaks.

A special feature of this study is that there are a few isolated bands within the broad emission band, which are effectively excited at photon energies of 5, 5.5 and 6.2 eV.

It is assumed that the observed excitation spectra of spectral regions around 5, 5.5 and 6-6.2 eV peaks of self-luminescence of  $\text{LiKSO}_4$  crystal correspond to the transition of electrons from the terms  $1t_1$ ,  $3t_2$ , e,  $2t_2$  of the ground state of the  $\text{SO}_4^{2-}$ . Intrinsic luminescence with several maxima occurs as a result of recombination of the excited electron in the conduction band with localized holes above the valence band.

[1] V. G. Sholokh, N. I. Aleshkevich, V. V. Syt'ko, Z. B. Perekalina, O. A. Baturina, B. Brezina,. Journal of Applied Spectroscopy 45 (1986) 1, 718-722

## INVESTIGATION OF ENERGY TRANSFER BETWEEN RARE EARTH IONS OF A 3D LANTHANIDE-ORGANIC FRAMEWORK

Carime V. Rodrigues<sup>a</sup>, Marcelo Oliveira Rodrigues<sup>a</sup>, Leonis L. Luz,<sup>b</sup> Ricardo O. Freire,<sup>c</sup> Severino A. Junior.<sup>b</sup>

<sup>a</sup> Instituto de Química, Campus Universitário Darcy Ribeiro, Brasília-DF, Brazil, carime.v.rodrigues@gmail.com

<sup>b</sup> Departamento de Química Fundamental, UFPE, Recife - PE, Brazil.

<sup>c</sup> Departamento de Química, UFS, São Cristóvão-SE, Brazil.

The present work reports an experimental and theoretical study of the Ln<sup>3+</sup>-Ln<sup>3+</sup> energy transfer (ET) and color tuning of [(La<sub>0.9</sub>Eu<sub>0.05</sub>Tb<sub>0.05</sub>)<sub>2</sub>(PDC)<sub>3</sub>(H<sub>2</sub>O)<sub>4</sub>]2H<sub>2</sub>O, herein designated as (1).[1] In this sample, Tb<sup>3+</sup>-Eu<sup>3+</sup> ET influences the luminescence decay profile of the donor species, Tb<sup>3+</sup>, in comparison with that presented by the LnMOF doped just with terbium. The emission of the compound has presented a sensible dependence on the excitation wavelength, enabling an efficient tuning of the photoluminescence color, as shown in figure 1.

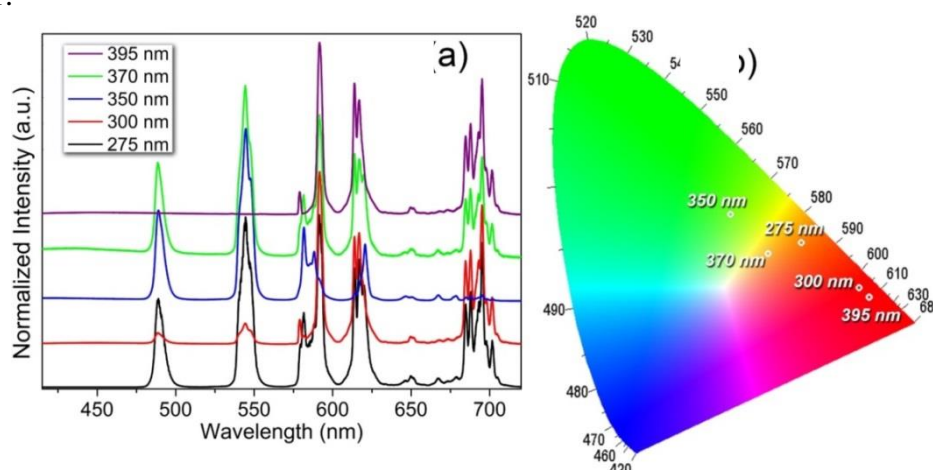


Figure 1- Emission spectra upon different excitations wavelengths and CIE diagram points of (1)

A theoretical methodology[2] was applied to calculate the single Tb<sup>3+</sup>-Eu<sup>3+</sup> energy transfer process by the mechanisms D–D, D–Q, Q–Q and Ex. The results arranged on table 1 indicate that the interactions are predominantly governed by D–Q and Q–Q mechanisms.

Table 1- Calculated values of intramolecular energy transfer between Tb<sup>3+</sup> and Eu<sup>3+</sup> ions

Mechanism	Tb( <sup>5</sup> D <sub>4</sub> ) → Eu( <sup>5</sup> D <sub>1</sub> ) (s <sup>-1</sup> )	Tb( <sup>5</sup> D <sub>4</sub> ) → Eu( <sup>5</sup> D <sub>0</sub> ) (s <sup>-1</sup> )
D–D	170.142	297.62
D–Q	446.512	657.73
Q–Q	442.97	652.52
Ex	1.22	7.11

[1] C. V. Rodrigues, L. L. Luz, J. D. Dutra, S. A. Junior, O. L. Malta, C. C. Gatto, H. C. Streit, R. O. Freire, C. Wickleder, M. O. Rodrigues, Phys. Chem. Chem. Phys. 16 (2014) 14858-14866.

[2] O. L. Malta, Journal of Non-Crystalline Solids 354 (2008) 4770-4776.

### Acknowledgements

This work was supported by INAMI, CAPES, CNPQ, DPP-UnB and FAPDF.

## DISCOLORATION EFFECTS OF DENTAL COMPOSITE MATERIALS STAINED IN BEER

Milica Antonov<sup>a</sup>, Bojana Milićević<sup>a</sup>, Lea Lenhardt<sup>a</sup>, Ivana Zeković<sup>a</sup>, Dragica Manojlović<sup>b</sup>,  
Miroslav D. Dramićanin<sup>a</sup>

<sup>a</sup>University of Belgrade, Vinča Institute of Nuclear Sciences, P.O. Box 522, Belgrade 11001, Serbia, email: mantonov@vinca.rs

<sup>b</sup>University of Belgrade, School of Dental Medicine, Rankeova 4, Belgrade, 11000, Serbia

Susceptibility to extrinsic colorants is one of the most important factors responsible for color instability of dental composite materials (in dynamical oral environment) which is unacceptable for aesthetic restorations. Changes of color and fluorescence of composite samples stained in different beer during 14 days are evaluated in this study. 20 microhybrid composite disk-shaped specimens (13 mm in diameter × 2 mm thick; Gradia Direct™ XBW shade) were divided in five groups and immersed in four different dark beers (Leffe, Bernard, Erdinger, Guinness) and one light beer (Tuborg). Samples immersed in distilled water at 37°C for 24h were used as the reference samples. Diffuse reflection spectra are measured in 360-830 nm range. CIELAB color analysis was used to calculate color coordinates L\* a\* and b\* for the standard D65 illuminant. Color stability was determined by the difference of total changes of color ( $\Delta E$ ) between the coordinates obtained from the specimens before and after immersion into the solutions. The largest color change is observed with staining in Bernard beer ( $\Delta E \approx 9$ ), while specimens immersed in Tuborg light beer showed the lowest color change of about 4.8. The Change of luminescence emission after staining is assessed from excitation-emission spectra measured over 300-650 nm emission and 270-550 nm excitation range, Figure 1. In general, all samples showed lower emission in the blue spectral range; the largest change is observed with UV excitations. Overall, dental composite samples undergo significant change in their optical (aesthetic) properties after exposure to beer. These changes are larger than clinically acceptable threshold ( $\Delta E < 3.3$ ).

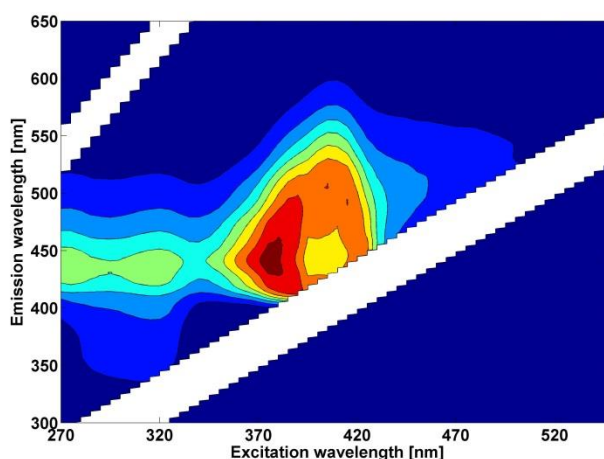


Figure 1. Excitation-emission spectrum of the Gradia Direct™ XBW composite after 14 day exposure to Guinness beer.

## INVESTIGATION OF THE OPTICAL AND LUMINESCENT PROPERTIES OF THE PURE QUARTZ USING SYNCHROTRON RADIATION

Vitaly N. Kolobanov<sup>a</sup>, Igor A. Markov<sup>a</sup>, Peter P. Shvansky<sup>b</sup>

<sup>a</sup>*Faculty of Physics, Moscow State University, 119899 Moscow, Russia*

<sup>b</sup>*All-Russian Research Institute for Synthesis of Materials (VNIISIMS), Alexandrov, Vladimir region, Russia*

High quality optical quartz was received in VNIISIMS by hydrothermal method on seeds of (0001) - orientation. Crystallization was provided from the solutions of sodium hydroxide with the admixture of lithium nitride in an interval of temperatures 330 – 345<sup>0</sup> C and pressures 100-130 MPa. Seeds were located under horizontal screens with the purpose of reduction of solid inclusions in growing crystals. Optical quartz crystals were grown free from Al and non-structural impurities in the pinacoidal growth sectors.

Luminescence excitation and emission spectra as well as reflectivity and emission kinetics were measured using synchratron radiation at DESY, Hamburg. Measurements were performed in the wide energy region 4 – 600 eV corresponding to the fundamental absorption region and upper core levels. Short wavelength transparency edge of the high quality SiO<sub>2</sub> single crystals located near 146 nm (8,5 eV) at near room temperature and shifted to 143 nm (8.66 eV) at near liquid helium temperature. Some peculiarities in the luminescence excitation spectra at the 100-115 eV can be assigned to the absorption transitions from the core 2p Si<sup>4+</sup> level.

Luminescence nature and specific of the electronic band structure SiO<sub>2</sub> single crystals were discussed.

Financial support of the RF Ministry of Education and Science grant RFMEFI61614X0006 is gratefully acknowledged.

## IR SPECTROSCOPY STUDY OF THE ORIENTATION ORDER OF NEMATIC LIQUID CRYSTALS DOPED QUANTUM DOTS

Cavrish E.O.<sup>a</sup>, Konshina E.A.<sup>a</sup>, Vangonen A.I.<sup>b</sup>

<sup>a</sup> *ITMO University, Kronverkskii pr., 49, 197101, Saint-Petersburg, Russia*

<sup>b</sup> *Scientific and Industrial Corporation "Vavilov State Optical Institute"*

Adding semiconductor quantum dots in a nematic liquid crystal (NLC) leads to a change in the optical, dynamic, dielectric and elastic properties [1-3]. These properties depend on the orientation order of the NLC molecules that may be violated as a result of doping. Therefore, the study of orientational order in the composite media based on the NLC doped nanoparticles are relevant. The main objective of this work was to study changes of an orientation order parameter and a dichroic ratio of the main bands in the NLC absorption spectrum as a result of changes in the concentration of CdSe/ZnS quantum dots using the IR Attenuated Total Reflection. This method is the highly sensitive in measuring molecular structure of thin layers.

The IR spectra were measured using Perkin-Elmer 2201 spectrometer. Ge prism on twelve reflections was used as an optical guide for IR beam. We used the NLC mixture on base cyan biphenyl (CB) molecules with a positive dielectric anisotropy and with a refractive index  $n_o=1.51$ . The CdSe/ZnS quantum dots (QDs) core-shell type with a core size of 5 nm were used for a preparation of the NLC suspensions. Cells were fabricated using Ge prism and a glass substrate covered with inner sides by the polyimide layer for homogeneous oriented NLC molecules. The polarized IR spectra for the *s*- and *p*-polarizations were obtained in the range 3500-850  $\text{cm}^{-1}$ , in which the electric vector of the radiation was polarized perpendicular ( $R_s$ ) and parallel ( $R_p$ ) to plane of incidence.

The higher value of the dichroic ratio was observed for bonds, which vibrate along the direction of the electric vector of incident IR radiation. For the CB molecule the higher dichroic ratio in the IR spectra there were the  $\text{C}\equiv\text{N}$  stretching ( $\sim 2226 \text{ cm}^{-1}$ ), the phenyl  $\text{C}-\text{C}$  stretching ( $\sim 1605 \text{ cm}^{-1}$  и  $\sim 1494 \text{ cm}^{-1}$ ) and the  $\text{C}-\text{C}$  stretching of biphenyl ring ( $\sim 1246 \text{ cm}^{-1}$ ). Our results showed that the dichroic ratio of the major stretching in the NLC spectra increased, for example, the phenyl  $\text{C}-\text{C}$  stretching ( $\sim 1605 \text{ cm}^{-1}$ ) of 4.4 to 5.5 with increasing of QDs concentrations from 5 to 13 mg/ml. The order parameter of the main absorption bands in the pure NLC spectra varied from 0.41 to 0.67 and its value increased to 0.74 with the QDs doping. The results show that the CdSe/ZnS QDs doping in the NLC led to improved the CB molecular orientation.

[1] E.A. Konshina, E.O.Gavrish, A.O. Orlova, M.V. Artem'ev, Tech Phys Lett. 37, pp. 011–1014, 2011.

[2] E.A. Konshina, I.F. Galin, E.O. Gavrish, Universal J Mater. Sci.;2, pp. 1–4 2014.

[3] E.A.Konshina, I.F.Galin, D.P.Shcherbinin, E.O.Gavrish, Liq Cryst.41, pp. 1229–1234, 2014.

[4] A.I Vangonen, E.A. Konshina Mol. Cryst.& Liq. Cryst.304, pp. 507-512, 1997.

## $\text{K}_2\text{SiF}_6:\text{Mn}^{4+}$ AS A RED PHOSPHOR FOR REMOTE LEDs

Heleen F. Sijbom<sup>a,b</sup>, Koen Van den Eeckhout<sup>a,b</sup>, Dirk Poelman<sup>a,b</sup>, Philippe F. Smet<sup>a,b</sup>

<sup>a</sup> *LumiLab, Department of Solid State Sciences, Ghent University, Krijgslaan 281-S1, 9000 Ghent, Belgium, Heleen.Sijbom@UGent.be*

<sup>b</sup> *Center for Nano- and Biophotonics (NB-Photonics), Ghent University, Ghent, Belgium*

$\text{K}_2\text{SiF}_6:\text{Mn}^{4+}$  is promising as a red phosphor in LEDs for general lighting and displays [1]. Its narrow red emission around 630 nm and good thermal stability make it suitable for improved colour rendering (CRI), while its excitation band around 455 nm is ideally suited for blue LED excitation [2]. Simulations show high CRI and luminous efficacy values for  $\text{K}_2\text{SiF}_6:\text{Mn}^{4+}$  combined with a green or yellow phosphor and a blue LED, for a wide range of colour temperatures. To maximize the application opportunities for this phosphor, the luminescence behavior at high excitation intensities and on a single particle scale should be known. This research presents a study of the saturation behaviour and thermal properties of  $\text{K}_2\text{SiF}_6:\text{Mn}^{4+}$ , complemented by a combined investigation of structural and luminescence properties in SEM-CL (cathodoluminescence in a scanning electron microscope) mappings.

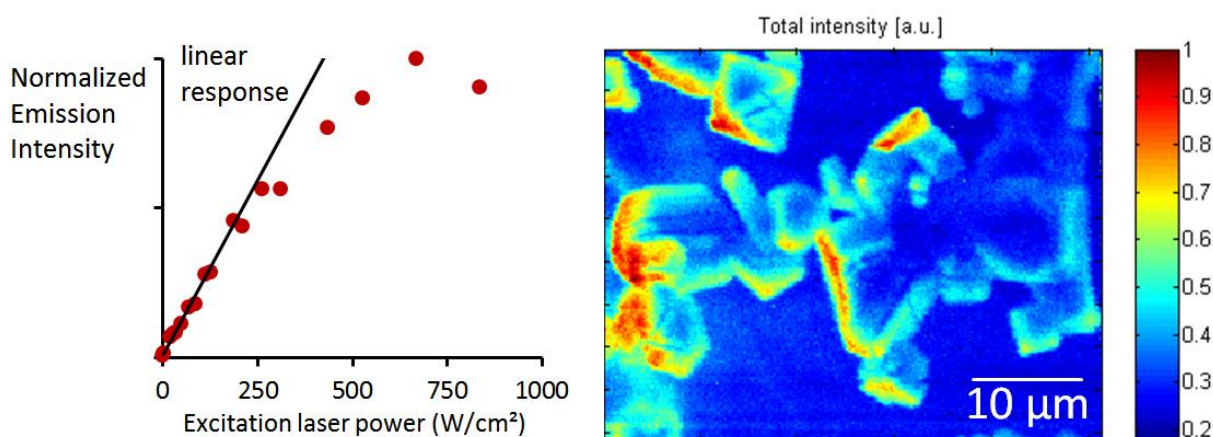


Figure 1: Sublinear response of  $\text{K}_2\text{SiF}_6:\text{Mn}^{4+}$  emission with increasing excitation power (left) and SEM-CL mapping of  $\text{K}_2\text{SiF}_6:\text{Mn}^{4+}$  particles (right).

The integrated emission intensity of  $\text{K}_2\text{SiF}_6:\text{Mn}^{4+}$  in Figure 1 (left) shows sublinear response at high excitation power due to the relatively long lifetime of the excited state of 8.1 ms at room temperature. Thermal quenching is limited since the emission intensity is unaffected up to 400 K, which is above the normal working temperature of most LEDs. Nevertheless, upon high incident laser intensity the phosphor is irreversibly damaged, as can be monitored by SEM-CL. A remote phosphor setup, where the phosphor is physically separated from the pumping LED, can overcome saturation issues at high excitation power by lowering the blue photon flux at the phosphor level.

EDX-mappings show a homogeneous incorporation of the Mn dopant. However, the SEM-CL mappings in Figure 1 (right) show higher emission intensities at the edges of the well crystallized, cubic particles. This peculiar phenomenon is a combination of selective light outcoupling, the direction of the light collection and the interaction volume of the electron beam.

[1] T. Takahashi, S. Adachi, *J. Electrochem. Soc.* 155 (2008) E183-E188.

[2] M.G. Brik, A.M. Srivastava, *J. Lumin.* 133 (2013) 69-72.



## KINETICS OF HOLOGRAM RECORDING IN REVERSIBLE HOLOGRAPHIC MEDIUM BASED ON CALCIUM FLUORIDE CRYSTALS WITH COLOR CENTERS

Aleksandr S. Shcheulin, Aleksandr E. Angervaks, Aleksandr I. Ryskin  
*ITMO University, 49 Kronverkskiy pr., St. Petersburg, Russia, angervax@mail.ru*

Holographic media could be divided into two classes, irreversible and reversible ones. For the former class, the recording light produces irreversible modification of optical constants in the maxima of the fringe pattern. The diffraction response of such media increases with increasing recording exposure, passes the peak value at the maximum possible changes of optical constants, and then decreases down to zero due to scattering light presented in the fringe pattern minima. The modification of optical constants with exposure for reversible media (the kinetics of the hologram recording) is of another nature due to existence of reverse process with respect to recording one. The diffraction efficiency, DE, of reversible media does not decrease to zero with exposure but reaches the saturation level which is determined by the rates' ratio of direct (recording) and reverse processes. However, the attainment of the saturation level could be a non-monotonous process. In this paper, the kinetics of hologram recording in reversible holographic medium, calcium fluoride ( $\text{CaF}_2$ ) crystal with color centers, is reported.

Additively colored (heated in a reducing atmosphere of calcium vapor)  $\text{CaF}_2$  crystals contain various color centers which consist of anion vacancies and electrons. They could be divided into "simple", *F*-, *M*-, *R*- and *N*-centers, formed by 1–4 vacancies/electrons and highly-aggregated centers: "colloidal" centers which are two-dimensional calcium islets, and "quasi-colloidal" centers. The structure and constitution of these centers are unknown at present, but probably take an intermediate position between simple and colloidal centers according to the number of vacancies/electrons.

Each type of color centers has characteristic absorption bands. Under illumination of the colored crystal in these bands at  $T \geq 70$  °C the center transformations take place. The specific diffusion-drift mechanism of hologram recording in  $\text{CaF}_2$  (at  $T = 150$ – $200$  °C) results both in the center transformation and in their spatial redistribution within the crystal bulk: color centers leave the maxima and concentrate in the minima of the fringe pattern (the direct process). The higher the recording exposure the narrower the regions of color centers concentration that leads to formation of non-sinusoidal holographic grating with increasing higher-order diffraction responses.

The reverse process for the  $\text{CaF}_2$  is a thermal ionization of color centers in the minima of the fringe pattern. As a result, the reverse flow of color centers with respect to recording one arises. Thus, DE of  $\text{CaF}_2$  reaches the saturation level, which depends on the power density of recording radiation, holographic grating frequency and recording  $T$ . However, before reaching the saturation level the DE versus exposure dependence passes several local maxima. The physical processes responsible for these maxima are discussed. The shape of the dependence allows highlighting the exposure ranges at which sinusoidal or non-sinusoidal holographic gratings can be recorded in  $\text{CaF}_2$ .

## LANGASITE AND LANGATATE CRYSTALS: OPTICAL CHARACTERIZATION AND POINT DEFECTS

Oleg A. Buzanov<sup>a</sup>, Nina S. Kozlova<sup>b</sup>, Anna P. Kozlova<sup>b</sup>, Dmitriy A. Spassky<sup>c,d</sup>, Nikita A. Siminel<sup>b</sup>, Evgeniya V. Zabelina<sup>b</sup>

<sup>a</sup>*Fomos-Materials 16 Buzheninova street, Moscow, Russia*

<sup>b</sup>*NUST "MISiS", 4, Leninskii pr., Moscow Russia, zabev@mail.ru*

<sup>c</sup>*Institute of Physics, University of Tartu, Ravila 14c, 50411, Tartu, Estonia*

<sup>d</sup>*Skobeltsyn Institute of Nuclear Physics, Moscow State University, Moscow, Russia*

Langasite (LGS,  $\text{La}_3\text{Ga}_5\text{SiO}_{14}$ ) and langatate (LGT,  $\text{La}_3\text{Ga}_{5.5}\text{Ta}_{0.5}\text{O}_{14}$ ) are crystals with calcium-gallogermanate structure. In consequence of the unique combination of piezoelectric, thermal, luminescent and nonlinear optical properties these crystals are expected to satisfy requirements for various applications including laser media or parametric quantum oscillators. The presence of point defects and their associations, in particular, color centers, in the crystals limits areas of their application. Different research groups develop the models of point defects in LGS and LGT [1-3]. But still these models are incomplete and contradictory.

Here we present the results of our studies of the optical and luminescent characteristics of LGT and LGS crystals depending on their composition, orientation and growth conditions. All investigated samples were cut from bulk crystals grown in Fomos-Materials using Czochralski method in Ir crucibles, growth atmosphere – Ar or Ar plus  $\text{O}_2$ . Optical transmission spectra were measured using UV-Vis-Nir spectrophotometer «Cary-5000» (Agilent Technologies). The luminescence was excited at  $T=300$  K by third harmonic of YAG:Nd<sup>3+</sup> ( $\lambda_{\text{ex}}=355$  nm) or by Xe lamp.

The growth atmosphere significantly influences the coloration and, as a consequence transmission spectra of LGT crystals [4]. Colorless LGT crystals are obtained in Ar atmosphere, while colored crystals – with addition of oxygen. In transmission spectra of LGS and LGT in visible and UV spectral regions we observed three absorption bands in the colored crystals (290, 380 and 490 nm) and only one band in the colorless crystals (290 nm). Also in transmission spectra of all investigated samples there are two bands in near infra-red region - 1850 and 2920 nm. We observed anisotropy of transmission spectra of samples – this effect in crystals with Ca-gallogermanate crystals is well-known [5]. However for the samples, which were cut in the direction parallel to axis Z we also observed dichroism. This effect occurs in some crystals with specific structure when naturally polarized light pass along directions perpendicular to the optical axis, and may be caused by the symmetry of the crystals' structure or by the anisotropy of color centers. First studies of luminescence in LGT and LGS crystals demonstrated considerable influence of growth conditions on the luminescent characteristics of these crystals. Therefore it shows that the method of luminescence spectroscopy is efficient for the studies of the origin of crystals structure defects in langasites and langatates.

[1] T. Taishi, T. Hayashi, N. Bamba, Y. Ohno, I. Yonenaga, W. Hoshikawa, *Physica B: Condensed Matter* 401-402 (2007) 437-440.

[2] A.V. Butashin, V.A. Fedorov, V.F. Mescheriakov, V.S. Mironov, L.G. Shilin, O.A. Busanov, A.N. Zabelin, S.A. Sakharov NCCG-2008. Book of abstracts, Moscow, 2008.

[3] G.M. Kuz'micheva, I.A. Kaurova, V.B. Rybakov, S.S. Khasanov, A. Cousson, O. Zaharko, E.N. Domoroshchina, A.B. Dubovskii, *Cryst. Res. Technol.* 47-2 (2012) 131-138.

[4] O.A. Buzanov, N.S. Kozlova, E.V. Zabelina, *Crystallography Reports* 52-4 (2007) 691-696.

[5] X.Shi, D. Yuan, A. Wei, Z. Wang, B. Wang, *Mat. Res. Bull.* 41 (2006) 1052-1055

## LANTANIDES BASED LUMINESCENT MATERIAL INCORPORATED INTO SILICA MATRIXES

Joanna Cybińska<sup>a,b</sup>, Magdalena Wilk<sup>b</sup>, Marta Kargol<sup>b</sup>, Katarzyna Komorowska<sup>b</sup>

<sup>a</sup> Faculty of Chemistry, University of Wrocław, Poland,

<sup>b</sup> Department of Nanotechnology, Wrocław Research Centre EIT+, Poland,  
marta.kargol@eitplus.pl

As it is well known during the sol-gel process, it is possible to synthesize at room temperature a porous glassy network. Pores several nanometers large with numerous pending Si-OH groups well fitted to nanoscale chemical reactions and the possibility of incorporating various heteroatoms into the silica framework [1,2] may result in a wide range of modified products. On the other hand incorporating the luminescent materials into silica matrix should stabilize and improve their optical performance. Thus macroscopic nanostructured monoliths synthesized via direct liquid crystal templating pathway in high-concentration amphiphilic solutions and possessing large internal surface area and high porosity with controllable and narrowly distributed pore sizes are promising candidates to accommodate optically active lanthanides ions, what makes them useful for photonic applications.

This research project was focus on obtaining the desired porous structures enable the luminescent centers to be effectively incorporated and thus chemically and optically stable hybrid materials to be developed. These materials were systematically studied by using various optical and surface characterization techniques so as to establish the relationship between the functionalization capacity and porous structures. The optically active ions as  $\text{Eu}^{3+}$  or  $\text{Tb}^{3+}$  were introducing to the matrices during the sol-gel process or by post synthesis impregnation. For the investigated samples spectroscopic properties were measured showing the influence of sample preparation on the optical properties was shown.

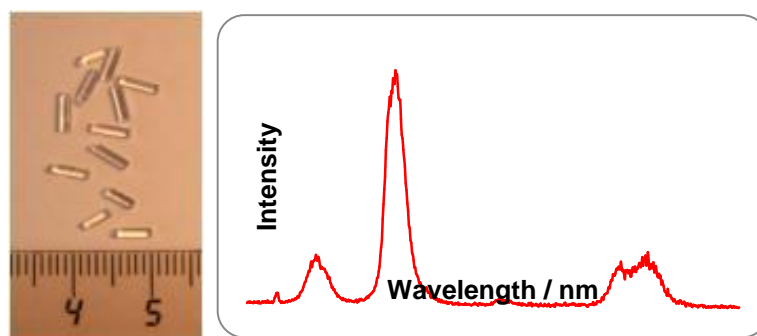


Fig. Monolithic sample image after calcination, before and after the  $\text{Eu}^{3+}$  ions introduction (left) The emission spectrum of aluminosilica monoliths doped with  $\text{Eu}^{3+}$  ions by the sol-gel method. The  $\text{Eu}^{3+}$  concentration is 2 % in relation to Si. The spectrum was obtained under excitation at 393 nm.

### Acknowledgement

The work was supported by Wrocław Research Centre EIT+ within the project "The Application of Nanotechnology in Advanced Materials" - NanoMat (POIG.01.01.02-02-002/08) co-financed by the European Regional Development Fund (Operational Programme Innovative Economy, 1.1.2)

[1] L. Y. Chen et. al, Microporous Mater. 12, 323 (1997)

[2] A. Tuel Microporous Mesoporous Mater. 27, 151 (1999)

## LATTICE DYNAMICS OF $\text{Ca}_2\text{Ge}_7\text{O}_{16}$ : A COMBINED EXPERIMENTAL-THEORETICAL STUDY

Vladislav P. Petrov<sup>a</sup>, Vladimir A. Chernyshev<sup>a</sup>, Ivan I. Leonidov<sup>a,b</sup>,  
Ekaterina I. Konstantinova<sup>b</sup>, Emma G. Vovkotrub<sup>c</sup>, Anatoliy E. Nikiforov<sup>a</sup>  
<sup>a</sup>*Ural Federal University, 19 Mira, Ekaterinburg, Russia, lancervlad@gmail.com*  
<sup>b</sup>*Institute of Solid State Chemistry, UB RAS, 91 Pervomaiskaya, Ekaterinburg, Russia*  
<sup>c</sup>*Institute of High-Temperature Electrochemistry, UB RAS,  
20 Akademicheskaya, Ekaterinburg, Russia*

$\text{Ca}_2\text{Ge}_7\text{O}_{16}$  belongs to a family of multifunctional germanates  $M_2\text{Ge}_7\text{O}_{16}$  ( $M = \text{Ca}, \text{Cd}$ ). While calcium heptagermanate has been extensively studied as 3D hierarchical nanowire arrays/carbon textile anodes for application in lithium-ion batteries with excellent cycling performance, high capacity and superior rate capability [1, 2],  $\text{Mn}^{2+}$ ,  $\text{Pb}^{2+}$  or  $\text{Tb}^{3+}$ -doped  $\text{Cd}_2\text{Ge}_7\text{O}_{16}$  exhibit persistent luminescence properties [3, 4]. A series of promising red emitting  $\text{Ca}_2\text{Ge}_7\text{O}_{16}:\text{Eu}^{3+}$  [5] and white-blue afterglow phosphors  $\text{Ca}_2\text{Ge}_7\text{O}_{16}$  doped with  $\text{Tb}^{3+}$  [6] and  $\text{Dy}^{3+}$  [7] have been recently elaborated. However, vibrational spectroscopic properties and non-radiative multiphonon relaxation processes have not been elucidated yet.

The present report is focused on lattice dynamics of  $\text{Ca}_2\text{Ge}_7\text{O}_{16}$  studied by an experimental-theoretical approach, included FTIR spectroscopy, Raman microscopy and periodic *ab initio* calculations using the CRYSTAL14 code and several hybrid functionals. The Ca, Ge and O basis sets have been re-optimized for  $\text{Ca}_2\text{Ge}_7\text{O}_{16}$  bulk calculations. An excellent agreement between the experimental crystal structure, vibrational spectra, band structure, and their computed counterparts has been obtained. Various percentage of HF contribution in the range of 16–25% in different hybrids has been previously analyzed in DFT calculations of vibrational spectra of the other layered-type germanate,  $\text{Y}_2\text{CaGe}_4\text{O}_{12}$  [8]. The results of *ab initio* calculations show that the recently established WC1LYP (16% HF) [9] is among the most suitable DFT functionals for the most accurate vibrational mode assignment and description of lattice dynamics of  $\text{Ca}_2\text{Ge}_7\text{O}_{16}$  and other related germanate compounds.

This work was partially supported by the FASO Program No. 01201364479, RFBR (Grant No. 14–03–31324–mol\_a), Ministry of Education and Science of Russia (Grant No. 3.571.2014/K), and the URAN Computing Platform (IMM UB RAS, Ekaterinburg, Russia).

- [1] W. W. Li, X. F. Wang, B. Liu, et al., *Chem. Eur. J.* 19 (2013) 8650–8656.
- [2] T. Lv, X. Li, J.M. Ma, *RSC Adv.* 4 (2014) 49942–49945.
- [3] G. Che, X. Li, C. Liu, H. Wang, Y. Liu, Z. Xu, *Phys. Stat. Sol. A* 205 (2008) 194–198.
- [4] S. Yi, Y. Liu, J. Zhang, et al., *Chin. J. Inorg. Chem.* 20 (2004) 247–250.
- [5] T. Wang, X. Xu, D. Zhou, J. Qiu, X. Yu, *Mater. Res. Bull.* 60 (2014) 876–881.
- [6] M. Li, X. Yu, T. Wang, J. Qiu, X. Xu, *Ceram. Int.* (2015) <http://dx.doi.org/10.1016/j.ceramint.2015.05.095>.
- [7] E.I. Konstantinova, A.V. Ishchenko, I.I. Leonidov, *RSC Adv.* (2015) in press.
- [8] I.I. Leonidov, V.P. Petrov, V.A. Chernyshev, et al., *J. Phys. Chem. C* 118 (2014) 8090–8101.
- [9] R. Demichelis, B. Civalleri, M. Ferrabone, et al., *Int. J. Quant. Chem.* 110 (2010) 406–415.

## COLLOID SYNTHESIS, PHOTOCATALYTIC AND PHYSICO-CHEMICAL PROPERTIES OF BiVO<sub>4</sub> NANOPARTICLES

Slobodan D. Dolić<sup>a</sup>, Dragana J. Jovanović<sup>a</sup>, Milena Marinović Cincović<sup>a</sup>, Biljana Babić<sup>a</sup>,  
Krisjanis Smits<sup>b</sup>, Miroslav D. Dramićanin<sup>a</sup>

<sup>a</sup>*Vinča Institute of Nuclear Sciences, P.O. Box 522, Belgrade, Serbia, slobodan@vin.bg.ac.rs*

<sup>b</sup>*Institute of Solid State Physics, University of Latvia*

Among many different semiconducting materials with photocatalytic properties (TiO<sub>2</sub>, ZnO etc.) [1], bismuth-vanadate (BiVO<sub>4</sub>) based materials show great photocatalytic features that match the needs for a novel, efficient and affordable photocatalyst [2]. Herein, colloid synthesis of BiVO<sub>4</sub> in ethylene-glycol with PEG-200 as a directing agent has been successfully achieved. Various synthesis conditions such as pH value, concentration of precursors and molecular weight of PEG have been optimized. Prepared colloid solutions have been characterized by UV-VIS spectroscopy. Measured absorption spectra, for lower concentrations of the precursors, showed blue shift and calculated band gap of the colloid particles ranged from 2.55 to 2.76 eV. Obtained colloid solutions have been mixed with water, centrifuged, and the residue washed with methanol. X-ray diffraction (XRD) patterns show that the BiVO<sub>4</sub> nanoparticles crystallize in pure tetragonal phase. In order to improve their crystallinity and to investigate in more detail the structural and photocatalytic properties, the obtained BiVO<sub>4</sub> nanoparticles have been annealed at 350°C for 3 hours. Thermogravimetric analysis has been utilized to obtain the optimal annealing temperature. In annealed samples, tetragonal phase completely transits to monoclinic structure for which it has been reported in the literature to be photocatalytically more active [3]. BET surface analysis showed the greater specific surface of the samples obtained from the less concentrated colloids. This difference is even more noticeable after the annealing of the samples. In order to investigate photocatalytic activity of the samples, their ability to degrade organic dyes has been tested. BiVO<sub>4</sub> nanoparticles prepared via colloid synthesis show great photocatalytic activity and further improvements as well as some other applications are to be expected in the future.

[1] J. Schneider, M. Matsuoka, M. Takeuchi, J. Zhang, Yu Horiuchi, M. Anpo, D.W. Bahnemann, *Chem. Rev.* 114 (2014) 9919–9986.

[2] J.H. Kim, J.S. Lee, *Energy Environ. Focus* 3 (2014) 339-353.

[3] H. Fan, T. Jiang, H. Li, D. Wang, L. Wang, J. Zhai, D. He, P. Wang, T. Xie, *J. Phys. Chem. C* 116 (2012) 2425–2430.

# LINEAR AND NONLINEAR OPTICAL ABSORPTION COEFFICIENTS IN AN OFF-CENTER SPHERICALLY CONFINED HYDROGEN ATOM

Vladan Pavlović, Ljiljana Stevanović

Faculty of Sciences and Mathematics, Višegradska 33, Niš, Serbia,

vladan.pavlovic@pmf.edu.rs

Developments in modern technology have allowed researchers to fabricate very small semiconductor structures. Among these quantum structures, quantum dots, in which electrons are confined in all three spatial dimensions, are of the particular interest. These nanostructures play an important role in nanoelectronic and optoelectronic devices, since additional confinement can change electrical and optical properties.

Optical properties in low-dimensional structures can also be modified by impurities. Therefore, understanding the effects of impurities on the optical properties of QDs is very important for nanoelectronic and optoelectronic devices and its applications.

In this paper, we investigated the linear, third-order nonlinear and total optical absorption coefficients of a single GaAs quantum dot with off-center hydrogenic impurity. It is found that total absorption peak position changes with changing the QD radius. Also, the total absorption of the quantum dot could be reduced by adjusting the optical field intensity.

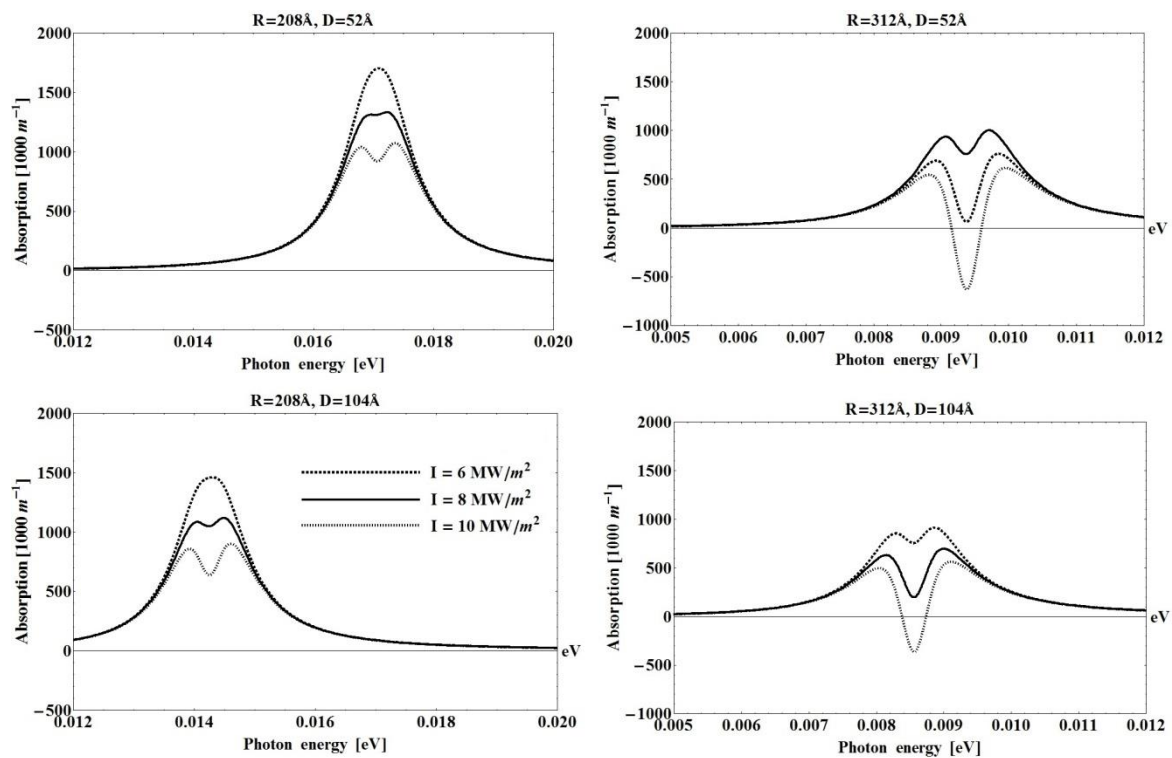


Figure 1. Total optical absorption coefficients as a function of the incident photon energy for two different positions of impurity, two different values of dot radius and three different values of the incident optical intensity.

## LOCALIZED SURFACE PLASMON RESONANCE IN THE IR REGIME

N. Sardana<sup>1</sup> and J.Schilling<sup>2</sup>

<sup>1</sup>*Institute of Nano Science and Technology, Mohali, India, nsardana@inst.ac.in*

<sup>2</sup>*Martin Luther University of Halle-Wittenberg, Halle, Germany, joerg.schilling@physik.uni-halle.de*

In the field of quantum optics, the possibility to enhance absorption or emission in a very small volume has been greatly influenced by high optical confinement and local field enhancement of the localized surface plasmons resonances (LSPR) occurring at metal nanoparticles, nanostructures or nanoantennas [1-3].

In our work, it is shown that for disk shaped nanoantennas the scattering resonances can be well predicted using Mie theory (as defined in [4]) shown in Figure 1a. Increasing the diameter shifts the particle resonances (especially the interesting dipole resonance A1,S1) towards the infrared.

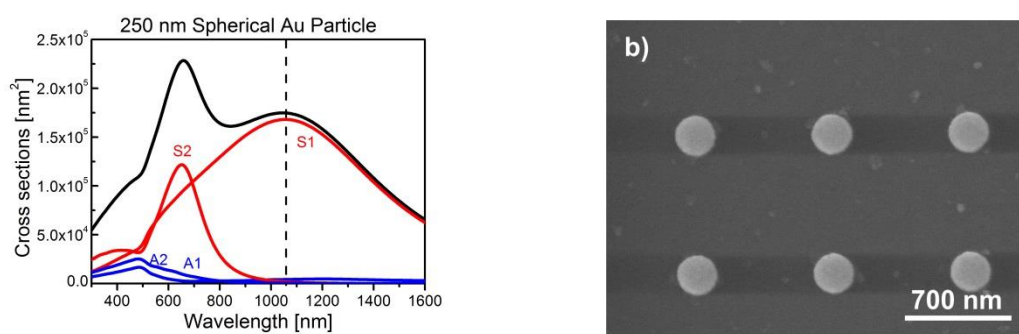


Figure 1: a) Mie Extinction calculation for 250 nm Spherical Au Particle b) SEM Images of disk shaped nanoantennas diameter  $\varnothing$  250nm

Experimentally such disk shaped nanoantennas have been produced by E-Beam Lithography in 2D periodic arrays (SEM of one of them is shown in Figure 1b). In all the measured transmission spectral of these samples, a broad single particle resonance and a sharper fano line shape at longer wavelengths are clearly visible. The sharper fano style resonances are formed due to mutual coupling of localized surface plasmon resonance (LSPR) resulting in the surface lattice resonance (SLR) to the red side of the Raleigh anomaly (RA). This can actually be observed twice - very clearly for the (1,0) RA and once in a much weaker form for the (1,1) RA. All single particle resonances show good theoretical fitting with a Lorentzian curves. On reducing the size of the disks (same periodicity), a blue shift of single particle resonance also leads to a reduced lattice coupling of the LSPRs.

Furthermore, embedded quantum dots surrounding the nanoantennas show up to 4-fold photoluminescence enhancement due to the coupling to the surface plasmon lattice resonances for larger disk diameters.

[1] Gavrilenko, V.I., Optics of Nanomaterials. 2010: Pan Stanford.

[2] Maier, S.A., Plasmonics: Fundamentals and Applications. 2007: Springer.

[3]Maier, S.A., et al., Nat. Mater., 2003. 2(4): p. 229 - 232.

[4] Hohenester, U. and A.Trugler, Comp. Phys. Commun., 2012. 183: p. 370-381.

## LOW-TEMPERATURE COMBUSTION SYNTHESIS AND PHOTOLUMINESCENCE PROPERTIES OF $Y_{2-x-y}Eu_xBi_yWO_6$

Darío Espinoza<sup>a</sup>, Jaime Llanos<sup>b</sup>

<sup>a</sup>*Dept. of Chemistry, Universidad de Chile, Las Palmeras 3425, Santiago, Chile,  
dario.jespinoza@gmail.com*

<sup>b</sup>*Dept. of Chemistry, Universidad Católica del Norte, Avda. Angamos 0610, Antofagasta,  
Chile, jllanos@ucn.cl*

The chemistry of rare-earth elements plays an important role due to its excellent luminescent properties. As is known luminescent materials are applied ion lighting, lasers, and recently are proposed for improving solar cells [1-3].

The literature reports that the exposure to UV light produces serious damages to the DSSC since the iodine present in the electrolyte is irreversibly consumed under UV radiation [4]. Inorganic phosphors are suitable materials for reducing this disadvantage in dye sensitized solar cells.

In this work, we report on the synthesis and optical properties of the orthorhombic low-temperature phase for  $Y_{2-x-y}Eu_xBi_yWO_6$ . The x-ray powder diffraction pattern for all phases indicated that they crystallized isostructurally with the Aurivillius phase,  $Bi_2WO_6$ , which crystallizes with the orthorhombic space group  $P2_1ab$  [5].

The emission spectra of  $Y_{2-x-y}Eu_xBi_yWO_6$  show similar features, and exhibit the characteristic emission originated from the transition between the excited state  $5D_0$  to the ground state  $7F_J$  ( $J=0,1,2,3,4$ ) of the  $4f_6$  configuration of  $Eu^{3+}$ .

The excitation spectra are characterized by a broad charge-transfer band centered at about 300 nm. The intensity of the charge-transfer band is much larger than the  $7F_0 \rightarrow 5L_6$  (395 nm) transition. An interesting feature of the CBT in the excitation spectrum of  $Y_{1.86}Eu_{1.04}Bi_{0.04}WO_6$  is its extended tail into the near UV range (~ 400 nm). This increase occurs due to extra absorption involving the Bi-O component in addition to Eu-O and W-O charge-transfer bands. The as prepared red phosphors can be used as either energy converters in SSLDs with InGaN-based LED as the excitation source or as ultraviolet-absorbing luminescent converter to improve the light harvesting process for DSSC solar cells.

[1] T. Jüstel; H. Nikols, C. Ronda, *Angew. Chem. Int. Ed.* 37 (1998) 3084.

[2] J. Llanos, D. Olivares, V. Manríquez, D. Espinoza and I. Brito, *J. Alloys and Compd.* 628 (2015) 352

[3] M.N. Huang, Y.Y. Ma, F. Xiao, Q.Y. Zhang, *Spectrochim. Acta, Part A* 120 (2014) 55

[4] N. Kato, Y. Takeda, K. Higuchi, A. Takeichi, E. Sudo, H. Tanaka, T. Motohiro, T. Sano, T. Toyoda, *Sol. Energy Mater. Sol. Cells* 93 (2009) 8903

[5] N.A. McDowell, K.S. Knight, P. Lightfoot, *Chem. Eur. J.* 12 (2006) 1493

**Acknowledgment:** The authors acknowledge Fondecyt-Chile for financial support (Grant 1130248).



## LUMINESCENCE AND SCINTILLATION PROPERTIES OF A Cs<sub>3</sub>BiCl<sub>6</sub> CRYSTAL

Makoto Shimizu<sup>a</sup>, Masanori Koshimizu<sup>a</sup>, Yutaka Fujimoto<sup>a</sup>, Takayuki Yanagida<sup>b</sup>,  
Shingo Ono<sup>c</sup>, and Keisuke Asai<sup>a</sup>

<sup>a</sup>*Department of Applied Chemistry, Tohoku University, 6-6-07 Aoba, Aramaki, Aoba-ku, Sendai 980-8579, Japan, koshi@qpc.che.tohoku.ac.jp*

<sup>b</sup>*Graduate School of Materials Science, Nara Institute of Science and Technology, 8916-5 Takayama-Cho, Ikoma, Nara 630-0192, Japan, t-yanagida@ms.naist.jp*

<sup>c</sup>*Department of Mechanical Engineering, Nagoya Institute of Technology, Gokiso-cho, Showa-ku, Nagoya, Aichi 466-8555, Japan, ono.shingo@nitech.ac.jp*

Bi-based inorganic crystals are potentially applicable as scintillation materials for high-energy photon detection because the atomic number of Bi is large (83). Therefore, Bi-based compounds generally have a high effective atomic number, leading to the ability to stop high-energy photons such as gamma rays.

In this paper, we report the optical and scintillation properties of a Cs<sub>3</sub>BiCl<sub>6</sub> single crystal. Because this compound has an effective atomic number of 60, it is expected to have high stopping power for high-energy photons. We analyzed the luminescence and scintillation properties of this compound.

Single crystals of Cs<sub>3</sub>BiCl<sub>6</sub> were grown by the Bridgman-Stockbarger method. First, a stoichiometric amount of CsCl (99.999%, High-purity Chemical, Japan) and BiCl<sub>3</sub> (99.99%, High-purity Chemical, Japan) were well mixed and dried at 453 K in vacuum for one night in order to remove adsorbed water. The crystals were grown in vacuum in sealed quartz tubes. The temperature gradient during the growth was estimated to be approximately 1 K/h. The crystal was not hygroscopic, and all the measurements were performed in air. In addition, thin films of Cs<sub>3</sub>BiCl<sub>6</sub> were prepared on quartz substrates by the pulsed laser deposition method and were used to measure the absorption spectra.

In the absorption spectrum of the Cs<sub>3</sub>BiCl<sub>6</sub> thin film, two significant absorption peaks were observed at approximately 220 nm (=5.64 eV) and 330 nm (=3.76 eV). A previous paper on Bi<sup>3+</sup>-doped Cs<sub>2</sub>NaLaCl<sub>6</sub> [1] reported two transitions, i.e., a <sup>1</sup>A<sub>1g</sub>→<sup>3</sup>T<sub>1u</sub> transition at 3.80 eV and a <sup>1</sup>A<sub>1g</sub>→<sup>1</sup>T<sub>1u</sub> transition at 5.60 eV. Based on the similarity, the absorption peaks at 220 nm and 330 nm are ascribed to the <sup>1</sup>A<sub>1g</sub>→<sup>1</sup>T<sub>1u</sub> transition and the <sup>1</sup>A<sub>1g</sub>→<sup>3</sup>T<sub>1u</sub> transition of Bi<sup>3+</sup>, respectively.

In the luminescence spectra of the Cs<sub>3</sub>BiCl<sub>6</sub> single crystal at low temperatures, a strong band was observed at approximately 390 nm. In the previous paper [1], broad quadruplet emission peaks at approximately 3.63 eV (=342 nm) in Cs<sub>2</sub>NaLaCl<sub>6</sub>:Bi<sup>3+</sup> were reported, which were ascribed to the <sup>3</sup>T<sub>1u</sub>→<sup>1</sup>A<sub>1g</sub> transition of Bi<sup>3+</sup>. We tentatively ascribe the peak at 390 nm to the same origin.

In the scintillation spectrum of the Cs<sub>3</sub>BiCl<sub>6</sub> single crystal excited by X-ray, we observed the peaking of two significant bands at approximately 400 nm and 600–700 nm. The band that peaked at 400 nm is ascribed to the same transition as that of the luminescence band at 390 nm. The band that peaked at 600–700 nm is ascribed mainly to the <sup>1</sup>T<sub>1u</sub>→<sup>3</sup>T<sub>1u</sub> transition according to ascription of a band at 1.74 eV in Cs<sub>2</sub>NaLaCl<sub>6</sub>:Bi<sup>3+</sup> to the <sup>1</sup>T<sub>1u</sub>→<sup>3</sup>T<sub>1u</sub> transition [1]. The observation of this band only in the case of scintillation may be related to different deexcitation processes between photoluminescence and scintillation.

[1] A. Wolfert, G. Blasse, J. Solid State Chem., 59 (1985) 133–142.

## LUMINESCENCE OF CO-DOPED $\text{Sr}_5\text{MgLa}_2(\text{BO}_3)_6:\text{Ce}^{3+},\text{Mn}^{2+}$ PHOSPHOR

Matthias Müller, Stefan Fischer, Thomas Jüstel

*Department of Chemical Engineering, Münster University of Applied Sciences,  
Stegerwaldstr. 39, 48565 Steinfurt, Germany,  
matthias\_mueller@fh-muenster.de; tj@fh-muenster.de*

Since the development of bright blue emitting LEDs by Nakamura *et al.* LEDs replace more and more common light bulbs and fluorescence lamps in domestic lighting [1]. This is due to the benefits LEDs possess compared to the common light sources. Usually, LEDs provide longer lifetimes, higher wall plug efficiency, as well as a higher colour rendering [2,3]. These days, most of the white emitting LEDs consist of a blue emitting (In,Ga)N-chip pumping a green emitting phosphor, *e.g.*  $(\text{Y,Gd})_3\text{Al}_5\text{O}_{12}:\text{Ce}^{3+}$ . Due to the green emission, this set-up provides a high luminous efficacy. On the other side these lamps suffer from a low colour rendering index and also a high colour temperature because of the deficiency of emission in the red spectral range [4]. A potential approach to avoid these drawbacks is the application of an ultraviolet (UV) emitting LED pumping a blend consisting of a blue, green, and red phosphor. This approach can provide warm and cold white emitting light sources with excellent colour points [5]. Unfortunately, these systems incur a loss in blue emission due to re-absorption by the green and red phosphor. Therefore, many research groups presently develop single phased white emitting phosphors pumped by UV LEDs. One option to realize such a white emitting phosphor is to use the ion couple  $\text{Ce}^{3+}$  and  $\text{Mn}^{2+}$ . The broad emission bands of  $\text{Ce}^{3+}$  and  $\text{Mn}^{2+}$  in many host materials can complement each other to white light due to additive colour mixing.

To investigate the photoluminescence (PL) of  $\text{Ce}^{3+}$  and  $\text{Mn}^{2+}$  in co-doped  $\text{Sr}_5\text{MgLa}_2(\text{BO}_3)_6$  a series of powder samples with various  $\text{Mn}^{2+}$  concentrations was synthesized *via* high temperature solid state reaction. Phase purity of the samples was investigated using X-ray powder diffractometry. Diffuse reflectance measurements reveal the optical properties of the synthesized phosphor powders. PL properties were evaluated by recording emission and excitation spectra. Moreover, fluorescence lifetime measurements were performed. Temperature behaviour of PL was investigated recording PL spectra as well as executing fluorescence lifetime measurements from 100 to 500 K.

It turned out that co-doped  $\text{Sr}_5\text{MgLa}_2(\text{BO}_3)_6:\text{Ce}^{3+},\text{Mn}^{2+}$  possesses two emission bands in the blue and red spectral range. The blue emission band was assigned to the completely allowed  $[\text{Xe}]5d^1 \rightarrow [\text{Xe}]4f^1$  ( $^2F_{5/2,7/2}$ ) transition of  $\text{Ce}^{3+}$ . The red emission band was designated to the relaxation from the excited  $^4T_1(^4G)$  state to the  $^6A_1(^6S)$  ground state. Furthermore, it was found that thermal quenching of the photoluminescence is primarily caused by the  $\text{Mn}^{2+}$  ions.

[1] S. Nakamura, P. Stephen, F. Gerhard, *The Blue Laser Diode: The Complete Story*, Springer-Verlag, Berlin/Heidelberg, 1997.

[2] C. Feldmann, T. Jüstel, C. R. Ronda, P. J. Schmidt, *Adv. Funct. Mater.* 13 (2003) 511–516.

[3] E. F. Schubert, J. K. Kim, *Science* 308 (2005) 1274-1278.

[4] H. S. Jang, W. B. Im, D. C. Lee, D. Y. Jeon, S. S. Kim, *J. Lumin.* 126 (2007) 371-377.

[5] Y. Uchida, T. Taguchi, *Opt. Eng.* 44 (2005) 124003.

## LUMINESCENCE OF InP/ZnS QUANTUM DOTS IN NANOPOROUS ANODIC ALUMINA

Sergey S. Savchenko, Ilya A. Weinstein, Alexander S. Vokhmintsev, Denis O. Ilin  
*Ural Federal University, Mira str., 19, Yekaterinburg, Russia, s.s.savchenko5@gmail.com*

Semiconductor nanocrystals or quantum dots (QDs) are functional nanomaterial with unique electrical and optical properties due to quantum-confinement effect in all three dimensions. At present, applications of QDs for color conversion to design white LEDs are investigated, in particular on the basis of non-toxic compounds of III-V elements. To create such luminescent composites the use of wide-band solids is promising as active substrate. Thus, the aim of the work is to study photoluminescence (PL) of the InP/ZnS QDs deposited into anodic aluminum oxide (AAO) matrices.

Investigated InP/ZnS QDs (labeled GA-150, Nanotech-Dubna Centre) had average size of 25 nm. Its three-layer structure consisted of the core of InP, the first shell of ZnS, the second one of polyethylene glycol with functionally active amino groups for ligand binding. Nanoporous matrices of Al<sub>2</sub>O<sub>3</sub> were obtained by two-step anodizing industrial Al foil at the constant current using ethane diacid electrolyte. Four samples were synthesized with the average pore size  $\approx$  50 nm. Three AAO matrices were annealed at 500 °C, 700 °C and 900 °C for 5 hours in ambient atmosphere. All the samples had amorphous structure in accordance with the X-ray diffraction analysis data. To deposit QDs the annealed substrates were placed in a InP/ZnS colloidal solution and treated in an ultrasonic bath Eurosonic 4D for 1 hour. Finally, the samples were disintegrated into powder in a mortar.

PL measurements of the samples were carried out by Perkin Elmer LS 55 luminescent spectrometer in fluorescence mode. Synthesized powders were fixed on silver plates to detect spectra. Measurements of the intrinsic fluorescence of QDs were performed for dry InP/ZnS precipitate, which was produced by coating and evaporation of the colloidal solution on Ag plate at room temperature.

The fluorescence spectra of annealed AAO are characterized by wide bands in the 2 - 4 eV range with the maxima of 2.77 eV (500 °C) and 2.93 eV (700 °C). QDs exhibit intrinsic emission with  $E_m = 2.26$  eV and FWHM = 0.23 eV. It is shown that the measured spectra of the synthesized phosphors contain luminescence band of the InP/ZnS. This fact testifies to the preservation of the integrity of the zinc sulfide shell and as a result, a reliable passivation of the QD surface. Thus, fluorescent properties of the quantum dots are found to be retained and the InP/ZnS@AAO composite structures are successfully synthesized. Chromaticity coordinates are calculated for all samples used. The color region covered by varying QD concentration and AAO annealing temperature up to 900°C are evaluated. The applications of the obtained structures for fabrication solid state emitters with adjustable color are discussed.

## LUMINESCENCE OF NEUTRON-IRRADIATED BERYLLIUM OXIDE CRYSTALS

Maxim D. Petrenko<sup>a</sup>, Igor N. Ogorodnikov<sup>a</sup>, Vladimir Yu. Ivanov<sup>a</sup>, Alexander V. Kruzhalov<sup>a</sup>

<sup>a</sup>*Ural Federal University, Mira St. 19, Yekaterinburg, Russia, md.petrenko@urfu.ru*

Beryllium oxide is well-known optical material for use in solid state dosimetry using both the thermoluminescence (TL) and optically-stimulated luminescence (OSL) methodologies. At present, many research groups are actively engaged in the study of the luminescence properties of beryllium oxide and the improvement of its dosimetric characteristics [see, for example [1]]. Similar to  $\alpha$ -Al<sub>2</sub>O<sub>3</sub> the creation of color centers in BeO leads to essential changes of its dosimetric properties [2]. In this work promising results were obtained in thermochemical additive coloration of BeO single crystals. However, apart from the thermochemical coloration there can also be possible a process of radiation-induced creation of lattice defects in the crystals.

The aim of this work is to study BeO single crystals irradiated with neutrons. All the crystals were grown by V.A.Maslov using flux method. We investigated the defect structure of irradiated BeO samples using experimental facilities of Experimental Physics Department of Ural Federal University. Spectra of optical absorption, photoluminescence, x-ray induced luminescence, and ESR were obtained under various experimental conditions at  $T=6$  K and room temperature. Thermoluminescence glow curves were investigated over the temperature range from  $T=6$  K up to  $T=800$  K.

PL emission band at 3.9 eV was found in the photoluminescence spectra. This band has been attributed to the emission of F<sup>+</sup> centers in beryllium oxide. The appropriate PL excitation band was found at 5.4 eV [3]. Additional information about the structure of the samples was obtained using X-ray induced luminescence and ESR spectroscopy techniques.

The presence of F<sup>+</sup> centers in the samples suggests that radiation exposure of BeO crystals also leads to the creation of color centers. Further studies aimed at expanding the information about the defects in these crystals and radiation coloration of single crystals using other methods of radiation impact.

[1] A.Jahn, M.Sommer, W.Ullrich, M.Wickert, J.Henniger, Radiation measurements, 56 (2013) 324.

[2] D.S.Tausenev, I.I.Milman, V.Yu.Ivanov, A.V.Kruzhalov, Radiation measurements, 43 (2008) 349.

[3] I. Ogorodnikov, A. Kruzhalov, Material Science Forum, 239-241 (1997) 51

## LUMINESCENCE OF RARE EARTH IONS IN PHOSPHATE GLASSES

Marta Soltys<sup>a</sup>, Joanna Pisarska<sup>a</sup>, Joanna Janek<sup>a</sup>, Lidia Żur<sup>a</sup>, Wojciech A. Pisarski<sup>a</sup>

<sup>a</sup>*Institute of Chemistry, University of Silesia, Katowice, Poland, martasoltys@interia.pl*

In recent years, the rare earth-doped phosphate glasses have been interested to industrial applications. Among oxide glasses, the systems based on P<sub>2</sub>O<sub>5</sub> are used in optoelectronics, and they are suitable for the fabrication of optical fibers, great importance in optical data transmission, detection, sensing and laser technologies [1]. Their application capabilities are caused by transparency in a wide spectral range, from the ultraviolet to the infrared. Furthermore, these systems have unique characteristics, for example low melting point, low refractive index and low dispersion [2]. On the other hand, disadvantages are hygroscopic properties of P<sub>2</sub>O<sub>5</sub> because contribute to the lower luminescence for rare earth-doped phosphate glasses [3].

This work presents the results for rare earth-doped phosphate glasses prepared in a glove box and then the fully amorphous samples studied using optical spectroscopy. Visible and near-infrared luminescence spectra for rare earth ions in phosphate glasses were registered. Moreover, luminescence lifetimes for the upper excited state of rare earth were also evaluated. An analysis of several spectroscopic parameters are necessary to characterize glass host in relation to potential applications for optoelectronic devices. Therefore, spectroscopic parameters like the phonon energy of the glass host, the luminescence linewidth, the measured lifetime and the fluorescence intensity ratio R/O of Eu<sup>3+</sup> ions and Y/B of Dy<sup>3+</sup> ions were determined. Furthermore, correlation between structural changes in the glass matrix of systems based on P<sub>2</sub>O<sub>5</sub> and spectroscopic properties of Ln<sup>3+</sup> ions can be made.

[1] C.C Santos, I. Guedes, C-K. Loong, L.A. Boatner, A.L. Moura, M.T. de Araujo, C. Jacinto, M.V.D. Vermelho, J. Phys. D: Appl. Phys. 43 (2010) 025102.

[2] K. Linganna, C.K. Jayasankar, Spectrochim. Acta A 97 (2012) 788-797.

[3] I.A.A. Terra, A.S.S. de Camargo, L.A. de O. Nunes, R.A. Carvalho, S.M. Li, J. Appl. Phys. 100 (2006) 123103.

## LUMINESCENCE PROPERTIES AND INFLUENCE OF AGING TIME ON STRUCTURE OF Sr<sub>3</sub>SiO<sub>5</sub> DOPED WITH Eu<sup>3+</sup> AND Eu<sup>2+</sup>

J. Barzowska<sup>a</sup>, N. Górecka<sup>b</sup>, K. Szczodrowski<sup>c</sup>, M. Grinberg<sup>d</sup>

<sup>a</sup> *Institute of Experimental Physics, University of Gdansk, Wita Stwosza 57, 80-952 Gdansk, Poland, fizjb@ug.edu.pl*

<sup>b</sup> *Institute of Experimental Physics, University of Gdansk, Wita Stwosza 57, 80-952 Gdansk, Poland, natalia.gorecka@ug.edu.pl*

<sup>c</sup> *Institute of Experimental Physics, University of Gdansk, Wita Stwosza 57, 80-952 Gdansk, Poland, fizks@ug.edu.pl*

<sup>d</sup> *Institute of Experimental Physics, University of Gdansk, Wita Stwosza 57, 80-952 Gdansk, Poland, fizmgr@ug.edu.pl*

Although the Sr<sub>3</sub>SiO<sub>5</sub>: Eu<sup>2+</sup> material is known, there is no information regarding spectral properties of Sr<sub>3</sub>SiO<sub>5</sub>: Eu<sup>3+</sup> and Sr<sub>3</sub>SiO<sub>5</sub>: Eu<sup>3+</sup>, Eu<sup>2+</sup>, therefore we made an attempt to obtain such material in pure phase. Sr<sub>3</sub>SiO<sub>5</sub> doped with Eu<sup>2+</sup> and Eu<sup>3+</sup> was obtained using solid state synthesis method. Due to problems related to synthesis of Sr<sub>3</sub>SiO<sub>5</sub> matrix, we examined one of the synthesis conception, which was described in literature. Therefore, a group of materials obtained by using different concentration of SiO<sub>2</sub> (from 0,95 to 1 mol) was synthesized to investigate the influence of silica concentration on phase composition. A two-step synthesis was applied. This synthesis involves an initial annealing of mixture of reagents under inert gas atmosphere and their reduction under hydrogen/nitrogen atmosphere. The phase composition analysis as well as spectroscopic measurements of products were performed to characterize the obtained phosphors. The XRD patterns show that all obtained products contain additional impurity phases, apart from expected Sr<sub>3</sub>SiO<sub>5</sub>. Emission spectra of materials obtained after first step of the synthesis consist of narrow bands, which are characteristic for f-f transitions in Eu<sup>3+</sup> ion. The emission spectra of materials, which were obtained after reduction process, are characterized by the intensive, broad band attributed to the d-f transitions in Eu<sup>2+</sup>. However in few cases, the complete reduction did not occur and the bands of Eu<sup>3+</sup> can be still observed.

Preliminary research concerning the influence of aging time on the material structure was also performed. It was noticed that with aging time the XRD patterns of materials have changed. The SrO was replaced with Sr(OH)<sub>2</sub>•H<sub>2</sub>O, due to reaction of SrO with the H<sub>2</sub>O from the moisture and additional reflects appeared. The materials were found to be unstable.

[1] L.Chen, A.Luo, Y.Jiang, F.Liu, X.Deng, S.Xue, X.Chen, Y.Zhang. *Materials Letters*. 106 (2013) 428-431.

[2] C.Shen, Y.Yang, S.Jin, J.Ming, H.Feng, Z.Xu. *Optik* 121 (2010) 1487-1491.

[3] Z.Wang, B.Yang, P.Li, Z.Yang, Q.Guo. *Physica B* 407 (2012) 1282-1286.

[4] C.Guang, L.Quansheng, C.Liqun, L.Liping, S.Haiying, W.Yiqing, B.Zhaohui, Z.Xiyan, Q.Guanming.

*JOURNAL OF RARE EARTHS*, Vol. 28, No. 4, Aug. 2010, p. 526

[5] W.Xiaochun, Z.Xiyan, W.Chen, Q.Weida, S.Jiaxun. *JOURNAL OF RARE EARTHS*, Vol. 31, No. 5, May 2013, P. 456

## LIGHT EMISSION FROM IONIC NHC-CYCLOPLATINATED COMPOUNDS

Andres Chueca<sup>a</sup>, Sara Fuertes<sup>a</sup>, Violeta Sicilia<sup>a</sup>.

<sup>a</sup>*Instituto de Síntesis Química y Catálisis Homogénea (ISQCH), CSIC - Universidad de Zaragoza, Departamento de Química Inorgánica, Facultad de Ciencias, Pedro Cerbuna 12, 50009 Zaragoza, España., achueca@unizar.es*

The use of  $[\{\text{Pt}(\mu\text{-Cl})(\eta^3\text{-2-Me-C}_3\text{H}_4)\}_2]$  as starting material allowed to accomplish a step by step cyclometallation of the NHCs<sup>[1]</sup> through the intermediate carbene complexes  $[\text{PtCl}(\eta^3\text{-2-Me-C}_3\text{H}_4)(\text{HC}^{\wedge}\text{C}^*-\kappa\text{C}^*)]$  (1A,  $\text{HC}^{\wedge}\text{C}^*-\kappa\text{C}^*=1\text{-}(4\text{-cyanophenyl})\text{-3-methyl-1}H\text{-imidazol-2-ylidene}$  (A); 1B,  $\text{HC}^{\wedge}\text{C}^*-\kappa\text{C}^*=3\text{-methyl-1-(naphthalen-2-yl)-1}H\text{-imidazol-2-ylidene}$  (B)), to give two new NHC-cyclometallated compounds,  $[\{\text{Pt}(\mu\text{-Cl})(\text{C}^{\wedge}\text{C}^*)\}_2]$  ( $\text{HC}^{\wedge}\text{C}^*-\kappa\text{C}^*=A$  (2A), B (2B)). Compounds 2A/2B were used as precursors to get the highly luminescent compounds  $(\text{NBu}_4)[\text{Pt}(\text{C}^{\wedge}\text{C}^*)(\text{CN})_2]$  ( $\text{HC}^{\wedge}\text{C}^*-\kappa\text{C}^*=A$  (3A) (see Figure 1), B (3B)) and  $[\text{Pt}(\text{C}^{\wedge}\text{C}^*)(\text{CNR})_2]\text{PF}_6$  ( $\text{HC}^{\wedge}\text{C}^*-\kappa\text{C}^*=A$ , R = 2,6-dimethylphenyl (4A), <sup>t</sup>Bu (5A); B, R = 2,6-dimethylphenyl (4B), <sup>t</sup>Bu (5B)).

Differences in the luminescent behavior of 3A/B-5A/B were found by modification of both the NHC and the ancillary ligands. To see, solid samples of compounds 3A and 3B show blue and yellow intense phosphorescence respectively ( $\Phi \approx 60\%$ ) (Figure 2) upon excitation at  $\lambda_{\text{exc}} = 365$  nm. On the other hand, the color modulation can be achieved by changing the ancillary ligands. For the isocyanide compounds 4A/B-5A/B the emission color ranges from green (4A) to orange (5A) (Figure 3). TD-DFT calculations for a better insight in the optical properties of these derivatives have been performed.

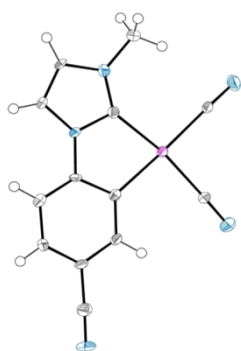


Figure 1. X-ray crystal structure of 3A.

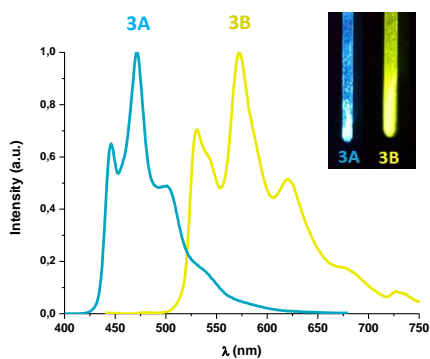


Figure 2. Normalized emission spectra of 3A and 3B in solid state at 298 K.

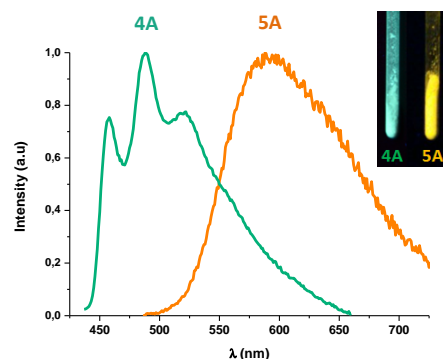


Figure 3. Normalized emission spectra of 4A and 5A in solid state at 298 K.

[1] S. Fuertes, H. García, M. Perálvarez, W. Hertog, J. Carreras, V. Sicilia, Chem. Eur. J. 21 (2015) 1620-1631.

## INVESTIGATION OF PHYSICAL AND CHEMICAL PROPERTIES OF WO<sub>3</sub>-FILMS OBTAINED BY SOL-GEL METHOD

Alexandr O. Trofimov, Elena V. Kolobkova, Nikolay V. Nikonorov  
*ITMO University, 4 Birjevaya line, Saint Petersburg, Russia, exeptional777@mail.ru*

The effect of changes in the conditions of sol-gel method [1] on the thermal characteristics and the structure electrochromic (EC) a-WO<sub>3</sub> films has been studied. DSC data has showed greater sensitivity of the structure to the peculiarities of the drying of the product poliperoxotungstic acid (fig. 1). The films were transparent over a wide range ( $E_g = 2,5$  eV).

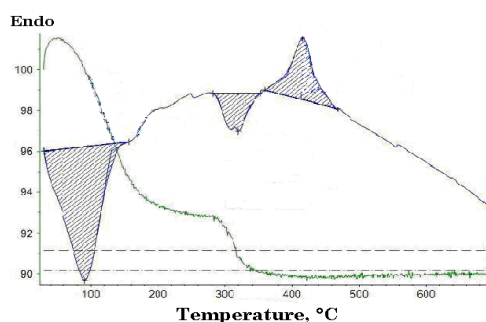


Fig. 1 – DSC films WO<sub>3</sub>, obtained at different drying conditions

All compositions were amorphous as measured by X-rays [2] diffraction (fig. 2). The presence in the structure of amorphous transparent glassy semiconductor a-WO<sub>3</sub> predominantly tetrahedral [WO<sub>4</sub>] groups was concluded based on the IR and Raman spectroscopy [3] dates. The precursor product and EC-films are glass material obtained by the sol-gel process with the composition WO<sub>3</sub> \* x H<sub>2</sub>O. Synthesis peculiarities of mesoporous a-WO<sub>3</sub> affects both the pore structure, which determines the concentration of the aqueous components and the ratio of the bridging W-O-W and unbridged W=O bonds, defining characteristics of the electrochromic materials.

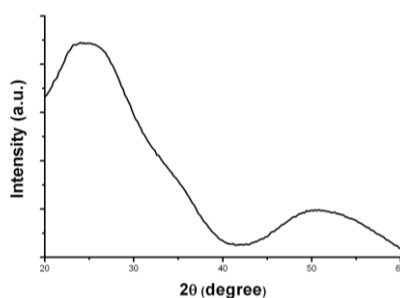


Fig. 2 – X-ray diffraction of the film obtained by sol-gel deposition from

- [1] U.S. Krasnov, G.Y. Kolbasov, S.V. Volkov, *Nanosystemi, nanomateriali, nanotehnologii* 6 No3 (2008). 845.
- [2] G.M. Ramans, J.V. Gabrusenoks, A.A. Veispals, *Phys. status solidia* 74 No1 (1982) 41.
- [3] M.H. Brodskii, *Rasseyanie sveta v tverdih telah*, 230 (1979).



## EFFECT OF ANNEALING CONDITIONS ON $\text{Eu}^{3+}$ -DOPED $\text{Gd}_2\text{Ti}_2\text{O}_7$ THIN FILM LUMINESCENCE

Željka Antić<sup>a</sup>, K. Prashanthi<sup>a</sup>, Sanja Čulubrk<sup>b</sup>, Miroslav D. Dramićanin<sup>b</sup> and Thomas Thundat<sup>a</sup>

<sup>a</sup>*Department of Chemical and Materials Engineering, University of Alberta, Edmonton, Canada, \*zeljkaa@gmail.com, antic@ualberta.ca*

<sup>b</sup>*Vinča Institute of Nuclear Sciences, University of Belgrade, P.O.Box 522, 11001 Belgrade, Serbia*

There is a growing interest in thin film phosphors due to their potential application in integrated optical and optoelectronic devices, active waveguides, energy-saving lighting, solar energy conversion, X-ray imaging and displays. Pulsed laser deposition (PLD) is a well-known, fast and effective technique to grow thin-films of complex-oxide materials. This technique uses short and intensive pulsed laser to transfer the material from a solid source to a substrate by evaporation without losing its stoichiometry.

Herein we will give detailed instructions on how to synthesize and design  $\text{Eu}^{3+}$ -doped  $\text{Gd}_2\text{Ti}_2\text{O}_7$  luminescent thin films by the PLD technique. Due to the high transparency requirements, quartz glass was used as a substrate for deposition. Thin films structure, morphology and optical properties were investigated, discussed and correlated. As-deposited films were of amorphous nature and with additional thermal treatment they become crystalline. Detail investigation of structural formation done in small,  $50^\circ\text{C}$  steps, showed that samples treated up to  $1000^\circ\text{C}$  show presence of secondary, non-pyrochlore phases. Pyrochlore phase is obtained at  $1000^\circ\text{C}$ , and in order to remove any minor impurities and to get well crystalline, pure-phase thin films, samples were heated at  $1050^\circ\text{C}$  and  $1100^\circ\text{C}$  also. Cross-sectional SEM of crystalline samples show relatively dense films, with uniform thickness ( $\sim 650$  nm) and grain size distribution in agreement with AFM results. Photoluminescent spectroscopy showed typical red emission of  $\text{Eu}^{3+}$  ions.

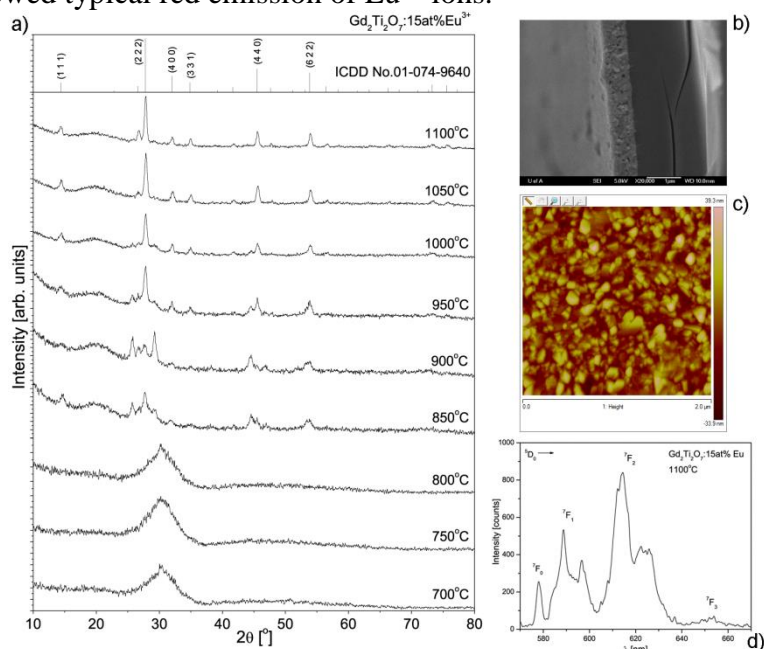


**Figure 1** a) XRD diffractograms, b) cross-sectional SEM, c) atomic force microscopy and d) photoluminescent emission spectrum of  $\text{GTO:15at\%Eu}^{3+}$  thin films.

## MULTISITE EXCITATION AND EMISSION PROPERTIES OF THE Nd<sup>3+</sup> AND Lu<sup>3+</sup> DOPED CaF<sub>2</sub> LASER CRYSTALS

S. Normani<sup>a</sup>, A. Braud<sup>a</sup>, J.L. Doualan<sup>a</sup>, R. Moncorgé<sup>a</sup>, C. Maunier<sup>b</sup>, D. Penninckx<sup>b</sup> and P. Camy<sup>a</sup>

<sup>a</sup>Centre de recherche sur les Ions, les Matériaux et la Photonique (CIMAP), UMR 6252 CEA-CNRS-ENSICAEN, Université de Caen, 6 Blvd Maréchal Juin, 14050 Caen, France  
simone.normani@ensicaen.fr

<sup>b</sup>CEA CESTA, 15 avenue des Sablières, CS 60001, 33116 Le Barp Cedex, France

It was recently demonstrated that efficient and broadband laser emission was possible with Nd-doped CaF<sub>2</sub> and SrF<sub>2</sub> single crystals around 1.055μm [1-3]. Such laser emission, known as completely quenched because of cross-relaxation in the singly doped materials [4], increases spectacularly by co-doping with non-optically active “buffer” ions like Y<sup>3+</sup> or Lu<sup>3+</sup>. Broadband laser emission and ultra-short laser operation could be already demonstrated [5] and large scale high peak power diode-pumped amplifiers can be anticipated. A deep investigation of both spectral and dynamical properties of CaF<sub>2</sub>:Nd<sup>3+</sup> crystals co-doped with various amounts of Lu<sup>3+</sup> was performed via conventional spectroscopy techniques including absorption, fluorescence and emission lifetime measurements: the results suggest that an increase in Lu<sup>3+</sup> concentration tends to increase the efficiency of Nd<sup>3+</sup> transitions, interpreted as a consequence of cluster breaking by the buffer ions. By employing the parameters from previous data, time-resolved spectroscopy has been employed in order to isolate the different centres, discerning them by their lifetime, main absorption peak and emission line. Two different spectra resulted from these measurements, and linear combinations of the two have been seen to recover fairly faithfully the different emission spectra at different co-doping levels and excitation wavelengths, as shown in figure 1.

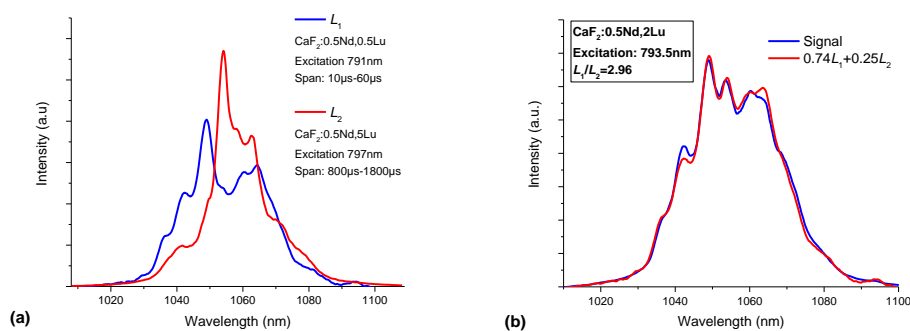


Fig. 1. Time-resolved measurements of CaF<sub>2</sub>:Nd, Lu. (a) Spectra of isolated luminescent centre types. (b) reconstruction of a fluorescence spectrum via a linear combination of the “pure” single-centre ones.

- [1] J. L. Doualan, L. B. Su, G. Brasse, A. Benayad, V. Ménard, Y. Y. Zhan, A. Braud, P. Camy, J. Xu, and R. Moncorgé, *J. Opt. Soc. Am. B* 30 (11), pp 3018-3021 (2013)
- [2] L B Su, Q G Wang, H J Li, G Brasse, P Camy, J L Doualan, Braud, R Moncorgé, Y Y Zhan, L H Zheng, X B Qian and J Xu, *Laser Phys. Lett.* 10, 035804 (4pp) (2013)
- [3] M. Jelínek, V. Kubeček, L. Su, D. Jiang, F. Ma, Q. Zhang, Y. Cao and J. Xu, *Laser Phys. Lett.* 11, 055001 (4pp) (2014)
- [4] S. A. Payne, J. A. Caird, L. L. Chase, L. K. Smith, N. D. Nielsen, and W. F. Krupke, *J. Opt. Soc. Am. B* 8 (4) pp 726-740 (1991)
- [5] Z. P. Qin, G. Q. Xie, J. Ma, W. Y. Ge, P. Yuan, L. J. Qian, L. B. Su, D. P. Jiang, F. K. Ma, Q. Zhang, Y. X. Cao, and J. Xu, *Opt. Lett.* 39 (7) 1737-1739 (2014)

## GRAPHENE UNROLLED FROM MULTI-WALLED CARBON NANOTUBES BY HIGH-INTENSITY ULTRASOUND

Jiří Henych<sup>a</sup>, Václav Štengl<sup>a</sup>, Petra Ecorchard<sup>a</sup>, Hynek Beneš<sup>b</sup>

<sup>a</sup>*Materials Chemistry Department, Institute of Inorganic Chemistry AS CR v.v.i., 25068 Řež, Czech Republic, henych@iic.cas.cz*

<sup>b</sup>*Institute of Macromolecular Chemistry AS CR v.v.i., 16206 Praha, Czech Republic*

2D single- or thin-layer graphene sheets are predicted for many applications thanks to its extraordinary mechanical, thermal, electrical, as well as optical and optoelectronic properties. Despite a myriad of demonstrated methods of graphene preparation a good balance of quality, productivity and cost remain unsolved. An interesting method for obtaining graphene can be “unrolling” or “unzipping” of carbon nanotubes. Multi-walled carbon nanotubes (MWCNT's) can be cut and unzipped to produce curved graphene nanosheets with enhanced supercapacitor performance [1]. Two-step solution-based method was advantageously used for unrolling of “cup-stacked” carbon nanotubes and relatively high-quality graphene was produced [2]. Recently, we participated on unrolling of MWCNT's with ionic liquids for epoxy-based nanocomposites [3]. Power ultrasound can be also employed for production of low dimensional materials, as was demonstrated in our previous studies, such as production of graphene from graphite [4], preparation of luminescent graphene [5], BN and BCN [6], or MoS<sub>2</sub> [7] quantum dots. Here, we introduce relatively easy process of using power ultrasound in a pressurized reactor for unrolling of MWCNT's to produce graphene flakes. Ultrasonication of suspension of MWCNT's in ethylene glycol lead to gradual unrolling of nanotubes and individual sheets of graphene are obtained as can be seen in Figure 1. The process can be controlled by time of ultrasonication, temperature or solvent used. Stabilization of the produced graphene can be controlled by an addition of various ionic liquids which is being now under further investigation.

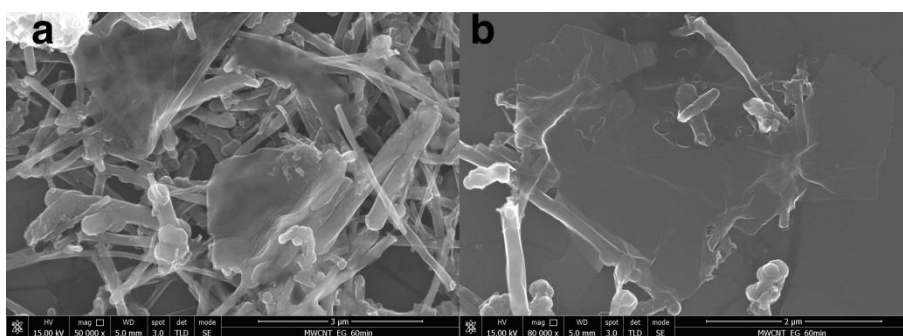


Figure 1. SEM micrographs of ultrasonic unrolling of MWCNT's

- [1] H. Wang, Y. Wang, Z. Hu, X. Wang, *ACS Appl. Mater. Inter.* 4 (2012) 6827–6834.
- [2] Q. Liu, T. Fujigaya, N. Nakashima, *Carbon* 50 (2012) 5421–5428.
- [3] A.C. Kleinschmidt, R.K. Donato, M. Perchaz., et al., *RSC. Adv.* 4 (2014) 43436–43443.
- [4] V. Štengl, *Chem. Eur. J.* 18 (2012) 14047–14054.
- [5] V. Štengl, S. Bakardjieva, J. Henych, K. Lang, M. Kormunda, *Carbon* 63 (2013) 537–546.
- [6] V. Štengl, J. Henych, M. Kormunda, *Sci. Adv. Mater.* 6 (2014) 1106–1116.
- [7] V. Štengl, J. Henych, *Nanoscale* 5 (2013) 3387–3394

## STRUCTURAL AND PHOTOLUMINESCENCE INVESTIGATION OF Pr<sup>3+</sup>-DOPED Gd<sub>2</sub>O<sub>3</sub> NANOMATERIALS BY SOL-GEL PROCESS

M. Seraiche<sup>a, b\*</sup>, L. Guerbous<sup>b</sup>

<sup>a</sup> *Department of Materials and Components, Faculty of Physics, USTHB, BP 32 El alia, Bab Ezzouar 16111, Algiers, Algeria. seraiche28@hotmail.fr, mseraiche@usthb.dz*

<sup>b</sup> *Laser Department, Nuclear Techniques Division, Algiers Nuclear Research Center, 02, bd Frantz Fanon, BP 399, Algiers 16000, Algeria. guerbous@yahoo.fr*

Gd<sub>2</sub>O<sub>3</sub>-sesquioxide has been studied many time as the host matrix for rare earth ions for both down-conversion and up-conversion luminescence phenomena, thanks to its interesting physical properties, such as chemical durability, high melting point (2320 °C), thermal stability and its low phonon energy (600 cm<sup>-1</sup>). In addition, it exhibit a high density of Gd<sub>2</sub>O<sub>3</sub> ( $\rho = 7.6 \text{ g/cm}^3$ ), which make it a suitable candidate for RE-doped for X-ray detector scintillators in imaging systems. Moreover, it is well known that the luminescent behavior of all RE-doped phosphors depends on the morphology, size and synthetic route. In this work, we report the results on structural and photoluminescence of Pr<sup>3+</sup>-doped Gd<sub>2</sub>O<sub>3</sub> nanomaterial. Nano-sized Gd<sub>1-x</sub>Pr<sub>x</sub>O<sub>3</sub> (x=0.5, 1, 2, 4) % mol have been successfully synthesized by sol gel method. X-ray powder diffraction (XRD), FT-IR, steady as well as time-resolved photoluminescence (PL) spectroscopy techniques were employed to characterize the obtained samples. It is found that 0.5 % concentration of Pr<sup>3+</sup> presents the quenching point of emission in Gd<sub>2</sub>O<sub>3</sub> host. Under UV excitation ( $\lambda_{ex}=230 \text{ nm}$ ), a number of emission peak in the red region assigned to <sup>1</sup>D<sub>2</sub>→<sup>3</sup>H<sub>4</sub> intraconfigurational transitions of the Pr<sup>3+</sup>. The luminescence decay curves evolution of Gd<sub>1-x</sub>Pr<sub>x</sub>O<sub>3</sub> monitored by <sup>1</sup>D<sub>2</sub>→<sup>3</sup>H<sub>4</sub> were measured and investigated. In addition, the variation of <sup>1</sup>D<sub>2</sub> lifetime in function of Gd<sub>1-x</sub>Pr<sub>x</sub>O<sub>3</sub> grain size studied and discussed.

## PHOTOCATALYTIC PERFORMANCE OF Mg<sub>2</sub>TiO<sub>4</sub> NANOPOWDER

Mina Medić,<sup>a</sup> Marija Vasić,<sup>b</sup> Aleksandra Zarubica,<sup>b</sup> Lidija Trandafilović,<sup>a</sup> Miroslav D. Dramićanin,<sup>a</sup> Jovan M. Nedeljkovića<sup>a</sup>

<sup>a</sup>*Institute of Nuclear Sciences Vinča, P.O. Box 522, 11001 Belgrade, Serbia*

<sup>b</sup>*Department of Chemistry, Faculty of Science and Mathematics, University of Niš, Višegradska 33, 18000 Niš, Serbia*

Magnesium-orthotitanate (Mg<sub>2</sub>TiO<sub>4</sub>) powder consisting of loosely agglomerated Mg<sub>2</sub>TiO<sub>4</sub> nanoparticles with the size of about 10 nm was prepared using Pechini-type synthetic route. Obtained material was characterized using transmission electron microscopy and X-ray diffraction measurements [1,2]. Band gap value of Mg<sub>2</sub>TiO<sub>4</sub> powder was estimated from diffuse reflection data. Possibility to use Mg<sub>2</sub>TiO<sub>4</sub> material for photocatalytic purposes was demonstrated in degradation reaction of organic dye crystal violet.

[1] M. Medić, M. Brik, G. Dražić, Ž. Antić, V. Lojpur, M. D. Dramićanin, J. Phys. Chem. C 119 (2015) 724–730

[2] K. Vuković, M. Medić, M. Sekulić, and M. D. Dramićanin, Adv. Cond. Matter Phys. 2015 (2015) 7

## FABRICATION OF $Y_2O_3$ and $Y_{1.94}Yb_{0.05}Er_{0.01}O_3$ THIN FILMS BY PULSED LASER DEPOSITION

Djordje Veljović<sup>a</sup>, Natalia Mihailescu<sup>b</sup>, Angela Stefan<sup>b</sup>, G. E. Stan<sup>c</sup>, Catalin Luculescu<sup>b</sup>,  
Djordje Janačković<sup>a</sup>, Vesna Đorđević<sup>d</sup>, Miroslav D. Dramićanin<sup>d</sup>, Radenka Krsmanović  
Whiffen<sup>d</sup>, Carmen Ristoscu<sup>b</sup>, Serban Georgescu<sup>b</sup>, Ion N. Mihailescu<sup>b</sup>

<sup>a</sup>*Faculty of Technology and Metallurgy, University of Belgrade, Serbia, e-mail:*  
*djveljovic@tmf.bg.ac.rs*

<sup>b</sup>*National Institute of Lasers, Plasma and Radiation Physics, Magurele, Ilfov, Romania; e-mail:*  
*natalia.serban@inflpr.ro*

<sup>c</sup>*National Institute of Materials Physics, Magurele, RO-077125, Romania*

<sup>d</sup>*Vinca Institute of Nuclear Sciences, University of Belgrade, Serbia, e-mail:*  
*radenka@vinca.rs*

Ultraviolet photons generated by a KrF\*-laser source ( $\lambda=248$  nm) were used for the synthesis by pulsed laser deposition (PLD) of nanometric  $Y_2O_3$  and  $Y_{1.94}Yb_{0.05}Er_{0.01}O_3$  thin films with controlled thickness, stoichiometry and photoluminescence properties. The expelled material was collected onto  $SiO_2$  and Si (100) wafers. We studied the effects of substrate temperature (500°C and 600°C) and Oxygen pressure (1Pa and 10 Pa) on the structural properties of the films. FTIR spectra demonstrated a congruent transfer of material from the target to the substrate. On the basis of FTIR analysis, we selected the regime 1Pa/600°C as the best one for the deposition of doped and undoped  $Y_2O_3$  layers. The deposited structures were characterized from physical-chemical point of view by Scanning Electron Microscopy in top- and cross-view modes, X-Ray Diffraction, Raman spectroscopy, Transmission Electron Microscopy and Energy Dispersive X-Ray Spectroscopy investigations. Optical activity of  $Y_{1.94}Yb_{0.05}Er_{0.01}O_3$  films was proved by photoluminescence and NIR spectroscopies as presented in Figure 1 below.

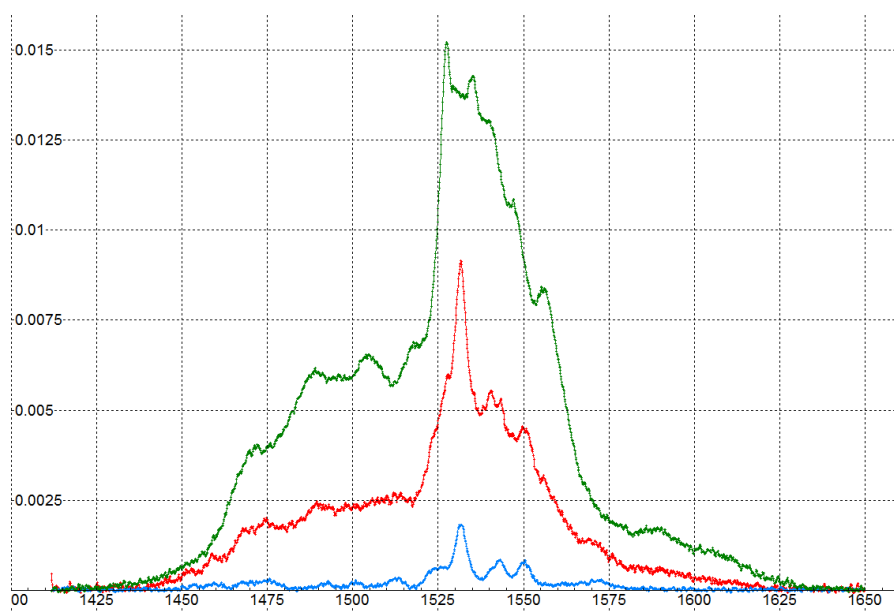


Figure 3 NIR spectra (excitation @980 nm) collected from the  $Y_{1.94}Yb_{0.05}Er_{0.01}O_3$  TFs. Green line –  $SiO_2$  substrate, thermally treated at 600°C; red – Si substrate, 600°C; blue – Si substrate, 500°C.

## SUBSTITUTIONAL METHODS IN SPECTRAL PARAMETERS' MANAGEMENT OF LED GARNET PHOTOLUMINOPHORES

*Naum Soschin<sup>a</sup>, Vladimir Bolshukhin<sup>a</sup>, Vladimir Ulasyuk<sup>b</sup>*

*<sup>a</sup>SRC «Luminophore», <sup>b</sup>Corp. «ELTAN LTD», Fryazino, Russia, v\_n\_ulas@mail.ru*

The most common Solid-State Light sources are binary LEDs based upon InN-GaN-AlN nitride heterostructure covered by heterophase converter layer of polymer media containing phosphor in granular phase. The wide range of the LEDs application requires colorimetric polychromy and spectral variability of the phosphors. Oxide compositions with crystalline garnet structure and  $(\text{Lu})_3\text{Me}^{\text{II}}_2\text{Me}^{\text{III}}_3\text{O}_{12}$  stoichiometric formula are optimal for meeting these spectral and colorimetric demands. Garnet unit cell contains 160 ions with coordination number (CN) 8 in case of lanthanides, CN=6 in case of B, Al, Ga row medium-size ions, or CN=4 in case of small-size ions of Mg, Si, Ti.

Common way of spectrum adjustment in the garnet structure is isovalent substitution of lanthanide ion with d-f transition ion of  $\text{Ce}^{3+}$ . If concentration of substituting  $\text{Ce}^{3+}$  ion in the Y-Gd-Ce-Gd cationic sublattice is low, then spectral maximum shifts by  $\Delta\lambda = \pm 10$  nm with spectrum semi-width shift of  $\Delta\lambda_{0.5}$  which is  $\pm 2$  nm. Isovalent substitution of  $\text{Ln}^{3+}$  in cationic sublattice allows changing spectral maximum in the Y→Gd row from  $\lambda=540$  nm to  $\lambda=580$  nm thus attaining orange-red phosphorescence with Ra=90% light purity whereas the same pattern of substitution in the CN=8 nodes following Y→Lu Y→Yb scheme leads to synthesis of narrow-band luminescent phosphors with green light radiation of  $\lambda=522-530$  nm and  $\Delta\lambda_{0.5}=105$  nm. Such green-radiating phosphor converters for In-GaN structure resulted in creation of LED with intensive green phosphorescence featuring luminous efficacy of  $\eta=180-195$  lm/W.

Homovalent substitution of B→Al→Ga in the CN=6 nodes of the anionic sublattice allows synthesis of luminescent phosphor with high quantum output of  $\eta>0.92$  and luminous efficacy of 160-200 lm/W featuring relatively high level of thermal stability.

Along with homovalent substitution, heterovalent scheme of  $2\text{Al}_{\text{Al}} \rightarrow \text{Mg}_{\text{Al}} + \text{Si}_{\text{Al}}$  is applied to anionic sublattice with CN=4 nodes resulting in bathochromic shift of  $\text{Ce}^{3+}$  luminescence to  $\lambda \approx 620$  nm with warm white light featuring correlated color temperature  $T_c \leq 2700$  K and abnormally wide spectrum half-width of 148 nm (Fig. 1).

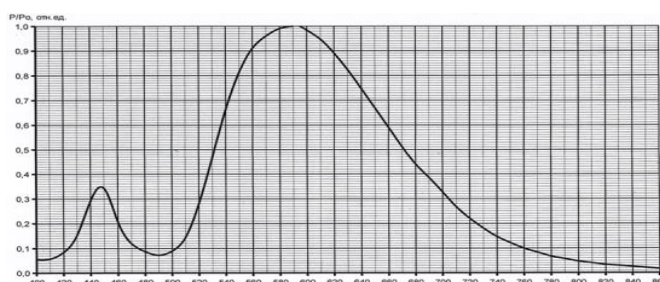


Fig. 1. Abnormally wide radiation spectrum of white binary LED

Heteroatomic substitution schemes of  $2\text{O}_0 \rightarrow \text{Hal}_0 + \text{N}_0 \dots 2\text{O}_0 \rightarrow \text{Hal}_0 + \text{P}_0$  have been proposed for the 96 oxygen nodes in the tetrahedron corners  $[\text{AlO}_4]$  which allowed adjustment spectrum maximum and asymmetry of spectral absorption curve as well.

All luminescent phosphors described above with atomic substitution in the nodes with different CNs allow creating materials with blue, green, yellow, orange, and red radiation featuring  $1500\text{K} < T_c \leq 10000\text{K}$ , high quantum yield and thermal stability.



## X-RAY SENSITIVE DETECTOR WITH A MATRIX OF SILICON PHOTODIODES FOR ENTERING THE X-RAY IMAGE INTO A COMPUTER

Vladimir Ulasyuk, Lyudmila Bikova, Nina Jelyabovskaya,  
Irina Lobanova, Vladimir Shukhtin and Naum Soschin  
*Corp. «ELTAN LTD», Fryazino, Russia, v\_n\_ulas@mail.ru*

Strict requirements are imposed on the main element of the X-ray scanners - X-ray detector for digital tomography (high information capacity, sensitivity in medium-energy X-ray range 22-50 keV, short duration of the afterglow of less than 100 microseconds, high contrast at a resolution of more than 5 line pairs/mm), to meet which we used pixelation of X-ray scintillating layer by separating elements obtained by deep anisotropic plasma etching of silicon wafers with a pitch of square cells of 48 micron and walls of 5...6 microns. The used depth of cells in silicone is 50 to 100 microns, with the mode of tilting silicon walls. The walls are covered with a reflective layer Al up to 0.2 microns thick, which allows to increase the light output from the structure by 80-90%. The cells are filled with X-ray phosphor grains with typical spectrum under X-ray excitation (Fig. 1). Instead of conventionally used CsJ\*TI, that has known disadvantages, heavy-type atomic grain X-ray phosphors are used of  $\sum Ln=(Gd,Lu,Tb,Ce)El_{VI}$  kind, where  $El_{VI}=S, Se, Te$ , while a portion of oxygen ions  $O^{2-}$  is substituted by  $2O_0=Hal_0+Ev$  scheme, where  $Ev N^{3-}$  or  $P^{3-}$ , and  $Hal_0=F^{1-}, Cl^{1-}, Br^{1-}$ .

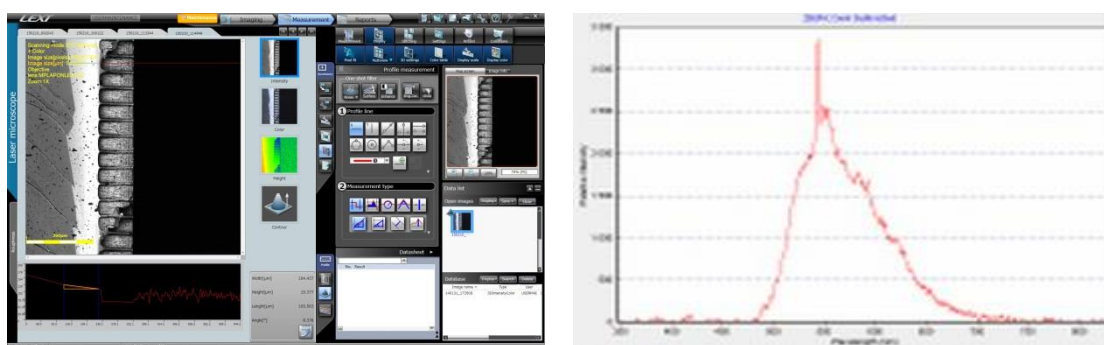


Figure 1. Cells filled with X-ray phosphor in silicon matrix

Also for conversion of X-ray radiation into visible heavy-type atomic compoundings are used with garnet structure and molecular mass of 900 amu with stoichiometric formulas  $(\sum Ln)_3Me^{III}_5O_{12}$ , where  $Me^{III}=Al, Ga, In$  and high effective atomic number of over 65 units. The length of afterglow of materials, activated by elements of Tb, Ce, Y group do not exceed 100 microseconds, allowing you to use the programs of tomosynthesis for creation of high resolution images.

The scintillator is aligned and optically glued with CMOS by RadEye1 photosensor, and provides high contrast and resolution power (Fig.2).



Figure 2. The obtained X-ray image of spine of salted fish



## STRUCTURE AND LUMINESCENCE PROPERTIES OF PURE AND EUROPIUM-DOPED $\text{Zn}_2\text{SnO}_4$

Tamara B. Ivetić<sup>a</sup>, Mirjana R. Dimitrievska<sup>b</sup>, Goran R. Štrbac<sup>a</sup>, Kristina O. Čajko<sup>a</sup>, Ljubica R. Đaćanin<sup>a</sup>, Dragoslav M. Petrović<sup>a</sup>, Svetlana R. Lukić-Petrović<sup>a</sup>

<sup>a</sup>*Department of Physics, Faculty of Sciences, University of Novi Sad, Trg Dositeja Obradovića 4, 21000 Novi Sad, Serbia, tamara.ivetic@df.uns.ac.rs*

<sup>b</sup>*Catalonia Institute for Energy Research (IREC), C. Jardis des les Dones de Negre 1, 08930 Sant Adrià del Besos, Barcelona, Spain, mdimitrievska@irec.cat*

Zinc stannate ( $\text{Zn}_2\text{SnO}_4$ ) is ternary zinc tin oxide transparent n-type semiconductor with a wide band gap [1]. Among numerous applications  $\text{Zn}_2\text{SnO}_4$  spinel has started to be used as the host material for making new red/green emitting phosphor [2]. Europium-doped (1 at. %) nanocrystalline zinc stannate ( $\text{Zn}_2\text{SnO}_4:\text{Eu}^{3+}$ ) was synthesized via high-energy ball-milling solid-state reaction method. The structural and optical properties were investigated in detail using several techniques: X-ray diffraction (XRD), scanning electron microscopy (SEM), Raman and diffuse reflectance spectroscopy (DRS). The PL spectra under UV ray excitation (Fig. 1) displayed strong, broad (green to red) emission where the intensity decreases when doped with europium. This emission does not originate from the band edge of  $\text{Zn}_2\text{SnO}_4$  matrix but from the oxygen vacancies or residual strain cause by preparation procedure [1] so it could be suggested that these intrinsic defects are being reduced with doping. The VIS ray excitation spectra showed PL intensity increase in 2 eV to 2.1 eV region when sample is doped with europium ions probably as a result of a luminescence that originates from lower  $\text{Eu}^{3+}$  ion energy states and could be taken as an indication of a very efficient non radiative relaxation from the matrix to  $^5\text{D}_0$  level of trivalent europium ion. The shift of a PL peak position towards higher energies compared to pure spinel sample is another confirmation of a change in band gap we've noticed from DRS analysis.

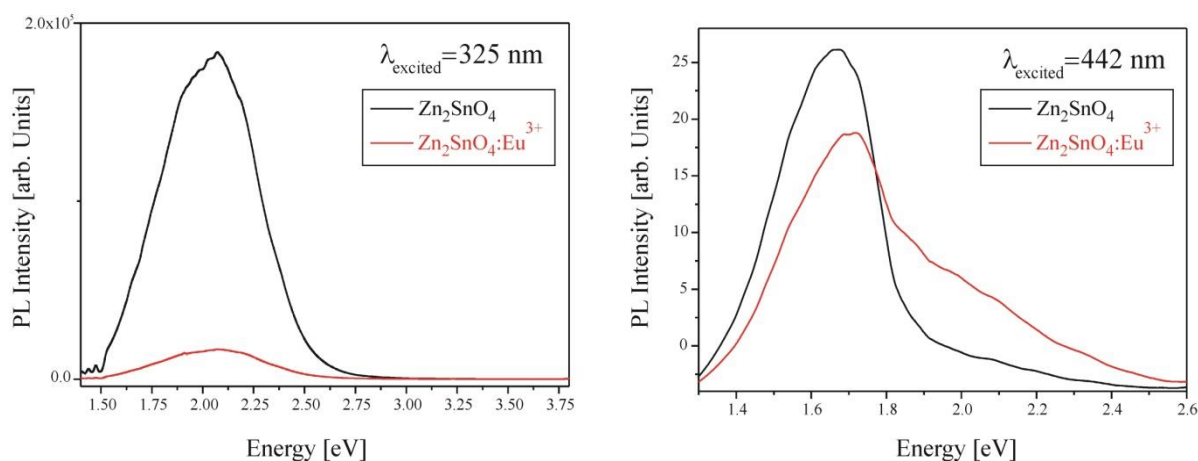


Fig. 1. PL spectra of pure and Eu-doped  $\text{Zn}_2\text{SnO}_4$  under 325 nm and 442 nm excitation.

Acknowledgments: APV Provincial Secretariat for Science and Technological Development and Ministry of Education, Science and Technological Development of the Republic of Serbia.

[1] S. Baruah, J. Dutta, *Sci. Technol. Adv. Mater.* 12 (2011) 013004 (1-18).

[2] Y-C. Chen, Y-H. Chang, B-S. Tsai, *Mater. Transactions* 45 (2004) 1684–1686.

## DIELECTRIC AND STRUCTURAL CHARACTERISTICS OF THE Bi-As<sub>2</sub>S<sub>3</sub> QUASIBINAR CHALCOGENIDES

M.V. Šiljegović<sup>a</sup>, S.R. Lukić Petrović<sup>a</sup>, D.M. Petrović<sup>a</sup>, D. L. Sekulić<sup>b</sup>, G.R. Štrbac<sup>a</sup>,  
F. Skuban<sup>a</sup>

<sup>a</sup>University of Novi Sad, Faculty of Sciences, Department of Physics, Trg Dositeja  
Obradovića 4, 21000 Novi Sad, Serbia, email: mirjana.siljegovic@df.uns.ac.rs

<sup>b</sup>University of Novi Sad, Faculty of Technical Sciences, Trg Dositeja Obradovića 6, 21000  
Novi Sad, Serbia, email: dalsek@yahoo.com

The results of the dielectric constant and dielectric loss measurement of Bi<sub>5</sub>(As<sub>2</sub>S<sub>3</sub>)<sub>95</sub> and Bi<sub>7</sub>(As<sub>2</sub>S<sub>3</sub>)<sub>93</sub> chalcogenides indicated their usual dispersion behavior. On the other hand, significantly higher values of these two parameters were obtained in the entire frequency measuring range (100 Hz-1 MHz), compared to those that generally characterize chalcogenide glasses. Very high dielectric constant obtained for the Bi<sub>7</sub>(As<sub>2</sub>S<sub>3</sub>)<sub>93</sub> sample was explained by charge carrier accumulation due to reduced mobility on the interface between the phases with different conductivity. The results of Raman spectroscopy have shown the complexity of the sample structure. Namely, significant number of narrower peaks observed in Raman spectrum proved the existence of several molecular species or clusters i.e. the occurrence of the phase separation. Also, the absence of the crystallization process in DSC curve of this sample was interpreted as a consequence of existence of the crystalline centers already at room temperature so it is necessary to analyze this composition as a glass-ceramic. Crystallization of the sample with lower bismuth content observed in DSC curve as a two-stage process is the reason why the significant increase of its dielectric constant value at higher temperatures could be attributed to the existence of two types of molecular dipoles that is molecular phase separation. Their identification was made by X-ray diffraction analysis of the annealed sample to the temperature of beginning of the first crystallization process.

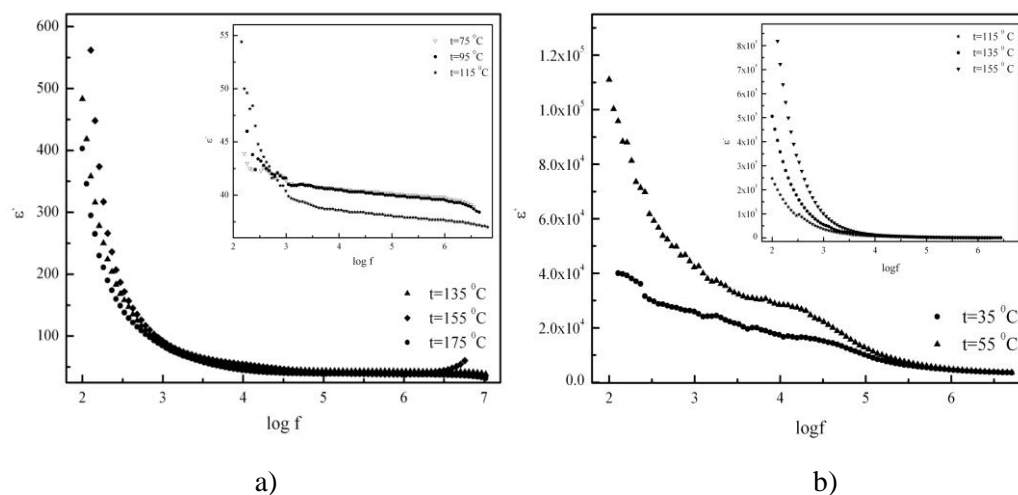


**Fig. 1.** Frequency dependence of dielectric constant for samples at different temperatures:  
a) Bi<sub>5</sub>(As<sub>2</sub>S<sub>3</sub>)<sub>95</sub>; b) Bi<sub>7</sub>(As<sub>2</sub>S<sub>3</sub>)<sub>93</sub>

Acknowledgments: APV Provincial Secretariat for Science and Technological Development and Ministry of Education, Science and Technological Development of the Republic of Serbia.

## RE<sup>3+</sup>-DOPED GdVO<sub>4</sub> THIN FILMS OBTAINED BY PULSED LASER DEPOSITION METHOD

Željka Antić<sup>a</sup>, K. Prashanthi<sup>a</sup>, Dragana Jovanović<sup>b</sup>, Miroslav D. Dramićanin<sup>b</sup> and Thomas Thundat<sup>a</sup>

<sup>a</sup>Department of Chemical and Materials Engineering, University of Alberta, Edmonton, Canada, \*zeljkaa@gmail.com, antic@ualberta.ca

<sup>b</sup>Vinča Institute of Nuclear Sciences, University of Belgrade, P.O.Box 522, 11001 Belgrade, Serbia

This report gives detailed instructions on how to design and fabricate Dy<sup>3+</sup>, Eu<sup>3+</sup> and Sm<sup>3+</sup>-doped GdVO<sub>4</sub> luminescent thin films by the pulsed laser deposition technique. GdVO<sub>4</sub> host in a form of thin film is chosen for few reasons:

- i) due to the similar ionic radii, electronic structures and electronegativities gadolinium ions can be replaced easily with luminescence-active rare earth (RE<sup>3+</sup>) ions in a wide range of concentrations, without strongly affecting the lattice structure,
- ii) reports [1–3] show that GdVO<sub>4</sub> crystals have more advantages over YVO<sub>4</sub>, most important being higher thermal conductivity, larger emission and absorption cross-sections and remarkable quantum efficiency of 95 %,
- iii) to investigate the influence of the materials morphology (powder vs. thin film) on its photoluminescent properties.

Thin films structure, morphology and optical properties were investigated and discussed in detail. Moreover, photoluminescent properties of thin films were compared with their nanopowder counterparts. In order to investigate substrate influence on structure and consequently on photoluminescence and due to the requirements for high transparency and high chemical and thermal stability substrates used for luminescent thin films deposition were quartz glass, sapphire, prime silicon and thermally grown SiO<sub>2</sub>.

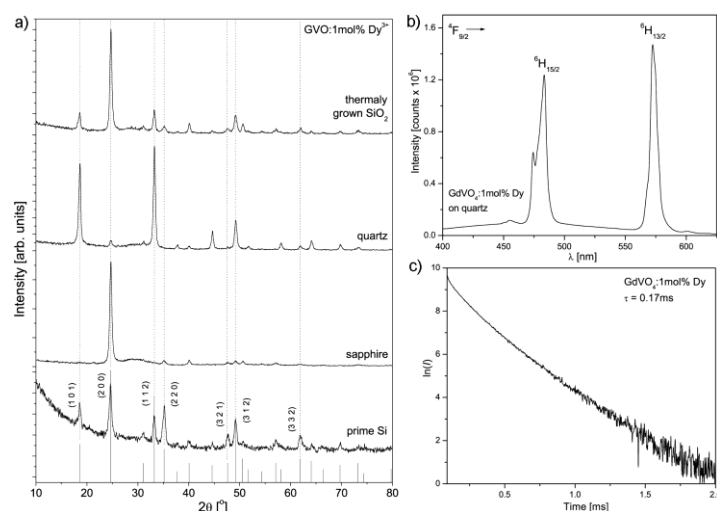


Figure 4 a) XRD diffractograms on different substrates, b) photoluminescent emission spectrum and c) decay curve of GdVO<sub>4</sub>:1mol%Dy<sup>3+</sup> sample.

[1] A. I. Zaguniennyi, V. G. Ostoumov, I. A. Shcherbakov, T. Jensen, J. P. Meyn, G. Huber, Sov. J. Quant. Electron. 22 (1992) 1071-1072.

[2] M. Anitha, P. Ramakrishnan, A. Chatterjee, G. Alexander, H. Singh, Appl. Phys. A 74 (2002) 153-162

[3] T. Gavrilović, D. Jovanović, V. Lojpur, M. D. Dramićanin, Sci. Rep. 4 (2014) 4209

## RARE-EARTH DOPED SILVER EXCHANGED SILICA-HAFNIA WAVEGUIDES FOR BROADBAND DOWNCONVERSION TO IMPROVE THE EFFICIENCY OF PV SOLAR CELLS

A. Bouajaj<sup>a</sup>, F. Enrichi<sup>b,c</sup>, C. Armellini<sup>c</sup>, G. Battaglin<sup>d</sup>, F. Belluomo<sup>e</sup>, E. Cattaruzza<sup>d</sup>, F. Gonella<sup>d</sup>, A. Łukowiak<sup>f</sup>, M. Mardegan<sup>d</sup>, S. Polizzi<sup>d</sup>, C. Sada<sup>g</sup>, M. Ferrari<sup>c</sup>

<sup>a</sup> *Laboratoire des Technologies Innovantes, LTI, Département de Génie industriel ENSA – Tanger, Université Abdelmalek Essaâdi. Tanger, Morocco*

<sup>b</sup> *Veneto Nanotech, Laboratorio LANN, C.so Stati Uniti 4, 35127 Padova, Italy*

<sup>c</sup> *CNR-IFN, Istituto di Fotonica e Nanotecnologie, CSMFO Lab. & FBK-CMM, Via alla Cascata 56/C, Povo, 38123 Trento, Italy*

<sup>d</sup> *Center for Nanosciences and Nanobiomaterials, Department of Molecular Sciences and Nanosystems, Università Ca' Foscari Venezia, via Torino 155/b, 30172 Venezia-Mestre, Italy*

<sup>e</sup> *Meridionale Impianti SpA, Via Senatore Simonetta 26/D, 20867 Caponago (MB), Italy*

<sup>f</sup> *Institute of Low Temperature and Structure Research, PAS, ul. Okolna 2, 50-422 Wrocław, Poland*

<sup>g</sup> *Dipartimento di Fisica G. Galilei, Università di Padova, Via Marzolo 8, 35131 Padova, Italy*

*Corresponding author. E-mail address: francesco.enrichi@venetonanotech.it*

*Presenting author. E-mail address: cattaruz@unive.it*

One of the major limits for the performance of silicon solar cells is due to spectral mismatch between the solar emission and the region of efficient energy conversion of the cell. In particular, about the 8% of the total power coming from the Sun on the Earth surface lies in the near-ultraviolet range ( $\lambda \leq 400$  nm), a region for which devices exhibit a very poor conversion efficiency [1]. Therefore, many strategies for the modification of the sunlight radiation by luminescent quantum cutting or downshifting materials have been reported [2]. In this paper we try to combine quantum cutting optical properties of rare-earth doped materials [3] with broadband absorption and emission properties of silver aggregates such as dimers, trimers or small multimers [4]. In particular, Tb<sup>3+</sup> / Yb<sup>3+</sup> codoped silica-hafnia sol gel waveguides were prepared by dip-coating deposition while the silver incorporation was experimented by ion exchange, immersing the waveguides in Ag-containing molten salt bath. Different rare-earth concentrations and silver ion exchange conditions were studied (as well as post-synthesis annealing) in order to obtain favorable conditions for improving the performance of photovoltaic solar cells.

### Acknowledgments

The research activity was performed in the framework of the CNR-CNRST joint project (2014-2015).

[1] X.Huang, S.Han, W.Huang, X.Liu, Chem. Soc. Rev. 42 (2013) 173–201.

[2] E.Klampafitis, D.Ross, K.R.McIntosh, B.S.Richards, Sol. Energy Mater. Sol. Cells 93 (2009) 1182–1194.

[3] G.Alombert-Goget, C.Armellini, S.Berneschi, A.Chiappini, A.Chiasera, M.Ferrari, S.Guddala, E.Moser, S.Pelli, D.N.Rao, G.C.Righini, Opt. Mat. 33 (2010) 227–230.

[4] E.Cattaruzza, V.M. Caselli, M.Mardegan, F.Gonella, G.Bottaro, A.Quaranta, G.Valotto, F.Enrichi, Ceram. Int. 41 (2015) 7221–7226.

## RARE EARTH DOPED LEAD-FREE GERMANATE GLASSES FOR OPTICAL ACTIVE FIBER TECHNOLOGY

Joanna Pisarska<sup>a</sup>, Wojciech A. Pisarski<sup>a</sup>, Marcin Kochanowicz<sup>b</sup>, Jacek Żmojda<sup>b</sup>,  
Dominik Dorosz<sup>b</sup>, Jan Dorosz<sup>b</sup>

<sup>a</sup> *Institute of Chemistry, University of Silesia, Katowice, Poland, joanna.pisarska@us.edu.pl*

<sup>b</sup> *Faculty of Electrical Engineering, Bialystok University of Technology, Bialystok, Poland*

Among several inorganic glass systems, glasses containing CdF<sub>2</sub> and/or PbF<sub>2</sub> are classified as toxic raw materials and consequently they are being often eliminated from various practical applications due to their hazardous effect on health and environment, but at the same time these fluoride components were established to play important role in glass formation and further strengthening of glass host network [1]. Alternatively, lead- and cadmium-free glasses are proposed for potential applications in photonics [2].

In this work, we present the results for Er<sup>3+</sup> ions in lead-free germanate glasses. In the studied BaO-Ga<sub>2</sub>O<sub>3</sub>-GeO<sub>2</sub> glass system, barium oxide was partially or totally substituted by BaF<sub>2</sub>. Luminescence properties of Er<sup>3+</sup> ions in germanate glasses have been examined as a function of BaF<sub>2</sub> concentration. Near-infrared luminescence spectra at 1530 nm correspond to main <sup>4</sup>I<sub>13/2</sub> - <sup>4</sup>I<sub>15/2</sub> transition of Er<sup>3+</sup>. Based on spectra and their decays, the <sup>4</sup>I<sub>13/2</sub> - <sup>4</sup>I<sub>15/2</sub> line widths and luminescence lifetimes for the <sup>4</sup>I<sub>13/2</sub> upper laser state of Er<sup>3+</sup> ions were determined. Our previously published work indicate that quite long-lived near-infrared luminescence of Er<sup>3+</sup> is observed for glass samples with low BaF<sub>2</sub> concentration [3]. Thermal properties are also presented and discussed in relation to practical applications in optical active fiber technology. Acknowledgment: The National Science Centre (Poland) supported this work under research project 2011/03/B/ST7/01743.

[1] G. Sharma, R. Bagga, N. Mahendru, M. Falconieri, V.G. Achanta, A. Goel, S.N. Rasool, N. Vijaya, *J. Lumin.* 159 (2015) 38.

[2] H. Lin, E.Y.B. Pun, B.J. Chen, Y.Y. Zhang, *J. Appl. Phys.* 103 (2008) 056103.

[3] W.A. Pisarski, J. Pisarska, D. Dorosz, J. Dorosz, *Mater. Chem. Phys.* 148 (2014) 485.

## RADIOPHOTOLUMINESCENCE PROPERTIES OF Ag-DOPED PHOSPHATE GLASSES

Hironori Tanaka<sup>a</sup>, Yutaka Fujimoto<sup>a</sup>, Masanori Koshimizu<sup>a</sup>, Takayuki Yanagida<sup>b</sup>, Keiichiro Saeki<sup>a</sup>, Takuma Yahaba<sup>a</sup>, Keisuke Asai<sup>a</sup>

<sup>a</sup>*Tohoku University, 6-6-07, Aramaki Aza-aoba, aoba-ku, Sendai, Japan,*  
*hironori.t@dc.tohoku.ac.jp*

<sup>b</sup>*Nara Institute of Science and Technology, 8916-5 Takayama, Ikoma, 630-0192, Japan*  
*t-yanagida@ms.naist.jp*

Passive dosimeters have conventionally used Ag-doped phosphate glass. The Ag ions are typically stable in their monovalent state in the glass host; however, the Ag<sup>+</sup> ions change to Ag<sup>0</sup> and Ag<sup>2+</sup> ions on exposure to X-ray and gamma ray irradiation or to high-intensity laser irradiation such as a femto-second laser pulse [1]. Thus, Ag-doped glass enables the estimation of the exposure dose using the relative intensity of the fluorescence, i.e. the radiophotoluminescence (RPL) resulting from the Ag<sup>0</sup> and Ag<sup>2+</sup> ions. However, there are remaining problems to solve, such as the build-up process, the disappearance of luminescence centers when the glasses are annealed at high temperature, and the influence of the phosphate glasses composition. Therefore, we began a detailed examination of the factors influencing the RPL properties. In this study, we focus on the composition of phosphate glasses containing Ag.

The glass samples were prepared according to a conventional melt-quenching method in air. The raw materials, AgCl and NaPO<sub>3</sub> (Na/Ag), were mixed, loaded into an alumina crucible, and melted at 800–1200°C for 30 min in an electric furnace. Finally, the glass melt was quenched on a stainless plate heated to 300°C, which is below the glass transition temperature. The X-ray irradiation was performed using an X-ray tube operated at 40 mA and 40 kV for 5 minutes. To assess the stability of the Ag fluorescence centers in the glasses, the measurements were taken 24 hours after the samples were irradiated with X-ray. The same operations were also performed for K(PO<sub>3</sub>)<sub>n</sub>, Sr(PO<sub>3</sub>)<sub>2</sub>, and Al(PO<sub>3</sub>)<sub>3</sub> instead of NaPO<sub>3</sub>. Moreover, we prepared the same composition sample (Na-Al/Ag) as the product by Chiyoda Technol for comparison. We measured the absorption spectra, fluorescence spectra, RPL spectra, fluorescence lifetimes, and electron spin resonance (ESR) for the samples.

The RPL spectra of the various Ag-doped (0.1 mol%) phosphate glasses, which contain a single s-block atom and were X-ray irradiated for 5 minutes, are shown in Fig. 1. The Na/Ag sample showed a similar spectrum to that of Na-Al/Ag. Moreover, K/Ag showed RPL but the peak was shifted to the short wavelength side. On the other hand, Al/Ag and Sr/Ag did not show RPL. The emission band observed at 400 nm is derived from the Al oxide in Al/Ag. Moreover, Al/Ag and Sr/Ag did not show blue fluorescence of Ag<sup>+</sup> in non-irradiated, showing that Ag was not doped in the glass as Ag<sup>+</sup> in the Al and Sr samples. The product contains Na and Al. Thus, alkali metals contained in the phosphate are required and influence the RPL fluorescent properties.

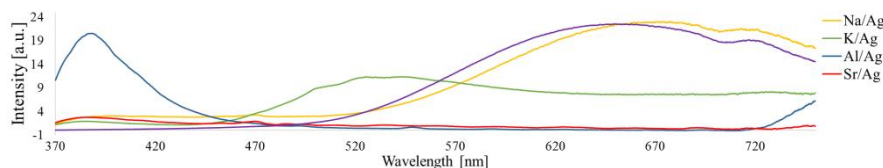


Fig.1 The RPL spectra of various phosphate glasses

[1] Y. Miyamoto, T. Yamamoto, K. Kinoshita, S. Koyama, Y. Takei, H. Nanto, Y. Shimotsuma, M. Sakakura, K. Miura, K. Hirao, *Radiation Measurements* 45(2010)546–549.

## RADIATION RESISTANCE DIAGNOSTICS OF OPTICAL MATERIALS

Eduard Feldbach<sup>a</sup>, Eliko Tõldsepp<sup>a</sup>, Marco Kirm<sup>a</sup>, Aleksandr Lushchik<sup>a</sup>,  
Kenichiro Mizohata<sup>b</sup>, Jyrki Räisänen<sup>b</sup>

<sup>a</sup>*Institute of Physics, University of Tartu, Ravila 14c, Tartu, Estonia, eduard.feldbach@ut.ee*

<sup>b</sup>*Department of Physics, University of Helsinki, P.O. Box 43, Finland*

Optical materials and insulators will play a substantial role in diagnostic systems of future deuterium-tritium fusion reactors, which have to withstand 14 MeV neutron irradiation of unprecedented intensity. Development of extremely neutron resistant optical materials is an important task of the EUROfusion consortium research programme started in 2014 [1]. Neutron radiation induces numerous different types of defects in the materials. For optical components (windows, lenses, fibers) radiation induced optical absorption and undesired light emission (luminescence) are the main problems. Also the investigation of these phenomena at the operating conditions of the future fusion reactors is still unresolved. Considerable damage level of the order of 0.1 – 1 displacements per atom (dpa) is needed for testing of optical materials [2], but at the moment there are no sources of 14 MeV neutrons with sufficient flux. Fortunately optical parameters can be determined in a very thin layer of tiny samples, which enable to use proton or molecular hydrogen [3] ion beams for this task. In this work MgO single crystals and Al<sub>2</sub>O<sub>3</sub> ceramics were irradiated by hydrogen ions to test our approach for diagnostic procedure using ion beams of moderate (hundreds of keV) energies. This level of energies differ considerably from 14 MeV, but enables to concentrate all induced damage in a thin surface layer and therefore the needed fluence is achievable using standard high current ion implanter within reasonable irradiation time. 200 keV molecular hydrogen beam was applied in this work using KIIA 500 kV implanter of Ion Beam Laboratory University of Helsinki. The SRIM calculations for MgO target enable to estimate the irradiated thickness (400-500 nm) and necessary fluence ( $10^{17}$  H ions/cm<sup>2</sup>) to get the damage level of ~0.5 dpa. To detect elementary defects (vacancies and interstitials) in this layer resulting from proton irradiation the highly sensitive luminescence spectroscopy can be used for identifying F-type centres (anion vacancy + electron). Luminescence bands of F and F<sup>+</sup> centres are well-known for most of the optical materials. Luminescence in irradiated layer of given thickness can be excited using electron beam with adjustable energy. In our experiments 7 keV electrons were used, which according to the CASINO simulation overlap well with penetration depth of ions into MgO. Luminescence of F<sup>+</sup> centres in irradiated MgO and Al<sub>2</sub>O<sub>3</sub> layers increased considerably indicating the creation of stable vacancies under used ion beam. Al<sub>2</sub>O<sub>3</sub> exhibit also drastic fading of well-known luminescence band of self-trapped excitons in the VUV spectral range, which is an evidence of considerable disordering of the crystal structure. In the irradiated MgO the VUV emission near band edge due to large radius excitons [4] was revealed evidencing higher radiation resistance of MgO. In conclusion, the standard ion implanters provide fluence of protons high enough in a thin irradiated layer. Applying the electron beam of adjustable energy exciting the full irradiated depth, cathodoluminescence was shown to be a versatile diagnostic tool for radiation resistance of optical materials in fusion technology.

[1] [www.euro-fusion.org/programme/](http://www.euro-fusion.org/programme/)

[2] S.J. Zinkle, NIM B 286 (2012) 4-19.

[3] A. Anttila, J. Räisänen, NIM 185 (1981) 601-602.

[4] E. Feldbach, I. Kuusmann, G. Zimmerer, J. Luminescence 24/25 (1981) 433-436.

## QUANTUM MECHANICAL TRANSMISSION WITH ABSORPTION OF ZnO THIN FILMS

Petya Petkova<sup>a</sup>, Darina Bachvarova<sup>a</sup>, Petko Vasilev<sup>a</sup>, Karem Boubaker<sup>b</sup> and Refka Mimouni<sup>c</sup>

<sup>a</sup>Laboratory of Photonics, 115 Universitetska street, Shumen, Bulgaria, Petya232@abv.bg

<sup>b</sup>École Supérieure de Sciences et Techniques de Tunis (ESSTT), Université de Tunis/63 Rue Sidi Jabeur, 5100, Mahdia, Tunisia

<sup>c</sup>Unité de physique des dispositifs à semi-conducteurs, Faculté des sciences de Tunis, Université de Tunis, El Manar, 2092 Tunis, Tunisia

In this work, we studied the undoped and co-doped ZnO as absorptive medium. We first observed the variation with energy the transmission and the reflection from a rectangular barrier and the corresponding well with out the presence of absorption [1]. Then, we described the variation of transmission, reflection and absorption generated by a purely absorptive domain of width  $a$  and strength  $W_0$ . The one dimensional time independent Schrödinger equation is solved in the case of ZnO thin films. In this connection, we determined the values of: real part of optical potential  $V_0$ , wave function  $\Phi$ , absorption potential strength  $W_0$  and incident energy  $E$ .

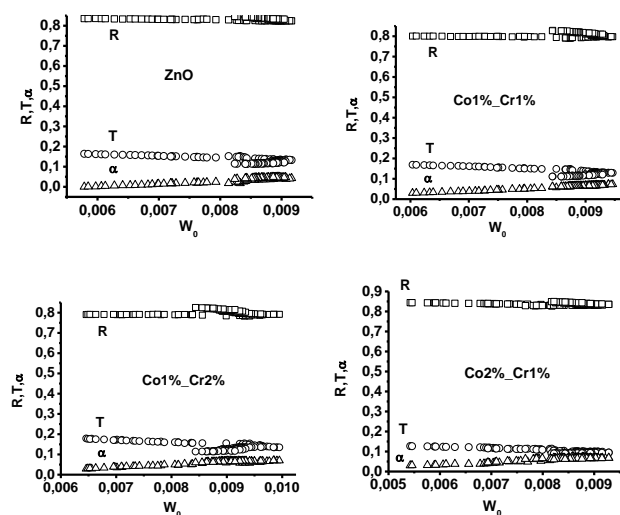


Figure 1. Reflection, transmission and absorption as a function of  $W_0$  for undoped and co-doped ZnO thin films.

### Acknowledgements

This paper is supported by the Project BG051PO001-3.3.06-0003 “Building and steady development of PhD students, post-PhD and young scientists in the areas of the natural, technical and mathematical sciences”. The Project is realized by the financial support of the Operative Program “Development of the human resources” of the European social fund of the European Union.

[1] S. Mahadevan, A. Uma Maneswari, P. Prema and C.S. Shastry, Physics Education, pp. 13 – 21, 2006



## PHOTOLUMINESCENCE PROPERTIES OF $\text{Sr}_2\text{GeO}_4:\text{Ce,Na}$

Karolina Fiaczyk, Eugeniusz Zych

Faculty of Chemistry, University of Wrocław

14. F. Joliot-Curie Street, 50-383 Wrocław, Poland, eugeniusz.zych@chem.uni.wroc.pl

Strontium germanate ( $\text{Sr}_2\text{GeO}_4$ ) can exist in two different crystallographic phases: monoclinic and orthorhombic. In this presentation we focus on  $\text{Ce}^{3+}$  luminescence in the orthorhombic phase (point group:  $Pbn2_1$ ), whose density is about  $5 \text{ g/cm}^3$  [1]. This powder were prepared by classic ceramic method at  $1350 \text{ }^\circ\text{C}$  in reducing atmosphere of forming gas.

Emission spectra show the well-known characteristic doublet of the  $\text{Ce}^{3+}$  emission. Luminescence properties  $\text{Sr}_2\text{GeO}_4:\text{Ce,Na}$  powders were measured in the range of 35-300 K. At room a significant temperature thermal quenching is observed. Average decay time at 300 K is 8.7 ns and the fit gave two components of  $\tau_1=5.1 \text{ ns}$  and  $\tau_2=16.0 \text{ ns}$ . Already at 240 K decay traces is almost mono-exponential, and upon further cooling becomes fully single-exponential and in the 35-150 K range of temperatures its time constant is  $\tau=33 \text{ ns}$ , a value which accords with not quenched  $\text{Ce}^{3+}$  luminescence around 400 nm. These data are presented in Fig. 1a. Fig. 1b shows changes in photoluminescence intensity of  $\text{Sr}_2\text{GeO}_4:\text{Ce,Na}$  powders in the 35-300 K range of temperatures. The possible reasons of the thermal quenching of Ce emission in  $\text{Sr}_2\text{GeO}_4:\text{Ce,Na}$  powders will be discussed in the presentation.

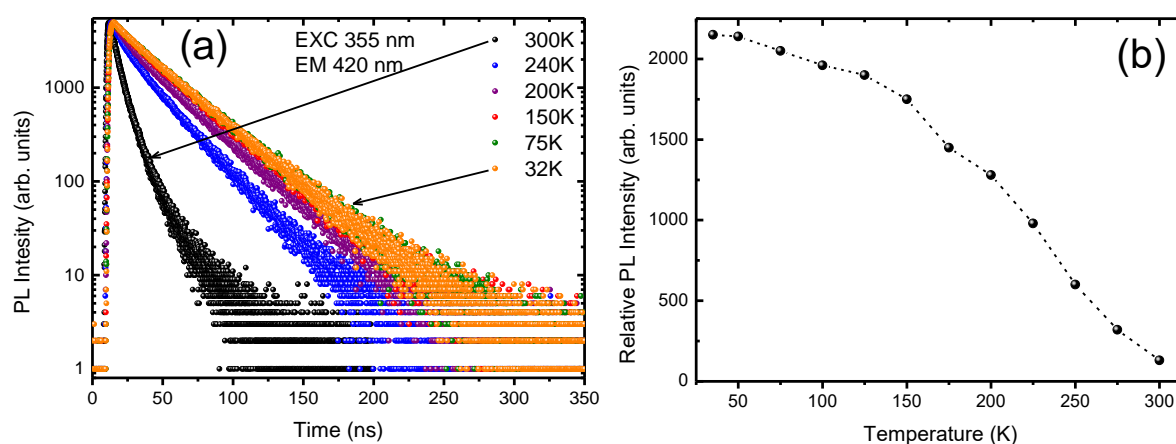


Figure 5. Luminescence decay traces of  $\text{Sr}_2\text{GeO}_4:0.5\%\text{Ce},0.5\%\text{Na}$  (a). Luminescence was monitored at 420 nm and excited at 355 nm. Temperature dependence of photoluminescence intensity upon 365 nm excitation (b).

### Acknowledgement

The work was supported by Wrocław Research Centre EIT+ within the project "The Application of Nanotechnology in Advanced Materials" - NanoMat (POIG.01.01.02-02-002/08) co-financed by the European Regional Development Fund (Innovative Economy Operational Program 1.1.2).

[1] F. Nishi, Y. Takeuchi, Z. Kristallogr. 211 (1996) 607-611.

## **PHOTOLUMINESCENCE FROM MAGNETOEXCITON IN NON-UNIFORM NANORING**

Luis C. Porras, William. Gutiérrez Niño, Ilia D. Mikhailov  
*Universidad Industrial de Santander, Calle 9 # 27, Bucaramanga, Colombia A.A. 678,  
luis.c.porras.m@gmail.com*

We present a theoretical analysis of the magneto-optical properties of a neutral exciton confined in a quantum ring of non-uniform thickness in the presence of a magnetic field applied along the ring's symmetry axis. By using the functional derivative technique [1] and considering a special case of parabolic non-uniformity, we show that in the structural adiabatic limit, when the width of the pattern of the particles pathways within the ring is much smaller than the ring's radius the wave equation for exciton is completely separable and its wave functions and corresponding energies can be found exactly. The found solution allows us to calculate the density of the states, oscillator strength and the photoluminescence spectrum for different ring radii and scales of the non-uniformity. The dependencies of the magneto-optical properties of the exciton on the magnetic field strength are discussed. Our results show a substantial change of the amplitudes of the Aharonov–Bohm oscillations of the energy levels, the density of states and the photoluminescence spectrum of neutral excitons induced by the non-uniformity.

[1] L. C. Porras and I. D. Mikhailov, *Physica E* 53 (2013) 41; L. F. García, S. Yu. Revinova and I. D. Mikhailov, *Physica E* 71 (2015) 101

## GROWTH AND SCINTILLATION PROPERTIES OF Eu AND Tb DOPED LiGdF<sub>4</sub>/LiF EUTECTIC SCINTILLATOR FOR NEUTRON DETECTION

Kei Kamada<sup>a,b</sup>, Kosuke Hishinuma<sup>c</sup>, Shunsuke Kurosawa<sup>b,c</sup>, Akihiro Yamaji<sup>c</sup>, Yasuhiro Shoji<sup>a,c</sup>, Jan Pejchal<sup>b,d</sup>, Yuji Ohashi<sup>c</sup>, Yuui Yokota<sup>a</sup>, and Akira Yoshikawa<sup>a,b,c</sup>

<sup>a</sup>Tohoku University, New Industry Creation Hatchery Center, Sendai, 980-8579, Japan

<sup>b</sup>C&A corporation, T-Biz, 6-6-10 Aoba, Aramaki, Aoba-ku, Sendai, 80-8579, Japan

<sup>c</sup>Tohoku University, Institute for Material Research, Sendai, 980-8577, Japan

<sup>d</sup>Institute of Physics AS CR, Cukrovarnicka 10, 16253 Prague, Czech Republic

In this decade, some novel inorganic scintillators for neutron detection have been reported. Among them, LiCaAlF<sub>6</sub> based scintillator is the most promising candidate [1]. LiCaAlF<sub>6</sub> includes Li in the host lattice and have a function of the pulse shape discrimination between neutrons and gamma-rays. As it is single crystal, Li content is limited by the chemical formula and can't be increased. Thus, if we need higher neutron detection efficiency, we have to find other way. As a candidate for novel neutron detectors, Eu activated LiF-CaF<sub>2</sub> eutectic scintillators were developed and their scintillation properties under <sup>252</sup>Cf neutron exposure were examined [2]. The most important advantage of eutectic scintillators is higher Li content than that of conventional neutron scintillators like Li-glass, Eu:LiI, LiFIZnS. The interest in this study is not only to increase Li content but also the possible design for high resolution neutron imager using the directionally solidified eutectic (DSE) system coupled with high resolution photo detectors. Possibility of high resolution using DSE system is proposed by GAP-Al<sub>2</sub>O<sub>3</sub> [3] and CsI-NaCl. DSE system for X-ray CT application.

In this research, exploration of PSSFs by directional crystal growth method will be reported. In this study, Eu and Tb doped LiGdF<sub>4</sub>/LiF eutectics were explored. Crystal growth was performed by the micro-pulling-down ( $\mu$ -PD) method at the eutectic point (LiF:75 mol%, GdF<sub>3</sub>:25 mol%) with growth rate of 0.1-1.5mm/min Fig.1 showed a example photograph of grown eutectic grown at a growth speed of 0.15mm/min. The sample was cut and polished along transverse cross-section. The sample was optically transparent and showed well aligned eutectic structure with 2-3  $\mu$ m diameter LiF fiber surrounded by LiGdF<sub>4</sub> Matrix. Radioluminescence spectra of grown Eu and Tb doped LiGdF<sub>4</sub>/LiF eutectics were observed by <sup>214</sup>Am alpha-ray excitation. Tb<sup>3+</sup> 4f4f and Eu<sup>3+</sup> 4f4f emissions were observed in 450-750nm. Results of investigations of their crystal structure, eutectic phase by TEM and evaluation of scintillation properties were also reported in the presentation.

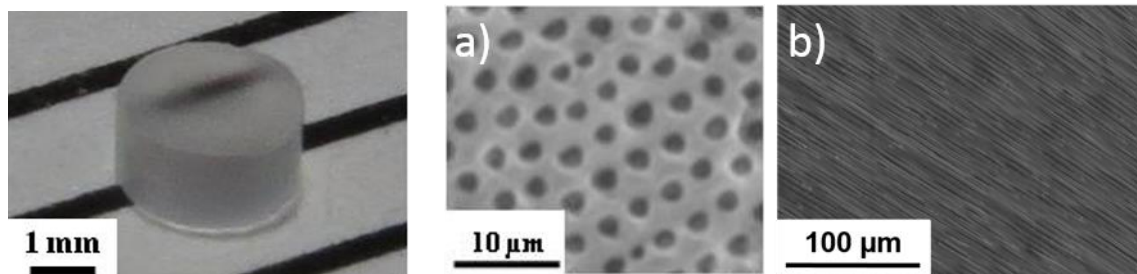


Fig. 1. Photographs of the 2mm thick polished eutectic sample along transverse cross-section.

Fig. 2. Back scattered electron image of a) transverse cross-section b) longitudinal cross-section of the eutectic. (White:LiGdF<sub>4</sub>, Black:LiF)

[1] N.Kawaguchi, et al., Nucl. Instrum. Methods. A, 652 (2011) 351.

[2] A.Yoshikawa, et al., Opt. Mater., 32 (2010) 845.

[3] Y. Ohashi, et. al., App. Phy. Lett. 102, (2013) 051907.

## PHOTOLUMINESCENCE AND RADIATION PROPERTIES OF Ce<sup>3+</sup>-DOPED CsCaCl<sub>3</sub> CRYSTALLINE SCINTILLATOR

Yutaka Fujimoto<sup>a</sup>, Keiichiro Saeki<sup>a</sup>, Hironori Tanaka<sup>a</sup>, Takuma Yahaba<sup>a</sup>, Takayuki Yanagida<sup>b</sup>, Masanori Koshimizu<sup>a</sup>, Keisuke Asai<sup>a</sup>,

<sup>a</sup>Department of Applied Chemistry, Graduate School of Engineering, Tohoku University, 6-6-07 Aoba, Aramaki, Aoba-ku, Sendai 980-8579, Japan

<sup>b</sup>Graduate School of Materials Science, Nara Institute of Science and Technology (NAIST), 8916-5 Takayama-Cho, Ikoma, Nara 630-0192, Japan

Inorganic crystalline scintillators have been used over the years to convert the incident X-ray and gamma-ray radiation into ultraviolet-visible photons. Therefore, there is a continuous need for development of new high-performance scintillators in most radiation detection applications. In recent years, various Ce<sup>3+</sup>- and Eu<sup>2+</sup>-doped halide based scintillators have been developed, exhibiting high light output and fast scintillation decay owing to the 5d–4f allowed transitions. Especially, Zhuravleva et al. [1] investigated the Eu<sup>2+</sup>-doped CsCaCl<sub>3</sub> crystal, obtaining high light yields (~18000 ph/MeV). In this paper, we report on the photoluminescence and radiation response properties involving radioluminescence, scintillation decay time, and absolute scintillation yield of the Ce<sup>3+</sup>-doped CsCaCl<sub>3</sub> crystal. A horizontal three-zone furnace was used to synthesize the crystal sample via the Bridgman method. The starting materials for Ce<sup>3+</sup>-doped CsCaCl<sub>3</sub> were 99.999% purity CsCl, 99.9% CaCl<sub>2</sub>, and 99.9% CeCl<sub>3</sub> · 7H<sub>2</sub>O powders. The concentration of the Ce dopants was 0.5 mol% for the luminescence center. After the synthesis process, an as-grown crystal was cut and polished into the dimensions of 3.0 × 3.0 × 2.0 mm<sup>3</sup>. The photoluminescence map was obtained with a Quantaaurus-QY (Hamamatsu) spectrofluorometer equipped with a Xenon lamp and calibrated integrating sphere. An emission band in the 350–420 nm wavelength range was obtained under excitation at 335 nm owing to the 5d–4f transition of Ce<sup>3+</sup>, as shown in Fig. 1. The fluorescence quantum efficiency of Ce<sup>3+</sup> was estimated to be approximately 76%. The photoluminescence decay curve was obtained by a DeltaFlex (Horiba) system. A light-emitting diode (LED) wavelength of 320 nm was used as the excitation source. Figure 2 shows the result. The decay time of the Ce<sup>3+</sup> emission was a fast component, which was calculated to be approximately 32 ns. A comparison of the absolute scintillation yield of the Ce<sup>3+</sup>-doped CsCaCl<sub>3</sub> crystal and that of a NaI:Tl commercial scintillator was performed with a <sup>137</sup>Cs gamma-ray irradiated pulse height spectrum measurement. A detailed description of the pulse height spectra has been provided in another paper [2]. From the spectra (Fig. 3), the absolute scintillation yield of the Ce<sup>3+</sup>-doped crystal was found to be approximately 7600 photons per MeV.

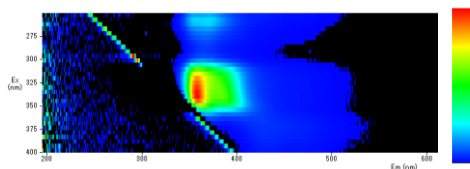


Fig. 1. Photoluminescence map.  
λ<sub>ex</sub> = 250–400 nm, λ<sub>em</sub> = 200–600 nm.

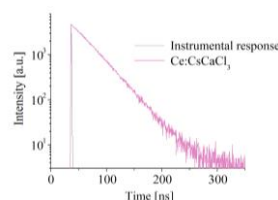


Fig. 2. Photoluminescence decay curve (λ<sub>ex</sub> = 320 nm, λ<sub>em</sub> = 375 nm).

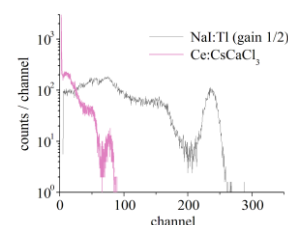


Fig. 3. <sup>137</sup>Cs-gamma-ray irradiated pulse height spectra.

- [1] M. Zhuravleva, B. Blalock, K. Yang, M. Koschan, Ch.L. Melcher, *J. Cryst. Growth* 352 (2012) 115–119.  
[2] T. Yanagida, Y. Fujimoto, K. Fukuda, V. Chani, *Nucl. Instrum. Methods A* 729 (2013) 58–63.

## PHOTOIONIZATION OF $\text{Ce}^{3+}$ IONS IN $\text{YAG}:\text{Ce}^{3+}$ , $\text{LiCaAlF}_6:\text{Ce}^{3+}$ , $\text{LiY}_x\text{Lu}_{1-x}\text{F}_4:\text{Ce}^{3+}$ ( $x = 0, 0.5, 1$ ) AND $\text{SrAlF}_5:\text{Ce}^{3+}$ CRYSTALS

Vitaly Pavlov<sup>a</sup>, Vadim Semashko<sup>a</sup>, Rafail Rakhmatullin<sup>a</sup>, Stella Korableva<sup>a</sup>

<sup>a</sup>*Kazan Federal University, 18 Kremlyovskaya str., Kazan 420008, Russian Federation,  
Vitaly.V.Pavlov@gmail.com*

The study of excited-state photoionization of impurity ions is very important for the search of UV/VUV solid-state laser media, operating on the 5d-4f transitions of trivalent rare earth ions. The photoionization processes lead to photoconductivity effect ( $\sigma$ ) and color center formation and they are an initial cause of unsatisfactory spectral and energy characteristic of the majority UV/VUV lasers [1].

Dielectric spectroscopy, which studies variations of the complex permittivity ( $\varepsilon = \varepsilon_1 - j\varepsilon_2$ ) of crystals under optical irradiation, is the powerful instrument for research of the photoionization processes in crystals. For instance, the variation of its imaginary part  $\delta\varepsilon_2$  can be caused by the appearance of free charge carriers generated as a result of one- or multi-photon impurity ionization ( $\delta\varepsilon_2 \sim \sigma$ ). On the other hand, the variation of real part ( $\delta\varepsilon_1$ ) is associated with a change of dielectric polarization of crystal due to the electronic transitions of impurity ions and color centers. There are two widely held methods of dielectric spectroscopy which make it possible to investigate the photoionization processes. One of them is a conventional technique based on the photocurrent registration by means of blocking electrodes [2]. The second one is a microwave resonant technique based on the measurements of parameters of the cavity resonator with sample [3].

In the first part of this work one- or two-photon ionization of  $\text{Ce}^{3+}$  ions in  $\text{YAG}:\text{Ce}^{3+}$  was investigated using both techniques. Results revealed that the signal registered by the conventional technique includes information about the variations of both parts of complex permittivity and there is no way to separate them. It creates difficulties in obtaining and interpreting the photoconductivity spectrum. Studies have shown that the most informative method for research of the photoionization processes is a microwave resonant technique, because it allows us to study timing and spectral characteristics of each parameter  $\delta\varepsilon_1$  and  $\delta\varepsilon_2$  individually. Moreover, in this case we were able to realize less than a 5-ns temporal resolution for the study of photostimulated processes.

In the second part of this work the microwave resonant technique was applied to study of impurity photoionization in  $\text{Ce}:\text{LiCaAlF}_6$ ,  $\text{Ce},\text{Yb}:\text{LiY}_x\text{Lu}_{1-x}\text{F}_4$  ( $x = 0, 0.5$  and  $1$ ) and  $\text{Ce},\text{Yb}:\text{SrAlF}_5$  crystals. Timing and spectral characteristics of complex permittivity of investigated crystals under laser irradiation in 240 – 310 nm spectral range are investigated. The lifetime of free charge carrier is estimated. The photoconductivity spectra for all investigated crystals have been determined. Interpretation of obtained spectra was carried out using the results of pump-probe experiments. It was found that photoconductivity of  $\text{Ce}:\text{LiCaAlF}_6$ ,  $\text{Ce},\text{Yb}:\text{LiY}_x\text{Lu}_{1-x}\text{F}_4$  ( $x = 0, 0.5$  and  $1$ ) crystals is caused by excited-state absorption of  $\text{Ce}^{3+}$  ions from 5d-states to 6s-state localized in the conduction band of these crystals.

[1] K.-S. Lim, D.C. Hamilton, *J. of Lum.* 40-41 (1988) 319–320

[2] C. Pedrini, D.S. McClure, C.H. Anderson, *J. Chem. Phys.* 70 (1979) 4959–4962

[3] M.-F. Joubert, S.A. Kazanskii, Y. Guyot, J.-C. Gacon, and C. Pedrini, *Phys. Rev. B.* 69 (2004) 165217

## PHOSPHOR IN GLASS BASED ON HIGH REFRACTIVE INDEX GLASSES DOPED WITH $\text{Eu}^{3+}$ AND $\text{Mn}^{2+}$ IONS FOR LEDS

Yana A. Nekrasova<sup>a</sup>, Vladimir A. Aseev<sup>a</sup>, Anastasiya Y. Bibik<sup>a</sup>, Julia V. Tuzova<sup>a</sup>, Mariya A. Shvaleva<sup>a</sup>, Nicolay V. Nikonorov<sup>a</sup>, Elena V. Kolobkova<sup>a</sup>, Oleg A. Usov<sup>b</sup>

<sup>a</sup>*ITMO University, St. Petersburg, Russia, nekrasova@oi.ifmo.ru*

<sup>b</sup>*Ioffe Physical-Technical Institute of the RAS, St. Petersburg, 194021 Russia*

White light-emitting diodes (LEDs) have attracted considerable attentions now due to promising features such as low energy consumption, long lifetime, small size, fast switching, as mercury free nonpolluting environment. For fixing powered phosphor on a chip usually use silicone resins. But these materials are unstable to UV exposure and temperatures above 150°C. Inorganic materials, like glasses and ceramics, are more stable as polymer binders.

One of the perspective material for phosphors is phosphor-in-glass (PiG). It is a simple mixture of typical commercial phosphor and glass powders (or frits). After a heat treatment, glass powders can be formed into a stable matrix for the phosphors through the viscous sintering process. The sintering temperature can be considerably lower (~600 °C) than those for phosphor ceramic sintering processes. In present work, we report  $\text{SiO}_2\text{-PbO-PbF}_2\text{-AlF}_3$  glass systems as silicate glass frit materials. An additional some glasses have been doped with  $\text{EuF}_3$  (1-3 mol %) and  $\text{MnF}_2$  (2-20 mol%).

Sample with different glass to  $\text{YAG:Ce}^{3+}$  phosphor ratios were prepared by sintering at different temperatures. Powders were pressed into disks and heat-treated at different temperatures and time durations.

The spectral and luminescent properties of these PiG samples have been investigated to define the relationships between light conversion efficiency, composition and structures. Optical properties of the phosphor have been investigated. It was shown that the optical properties of WLED based of such material can be easily adjusted by changing thickness of phosphor, ratio of glass to phosphor and concentration of dopants. It was demonstrated that the new phosphor is very attractive medium for fabrication the phosphor-converted white LEDs.

## PHONON SPECTRA OF EULYTITE CRYSTALS $\text{Bi}_4\text{M}_3\text{O}_{12}$ (M=Ge, Si): AB INITIO STUDY

N. M. Avram<sup>a,b</sup>, V.A.Chernyshev<sup>c</sup>, E.-L.Andreici<sup>a</sup>, V.P. Petrov<sup>c</sup>, P.Petkova<sup>d</sup>

<sup>a</sup>*Department of Physics, West University of Timisoara, V. Parvan 4, Timisoara 300223, Romania*

<sup>b</sup>*Academy of Romanian Scientists, Independentei Street 54, Bucharest 050094, Romania*  
<sup>c</sup>*Ural Federal University, 620002 Ekaterinburg, Russia*

<sup>d</sup>*Shumen University "Konstantin Preslavsky", 115 Universitetska street, 9712 Shumen, Bulgaria*

*e-mail:n1m2marva@yahoo.com*

The eulytite crystals  $\text{Bi}_4\text{Ge}_3\text{O}_{12}$  and  $\text{Bi}_4\text{Si}_3\text{O}_{12}$ , undoped and doped with rare earth ions, present important electronic and spectral properties and have many applications as scintillators, optical devices and laser materials.

In this paper we give the results of a DFT calculation of phonon spectra of these crystals, in the center of the first Brillouin zone. First, the geometry optimization was performed using the analytical energy gradients, with respect to atomic coordinates and unit cell parameters. Vibrational wave number and normal modes were calculated within the harmonic approximation by diagonalizing the mass-weighted Hessian matrix.

The IR and Raman spectra of both crystals were simulated with the periodic ab initio CRYSTAL 09 cod [1], by adopting an all-electron Gaussian-type basis set and the B3LYP HF-DFT hybrid functional. The two sets of Transverse-Optical and Longitudinal-Optical frequencies are generated, together with their intensities. Also, the influence of isotopic substitution for Bi,Ge and O in phonon modes and the picture with values of frequencies shift in each mode by isotopic substitution are given.

The obtained results are discussed and the agreement between the computed spectra and experimental data [2, 3] are quite satisfactory, which justify the model and simulation scheme used for the title system.

[1]. R.Dovesi, R. Orlando, B.Civalleri, C. Roetti, V. R. Saunders and C. M Zicovich-Wilson, *Kristallogr.* **220** 571(2005).

[2] P. Beneventi, D. Bersani, P.P. Lottici, L. Kovaks, *Solid State Comm.* **93**, 3865(1996).

[3]. M.Couzi, J.R.Vignalou, C.Boulon, *Solid State Comm.* **20**, 461 (1977).

## PHONON SPECTRA AND ELASTIC CONSTANTS OF RARE-EARTH TITANATE PYROCHLORES $R_2Ti_2O_7$ (R = Gd, Tb, Dy, Ho, Er, Tm, Yb, Lu, Y) FROM FIRST PRINCIPLES

Vladislav P. Petrov<sup>a</sup>, Vladimir A. Chernyshev<sup>a</sup>, Anatoliy E. Nikiforov<sup>a</sup>

<sup>a</sup>*Ural Federal University, 19 Mira, Ekaterinburg, Russia, lancervlad@gmail.com*

Rare earth titanates family  $R_2Ti_2O_7$  (R = Gd–Lu, Y) attracting attention through a variety of optical and magnetic properties of these materials [1,2]. The optical spectrum  $f$ – $f$  transitions of rare earth ions contains a large number of phonon replicas [3], for its interpretation and selection of electronic transitions need information about the frequencies and types of lattice vibrations. The elastic properties of pyrochlore were investigated in number of works [4,5]. The measured elastic constants of the same rare earth titanate pyrochlore from studied row are different significantly [4,5]. Therefore it is necessary to perform *ab initio* calculations of structural, vibrational and elastic properties for the whole pyrochlore row  $R_2Ti_2O_7$  (R = Gd – Lu, Y) taking a unified *ab initio* approach.

In this work, we report on theoretical studies of lattice dynamics of rare-earth titanates pyrochlore family (R = Gd–Lu). *Ab initio* CRYSTAL14 MO LCAO code [6] and the hybrid B3LYP and PBE0 Hamiltonians have been used for the calculations in the DFT approach. All electron basis set were chosen for titanium and oxygen while the pseudopotential method were used for describing the rare earth ion. The crystal structure has been preliminary optimized. Calculations of the phonon frequencies at Gamma point have been carried out within the harmonic approximation. The calculations of the crystal structure and vibrational spectra are in good agreement with the experimental data. The calculations do not reproduce abnormally low values of the elastic constants obtained by Nakanishi et al [5].

This work was partially supported by Ministry of Education and Science of Russia (Grant No. 3.571.2014/K).

[1] M.A. Subramanian, G. Aravamudan, G.V. Subba Rao., Prog. Solid State Chem. 15 (1983) 2.

[2] M.N. Popova, S.A. Klimin, B.Z. Malkin, E.P. Chukalina, E.A. Romanov, E. Antic-Fidancev, B.V. Mill, G. Dhalenne, Physics of the Solid State, 47 (2005) 8, 1425.

[3] B.Z. Malkin, T.T.A. Lummen, P.H.M. van Loosdrecht, G. Dhalenne, A.R. Zakirov, J. Phys.: Condens. Matter 22 (2010) 276003.

[4] Luan Y. Elastic properties of complex transition metal oxides studied by Resonance Ultrasound Spectroscopy, University of Tennessee, PhD thesis, [http://trace.tennessee.edu/utk\\_graddis/993](http://trace.tennessee.edu/utk_graddis/993) (2011)

[5] Y. Nakanishi, T. Kumagai, M. Yoshizawa et al. Phys Rev B 83 (2011) 184434.

[6] R. Dovesi, R. Orlando, A. Erba, C.M. Zicovich-Wilson, B. Civalleri, S. Casassa, L. Maschio, M. Ferrabone, M.De La Pierre, P.D'Arco, Y. Noel, M. Causa, M. Rerat, B. Kirtman, Int. J. Quantum Chem. 114 (2014).1287.



## PERMITTIVITY AND PERMEABILITY OF SEMI-INFINITE METAMATERIAL

Olga V. Porvatkina, Alexey A. Tishchenko, Mikhail N. Strikhanov

*National Research Nuclear University "MEPhI" 31 Kashirskoe Highway, Moscow, Russia,  
OVPorvatkina@mephi.ru*

Metamaterials are artificial materials demonstrating unusual electromagnetic and optical properties, e.g., negative refractive index and subwavelength focusing [1],[7]. Due to their properties metamaterials are in the center of modern investigations. They find use in various applications: for instance, metamaterial coatings have been employed to enhance the radiation and matching properties of electrically small electric and magnetic dipole antennas and for engineering sensors with specified sensitivity [8].

In our work we investigate dielectric and magnetic properties of semi-infinite metamaterial consisting of particles of different possible nature: atoms, molecules, nanoparticles, etc. It is important that these particles would have magnetic properties. Polarization of a near-surface layer is known to differ from its bulk value for non-magnetic materials [9],[10]; for magnetic materials, including metamaterials, the situation should be the similar, which is the subject of our research. We obtain analogues of the Clausius-Mossotti relation both for permittivity and permeability taking into account local field effects in the long-wave approximation (for infinite metamaterial see our recent paper [11], for 2D-metamaterial see [7]). These relations describe the connection between macroscopic characteristics of the semi-infinite metamaterial (permittivity and permeability) and characteristics of constituent particles (dielectric polarizability and magnetic polarizability), which is a bright example of multi-scale approach - method very popular today in physical and computer simulating.

[6] J. B. Pendry, Phys. Rev. Lett. 85 (2000) 3966-69.

[7] D.R. Smith, J.B. Pendry, M.C.K. Wiltshire, Science 305 (2004) 788-792.

[8] K. Gangwar, Dr. Paras, Dr. R.P.S. Gangwar, AEEE 4 (2014) 97-106.

[9] M.I. Ryazanov, Zh. Eksp. Teor. Fiz. 110 (1996) 959-965.

[10] W.L. Mochan, R.G. Barrera, Phys. Rev. Lett. 55 (1985) 1192-1195.

[11] O.V. Porvatkina, A.A. Tishchenko, M.I. Ryazanov, M.N. Strikhanov, IOP Conf. Ser. 541 (2014) 012024.

[12] O.V. Porvatkina, A.A. Tishchenko, M.N. Strikhanov, IOP Conf. Ser. (2015), accepted.

## OPTICALLY- AND THERMALLY-STIMULATED LUMINESCENCES OF Ce-DOPED SiO<sub>2</sub> GLASS PREPARED BY SPARK PLASMA SINTERING

Go Okada<sup>a</sup>, Safa Kasap<sup>b</sup>, Takayuki Yanagida<sup>a</sup>

<sup>a</sup>Graduate School of Materials Science, Nara Institute of Science and Technology, Nara Japan

<sup>b</sup>Electrical and Computer Engineering, University of Saskatchewan, Saskatoon, Canada

Rare-earth doped inorganic materials have found practical applications in a number of areas. In radiation measurements, such materials are used in order to convert incident radiation to light so that the radiation is indirectly detected using a conventional photodetector. Examples of applications include radiograph imaging plates [1], scintillators [2], and dosimeters [3].

In this study, we have prepared and investigated the dosimetric properties of a SiO<sub>2</sub> glass doped with Ce<sup>3+</sup>. The sample was synthesized by a Spark Plasma Sintering (SPS) technique after [4]. SiO<sub>2</sub>:Ce<sup>3+</sup> is very appealing dosimetric material because the host material is considered to be equivalent to tissue, which means that that radiation energy deposited in SiO<sub>2</sub> should be the same as that of human tissue. The SiO<sub>2</sub>:Ce<sup>3+</sup> samples synthesized in this work exhibit a strong photoluminescence (PL) band emission in the range of 400 – 550 nm, which is due to the 5d<sup>1</sup>4f transitions by the Ce<sup>3+</sup> ion. After irradiating the sample by X-rays, both an optically-stimulated luminescence (OSL) by a 630-nm stimulation as well as thermally-stimulated luminescence (TSL) are observed. The structure of TSL glow peak is very broad with the center around 200 °C. With these radiation induced effects, we have confirmed, with the measurement instruments available to us, the dose detection ranges are at least 1 mGy and 1 Gy for both OSL and TSL.

[1] J. A. Rowlands, *Phys. Med. Biol.*, 47 (2002), R123-66.

[2] T. Yanagida, *Opt. Mater.*, 35, (2013) 1987-1992.

[3] G. Okada, B. Morrell, C. Koughia, A. Edgar, C. Varoy, G. Belev, T. Wysokinski, D. Chapman, S. Kasap, *Appl. Phys. Letters*, 99 (2011), 121105

[4] J. Zhan, R. Tu, T. Goto, *Ceram. Int.*, 38 (2012), 2673-2678

## NON-ISOTHERMAL CRYSTALLIZATION PROCESS OF $\text{Eu}^{3+}$ DOPED $\text{Zn}_2\text{SiO}_4$ POWDERS

Milena Marinović-Cincović<sup>a</sup>, Bojan Janković<sup>b</sup>, Bojana Milićević<sup>a</sup>, Miroslav D. Dramićanin<sup>a</sup>  
<sup>a</sup>*Vinča Institute of Nuclear Sciences University of Belgrade, Mike Petrovića Alasa 12-14, P. O. Box 552, 11001 Belgrade, Serbia*

<sup>b</sup>*Faculty of Physical Chemistry, Department of the Dynamics and Structure of Matter, University of Belgrade, Studentski trg 12-16, P. O. Box 137, 11001 Belgrade, Serbia*

Kinetic analysis of non-isothermal crystallization process of  $\text{Eu}^{3+}$  doped  $\text{Zn}_2\text{SiO}_4$  powders prepared by sol-gel procedure was performed using simultaneous TG-DTA measurements. Investigated samples were subjected to firing under influence of microwave (MW) heating. Kinetic study was based on application of generalized time approach with defined analytical form of heating rate function [1, 2]. It was found that crystallization process can be best described by Šesták-Berggren (SB) ( $M,N$ ) autocatalytic model. Also, it was found that behavior of  $N$  values with changing of heating rate can be linked to shift of mechanism from Langmuir-Hinshelwood to Eley-Rideal. Based on calculated values of  $M$  and  $N$  exponents, and for middle-sized nano-powder fraction (60 - 65 nm), we conclude that there is a combined pathways, which includes a quite large number of surface defects producing surface nuclei, and at same time, relatively high number of bulk nuclei in latter stage of process. It was concluded that occurrence of higher and sharper crystallization rate peaks on side of higher heating rates indicate increase in nucleation time and more pronounced bulk mechanism. Deviations from Arrhenius plot dependence is found in a form of “concave” manner relationship. This phenomenon describe the case of competing mechanisms of crystallization.

[1] B. Janković, M. Marinović-Cincović, M. D. Dramićanin, *J. Alloy. Compd.* 587 (2014) 398-414

[2] R. Krsmanović Whiffen, Ž. Antić, A. Speghini, M. I. G. Brik, B. Bártová, M. Bettinelli, M. D. Dramićanin, *Opt. Mater.*, 36 (2014) 1083-1091

## OPTICAL PROPERTIES OF HYBRID ASSOCIATES COLLOIDAL Ag<sub>2</sub>S QUANTUM DOT WITH J-AGGREGATES OF DEC ORGANIC DYE

Tamara Shatskikh, Oleg Ovchinnikov, Irina Grevtseva, Michail Smirnov  
Voronezh State University, 1 Universitetskay sq., Voronezh, Russia, tamara-shatskikh@rambler.ru

Investigation of optical properties of semiconductor nanoparticles and nanostructures, formed from them is one of the important directions of nanophotonics. The most actual applications of colloidal quantum dots photonics are fluorescent labeling of biological objects and biosensors [1,2]. Colloidal Ag<sub>2</sub>S quantum dots (QDs) are perspective for this purpose. They are characterized by photoluminescence at 1100-1200 nm. However, the optical absorption of particles with size of 2-3 nm is located in the region of 350-450 nm. During conjugation of Ag<sub>2</sub>S QDs with organic dye molecules efficient excitation of infrared (600-700 nm) is possibly [3]. This work is devoted to the analysis of this possibility for hybrid associates, constructed from colloidal Ag<sub>2</sub>S QDs with organic dye molecules of 3,3'-di-( $\gamma$ -sulfopropyl)-4,4',5,5'-dibenzo-9-ethylthiacarbocyanine betaine pyridinium salt (DEC).

Ag<sub>2</sub>S QDs, obtained by sol-gel method and conjugated with DEC were investigated. The conjugation of Ag<sub>2</sub>S QDs with DEC dye molecules was realized by introducing an ethanol solution of the dye in the gelatin sol. The dye concentration was 10<sup>-2</sup> mol.f. (mol DEC / mol QDs). The UV-vis absorption spectra of Ag<sub>2</sub>S-DEC hybrid associates show two absorption peaks at 632 nm and 653 nm. They are related to J<sub>cis</sub>- and J<sub>trans</sub>-aggregates, respectively. Thus, the conjugation of Ag<sub>2</sub>S QDs with polymethine dye molecules leads to the formation of associates of Ag<sub>2</sub>S QDs with J<sub>trans</sub>-aggregates and Ag<sub>2</sub>S QDs with J<sub>cis</sub>-aggregates. It is important to notice, that the peak position of absorption J-band in DEC solutions and in mixtures with Ag<sub>2</sub>S QDs is almost invariably. Probably, the presence of Ag<sub>2</sub>S QDs does not affect on the distribution of  $\pi$  electron density in J-aggregate.

Under excitation of associate by radiation of 660 nm, that is corresponded to absorption region of dye J<sub>trans</sub>-aggregates and impurity absorption of Ag<sub>2</sub>S QDs luminescence in the band of QDs (1200 nm) is increased. Possibility, the excitation of Ag<sub>2</sub>S QDs luminescence is due to direct excitation of luminescence center, which is caused by defects in the band gap of QDs with participation of discrete levels of the conduction and valence bands of Ag<sub>2</sub>S. And dye sensitizes this transition. Defects of crystal structure are characteristic of Ag<sub>2</sub>S QDs due to non-stoichiometry of silver sulphide. These defects are expressed as impurity absorption in long-wavelength spectral region relative to the exciton transition in the electronic absorption spectra.

Thus, when the energy levels of Ag<sub>2</sub>S QDs and dye molecules are close, it is possible efficiently interaction between two systems. Under excitation of 660 nm it is possible efficient transfer of electronic excitation energy between components of Ag<sub>2</sub>S QDs-DEC associate.

This work was supported by President grant CII-1161.2015.4.

[1] Sh. K. Murti, Int. J. Nanomedicine. 2 (2007) 129-141.

[2] P. Journey, R. Agarwal, V. Singh, K. Roy, S.V. Sreenivasan, L. Shi, J. Nanotechnol. Eng. Med. 4 (2013) 031002.

[3] P. Jiang, C. Zhu, Z. Zhang, Z. Tian, D. Pang, Biomaterials. 33 (2012) 5130-5135.

## OPTICAL PROPERTIES OF CONVENTIONAL AND LOW-SHRINKAGE MODEL COMPOSITES

Dragica Manojlovic<sup>a</sup>, Miroslav D. Dramićanin<sup>b</sup>, Maja Lezaja<sup>a</sup>, Pong Pongprueksa<sup>c</sup>, Bart Van Meerbeek<sup>c</sup>, Vesna Miletic<sup>a</sup>

<sup>a</sup> *University of Belgrade, School of Dental Medicine, DentalNet Research Group, Rankeova 4, Belgrade, Serbia*

<sup>b</sup> *University of Belgrade, Institute of Nuclear Sciences „Vinča“, P.O. Box 522, Belgrade, Serbia*

<sup>c</sup> *BIOMAT, Department of Oral Health Sciences, KU Leuven (University of Leuven) & Dentistry, University Hospitals Leuven, Leuven, Belgium*

Ideal resin-based composites (RBCs) should mimic the optical properties of natural teeth and have color stability throughout the functional life-time of the restoration. However, RBCs have a tendency to discoloring when exposed to the oral environment.

The aim of this study was to determine the effect of a conventional and a low-shrinkage methacrylate monomer as well as conventional and alternative photoinitiators on color, translucency, and color stability of model RBCs.

Four microhybrid RBCs were prepared containing 30wt% of an organic matrix and 70wt% of silanated Ba-glass fillers. The organic matrix consisted of 70:30wt% of Bisphenol A-glycidyl-methacrylate (BisGMA) / triethyleneglycol-dimethacrylate (TEGDMA) or FIT-852 (FIT; Esstech Inc.) / TEGDMA monomers and 1wt% of camphorquinone (CQ) / amine or Lucirin TPO photoinitiators. Color and translucency were measured using Thermo Scientific Evolution (Thermo Fisher Scientific) and SpectroShade™Micro (MHT Optic Research) spectrophotometers. Color stability was evaluated after immersion in black tea (pure, with milk or lemon) and distilled water. Data were analyzed using two-way and one-way ANOVA with Tukey's post-test ( $\alpha=0.05$ ).

Low-shrinkage FIT-based RBCs were considerably brighter, showed lower deviation from the ideal white color and had almost 5 times lower translucency than conventional BisGMA-based RBCs. Photoinitiators had no significant effect on the baseline color. Initially whiter FIT-based RBCs showed greater staining in all staining solutions compared to BisGMA-based RBCs. TPO-containing RBCs showed better color stability than CQ-containing RBCs irrespective of the base monomer. Greatest color changes occurred after immersion in tea with lemon. Adding milk to tea significantly reduced material staining.

Urethane-based low-shrinkage monomer FIT and conventional monomer BisGMA greatly affected color, translucency and color stability of their respective RBCs. Differences in optical properties of low-shrinkage RBCs compared to BisGMA-based RBCs seem to be associated primarily with the type of monomer. Staining of RBCs is influenced by initial color, the type of base monomer, pH values and staining ability of media.

## OPTICAL PROPERTIES OF CdMoO<sub>4</sub>:RE<sup>3+</sup> (RE = Nd, Eu, Yb) SINGLE CRYSTALS

Małgorzata Guzik<sup>a</sup>, Elżbieta Tomaszewicz<sup>b</sup>, Yannick Guyot<sup>c</sup>, Marek Berkowski<sup>d</sup>,  
Kheirredine Lebbou<sup>c</sup>, Janina Legendziewicz<sup>a</sup>, Georges Boulon<sup>c</sup>

<sup>a</sup>*Faculty of Chemistry, University of Wrocław, 14 F. Joliot-Curie,  
50-383 Wrocław, Poland,*

<sup>b</sup>*Department of Inorganic and Analytical Chemistry, West Pomeranian University of  
Technology, Al. Piastów 42, 71-065 Szczecin, Poland*

<sup>c</sup>*Institute Light Matter (ILM), UMR5306 CNRS-University Lyon1, University of Lyon, 69622  
Villeurbanne, France*

<sup>d</sup>*Institute of Physics, Polish Academy of Sciences, Al. Lotników 32/46,  
02-668 Warszawa, Poland*

Molybdates and tungstates containing rare-earth ions are attractive luminescent materials due to a very high-stability of light emission, high efficiency, long lifetime and low excitation threshold as well as their chemical and thermal durability in air [1]. Our earlier studies have revealed the existence of limited tetragonal scheelite type Cd<sub>1-3x</sub>RE<sub>2x</sub>□<sub>x</sub>MoO<sub>4</sub> solid solutions, where □ denotes cationic vacancies [2,3]. Presence of vacancies is caused by a compensation of an excessive positive charge which resulted from the replacement of divalent Cd<sup>2+</sup> ions by trivalent rare-earth ones in a CdMoO<sub>4</sub> framework. When RE = Pr, Nd, Sm–Gd, the homogeneity range of solid solutions under study is 0 < x ≤ 0.25 [2,3]. For heavier rare earths, this range is clearly narrower. Very interesting optical results presented in our previous papers for polycrystalline samples of Cd<sub>1-3x</sub>RE<sub>2x</sub>□<sub>x</sub>MoO<sub>4</sub> (RE=Nd, Eu, Yb) motivated us to undertake of studies on their single crystals [4-6]. Cadmium and rare-earth molybdates in a single crystals form have been successfully grown by the Czochralski method in an inductively heated platinum crucible in air atmosphere. The starting materials for crystallization processes were following metal oxides: RE<sub>2</sub>O<sub>3</sub> (RE=Nd, Eu, Yb, with purity over 99.99%), CdO (99.998%) and MoO<sub>3</sub> (99.95%). The single crystals were grown on <001> oriented seed prepared from a single crystal of cadmium molybdate. The content of RE<sup>3+</sup> ions was confirmed by ICP-MS method after dissolving monocrystalline samples in dilute and hot aqueous hydrochloric acid solution.

Our previous studies performed for the analogues in the form of microcrystalline powders revealed that Eu<sup>3+</sup>, Nd<sup>3+</sup>, Yb<sup>3+</sup>-doped cadmium molybdates, which contain a define amount of the cationic vacancy exhibit very intense luminescence, so that could be applied for WLEDs with Eu<sup>3+</sup> ions and for laser materials with Nd<sup>3+</sup>/Yb<sup>3+</sup> ions.

So, it is very important task to analyse the structure and optical properties of mentioned above compositions in the form of single crystals.

[1] G. Boulon, *Opt. Mat.*, 34 (2012) 499.

[2] E. Tomaszewicz, S.M. Kaczmarek, H. Fuks, *Mat. Chem. Phys.*, 122 (2010) 595.

[3] E. Tomaszewicz, E. Flipek, H. Fuks, J. Typek, *J. Eur. Ceram. Soc.*, *J. Eur. Ceram. Soc.*, 34 (2014) 1511.

[4] M. Guzik, E. Tomaszewicz, Y. Guyot, J. Legendziewicz, G. Boulon, *J. Lumin.*, <http://dx.doi.org/10.1016/j.jlumin.2015.02.043>

[5] M. Guzik, E. Tomaszewicz, Y. Guyot, J. Legendziewicz, G. Boulon, *J. Mat. Chem. C*, 3 (2015) 4057.

[6] M. Guzik, E. Tomaszewicz, Y. Guyot, J. Legendziewicz, G. Boulon, *J. Mat. Chem. C*, in revision.

## OPTICAL PROPERTIES OF $^{40}\text{Ca}^{100}\text{MoO}_4$ SINGLE CRYSTALS FOR THEIR APPLICATION IN THE CRYOGENIC SCINTILLATION DETECTOR

Anastasiia Chernykh<sup>a</sup>, Oleg Buzanov<sup>b</sup>, Marina Bykova<sup>a</sup>, Evgeniya Zabelina<sup>a</sup>, Anna Kozlova<sup>a</sup>,  
Nina Kozlova<sup>a</sup>

<sup>a</sup>*NUST MIS&S, 119049, Moscow, Russia chernykh.anastasya@yandex.ru*

<sup>b</sup>*OAO Fomos-Materials, 107023, Moscow, Russia buzanov@newpiezo.com*

Calcium molybdate single crystal ( $\text{CaMoO}_4$ ) is a material widely used in laser physics and acoustic optics due to a combination of unique properties and manufacturability [1]. At the same  $\text{CaMoO}_4$  attracts attention as a possible material for scintillation cryogenic detector because of the ability for isotope  $^{100}\text{Mo}$  to demonstrate the neutrinoless  $2\beta$  decay. The main requirement for working detector's element is light attenuation coefficient ( $\mu$ ) of the crystal less than  $0.01 \text{ cm}^{-1}$  at the wavelength of 520 nm. However, grown  $\text{CaMoO}_4$  single crystals are blue. This is highly undesirable for practical use. It is known that in order to reduce the intensity of the calcium molybdate crystals' color the continuous oxidation annealing (over 600 hours) is required.

In this paper we present the results of our studies of  $\text{CaMoO}_4$  optical properties depending on the annealing conditions. All crystals were grown in Fomos-Materials. Specimens' crystallographic orientations were Z- and Y- $25^\circ$ . Optical spectra were measured using spectrophotometer "Cary-5000" (Agilent Technologies) equipped with DRA-2500 console. Refractive indices were measured using goniometer-spectrometer GS-2.

Along directions perpendicular to the optical axis we observed the dichroism phenomenon, which is associated with anisotropy of color centers and their complexes in the crystals. In order to determine nature of the defects we studied light scattering and diffuse reflection spectra of the single crystals in the spectral region 250 – 800 nm.

The values of spectral transmittance and the refractive index are necessary to calculate the spectral values of the attenuation coefficient  $\mu(\lambda)$ . There are various refractive indices values for calcium molybdate measured by different authors [2,3,4], so refractive indices and their dispersions for prism-shaped *as-grown* and annealed samples in the wavelength range 250 – 800 nm was measured. Transmission spectra and the refractive indices along the length of the prisms were used in comparative study of optical homogeneity of the crystals.

[1] L. F. Jounson, J. of Appl. Phys., 34 (1963) 897.

[2] W. L. Bond, J. of Appl. Phys., 36 (1965) 1674-1677.

[3] T.A. Davis, K. Vedam, JOSA, 58 (1968)1446-1451.

[4] A.N. Annenkov et al., Nuclear Instruments and Methods in Physics Research Section A: Accelerators, Spectrometers, Detectors and Associated Equipment, 584 (2008) 334-345.

## OPTICAL PROPERTIES OF DOPED TRANSPARENT $Y_2O_3$ AND $Y_3Al_5O_{12}$ CERAMICS

V.V.Balashov, Y.L.Kopylov, V.B.Kravchenko, K.V.Lopukhin, V.V.Shemet  
*Fryazino branch of Kotel'nikov Institute of Radioengineering and Electronics,  
of RAS, Fryazino, Moscow region, Russia, ylk215@yandex.ru*

Highly transparent  $Y_2O_3$  and  $Y_3Al_5O_{12}$  ceramics are new and very interesting materials which can be used as active laser media and different kinds of scintillators.  $Y_2O_3$  ceramics doped with Nd, Yb, Er, Ho, Tm cations as well as  $Y_3Al_5O_{12}$  ceramics with Nd and Yb ions were manufactured by solid state reactive sintering method in vacuum atmosphere. Yttria commercial oxide powders and chemically precipitated all oxides' powders were used as starting materials. Stoichiometric amounts of oxide powders were mixed and ball milled with anhydrous alcohol as dispersing media. After milling and subsequent drying the powders were compacted by dry and wet methods. In the case of dry compaction process the powders were preliminary pressed uniaxially at low (about 20-50 MPa) pressures and finally pressed isostatically at 200 - 300 MPa. For wet compaction process the High Pressure Colloidal Slip Casting method [1] was used. Sintering process was produced in vacuum furnace with carbon heater at different temperatures and different keeping time. All set of thermal methods (DTA, DG, DSC etc.) was used to investigate and optimize the compaction and sintering processes. The main optical and microstructural properties such as spectra of inline transmission, luminescence spectra, ceramics grain size and residual pores concentration and pores volume distribution were investigated for obtained samples of ceramics. The parameters values of these properties were discussed in dependence on samples manufacturing conditions. It is important to use the optimal sintering aids in ceramic processing to improve the sintering conditions and decrease the residual porosity, etc. For  $Y_3Al_5O_{12}$  ceramics oxides  $SiO_2$ ,  $MgO$ ,  $B_2O_3$  in different combinations and concentrations were used as sintering aids. Combination of  $ZrO_2$  and  $La_2O_3$  oxides were used for ceramics based on  $Y_2O_3$ . Phenomenological model of influence of different oxides on sintering kinetics is proposed and discussed. The best ceramics samples have optical transmittance practically equal to theoretical values for the corresponding crystals.

[1] A. A. Kaminskii, V. B. Kravchenko, Yu. L. Kopylov, et al. (HPCSC) method. Phys. Stat. Sol. (a), 204 (2007) 2411-2415.



## OPTICAL CHARACTERIZATION OF ZnSe/CdSe NANOCRYSTALS WITH $\pi$ -CONJUGATED ORGANIC LIGANDS

Takuma Yahaba, Shigeru Kaida, Masanori Koshimizu, Yutaka Fujimoto, Keisuke Asai  
 Department of Applied Chemistry, Graduate School of Engineering, Tohoku University,  
 Aramaki Aza Aoba 6-6-04, Aoba-ku, Sendai, Miyagi, JAPAN  
 takuma.yahaba.s1@dc.tohoku.ac.jp

Organic–inorganic heterostructures provide the possibility for observing new types of excitons that are expressed by the wave function mixing of Frenkel and Wannier excitons. The new excitons are expected to possess large oscillator strengths from the Frenkel exciton and non-linear sensitivity from the Wannier exciton. The formation of the new excitons requires that the organic and inorganic energy levels must be resonantly adjusted. In this study, we synthesized organic–inorganic heterostructures by covering ZnSe/CdSe core/shell nanocrystals (inorganic) with 2-aminoanthracene (AAn),  $\pi$ -conjugated organic ligands. The photoluminescence (PL) peak wavelength of ZnSe/CdSe nanocrystals can be controlled by the thickness of the CdSe shell layer. We planned the realization of the excitation resonance state and composed ZnSe/CdSe–AAn to ensure the PL peak wavelength of ZnSe/CdSe nanoparticles was as close as possible to 480 nm, which is the PL peak wavelength of AAn. Finally, we evaluated the optical characteristics of the heterostructures.

The ZnSe/CdSe nanocrystals possessing a PL peak at 481 nm (ZnSe/CdSe481) were used in the synthesis of ZnSe/CdSe–AAn. ZnSe/CdSe–AAn was obtained by adding the AAn chloroform solution (2.0 mM) to the ZnSe/CdSe solution and heating to 50°C. The PL spectra and decay curve were measured and the relative quantum yield (QY) was calculated for each of the samples.

Fig. 1 shows the PL spectra of ZnSe/CdSe481–AAn. With the increase of AAn, the PL peak wavelength shifts by about 20 nm. These ZnSe/CdSe481–AAn spectra cannot be represented by either the ZnSe/CdSe481 or AAn spectra. Table 1 shows the decay time constant and QY of ZnSe/CdSe481–AAn. With the increase of AAn, the decay time constant of the short-lifetime component shows almost no changes while that of long-lifetime component decreases. Moreover, under 360-nm excitation, QY increases. Consequently, the decrease in the long-lifetime component derived from ZnSe/CdSe481 indicates an increase of radiative relaxation. These results strongly suggest resonance between the excited states of ZnSe/CdSe481 and AAn.

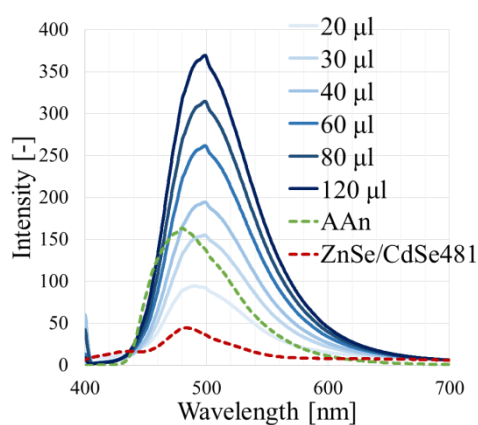


Fig. 1. The PL spectra of ZnSe/CdSe481–AAn

Table 1. Decay time constant and QY of ZnSe/CdSe481–AAn for each AAn addition

AAn additional volume [μl]	Short-life component		Long-life component		QY [%]
	Decay time constant [ns]	Relative intensity [%]	Decay time constant [ns]	Relative intensity [%]	
20	11.1	63.3	49.8	36.7	3.22
30	11.8	74.5	53.0	25.5	7.58
40	12.1	78.3	51.6	21.7	8.48
60	12.6	82.5	49.1	17.5	9.77
80	12.5	85.3	45.9	14.7	10.2
120	12.1	83.5	37.5	16.5	9.79
ZnSe/CdSe481	5.30	26.5	44.4	73.5	1.46
AAn	10.0	81.1	18.3	18.9	93.6

## OPTICAL BIOSENSOR FOR DETECTION OF FORMALDEHYDE BASED ON AOX ENZYME ON POLY-N-BUTYL ACRYLIC-CO-N- ACRYLOXYSUCCINIMIDE FILM

Nurlely Kusuma<sup>a</sup>, Musa Ahmad<sup>a,b</sup>, Lee Yook Heng<sup>a</sup>

*Department of Physics, Faculty mathematics and natural science, University of Indonesia,  
Kampus UI Depok, Jawa Barat, Depok, 16424, Indonesia.*

<sup>a</sup>*School of Chemical Sciences and Food Technology, Faculty of Science and Technology,  
Universiti Kebangsaan Malaysia (UKM), 43600 Bangi, Selangor D.E., Malaysia*

<sup>b</sup>*Industrial Chemical Technology Programme, Faculty of Science and Technology, Universiti  
Sains Islam Malaysia, Bandar Baru Nilai, 71800 Nilai, Negeri Sembilan D.K., Malaysia*

Optical biosensors for the detection of formaldehyde in solution have been developed. The biosensor have been designed from poly n-butyl acrylic-co-N-acryloxysuccinimide (NBA-co-NAS) membrane as a pH-sensitive transducer. Alcohol oxidase (AOX) enzyme was immobilized on the membrane by covalent binding between the amine groups of AOX with the succinimide group of poly (nBA-co-NAS) membrane which containing a chromoionofor (ETH5294) and lipophilic salt (NaTFPB). The biosensor showed high sensitivity, good linearity and exhibited high reproducibility towards formaldehyde in the concentration range of  $10^{-4}$  - 10 mM ( $R^2=0.998$ ) at room temperature. Furthermore, the biosensor was highly selective for formaldehyde with no disturbance by acetaldehyde, methanol, ethanol, glucose and glyserol. The biosensor is stable up to 15 days if stored at 4°C with a 10 min response time.

- [1] Patel, N.G., Meier, S., Cammann, K. & Chemnitius, G.C. 2001. Screen-printed biosensor using different alcohol oxidase. *Sensors and Actuators B* 75: 101-110.
- [2] Siti, A.H., Lee, Y.H. & Musa, A. 2006. A formaldehyde biosensor base on potentiometric pH transducer and immobilize enzyme alcohol oxidase. *Malaysian Journal of Chemistry* 8: 016-021.
- [3] Kawamura, K., Kerman, K., Fujihara, M., Nagatani, N., Hashiba, T. & Tamiya, E., 2005. Development of a novel hand-held formaldehyde gas sensor for the rapid detection of sick building syndrome. *Sensors and Actuators B* 105: 495-501.
- [4] Tan, L.L., Musa, A., Lee, Y.H. 2012. A novel optical ammonia sensor based on reflectance measurements for highly polluted and coloured water. *Sensors and Actuators B* 171-172: 994-100.
- [5] Lee, Y.H., Teh, H. F., Loh, H. C. & Musa, A. 2003a. Influence of Methacrylic-Acrylic Copolymer Composition on Plasticiser-free Optode Films for pH Sensors. *Sensors* 3: 83-90.
- [6] Lee, Y.H. & Hall, E.A.H. 1996. Methacrylate-acrylate based polymers of low plasticiser content for potassium ion-selective membranes. *Analytica Chimica Acta* 324: 47-56.
- [7] Levichev, S. S., Bratov, A. V. & Vlasov, Y. G. 1994. New photocurable composition for ISFET polymer membrane. *Sensors and Actuators B* 19: 625-628.
- [8] Lee, Y.H. & Hall, E.A.H. 2000. Methacrylic-acrylic polymers in ion-selective membranes: achieving theright polymer recipe. *Analytica Chimica Acta*. 403: 77-89.
- [9] Khor, S.M., Lee, Y.H. & Musa, A. 2006. Pemegunaan enzim urease dalam bahan hidrogel metakrilat untuk menghasilkan membran biosensor urea. *Jurnal Teknologi* 45: 53-66.

## OPTICAL AND MORPHOLOGICAL PROPERTIES OF NEW RED $\text{Y}_2\text{Hf}_2\text{O}_7:\text{Eu}^{3+}$ NANOPHOSPHORS

Jelena Papan<sup>a</sup>, Milica Sekulić<sup>a</sup>, Dragana J. Jovanović<sup>a</sup>, Vesna Đorđević<sup>a</sup>, Miroslav Dramićanin<sup>a</sup>

<sup>a</sup>Vinča Institute of Nuclear Sciences, University of Belgrade, P.O. Box 522, 11001 Serbia, [jelenap@vin.bg.ac.rs](mailto:jelenap@vin.bg.ac.rs)

Ternary oxides with the formula of  $\text{A}_2\text{B}_2\text{O}_7$ , where A is a 3+ ion and B a 4+ ion, have been of great interest for many researchers over a number of years. Different methods for the  $\text{A}_2\text{B}_2\text{O}_7$  compounds were developed. Among them,  $\text{Y}_2\text{Hf}_2\text{O}_7$  is a promising candidate for scintillator, which has potential application in high-energy nuclear medical fields such as computer tomography (CT) and positron emission tomography (PET). However, to the best of our knowledge, synthesis and studies of  $\text{Eu}^{3+}$ -doped  $\text{Y}_2\text{Hf}_2\text{O}_7$  have not been investigated yet. In this work, we studied optical and morphological properties of  $\text{Y}_2\text{Hf}_2\text{O}_7:\text{Eu}^{3+}$  nanophosphors prepared with soft chemical sol-gel synthesis. The phase identity and purity of all of prepared powders was investigated by XRD. All the samples were found to be nanocrystalline with cubic fluorite type of crystal structure ( $Fm\bar{3}m (2\ 2\ 5)$ ) space group. In order to improve the crystallinity of the nanoparticles, the samples were additionally heat-treated at three different temperatures ( $T = 800, 1100$  and  $1400$  °C). Also, in order to observe the dependence of emission intensities with doping concentration,  $\text{Y}_2\text{Hf}_2\text{O}_7$  was doped with different atomic percentages of  $\text{Eu}^{3+}$  (1, 2, 4, 8 and 12 %) ions. Representative emission spectrum of  $\text{Y}_2\text{Hf}_2\text{O}_7:2\text{at}\%\text{Eu}^{3+}$  nanophosphor is shown on the Figure 1.

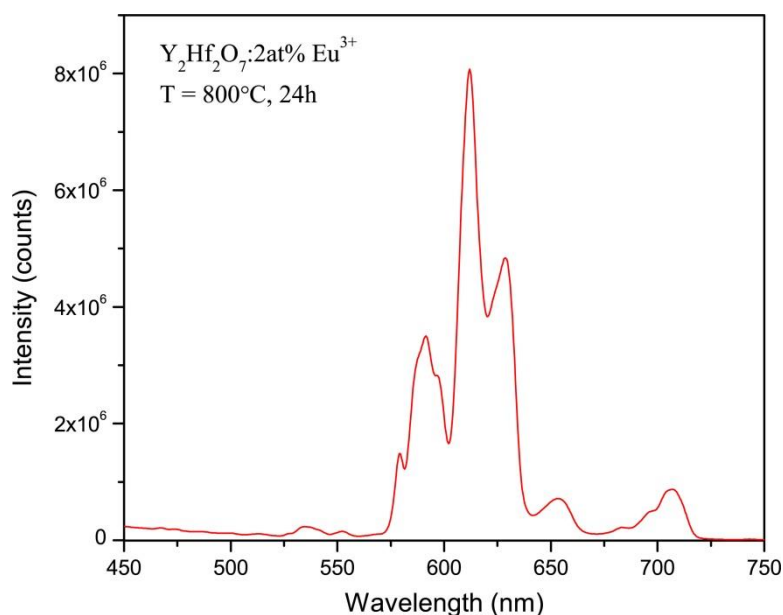


Figure 1. Emission spectrum of synthesized  $\text{Y}_2\text{Hf}_2\text{O}_7:2\text{at}\%\text{Eu}^{3+}$  nanophosphor.

## OPTICAL AND LUMINESCENT PROPERTIES OF RARE-EARTH GALLIUM BORATES $RGa_3(BO_3)_4$ , WHERE $R = Nd, Sm - Er, Y$

Elena A. Dobretsova<sup>a</sup>, Kirill N. Boldyrev<sup>a</sup>, Elena Yu. Borovikova<sup>b</sup>

<sup>a</sup>*Institute for Spectroscopy RAS, 142190, Fysicheskaya 5, Moscow, Troitsk, Russia,  
elena-dobrecova@yandex.ru*

<sup>b</sup>*Department of Crystallography and Crystal Chemistry, Faculty of Geology, Moscow State  
University, 119991, GSP-1, Moscow, Russia*

The family of rare-earth borates with general formula  $RM_3(BO_3)_4$ , where  $R = Nd, Sm - Er, Y$  and  $M = Al, Ga, Fe, \text{ and } Cr$  possesses an application potential. The aluminum borates  $RA_3(BO_3)_4$  exhibit excellent luminescent and nonlinear optical properties combined with chemical stability and good physical parameters. They are used in self-frequency doubling and mini-lasers. Gallium borates are much less studied.

The crystals of rare-earth gallium borates  $RGa_3(BO_3)_4$ ,  $R = Nd, Sm - Er, Y$ , were grown by the flux method. All gallium borates were investigated by infrared (IR) spectroscopy technique in a middle- and far IR regions. The factor group and correlational analyses were carried out [1,2]. External modes include the translational modes of  $R^{3+}$ ,  $Ga^{3+}$ , and  $BO_3^{3-}$  ions and the  $BO_3$  librations, whereas the internal modes are related to the vibrations of  $BO_3$  groups. In the IR spectra of gallium borates with  $Eu^{3+}$  and  $Nd^{3+}$  ions, we can see additional bands in the region of  $\nu_1$  vibrations of the  $BO_3^{3-}$  units. The appearance of these bands must be related to an admixture of a monoclinic phase.

Luminescence spectra and luminescence decay curves for  $EuGa_3(BO_3)_4$  and  $HoGa_3(BO_3)_4$  were measured at room temperature using a laboratory setup of the Skobeltsyn Institute of Nuclear Physics. A nitrogen laser ( $\lambda=337$  nm) was used as an excitation source. The spectrum of the Eu gallium borate exhibits typical features in the region 500–750 nm, caused by intraconfigurational  $4f^6 \rightarrow 4f^6$  transitions of  $Eu^{3+}$ . The most intensive peak is attributed to the electric-dipole (ED) hypersensitive transition  $^5D_0 \rightarrow ^7F_2$  (~614 nm). The fluorescence decay curve observed for the 614 nm emission band after pumping at 337 nm shows a single exponential decay with a lifetime of about 940  $\mu s$ . A broad luminescence band with a maximum at about 430 nm was observed for  $HoGa_3(BO_3)_4$ . The decay curve for this band shows a simple exponential decay with a lifetime of about 140  $\mu s$ .

Support by the President of Russian Federation (D.E.A. project CII-754.2015.1) and by the Russian Science Foundation (grant No 14-12-01033) is acknowledged.

[1] D. Fausti, A. Nugroho, P. v. Loosdrecht, S. Klimin, M. Popova, L. Bezmaternykh, PRB 74 (2006) 024403.

[2] E.Yu. Borovikova, E.A. Dobretsova, K.N. Boldyrev, V.S. Kurazhkovskaya, V.V. Maltsev, N.I. Leonyuk, Vibr. spectr. 68 (2013) 82–90.

## **NONLINEAR OPTICAL PROPERTIES OF $\text{TeO}_2\text{-P}_2\text{O}_5\text{-ZnO-LiNbO}_3$ GLASSES DOPED BY $\text{Er}_2\text{O}_3$ , $\text{Nd}_2\text{O}_3$ AND $\text{Gd}_2\text{O}_3$ RARE EARTH IONS**

Rafał Miedziński<sup>a</sup>, Izabela Fuks-Janczarek<sup>b</sup>, El Sayed Yousef<sup>c</sup>

<sup>a</sup>*Institute of Physics, J. Dlugosz University, Al. Armii Krajowej 13/15, Czestochowa, Poland, r.miedzinski@ajd.czyst.pl*

<sup>b</sup>*Institute of Physics, J. Dlugosz University, Al. Armii Krajowej 13/15, Czestochowa, Poland, i.fuks@ajd.czyst.pl*

<sup>c</sup>*Department, Faculty of Science, King Khalid University, P. O. Box 9004, Abha, Saudi Arabia*

This paper presents measurements of nonlinear optical properties of  $\text{TeO}_2\text{-P}_2\text{O}_5\text{-ZnO-LiNbO}_3$  glasses doped by  $\text{Er}_2\text{O}_3$ ,  $\text{Nd}_2\text{O}_3$  and  $\text{Gd}_2\text{O}_3$  using single beam z-scan technique. The sample was moved along z-axis in range of 50 mm experiencing different levels of irradiance. The pulsed Nd:YAG laser were used at 532 nm wavelength and 5ns pulse width. The z-scan results are fitting by using mathematical software in order to obtain nonlinear refractive index and nonlinear absorption coefficient of the investigated material. The lowest nonlinear absorption coefficient obtained for undoped glass (0.41 cm/GW) and the highest for glass containing  $\text{Er}_2\text{O}_3$  ions (0.54 cm/GW).

## NON-ISOTHERMAL KINETIC BEHAVIOR OF CRYSTALLIZATION PROCESS OF $Y_2Ti_2O_7$

Bojana Milićević<sup>a</sup>, Sanja Čulubrk<sup>a</sup>, Željka Antić<sup>b</sup>, Miroslav D. Dramićanin<sup>a</sup>, Milena Marinović-Cincović<sup>a</sup>

<sup>a</sup>*Institute of Nuclear Sciences "Vinča", University of Belgrade, P.O.Box 522, 11000 Belgrade, Serbia, milena@vinca.rs*

<sup>b</sup>*Department of Chemical and Materials Engineering, University of Alberta, Edmonton, Canada*

The crystallization process of  $Y_2Ti_2O_7$  powders prepared by Pechini-type polymerized complex route has been studied under non-isothermal conditions [1]. In order to characterize the precursor's powders and final product of the crystallization, a variety of experimental techniques, such as simultaneous thermogravimetric (TG) and differential thermal analysis (DTA), Fourier transform infrared (FTIR) spectroscopy, X-ray diffraction (XRD) analysis, the scanning electron microscopy (SEM) and transmission electron microscopy (TEM) analyses were used. Samples were characterized with differential thermal analysis (DTA) using different heating rates (5, 10, 20, 40 °C /min) to study the kinetics of crystallization process. The value of apparent energy activation of investigated process was calculated with two non-isothermal methods based on the Arrhenius equation: Kissinger and Ozawa, as well as isoconversional analysis. The average values of activation energy in  $Y_2Ti_2O_7$  ceramics were 820 kJmol<sup>-1</sup> in both transformation process.

Based on the results of DTA analysis and calculated crystallization values (n=3, m=2) it was concluded that the apparent isothermal crystallization process include a constant rate of nucleation and two-dimensional growth of nuclei, and excludes the possibility of surface crystallization. A special relationship between degree of conversion, energy activation and temperature was discussed in detail.

[1] B. Janković, M. Marinović-Cincović, M. Dramićanin, J. Phys. Chem. Solids 85 (2015) 160-172

## OPTICAL STUDIES OF THE ABSORPTION CURVES OF KDP CRYSTAL

Temirgaly Koketai, Ainura Tussupbekova, Askhat Baltabekov, Batima Tagayeva, Anel Ibrayeva, Elmira Mussenova  
*Academician Y.A. Buketov Karaganda State University, 28 Universitetskaya Street  
 Karaganda, Kazakhstan, aintus\_070482@mail.ru*

This paper presents results of the optical study of the adsorption curves of doped KDP crystal. For this purpose crystal KDP ( $\text{KH}_2\text{PO}_4$ ) was activated by divalent manganese ions. The main research methods were the methods of thermoactivation spectroscopy.

Obtained for these objects absorption curve (Fig. 1) were compared with curve for pure KDP crystal from [1]. There are two broad bands of non-elementary optical absorption in the area of transparency of the matrix: in 1.5-2.2 eV region and in 5.7-6.2 eV region. It is obvious that the emergence of these absorption bands associated with electron transitions of impurity metal ions.

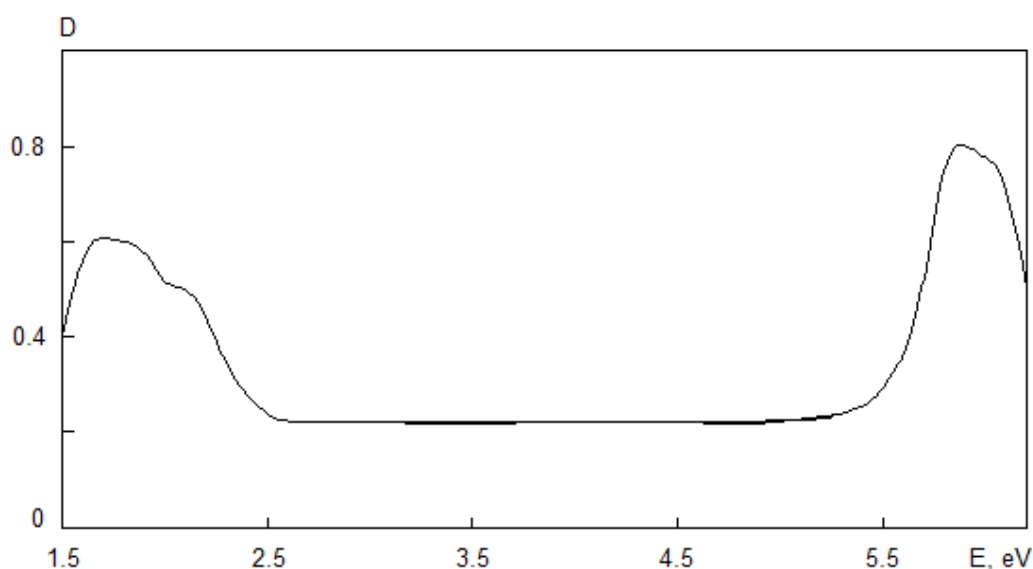


Figure 1. Absorption spectrum KDP- $\text{MnSO}_4$  crystal ( $T=80\text{K}$ )

This result leads to the following conclusion: the manganese ions in the activation of KDP by sulfate are forming two types of impurity centers in the crystal lattice.

[1] T.A. Koketai, B.S. Tagayeva, A.K. Tussupbekova, G.I. Mussina, B.A. Baizhitova, Book of abstracts. International conference on Radiation Physics and Chemistry of Condensed Matter, (2014) 443.

## NATURE AND FORMATION ENERGY OF ABSORBING CENTRES CAUSED BY REDUCING HEAT TREATMENT IN $\text{LiNbO}_3$ , $\text{LiNbO}_3\text{:Mg}$ AND $\text{LiNbO}_3\text{:Fe}$ CRYSTALS

Dmitro Sugak<sup>a,b</sup>, Oleg Buryy<sup>a</sup>, Yuriy Sugak<sup>c</sup>, Klaus-Dieter Becker<sup>d</sup>, Ivan Solskii<sup>b</sup>, Sergii Ubizskii<sup>a</sup>

<sup>a</sup>*Lviv Polytechnic National University, 12 Bandera St., Lviv, Ukraine, dm\_sugak@yahoo.com*

<sup>b</sup>*Scientific Research Company "Carat", 202 Stryjska St., Lviv, Ukraine*

<sup>c</sup>*Institute of Energy Research and Physical Technologies, TU Clausthal, Germany*

<sup>d</sup>*Institute of Physical and Theoretical Chemistry, TU Braunschweig, Germany*

The reducing annealing of lithium niobate (LN) is used in acoustoelectronic and electrooptic active elements manufacturing technology to reduce the impact of pyroelectric effects on device characteristics [1, 2]. Despite the large number of publications devoted to the occurrence of induced absorption (IA), the nature of the centers and mechanisms of their formation under the influence of thermal treatment remains the subject of debate. In particular, this concerns the determination of activation energy of absorbing centers formation processes directly during reducing annealing.

Congruent  $\text{LiNbO}_3$ ,  $\text{LiNbO}_3\text{:Mg}$  (LN-Mg) and  $\text{LiNbO}_3\text{:Fe}$  (LN-Fe) crystals were grown by the Czochralski method. MgO content was 5 mol.%. The content of Fe ions was 0.2 at.%. Investigation of IA was performed *in-situ* during heating samples up to  $T \sim 1200$  K in 95% Ar + 5%  $\text{H}_2$  gas mixture using a spectrophotometer Perkin-Elmer Lambda9, equipped with a special oven [3].

The coloration of undoped LN crystals occurs in two stages. Firstly, the IA appears at the  $10000\text{ cm}^{-1}$  region at temperatures 700-870 K. The formation of this absorption band is connected with the appearance of  $\text{Nb}_{\text{Li}}^{4+}$  polarons. Further heating causes the appearance of IA at the region of about  $16000\text{ cm}^{-1}$ . The appearance of this band is associated with the formation of bipolarons ( $\text{Nb}_{\text{Li}}^{4+} - \text{Nb}_{\text{Nb}}^{4+}$ ). Cooling of the LN from 870 K to 300 K leads to the transformation of polarons in bipolarons, accompanied by conversion of low energy band to the high energy band. Cooling from temperatures, higher than 870K does not change the shape of LN spectrum. The coloration of LN-Mg crystals has different features due to the fact that  $\text{Mg}^{2+}$  ions prevent  $\text{Nb}_{\text{Li}}$  formation. That is why at the first stage the IA band at  $8000\text{ cm}^{-1}$  appears which is connected with the free polarons. Cooling of LN-Mg from 870 K to 300 K does not change the spectrum - the IA at  $8000\text{ cm}^{-1}$  remains hence the transformation of free polarons into bipolarons does not happen. LN-Mg reducing from  $T > 870$  K leads to the appearance of IA band connected with bipolarons. Cooling of the LN-Mg from  $T > 870$  K to 300 K does not change the IA spectrum. The coloration of LN-Fe crystals occurs in three stages. At  $T \geq 470$  K the IA band appears at about  $20000\text{ cm}^{-1}$  caused by  $\text{Fe}^{3+} \rightarrow \text{Fe}^{2+}$  recharging. Further LN-Fe heating leads to changes similar to those occurring in the LN and LN-Mg crystals. Approximation of temperature increase of IA allowed to determine activation energies of  $\text{Nb}_{\text{Li}}^{4+}$  formation (0,6-1,0 eV); bipolarons formation (0,30-0,45 eV);  $\text{Nb}_{\text{Nb}}^{4+}$  formation (1,04...1,07 eV) and  $\text{Fe}^{3+} \rightarrow \text{Fe}^{2+}$  recharging (0,66...0,69 eV) for the first time. The nature of investigated processes is discussed in terms of oxygen outdiffusion.

[1] P.F. Bordui, D.H. Jundt, E.M. Standifer, R.G. Norwood, R.L. Sawin, J.D. Galipeau, J. Appl. Phys. 5 (1999) 3766

[2] B. Brickeen, C. Shanta, Opt. Eng. 49 (2010) 124201.

[3] D. Sugak, Ya. Zhydachevskii, Yu. Sugak, O. Buryy, S. Ubizskii, I. Solskii, M. Schrader, K-D Becker, J. Phys.: Cond. Matter. 19 (2007) 086211.



## MODEL OF NANOCONE STRUCTURE WITH GIANT POLARIZABILITY

William Gutiérrez Niño, Luis Francisco García, Ilia D. Mikhailov  
*Universidad Industrial de Santander, Calle 9 # 27, Bucaramanga, Colombia A.A. 678,*  
*willigun@gmail.com*

Currently semiconductor nanowires are considered as one of the most promising building blocks for the design of a variety of photonic devices. Light emitting diodes, photodetectors, solar cells and solid-state sources of single-photons are some of their potential applications. Today, the ability to control the growing of nanowires has become possible fabricating different 1D nanostructures such as nanowire superlattices [1] and nanocones [2] and nanotubes [3] offering several attractive routes to design novel materials with particular properties by varying the composition or the geometry. As example, we consider a model of a cone-shaped nanowire structure with n-type top layer in the presence of the electric field applied along the symmetry axis. A simple mathematical model describing the electronic properties of such system is the Schrödinger equation for the electron confined inside of a nanowire in a form of a truncated cone with a shallow donor situated at its upper surface. Our calculations reveal that in the ground state the electron is mainly located close to the donor while in the first excited states it is found predominantly nearly the bottom and the energy gap between these states is very sensitive to the variation of the cone's aperture angle and the external electric field. The larger the aperture angle, the smaller is the energy gap and the superior is a dipole moment of the excited state. We show that the increasing external electric field induces a lowering of the donor ionization potential, diminishing successively the energy gap until it becomes equal to zero for a critical value of the external electric field. As the electric field further increases, the electron in its ground state jumps from the upper region toward the bottom of the nanocone, generating a giant dipole moment.

[1] M.S. Gudiksen, J.L. Lauhon, J. Wang, D.C. Smith, C.M. Lieber, *Nature* 415 (2002) 617-620

[2] Rui Yu, Qingfeng Lin, Siu-Fung Leung, Zhiyong Fan, *Nano Energy* 1 (2012) 57-72

[3] P. Mohan, J. Motohisa, and T. Fukui, *Nanotechnology* 16 (2005) 2903-2907; *Appl. Phys. Lett.* 88 (2006) 133105-133110

## LUMINESCENCE PROPERTIES, JUDD-OFELT ANALYSIS AND EMISSION ON UP-CONVERSION UNDER 612 NM EXCITATION IN A NEW ERBIUM DOPED GERMANO-TELLURITE GLASS

Y. Benmadani<sup>a,b</sup>, A. Kermaoui<sup>a</sup>, R. Si Fodil<sup>a</sup>, A. Kellou<sup>a</sup>, M. Benabdesselam<sup>c</sup>

<sup>a</sup> *Laboratory of Quantum Electronics, Faculty of physics, U.S.T.H.B., B.P. :32, El-Alia, 16111 Bab- Ezzouar, Algiers, Algeria*

<sup>b</sup> *Department of physics, Faculty of sciences and Technology, University Doctor YAHIA FARES, Medea, Algeria*

<sup>c</sup> *Université Nice Sophia Antipolis, Laboratoire Physique de la Matière Condensée, CNRS UMR 7336, Parc Valrose, F06108 Nice cedex 2, France*

*Corresponding Author: yanis\_phy@live.fr*

In this work, a new transparent Erbium doped Germano-Tellurite glass has been synthesized by the melt-quenching method. The studied glass has a high thermal stability and a strong mechanical hardness [1] and might be suitable for developing optical fiber and broadband amplifiers.

According to the visible- near infrared absorption spectrum, the optical transitions of absorption have been assigned and the up-conversion emissions have been investigated.

The Judd-Ofelt (J-O) intensity parameters ( $\Omega_2$ ,  $\Omega_4$ ,  $\Omega_6$ ) were determined and then used to calculate the radiative transition probabilities of excited states of Erbium ions.

The obtained results were compared to those of other glasses given in the literature [2]. Thus the studied glass shows a good disposition to emit a visible green luminescence, corresponding to the radiative electronic transitions from  $^4S_{3/2}$  and  $^2H_{11/2}$  levels to the ground state  $^4I_{15/2}$  of trivalent Erbium ions.

These two transitions centred at around 523 and 547nm respectively, have been obtained in up-conversion emissions under laser diode excitation at 612nm.

The dependence of these anti-Stokes green emissions as a function of pump power excitation has been studied and confirmed the non linear phenomenon of Two-Photons absorption. Indeed, this variation was represented by the slopes of the linear regression of 1.75 for both green emissions. The value of this slopes confirmed that two photons absorption processes which contribute to the up-conversion of the two visible green emission bands.

[1] Y. Yang, B.Chen, C.Wang, G.Ren, Q.Meng, X.Zhao, W.Di, X.Wang, J.Sun, L.Cheng, T.Yu, Y.Peng, *Journal of non Crystalline Solids*, 354 (2008) 3747-3751.

[2] Y.Benmadani, A.Kermaoui, M.Chalal, W.Khemici, A.Kellou, F.Pellé, *Optical Materials*, 35 (2013) 2234-2240.

## LUMINESCENCE SPECTROSCOPY OF $\text{Eu}^{3+}$ IONS IN $\text{Lu}_3\text{Ga}_5\text{O}_{12}$ GARNET

A.P. Luचेchko<sup>a</sup>, I.I. Syvorotka<sup>b</sup>, I.M. Syvorotka<sup>b</sup>

<sup>a</sup>*Ivan Franko National University of L'viv, Faculty of Electronics, 107 Tarnavskogo Str.,  
L'viv 79017, Ukraine, luचेchko@electronics.lnu.edu.ua*

<sup>b</sup>*SRC "Carat", 202 Stryjska Str., 79031 L'viv, Ukraine, syvorotka.jr@gmail.com*

In recent years, many researchers give attention to the oxide-based phosphors in order to obtain efficient luminescent materials for solid state lasers, luminophores and scintillators. The oxides with garnet structure, in particular lutetium gallium garnet ( $\text{Lu}_3\text{Ga}_5\text{O}_{12}$ ), are perspective materials for phosphors and X-ray screens. The luminescent properties of garnets can be modified by doping with rare earth ions.  $\text{Eu}^{3+}$ -activated  $\text{Lu}_3\text{Ga}_5\text{O}_{12}$  have attracted the most attention because of its higher density in comparison with many other oxide materials as well as excellent luminescence properties in orange and red spectral region [1-3].

Epitaxial films  $\text{Lu}_3\text{Ga}_5\text{O}_{12}:\text{Eu}^{3+}$  were grown on 2 inch (111)-oriented  $\text{Gd}_3\text{Ga}_5\text{O}_{12}$  substrates by conventional dipping LPE technique using lead-free flux based on  $\text{Bi}_2\text{O}_3$ -  $\text{B}_2\text{O}_3$ . The substrate and film lattice parameters were determined by standard X-ray diffractometry (XRD) method using the DRON-3 diffractometer. The X-ray and photoluminescence properties of the  $\text{Lu}_3\text{Ga}_5\text{O}_{12}$  with  $\text{Eu}^{3+}$  ions concentration equal 1-2 at.% were investigated in the temperature range 77-550 K.

It has been established that emission intensity of the  $\text{Lu}_3\text{Ga}_5\text{O}_{12}$  epitaxial films depends on the growing features, type of excitation, activator concentration and temperature.

Photoluminescence of  $\text{Eu}^{3+}$  ions is mainly excited in broad UV band 210-340 nm (charge-transfer  $\text{O}^{2-} \rightarrow \text{Eu}^{3+}$ ) and in the sharp lines corresponded to  $4f-4f$  forbidden transitions of  $\text{Eu}^{3+}$  ions. The most intense excitation line of  $\text{Eu}^{3+}$  ions in  $\text{Lu}_3\text{Ga}_5\text{O}_{12}:\text{Eu}^{3+}$  epitaxial films is observed at 393 nm ( ${}^7\text{F}_0 \rightarrow {}^5\text{L}_6$  transitions in  $\text{Eu}^{3+}$  ions).

The X-ray and photoluminescence spectra of  $\text{Eu}^{3+}$  ions in  $\text{Lu}_3\text{Ga}_5\text{O}:\text{Eu}^{3+}$  epitaxial films are characteristic to the  $f \rightarrow f$  transition in the  $\text{Eu}^{3+}$  ions that occupied dodecahedral sites in the garnet structure. The strong characteristic lines assigned to the  ${}^5\text{D}_0 \rightarrow {}^7\text{F}_j$  ( $j = 1, 2, 4$ ) transitions in the  $\text{Eu}^{3+}$  ions were observed in the luminescence spectra of all investigated films. It should be also noted that the long-wavelength luminescence band at about 706 nm ( ${}^5\text{D}_0 \rightarrow {}^7\text{F}_4$  transition) is dominant under X-ray excitation. The temperature dependences of X-ray luminescence at the monitoring spectra on 591 and 706 nm were investigated in the temperature range 85-550 K.

[1] H. Ogino, A.Yoshikawa, M. Nikl, J.A. Mares et al, Journal of Crystal Growth 311 (2009) 908-911.

[2] A. Luचेchko, I.I. Syvorotka, Ya. Zakharko, I.M. Syvorotka, Solid State Phenomena 230 (2015) 166-171.

[3] V. Venkatramu, M. Giarola, G. Mariotto, S. Enzo, S. Polizzi et al, Nanotechnology 21 (2010) 175703+12.

## LUMINESCENT LABELING OF NANOCRYSTALS: SiO<sub>2</sub> @ LaPO<sub>4</sub>

Jacobine van Hest<sup>a</sup>, Andries Meijerink<sup>b</sup>

<sup>a</sup>*Utrecht University, Princetonplein 1, Utrecht, The Netherlands, J.J.H.A.vanHest@uu.nl*

<sup>b</sup>*Utrecht University, Princetonplein 1, Utrecht, The Netherlands, A.Meijerink@uu.nl*

Nanomaterials are embedded in a variety of products we use daily, e.g. silica nanocrystals are applied in rubber, paper and cement. However, not much is known about the environmental and health risks of nano-enabled products. For this reason, it is necessary to study these systems in more detail. The demand for guidelines for nanomaterials asks for model-nanosystems that can be followed and identified during their life cycle.

In this project, we have synthesized silica nanocrystals with a luminescent LaPO<sub>4</sub> core. The size of the luminescent core was varied between 4 and 8 nm by changing the lanthanide precursor to ligand ratio using the method of Hickmann [1]. The luminescent properties of the nanocrystal were varied by changing or combining the nature of the lanthanide dopants in the LaPO<sub>4</sub> nanocrystal. In this way, it is possible to obtain a lot of unique luminescent labels.

Silica was grown around the luminescent LaPO<sub>4</sub> cores using the reverse micelle method [2]. Silica spheres with sizes between 35 and 85 nm could be obtained. The size of the silica particles could be increased by changing the dispersion medium of the LaPO<sub>4</sub> nanocrystals to a more polar one. The nanocrystals preserved their luminescence properties after silica coating.

The next step is to study the spreading and properties like clustering behavior of the nanocrystals with fluorescence microscopy. The fluorescent nanoparticles make it possible to use combined fluorescence and electron microscopy for the analysis of the nanoparticles, down to the single particle level – and is in progress.

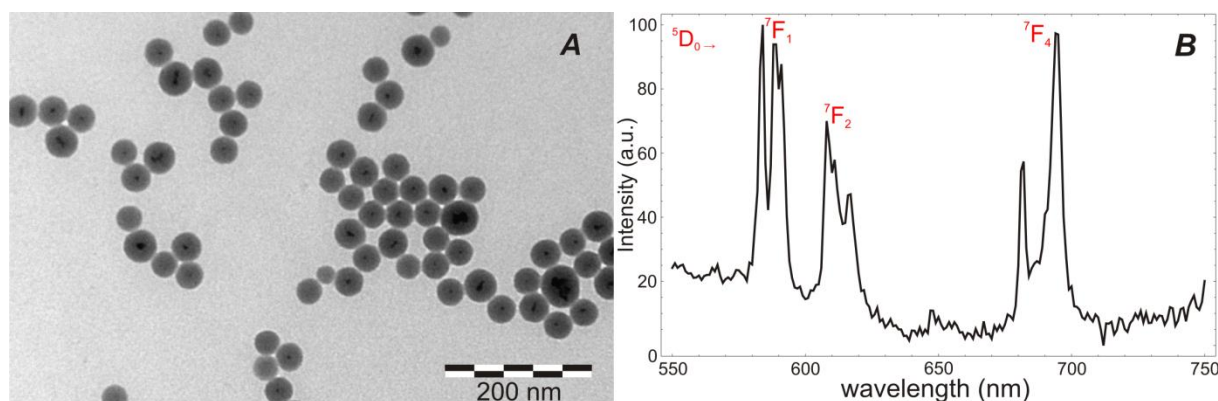


Figure 1. A: TEM image of LaPO<sub>4</sub>:Eu<sup>3+</sup> nanocrystals incorporated into silica spheres of  $36.9 \pm 3.9$  nm. B: emission spectrum of these particles upon excitation at 280 nm.

[1] K. Hickmann, K. Kömpe, A. Hepp, M. Haase, *Small*, 4 (2008) 2136-2139

[2] R. Koole, M. van Schooneveld, J. Hilhorst, C. de Mello Donegá, D. C. 't Hart, A. van Blaaderen, D. Vanmaekelbergh, A. Meijerink, *Chem. Mater.* 20 (2008) 2503-2512

## LUMINESCENT PROPERTIES OF FLUOROPHOSPHATE GLASS DOPED WITH COPPER IONS

*Anastasiia N. Babkina, Pavel S. Shirshnev, Nikolay V. Nikonorov, Elena V. Kolobkova  
ITMO University, 4 Birjevaja line, Saint-Petersburg, Russia, babkina.anastasya@email.com*

Glasses and polymers, containing copper (I) ions ( $\text{Cu}^+$ ) or copper chemical compounds have attracted considerable attention because of their specific optical properties.  $\text{Cu}^+$  ions in an oxide glass matrix is well known to produce blue emission under ultraviolet (UV) excitation ( $\lambda_{\text{exc}} = 250\text{-}260\text{ nm}$ ) [1]. The given research is aimed to investigate the influence of temperature on the luminescence spectra and the total intensity of luminescence of the phosphate glasses with univalent copper ions in the temperature interval from 77K up to 623K. The phosphate glasses have the following composition:  $\text{NaPO}_3(40)\text{-Ba}(\text{PO}_3)_2(19,5)\text{-AlF}_3(40,5)$  (mol%) matrix with  $\text{CuCl}$  as a dopant. The glass was synthesized in the corundum crucibles at  $1100\text{ }^\circ\text{C}$  for 1 h. The irradiation of the glasses by 260-320nm induce the luminescent band with the maximum on 460 nm, the excitation by 330 nm and more shows the band with the maximum on 580 nm. It means there are several luminescent centers:  $\text{Cu}^+$  ions in the shortwavelength region and the  $(\text{Cu}_2\text{O})_n$  molecular clusters in the long wavelength region [2].

The main source of irradiation during temperature experiments is the semiconductor laser with ( $\lambda_{\text{exc}} = 405\text{ nm}$ ). Thus the luminescence of molecular clusters only is reached. While heating the sample from the room temperature up to 623K the color of the luminescence changes from red to green-blue one. In case of cooling the sample of the glass from the room temperature down to the liquid nitrogen boiling temperature the color changes to deep red. The obtained experimental data reveals that the luminescent band has shifted on 45nm during the heating period from 293K up to 543K. During heating the intensity increases by almost 2 times.

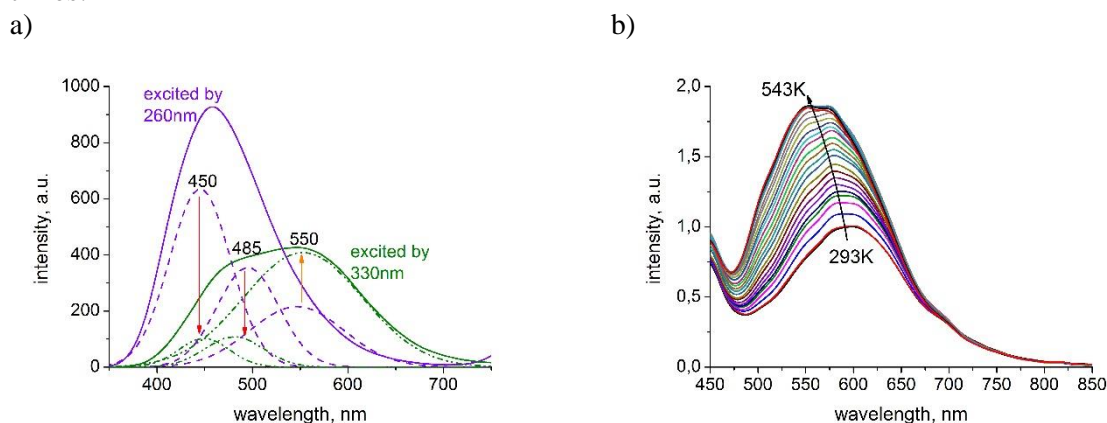


**Fig.1** - Luminescence spectra, obtained at a) - 293K under different excitation wavelengths, b – different temperatures under excitation by 405 nm.

As a result the phosphate glasses can be used as the materials for the sensitive core of the luminescent temperature sensor. They can provide not only measuring the temperature in one point but also calculating the temperature gradient spread over long-distance objects and comparing temperature of different objects.

[1] H. Chen, M. Matsuoka, J. Zhang, M. Anpo, J. Catal. 228 (2004) 75-78.

[2] .N. Babkina, N.V. Nikonorov, T.A. Shakhverdov, P.S. Shirshnev, A.I. Sidorov. Opt. Mat. 36 (2014) 773–777.

## LUMINESCENT PROPERTIES OF SILVER MOLECULAR CLUSTERS IN PHOTO-THERMO-REFRACTIVE GLASSES CONTAINING CHLORIDE AND BROMIDE AGENTS

Victor D. Dubrovin, Aleksander I. Ignatiev, Nikolai V. Nikonorov

*Saint-Petersburg National Research University of Information Technologies, Mechanics and Optics, 49, Kronverkskiy pr., 197101 Saint-Petersburg, Russia*

The most widely used material for solar panels is silicon, due to its low cost and prevalence, but it also has some disadvantages like a limited operating range (400-1100nm) and relatively low efficiency, about 12-20%. One of the materials, which allow to extend operation range and consequently increase the solar cell efficiency, is photo-thermo-refractive glasses (PTR). These glasses are perspective for use as spectral down-converters in solar energy and LED white light. PTR glasses other than the above applications may be used for the optical recording and storage of information by allowing the local transformation of charged molecular clusters in neutral by UV irradiation.

In the work we investigated the PTR glasses based on the  $\text{Na}_2\text{O-ZnO-Al}_2\text{O}_3\text{-SiO}_2\text{-NaF-NaHal}$  (Hal being Cl or Br 0 - 2,2 mol.%) and doped with photo-sensitive dopant of  $\text{CeO}_2$  (0.007 mol.%), reductant dopant of  $\text{Sb}_2\text{O}_3$  (0.04 mol.%) and also  $\text{Ag}_2\text{O}$  were synthesized.

For the UV irradiation of PTR glass samples under study, a mercury lamp was used, one of the radiation maxima of the lamp coinciding practically in location ( $\lambda=305\text{-}315\text{ nm}$ ) with the absorption maximum of  $\text{Ce}^{3+}$  ions. For heat-treating the samples, Heat treatment was carried out at different temperatures (250, 300, 350, 400 °C) with in 1h.

Fig. 1 shows the luminescence spectra of PTR glasses containing NaCl and NaBr, for different halides concentration after UV irradiation.

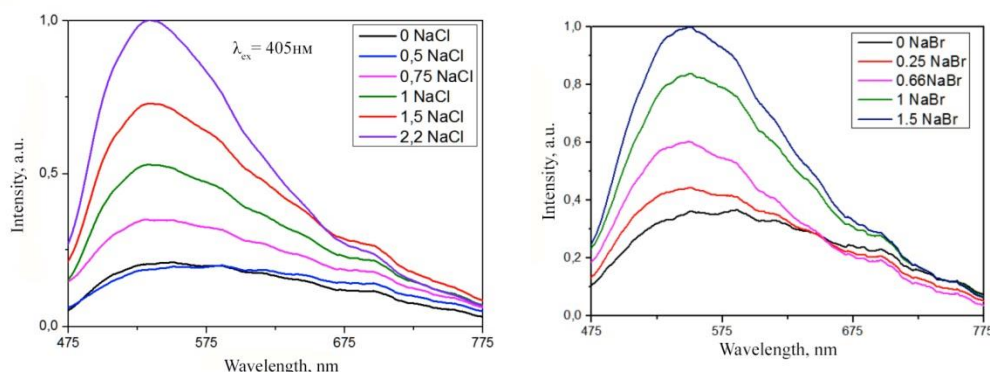


**Fig. 1** – Luminescence spectra of PTR(Cl) (a) and PTR(Br) (b) glasses samples after the UV irradiation

Increasing halides concentration in glass results in significant increase of silver MC luminescence intensity, up to 6,5 times for PTR(Cl) glasses and 2,5 for PTR(Br) glasses. Subsequent heat treatment of PTR glasses below glass transition temperature leads to a significant increase of neutral silver molecular clusters luminescence intensity because of an increase in their number.

Chlorides and bromides injection in PTR glass composition leads to the formation of neutral clusters such as  $\text{Ag}_n\text{Cl}$  &  $\text{Ag}_n\text{Br}$  respectively, which results in the luminescence peak shift. Because of rather big value of quantum yield (up to 50%) these glasses could be used as replacement of usual cover glasses to increase silicon solar cells efficiency.

## LUMINESCENT PROPERTIES OF YAG: Gd, Ce PHOSPHORS UNDER PHOTO- AND ELECTRONIC EXCITATION

Damir Valiev, Sergey Stepanov, Viktor Lisitsyn  
National Research Tomsk Polytechnic University, 30 Lenin Avenue, Tomsk, Russia,  
stepanovsa@tpu.ru

The results of research of spectral-kinetic characteristics of the luminescence of a series industrial phosphors YAG:Gd, Ce («FL5049», «AWB3» and «LEUD560») under influence different sources of excitation (pulsed electron accelerator  $E_e=280$  KeV, nitrogen laser  $E_{hv}=3.68$  eV and LED  $E_{hv}=2.76$  eV) are compared. These phosphors are promising for use as transducers of emission in the range 400-500 nm [1-2], but the process of energy transfer to luminescence centers, as well as the composition investigated not enough.

The obtained spectra of pulse cathodoluminescence and photoluminescence under these types of excitation have a similar shape. Consequently excited same luminescence centers. Perhaps the luminescence centers are components of the cluster. To confirm are investigated characteristics decay kinetic of luminescence.

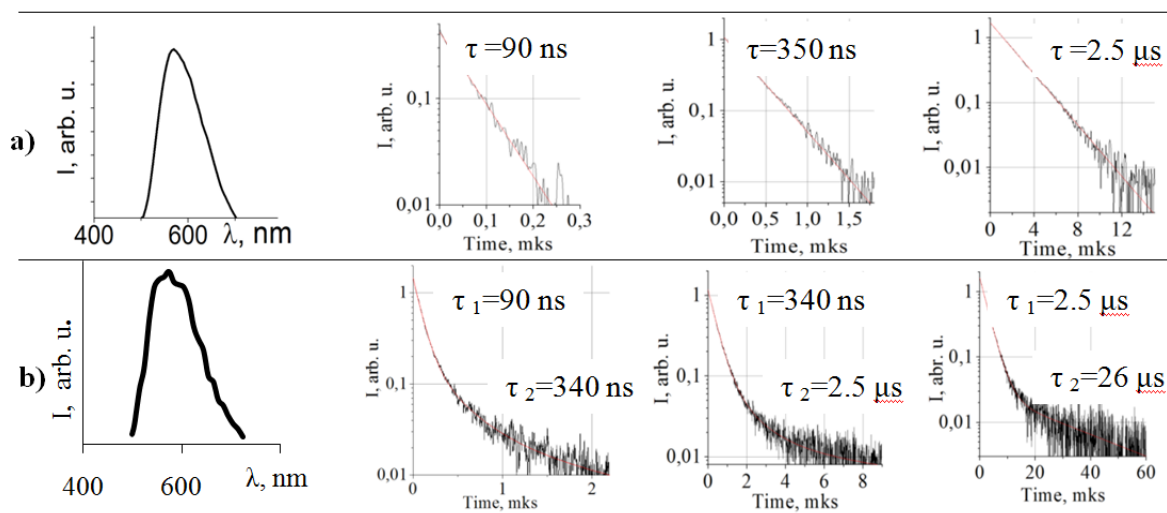


Fig. 1. Spectral and kinetic characteristics of pulse luminescence of YAG:Gd, Ce phosphor (FL5049) under influence nitrogen laser (a) and pulse electron accelerator (b).

From the results of the decomposition decay kinetic curves of luminescence for all the used excitation sources are allocated similar characteristic times was found. The difference in the form of decay kinetic curves photo- and cathodoluminescence by different ratios of localization of energy levels of defects can be explained. Consequently, the excitation energy localizes on defects (traps), spatially close to the luminescence center. The efficiency of energy transfer to a luminescence center is determined by space and energy correlated pairs: trap - luminescence center. Formation of such pairs occurs during the synthesis. These pairs may be part of the cluster [3], which is an effective capture area of ionizing excitation.

This study was financially supported by grants of the Ministry of Education and Science of Kazakhstan Republic (a. N 32, 349).

[1] S. Nishimira, S. Tanabe, K. Fujoka, Y. Fujimoto, Opt. Mater. 33 (2011) 688–691.

[2] S. Nakamura, Blue laser Diode, Springer-Verlag, Berlin, 1997.

[3] V.M. Lisitsyn, D.T. Valiev, I.A. Tupitsyna, E.F. Polissadova, V.I. Oleshko, L.A. Lisitsyna, L.A. Andryuschenko, A.G. Yakubovskaya, O.M. Vovk, J. Lumin. 153 (2014) 130–135.



## MAGNETIC FEATURES AND PHASE TRANSITIONS OF $\text{Ni}_3(\text{BO}_3)_2$ SINGLE CRYSTAL

Anastasiia D. Molchanova<sup>a</sup>, Kirill N. Boldyrev<sup>a</sup>, Roman V. Pisarev<sup>b</sup>

<sup>a</sup>*Institute of Spectroscopy RAS, 5 Fizicheskaya, Troitsk, Moscow, Russia,  
nastyamolchanova@list.ru*

<sup>b</sup>*Ioffe Physical Technical Institute RAS, 26 Politekhnickeskaya, St Petersburg, Russia,  
pisarev@mail.ioffe.ru*

$\text{Ni}_3(\text{BO}_3)_2$  belongs to the group of the transition metal oxyborates  $\text{Me}_3(\text{BO}_3)_2$ , where  $\text{Me} = \text{Mg}, \text{Mn}, \text{Co},$  and  $\text{Ni}$ . These orthorhombic materials crystallize in the kotoite structure with two nonequivalent octahedral positions for  $\text{Me}$  in the unit cell ( $2a$  and  $4f$ ). All of them are antiferromagnetics (for  $\text{Ni}_3(\text{BO}_3)_2$   $T_N=46\text{K}$ ). However, up to now many physical properties of this group of oxyborates remain unexplored. The present work is devoted to the first optical study of  $\text{Ni}_3(\text{BO}_3)_2$ . Infrared (IR) reflection and transmission spectra at the nearly normal incidence (at an angle  $\sim 10^\circ$ ) were registered in a broad spectral range using a Fourier-transform infrared spectrometer Bruker IFS 125HR. Modeling of infrared reflection spectra made it possible to establish TO-frequencies, damping coefficients ( $\gamma$ ) and oscillator strengths ( $f_j$ ) for all of the infrared-active phonons. High-frequency dielectric constants  $\epsilon_\infty$  were also determined for different directions of the light propagation. Below  $T_N$ , infrared transmission spectra of  $\text{Ni}_3(\text{BO}_3)_2$  show narrow satellites near strong phonon absorption lines. These satellites don't shift with a further decrease of the temperature (see. Fig. 1). Perhaps, they are associated with a doubling or quadrupling of the crystal unit cell, which occurs simultaneously with the magnetic ordering. Thus, we can explain the phenomenon by a folding of the Brillouin zone, so that we observe the edge of the zone in the spectra [1].

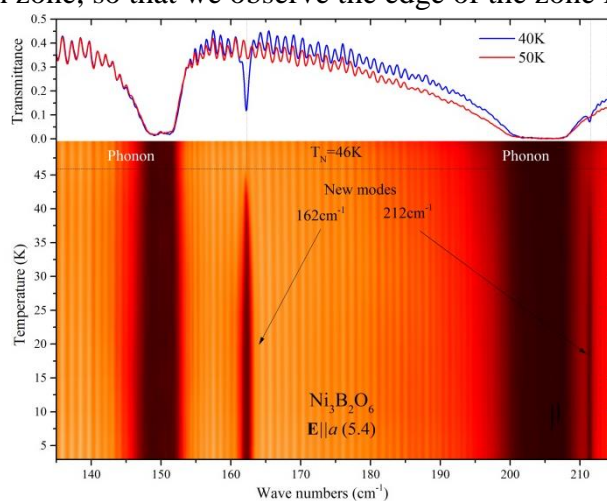


Fig. 1. Colormap of the transmission spectra in the far infrared region. The upper part shows the spectra above and below  $T_N$ .

Below  $T_N$ , new absorption bands appear at about  $17$  and  $26\text{ cm}^{-1}$ . They grow in intensity, narrow, and shift to higher frequencies with further lowering the temperature. These features were assigned to magnetic excitations (spin waves). Narrow lines associated with d-d transitions of the  $\text{Ni}^{2+}$  ion were also observed.

This work was supported by the RFBR Grant No 15-02-04222a and the President of the Russian Federation (Grant No MK-3521-2015.2).

[1] M.N.Popova, A.B.Sushkov, A.N.Vasil'ev, M.Isobe, Yu.Ueda, JETP Lett. 65 (1997) 743-748.



## SYNTHESIS AND PROPERTIES OF $\text{Eu}^{3+}$ DOPED $\text{Lu}_2\text{Ti}_2\text{O}_7$

Sanja Čulubrk, Katarina Vuković, Milena Marinović-Cincović, Miroslav D. Dramićanin  
*Vinča Institute of Nuclear Sciences, University of Belgrade, P.O. Box 522, 11001 Belgrade,  
Serbia, email: kvukovic@vinca.rs*

This paper reports chemical synthesis, structural and luminescent characterization, and Judd-Ofelt analysis of emission of  $\text{Eu}^{3+}$ -doped lutetium-titanate powders. We present fast and effective method for synthesis of  $\text{Lu}_2\text{Ti}_2\text{O}_7:\text{Eu}^{3+}$  based on polyesterification between citric acid (CA) and ethylene glycol (EG) [1,2]. An important aspect of this method is to use mixed metal-CA complex with stoichiometric Lu:Ti ratio of 1:1, rather than a simple mixture of individual metal-CA complexes. Set of six  $\text{Lu}_2\text{Ti}_2\text{O}_7$  samples are prepared with different  $\text{Eu}^{3+}$  concentrations (1; 3; 5; 7; 10 and 15 at.%). Thermal analysis made with TG-DTA revealed that the temperature required for the transformation to the pure pyrochlore phase was  $820^\circ\text{C}$ . X-ray diffraction measurements showed that  $\text{Lu}_2\text{Ti}_2\text{O}_7$  nanoparticles crystallized in the face-centered cubic lattice. Photoluminescence measurements are performed to analyze emission and emission decay characteristics of nanophosphors. Optical properties were examined by photoluminescence spectroscopy and spectra of all samples showed intense red emission, typical for f-f electronic transitions of the  $\text{Eu}^{3+}$  ions. Emission increase above 1 at.% of  $\text{Eu}^{3+}$ , reaching maximum at 15 at.%. Photoluminescence spectra of all samples clearly show characteristic lines centered around 579, 590, 654, 708 nm that correspond to  $^5\text{D}_0 \rightarrow ^7\text{F}_0$ ,  $^7\text{F}_1$ ,  $^7\text{F}_2$ ,  $^7\text{F}_3$  electronic transitions of  $\text{Eu}^{3+}$  ions, respectively. Judd-Ofelt theory was applied to experimental data for the quantitative determination of optical parameters such as  $\Omega_2$ ,  $\Omega_4$  Judd-Ofelt parameters, radiative and nonradiative transition rates and emission quantum efficiency. It was observed that, for all the samples,  $\Omega_2 > \Omega_4$ . This indicated the existence of a fair degree of covalency in the metal and ligand bonding. The luminescence quantum yields were calculated by for the different levels of doping.

- [1] S. Čulubrk, Ž. Antić, V. Lojpur, M. Marinović-Cincović, M. D. Dramićanin, *J. Nanomater.* 2015 (2015) 8  
[2] S. Čulubrk, Ž. Antić, M. Marinović-Cincović, P. S. Ahrenkiel, M. D. Dramićanin, *Opt. Mater.* 37 (2014) 598-606

## MOLTEN LIGAND SYNTHESIS METHOD AND LUMINESCENCE STUDY OF RE<sup>3+</sup> COMPLEXES WITH PIMELATE

Israel P. Assunção<sup>a</sup>, Hermi F. Brito<sup>a</sup>, Maria C.F.C. Felinto<sup>b</sup>, Oscar L. Malta<sup>c</sup>

<sup>a</sup>Instituto de Química da Universidade de São Paulo, São Paulo, SP, Brasil *ipassunc@iq.usp.br*

<sup>b</sup>Química e Meio Ambiente, Instituto de Pesquisas Energéticas e Nucleares, São Paulo, SP, Brasil.

<sup>c</sup>Departamento de Química Fundamental, Universidade Federal de Pernambuco, Recife, PE, Brasil.

For decades, the rare earth ions (RE<sup>3+</sup>) luminescent complexes have attracted much interest due to their intrinsic spectroscopic behavior and commercial applications in different areas such as: organic light-emitting diodes (OLEDs), luminescent security inks, sensors, optical markers, *etc* [1]. This work presents the molten ligand synthesis method of RE<sup>3+</sup> complexes, characterization and luminescent properties of the [RE<sub>2</sub>(PIM)<sub>3</sub>(DPSO)<sub>3</sub>] compound where RE: Eu<sup>3+</sup> and Tb<sup>3+</sup>; PIM: pimelic acid (heptanedioic acid) and DPSO: diphenyl sulfoxide. The lanthanides complexes were synthesized by molten ligand solid state method using the rare earth chloride and the PIM and DPSO ligands, which have the advantage of present low melting points at around 104 and 70 °C, respectively. The RE<sup>3+</sup> complexes were characterized via elemental analysis (CHN), thermal analysis coupled with mass spectrometry (TG/MS), x-ray diffraction by the powder method (XPD) and infrared spectroscopy (FTIR). The infrared absorption spectra indicate that the ligand-metal interaction is via chelate-bridging and their XPD patterns suggest high crystallinity and that the complexes present isomorphic character. The principal photoluminescence properties were determined based on the emission spectra of the Eu<sup>3+</sup> (Fig. 1, left) and Tb<sup>3+</sup> (Fig. 1, right) complexes, showing a highly intense red and green emission colors, under UV excitation at 394 and 369 nm, respectively. Moreover, the spectra show narrow emission bands characteristic of the <sup>5</sup>D<sub>0</sub>→<sup>7</sup>F<sub>0-4</sub> transitions of the Eu<sup>3+</sup> and the <sup>5</sup>D<sub>4</sub>→<sup>7</sup>F<sub>6-0</sub> transitions of Tb<sup>3+</sup> ion. The absence of the broad emission band from the triplet states (T<sub>1</sub>) of the organic ligands in the spectral range from 400 to 600 nm is also consistent with an efficient ligand-to-metal intramolecular energy transfer to the emitting levels of Eu<sup>3+</sup> and Tb<sup>3+</sup> in the complexes [2]. The emission quantum efficiency of <sup>5</sup>D<sub>0</sub> level and the 4f–4f experimental intensity parameters of the Eu<sup>3+</sup> ion will be discussed.

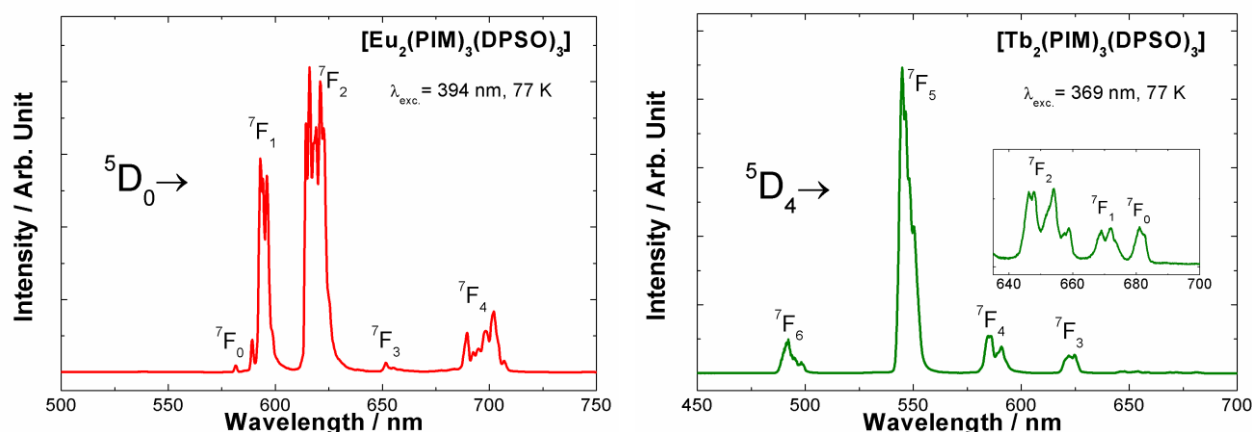


**Fig. 1 - Emission spectra of [Eu<sub>2</sub>(PIM)<sub>3</sub>(DPSO)<sub>3</sub>] (left) and [Tb<sub>2</sub>(PIM)<sub>3</sub>(DPSO)<sub>3</sub>] (right) complexes recorded at low temperature.**

[1] J.-C.G. Bunzli, C. Piguet, *Chem. Soc. Rev.* 34 (2005) 1048-1059.

[2] E. R. Souza, I. G. N. Silva, E. E. S. Teotonio, M.C.F.C. Felinto, H.F. Brito *J. Lumin.* 130 (2010) 283-291.

## MONOCRYSTALLINE PHOSPHOR WITH ENHANCED LIGHT EXTRACTION

Tomáš Fidler<sup>a</sup>, Jan Kubát<sup>a</sup>, Peter Matvija<sup>a</sup>, Ondřej Bečička<sup>a</sup>, Martin Rejman<sup>a</sup>, , Štěpán Novotný<sup>a</sup>

<sup>a</sup>CRYTUR spol. s r.o., Palackého 175, 51101 Turnov, Czech Republic, fidler@crytur.cz

Light emitting diodes (LEDs) are more and more employed in lighting industry to obtain white light with combination of blue LED and yellow emitting powder phosphor dispensed in encapsulant (silicone or epoxy resins).

For high-power application standard approach is not sufficient for long and stable life-time use due to ageing of encapsulants, device over-heating and efficiency droop. As an alternative a phosphor-in-glass, a ceramic phosphor, plasma sprayed phosphor [1] and recently single-crystalline phosphor can be used for converting of part of blue light to yellow light. More recently powerful blue laser diodes (LD) were utilized as excitation sources which place additional demands on phosphor material.

In this work high quality Ce doped  $Y_3Al_5O_{12}$  single crystals were grown by CRIG method and after that manufactured to rectangular shape. Combination of blue LED and YAG:Ce single crystal phosphor produces intense “cool white” light which is not acceptable for all applications, e.g. in household it is convenient to generate light with lower colour temperatures closer to “warm white” light. For changing resulting properties such as CIE coordinates and correlated colour temperature (CCT) chemical composition of single crystals was modified.

Main advantages of single crystal phosphor consist of high internal quantum efficiency, absence of any scattering centres which allows using lower doping concentrations and eliminate lower heat generation due to Stokes shift. Thanks to high thermal conductivity of single crystalline material generated heat is effectively distributed along whole phosphor plate.

Remaining issue is relatively high value of index of refraction which limits extraction of converted light from a body of phosphor plate. Reduction of this effect can be achieved by surface modification. In comparison with polished surface its grinding enhances light output by factor about two. More sophisticated method is preparation of defined features on emitting surface of phosphor plate. Resulting light extraction in desired direction is thus further increased and allows assembling high-power LED and LD devices.

[1] P. Ctibor, J. Kubát, B. Nevrlá, Z. Pala, J. Mat. Res. 29 (2014) 2344-2351.

## LIGHT EMITTERS BASED ON ELECTROCHEMILUMINESCENT PHENOMENA IN NANOSIZED CAVITIES

Aliaksandr Smirnov, Andrei Stepanov

*Belarusian State University of Informatics and Radioelectronics, 6 P. Brovka, Minsk, Belarus, smirnov@bsuir.by*

Being in a liquid form, electrogenerated chemiluminescence (EGCL) is a self-regenerated process, which has potentially the quantum efficiency close to 100% and is characterized by stability of properties, which is a clear advantage compared with common OLED-structures [1, 2]. Thus, the liquid EGCL cell holds the key for solving the lifetime issues of solid state OLED. A common EGCL cell consists of two closely placed (10-100 $\mu\text{m}$ ) flat electrodes [3, 4], where at least one of them is transparent. Usually, it is an ITO covered glass substrate. The cell may contain a polar solvent, luminophor and background electrolyte [3]. We have fabricated of EGCL cell with nanosized cavities in a solid layer, cavities being filled with light-emitting material (Fig. 2).

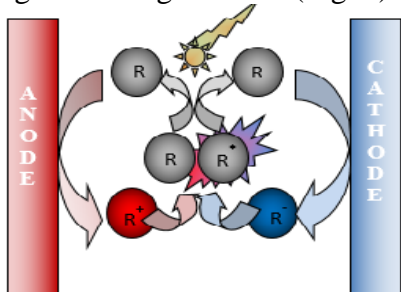


Figure 1. An EGCL cell

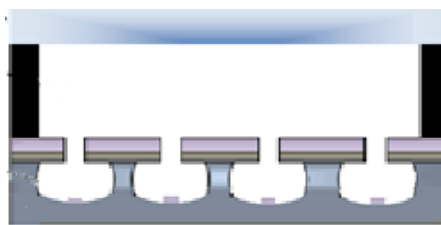


Figure 2. Construction of EGCL cell on a silicon substrate

For producing of a luminescence cell with nanosized cavities on the silicon substrate, a  $\langle 111 \rangle$  or  $\langle 100 \rangle$  silicon wafer with low resistivity ( $\rho=0,01$  Ohm-cm). Standard wafer cleaning was applied. 0,1 micron  $\text{SiO}_2$  film was produced by thermal oxidation of Si. 0,8 micron  $\text{Si}_3\text{N}_4$  film was coated by PECVD with  $\text{SiH}_4 - \text{N}_2$  (5:1) gas mixture at the temperature of  $850^\circ\text{C}$ .  $\text{SiO}_2$  sub layer was used as a damper to reduce the mechanical stresses. Cavity regions were defined by a photolithography process. Removal was done by plasma etching of  $\text{Si}_3\text{N}_4\text{-SiO}_2$  in  $\text{SF}_6$ . Formation of nanosized cavities in the silicon layer was held in two stages. In the first stage, anodizing of Si in HF – ethanol mixture with a weight ratio 3:1 was performed in regions not covered by  $\text{Si}_3\text{N}_4\text{-SiO}_2$  layers to the depth of 50-150 micron (current density  $30\text{mA}/\text{cm}^2$ ). In the second stage, alkaline etching of porous Si was carried out in boiling 10% KOH. Formation of transparent conductive electrodes was produced by RF magnetron sputtering (current density  $1\text{mA}/\text{cm}^2$ ) of  $\text{SnO}_2\text{-In}_x\text{O}_y$ .

[1] H. Schapper et al., New aspects of DC electrochemiluminescence, J. Electrochem. Soc. 1982, v.129, N 6, pp.1289-1294

[2] P. Jaguiro, Physical model of electrochemiluminescence, in «inorganic and organic electroluminescence», ed. by R.Mauch, 1996; pp. 47-52.

[3] Y. Hamada et al., “Luminescent element”, US patent No 2004/0106005 A1, Jun. 3, 2004.

[4] P.Jaguiro, A.Smirnov, X.Sun (Singapore), C.H.Kam (Singapore), Electrolyteless electrochemiluminescent displays, Proc. 29<sup>th</sup> Int. Display Research Conf., September 2009, Rome, Italy, p. 257-259

[5] P. Jaguiro, A. Stsiapanau, A. Smirnov, Chemiluminescent display, Semiconductor Physics, Quantum Electronics & Optoelectronics, 2010. V. 13, N 3. P. 298-301.

[6] A.Smirnov, A.Stsiapanau, Xiaowei Sun, Chan Hin Kam, Liquid Electrochemiluminescent Organic Light Emitting Cell, Abstracts of Int. Conf. “Global Photonics-2010”, Singapore, December 2010, p.56-57.

## OSL PROPERTIES OF NEW HYBRID DETECTORS

Ewa Mandowska<sup>a</sup>, Arkadiusz Mandowski<sup>a</sup>, Barbara Marczevska<sup>b</sup>, Paweł Bilski<sup>b</sup>,

<sup>a</sup>*Institute of Physics, Jan Długosz University, Armii Krajowej 13/15, Częstochowa, Poland, e.mandowska@ajd.czyst.pl*

<sup>b</sup>*Institute of Nuclear Physics, Polish Academy of Sciences, Radzikowskiego 152, Krakow, Poland*

Optically stimulated luminescence (OSL) is the luminescence emitted from irradiated insulator or semiconductor during stimulation with light of appropriate energy [1]. The OSL intensity is a function of the dose of absorbed ionizing radiation and therefore is a technique increasingly used in dosimetry.

The most popular OSL detectors are made of  $\text{Al}_2\text{O}_3:\text{C}$  as well as BeO crystals. For some applications (e.g. in medicine) it would be desirable to construct detectors in the form of high-area flexible foils. This could be achieved by incorporating small grains of typical inorganic crystalline OSL phosphors into organic (polymer) matrix. For present studies we applied such hybrid technique to prepare samples containing  $\text{Al}_2\text{O}_3:\text{C}$  microcrystalline grains in poly-(N-vinyl carbazole) (PVK) and chitosan (CH) matrices. Typical OSL response curves for PVK and CH with  $\text{Al}_2\text{O}_3:\text{C}$  are presented in Fig. 1. This hybrid structure gives more possibilities in construction of new OSL detectors. CW-OSL after excitation of beta and gamma radiation was not observed for pure polymer matrices contrary to polymer blends with  $\text{Al}_2\text{O}_3:\text{C}$  [2]. The dependence of OSL response normalized to sample mass on dose was studied. This dependence is linear for PVK and CH with 10%  $\text{Al}_2\text{O}_3:\text{C}$  in wide dose ranges for beta and gamma irradiations (Fig. 2).

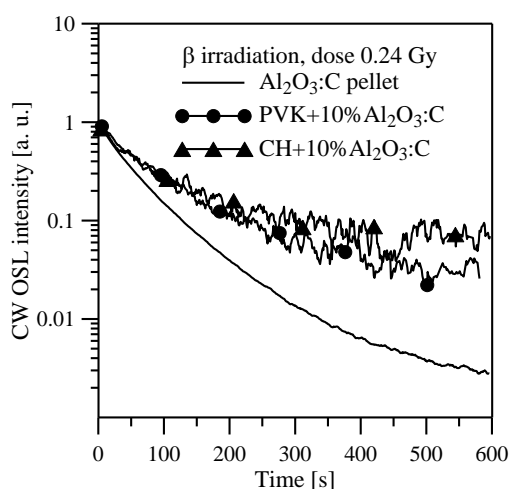


Fig. 1 Normalized CW OSL decay of  $\text{Al}_2\text{O}_3:\text{C}$  pellet, PVK with 10%  $\text{Al}_2\text{O}_3:\text{C}$  and CH with 10%  $\text{Al}_2\text{O}_3:\text{C}$ , after beta irradiation.

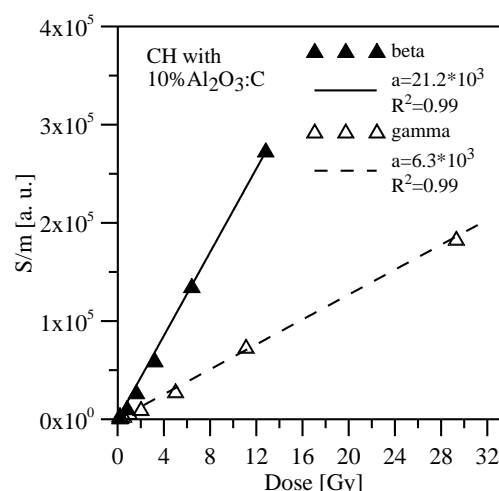


Fig. 2 Dose response normalized to the sample mass of CH with 10%  $\text{Al}_2\text{O}_3:\text{C}$  after gamma irradiation, at room temperature. S is integrated CW OSL signal intensity (total luminescence during 600s of stimulation) and m is sample mass.

[1] E. G. Yukihara, S. W. S. McKeever, „Optically stimulated luminescence fundamentals and applications”, Wiley, 2011.

[2] E. Mandowska, A. Mandowski, B. Marczevska, P. Bilski, *Radiat. Meas.*, 71 (2014) 174-177.

## AN EXOTIC REMOTE PHOSPHOR WITH HIGH QUANTUM YIELD FOR WARM WHITE LIGHT PRODUCTION: MANIFESTATION OF SILICA NANOPARTICLES

Kiwan Jang<sup>a</sup>, Sakthivel Gandhi<sup>a</sup>, Ho Sueb Lee<sup>a</sup>, Dong Soo Shin<sup>b</sup>, Jung Hyun Jeong<sup>c</sup>

<sup>a</sup>*Department of Physics, Changwon National University, Changwon, Republic of Korea*

<sup>b</sup>*Department of Chemistry, Changwon National University, Changwon, Republic of Korea*

<sup>c</sup>*Department of Physics, Pukyong National University, Busan, Republic of Korea*

Single phosphor converted warm white LEDs draw a lot of attention due to its notable advantages including power consumption, compactness and environmentally benign nature. The great challenge associated with the improvisation in performance of warm white LEDs can be achieved by fine tuning of the emission wavelength. In connection with that, a novel attempt towards the development of  $\text{Eu}^{2+}$  doped  $\text{M}_2\text{SiO}_4$  ( $\text{M}=\text{Ca}$  &  $\text{Sr}$ ) have been put forth using a silica nanoparticles through a convenient wet-solid phase reaction. The developed phosphor can be efficiently excited in a broad spectral range of 200 – 500 nm, and gets emitted strongly in the green region. On introduction of high concentration of dopant into the host, a clear red shift has been recorded in the photoluminescence spectra. These silica nanoparticle assisted synthesis of  $\text{M}_{2-x}\text{Eu}_x^{2+}\text{SiO}_4$  phosphors showed a good thermal luminescence stability and high quantum efficiency of about 85 %. It has also been successfully used for the fabrication of a flexible and translucent remote phosphor. The fabricated remote phosphor attached proto-type LED exhibits a very strong warm white emission along with lower CCT and higher CRI.

## DUAL-MODE LUMINESCENCE WITH BROAD NEAR UV AND BLUE EXCITATION BAND FROM $\text{Sr}_2\text{CaMoO}_6:\text{Sm}^{3+}$ PHOSPHOR FOR WHITE LEDs

Lili Wang<sup>a</sup>, Byung Kee Moon<sup>a</sup>, Byung Chun Choi<sup>a</sup>, Jung Hyun Jeong<sup>a</sup>,  
Jung Hwan Kim<sup>b</sup>, Kiwan Jang<sup>c</sup>, Ho Sueb Lee<sup>c</sup>, Dong Soo Shin<sup>d</sup>

<sup>a</sup>*Department of Physics, Pukyong National University, Busan 608-737, Republic of Korea,  
jhjeong@pknu.ac.kr*

<sup>b</sup>*Department of Physics, Donggeui University, Busan 614-714, Republic of Korea*

<sup>c</sup>*Department of Physics, Changwon National University, Changwon 641-773, Republic of  
Korea*

<sup>d</sup>*Department of Chemistry, Changwon National University, Changwon 641-773, Republic of  
Korea*

Dual-mode excitation properties were introduced in  $\text{Sm}^{3+}$  doped  $\text{Sr}_2\text{CaMoO}_6$  prepared by a high temperature solid state reaction technique. Two approaches to warm white emission can be realized in the  $\text{Sm}^{3+}$  doped single-component phosphor. Warm white light can be obtained from  $\text{Sr}_{1.995}\text{Sm}_{0.005}\text{CaMoO}_6$  phosphor with 380 nm or 410 nm excitation energy. The full visible spectral emission of the single-phase phosphor comes from the high and low level emission lines of  $\text{Sm}^{3+}$  ions as well as the intrinsic luminescence of  $\text{MoO}_6$  group. It is also competitive as a blue-pumped yellow-emitting phosphor and gives three emission bands at 567, 603 and 650 nm, respectively presenting yellow luminescence upon 466 nm radiation. The 650 nm red emission band corresponding to  $^4\text{G}_{5/2} \rightarrow ^6\text{H}_{9/2}$  transition of  $\text{Sm}^{3+}$  can improve its color rendering. The excellent photoluminescence of  $\text{Sr}_2\text{CaMoO}_6$  is related to the partial tilting  $(\text{Ca}/\text{Mo})\text{O}_6$  and octahedra and therefore lowered symmetry, which were confirmed by General Structure Analysis System. Band gap of  $\text{Sr}_2\text{CaMoO}_6$  estimated from the diffuse reflection spectra and also calculated by CASTEP mode shows its semi-conducting character. All the results show that  $\text{Sr}_{2-x}\text{Sm}_x\text{CaMoO}_6$  phosphors have considerable potential for use in near UV LED or pumped by blue LED chip.

## WHITE UPCONVERSION EMISSION AND TEMPERATURE DEPENDENCE OF Er<sup>3+</sup>, Yb<sup>3+</sup> AND Tm<sup>3+</sup> TRI-DOPED Y<sub>2</sub>O<sub>3</sub> NANOPHOSPHORS

Hyeon Mi Noh<sup>a</sup>, Jung Hyun Jeong<sup>a</sup>, Jung Hwan Kim<sup>b</sup>, Kiwan Jang<sup>c</sup>, Ho Sueb Lee<sup>c</sup>,  
Dong Soo Shin<sup>d</sup>

<sup>a</sup>*Department of Physics, Pukyong National University, Busan 608-737, Republic of Korea,  
jhjeong@pknu.ac.kr*

<sup>b</sup>*Department of Physics, Dongeui University, Busan 614-714, Republic of Korea*

<sup>c</sup>*Department of Physics, Changwon National University, Changwon 641-773, Republic of  
Korea*

<sup>d</sup>*Department of Chemistry, Changwon National University, Changwon 641-773, Republic of  
Korea*

Over the past few decades, upconversion(UC) materials have received considerable attention due to their potential applications in bioimaging and biological labelling [1-3]. UC luminescence is nonlinear process that re-emits a short wavelength photon by absorbing more than one photon successfully at longer wavelengths via the long-life intermediate energy states in UC luminescence materials [4]. Y<sub>2</sub>O<sub>3</sub> is an excellent host material because its high chemical stability, low phonon energy and high efficiency. During the past few years, many investigations on white upconversion luminescence in rare earth doped oxides by different approaches were performed.

In this paper, the upconversion properties and temperature dependence of Er<sup>3+</sup>, Yb<sup>3+</sup> and Tm<sup>3+</sup> tri-doped Y<sub>2</sub>O<sub>3</sub> phosphors were synthesized by solvothermal method. Crystallinity and structures of the samples were determined using X-ray diffraction and the emission spectra were obtained by 975 nm diode laser (LD). Their upconversion processes were explained by measuring the upconversion luminescence spectra and pump power dependence.

[1] Z Chen, H. Chen, H. Hu, M. Yu, F. Li, Q. Zhang, J. Amer. Chem. Soc.130, (2008) 3023–3029.

[2] H. Hu, M. Yu, F. Li, Z. Chen, X. Gao, L. Xiong, Chem. Mater. 20, (2008) 7003–7009.

[3] S. A. Hilderbrand, F. Shao, C. Salthouse, .U. Mahmood, R Weissleder, Chem. Commun. 28, (2009) 4188–4190.

[4] T. S. Atabaev, Z. Piao, Y. H. Hwang, H. K. Kim, N. H. Hong, J. Alloys Comp. 572, (2013) 113–117.



## BLUE LUMINESCENCE IN MWO<sub>4</sub>:Tm<sup>3+</sup> (M= Ba, Sr) PHOSPHORS

Edson L. Gaiollo<sup>a</sup>, Renan P. Moreira<sup>a</sup>, Helliomar P. Barbosa<sup>b</sup>, Cassio C. S. Pedroso<sup>b</sup>, Lucas C.V. Rodrigues<sup>b</sup>, Oscar M. L. Malta<sup>c</sup>, Hermi F. Brito<sup>b</sup>, Maria C.F.C. Felinto<sup>b</sup>

<sup>a</sup>Centro de Química e Meio Ambiente, IPEN, São Paulo, Brazil

<sup>b</sup>Instituto de Química, Universidade de São Paulo, São Paulo, Brazil

<sup>c</sup>Departamento de Química, Universidade Federal de Pernambuco, Pernambuco, Brazil  
mfelinto@ipen.br

Highly luminescent emission from trivalent rare earth (R<sup>3+</sup>) doped tungstates [WO<sub>4</sub>]<sub>2</sub>- have been extensively studied during the past century, especially on their very interesting luminescence, structural properties and electro-optical applications [1]. Nowadays they have awakened the curiosity of nano world. This work reports the investigation of MWO<sub>4</sub>:Tm<sup>3+</sup> (M=Ba, Sr) materials with blue emission luminescence prepared with a low cost and easy synthesis route. The materials were prepared by the co-precipitation method with stoichiometry aqueous solutions of Na<sub>2</sub>WO<sub>4</sub>, BaCl<sub>2</sub> or SrCl<sub>2</sub> and TmCl<sub>3</sub> (Tm<sup>3+</sup> in 0.02 to 0.1 mol-% of the M<sup>2+</sup> amount). The as-prepared materials were characterized by infrared spectroscopy showing strong vibrations in the range 700-1000 cm<sup>-1</sup> attributed to stretching vibration (ν) symmetrical and asymmetrical of the tetrahedral group (WO<sub>4</sub><sup>2-</sup>). The XRD measurements reveal that the majority phase is tetragonal scheelite phase with I41/a (#88) space group. The emission spectra of MWO<sub>4</sub>:Tm<sup>3+</sup> (M= Ba, Sr) materials are dominated by high intensity 1D<sub>2</sub>→3F<sub>4</sub> transition in blue region (~452nm) and <sup>1</sup>G<sub>4</sub>→<sup>3</sup>H<sub>6</sub> (~475nm) and also other transitions of Tm<sup>3+</sup>, in red <sup>1</sup>G<sub>4</sub>→<sup>3</sup>F<sub>4</sub> (654 nm) and close to infrared <sup>3</sup>H<sub>4</sub>→<sup>3</sup>H<sub>6</sub> (~780 nm) transitions observed in the spectra. These transitions, although with low intensity, means that different Tm<sup>3+</sup>-related emitting centers coexist in the same sample suggesting that the ions must be placed in different site of symmetry. (Fig. 1; left and center). The chromaticity diagram (Fig. 1;right) exhibit emission color tuning of of MWO<sub>4</sub>:Tm<sup>3+</sup> (M= Ba, Sr) materials phosphors by changing the dopant concentration from 0.2 to 1.0 mol-%. These results suggest that the material can be used as an alternative to blue marker.

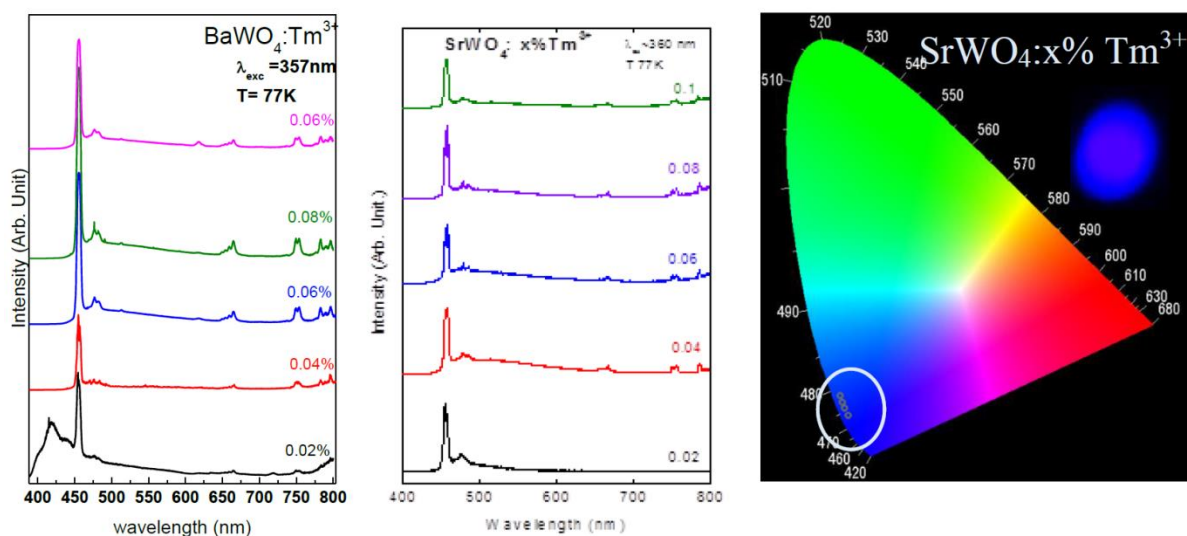


Figure 1. Emission spectra; (left and center) and CIE color coordinates; (right) of the MWO<sub>4</sub>:Tm<sup>3+</sup> phosphors.

[1] Kodaira, C. A.; Brito, H. F.; Malta O. L.; Serra, O. A. J. Lumin. 2003, 101, 11–21.

## **ZnO NANOPOWDERS BY A MICROWAVE HYDROTHERMAL METHOD – INFLUENCE OF EUROPIUM DOPING ON LUMINESCENCE PROPERTIES**

E. Wolska-Kornio<sup>1</sup>, J. Kaszewski<sup>1</sup>, B.S. Witkowski<sup>1</sup>, Ł. Wachnicki<sup>1</sup>, M. Godlewski<sup>1,2</sup>

<sup>1</sup>*Institute of Physics, Polish Academy of Sciences, Al. Lotników 32/46, 02-668 Warsaw, Poland*

<sup>2</sup>*Dept. of Mathematics and Natural Sciences College of Science, Cardinal S. Wyszyński University, Dewajtis 5, 01-815 Warsaw, Poland*

ZnO is very intensively investigated material with a range of possible applications in electronics (in cross-bar memories [1]), photovoltaics (as transparent conductive electrodes [2]) or spintronics (when doped with transition metal ions [3]). Decreasing to nanometer scale results in the new interesting physical features of this material, which may lead to new potential applications of nano-ZnO in medicine and biology as fluorescence labels [4]. In fact, ZnO nanopowders have several advantageous properties to be used as e.g. luminescence markers for cancer cells in living organisms. For such applications nanopowders should be small (of nanometer sizes [4]) and show highly efficient visible luminescence.

Doping with Europium, a rare earth element with a characteristic energy structure may result in visible and/or infrared emission. Thus, Eu is often applied as a luminescence activator. The sharp luminescence peaks and a low sensitivity to temperature are the characteristics of the 4f – 4f transitions. Importantly 4f -4f emission of Eu can be effectively excited by 4f- 5d excitation process, whereas, due to the atomic character of the 4f shell, the 4f-4f excitation is ineffective. The transition is forbidden due to the same parity of the initial and excited state for the 4f – 4f transitions.

In this work we analyze optical properties of Europium doped ZnO nanopowders obtained by a hydrothermal method. We show series of the samples with changing content of the dopant. Nanopowders were made using a zinc nitrate hexahydrate ( $N_2O_6Zn \times 6H_2O$ ) and distilled water.

The research was partially supported by the National Science Centre project 20/0139/N/ST3/04189

[1] M. Godlewski, E. Guziewicz, T. Krajewski, P. Kruszewski, Ł. Wachnicki, K. Kopalko, A. Wójcik, and V. Osinniy, *Microelectronic Engineering* **85**, 2434 (2008).

[2] M. Godlewski, E. Guziewicz, G. Łuka, T. Krajewski, M. Łukasiewicz, Ł. Wachnicki, A. Wachnicka, K. Kopalko, A. Sarem, and B. Dalati, *Thin Solid Films* **518**, 1145 (2009).

[3] T. Dietl, H. Ohno, and F. Matsukura, *Science* **287**, 1019 (2000).

[4] M. Godlewski, S. Yatsunencko, A. Nadolska, A. Opalińska, W. Łojkowski, K. Drozdowicz - Tomsia, and E.M. Goldys, *Opt. Mater.* **31**, 490 (2009).

## WHITE-LIGHT-EMITTING KCl:Eu<sup>2+</sup>/KCN CRYSTAL

Luis H. Andrade<sup>a,□</sup>, Sandro M. Lima<sup>a</sup>, Rogerio Ventura da Silva<sup>a</sup>, Mauro L. Baesso<sup>b</sup>,  
Yannick Guyot<sup>c,\*</sup> and Luiz Antonio de Oliveira Nunes<sup>d</sup>

<sup>a</sup>*GEOF, Universidade Estadual de Mato Grosso Sul, Dourados, MS, Brazil,*  
<sup>□</sup>*luishca@me.com*

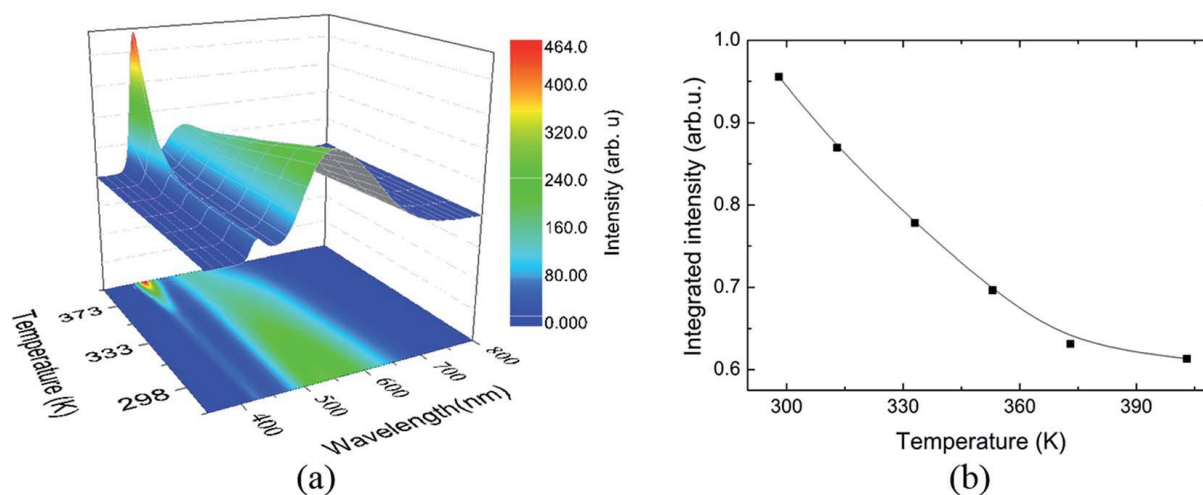
<sup>b</sup>*Departamento de Fisica, Universidade Estadual de Maringá, Maringá, PR, Brazil*

<sup>c</sup>*Institut Lumière Matière, Université Lyon1, Villeurbanne, France,*

<sup>\*</sup>*yannick.guyot@univ-lyon1.fr*

<sup>d</sup>*Instituto de Fisica de São Carlos, Universidade de São Paulo, São Carlos, SP, Brazil*

The optical and colorimetric properties of a KCl:Eu<sup>2+</sup>/KCN crystal are analyzed in this work [1] to verify its potential for the development of white-light-emitting diode (WLED) devices. An unusual broad and intense yellow-green emission band is observed at 530 nm when this crystal is excited with UV radiation. This emission originates from the coupling between the Eu<sup>2+</sup> ions and multiple CN<sup>-</sup> molecular ions. Luminescence experiments, at middle infrared and visible spectral regions, at different temperatures and excitations indicate that both emissions are characteristic of the energy transfer from the Eu<sup>2+</sup> ions to the CN<sup>-</sup> molecular ions. The luminescence quantum efficiency of this material was measured using thermal lens spectroscopy, which provided a high value of 95%. Based on the experimental results, a model to explain the Eu–CN coupling is proposed. A WLED prototype was assembled using an UV LED to excite the KCl:Eu<sup>2+</sup>/KCN crystal and using a small amount of Y<sub>2</sub>O<sub>3</sub>:Eu<sup>3+</sup> phosphor powder to compensate for the red color. The results showed a correlated color temperature of 3300 K; the u',v' color coordinate distance to the Planckian Locus (Du'v') was 0.0008, and the Color Rendering Index(CRI) was approximately 90.



(a) Emission plot for the KCl:Eu<sup>2+</sup>/KCN crystal as a function of temperature for excitation at 325 nm.

(b) Integrated intensity of the yellow emission as a function of temperature.

[1] Luis H. Andrade et al. J. Mater. Chem. C, 2014, 2, 10149–10156

## **OPTIMIZATION OF EMULSION POLYMERIZATION OF SELF-ASSEMBLED COLLOIDAL CRYSTALS FOR LASER APPLICATION**

S.H. Vakili Tahami<sup>a\*</sup>, S. Pourmahdian<sup>a,b</sup>, B. Shirkavand<sup>a</sup>, M. M. Tehrani<sup>c</sup>

<sup>a</sup>*Department of Resin and Additives, Institute for Color Science and Technology, Tehran, Iran, Hdtahami@icrc.ac.ir*

<sup>b</sup>*Polymer Engineering Department, Amirkabir University of Technology, P.O. Box 15785, Tehran, Iran*

<sup>c</sup>*Laser and Plasma Research Institute, G. C., Shahid Beheshti University, Tehran, Iran*

Nano-sized Polymeric colloidal particles could be self-organized into three dimensional structures to obtain desired optical properties. In this research, a facile emulsifier-free emulsion polymerization method was used to synthesize highly mono-disperse sub-micron polystyrene colloids. By controlling of the reaction parameters, various sizes of colloidal particles were prepared in the range of 190 nm up to 400 nm. The colloidal particles were used to prepare a uniform colloidal crystal (CC) films. These CC films showed bright colours and a characteristic reflection bands according to the size of colloidal particles (photonic band gap). The Bragg reflection of the CC films was optimized to overlap with the wavelength of the light emitting of a fluorescent dye. The fluorescent dye was applied between two CC films as planer light emitting layer. The prepared CC films with the planer defect were used in low-threshold laser application by optical excitation. The low-threshold lasing action can be realized by the confinement of photons emitted from the intermediate light-emitting defect layer.

## WAVELENGTH-CONVERSION EFFICIENCY ENHANCEMENT IN NANO-TEXTURED FLUORESCENT 6H-SiC PASSIVATED BY ATOMIC LAYER DEPOSITED TITANIUM OXIDE

Weifang Lu<sup>a</sup>, Yiyu Ou<sup>a</sup>, Valdas Jokubavicius<sup>b</sup>, Ahmed Fadil<sup>a</sup>, Mikael Syväjärvi<sup>b</sup>, Paul Michael Petersen<sup>a</sup>, and Haiyan Ou<sup>a</sup>

<sup>a</sup> Department of Photonics Engineering, Technical University of Denmark, DK-2800, Lyngby, Denmark, [weilu@fotonik.dtu.dk](mailto:weilu@fotonik.dtu.dk)

<sup>b</sup> Department of Physics, Chemistry and Biology, Linköping University, SE-58183, Linköping, Sweden

In the state-of-the-art technologies, nano-textured surface is an effective approach to boost wavelength-conversion efficiency in fluorescent 6H-SiC based white light-emitting diodes (LEDs) [1]. Surface nanostructures can enhance the light emission in a broad spectral range and omnidirections compared with as-grown 6H-SiC [2]. However, the surface recombination needs to be suppressed to further improve the conversion efficiency. Up to now, still very little work has been reported on surface passivation of fluorescent 6H-SiC. The atomic layer deposited (ALD) TiO<sub>2</sub> thin film has been reported to passivate the Si based solar cells [3]. In this work, we investigate the surface passivation effect on nano-textured fluorescent 6H-SiC by (ALD) TiO<sub>2</sub> thin films.

Nitrogen and boron co-doped 6H-SiC epilayers (100 μm) were grown on 1.4° off-axis 6H-SiC substrate by the Fast Sublimation Growth Process (FSGP) [4]. Based on the self-assembled nano-patterned reactive-ion etching (RIE) method [5], nano-textured surfaces were fabricated on three samples (a, b, c). Prior to TiO<sub>2</sub> film deposition, sample b and c were cleaned by oxygen plasma and dilute HF for 15min and 5min, respectively. A 20nm thick layer was deposited on sample b and c by thermal ALD (Picosun R200). The TiO<sub>2</sub> films were synthesized using titanium tetrachloride (TiCl<sub>4</sub>) and H<sub>2</sub>O gas as precursors. The deposition was performed at 300°C with a growth rate of 0.4Å per cycle. After TiO<sub>2</sub> deposition, sample c was annealed at 500°C for an hour in N<sub>2</sub> atmosphere.

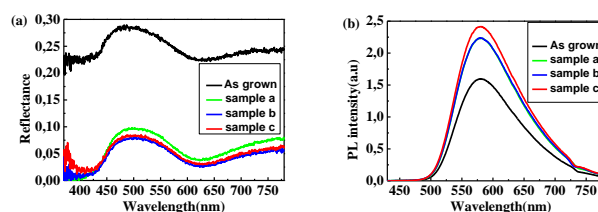


Fig. 1. (a) Reflectance and (b) photoluminescence spectra of as-grown sample, sample a (nano-textured), sample b (covered with 20nm thick TiO<sub>2</sub>) and sample c (covered with 20nm thick TiO<sub>2</sub> and annealed at 500°C for 1h). The reflectance of sample b and c covered with 20nm thick TiO<sub>2</sub> slightly decreases compared to sample a, as shown in Fig. 1(a). After deposition of 20nm thick TiO<sub>2</sub> layer, the photoluminescence (PL) intensity remains the same. However, the annealed sample c has stronger photoluminescence than the other samples, i.e. the PL has been improved by 8.05% compared to sample b, as shown in Fig. 1(b).

Our experiments show that TiO<sub>2</sub> film has an efficient passivation effect on nano-textured fluorescent 6H-SiC after the annealing. The effective passivation is likely to be further improved when the thickness of TiO<sub>2</sub>, deposition conditions of TiO<sub>2</sub> and the annealing conditions.

[1]H. Ou, Y. Ou, A. Argyraki, et al., European Physical Journal B: Condensed Matter Physics 87 (2014) 58.

[2]Y. Ou, V. Jokubavicius, P. Hens, et al., Optics express 20 (2012) 7575.

[3]B. Liao, B. Hoex, A.G. et al., Applied Physics Letters 104 (2014) 253903.

[4]M. Syväjärvi, J. Müller, J.W. Sun, et al., Physica Scripta T148 (2012) 014002.

[5]Y. Ou, I. Aijaz, V. Jokubavicius, et al., Optical Materials Express 3 (2013) 86.

## UPCONVERSION WHITE LIGHT AND MULTICOLOR LUMINESCENCE IN $\text{GdVO}_4\text{:Ln}^{3+}/\text{Yb}^{3+}$ ( $\text{Ln}^{3+} = \text{Ho}^{3+}, \text{Er}^{3+}, \text{Tm}^{3+},$ $\text{Ho}^{3+}/\text{Er}^{3+}/\text{Tm}^{3+}$ ) NANORODS

Tamara Gavrilović<sup>a</sup>, Dragana J. Jovanović<sup>a</sup>, Sanja Čulubrk<sup>a</sup>, Krisjanis Smits<sup>b</sup>, Miroslav D. Dramićanin<sup>a</sup>

<sup>a</sup>*Vinča Institute of Nuclear Sciences, University of Belgrade, P.O. Box 522, 11001 Serbia, tamarag@vinca.rs*

<sup>b</sup>*Institute of Solid State Physics, University of Latvia*

Up-converting lanthanide-doped  $\text{GdVO}_4$  nanocrystalline powders have been synthesized via co-precipitation method followed by subsequent annealing at higher temperatures, up to  $1000^\circ\text{C}$ . The average crystallite size, calculated by the Halder–Wagner method, changes from around 14 nm to 59 nm for the as-prepared samples and samples annealed at  $1000^\circ\text{C}$ , respectively. TEM and SEM measurements indicate that the as-prepared powders are self-organized in bundles of 5-6 individual nanorods up to 20 nm in length and from 5 nm in diameter, while powders annealed at  $800^\circ\text{C}$  and  $1000^\circ\text{C}$  contain non-regular spheres with size about 100 nm and few microns long rods with diameters about 1-2  $\mu\text{m}$ , respectively. It was demonstrated that by controlling the concentration ratio of dopant ions  $\text{Ho}^{3+}/\text{Er}^{3+}/\text{Tm}^{3+}/\text{Yb}^{3+}$  in  $\text{GdVO}_4$  powders, this materials can be optimized to produce multicolor emission and a tunable white light under irradiation at a single wavelength of 980 nm [1,2]. A pure white light emission was obtained in two samples of  $\text{Tm}^{3+}/\text{Er}^{3+}/\text{Ho}^{3+}/\text{Yb}^{3+}$ -co-doped  $\text{GdVO}_4$  powders with different doping concentration which were annealed at  $800^\circ\text{C}$ , and the calculated chromaticity coordinates (x, y) for them are (0.326, 0.339) and (0.323, 0.327). These coordinates fall in the white region and are very close to the standard equal energy white light coordinates (0.333, 0.333) according to the 1931 CIE diagram. Hence, the color output of the emission of lanthanide-doped  $\text{GdVO}_4$  nanorods, under excitation at 980 nm, can be precisely tuned by varying doping composition and concentration, providing their potential applications in white-light, display and lighting technology. The chromaticity coordinates (x, y) for all prepared samples are shown in Figure 1.

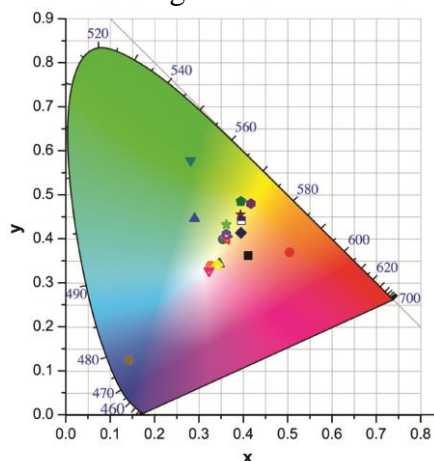


Figure 1. The CIE 1931 chromaticity diagram of  $\text{Gd}_{1-x-y-z-w}\text{Tm}_x\text{Er}_y\text{Ho}_z\text{Yb}_w\text{VO}_4$  powders excited with a 980 nm laser.

[1] T. Gavrilović, D. Jovanović, V. Lojpur, M. D. Dramićanin, *Sci. Rep.* 4 (2014) 4209

[2] T. V. Gavrilović, D. J. Jovanović, L. Trandafilović, M. D. Dramićanin, *Opt. Mater.* 45 (2015) 76–81

## UPCONVERSION LUMINESCENCE IN $\text{LaInO}_3:\text{Er}^{3+}$

Nina Mironova-Ulmane<sup>a</sup>, Vera Skvorcova<sup>a</sup>, Kristaps Strals<sup>a</sup>, Guna Kriekē<sup>a</sup>, Anatolijs Sarakovskis<sup>a</sup>, Leonid Bashkirov<sup>b</sup>, Elena Juhno<sup>b</sup>

<sup>a</sup>*Institute of Solid State Physics University of Latvia, 8 Kengaraga str., Riga, Latvia, nina@cfi.lu.lv*

<sup>b</sup>*Belarusian State Technological University, 13a, Sverdlova str., Minsk, Belarus bashkirov@belstu.by*

High efficiency up-conversion luminescence processes are observed in various rare-earth doped materials. In this work  $\text{LaInO}_3:\text{Er}^{3+}$  samples with different  $\text{Er}^{3+}$  concentrations (0.01 – 10 mol%) have been synthesized.

Up-conversion luminescence and luminescence decay kinetics excited in the infrared spectral region have been measured.

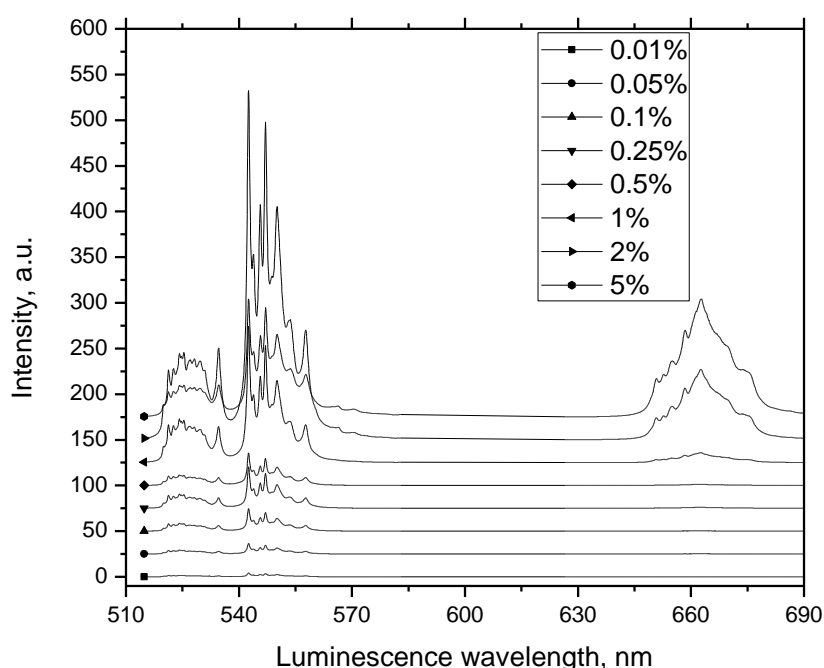


Figure 1. Upconversion luminescence spectra of  $\text{LaInO}_3:\text{Er}^{3+}$  with different  $\text{Er}^{3+}$  concentration

The analysis of the up-conversion luminescence spectra measured for the samples with different  $\text{Er}^{3+}$  content revealed presence of the concentration quenching (starting at 2 mol%). The transformation of excited state absorption mechanism to energy transfer mechanism of the up-conversion luminescence was noticed when the concentration of  $\text{Er}^{3+}$  was increased. The impact of  $\text{Er}^{3+}$  concentration on the luminescence processes in the material is discussed in the presentation.

This work was supported by Latvia-Belarus bilateral research project and Latvian Science Council Grant No.187/2012

## UPCONVERSION LUMINESCENCE IN $\text{CaYb}_{2-x}\text{Er}_x\text{Ge}_3\text{O}_{10}$ ( $x = 0-2$ )

Olga A. Lipina, Ivan I. Leonidov, Ludmila L. Surat, Alexander P. Tyutyunnik,  
Vladimir G. Zubkov

*Institute of Solid State Chemistry, UB RAS, 91, Pervomaiskaya, Ekaterinburg, Russia,  
LipinaOlgaA@yandex.ru*

In recent decades, lanthanide-doped upconversion (UC) materials have attracted burgeoning research interest. Initially, the studies of UC materials had been related to infrared detectors and UC lasers, and recently, new advanced applications have emerged, such as biolabeling, bioimaging, drug delivery, 3D displays, and efficiency improvement for solar cells [1–5]. Simple and fast solution-based methods are often used for the preparation of upconversion compounds doped with lanthanide ions at room-temperature. The surfactants introduced in the synthesis process have an impact on the crystal size, morphology, as well as luminescence properties by affecting the nonradiative process [5–7].

The present report summarizes the UC luminescence properties of a new series of germanates  $\text{CaYb}_{2-x}\text{Er}_x\text{Ge}_3\text{O}_{10}$  ( $x = 0-2$ ) studied by means of luminescence spectroscopy and excited state dynamics experiments. The solid solutions have been prepared using an EDTA-assisted route and conventional solid-state reaction. Powder XRD study shows that the samples crystallize in the monoclinic system with the space group  $P2_1/c$ ,  $Z = 4$ . The effect of the synthesis methods, dopant concentrations, and excitation wavelengths on luminescence properties of the compounds has been determined.

The solid solutions reveal UC emission in visible spectral range under excitation at 980 nm, resonant with both  $^4\text{I}_{15/2} \rightarrow ^4\text{I}_{11/2}$   $\text{Er}^{3+}$  and  $^2\text{F}_{7/2} \rightarrow ^2\text{F}_{5/2}$   $\text{Yb}^{3+}$  transitions. Concentration dependent studies show that the highest intensity of the lines around 408 nm ( $\text{H}_{9/2} \rightarrow ^4\text{I}_{15/2}$ ), 524 nm ( $\text{H}_{11/2} \rightarrow ^4\text{I}_{15/2}$ ), 548 nm ( $^4\text{S}_{3/2} \rightarrow ^4\text{I}_{15/2}$ ) and 660 nm ( $^4\text{F}_{9/2} \rightarrow ^4\text{I}_{15/2}$ ) is observed for the sample  $x = 0.2$ , strong upconversion luminescence could still be easily observed by the naked eye. Power dependence and lifetime measurements were performed to understand the mechanisms responsible for the efficient upconversion luminescence.

The Stokes luminescence in the infrared range (excitation = 808 nm) has been also studied. The intensive peak centered at 1538 nm corresponds to the characteristic transitions  $^4\text{I}_{13/2} \rightarrow ^4\text{I}_{15/2}$   $\text{Er}^{3+}$ .

As a conclusion,  $\text{CaYb}_{2-x}\text{Er}_x\text{Ge}_3\text{O}_{10}$  ( $x = 0-2$ ) promise to be a new class of upconversion materials with many applications such as solar energy conversion, novel three-dimensional solid-state display, UC LED lighting, biomedical multi-color imaging and low threshold UC lasers.

This work was partially supported by the FASO program no. 01201364479 and RFBR (grant no. 13–03–00047a).

- [1] S. Sivakumar, P.R. Diamente, F.C.J.M. van Veggel, *Chem. Eur. J.* 12 (2006) 5878–5884.
- [2] M. Nyk, R. Kumar, T.Y. Ohulchanskyy, E.J. Bergey, P.N. Prasad, *Nano Lett.* 8 (2008) 3834–3838.
- [3] B.M. van der Ende, L. Aarts, A. Meijerink, *Phys. Chem. Chem. Phys.* 11 (2009) 11081–11095.
- [4] R. Martín-Rodríguez, S. Fisher, A. Ivaturi, B. Froehlich, K.W. Krämer, J.C. Goldschmidt, B.S. Richards, A. Meijerink, *Chem. Mater.* 25(2013) 1912–1921.
- [5] P. Ramasamy, P. Manivasakan, J. Kim, *RSC Adv.* 4 (2014) 3487–34895.
- [6] F. Hei, N. Niu, L. Wang, J. Xu, Y. Wang, G. Yang, S. Gai, P. Yang, *Dalton Trans.* 42 (2013) 10019–10028.
- [7] R. Dey, V.K. Rai, *Dalton Trans.* 43 (2014) 111–118.



## UP-CONVERSION EMISSIONS IN WATER-SOLUBLE Yb<sup>3+</sup>, Tm<sup>3+</sup>, Gd<sup>3+</sup> DOPED β-NaYF<sub>4</sub> NANOPARTICLES FOR IN VIVO THERANOSTIC

N. Francolon<sup>1</sup>, F. Leccia<sup>2</sup>, E. Jouberton<sup>3</sup>, D. Boyer<sup>1</sup>, I. Miladi<sup>3</sup>, Delphine Felder-Flesch<sup>4</sup>,  
Sylvie Begin-Colin<sup>4</sup>, L. Morel<sup>2</sup>, E. Miot-Noirault<sup>3</sup>, J-M. Chezal<sup>3</sup>, R. Mahiou<sup>1\*</sup>

Rachid.Mahiou@univ-bpclermont.fr

<sup>1</sup>Université Clermont Auvergne, Institut de Chimie de Clermont-Ferrand, UMR 6296 CNRS / UBP / ENSCCF - 63171 AUBIERE, France

<sup>2</sup>Université Clermont Auvergne, Génétique Reproduction et Développement, CNRS, UMR 6247, INSERM, U931 - 63000 CLERMONT-FD, France

<sup>3</sup>Université Clermont Auvergne, Imagerie Moléculaire et Thérapie Vectorisée, UMR 990, INSERM, Uda - 63000 CLERMONT-FD, France

<sup>4</sup>Université de Strasbourg, Institut de Physique et Chimie des Matériaux de Strasbourg, CNRS, UMR 7504, 67034 STRASBOURG, France

Currently, targeted fluorescent nanoparticles (NPs) have become a major interest in the field of nanomedicine. Especially, upconverting nanoparticles (UCNPs) have attracted much attention due to their peculiar properties, relevant for bioimaging applications in the infrared range. In this work, we developed new multifunctional UCNPs for *in vivo* theranostic, particularly in the case of prostate cancer.

These materials permit the conversion of near infrared (NIR) radiations into photons of higher energy (NIR, visible and ultraviolet) *via* a multiphoton mechanism. In comparison with UV excitation, fluorescence imaging based on NIR light, which is only weakly absorbed by biological tissue, leads to deeper and non-invasive diagnosis. Among the lanthanide doped materials, NaYF<sub>4</sub> was reported as the most efficient lattice for UC process.

This well-known host was synthesized via a thermolysis process using oleic acid and octadecene in order to obtain spherical and crystallized nanoparticles with a narrow size distribution. Moreover the UCNPs are functionalized in order to make them biocompatible and decrease their toxicity. To this aim, we have used the ligand exchange method, with two types of molecules: PEG-phosphate and dendronized molecules. In fact these previous molecules are more and more developed for biomedical applications. Then, the interaction of the water-soluble UCNPs with living cells was investigated. In particular, LNCaP prostate cancer cells were incubated with nanoparticles and have shown low toxicity.

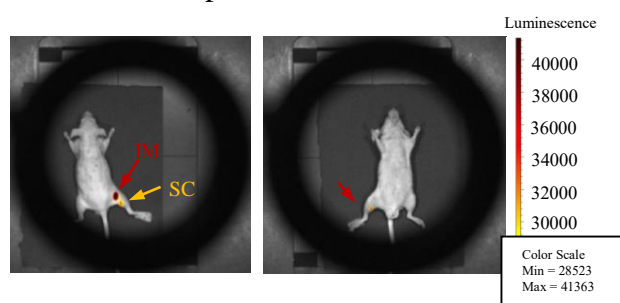


Fig 1 : In vivo imaging of NPs@dendrons injected in mice (power of the laser = 71mW/cm<sup>2</sup>).

Finally, some *in vivo* tests have been done on mice in order to show the feasibility of our UCNPs for biological application. Figure 1 presents the *in vivo* whole body images of nude mice with injections of a solution at 1 mg/mL of NaYF<sub>4</sub>@dendrons (50μL intramuscular –IM- and 20μL subcutaneous – SC). A significant UCL signal was observed for both injections and show the potential of these UCNPs. In addition, UV emission can be generated under NIR excitation, wavelength which can be used for *in-situ* therapy by killing the cancerous cells.

Acknowledgment: The authors would like to thanks the Région Auvergne and the Fonds Européen de Développement Régional (R72-p2 : 2012-2015) for their financial support.

## UPCONVERSION STUDIES ON Mg<sup>2+</sup> DOPED La<sub>2</sub>O<sub>3</sub>: Er<sup>3+</sup>/Yb<sup>3+</sup> NANOPHOSPHORS FOR TEMPERATURE SENSING AND SECURITY

Surya P. Tiwari, Sanjeet Singh, Kaushal Kumar, Vineet K. Rai  
*Department of Applied Physics, Indian School of Mines, Dhanbad-826004 (India)*  
*sptiwari.ism@gmail.com*

This report describes the synthesis, characterization and optical properties of Mg<sup>2+</sup> doped La<sub>2</sub>O<sub>3</sub>: Er<sup>3+</sup>/Yb<sup>3+</sup> phosphors through combustion process. The amounts of Mg<sup>2+</sup> are taken as 2, 4, 6, 8 and 10 mol%. The samples were characterized by using XRD, AFM and FTIR. The samples are excited by a 980 nm diode laser and recorded their upconversion emission spectra at room temperature. The optimum luminescence intensity is found for 8 mol% Mg<sup>2+</sup> doped La<sub>2</sub>O<sub>3</sub>: Er<sup>3+</sup>/Yb<sup>3+</sup>. Four dominant upconversion emission bands have been observed around 411nm (<sup>2</sup>H<sub>9/2</sub>→<sup>4</sup>I<sub>13/2</sub>), 524 nm (<sup>2</sup>H<sub>11/2</sub>→<sup>4</sup>I<sub>15/2</sub>), 548 (<sup>4</sup>S<sub>3/2</sub>→<sup>4</sup>I<sub>15/2</sub>) and 661 nm (<sup>4</sup>F<sub>9/2</sub>→<sup>4</sup>I<sub>15/2</sub>) through different transitions of Er<sup>3+</sup> ions. The lifetime of <sup>4</sup>S<sub>3/2</sub> level for 0 mol% Mg<sup>2+</sup> doped La<sub>2</sub>O<sub>3</sub>: Er<sup>3+</sup>/Yb<sup>3+</sup> and 8 mol% Mg<sup>2+</sup> doped La<sub>2</sub>O<sub>3</sub>: Er<sup>3+</sup>/Yb<sup>3+</sup> samples are measured and found 752 and 557 μs, respectively. Color co-ordinate diagram of the sample is found variant for different laser power that shows the applicability of present material as LED.

## UNCONTROLLED IMPURITY OF Bi<sup>3+</sup> IN RARE-EARTH IRON BORATES RFe<sub>3</sub>(BO<sub>3</sub>)<sub>4</sub>

Kirill N. Boldyrev<sup>a</sup>, Marina N. Popova<sup>a</sup>, Leonard N. Bezmaternykh<sup>b</sup>, Irina A. Gudim<sup>b</sup>

<sup>a</sup>*Institute of spectroscopy, Russian Academy of Sciences, 5 Fizicheskaya str., Troitsk, Moscow, Russia, kn.boldyrev@gmail.com*

<sup>b</sup>*Kirensky Institute of Physics, Siberian Branch of the Russian Academy of Sciences, Krasnoyarsk, Russia*

Rare-earth iron borates with general formula RFe<sub>3</sub>(BO<sub>3</sub>)<sub>4</sub> ( $R = Y, \text{Pr-Er}$ ) have a structure of the natural mineral huntite (SG  $R32$ ). These crystals are interesting due to their nonlinear optical and magnetic properties. Iron borates with an ionic radius of  $R$  smaller than that of Sm undergo a structural phase transition into the SG  $P3_121$  at the temperature  $T_S$  inversely proportional to the ionic radius of the  $R^{3+}$  ion. In this study, we investigate EuFe<sub>3</sub>(BO<sub>3</sub>)<sub>4</sub>, the compound that possesses the lowest temperature of the structural phase transition among members of the RFe<sub>3</sub>(BO<sub>3</sub>)<sub>4</sub> family. Interestingly enough, strongly different  $T_S$  temperatures,  $T_S = 88$  K and  $T_S = 58$  K were reported for powder samples prepared by solid-phase synthesis [1] and for a single crystal grown by the solution-melt technique using the Bi<sub>2</sub>Mo<sub>3</sub>O<sub>12</sub> based flux [2], respectively.

To find a reason for such discrepancy, we compare here optical spectra of EuFe<sub>3</sub>(BO<sub>3</sub>)<sub>4</sub> single crystals grown on the seeds from the solution-melts on the base of (i) Bi<sub>2</sub>Mo<sub>3</sub>O<sub>12</sub> and (ii) Li<sub>2</sub>WO<sub>4</sub>. The spectra clearly evidence  $T_S = 58$  K for the sample (i) and  $T_S = 83$  K for the (ii) one, whereas  $T_N = 34$  K for both samples. Obviously, lower  $T_S$  for the sample (i) is connected with entering of a “big” Bi<sup>3+</sup> ion from the flux into positions of Eu<sup>3+</sup>. Our estimate gives  $7 \pm 2$  % for Bi concentration in the sample (i). Bi impurity manifests itself also by a presence of extra lines in the spectra of  $f-f$  europium transitions, due to the Eu<sup>3+</sup> ions located near Bi impurity centers. Using our data on other RE iron borates (with  $R = \text{Gd, Tb, Dy, and Ho}$ ) grown with the Bi<sub>2</sub>Mo<sub>3</sub>O<sub>12</sub> based flux we have found a considerable concentration of Bi in the range 3-10 %, also in these cases. This result indicates the need to take into account uncontrolled impurities when considering optical and magnetic properties of compounds grown by flux-melting technique.

This work was supported by the Russian Science Foundation (Grant № 14-12-01033).

[1] Y. Hinatsu et.al., J. Solid State Chem. 172 (2003) 438-445.

[2] M. N. Popova, J. Magn. Magn. Mater. 321 (2009) 716-719.

## TUNING OF THE PHOTOPHYSICAL PROPERTIES OF PYRIMIDINE AND PYRROLO[2,3-D]PYRIMIDINE CORE BASED DERIVATIVES AND THEIR APPLICATIONS FOR FLUORESCENCE SENSING

Arunas Miasojedovas<sup>a</sup>, Lina Skardžiūtė<sup>a</sup>, Justina Jovaišaitė<sup>a</sup>, Jelena Dodonova<sup>b</sup>, Jonas Bucevičius<sup>b</sup>, Sigitas Tumkevičius<sup>b</sup>, Saulius Juršėnas<sup>a</sup>

<sup>a</sup> *Institute of Applied Research, Vilnius University, Saulėtekio 9-III, LT-10222 Vilnius, Lithuania, arunas.miasojedovas@ff.vu.lt*

<sup>b</sup> *Department of Organic Chemistry, Faculty of Chemistry, Vilnius University, Naugarduko 24, LT-03225 Vilnius, Lithuania*

Organic molecules with a  $\pi$ -conjugated backbone are extensively researched due to their applications in a wide range of electronic and optoelectronic devices, such as organic light emitting devices (OLEDs), solar cells, sensors etc. The variety of applications is enabled by the possibility to tune their structural, electronic and photophysical properties via introduction of heteroaryl moieties into the backbone of extended  $\pi$ -systems. Due to strong aromaticity, significant  $\pi$ -deficiency, n- $\pi$  electronic states, pH sensitivity, and ability of their nitrogen atoms to take part in specific intermolecular bonding and interactions in the solid state pyrimidines and pyrrolo[2,3-d]pyrimidines are functional groups often used in more complex donor-acceptor organic structures. They also demonstrate bio-medical activity as various antiviral, antibacterial and even antitumorous agents. Moreover, they share very similar structure with the DNA nucleobases. The combination of the previously mentioned properties could lead to successful application of pyrimidine and pyrrolo[2,3-d]pyrimidine derivatives in bio-sensing and bio-labeling.

In this work we report on the photophysical properties of novel derivatives based on pyrimidine and pyrrolo[2,3-d]pyrimidine cores. The impact of the polar and steric substituents on the photophysical properties of the synthesized donor-acceptor chromophores was evaluated by investigating their optical and electrochemical properties in surroundings of increasing polarity. The results were supplemented by DFT modelling. Substituent induced non-monotonous variation of fluorescence efficiency and optical properties was revealed and is discussed with special emphasis on intramolecular charge transfer and intersystem crossing processes. In addition, highly selective fluorescence sensing of Hg and Fe ions by acceptor-substituted pyrimidine and pyrrolo-pyrimidine derivatives was demonstrated. Different ion sensing mechanisms, determined by the polar substituents, resulting in either enhancement or decrease of the fluorescence intensity and alteration of absorbance spectra, were revealed. Extreme enhancement of fluorescence intensity, up to 400 times, was found for dimethylamine substituted pyrrolo-pyrimidine derivative, manifesting pronounced selectivity to Hg ions.

## THEORY OF OPTICAL CENTRES WITH JAHN-TELLER EFFECT IN EXCITED STATES – CONTRIBUTION OF PHONONS

Kaja Pae, Vladimir Hizhnyakov

*Institute of Physics University of Tartu, Ravila 14c, Tartu, Estonia, kaja.pae@gmail.com*

We have developed a method of calculating of vibronic states and optical spectra of impurity centers in crystals with degenerated electronic states. The method allows one to take into account the Jahn-Teller effect in the degenerate state. The vibronic interaction with non-totally symmetrical local (pseudolocal) modes and with phonon continuum is taken into account. The vibronic interaction with local modes leads to strong hybridization of the quantum states of the modes with the electronic states resulting in formation of complicated vibronic states. Non-totally symmetric phonons cause decay of the vibronic states by emission of phonon quanta to the bulk. The method allows one to calculate both these effects. The method is fully quantum-mechanical. It is based on the time-representation and it considers the time evolution of the excited states. It works for an arbitrary vibronic interaction with a few local modes and weak interaction with an arbitrary number of other modes, including the modes of the phonon continuum [1].

We present the results of explicit calculations of vibronic states and optical spectra of optical centers of trigonal symmetry with two-fold degenerated electronic state of E-representation. In these centers the vibronic interaction with doubly degenerate vibrational mode of *e*-symmetry leads to Jahn-Teller effect known as the *E x e*-problem with the Mexican hat-type adiabatic potential. The method allows one to include all the JTE vibronic states of this problem remarkably contributing to the optical spectrum. The interaction of local mode with phonons results in the replacement of vibronic lines in the spectrum by phonon-assisted bands. The results are illustrated by the calculations of optical spectra in Debye–Van Hove model of phonons. Series of numerical calculations of absorption and resonant Raman scattering spectra are performed using different vibronic and phonon coupling [2]. We also study relaxation process from excited Jahn-Teller state due to phonons and present numerical calculations, which give detailed description of time evolution of the system through the conical intersection of the Mexican hat potential [3].

There are several experimental studies of crystal centres, where theory of Jahn-Teller *E x e*-problem is needed to explain the optical spectra. To name a few - for example study of Raman scattering and photoluminescence of  $\text{LaMnO}_3$  [4,5], the tunneling splitting in the impurity crystal  $\text{MgO} : \text{Cu}^{2+}$  [6]. A theoretical description of some of observed effect will be presented.

[1] V. Hizhnyakov, K. Pae, T. Vaikjärv, *Chemical Physics Letters*. (2012) 525–526, 64 - 68.

[2] K. Pae, V. Hizhnyakov, *Journal of Chemical Physics*. (2013) 138(10), 104103.

[3] K. Pae V. Hizhnyakov, *Journal of Chemical Physics*. (2014)141(23), 234113.

[4] N. N. Kovaleva, O. E. Kusmartseva, K. I. Kugel et al, *J. Phys.: Condensed Matter* 25 (2013) 155602.

[5] N. N. Kovaleva, K. I. Kugel, Z. Potucek et al, *J Phys.: Condensed Matter*. <http://arxiv.org/abs/1407.1475>.

[6] I. B. Bersuker, Isaac in: M. Atanasov, C. Daul, P. L. W (Eds.), *Vibronic Interactions and the Jahn-Teller Effect*. Springer, 2012, pp. 1-22.

## THEORETICAL STUDY ON ZNHGSSE ALLOYS FOR WIDE RANGE OPTOELECTRONIC APPLICATIONS

Mehmet Ustundag<sup>1</sup>, Sadik Bagci<sup>1</sup>, Battal G. Yalcin<sup>1</sup>, Metin Aslan<sup>1</sup>

<sup>1</sup>*Sakarya University, Art and Science Faculty, Department of Physics 54187 Sakarya, Turkey*

We present a calculation of the structural, electronic and optical properties of the four binary members of ZnHgSSe quaternary system by means of wien2k software package [1]. The exchange-correlation potential is treated by generalized gradient approximation (GGA) within the scheme of Wu and Cohen [2]. Also, we have used modified Becke-Johnson (mBJ) formalism [3] to improve the band gap results. All the calculations have been performed after geometry optimization. We have determined that the direct band gap of the system can vary from 0.06 eV (HgSe) to 3.6 eV (ZnS) as shown in Figure 1. ZnHgSSe alloys have also provided the possibility of grown on lattice matched to the common substrates of GaAs and InP as well. Because of the band gap range cover near UV, visible and IR spectrum regions, and lattice match properties, ZnHgSSe alloys are candidate materials for many optoelectronic applications.

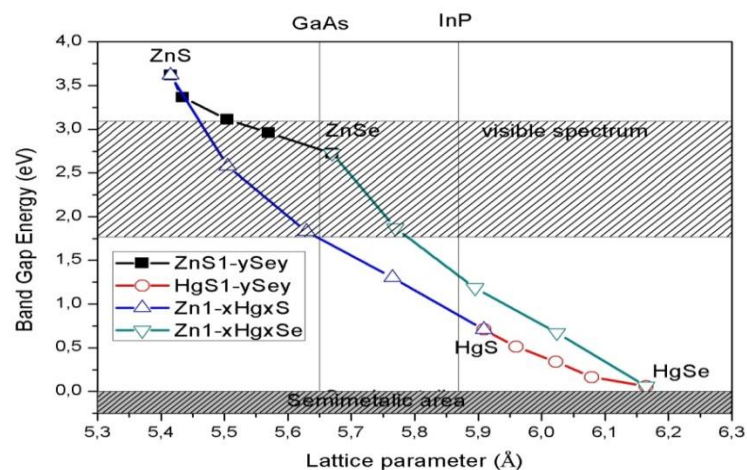


Figure 1. Energy band gap versus lattice constant diagram.

[1] P. Blaha, K. Schwarz, G. K. H. Madsen, D. Kvasnicka, and J. Luitz, WIEN2K: An Augmented Plane Wave Plus Local Orbitals Program for Calculating Crystal Properties, edited by K. Schwarz, Vienna University of Technology, Austria, 2001.

[2] Z. Wu, R. E. Cohen, Phys. Rev. B 73 (2006) 235116.

[3] F. Tran, P. Blaha, Phys. Rev. Lett. 102 (2009) 226401.

## THE UNIT CELL PARAMETER OF THE CUBIC BIXBYITE SESQUIOXIDES VS. STARK SPLITTING OF THE EUROPIUM ${}^7F_1$ MANIFOLD

Željka Antić<sup>a,\*</sup>, Vesna Đorđević<sup>b</sup>, Miroslav D. Dramićanin<sup>b</sup> and Thomas Thundat<sup>a</sup>

<sup>a</sup>*Department of Chemical and Materials Engineering, University of Alberta, Edmonton, Canada, \*zeljkaa@gmail.com, antic@ualberta.ca*

<sup>b</sup>*Vinča Institute of Nuclear Sciences, University of Belgrade, P.O.Box 522, 11001 Belgrade, Serbia*

A set of  $\text{Eu}^{3+}$ -doped  $(\text{Y}_x\text{Sc}_{1-x})_2\text{O}_3$  ( $x = 0, 0.25, 0.5, 0.75, 1$ ) nanocrystalline powders was synthesized using polymer complex solution method. Comparative structural and optical characterization was carried out by powder X-ray diffraction and photoluminescence (PL) excitation, emission and emission decay measurements. The second order crystal field parameters ( $B_0^2$ ) and ( $B_2^2$ ) and crystal field strength ( $N_v$ ) were calculated for the compositions using Stark components of the  ${}^7F_1$  manifold of the  $\text{Eu}^{3+}$  ion in the  $C_2$  point symmetry.

Up to date, we reported studies on the following pure and mixed  $\text{Eu}^{3+}$ -doped rare-earth sesquioxides,  $\text{RE}_2\text{O}_3\text{--RE}'_2\text{O}_3$  ( $\text{RE}, \text{RE}' = \text{Y}, \text{Gd}, \text{La}$  and  $\text{Lu}$ ) [1-5]. Herein we joined all data, including the new ones obtained with  $(\text{Y}_x\text{Sc}_{1-x})_2\text{O}_3\text{:Eu}^{3+}$  solid solutions. We showed that the crystal field parameters linearly depend on unit cell parameter and that these dependencies may be considered as part of an overall dependence for the entire sesquioxide family. From these dependences, we derived a simple, semi-empirical equation that relates the unit cell parameter of the cubic host material and the energy of splitting of  ${}^7F_1$  emission of dopant  $\text{Eu}^{3+}$  ions, ( $\Delta E$ ). The relation is applicable to all cubic sesquioxide hosts and indicates the sensitivity of  $\text{Eu}^{3+}$  emission on the structure of the host material.

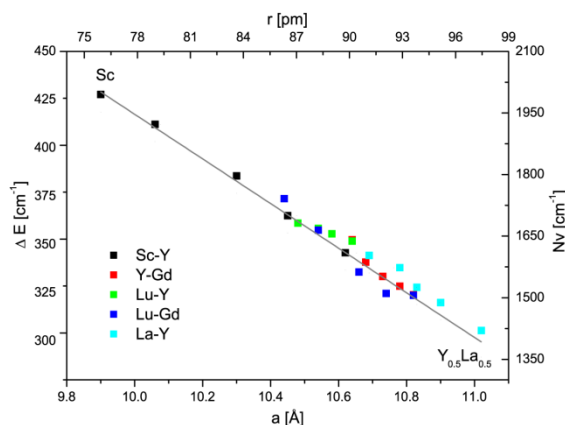


**Figure 1** Graphical representation of maximum splitting ( $\Delta E$ ) of  ${}^7F_1$  manifold and crystal field parameter ( $N_v$ ) as a function of cell parameters (down x-axis) and cation radius (upper x-axis) for a full range rare-earth sesquioxide binary systems,  $\text{RE}_2\text{O}_3\text{--RE}'_2\text{O}_3$  ( $\text{RE}, \text{RE}' = \text{Sc}, \text{Y}, \text{La}$  to  $\text{Lu}$ ).

[1] Ž. Andrić, M.D. Dramićanin, M. Mitrić, V. Jokanović, A. Bessière, B. Viana, *Opt. Mater.* 30 (2008) 1023-1027.

[2] Ž. Antić, R. Krsmanović, M. Wojtowicz, E. Zych, B. Bártová, M.D. Dramićanin, *Opt. Mater.* 32 (2010) 1612-1617.

[3] V. Đorđević, M.G. Nikolić, B. Bartova, R.M. Krsmanović, Ž. Antić, M.D. Dramićanin, *J. Nanopart. Res.* 15 (2013) 1322.

[4] R.M. Krsmanović, Ž. Antić, B. Bártová, A. Speghini, M. Bettinelli, M.G. Brik, M.D. Dramićanin, *Opt. Mater.* 36 (2014) 1083-1091.

[5] V. Đorđević, Ž. Antić, V. Lojpur and M.D. Dramićanin, *J. Phys. Chem. Solids*, 75 (2014) 1152-1159.

## THE EFFECT OF Li<sup>+</sup> CO-DOPING ON STRUCTURAL, MORPHOLOGICAL AND OPTICAL PROPERTIES OF TiO<sub>2</sub>:Eu<sup>3+</sup> NANOPOWDERS

Vesna Đorđević<sup>a,\*</sup>, Bojana Milićević<sup>a</sup>, Goran Dražić<sup>b</sup> and Miroslav D. Dramićanin<sup>a</sup>

<sup>a</sup>Vinča Institute of Nuclear Sciences, University of Belgrade, P.O.Box 522, 11001 Belgrade, Serbia, vesipka@vinca.rs

<sup>b</sup>Laboratory for Materials Chemistry, National Institute of Chemistry, Hajdrihova 19, 1000 Ljubljana, Slovenia

A set of anatase TiO<sub>2</sub>:3at.% Eu<sup>3+</sup> nanocrystalline powders co-doped by Li<sup>+</sup> ions was synthesized by hydrolytic sol-gel route [1]. The effect of Li<sup>+</sup> co-dopant was studied in the concentrations from 0 up to 12at.%, in the 3at.% step are studied by X-ray powder diffraction (XRD), transmission electron microscopy (TEM), and photoluminescence emission and lifetime spectroscopy. XRD patterns showed that the samples of TiO<sub>2</sub>:Eu,Li crystallize same as pure TiO<sub>2</sub> anatase in addition of 3at.% Eu<sup>3+</sup> and addition of Li<sup>+</sup> ions up to 9at.%. XRD and TEM results showed that using proposed synthetic approach, pure TiO<sub>2</sub> anatase powders crystallize as nanopowders with crystallite size of ~10 nm and particle size of around 10–20 nm range. Introducing Eu<sup>3+</sup> ions in the TiO<sub>2</sub> matrix significantly disturbs the structure by lowering crystallite size to ~4 nm, giving the powders with substantial amount of amorphous phase. Addition of Li<sup>+</sup> co-dopant partially compensates the disturbance between Eu<sup>3+</sup> and Ti<sup>4+</sup> ions, ordering the structure and improving the crystallinity. Increase in emission intensity of Eu<sup>3+</sup> ion and lifetime value was observed with all co-doped samples. The largest effect, in which the emission intensity was two times larger (compared with the sample without Li<sup>+</sup> ions), was achieved with the addition of 6 at.% of Li<sup>+</sup> ions. The largest effect on lifetime of Eu<sup>3+</sup> <sup>5</sup>D<sub>0</sub> level was achieved with the addition of 9 at.% of Li<sup>+</sup> ions where lifetime value was 0.82 ms, which is ~30% more than the sample without Li<sup>+</sup> ions.

[1] Ž. Antić, R. Krsmanović, M. Nikolić, M. Marinović-Cincović, M. Mitrić, S. Polizzi, M. Dramićanin, Mater. Chem. Phys. 135 (2012) 1064–1069.



## THE LUMINESCENCE BUILD UP OF EXCITON-LIKE NATURE IN ALKALI HALIDE CRYSTALS AT REDUCED LATTICE SYMMETRY

Kuanyshebek Sh. Shunkeyev<sup>a</sup>, Shynar Zh. Sagimbayeva<sup>a</sup>, Zuchra K. Aimaganbetova<sup>b</sup>,  
Sagynbek K. Shunkeyev<sup>a</sup>, Daulet M. Sergeev<sup>a</sup>

<sup>a</sup>*Zhubanov Aktobe Regional State University, 34A Moldagulova avenue, Aktobe, Kazakhstan,  
shunkeev@rambler.ru*

<sup>b</sup>*al-Farabi Kazakh National University, 71 al-Farabi Avenue, Almaty, Kazakhstan*

The intrinsic luminescence of alkali halide crystals (AHC) is characterized by the luminescence of self-trapped exciton (STE) at regular lattice sites with only primary particles of crystal matrix [1]. STE structure in AHC is a dihalogen molecule engaged in two anion lattice sites and having orientation  $\langle 100 \rangle$  or  $\langle 110 \rangle$ . Changing the STE's inner circle by local lattice symmetry lowering with low-temperature deformation or light cation homologue makes the demonstration of the broad spectrum of exciton-like luminescence of varying intensity, nature and structure possible [1-3].

In crystals, where the luminescence quantum yield is high enough ( $\eta = 0.1 \div 0.9$ ) low-temperature uniaxial deformation leads to the effect of STE intensity buildup (in NaCl and NaBr to 50 times, in KI and RbI to 15 times, in CsBr to 8 times, in CsI to 1.5 times), which is interpreted by the reduction of the exciton's mean free path to self-trapping. In these crystals no new luminescence bands are registered, except for STE.

The minor strengthening of the STE luminescence intensity (in KBr to 2 times, KCl to 1.6 times) and the appearance of new luminescence bands at 3.58 and 2.75 eV in KBr and 3.88 and 3.1 eV in KCl are registered at low-temperature deformation in the crystals having a very low luminescence quantum yield ( $\eta = 0.002 \div 0.02$ ) and high efficiency of radiation defect creation. It is assumed that the nature of the STE luminescence intensity strengthening and new luminescence bands' nature are associated with the tunneling recharge between the ground states  $F'$ - and  $V_K$  centers that are effectively created by radiation in the low-temperature deformation.

On the example of KCl-Na crystal the assembly of electron-hole pairs in the sodium is demonstrated; the radiative relaxation of the sodium leads to the increased luminescence at 2.8 eV to 30 times in the temperature range from 120 K to 300 K, which is very important for the search of scintillation detectors on the basis of AHC.

The crystals' discrete influence on the structure of central-symmetric and asymmetric STE configuration in AHC is found through the implementation of a low-temperature deformation on two crystallographic directions ( $\langle 100 \rangle$ ,  $\langle 110 \rangle$ ): in face-centered crystals the luminescence intensity redistribution takes place in favor of the symmetrical configuration of STE (strong  $\rightarrow$  weak  $\rightarrow$  on or III  $\rightarrow$  II  $\rightarrow$  I-type), and in volume-centered crystals, on the contrary, in favor of the asymmetric configuration STE (on  $\rightarrow$  weak or I  $\rightarrow$  II - types).

This work was supported by grants from the Ministry of Education and Science of the Republic of Kazakhstan (project 4903/GF4, 4904/GF4).

[1] V. Babin, A. Bekeshev, A. Elango, K. Kalder, A. Maaros, K. Shunkeev, E. Vasilchenko, S. Zazubovich, *J.Phys.: Condens. Matter* 11 (1999) 2303–2317.

[2] A. Elango, Sh. Sagimbaeva, E. Sarmukhanov, T. Savikhina, K. Shunkeev, *Radiation Measurements* 33 (2001) 823–827.

[3] K. Shunkeev, E. Sarmukhanov, A. Barmina, L. Myasnikova, S. Shunkeyev, *J. of Applied Spectroscopy* 74 (2007) 67–72.

## THE LORENTZ OSCILLATOR MODEL AND COVALENT BONDS OF AQUEOUS SOLUTIONS

Petya Petkova<sup>a</sup>, Darina Bachvarova<sup>a</sup> and Petko Vasilev<sup>a</sup>

<sup>a</sup>*Laboratory of Photonics, 115 Universitetska street, Shumen, Bulgaria, Petya232@abv.bg*

In this work, the absorption spectrum of the complex  $[\text{Co}(\text{H}_2\text{O})_6]^{2+}$  is measured in the spectral region 400-600 nm. The aqueous solutions of  $\text{CoSO}_4 \cdot 7\text{H}_2\text{O}$  are prepared with the concentrations 1%, 1.5% and 2%. The refractive index of the investigated solutions is calculated. The Rydberg potential energy function [1, 2] and the generalized Morse function [3] are have been investigated together for  $[\text{Co}(\text{H}_2\text{O})_6]^{2+}$ . The linearized experimental and calculated Lorentz curves are compared for the investigated octahedral complex. The oscillator resonance frequency  $\omega_0$ , plasma frequency  $\omega_p$  and damping parameter  $\Gamma$  are determined also [4].

[1] R. Rydberg, Z. Physik 73 (1931) 376-.

[2] R. Rydberg, Z. Physik 80 (1933) 514-.

[3] R. Biswas and D.R. Hamann, Phys. Rev. Lett. 55 (1985) 2001-.

[4] M.J. Mageto, C.M. Maghanga and M. Mwamburi, The African Review of Physics (2012) 95-105.

## **SPECTRAL-LUMINESCENT PROPERTIES OF ZINC ALUMINOSILICATE GLASS-CERAMICS DOPED WITH NiO**

Alexandr Zhilin<sup>a</sup>, Irina Alekseeva<sup>a</sup>, O Dymshits<sup>a</sup>, Valery Golubkov<sup>b</sup>, Marina Tsenter<sup>a</sup>,  
Michael Shepilov<sup>a</sup>, Pavel Loiko<sup>c</sup>, Konstantin Yumashev<sup>c</sup>, Kirill Bogdanov<sup>d</sup>

<sup>a</sup>*NITIOM Vavilov State Optical Institute, 36/1, Babushkina ul., St. Petersburg, Russia,  
vodym1959@gmail.com*

<sup>b</sup>*Grebenshchikov Institute of Silicate Chemistry, St. Petersburg, Russia, golubkov@isc1.nw.ru*

<sup>c</sup>*Center for Optical Materials and Technologies, Belarusian National Technical University,  
65/17 Nezavisimosti Ave, Minsk, Belarus, kinetic@tut.by*

<sup>d</sup>*National Research University of Information Technologies, Mechanics and Optics,  
Kronverkskiy pr., 49, St. Petersburg, Russia, kirw.bog@gmail.com*

Zinc aluminosilicate glasses nucleated either by TiO<sub>2</sub> or by a mixture of TiO<sub>2</sub> and ZrO<sub>2</sub> and doped with 0.01 – 3.0 mol% NiO were prepared by a conventional melt-quenching technique and heat-treated in the temperature range of 700 – 1200 °C.

Their structure and phase transformations were studied using small angle X-ray scattering, X-ray diffraction analysis and Raman scattering. The absorption and luminescence properties of the two types of glass-ceramics were recorded and discussed.

It was experimentally shown that small additives of nickel oxide (0.01-0.15 mol.%) quantitatively and qualitatively change light-scattering properties of zinc spinel (gahnite) based glass-ceramics.

### Acknowledgments

This work was partially supported by the RFBR (Grant 13-03-01289 A) and performed under the task of Ministry of Education and Science of Russian Federation (task No. 3.109.2014/K).

## THE EFFECT OF ELECTRON BEAM AND THERMAL TREATMENTS ON THE SODIUM NANOPARTICLES FORMATION IN SODA-LIME GLASSES

Elizaveta. S. Bochkareva<sup>a</sup>, Nikolay V. Nikonorov<sup>a</sup>, Oleg A. Podsvirov<sup>b</sup>, Mikhail A. Prosnikov<sup>c</sup>, Alexander.I. Sidorov<sup>a</sup>

<sup>a</sup>*ITMO University, 49 Kronverksky ave., St. Petersburg, Russian Federation, sidorov@oi.ifmo.ru, b.elizaveta.s@gmail.com*

<sup>b</sup>*St.Petersburg Polytechnical University, 29 Polytechnicheskaya str., St. Petersburg, Russian Federation*

<sup>c</sup>*Ioffe Physical-Technical Institute RAS, 26 Polytechnicheskaya str., St. Petersburg, Russian Federation*

It is shown experimentally that the processing of sodium-containing silicate glasses with the electron beam with energy 35 keV and doses 20-65 mC/cm<sup>2</sup> and the subsequent thermal treatment result in the formation of the sodium nanoparticles (NPs) under the glass surface that manifest themselves in the plasmon resonance absorption band in the 405-410 nm region. The main mechanisms of this effect are the field migration of the positive sodium ions into the negatively charged region under the glass surface, produced by the thermalized electrons, reduction of sodium ions by the thermalized electrons, and NPs growth as a result of thermal diffusion of sodium atoms during the thermal treatment. These results are compared with the described in [1], where silver NPs were synthesized in the silver-containing glasses by the same method. The computer simulations in the dipole quasi-static approximation have shown that the most realistic model of the NP structure is the solid or liquid sodium core with two shells, the inner shell of sodium oxide and the external one being vacuum or gas.

[1] A.I. Ignat'ev, A.V. Nashchekin, V.M. Nevedomskii, O.A. Podsvirov, A.I. Sidorov, *Techn. Phys.* 56 (2011) 662–667.

## THE EFFECT OF CHARGE COMPENSATION BY MEANS OF Na<sup>+</sup> IONS ON THE LUMINESCENT PROPERTIES OF Nd<sup>3+</sup>-DOPED CaAl<sub>4</sub>O<sub>7</sub> AND CaGa<sub>4</sub>O<sub>7</sub>

Malgorzata Puchalska

*Faculty of Chemistry, University of Wrocław, 14 F. Joliot Street., 50-383 Wrocław, Poland,  
malgorzata.puchalska@chem.uni.wroc.pl*

Two series of powder materials: singly (Nd<sup>3+</sup>) and doubly (Nd<sup>3+</sup>,Na<sup>+</sup>) doped calcium aluminates and gallates - Ca<sub>1-x</sub>Nd<sub>x</sub>M<sub>4</sub>O<sub>7</sub> and Ca<sub>1-2x</sub>Nd<sub>x</sub>Na<sub>x</sub>M<sub>4</sub>O<sub>7</sub> (M=Al, Ga; x=0.001-0.1) were synthesized by a Pechini citrate process and their optical properties at 298 K and 77 K were investigated. XRD patterns of these samples proved the presence of a single grossite monoclinic phase with a space C2/c group. Upon excitation at 585 nm all obtained powders yielded relatively strong Nd<sup>3+</sup> luminescence corresponding to <sup>4</sup>F<sub>3/2</sub>→<sup>4</sup>I<sub>J</sub> (J=9/2-11/2) with the dominant component around 1080 nm. The effects of activator content as well as charge compensation by co-doping with monovalent Na<sup>+</sup> ions on the luminescence properties and decay kinetics of both luminescent materials were studied.

Low temperature emission spectra of singly doped calcium aluminates and gallates showed an increasing disturbance of the Nd<sup>3+</sup> local symmetry with raising dopant concentration. On the other hand, in Na co-doped materials the optical centers are much less perturbed due to lower accumulation of defects in their surroundings. It leads to a reduction of the number of Nd<sup>3+</sup> emission bands and their significant narrowing (see Fig. 1).

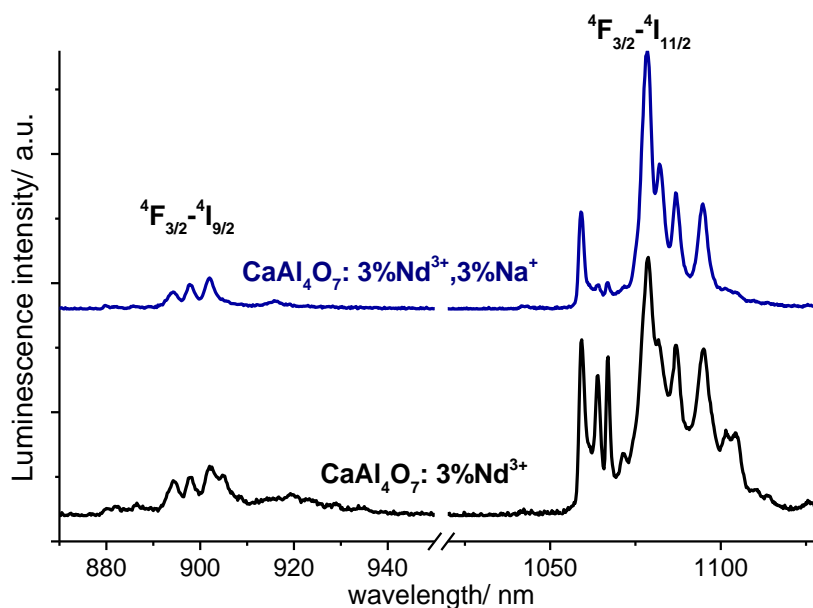


Fig. 1 Luminescence spectra of Nd<sup>3+</sup> doped and Nd<sup>3+</sup>,Na<sup>+</sup> co-doped CaAl<sub>4</sub>O<sub>7</sub> at 77 K

It was also found that charge compensation through Na<sup>+</sup> co-doping improved the luminescence brightness and decreased concentration quenching of fluorescence. These results basically proved that Nd<sup>3+</sup> ions substitute Ca<sup>2+</sup> ions in crystal lattices and tend to create pairs. In order to determine the dominant mechanism of the ion-ion interaction the non-exponential decay curves will be analyzed by Inokuti-Hirayama model.

## TEMPERATURE DEPENDENT LUMINESCENCE OF Cr<sup>3+</sup> DOPED YAl<sub>3</sub>(BO<sub>3</sub>)<sub>4</sub> and GdAl<sub>3</sub>(BO<sub>3</sub>)<sub>4</sub>

Beata Malysa<sup>a</sup>, Andries Meijerink<sup>b</sup>, Thomas Jüstel<sup>a</sup>

<sup>a</sup> Münster University of Applied Sciences, Stegerwaldstrasse 39, D-48565 Steinfurt, Germany,  
beata.malysa@fh-muenster.de, tj@fh-muenster.de

<sup>b</sup> Universiteit Utrecht, Princetonplein 5, 3584 CC Utrecht, The Netherlands,  
a.meijerink@uu.nl

A series of chromium activated YAl<sub>3</sub>(BO<sub>3</sub>)<sub>4</sub> (YAB) and GdAl<sub>3</sub>(BO<sub>3</sub>)<sub>4</sub> (GAB) samples were synthesized by a solid state reaction method. YAB and GAB are excellent hosts for Cr(III)-substitution because they offer only one kind of cation site with octahedral coordination. Hence, the chromate phase [CrO<sub>4</sub>]<sup>2-</sup> which strongly reduce the luminescence efficiency does not appear in these compounds because of the lack of the tetrahedral sites which are suitable for Cr<sup>6+</sup> ions [1]. The luminescent powders are well excitable in the blue and orange part of the spectrum. At lower temperature the narrow <sup>2</sup>E<sub>g</sub> emission dominates and the gradual increasing of the temperature causes broadening of the spectra because of the thermal population of <sup>4</sup>T<sub>2g</sub> state (Fig. 1a). The temperature dependence of the emission spectra monitored between 77 and 800 K shows that the photoluminescence intensity of YAB:1%Cr<sup>3+</sup> and GAB:1%Cr<sup>3+</sup> is nearly constant up to 350 K and the quenching temperature for the broad band Cr<sup>3+</sup> emission is at 550 and 650 K, respectively (Fig. 1b).

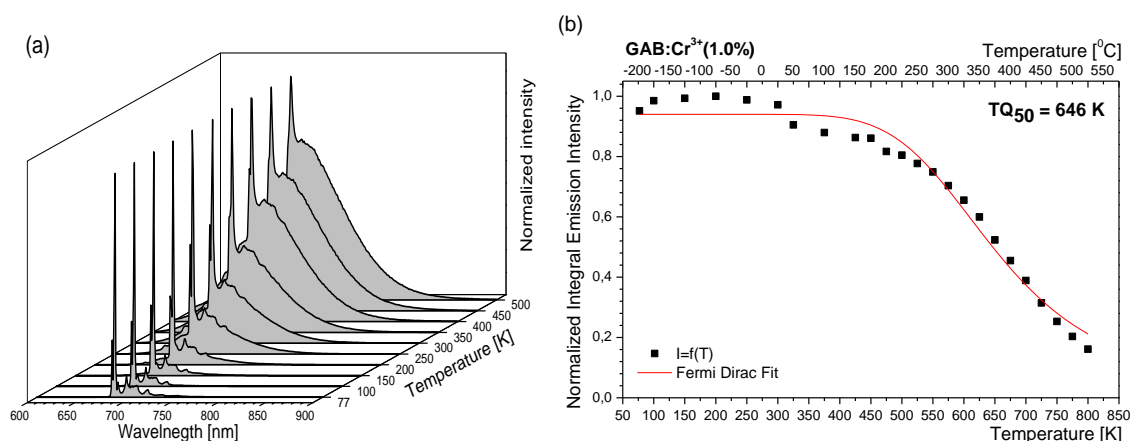


Fig. 1. Temperature dependent: a) emission spectra and b) normalized integral emission intensity of GdAl<sub>3</sub>(BO<sub>3</sub>)<sub>4</sub>:Cr<sup>3+</sup>(1.0%) upon excitation at 420 nm.

In order to compare the temperature dependent properties of YAB:Cr<sup>3+</sup> and GAB:Cr<sup>3+</sup>, the crystal field strength, Racah parameters, nephelauxetic effect and phonon coupling parameters have been determined. Both luminescent compounds belong to the intermediate crystal field materials and exhibit similar crystal field strength (around 1670 cm<sup>-1</sup>). However, the calculated B Racah parameters points to a higher global covalency in GAB. The electron phonon-coupling parameter (S) and the effective phonon energy ( $\hbar\omega$ ) were determined to be 5.9 and 263 cm<sup>-1</sup> for YAB and 5.4 and 309 cm<sup>-1</sup> for GAB, respectively. The larger electron-phonon coupling strength in YAB:Cr confirms the lower quenching temperature in comparison with GAB:Cr.

[1] F. Rasheed, K.P. O'Donnell, B. Henderson, D.B. Hollis, J. Phys.: Condens. Matter 3 (1991) 1915-1930.

## TEMPERATURE DEPENDENCE OF Y-ADMIX GAGG SCINTILLATOR GROWN BY THE CZOCHRALSKI PROCESS

Shunsuke Kurosawa <sup>a, b</sup>, Mafuyu Seki <sup>a</sup>, Kei Kamada <sup>a, c</sup>, Jan Pejchal <sup>d</sup>, Yasuhiro Shoji <sup>a, c</sup>, Yuji Ohashi <sup>a</sup>, Yuui Yokota <sup>b</sup>, Akira Yoshikawa <sup>a, b, c</sup>

<sup>a</sup> *Tohoku University, Institute for Material Research, 2-1-1 Katahira Aoba-ku, Sendai, Miyagi 980-8577, Japan, kurosawai@imr.tohoku.ac.jp*

<sup>b</sup> *Tohoku University, New Industry Creation Hatchery Center, 6-6-10 Aoba, Aramaki, Aoba-ku, Sendai, Miyagi 980-8579, Japan*

<sup>c</sup> *C&A Corporation, T-Biz, 6-6-10 Aoba, Aramaki, Aoba-ku, Sendai, Miyagi 980-8579, Japan*

<sup>d</sup> *Institute of Physics CAS, Cukrovarnicka 10, 16253 Prague, Czech Republic*

Ce-doped  $Gd_3(Ga, Al)_5O_{12}$  (GAGG) scintillator has excellent scintillation properties: high light output, good energy resolution, etc. [1], and we have developed a Compton camera using GAGG scintillator used in various fields such as dose-meter, astronomy and medical imaging. Here, the Compton camera consists of Compton scatter part and absorption part, and scintillators are available for use in both parts; Small-effective-atomic-number material is suitable for the scatter part to enhance the probability of Compton scatter. Since GAGG has an effective-atomic-number of over 50, we have developed a new material with that of less than 50. In this paper, we report the scintillation properties of Ce-doped  $(Gd, Y)_3(Ga, Al)_5O_{12}$  (GYAGG) scintillator grown by the Czochralski process.

Figure 1 show the as-grown  $Ce:(Gd_{3-x}, Y_x)Al_2Ga_3O_{12}$  crystals with a diameter of 1 inch, where  $x=0.5, 1.0, 1.5$ , and these crystals have effective-atomic-numbers of less than 50. The crystals were cut and polished into 5 mm x 5 mm x 1 mm (thickness), and all samples from tail, middle and seed side of the  $Ce:(Gd_{2.5}, Y_{0.5})Al_2Ga_3O_{12}$  bulk had light outputs of over 40,000 photons/MeV using a photomultiplier (PMT). On the other hand, other samples from the  $Ce:(Gd_{3-x}, Y_x)Al_2Ga_3O_{12}$  ( $x=1.0, 1.5$ ) bulks had that of 30,000 – 40,000 photons/MeV.

Since the Compton camera can be used in various temperature condition; as a dose-meter it can be -30 to 40 °C. Thus, the temperature dependence of scintillation properties such as light outputs, energy resolution, were investigated using the PMT and Si-avalanche photodiode for  $Ce:(Gd_{3-x}, Y_x)Al_2Ga_3O_{12}$  samples. Moreover, temperature dependence of photo-luminescence, including quantum yield up to 150 °C., were measured.

In this presentation, we show the above optical properties, scintillation properties and their temperature dependence.

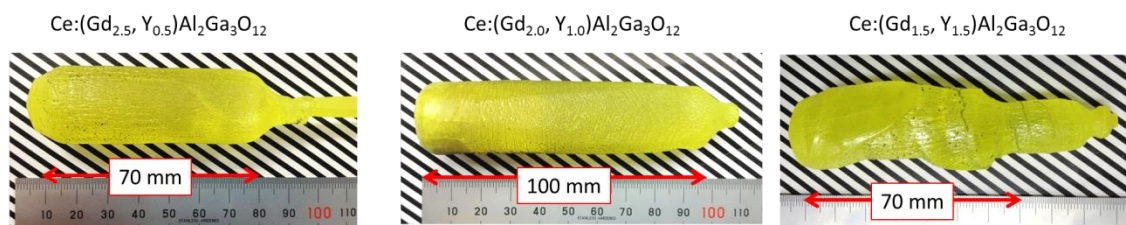


Fig. 1 photographs of 1-inch  $Ce:(Gd_{3-x}, Y_x)Al_2Ga_3O_{12}$  crystals grown by the Czochralski process.

[1] K. Kamada, A. Yoshikawa, *et al.*, *Crystal Growth & Design*, 11(2011) 4484-4490.

## SYNTHESIS, STRUCTURE AND LUMINESCENT PROPERTIES OF Eu<sup>3+</sup>- DOPED Zn<sub>2</sub>TiO<sub>4</sub> NANOPARTICLES

Mina Medić<sup>a</sup>, Vesna Lojpur<sup>a</sup>, Željka Antić<sup>b</sup>, Miroslav D. Dramićanin<sup>a</sup>

<sup>a</sup>University of Belgrade, Vinča Institute of Nuclear Sciences, P.O. Box 522, Belgrade 11001,  
Serbia, mina@vinca.rs

<sup>b</sup>Department of Chemical and Materials Engineering, University of Alberta, Edmonton, T6G  
2V4, Canada

Zinc-orthotitanate (Zn<sub>2</sub>TiO<sub>4</sub>) is used as an efficient catalyst, pigment, sensor, and ceramic for microwave dielectrics, thermoelectric materials, and for solid oxide fuel cells [1, 2]. So far, this material has been rarely investigated as a host matrix for rare earth elements [2]. In this work, we used simple Pechini-type polymerized complex route method to obtain Zn<sub>2</sub>TiO<sub>4</sub> nanopowders. This method is based on the polyesterification between citric acid (CA) and ethylene glycol (EG) [3]. It is important to note that we used mixed metal-CA complex with stoichiometric Zn:Ti ratio of 2:1 at low working temperatures necessary for nanoparticles formation. Eu<sup>3+</sup>- doped Zn<sub>2</sub>TiO<sub>4</sub> were calcined at 650°C for 1h to obtain pure phase. Detailed characterization of nanoparticles was done through several analysis: X-ray diffraction (XRD) confirmed cubic system with inverse spinel structure. Photoluminescence (PL) spectroscopy measurements included excitation and emission spectra. The materials exhibit characteristic strong red emission bands from <sup>5</sup>D<sub>0</sub>→<sup>7</sup>F<sub>J</sub> spin forbidden f–f electronic transitions in Eu<sup>3+</sup>.

[1] K.M. Girish, Ramachandra Naik, S.C. Prashantha, H. Nagabhushana, H.P. Nagaswarupa, K.S. Anantha Raju, H.B. Premkumar, S.C. Sharma, B.M. Nagabhushana, *Spectrochim. Acta Mol. Biomol. Spectrosc.* 138 (2015) 857–865

[2] J. Mrázek, L. Spanhel, M. Surýnek, M. Potel, V. Matějec, *J. Alloys Compd.* 509 (2011) 4018–4024

[3] M. M. Medić, M. G. Brik, G. Dražić, Ž. M. Antić, V. M. Lojpur, M. D. Dramićanin, *J. Phys. Chem. C.* 119 (1) (2014) 724–730



## SYNTHESIS, LUMINESCENCE AND SILICA COATING OF $\text{Eu}^{3+}$ -DOPED $\text{LaVO}_4$ NANOPARTICLES

Robin Geitenbeek and Andries Meijerink

<sup>a</sup>*Utrecht University, Princetonplein 5, Utrecht, Netherlands, R.G.Geitenbeek@uu.nl*

Extensive research on luminescent nanomaterials has enabled monitoring of reaction parameters and phenomena at the nanoscale. For instance, luminescent nanoparticles can be used as biolabels to monitor transport of (nano)particles in biological systems.

An important reaction parameter is temperature. Conventional thermometry is not always able to measure the temperature with a sufficient spatial resolution. Luminescent thermometers based on f-f transitions of lanthanides incorporated in nanoparticles can be used to determine the temperature with high spatial resolution in a wide range (4-1000 K)<sup>[1,2]</sup>.

The nanoparticles used for nanothermometry should be stable and robust under working conditions to be applicable as nanoprobes. In the case of physiological systems, toxicity and chemical stability are important factors. In industrial use, at elevated temperatures, the chemical and thermal stability are very important. These factors can be improved by encapsulating the nanoparticles in an inert protective shell material.

In this work we have prepared  $\text{LaVO}_4$  nanoplatelets doped with europium<sup>[3]</sup> and subsequently encapsulated these particles in inert silica via a micro-emulsion method<sup>[4]</sup>. Using TEM it was confirmed that the overgrowth with silica was successful. The luminescence measurements before and after silica overgrowth suggests that the silica has no effect on the europium emission. In the next step we will investigate the temperature-dependence of the luminescence for particles with and without silica overgrowth and test the applicability of these silica coated nanoparticles as nanothermometers under industrial reaction conditions.

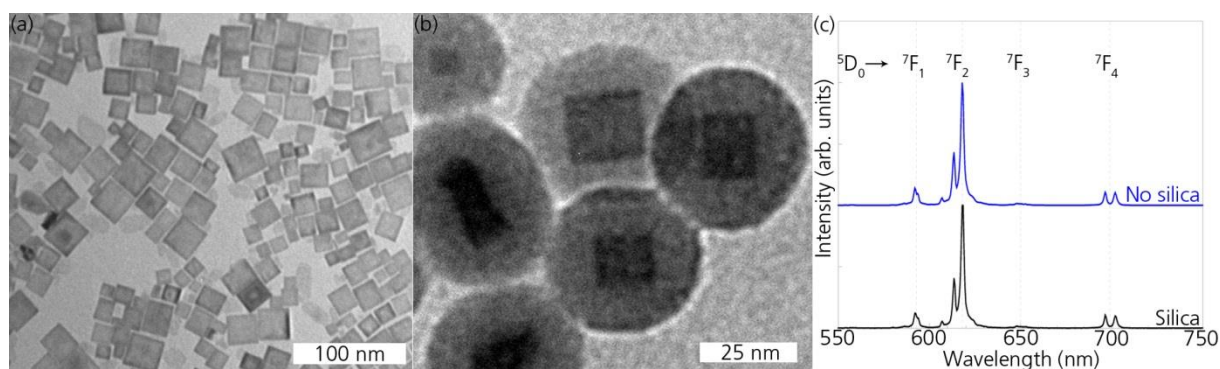


Figure 1: A TEM image of  $\text{Eu}^{3+}$ -doped  $\text{LaVO}_4$  nanoplatelets with an average diameter of 25 nm and a thickness of 5 nm (a), a TEM image of the nanoplatelets after overgrowth with silica (b) and the europium emission of nanoplatelets before and after silica encapsulation (c).

[1] C. Brites et al, *Nanoscale* 4 (2012) 4799-4829

[2] D. Jaque, F. Vetrone, *Nanoscale* 4 (2012) 4301-4326.

[3] J. Liu, Y. Li, *Adv. Mat.* 19 (2007) 1118-1122.

[4] R. Koole et al., *Chem. Mater.* 20 (2008).

## Ag AND TiO<sub>2</sub> NANOPARTICLES ON POLYMER SUPPORT

Ivana D. Vukoje<sup>a</sup>, Lidija V. Trandafilović<sup>a</sup>, Tijana S. Radoman<sup>b</sup>, Enis S. Džunuzović<sup>c</sup>,  
S. Phillip Ahrenkiel<sup>d</sup>, Jovan M. Nedeljković<sup>a</sup>

<sup>a</sup>*Institute of Nuclear Sciences Vinča, University of Belgrade, P. O. Box 522,  
Belgrade, Serbia, ivanav@vinca.rs*

<sup>b</sup>*Innovation center, Faculty of Technology and Metallurgy, University of Belgrade,  
Karnegijeva 4, 11120 Belgrade, Serbia*

<sup>c</sup>*Faculty of Technology and Metallurgy, University of Belgrade, Karnegijeva 4,  
11120 Belgrade, Serbia*

<sup>d</sup>*South Dakota School of Mines and Technology, 501 E Saint Joseph Street, Rapid City,  
SD 57701, USA*

Poly(GMA-co-EGDMA) macroporous copolymer was used as a support for preparation and functionalization of Ag and TiO<sub>2</sub> nanoparticles. Obtained nanocomposites were characterized using elemental analysis, transmission electron microscopy and X-ray diffraction analysis. UV-Vis reflection spectroscopy was used for optical characterization of Ag and TiO<sub>2</sub> nanoparticles on polymer support, while the coordination of nanoparticles to the poly(GMA-co-EGDMA) copolymer was studied using infrared spectroscopy. Antimicrobial efficiency of Ag nanoparticles on polymer support was tested against *Escherichia coli*, *Staphylococcus aureus*, and *Candida albicans*. On the other hand, the photocatalytic ability of red-shifted TiO<sub>2</sub> nanoparticles on polymer support was tested under visible light illumination by following the degradation of organic dye crystal violet. The preliminary results clearly indicate that surface-modified TiO<sub>2</sub> nanoparticles are able to photocatalytically perform under visible light illumination.

## STUDY OF LUMINESCENCE MECHANISMS AND EXCITATION ENERGY TRANSFER IN THE Yb-DOPED PbWO<sub>4</sub> CRYSTALS

Oksana Chukova, Sergiy G. Nedilko

*Physics Faculty, National Taras Shevchenko University of Kyiv  
4-b, acad. Hlushkov Ave., 03680, Kyiv, Ukraine*

Tungstate crystals (PbWO<sub>4</sub>, CdWO<sub>4</sub>, CaWO<sub>4</sub>) are successfully used as scintillators. Development of their characteristics and understanding of physical processes responsible for changes of their properties are important tasks for future applications of tungstates. The RE doping can decrease content of lead and oxygen vacancies, those are the most probable defects in the PWO crystals grown by Czochralsky method. That is why, adding of RE impurities changes significantly the defect composition of the crystal lattice and can effect on centres responsible for matrix emission. With this aim, we have carried out investigation of correlations in behaviour of matrix and impurity emission and used complex approach that included spectral investigations and mathematical analysis of the emission spectra.

The PWO crystals were grown by the Czochralski method using the "Crystal-617" installation. Spectral measurements were carried out using synchrotron radiation at SUPERLUMI station at HASYLAB (DESY), Hamburg, Germany and R&D Laboratory "Spectroscopy of condensed state of matter" at Physical Faculty of Taras Shevchenko National University of Kyiv.

The Yb<sup>3+</sup> ions in the PWO crystals form two emission centers. Origin and spectral properties of these centers are studied. Matrix emission spectra of the un-doped and Yb<sup>3+</sup> - doped PWO crystals are presented by five strongly overlapped bands at 3.0, 2.7, 2.45, 2.2 and 1.95 eV. The Yb<sup>3+</sup> doping increases intensity of the 3.0 eV band by formation of additional RE - induced channel of creation of excitons. The observed suppression in the Yb<sup>3+</sup>- doped crystals of the 1.95 eV band is caused by decreasing of Pb vacancies content in the doped crystals.

Excitation spectra of the investigated crystals are characterized by the sharp peak and wide asymmetric bands in 8.0 – 5.5 and 5.5 – 4.3 eV energy ranges. Positions of the sharp exciton peaks are 4.1 and 4.2 eV for the undoped and RE<sup>3+</sup>- doped crystals, respectively. We assume, that creation of excitons occurs only on that Pb states those are part of absorption centers involving Pb ions and neighbor defects. For the undoped crystals the most probable defects, taking part in such centers, are oxygen vacancies. The main type of defects in the doped crystals could be the RE<sup>3+</sup> ions arranged in the Pb sites. Then, independently on structure of centres of their creation, the described two types of excitons are supposed to localize and disintegrate at the same elements of crystal lattice (the regular WO<sub>4</sub><sup>2-</sup> groups) and give the same emission band at 3.0 eV. Thus, effect of the Yb ions on the blue emission is a result of formation by the RE ions of additional channel of energy transfer for creation of excitons.

Enhancement of the blue band and suppression of the red band are desirable for scintillation applications of the PWO crystals, therefore RE ions could improve spectral characteristics of the PWO scintillators.

## STUDIES ON YSO:Ce BASED PHOSPHORS PREPARED BY GEL COMBUSTION USING NEW SILICON SOURCE

Ioana Perhaita<sup>a</sup>, Laura E. Muresan<sup>a</sup>, Adrian I. Cadis<sup>a</sup>, Oana Ponta<sup>b</sup>, Laima Trinkler<sup>c</sup>

<sup>a</sup>Raluca Ripan Institute for Research in Chemistry-UBB, 30 Fantanele, Cluj-Napoca, Romania, laura\_muresan2003@yahoo.com

<sup>b</sup>Faculty of Physics-UBB, 1 Kogalniceanu, Cluj-Napoca, Romania, oanaponta@yahoo.com

<sup>c</sup>Institute of Solid State Physics, University, 8 Kengaraga, Riga, Latvia, trinkler@latnet.lv

A variety of cerium doped yttrium silicate based phosphors (YSO:Ce) were prepared by gel combustion using vinyltriethoxysilane (VTEOS) as silicon source, aspartic acid as fuel and Y-Ce nitrate as oxidiser. The study aims to investigate the effect of VTEOS molar amount, (used for the first time) on the structural and luminescent characteristics of YSO:Ce.

The structural composition of phosphors is changing from  $X_2\text{-Y}_2\text{SiO}_5$  to  $\alpha\text{-Y}_2\text{Si}_2\text{O}_7$  as the VTEOS amount is increased from 1 to 3 mole. The results are confirmed by FTIR and XRD investigations. The luminescent characteristics of YSO:Ce samples were evaluated at room and low temperature (10K÷300K) based on excitation and emission spectra (Figure1). Incorporation of cerium in different sites (Ce1 and Ce2) is discussed based on low temperature (10K).

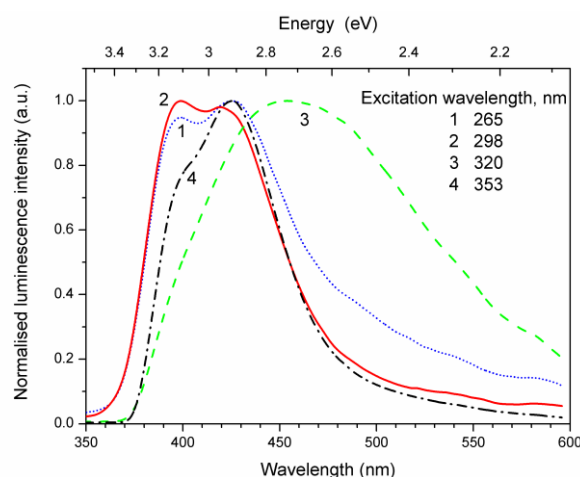


Figure 1 Normalised PL spectra at 10K for sample prepared with 1 mole VTEOS

Under UV excitation YSO:Ce exhibit blue emission due electron transition in  $\text{Ce}^{3+}$  from 5d level to the ground state levels ( $^2\text{F}_{5/2}$ ,  $^2\text{F}_{7/2}$ ). The emission intensity increase from 70 % to 120 % as VTEOS amount is increased, explained by the improvements in structural homogeneity.

### Acknowledgments

This work was supported by a grant of the Romanian National Authority for Scientific Research, CNCS – UEFISCDI, project number PN-II-RU-TE-2012-3-0360.

## STRUCTURAL PROPERTIES OF BISMUTH–LEAD-GERMANATE GLASSES

Simona Rada<sup>b</sup>, Marius Rada<sup>a</sup>, Nicolae Aldea<sup>a</sup>, Ramona - Crina Suciuc<sup>a</sup>, Sergiu Macavei<sup>a</sup>,  
Adrian Bot<sup>a</sup>, Eugen Culea<sup>b</sup> and Radu Balan<sup>c</sup>

<sup>a</sup> *National Institute for Research and Development for Isotopic and Molecular Technologies, 400293 Cluj-Napoca, Romania*

<sup>b</sup> *Department of Physics & Chemistry, Technical University of Cluj-Napoca, 400020 Cluj-Napoca, Romania*

<sup>c</sup> *The Department of Mechanisms, Fine Mechanics and Mechatronics, Technical University of Cluj-Napoca, 400020 Cluj-Napoca, Romania*

The present work is focused on the enhancement of network former environment in lead-germanate glasses by bismuth ions doping. A series of bismuth–lead-germanate glasses with the  $x\text{Bi}_2\text{O}_3(100-x)[7\text{GeO}_2\bullet 3\text{PbO}]$  composition glass where  $0 \leq x \leq 30$  mol%  $\text{Bi}_2\text{O}_3$  were synthesized by melt-quenching method. The FTIR, UV–VIS spectroscopy and cyclic voltammetry were conducted on these samples to evaluate the doping effect of structure of the host matrix network[1,2,3]. Our results indicate that direct incorporation of  $\text{Bi}_2\text{O}_3$  into the lead-germanate network modifies the lead-germanate network and the internal structure of glass network is rearranged. The structural flexibility of the lead-germanate network is possible due to its incapacity to accommodate with the excess of oxygen atoms and the creation of bridging oxygen ions. Optical gap energy and refractive index were obtained as a function of  $\text{Bi}_2\text{O}_3$  content. Gap energy values decrease as  $\text{Bi}_2\text{O}_3$  content increased from 0 to 10 mol% [4]. Further increase of  $\text{Bi}_2\text{O}_3$  concentration beyond 10 mol% increased the gap energy values. These behaviors of the glass system can be explained by two mechanisms: (i) for  $x \leq 10$  mol%  $\text{Bi}_2\text{O}_3$  – increase of degree of disorder of the host matrix because  $\text{Bi}_2\text{O}_3$  is network modifier and (ii) for  $x > 10$  mol% –  $\text{Bi}_2\text{O}_3$  acts as a network former. Cyclic voltammetry measurements using the glass system with  $10\text{Bi}_2\text{O}_3\bullet 90[7\text{GeO}_2\bullet 3\text{PbO}]$  composition as working electrode show the mobility of the lead ions, in agreement with UV–VIS data.

[1] Y.G. Choi, K.H. Kim, V.A. Chernov, J. Heo, J. Non-Cryst. Solids, 259 (1999), p. 205

[2] S. Rada, P. Pascuta, M. Bosca, M. Culea, L. Pop, E. Culea, Vib. Spectrosc., 48 (2) 2008), p. 255

[3] S. Rada, E. Culea, M. Bosca, M. Culea, R. Muntean, P. Pascuta, Vib. Spectrosc., 48 (2) (2008), p. 285

[4] J. Kaufmann, C. Russel, J. Non-Cryst. Solids, 356 (2010), p. 1158

## STRUCTURAL AND OPTICAL PROPERTIES OF PEROVSKITE-TYPE COMPOUNDS: NaTaO<sub>3</sub> AND NaNbO<sub>3</sub>

Paula Sfirloaga<sup>1</sup>, Maria Poienar<sup>1</sup>, Marcela Stoia<sup>2</sup>, Paulina Vlazan<sup>1</sup>

<sup>1</sup>National Institute for Research and Development in Electrochemistry and Condensed Matter, Timisoara, Condensed Matter Department, P. Andronescu no.1, 300254, Romania,

<sup>2</sup> "Politehnica" University of Timisoara, P-ta Victoriei no. 2, Timisoara 300006, Romania  
psfirloaga@yahoo.com

Alkali metal tantalates and niobates have excellent electro-optical and photorefractive properties and find extensive applications as optical wave guides and modulators and surface acoustic wave devices [1,2]. Traditionally these materials were prepared by solid state reaction which leads to inhomogeneity in composition and coarse particles. Chemical methods, e.g. co-precipitation, sol-gel, hydrothermal and colloid emulsion techniques, allow to efficiently control the morphology and chemical composition of the prepared powders [3]. The purpose of this study was to prepare NaTaO<sub>3</sub> (Nat) and NaNbO<sub>3</sub> (Nan) materials by ultrasonic method with immersed sonotrode in the reaction medium, followed by annealed at 600°C, for 6 h.

The phase purity and lattice parameters were studied by powder X-ray diffraction (XRD). The particle size and morphology were studied by scanning electron microscopy (SEM).

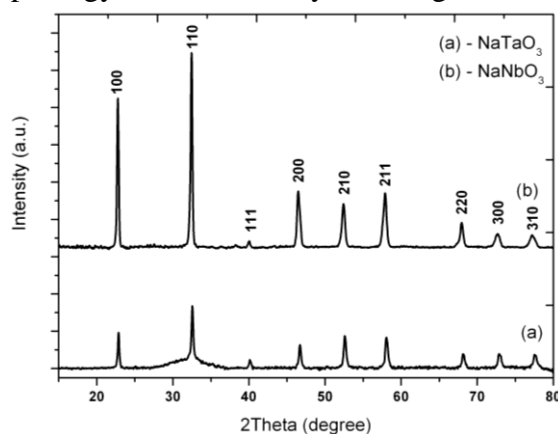


Figure 1. XRD patterns of NaTaO<sub>3</sub> (a) and NaNbO<sub>3</sub> (b)

Figure 1(a) and (b) show X-ray diffraction patterns of NaTaO<sub>3</sub> and NaNbO<sub>3</sub>, respectively. Ultrasonically obtained NaTaO<sub>3</sub> and NaNbO<sub>3</sub> nanomaterials display single phase without any secondary phases.

### Acknowledgements

Financial support for this work was provided by National Project 09 34 02 09/2015 and by the Collaborative applied research project 177/2014 PESTI-SENZ.

[1] Aydi A, Khemakhem H, Boudaya C, Muhll R V and Simon A Solid State Sci. 6 (2004) 333-337.

[2] Raveski I P and Prosandeev S A J. Phys. & Chem. Solids 63 (2002) 1939-1950.

[3] V. Samuel, A. B. Gaikwad and V Ravi, Bull. Mater. Sci. 29 (2006) 123-125.

## STANDARD THERMAL CONTRAST DEPENDENCE ON THE SUBSURFACE DEFECT DEPTH FOR THE DIFFERENT MATERIALS

Ljubiša D. Tomić<sup>a</sup>, Vesna M. Damnjanović<sup>b</sup>, Goran D. Dikić<sup>c</sup>,  
Bojan Č. Milanović<sup>c</sup>, Boban M. Bondžulić<sup>c</sup>

<sup>a</sup>*Technical Test Center, 445 Vojvode Stepe, Belgrade, Serbia, ljubisa.tomic@gmail.com*

<sup>b</sup>*Faculty of Mining and Geology, University of Belgrade, 7 Đušina, Serbia,  
vesna.damnjanovic@rgf.bg.ac.rs*

<sup>c</sup>*Military Academy, University of Defence in Belgrade, 33 Pavla Jurišića Šturma, Serbia,  
goran.dikic@mod.gov.rs, bojan.milanovic@va.mod.gov.rs, bondzulici@yahoo.com*

Pulsed thermography (PT) is non-destructive testing method based on the short thermal stimulation of a specimen surface and observation of its cooling process. Mainly due to thermal diffusion process, after heating by the pulse, the temperature of the material surface decreases rapidly. Thermal properties of the defects, which are similar to the sound material, introduce change of the temperature diffusion rate. Thus, the time dependence of the temperature distribution on a surface over defect is different in comparison with the surface with no subsurface defects. This difference is an indicator of the defect's presence. After detection of the defect, next goal is to find the parameter which provides determination of the depth of the defect. The aim of this paper is to determine the relation between standard thermal contrast and the depth of the subsurface defect for the different materials [1-5].

The experiments are performed on the specimens made of iron, brass and aluminum plate with the defects of the flat-bottom cylindrical holes shape. The diameters of the defects are 3 mm, 8 mm and 15 mm, with the different depths. The surface of the specimens was coated by the black mat paint and uniformly heated, using the flash lamp (BOWENS BW-3955), with the pulse energy of 1.5 kJ. Duration of the pulse was 2 ms and the distance from the lamp to the specimen was 0.5 m. The temperature distribution on the surface, during its self cooling process, was measured by the FLIR SC620 IR camera with a frame rate of 120 Hz [1, 3].

The standard temperature contrast of considered defects, regardless of the depth, is calculated from experimental data. The time of reaching the maximum temperature contrast (MTC) is different for each defect depth. Defects that are in the lower depth below the surface, gave the shorter time of reaching the MTC. The dependence of the defect depth on the time of reaching the MTC is linear. First derivative of the time distribution of the MTC can be used as a parameter for the quantitative assessment of the depth of the defect. For the purpose of numerical analysis of temperature distribution on the surface of the sample, 3D model was developed in GetDP [3]. The simulation results are verified by experimental results. Good correlation is achieved.

[1] Lj. Tomić, J. Elazar, NDT and E. Inter. 60 (2013) 132–135.

[2] S. Marinetti, V. Vavilov, Corros. Sci. 52 (2010) 865–872.

[3] G. Dikić, Lj. Tomić, V. Damnjanović, B. Milanović, Surf. Rev. and Lett. 22 2 (2015) 1550032–11.

[4] X.P.V. Maldague, Active Thermography, in: Nondestructive evaluation of materials by infrared thermography, ch. 9, sec. 9.2, New York, USA: John Wiley & Sons, 2001, pp. 347–348.

[5] Lj.D. Tomić, Nondestructive evaluation of the thermophysics properties materials by IR thermography, Ph.D. dissertation, School of Electrical Engineering, University of Belgrade, Belgrade, Serbia, 2013.

## SPECTROSCOPIC STUDY OF LUMINESCENT PROPERTIES OF Li-DOPED SCREEN-PRINTED ZnO FILMS

T.V. Zashivailo<sup>a</sup>, V.I. Kushnirenko<sup>b</sup>

<sup>a</sup>*National Technical University of Ukraine "KPI", 37 Pr. Pobedy, Kiev, Ukraine*

<sup>b</sup>*V. Lashkarev Institute of Semiconductor Physics, NASU, 45 Pr. Nauki, Kiev, Ukraine*

Zinc oxide (ZnO) attracts considerable attention for its possible application in optoelectronics. Lithium (Li) is considered as a promising dopant to obtain p-type ZnO because Li incorporation on the Zn-lattice site ( $\text{Li}_{\text{Zn}}$ ) is theoretically predicted to produce a shallow acceptor level. The aim of this work was to study the effect of Li doping on the luminescent properties of ZnO films.

The films of undoped and Li-doped ZnO were produced by a screen printing method on sapphire substrates. The ZnO paste was made from the ZnO powder mixed with distillate water or with  $\text{LiNO}_3$  aqueous solution. The concentration of Li in the films was about 0.003, 0.03 and 0.3 wt %. The films were annealed at  $T_S=800, 900$  and  $1000^\circ\text{C}$  for 30 min in air. The photoluminescence (PL) and PL excitation (PLE) spectra were studied at 77 and 300 K.

The PL spectra showed an excitonic UV band and a wide defect-related band peaked in the green-orange spectral range. In the undoped films, the increase of  $T_S$  up to  $1000^\circ\text{C}$  resulted in the tenfold increase in the intensity of excitonic PL band which can be ascribed to the improvement of crystalline quality of the films. The doping of ZnO with Li was found to induce following effects in the films: (i) an increase in concentration of acceptor-related defects; (ii) a change of the film crystallinity both in the bulk and at  $\text{ZnO}/\text{Al}_2\text{O}_3$  interface. The former effect was verified by an enhancement of Li-related PL band observed at about 580 nm and caused by a recombination in donor–acceptor pairs including the deep acceptor  $\text{Li}_{\text{Zn}}$ . For the latter effect, an improvement of crystalline quality of the ZnO:Li films was found at low sintering temperature ( $T_S=800^\circ\text{C}$ ). This was confirmed by a pronounced enhancement of the excitonic PL band accompanied by a specific transformation of PL excitation spectra of the defect-related band. These changes are ascribed to the effect of  $\text{LiNO}_3$  as a flux that lowers the melting point of the ceramic. Moreover, in the PL spectra of the film doped with Li of 0.3 wt % and recorded from the “back-side” of the films the excitonic PL band was found to be shifted to the UV spectral region and reached 330 nm for  $T_S=1000^\circ\text{C}$ . It is assumed that a strong diffusion of Al from the substrate into ZnO and a formation of solid solution with larger band gap energy occur.



## SPECTROSCOPIC PROPERTIES OF TRIVALENT SAMARIUM IONS IN BORATE GLASSES

Ihor I. Kindrat<sup>a</sup>, Bohdan V. Padlyak<sup>a,b</sup>

<sup>a</sup>*Division of Spectroscopy of Functional Materials, Institute of Physics, University of Zielona Góra, 4a Szafrana Str., Zielona Góra, Poland, igor.k.physics@gmail.com*

<sup>b</sup>*Sector of Spectroscopy, Vlokh Institute of Physical Optics, 23 Dragomanov Str., Lviv, Ukraine, bohdan@mail.lviv.ua*

Spectroscopic and luminescent properties of a series Sm-doped borate glasses as well as local structure of the Sm<sup>3+</sup> centers in these glasses are investigated using electron paramagnetic resonance (EPR), optical spectroscopy (absorption, photoluminescence, decay kinetics), Judd–Ofelt (J–O) analysis, and X-ray diffraction (XRD) techniques.

Borate glasses with Li<sub>2</sub>B<sub>4</sub>O<sub>7</sub>, LiKB<sub>4</sub>O<sub>7</sub>, CaB<sub>4</sub>O<sub>7</sub> and LiCaBO<sub>3</sub> compositions doped with Sm<sub>2</sub>O<sub>3</sub> in amounts of 0.5 and 1.0 mol. % have been obtained from the corresponding polycrystalline compounds in the air atmosphere using corundum crucibles and standard glass synthesis technology. The absence of discrete sharp peaks in the XRD patterns confirms the disordered glassy-like structure of the investigated glasses.

In all investigated Sm-doped glasses at low temperatures (4.2 ÷ 20 K) has been clearly observed broad EPR signal with  $g_{\text{eff}} \approx 9.7$ , related to the Sm<sup>3+</sup> isolated centers. At low and room temperatures in all investigated glasses also is observed additional broad EPR signals with  $g_{\text{eff}} \approx 2.1 \div 2.2$ , which belong to the Sm<sup>3+</sup> – Sm<sup>3+</sup> pair centers, coupled by magnetic dipolar and exchange interactions.

Optical absorption spectra of the Sm-doped glasses consist of intense broad band (fundamental absorption edge of the glass host), several weak bands in the visible spectral range, and several intense bands in the infrared spectral range. The J–O intensity parameters ( $\Omega_2$ ,  $\Omega_4$ ,  $\Omega_6$ ) have been calculated using the spectral intensities of the observed absorption bands and least-square approximation.

The photoluminescence spectra registered under excitation with  $\lambda_{\text{exc}} = 402 \text{ nm}$  (<sup>6</sup>H<sub>5/2</sub> → <sup>6</sup>P<sub>3/2</sub> absorption transition) are closely similar and contain 3 characteristic emission bands peaked at 562, 598, and 645 nm, which correspond to the <sup>4</sup>G<sub>5/2</sub> → <sup>6</sup>H<sub>5/2</sub>, <sup>6</sup>H<sub>7/2</sub>, <sup>6</sup>H<sub>9/2</sub> transitions of the Sm<sup>3+</sup> ions. The radiative properties such as transition probabilities, branching ratios, stimulated emission cross-sections, radiative lifetimes, and quantum efficiencies are estimated for observed emission transitions of the Sm<sup>3+</sup> ions and compared with corresponding values for other Sm-doped glasses.

Luminescence kinetics of the Sm<sup>3+</sup> centers for <sup>4</sup>G<sub>5/2</sub> → <sup>6</sup>H<sub>7/2</sub> transition is satisfactory described by a single exponent decay curves. Obtained lifetimes lie in the 2.13 ÷ 2.78 ms region and depend on both, the basic glass composition due to some differences in the local structure of Sm<sup>3+</sup> centres and Sm concentration due to cross-relaxation processes between the Sm<sup>3+</sup> – Sm<sup>3+</sup> pair centers.

Peculiarities of local structure of the Sm<sup>3+</sup> centers in the network of investigated glasses have been discussed being based on obtained spectroscopic results and XRD structural data.

## SPECTROSCOPIC PROPERTIES OF Lu<sub>2</sub>O<sub>3</sub>:Pr,Ti

Paulina Bolek<sup>a</sup>, Aneta Wiatrowska<sup>b</sup>, Dagmara Kulesza<sup>a</sup> Eugeniusz Zych<sup>a</sup>

<sup>a</sup>Faculty of Chemistry, University of Wrocław,

14. F. Joliot-Curie Street, 50-383 Wrocław, Poland, eugeniusz.zych@chem.uni.wroc.pl

<sup>b</sup> Philips Research, Materials Technology Department,

High Tech Campus 4, 5656 AE Eindhoven, The Netherlands,

Last years we have presented some Lu<sub>2</sub>O<sub>3</sub>-based ceramic storage phosphors and their properties [1,2]. Recently, we discovered a new member of this family, Lu<sub>2</sub>O<sub>3</sub>:Pr,Ti, which was received upon sintering at 1700°C for 5 hours in reducing (preferentially) atmosphere of forming gas (25% H<sub>2</sub> +75%N<sub>2</sub>). In this presentation we will discuss basic spectroscopic properties of the Lu<sub>2</sub>O<sub>3</sub>:Pr,Ti ceramic storage phosphors.

The glow curve of the Lu<sub>2</sub>O<sub>3</sub>:Pr,Ti storage phosphor contains one slightly structured band peaking at 350 °C (5 °C/s heating rate) as seen in Fig. 1a. We found that during irradiation with X-rays or high-energy UV rays a new broad absorption band is generated around 400 nm (Fig. 1b). This band is also well exposed in excitation spectrum of the red Pr<sup>3+</sup> luminescence of the irradiated material, see Fig. 1c. Yet, a prolonged stimulation into this band bleaches it out and both the absorption and excitation spectra revert to their original traces (see Figs. 1b,c). These and other results will be presented in detail and discussed. This may be done repeatedly with the same effect. First approach of linking various experimental results with the possible mechanisms of energy storing and releasing will be presented.

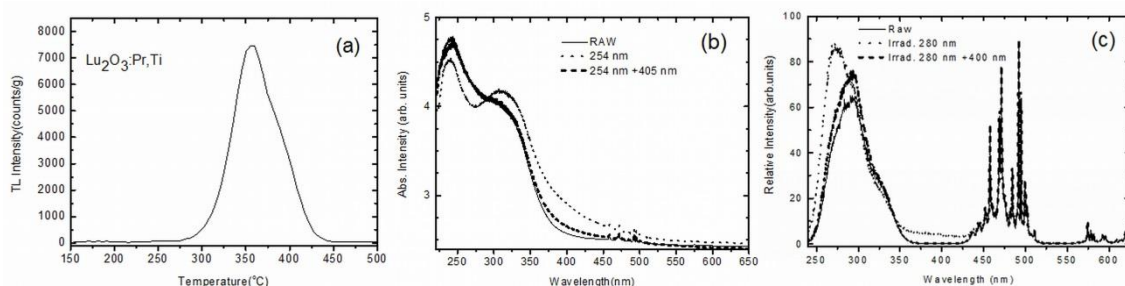


Fig. 1. Glow curve of Lu<sub>2</sub>O<sub>3</sub>:Pr,Ti (a), absorption spectra of raw, UV-irradiated and UV+405 nm irradiated Lu<sub>2</sub>O<sub>3</sub>:Pr,Ti ceramics (b), and excitation spectra of raw, UV irradiated, and UV+405 nm irradiated Lu<sub>2</sub>O<sub>3</sub>:Pr,Ti ceramics (c).

### Acknowledgement

The work was supported by Wrocław Research Centre EIT+ within the project "The Application of Nanotechnology in Advanced Materials" - NanoMat (POIG.01.01.02-02-002/08) co-financed by the European Regional Development Fund (Innovative Economy Operational Program 1.1.2).

[1] A. Wiatrowska, E. Zych, *J. Phys. Chem. C* 117 (2013) 11449–11458.

[2] D. Kulesza, E. Zych, *J. Phys. Chem. C* 117 (2013) 26921–26928.

## THE OPTICAL SPECTRUM OF TERNARY ALLOY $\text{BBi}_{1-x}\text{As}_x$

Battal G. Yalcin<sup>1</sup>, M. Aslan<sup>1</sup>, M. H. Ozcan<sup>1</sup>, H. A. Rahnamaye Aliabad<sup>2</sup>

<sup>1</sup>*Sakarya University, Art and Science Faculty, Department of Physics 54187 Sakarya, Turkey*

<sup>2</sup>*Hakim Sabzevari University, Department of Physics, Sabzevar, Iran*

Among the III-V semiconductors the boron: BBi and BAs as well as their alloys have attracted both scientific and technological interest in recent years. We present a calculation of the structural, electronic and optical properties of ternary alloy  $\text{BBi}_{1-x}\text{As}_x$  by means of wien2k software package [1]. The exchange-correlation potential is treated by generalized gradient approximation (GGA) within the schema of Wu and Cohen [2]. Also, we have used modified Becke-Johnson (mBJ) formalism [3] to improve the band gap results. All the calculations have been performed after geometry optimization. In this study, we have investigated structural properties such as lattice constant ( $a_0$ ), bulk modulus ( $B_0$ ) and its pressure derivative ( $B'$ ) and calculated the electronic band structures of studied materials. Accurate calculation of linear optical properties such as real ( $\epsilon_1$ ) and imaginary ( $\epsilon_2$ ) dielectric functions, refractive index ( $n$ ), extinct coefficient ( $\kappa$ ), absorption coefficient ( $\alpha$ ), reflectivity ( $R$ ), loss function ( $L$ ) and optical conductivity ( $\sigma$ ) are investigated. Our obtained results for studied binary compounds, BBi and BAs, fairly coincide with other theoretical calculations and experimental measurements. According to the best of our knowledge, no experimental or theoretical data are presently available for the studied ternary alloy  $\text{BBi}_{1-x}\text{As}_x$  ( $0 < x < 1$ ). The role of electronic band structure calculation as regards the linear optical properties of  $\text{BBi}_{1-x}\text{As}_x$  is discussed. The effect of the spin-orbit interaction (SOI) on the structural and optical properties is also investigated and found to be quite small.

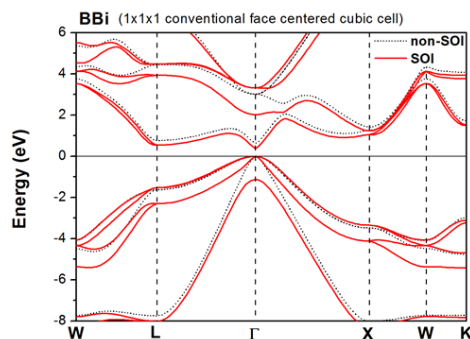


Figure 1. Calculated electronic band structure of BBi compound within mBJ calculation.

[1] P. Blaha, K. Schwarz, G. K. H. Madsen, D. Kvasnicka, and J. Luitz, WIEN2K: An Augmented Plane Wave Plus Local Orbitals Program for Calculating Crystal Properties, edited by K. Schwarz, Vienna University of Technology, Austria, 2001.

[2] Z. Wu, R. E. Cohen, Phys. Rev. B 73 (2006) 235116.

[3] F. Tran, P. Blaha, Phys. Rev. Lett. 102 (2009) 226401.

## SPECTRAL-LUMINESCENCE PROPERTIES OF $\text{ZrO}_2\text{-Y}_2\text{O}_3\text{-Er}_2\text{O}_3$ CRYSTALS

Natalya V. Sidorova<sup>a</sup>, Elena E. Lomonova<sup>b</sup>, Andrey A. Lyapin<sup>a</sup>, Alexey N. Chabushkin<sup>a</sup>,  
Polina A. Ryabochkina<sup>a</sup>

<sup>a</sup>*N.P. Ogarev Mordovian State University, 68 Bolshevistskaya. Str., Saransk, Russia,  
ya.natalka2112@yandex.ru*

<sup>b</sup>*Prokhorov General Physics Institute, Russian Academy of Sciences, 38 Vavilova Str.,  
Moscow, Russia, lomonova@lst.gpi.ru*

Laser emission in the 1.5 – 1.7  $\mu\text{m}$  is of interest for various applications in medicine, lidars, etc.). 1.5-micron laser radiation can be obtained on matrix doped  $\text{Er}^{3+}$  ions on the transition  ${}^4\text{I}_{13/2} \rightarrow {}^4\text{I}_{15/2}$  under selective laser pumping of  ${}^4\text{I}_{13/2}$  level. Er-doped yttria-stabilised zirconia (YSZ) crystals are possible candidates for solid-state laser emitting in 1.5-1.7  $\mu\text{m}$  spectral region [1].

The aim of the present paper is to investigate the spectral-luminescence properties of YSZ:Er for laser application. The absorption and luminescence spectra of the  $\text{ZrO}_2\text{-13.4mol\%Y}_2\text{O}_3\text{-0.6mol\%Er}_2\text{O}_3$  crystal have been measured. We have estimated the shape of the gain band for laser transition  ${}^4\text{I}_{13/2} \rightarrow {}^4\text{I}_{15/2}$  at different relative population inversion parameters. The gain band of the crystal extends from 1620 to 1700 nm for  $P=0.07$ .

The upconversion luminescence in the visible and near IR regions of  $\text{Er}^{3+}$  ions in YSZ:Er was observed upon excitation of  ${}^4\text{I}_{13/2}$  level. Fig. 1 shows luminescence spectra of  $\text{Er}^{3+}$  ions upon excitation of  ${}^4\text{I}_{13/2}$  level by 1.5-micron laser. Anti-stokes luminescence depopulates of the upper laser level and reduces the inversion population of  ${}^4\text{I}_{13/2}$  level. Therefore, mechanisms responsible for upconversion luminescence of  $\text{Er}^{3+}$  ions were also investigated. Luminescence rise and decay from  ${}^4\text{S}_{3/2}$  and  ${}^4\text{F}_{9/2}$  levels of  $\text{Er}^{3+}$  ions upon excitation of  ${}^4\text{I}_{13/2}$  level was recorded.

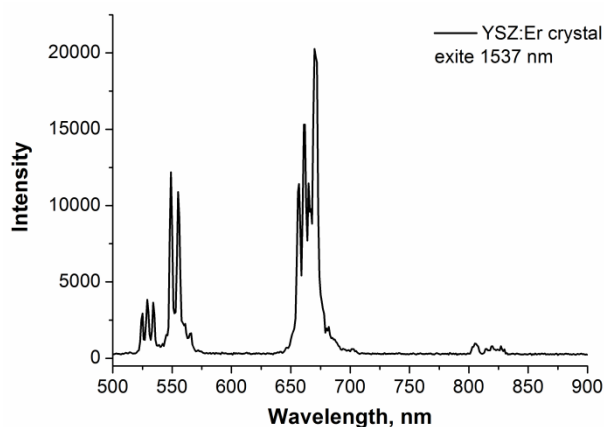


Fig. 1. Upconversion luminescence of  $\text{Er}^{3+}$  ions doped YSZ crystal.

This work were supported by The Ministry of Education and Science of the Russian Federation State Order for Research (Project No. 3.384.2014/K and Project No. 07080210059611) and Russian Foundation for Basic Research of (projects № 13-02-051).

[1] P.A. Ryabochkina, N.V. Sidorova, E.E. Lomonova, Quantum Electronics 44 (2014) 135 – 137.

## SIMULATION AND NUMERICAL ANALYSIS OF HIGHLY BIREFRINGENT PHOTONIC CRYSTAL FIBER TEMPERATURE SENSOR

R.Boufenar<sup>a, b</sup>, M. Bouamar<sup>a</sup>, A.Hocini<sup>a</sup>

<sup>a</sup>Laboratory analysis of signals and systems Department of Electronics, Mohamed Boudiaf University BP.166, road Ichebilia, M'sila 28000 Algeria, Rabouf@yahoo.fr

<sup>b</sup>Nuclear research center, BP 180 Ain Oussera/Djelfa 17000/Algeria.

Photonic crystal fibers (PCFs) [1] are a class of optical fibers constituting wavelength-scale microstructure running along fiber length. They possess a number of novel properties and significant applications owing to novel guiding mechanisms and flexible design. Among the properties, there have been more interests to explore birefringence property, by use of an asymmetric cladding or core structure.

PCFs with high birefringence [2] are of significant research interest as they could be widely used in fiber sensors [3].

In this paper, we propose a high sensitivity temperature sensor, where the fiber includes a solid silica core and a cladding with square lattice elliptical air holes infiltrated with ethanol along the fiber length (Fig.1).

Thermo-optical response of the design is theoretically investigated by Full-Vectorial Finite element Method with anisotropic perfectly matched layers (PMLs) [4, 5].

The temperature impact on the fiber birefringence were numerically analyzed using FEM based software. Results shows a linear dependence between the PCF birefringence and the temperature (Fig.2). The sensitivity can easily reach  $10^{-5}$  order of magnitude by Celsius degree. In comparison with other temperature sensor based on birefringent Photonic crystal Fiber, our designed sensor has higher sensitivity.

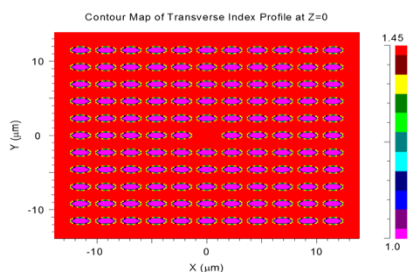


Fig.1 Contour map of transverse index profile

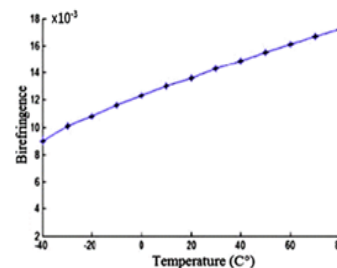


Fig.2 PCF birefringence versus temperature

[1] J.C. Knight, Photonic crystal fibres, Nature 424 (2003) 847.

[2] A. Ortigosa-Blanch, J.C. Knight, W.J. Wadsworth, J. Arriaga, B.J. Mangan, T.A.Birks, P.S.J. Russell, Highly birefringent photonic crystal fibers, Opt. Lett. 25(2000) 1325.

[3] Yongjin Hu, Jingyuan Wang and Ke Wen, "Temperature Sensor Based on Birefringent Properties of Photonic Crystal Fiber", Journal of Military Communications Technology, 29(2): 35-37(2008).

[4] K. Saitoh, M. Koshiba, Full-vectorial imaginary-distance beam propagation method based on a finite element scheme: application to photonic crystal fibers, IEEE J. Quantum Electron. 38 (2002) 927.

[5] S. Selleri, L. Vincetti, A. Cucinotta, M. Zoboli, Complex FEM modal solver of optical waveguides with PML boundary conditions, Opt. Quant. Electron. 33 (2001) 359–371.

## SCINTILLATION PROPERTIES OF Eu-DOPED CsCl AND CsBr CRYSTALS

Keiichiro Saeki<sup>a</sup>, Masanori Koshimizu<sup>a</sup>, Takayuki Yanagida<sup>b</sup>, Yutaka Fujimoto<sup>a</sup>,  
Takuma Yahaba<sup>a</sup>, Hironori Tanaka<sup>a</sup>, Keisuke Asai<sup>a</sup>

<sup>a</sup>Tohoku University, 6-6-07, Aoba, Aramaki, Aoba-ku, Sendai, Japan, saeki@dc.tohoku.ac.jp

<sup>b</sup>Nara Institute of Science and Technology, 8916-5, Takayama, Ikoma, Japan,  
t-yanagida@ms.naist.jp

A scintillation detector is composed of a scintillator, which converts absorbed ionizing radiation into multiple low-energy (~eV) photons, and a photomultiplier tube (PMT), which can detect the photons as an electrical signal. The characteristics of the scintillator play an important role in the performance of the radiation detector. The recently discovered Eu<sup>2+</sup>-doped halide-based scintillators have been reported to display excellent properties caused by the 4f<sup>6</sup>5d–4f<sup>7</sup> (<sup>8</sup>S<sub>7/2</sub>) transitions of Eu<sup>2+</sup> [1]. We therefore focused on Eu<sup>2+</sup>-doped CsCl and CsBr crystals in this investigation; to the best of our knowledge, there have been no previous reports of the scintillation properties of these crystals. In this article, the scintillation properties, including X-ray excited radioluminescence, decay time profiles, and <sup>137</sup>Cs-gamma-ray pulse height spectra of the Eu<sup>2+</sup>-doped crystals are reported.

CsCl:Eu (1 mol%) and CsBr:Eu (1 mol%) crystals were prepared using the Bridgman–Stockbarger method and grown under a vacuum in sealed quartz tubes. After the crystals had been cut and polished, their <sup>137</sup>Cs-gamma-ray (662 keV) irradiated pulse-height spectra, X-ray excited radioluminescence (XRL) spectra, and scintillation decay curves were investigated.

Figure 1 presents the <sup>137</sup>Cs-gamma-ray irradiated pulse-height spectra for the two compounds. We cannot clearly observe the peaks for these crystals. For this reason, we consider channels 70 and 280 to be the locations of the CsCl:Eu and CsBr:Eu peaks, respectively. We estimate the luminescence to be 600 photons/MeV for CsCl:Eu and 6100 photons/MeV for CsBr:Eu. For the CsBr:Eu crystal, the luminescence is three-fifths of that of a GSO crystal. The XRL spectra are shown in Fig. 2. The CsCl:Eu crystal showed emission bands at 250–280 nm and 450 nm, while, a broad emission band at 435 nm was observed for CsBr:Eu. The emission bands at 450 nm for CsCl:Eu and at 435 nm for CsBr:Eu can be attributed to the Eu<sup>2+</sup> 5d–4f transition. We additionally measured the scintillation decay time profiles for the two crystals. As a result of fitting these profiles, the decay time constants were found to be about 0.38 μs for CsCl:Eu and 0.58 μs for CsBr:Eu, both of which may be attributed to the Eu<sup>2+</sup> 4f<sup>6</sup>5d–4f<sup>7</sup> transitions.

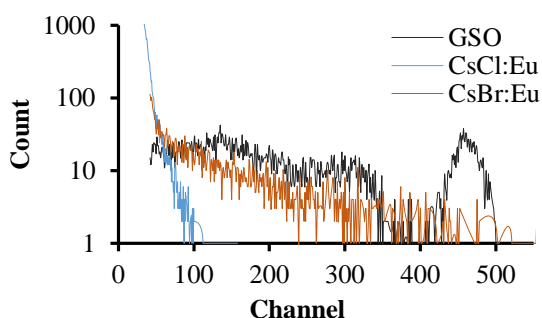


Fig. 1 <sup>137</sup>Cs-gamma-ray (662 keV) irradiated pulse height spectra.

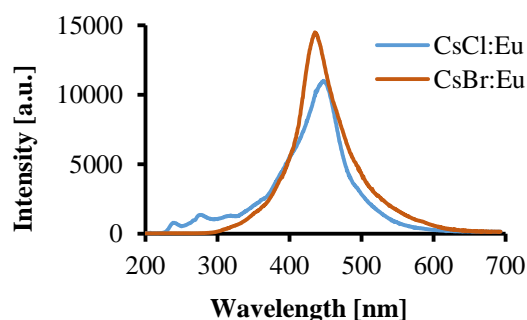


Fig. 2 XRL spectra.

[1] T. Yanagida, N. Kawaguchi, Y. Fujimoto, K. Fukuda, Y. Yokota, A. Yamazaki, K. Watanabe, J. Pejchal, A. Uritani, T. Iguchi, A. Yoshikawa, Opt. Mater. 33 (2011) 1243–1247.

## ROOM TEMPERATURE TIME-RESOLVED LUMINESCENCE OF OXYGEN-VACANCY DEFECT IN ZnO NANOSTRUCTURES SYNTHESIZED BY HYDROTHERMAL ROUTE

Widad Bekhti<sup>a,b</sup>, Mostefa Ghamnia<sup>a</sup>, Lakhdar Guerbous<sup>c</sup>

<sup>a</sup>*Laboratoire des Sciences de la Matière Condensée, Département de physique, Faculté des Sciences, Université d'Oran Es-Sénia, BP 1620 El-Ménaouer, 3100 Oran, Algeria.*

<sup>b</sup>*Département de Physique, Université de Blida 1 Saad-Dahleb, Route de soumaa BP 270 Blida, Algeria.*

<sup>c</sup>*Département Laser, DTN-C.R.N.A 02, Bd Frantz Fanon, BP 399, Algiers 16000, Algeria.*

ZnO is one of the most promising semiconductors due to its intrinsic properties that are enhanced at the nanoscale. In particular, one can cite the wide direct band-gap (3.37 eV), the large exciton binding energy (60 meV) at room temperature and an excellent chemical and thermal stability. Moreover, it is a versatile smart material with unique applications in sensors, photovoltaic, surface acoustic wave devices, light emitting diodes and luminescent devices, transparent conductive coatings and others [1-4]. Furthermore, the study of light emission phenomena in ZnO nanomaterial has gained a great interest during the last decade. Particularly, the origin and nature of the visible luminescence in ZnO (so called “green-yellow” emission) which are still under discussion.

Different methods are used to synthesize ZnO nanostructures such as conventional vapor-phase methods or organic solvents routes. In the present work, we describe the hydrothermal synthesis of different shaped ZnO nano/microrods. The impact of type and concentration of cations presents in solutions on the morphology and optical properties of the obtained rods will also be presented and discussed. In addition, more attention is focused on the study and investigation of time resolve photoluminescence of oxygen-vacancy defect in the green region.

[1] Z.W. Pan, Z.R. Dai, Z.L. Wang, Science 291 (2001) 1947.

[2] N. Saito, H. Haneda, T. Sekiguchi, N. Ohashi, I. Sakaguchi, K. Koumoto, Adv.Mater. 14 (2002) 418.

[3] J. Zhou, P. Fei, Y. Gao, Y. Gu, J. Liu, G. Bao, Z. L. Wang, Nano Lett. 8 (2008) 2725.

[4] C. Klingshirna, J. Fallerta, O. Gogolinb, M. Wissingera, R. Hauschilda, M. Hausera, H. Kalta, H. Zhoua, J. Lumin. 128 (2008) 792

**RELATIONSHIP BETWEEN STRUCTURE AND LUMINESCENCE  
PROPERTIES IN Ce<sup>3+</sup> OR Ce<sup>3+</sup>, Mn<sup>2+</sup>-DOPED GARNET PHOSPHORS  
FOR USE IN WHITE LEDS**

Damian Pasiński, Eugeniusz Zych, Jerzy Sokolnicki

*Faculty of Chemistry, University of Wrocław, 14 F. Joliot-Curie Street, 50-383 Wrocław,  
jerzy.sokolnicki@chem.uni.wroc.pl*

A series of Ce<sup>3+</sup> or Ce<sup>3+</sup> and Mn<sup>2+</sup> doped garnets of the general formula A<sub>3</sub>B<sub>2</sub>X<sub>3</sub>O<sub>12</sub> (A=Sr, Ca; B=Sc, Y; X=Si, Ge) was obtained using a high temperature solid state reaction. These compounds were characterized by X-ray diffraction and photoluminescence spectroscopy. The relation between luminescence properties of phosphors and their host lattice composition was studied. It was found that Ce<sup>3+</sup> ions occupied the A site and emitted in the green spectral region. Mn<sup>2+</sup> ions can exchange cations in both A and B site showing green and red emission, respectively and getting excited due to an energy transfer from Ce<sup>3+</sup>. This study showed the relationship between Ce<sup>3+</sup> and Mn<sup>2+</sup> emission/excitation wavelengths and the symmetry around the activator ions expressed by means of the distortion factor of the dodecahedral A site ( $d_{88}/d_{81}$ ). Decay times of the Ce<sup>3+</sup> and Mn<sup>2+</sup> luminescence were measured and correlated with the compositional dependent structural changes.



## REFRACTIVE INDEX SENSING USING TAPERED MICROCAVITIES PHOTONIC-CRYSTAL

Ahlam Harhouz, Abdesselam Hocini

*Laboratoire d'Analyse des Signaux et Systèmes BP.166, Route Ichebilia, Université  
Mohamed Boudiaf de M'sila, M'sila 28000, Algeria, hocini74@yahoo.fr,  
harhouz7ahlam@gmail.com*

In this work, we design new Infiltrated liquid sensor based on a 2D photonic crystal waveguide incorporating with microcavity to sense small refractive index changes. The refractive index (RI) sensor is formed by a point-defect resonant cavity in the sandwiched waveguide with triangular lattice of air holes (index profile of silicon slab  $n_{\text{si}}=3.42$  and air  $n_{\text{air}}=1$ ). The properties of the sensor are simulated using the finite-difference time-domain (FDTD) algorithm and the plane wave expansion (PWE) method (RSoft Photonic Suite). Sensors based on photonic crystal (PhC) waveguides incorporating with microcavities have many advantages in compactness, high sensitivity and quality (Q) factor, easy extension to sensor arrays and various choices of materials, and capability of parallel measurement [1-4]. On the other hand, a tapered-shift structure along the line defect increased quality factor of microcavity [5]. So, the proposed RI sensor is formed with two waveguide couplers and microcavity in the PhC with a triangular lattice of air holes which is shown in Fig.1. The microcavity is formed by change of the size of 14 air holes in the centre of the of the line defect. The hole's radius are:  $r_A=200\text{nm}$ ,  $r_B=180\text{nm}$ . The sensing principle is based on the shift of resonance wavelength  $\lambda_0$ , which occurs due to the change in RI of the sensor when the PhC's air holes are full of homogenous liquid. Several liquids with refractive indices ranging from 1 (the air) to 1.4 (Fig.2) were studied and showed that the best sensitivity of 475 nm/RIU and limit of detection of 0.01 RIU can be achieved (Fig.3). The varied resonance wavelength as a first degree polynomial function of refractive index was observed. The sensor is appropriate for detecting homogeneous medium.

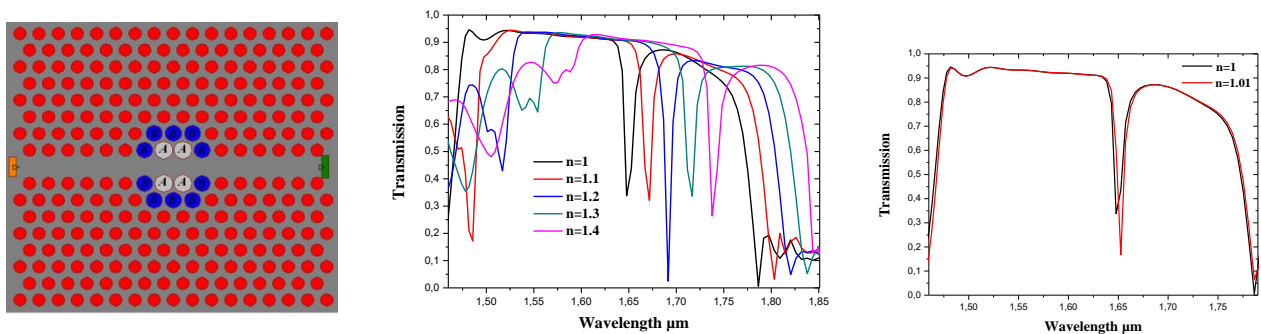


Fig.1 The proposed RI sensor. Fig.2 Calculated transmission spectra for TM polarization of the RI sensor

Fig.3 transmission spectra for TM polarization for  $n=1$  and  $n=1.01$

- [1] S. Mandal, D. Erickson, "Nanoscale optofluidic sensor arrays", *Optics. Ex*, pp.1623-1631, 2008;
- [2] L. Huang, H. Tian, D. Yang, J. Zhou, Q. Liu, P. Zhang, Y. Ji, "Optimization of figure of merit in label-free biochemical sensors by designing a ring defect coupled resonator", *Opt. Commun*, pp. 42-49, 2014.
- [3] L. Huang, H. Tian, D. Yang, J. Zhou, Q. Liu, P. Zhang, Y. Ji, "Label-free optical sensor by designing a high-Q photonic crystal ring-slot structure", *Opt. Commun*, pp.73-77, 2015.
- [4] J. Zhou, H. Tian, D. Yang, Q. Liu, Y. Ji, "Integration of high transmittance photonic crystal H2 nanocavity and broadband W1 waveguide for biosensing applications based on Silicon-on-Insulator substrate", *Opt. Commun*, pp.175-183, 2014.
- [5] E. Kuramochi, M. Notomi, S. Mitsugi, A. Shinya, T. Tanabe, and T. Watanabe, "Ultrahigh-Q photonic crystal nanocavities realized by the local width modulation of a line defect," *Appl. Phys. Lett.* 88, 041112, 2006.

## RED-TO-GREEN PHOTON UPCONVERTING MICROCRYSTALS FOR TEMPERATURE SENSING

Gary Degliame<sup>a</sup>, Nathalie Trannoy<sup>a</sup>, Jean-Pierre Jouart<sup>a</sup>, Madjid Diaf<sup>b</sup>

<sup>a</sup> Research Group for Engineer Science, University of Reims Champagne-Ardenne, Reims, France, gary.degliame@univ-reims.fr

<sup>b</sup> Laboratory of Lasers Physics, Optical Spectroscopy and Opto-Electronic, Badji Mokhtar-Annaba University, Annaba, Algeria

The intensities of emission lines from thermally coupled energy levels of lanthanide ions doped into host crystals are temperature interdependent and therefore usable in luminescence thermometry [1-3]. This communication reports on the temperature behavior of erbium-doped fluorite-type microcrystals ( $\text{CaF}_2:\text{Er}^{3+}$ ,  $\text{Cd}_x\text{Sr}_{1-x}\text{F}_2:\text{Er}^{3+}$ ) individually glued at the tip of a Joule-heated thermo-resistive probe and excited with a low power red laser (fig.1). Microcrystals of various sizes were selected with a view to their use as temperature sensors for scanning thermal microscopy. The Fluorescence Intensity Ratio method using the green upconversion luminescence from thermally coupled energy levels of  $\text{Er}^{3+}$  ions [4] was applied to appraise the microcrystal's temperature as a function of the electrical current intensity going through the thermo-resistive probe.

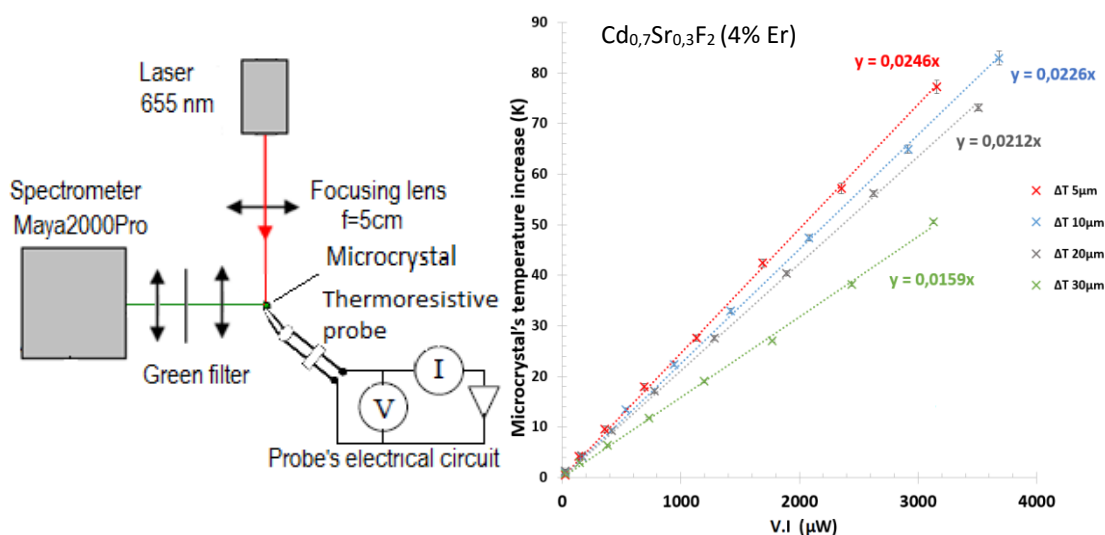


Figure 1: Experimental Set-Up

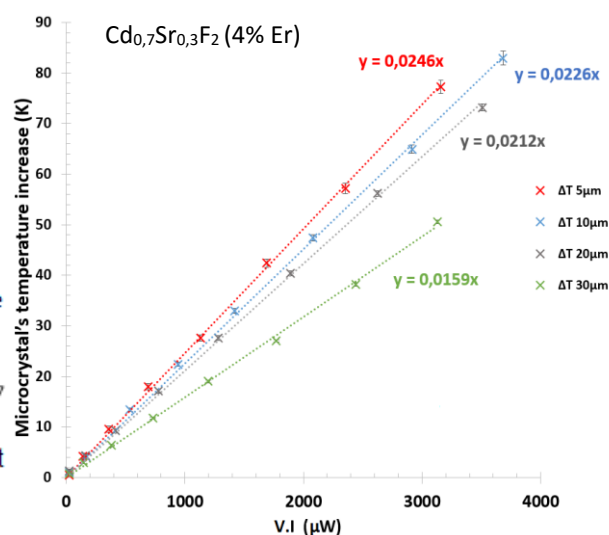


Figure 2: Temperature increase (for various sizes of microcrystals) versus the electrical power ( $P = V.I$ )

We checked that the microcrystal's temperature increased quadratically with the electrical current intensity and that the temperature appraised by this method was dependent on the microcrystal's size (fig.2). The causes of such dependence will be discussed.

[1] L. Aigouy, J. Lesueur, N. Bergeal, and M. Mortier, Appl. Phys. Lett. 101 (2012) 123113

[2] D. Jaque and F. Vetrone, Nanoscale 4 (2012) 4301-4326

[3] L. H. Fischer, G. S. Harms and O. S. Wolfbeis, Angew. Chem. Int. Ed. 50 (2011) 4546-4551

[4] N. Trannoy, A. Sayoud, M. Diaf, T. Duvaut, J.P. Jouart and P. Grossel, Optical Materials 42 (2015) 526-531

## OPTICAL CHARACTERIZATION OF RADIATION-INDUCED STRUCTURAL TRANSFORMATIONS IN CHALCOGENIDE SEMICONDUCTOR GLASSES

Oleh I. Shpotyuk<sup>a,b</sup>, Mykhaylo V. Shpotyuk<sup>c</sup>, Sergii B. Ubizskii<sup>c</sup>

<sup>a</sup>*Vlokh Institute of Physical Optics, 23 Dragomanov str., Lviv, Ukraine,  
olehshpotyuk@yahoo.com*

<sup>b</sup>*Jan Dlugosz University of Czestochowa, 13/15 al. Armii Krajowej, Czestochowa, Poland*

<sup>c</sup>*Lviv Polytechnic National University, 12 Bandera str., Lviv, Ukraine,  
shpotyukmy@yahoo.com*

Radiation-induced metastability in chalcogenide semiconductor glasses (ChSG) deals with specific defective states caused by destruction of existing bond arrangement following structural relaxation towards state with new distribution of covalent chemical bonds. The covalent bonds destructed by high-energy gamma-irradiation can be renewed *intrinsically* via direct interaction of bond-constituting atoms with nearest neighbors forming a channel for *own (intrinsic) bond switching*, or *extrinsically* due to interaction with impurity chemical environment. In the first case, the diamagnetic pairs of over- and under-coordinated atoms possessing an excess of positive and negative electric charge (*charged defects*), respectively, appear in a glassy backbone. In the latter case, some kinds of impurity products can be formed preferentially at the surface of ChSG, the most essential being induced by interaction with absorbed oxygen, which replace chalcogen in its bonding within glassy network. Thus, *the intrinsic radiation-induced effects* occur to be permanently admixed with *extrinsic impurity-related* ones, forming a complicated picture of competitive relaxation input in the overall balance of radiation-induced physical effects, where these channels cannot be well separated. Under such condition, the methodological route allowing unbiased observation of these channels has attained a vital importance, especially from viewpoint of practical implementation of induced functionality in a variety of ChSG systems. In this work, we shall present an adequate methodological solution of this problem exemplified by high-dose gamma-induced effects in glassy g-As<sub>2</sub>S<sub>3</sub>.

Two types of experimental measuring protocols was utilized to study gamma-induced optical effects in g-As<sub>2</sub>S<sub>3</sub>, these being realized in *direct* and *backward measuring chronology*. In the former, the optical transmission spectra in the visible region were recorded *ex-situ* for the same glass sample taken in non-irradiated (just before irradiation) and gamma-irradiated (one month after irradiation) states. The second type of optical measurements was performed *in-situ*, recording optical transmission spectra for the same gamma-irradiated and further annealed sample. The smallest inaccuracies were shown to be provided within the latter measuring protocol owing to elimination of measuring errors associated with (1) sample reinstallation in the spectrometer chamber and (2) time separation between subsequent cycles of optical spectra recording for initial unirradiated and gamma-irradiated samples. As a result, the impacts of impurity-related and intrinsic  $\gamma$ -induced effects on the optical transmission spectra can be reasonably separated. It is shown that impurity-related radiation processes (connected mainly with surface oxidation) depress optical transmission in near-band-gap region, while intrinsic ones (realized as defect formation) shift optical absorption edge towards larger wavelengths.

## NEW METHODS FOR STUDYING EXTREMELY LONG LASTING LUMINESCENCE PHENOMENA IN OSL DETECTORS

Arkadiusz Mandowski<sup>a</sup>, Ewa Mandowska<sup>a</sup>, Magdalena Biernacka<sup>a</sup>, Renata Majgier<sup>a</sup>,  
<sup>a</sup>*Jan Dlugosz University, Institute of Physics, Armii Krajowej 13/15, Czestochowa, Poland,*  
*a.mandowski@ajd.czyst.pl*

Optically stimulated luminescence (OSL) and thermoluminescence (TL) are two-stage luminescence phenomena [1]. First, the material has to be irradiated. The metastable excited states may last even for many years. Luminescence is triggered by optical stimulation (OSL) or heating (TL). Many materials exhibit both TL and OSL properties. In OSL the light emission is observed at shorter wavelengths than the stimulation wavelength. In general, the total concentration and distribution of charge carriers in trap levels corresponds to the absorbed dose of ionizing radiation. Nevertheless, these two parameters (distribution and concentration) are not always constant. Some OSL and TL materials exhibit undesirable fading, i.e. loss of the signal during longer period of time. The effect may relate e.g. to non-radiative tunneling or thermally activated transitions. These long lasting luminescence phenomena are usually very slow and consequently difficult to study.

This paper presents mathematical background and preliminary experimental results of the two methods: variable delay OSL (VD-OSL) and OSL-probe method. These methods allow to study luminescence properties of the studied material in a time scale of many days or weeks.

The most typical mode of OSL measurement is continuous wave OSL (CW-OSL). In this mode the sample is stimulated for several seconds to record the decay curve until all trapped charge carriers are released. The VD-OSL method consists of many steps including: - OSL signal zeroing by optical bleaching; - excitation of the sample by ionizing radiation with a defined dose; - repeating short CW-OSL measurements for a fixed time delay between readouts. Then the procedure is repeated for a different time delay. Finally, the series of readouts for particular time delay are normalized to the first readout. Then, relative OSL readouts are plotted vs. time delay or the total time from the beginning of the experiment [2]. Similarly the OSL-probe is performed as a series of very short pulsed OSL readouts during very long time period. Interesting correlations between VD-OSL and the OSL-probe methods are discussed based on current theoretical models for localized and delocalized transitions [3].

Both methods were implemented in custom made HELIOS-3 OSL reader [4]. Its software allows for full control of the stimulation time period and time intervals between pulses. The luminescence could be measured during and after the pulse stimulation. Typical measurement time ranges from several hours to several weeks.

**Acknowledgements.** This work was partially supported by research project PBS1/A9/4/2012 from the National Centre for Research and Development

[1] E. G. Yukihara, S. W. S. McKeever, „Optically stimulated luminescence fundamentals and applications”, Wiley, 2011.

[2] A. Mandowski, M. Biernacka, *Radiat. Meas.* 71 (2014) 265-269.

[3] A. Mandowski, A., *J. Phys. D: Appl. Phys.*, 38 (2005) 17-21

[4] A. Mandowski, E. Mandowska, L. Kokot, P. Bilski, P. Olko, B. Marczewska, *Elektronika*, 51 (2012) 136-138.

## NANOSCALE CHARACTERISATION OF OPTICAL MATERIALS BY MAPPING OF LOCAL REFRACTIVE INDEX VALUES AS MEASURED WITH SINGLE-MOLECULE SPECTROMICROSCOPY

Tatiana A. Anikushina<sup>a,b</sup>, Maxim G. Gladush<sup>a</sup>, Aleksei A. Gorshelev<sup>a</sup>, Andrei V. Naumov<sup>a,b</sup>

<sup>a</sup>*Institute for Spectroscopy of Russian Academy of Sciences, 5 Fizicheskaya Str., Troitsk, Moscow, Russia, naumov@isan.troitsk.ru*

<sup>b</sup>*Moscow State Pedagogical University, 1/1 M. Pirogovskaya Str, Moscow, Russia  
anikushina@list.ru*

One of the most important characteristics of a material that determines many of its macroscopic properties and is included as a parameter in many classical equations (Fresnel's, Maxwell's, etc.) is the refractive index  $n$ . In view of the growing interest to nanophotonics, it is important to know whether there is a relation between  $n$  and micro- and nanoscopic structure of solids. In order to give the answer to this question some special instruments for probing the local  $n$  values on the sub-diffraction (nanometer) level must be developed.

Here we propose a method for probing of the local fluctuations of  $n$  in solids by the analysis of zero-phonon spectral lines (ZPL) of single dye molecules at ultra-low temperatures and out of saturation effects due to laser excitation. ZPL spectral width is limited by excited state natural lifetime:  $\Gamma_0=1/2\pi T_1$ , whereas  $T_1$  is a function of  $n$  due to local field effects:  $T_1(n)=\tau_0/nf(n)$ , where  $f(n)$  depends on the theoretical model [1].

In present study, we take for further analysis the unique experimental data on SM ZPL width distributions in amorphous polyethylene and polycrystalline naphthalene as measured at milliKelvin temperatures in order to find the distribution of  $n$  local values in real Tr-doped solids [2, 3]. The distributions of lifetime-limited SM ZPL widths  $\Gamma_0$  were obtained. These distributions  $P_{\Gamma_0}(\Gamma_0)$  can be recalculated into the distributions of  $P_{T_1}(T_1)$  and then into the distributions of refraction indices  $P_n(n)$ . In the context of the present work we have found the dependence  $T_1(n)$  for terrylene (Tr) molecules in different matrixes (polyethylene, polystyrene, polyvinyl-butylal, polymethyl-methacrylate, and solid n-hexadecane).

In summary: (a) We show that in the real samples, there are considerable fluctuations of the refractive index, which are more notable in the disordered material. It is remarkable that the maximum of the refractive index distribution corresponds to the average value of  $n$ , obtained by traditional methods. (b) We propose a unique method for the probing of the local refractive index fluctuations in solids. It is based on the detection of SM ZPLs at conditions allowing lifetime-limited spectral line widths. This method is promising as it potentially allows simultaneous reconstruction of SM spatial coordinates with the nanometre accuracy by super-resolution fluorescence microscopy [4].

The support from Russian Foundation for Basic Research is acknowledged (project 14-29-07270), and from Russian Science Foundation (14-12-01415).

[1] D. Kuznetsov, V. Roerich, M. Gladush, Journal of Experimental and Theoretical Physics, 113 (2011), 647.

[2] E.A. Donley, V. Burzomato, U.P. Wild, T. Plakhotnik, Journal of Luminescence, 8384 (1999), 255-259.

[3] E.A. Donley, S. Bonsma, V. Palm, V. Burzomato, U.P. Wild, T. Plakhotnik, 8789 (2000), 109-114.

[4] A.V. Naumov, I.Y. Eremchev, A.A. Gorshelev, European Physical Journal D, 68 (11) (2014), 348.

## FABRICATION OF $Y_2O_3$ and $Y_{1.94}Yb_{0.05}Er_{0.01}O_3$ THIN FILMS BY PULSED LASER DEPOSITION

Djordje Veljović<sup>a</sup>, Natalia Mihailescu<sup>b</sup>, Angela Stefan<sup>b</sup>, G. E. Stan<sup>c</sup>, Catalin Luculescu<sup>b</sup>,  
Djordje Janačković<sup>a</sup>, Vesna Đorđević<sup>d</sup>, Miroslav D. Dramićanin<sup>d</sup>, Radenka Krsmanović  
Whiffen<sup>d</sup>, Carmen Ristoscu<sup>b</sup>, Serban Georgescu<sup>b</sup>, Ion N. Mihailescu<sup>b</sup>

<sup>a</sup>*Faculty of Technology and Metallurgy, University of Belgrade, Serbia, e-mail:*  
*djveljovic@tmf.bg.ac.rs*

<sup>b</sup>*National Institute of Lasers, Plasma and Radiation Physics, Magurele, Ilfov, Romania; e-*  
*mail: natalia.serban@inflpr.ro*

<sup>c</sup>*National Institute of Materials Physics, Magurele, RO-077125, Romania*

<sup>d</sup>*Vinca Institute of Nuclear Sciences, University of Belgrade, Serbia, e-mail:*  
*radenka@vinca.rs*

Ultraviolet photons generated by a KrF\*-laser source ( $\lambda=248$  nm) were used for the synthesis by pulsed laser deposition (PLD) of nanometric  $Y_2O_3$  and  $Y_{1.94}Yb_{0.05}Er_{0.01}O_3$  thin films with controlled thickness, stoichiometry and photoluminescence properties. The expelled material was collected onto  $SiO_2$  and Si (100) wafers. We studied the effects of substrate temperature (500°C and 600°C) and Oxygen pressure (1Pa and 10 Pa) on the structural properties of the films. FTIR spectra demonstrated a congruent transfer of material from the target to the substrate. On the basis of FTIR analysis, we selected the regime 1Pa/600°C as the best one for the deposition of doped and undoped  $Y_2O_3$  layers. The deposited structures were characterized from physical-chemical point of view by Scanning Electron Microscopy in top- and cross-view modes, X-Ray Diffraction, Raman spectroscopy, Transmission Electron Microscopy and Energy Dispersive X-Ray Spectroscopy investigations. Optical activity of  $Y_{1.94}Yb_{0.05}Er_{0.01}O_3$  films was proved by photoluminescence and NIR spectroscopies as presented in Figure 1 below.

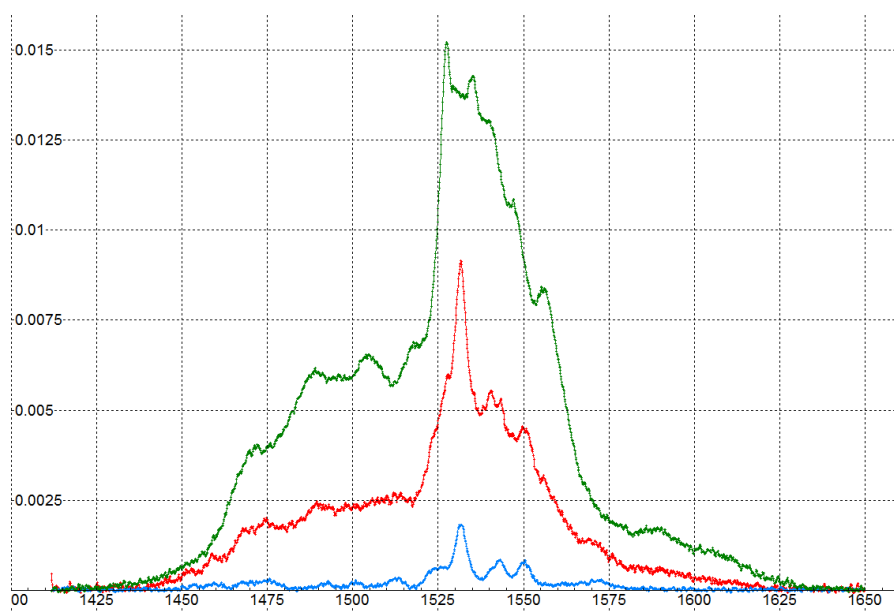


Figure 6 NIR spectra (excitation @ 980 nm) collected from the  $Y_{1.94}Yb_{0.05}Er_{0.01}O_3$  TFs. Green line –  $SiO_2$  substrate, thermally treated at 600°C; red – Si substrate, 600°C; blue – Si substrate, 500°C

## MODELLING LIGHT EMISSION FROM DC DISCHARGE TUBE FILLED WITH CH<sub>4</sub> GAS

V. Stojanović, Ž. Nikitović and Z. Lj. Petrović

*Institute of Physics, University of Belgrade, P.O. Box 57, 11080 Beograd, Serbia,  
zeljka@ipb.ac.rs*

In this work we modelled spatially resolved light emission from DC discharge tube filled with pure CH<sub>4</sub> gas by using Monte Carlo simulation technique. Methane DC discharges are widely used in plasma polymerisation, for obtaining diamond-like films and carbon nanostructures. Methane may also be applied in etching of low dielectric permeability (k) materials as they replace SiO<sub>2</sub> in higher frequency integrated circuits. Methane is one of the most popular molecular additives in gas mixtures for drift chambers used as track detectors for high energy particles.

Light emission produced in CH<sub>4</sub> discharge tube is modeled by following transport of electrons, positive ions (C<sup>+</sup>, CH<sup>+</sup>, CH<sub>2</sub><sup>+</sup>, CH<sub>3</sub><sup>+</sup>, CH<sub>4</sub><sup>+</sup>, H<sup>+</sup>, H<sub>2</sub><sup>+</sup>) and fast neutrals (CH and CH<sub>3</sub>) and accounting electron backscattering at the electrodes (graphite anode and stainless steel cathode). For conditions from low to high  $E/N$  (E-electric field, N-gas density) we calculated spatially dependent emission between two plan-parallel plates made of graphite. Excellent agreement between results of numerical simulation and measurements is achieved. It is found that light emission at low and moderate  $E/N$  mostly correspond to electron impact dissociative excitation of CH<sub>4</sub> while at high  $E/N$  apart from electron contribution shows contribution close to the cathode that belong to a heavy particles excitation. In this work we present spatially dependent H $\alpha$  emission as a function of  $E/N$ . The calculations were based on the heavy particle cross sections of Petrović and Phelps [1].

[1] Z. Lj. Petrović A. V. Phelps (1992) unpublished

## NOVEL ENERGY-SAVING (NANO) PHOSPHORS

Claudia Wickleder

*Inorganic Chemistry, Faculty for Science and Technology, University of Siegen,  
Germany, wickleder@chemie.uni-siegen.de*

Due to the continuous miniaturization of electronic and optical devices, the importance of functionalized nanomaterials has drastically increased in the past few years. Examples of nanoscopic materials are nanoparticles (NPs) and nanoporous metal-organic frameworks (MOFs). In contradiction to the analogous bulk samples, luminescent NPs present several advantages as high packing density, low light scattering effects, energy saving synthesis (with shorter preparation time and lower sintering temperatures) and are easily suspendable in liquid media [1]. Due to the small size, nanophosphors are able to build thinner films e.g. on the surface of light emitting diodes (LEDs) and are less subjected to concentration quenching effects, in comparison to doped micron-sized phosphors. Nanoporous MOFs offer the possibility of embedding and homogeneously mixing luminescent materials for fine tuning the emission color and also build thin films by means of liquid-phase epitaxy [2].

In this presentation, several optical materials for different applications, like LED phosphors, will be presented in bulk as well as in nanoparticle form. Furthermore, the advantages of nanostructured materials will be highlighted, especially those containing  $\text{Eu}^{2+}$  ions due to their outstanding luminescent properties (Fig. 1) [3, 4]. In general, luminescent materials with  $\text{Eu}^{2+}$  ions cannot be prepared by conventional methods in aqueous solution, thus novel synthesis for these materials will be presented yielding promising materials. Finally, multifunctional nanoparticles and highly luminescent MOFs will be presented.



Fig. 1 Tuning of the emission colour of  $\text{Eu}^{2+}$  doped alkaline earth silicates

[1] H. Cerqueira Streit, J. Kramer, M. Suta, C. Wickleder, *Materials* 6 (2013) 3079.

[2] H. C. Streit, M. Adlung, O. Shekhah, X. Stammer, H. K. Arslan, O. Zybalyo, T. Ladnorg, H. Gliemann, M. Franzreb, Ch. Wöll, C. Wickleder, *Chem. Phys. Chem.* 13 (2012) 2699.

[3] M. Krings, G. Montana, R. Dronskowski, C. Wickleder, *Chem. Mater.* 23 (2011) 1694.

[4] H. Terraschke, M. F. T. Meier, Y. Voss, H. Schönherr, C. Wickleder, *J. Cer. Proc. Res.* 16 (2015) 59.



## STAINING KINETICS OF DENTAL RESIN COMPOSITES

D. Manojlović,<sup>1</sup> M. Antonov,<sup>2</sup> B. Milićević,<sup>2</sup> L. Lenhardt,<sup>2</sup> M.D. Dramićanin<sup>2</sup>

<sup>1</sup> *University of Belgrade, School of Dental Medicine, Rankeova 4, Belgrade, Serbia*

<sup>2</sup> *University of Belgrade, Vinča Institute of Nuclear Sciences, P.O.Box 522, Belgrade, Serbia*

After daily exposure to different colorants from food and beverages, dental resin composites change color making the restoration aesthetically displeasing. Many studies have shown that red wine has a strong staining potential. Though total color change has been widely investigated in a number of reports, the knowledge on the mechanisms of staining and physicochemical processes during staining causing color instability are poorly documented. Optical properties of materials are affected to a different extent by adsorption and absorption of colorants from the staining solutions. In this report we present results of an analysis of staining kinetics on a microhybrid composite Gradia Direct, extra bleach white (XBW) shade exposed to red. Description of optical properties of materials surface is done through color space coordinates. Diffuse reflection spectra of composite samples were measured at several intervals during staining, as well as after immersion in distilled water for different times. CIELAB color coordinates are calculated. From these data kinetics of adsorption and desorption is followed.

## THE EFFECTS OF DOPING ON CRYSTAL STRUCTURE AND PHOTOLUMINESCENCE OF $\text{LaVO}_4:\text{Eu}^{3+}$

Andrii Shyichuk<sup>a</sup>, Mohammad Zarad<sup>a</sup>, Marcin Runowski<sup>a</sup>, Agata Szczeszak<sup>a</sup>, Renaldo T. Moura Jr.<sup>b</sup>, Albano N. Carneiro Neto<sup>b</sup>, Stefan Lis<sup>a</sup>, Oscar L. Malta<sup>b</sup>

<sup>a</sup>*Department of Rare Earth, Faculty of Chemistry, Adam Mickiewicz University, Umiltowska 89b, 61-614 Poznań, Poland; andrii.shyichuk@gmail.com*

<sup>b</sup>*Department of Fundamental Chemistry, Federal University of Pernambuco, Prof. Moraes Rego Ave., University city, CEP 50.740-560, Recife, PE, Brazil.*

The series of  $\text{LaVO}_4:\text{Eu}^{3+}$  was obtained via a hydrothermal route. The overall composition was  $\text{La}_{(1-x)}\text{Eu}_x\text{VO}_4$ , where  $x$  was equal 0.0, 0.02, 0.04, 0.06, 0.08 and 0.1.

Samples were analyzed using powder X-ray diffraction, XRD. The diffraction patterns were analyzed using Rietveld refinement by means of the MAUD software. The samples were confirmed to contain only one phase of the tetragonal lanthanum vanadate, t- $\text{LaVO}_4$ . The refinement provided experimental data on the crystal cell dimensions. Both crystal cell dimensions  $a$  and  $c$  showed a clear dependence on the amount of the introduced dopant. The increase of the amount of dopant from 0 to 10% resulted in a gradual decrease of the cell dimensions by about 0.1%.

Photoluminescence properties of the obtained samples were studied with the use of their emission and excitation spectra in the UV-Vis range. The excitation spectra contained both characteristic of  $\text{Eu}^{3+}$  (f-f transitions) and the  $\text{O}^{2-} \rightarrow \text{V}^{5+}$  charge transfer bands. The emission spectrum contained the bands of  $\text{Eu}^{3+}$  corresponding to the  ${}^5\text{D}_0\text{-}{}^7\text{F}_{0-4}$  transitions. The spectroscopic data were used to calculate experimental Judd-Ofelt intensity parameters. The intensity of the  ${}^5\text{D}_0\text{-}{}^7\text{F}_1$  magnetic dipole transition was used as a reference [1]. Both  $\Omega_2$  and  $\Omega_4$  intensity parameters were gradually decreasing with the increasing amount of dopant. Considering the changes in the cell dimensions; such behavior of the parameters might be attributed to the alterations in the chemical environment of the dopant ions caused by the cell dimensions' changes. However, theoretical calculations (from scratch [1]) of the intensity parameters suggest that decrease in the cell dimensions must cause an increase in the intensity parameters, provided that the chemical surround polarizability  $\alpha$  of dopant ions and charge donation factor  $g$  are constant. Fitting the  $\alpha$  and  $g$  parameters to the experimental trend suggests a decrease in both parameters with the increasing amount of the dopant.

Summarizing, in this study we have shown that introduction of the  $\text{Eu}^{3+}$  dopant to t- $\text{LaVO}_4$  causes a decrease in crystal cell dimensions of the material. Also, experimental Judd-Ofelt intensity parameters decrease gradually with the increase of the dopant concentration. As the crystal structure and synthesis conditions of the samples were the same, the decrease of the intensity parameters must be caused by the increase of the dopant amount. Most likely, the decrease of cell dimensions of the materials affects their electronic structure and, consequently, affects the  $\alpha$  and  $g$  parameters and the intensity parameters.

[1] G.F. de Sá, O.L. Malta, C. de Mello Donegá, A.M. Simas, R.L. Longo, P.A. Santa-Cruz, E.F. da Silva, *Coord. Chem. Rev.* 196 (2000) 165–195.

[2] A. Szczeszak, T. Grzyb, Z. Śniadecki, N. Andrzejewska, S. Lis, M. Matczak, G. Nowaczyk, S. Jurga, B. Idzikowski, *Inorg. Chem.* 53 (2014)12243–12252.

## **IMPROVEMENT OF MATERIAL SURFACE PROPERTIES BY USING LASER SHOCK WAVE TECHNIQUE**

Abdulhadi Kadhim<sup>1</sup> , Haitham T. Hussein<sup>2</sup> , Zahraa J. Muhammad<sup>2</sup>, Ayad Zwayen Mohammed<sup>1</sup>

<sup>1</sup>*Laser and Optoelectronic Eng. Dept. University of Technology, Baghdad, Iraq*

<sup>2</sup>*Applies science Dept. University of Technology, Baghdad, Iraq*  
*ayad\_1967\_2005@yahoo.com*

The utilization of a laser to change the surfaces of different materials designing is a vital subjects in the present time. Two types of alloys were utilized as a part of this work; 6063Al and C11000 alloys. The specimens were prepared by cutting into plate state of diameter 12 mm and after that cleaning and polishing procedure to create same surface roughness for all specimens. Surface roughness and micro hardness were measured for all specimens before and after laser shock wave treatment. distinctive laser parameters impact on alloys surface properties were considered, for example, laser energy, confinement layer(different depth of double deionized distilled water - DDDW), and number of laser pulses. The outcomes uncover that the surface roughness are increased by 200% for 6063Al alloy and by 120% for C11000 alloy when we utilized laser energy of 400mj, number of laser pulses of 100 and imprisonment layer of 5mm. While the micro hardness increment by 80% for the two types of alloys and at the same conditions. Diverse estimations and distinctive mechanical tests were completed for all specimens to produce exact and precise results.